

**Synthesis, structure, and reactivity of Omeprazole and
related compounds**

Judith Spence

Submitted in accordance with
the requirements for the degree of
Doctor of Philosophy

University of Leeds
School of Chemistry

August 2018

The candidate confirms that the work submitted is her own and that appropriate credit has been given where reference has been made to the work of others.

This copy has been supplied on the understanding that it is copyright material and that no quotation from the thesis may be published without proper acknowledgement.

The right of Judith Spence
to be identified as Author of this work
has been asserted by her in accordance with the
Copyrights, Designs and Patents Act 1988
© 2018 The University of Leeds and Judith Spence

To my family,
and
James and Peggy

Acknowledgement

Firstly I would like to thank my supervisor Prof. Chris Rayner for his support, advice and guidance, which has been invaluable to me throughout my PhD. I am also very thankful for his patience and understanding. I would also like to express my gratitude to AstraZeneca for funding this PhD, and thank my industrial supervisors Will Goundry, Martin Jones, and Andy Wells.

I also thank the members of the Rayner group from over the past few years, particularly Douglas Barnes for his companionship during the earlier years, and Meryem Benohoud, Lauren Ford, and Franziska Scheil, Henry Spurr, and Lissie Dufton who all made G.39 a pleasure to work in during the last year of my PhD.

I have made many good friends since coming to Leeds who have made these last few years tolerable, my great thanks goes to Fraser Cunningham, Katie Marriot, Chris Pask (thank you for the lovely crystal structures), and Felix Janeway

I would like to express my gratitude to the many people behind the scenes who have enabled this research, Dr. Terry Kee, Dr. Julie Fisher, and Prof Andy Wilson for their pastoral care, Martin Huscroft, Simon Barrett and Tanya Marinko-Covell for their technical support, and Francis and all the other members of staff at Stores for their tireless efforts. I am also thankful for all the help from Rachel Sherwin, Gail Hardwick, and Anna Luty over the past few years.

I am grateful to my family, my mum Sandra, Ray, Alex, Victoria, and Tom, for their endless love and support. A special thanks goes to my sister Alex who has been great company throughout during my time in Leeds. I would also like to thank Deborah, Helen, and Jennifer Adcott for welcoming me into their family.

Finally I would like to thank my wonderful partner James, without whom I probably would not have made it this far. Thank you for everything you have done for me.

Update: Since embarking upon the writing of this thesis I have gained another very important person in my life to which I would like to give special mention, my wonderful daughter Peggy. I was working on the first chapter of this thesis when I felt your first kicks, and I can hear you playing and laughing downstairs as I am typing this now. Thank you for coming into my life and making it infinitely more joyous. I love you, and I hope I can make you proud of me.

Abstract

This thesis is concerned with the synthesis and properties of racemic and enantiopure sulfoxides, compounds which have application as biologically active agents and are useful tools for chemical synthesis. Particular focus is placed on the sulfoxide Omeprazole, which is one of the world's best selling pharmaceutical products, and the single isomer form of the drug (*S*)-Esomeprazole.

Chapter one covers the fundamental aspects of sulfoxide chemistry, the synthesis of racemic sulfoxides, and describes various approaches to the production of chiral sulfoxides in optically pure form such as resolution, nucleophilic substitutions methodologies, and non-metal based oxidative processes which use either chiral catalysts or chiral oxidants. Chapter two continues this review discussing stereoselective sulfide oxidations using metal catalysts.

The discovery, mechanism of action, and large scale synthesis of Omeprazole, a biologically active sulfoxide used to treat ailments associated with excess stomach acid, is discussed in chapter three. In addition, this chapter examines the developments of the single enantiomer drug (*S*)-Esomeprazole and the various synthetic strategies employed in the production of this chiral sulfoxide.

The ensuing chapters describe my own work: chapter four contains work on the synthesis of a range of sulfides, racemic sulfoxides, and sulfones. Following on from this the asymmetric synthesis of chiral sulfoxides, including (*S*)-Esomeprazole, using a modified Kagan type titanium tartrate catalyst system was investigated, with the achievement of sulfoxidation enantioselectivities of up to > 99.5% ee.

In chapter five the development of a new method for the determination of enantiomeric excess of (*S*)-Esomeprazole by ^1H NMR is examined. Chiral tartrates were employed as chiral shift agents (CSA) and were found to provide efficient and accurate measurement of sulfoxide ee. The choice of NMR solvent, the host:guest ratio, and the efficacy of the tartrates to act as CSA for a range of structurally diverse sulfoxides was also investigated.

Chapter six covers three studies on the structures and reactivities of Omeprazole and related sulfoxides. X-ray crystallographic diffraction (XRD) was employed to investigate the solid state structures and packing a range of sulfoxides. The effect of annular tautomerism was explored by ^1H and ^{13}C NMR for a series of benzimidazole based sulfoxide species, including Omeprazole. Finally, ^1H NMR was employed to investigate the selective deuteration of sulfoxides such as Omeprazole, including the examination of H/D-exchange observed by NMR in DMSO-d_6 .

Abbreviations

Ac	Acetyl
acac	Acetylacetyl
ACAT	Acyl coenzyme A (CoA):cholesterol acyltransferase
benz	Benzimidazolyl
BINAP	2,2'-Bis(diphenylphosphino)-1,1'-binaphthyl
BINASO	1,1'-Binaphthalene-2,2'-diyl-bis(<i>p</i> -tolylsulfoxide)
BINOL	1,1'-Bi-2-naphthol
BMVO	Baeyer Villiger Monooxygenase
Bn	Benzyl
Boc	^t Butoxycarbonyl
br	Broad singlet
BSA	Bovine serum albumin
cat	Catalytic
CD	Cyclodextrins
CDA	Chiral derivitisation agent
CHP	Cumene hydroperoxide
CLC	Chiral liquid crystals
CMO	Cyclohexanone monooxygenase
COD	1,5-Cyclooctadiene
COSY	Correlation spectroscopy
CPO	Chloroperoxidase
CSA	Chiral shift agent
CSP	Chiral stationary phase
CTAB	Cetyltrimethylammonium bromide
DAG	Diacetone-D-glucose
DBU	1,8-Diazabicyclo[5.4.0]undec-7-ene
DCC	<i>N,N'</i> -Dicyclohexylcarbodiimide
DCE	Dichloroethane
DCG	Dicyclohexyl-D-glucofuranose
DET	Diethyl tartrate
(DHQD) ₂ -PYR	Hydroquinidine-2,5-diphenyl-4,6-pyrimidinediyl diether
DIPEA	Diisopropylethylamine
DIPT	Diisopropyl tartrate
DKR	Dynamic kinetic resolution

DMAP	4-Dimethylaminopyridine
dme	1,2-Dimethoxyethane
DMSO	Dimethyl sulfoxide
EDTA	Ethylenediamine tetraacetic acid
ee	Enantiomeric excess
ESCA	Electron spectroscopy for chemical analysis
Fc	Ferrocenyl
GC	Gas chromatography
HAPMO	4-Hydroxyacetophenone monooxygenase
hfc	3-(Heptafluoropropyl-hydroxymethylene)-d-camphorate
HMBC	Heteronuclear multiple-bond correlation spectroscopy
HMPA	Hexamethylphosphoramide
HMQC	Heteronuclear multiple quantum coherence
HPLC	High performance liquid chromatography
HQA	Hydroquinine acetate
HRP	Horse radish peroxidase
IBX	2-Iodoxybenzoic acid
IR	Infrared
LC	Liquid chromatography
LDH	Layered double hydroxides
MA	Mandelic acid
<i>m</i> CPBA	<i>m</i> -Chloroperbenzoic acid
MHz	Megahertz
MnP	Manganese peroxidase
MPO	Myeloperoxidase
MS	Molecular sieves
NaHMDS	Sodium hexamethyldisilazide
nb	Norbornadiene
NDO	Naphthalene dioxygenase
NMO	4-Methylmorpholine- <i>N</i> -oxide
NMR	Nuclear magnetic resonance
NOESY	Nuclear Overhauser effect spectroscopy
PAMO	Phenylacetone monooxygenase
PMB	<i>p</i> -Methoxy benzyl
PPHA	Phthalimidoperhexanoic acid
pyr	Pyridyl

QDA	Quinidine acetate
R _f	Retardation factor
SAE	Sharpless asymmetric epoxidation
SDE	Self-disproportionation of enantiomers
TBHP	^t Butyl hydrogen peroxide
TDO	Toluene dioxygenase
Tf	Trifluoromethanesulfonyl
THF	Tetrahydrofuran
TLC	Thin layer chromatography
TMAO	Trimethylamine <i>N</i> -oxide
tms	Tetramethylsilyl
TOCSY	Total correlation spectroscopy
tol	Tolyl
Tr	Trityl (triphenylmethyl)
Ts	<i>p</i> -Toluenesulfonyl
UHP	Urea-hydrogen peroxide
UV	Ultra violet
VBrPO	Vanadium bromoperoxidase
[O]	Oxidizing agent

Contents

Acknowledgement	vii
Abstract	ix
Abbreviations	xi
Contents	xv
1 Introduction: Synthesis and application of sulfoxides	1
1.1 Sulfoxides	1
1.2 Biologically important sulfoxides	1
1.3 Applications of sulfoxides	3
1.4 Synthesis of sulfoxides	7
1.4.1 Racemic sulfoxides	7
1.4.2 Chiral sulfoxides	8
1.4.2.1 Resolution of chiral sulfoxides	10
1.4.2.1.1 Classical resolution	10
1.4.2.1.2 Kinetic resolution	12
1.4.2.1.3 Enantiomeric enrichment via achiral chromatography	16
1.4.2.2 Synthesis of chiral sulfoxides via nucleophilic displacement at sulfur	18
1.4.2.2.1 The Andersen method	18
1.4.2.2.2 Alternative sulfinylating agents	20
1.4.2.2.3 Double nucleophilic displacement at sulfur	24
1.4.2.3 Non-metal based oxidation of prochiral sulfides	29
1.4.2.3.1 Oxidations performed using a chiral oxidant	29
1.4.2.3.2 Oxidations performed in presence of a chiral catalyst	43
1.4.2.3.3 Biological asymmetric sulfide oxidations	47
1.4.2.3.3.1 Oxidations using whole cells	48
1.4.2.3.3.2 Oxidations using isolated enzymes	51
1.4.2.3.3.3 Oxidations in the presence of bovine serum albumin	54
1.5 Summary	56
2 Introduction: Metal-catalyzed asymmetric sulfide oxidation	59
2.1 Titanium-catalyzed S-oxidations	59
2.2 Vanadium-catalyzed S-oxidations	81
2.3 Manganese-catalyzed S-oxidations	88
2.4 Iron-catalyzed S-oxidations	92
2.5 Molybdenum-catalyzed S-oxidations	96
2.6 Ruthenium-catalyzed S-oxidations	98
2.7 Copper-catalyzed S-oxidations	99

2.8	Aluminium-catalyzed S-oxidations.....	100
2.9	Zirconium-catalyzed S-oxidations	101
2.10	Tungsten-catalyzed S-oxidations	102
2.11	Platinum-catalyzed S-oxidations.....	103
2.12	Osmium-catalyzed S-oxidations	103
2.13	Niobium-catalyzed S-oxidations.....	104
2.14	Bismuth-catalyzed S-oxidations.....	105
2.15	Summary	105
3	Introduction: Omeprazole and Esomeprazole	107
3.1	Omeprazole: A Proton Pump Inhibitor	107
3.2	Development of Omeprazole	108
3.3	Mechanism of Action.....	111
3.4	Synthesis of Omeprazole	113
3.4.1	Structure and nomenclature of Omeprazole	113
3.4.2	Synthesis of Omeprazole.....	114
3.5	Esomeprazole: A single enantiomer proton pump inhibitor	116
3.5.1	Development of a new proton pump inhibitor	116
3.5.2	The Chiral Switch.....	118
3.5.3	Asymmetric synthesis of Esomeprazole.....	119
3.5.3.1	Industrial Process Development of Esomeprazole	119
3.5.3.2	Alternative syntheses of Esomeprazole	123
3.5.3.2.1	Resolution of racemic Omeprazole	123
3.5.3.2.2	Non-metal based oxidations	125
3.5.3.2.3	Metal based oxidations	126
3.6	Summary	134
4	Results and Discussion: Asymmetric synthesis of Esomeprazole.....	137
4.1	Project aims.....	137
4.2	Preparation of racemic Omeprazole and related compounds.....	138
4.2.1	Spectroscopic and chromatographic analysis of Omeprazole and related compounds	141
4.2.2	¹ H NMR characterization of Omeprazole vs. Esomeprazole	145
4.3	The Asymmetric synthesis of Esomeprazole	148
4.4	Enhancement of optical purity by crystallization.....	153
4.5	Synthesis of sulfides, sulfoxides, and sulfones analogous to the Omeprazole series. 154	
4.5.1	Synthesis of sulfides.....	155
4.5.2	Synthesis of racemic sulfoxides	156

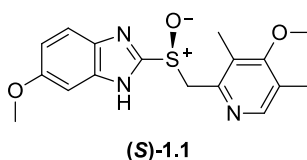
4.5.3	Synthesis of sulfones	157
4.6	Titanium mediated asymmetric synthesis of chiral sulfoxides	159
4.7	Improving the understanding if the Ti-tartrate asymmetric S-oxidation reaction: NMR studies of the catalyst components	160
4.7.1	NMR studies of the catalyst components: Ti(OiPr) ₄ + Pyrimetazole sulfide	161
4.7.2	NMR studies of the catalyst components: Ti(OiPr) ₄	162
4.7.2.1	Ti(OiPr) ₄ concentration studies	162
4.7.2.2	Implications for the Ti-mediated synthesis of Esomeprazole	168
4.7.3	NMR studies of the catalyst components: Ti(OiPr) ₄ + DET + H ₂ O	169
4.8	Conclusions and future direction	171
5	Evaluation of chiral tartrates for use as chiral solvating agents	175
5.1.1	NMR spectroscopy as a tool for quantitative stereochemical analysis	175
5.1.2	CSA for the enantiodiscrimination of chiral sulfoxides	177
5.2	NMR enantiodiscrimination of Omeprazole, Esomeprazole, and related PPIs	178
5.3	Chiral tartrates as CSA for ee determination in Esomeprazole	179
5.3.1	(<i>S</i>)-BINOL vs. (<i>S,S</i>)-DET as chiral shift agents	179
5.3.2	Choice of NMR solvent	181
5.3.3	Host-guest ratio	184
5.3.4	Determination of enantiomeric excess	190
5.4	Contrasting enantiodiscriminatory action of CSAs: DET vs. BINOL	193
5.5	Conclusions and future directions	197
6	Studies on the structure and reactivity of Omeprazole and related compounds	199
6.1	X-ray crystallography of Omeprazole and related compounds	199
6.1.1	X-ray structures of the Omeprazole family	199
6.1.2	Structural analysis of the Omeprazole family	209
6.1.3	X-ray structures of selected racemic sulfoxides	212
6.1.4	Structural analysis of racemic sulfoxides	215
6.2	Tautomerism of Omeprazole and related compounds	218
6.2.1	Prototropic exchange of Omeprazole and related species	218
6.2.2	Synthesis and characterization of derivatized Omeprazole and related species	224
6.3	Selective deuteration of Na-Omeprazole and related compounds	227
6.3.1	Deuteration of Na-Omeprazole in an aprotic solvent	227
6.3.2	Deuteration of Na-Omeprazole and related compounds in protic solvents	232
6.4	Conclusion and Future direction	238
7	Appendix	241
8	Experimental	243

8.1	General Experimental	243
8.2	Synthetic Protocols	245
8.3	NMR studies	267
	References.....	273

1 Introduction: Synthesis and application of sulfoxides

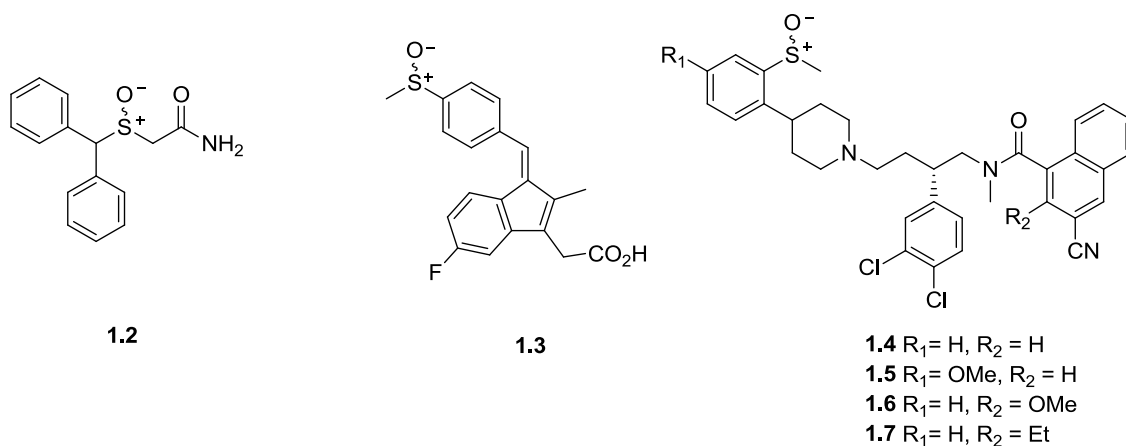
1.1 Sulfoxides

To the synthetic chemist the sulfoxide is a useful and versatile functional group, with uses as chiral auxiliaries and synthons for stereoselective carbon–carbon bond formation.¹⁻⁹ Furthermore, the sulfinyl functionality is regularly found in biologically active materials, both naturally occurring and manmade.¹⁰⁻¹² Over the past century great efforts have been made to fully understand and exploit the utility of the sulfoxide, from the early debates over the nature of the bonding in the group right through to the challenges presented in the development of an asymmetric synthesis of the modern day “blockbuster” drug Esomeprazole (*S*)-**1.1**.¹³⁻¹⁶ The aim of this chapter is to present an overview of the occurrence, application, and synthesis of sulfoxides, with particular emphasis given to the formation of chiral sulfoxides.

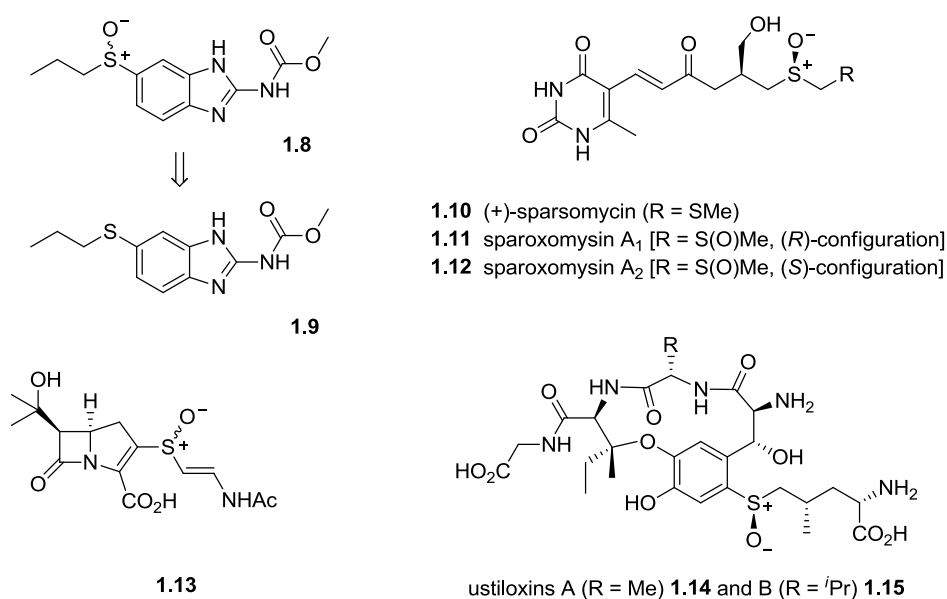


1.2 Biologically important sulfoxides

The sulfoxide functional group is found in a large number of molecules of biological interest, many of which have application as pharmaceuticals for the treatment of a wide range of conditions.¹⁷ Modafinil **1.2** is a psychostimulant used to treat sleep disorders such as narcolepsy and sleep apnea.¹⁸⁻²⁰ Although typically prescribed in the racemic form, the two enantiomers of Modafinil have been shown to have differing pharmacological effects, with the (*S*)-isomer being eliminated from the body at a rate three times faster than that of the (*R*)-isomer.²¹ The anti-inflammatory drug Sulindac **1.3** is employed in the treatment of arthritic conditions and has, over the past ten years, gained interest as an anti-cancer treatment.²² Four neurokinin antagonists **1.4-1.7** have been investigated for their potential for use in treatments against depression, urinary incontinence and asthma.²³



The efficacy of some medicinal therapies can be attributed to the sulfoxide metabolite of the administered drug. One example of this is found in the treatment for neurocysticercosis where the active sulfoxide **1.8** is believed to be responsible for the anthelmintic properties of the antiparasitic drug Albendazole **1.9**.²⁴ (+)-*Sparsomycin* **1.10**, a metabolite of *Streptomyces sparsogenes* and *Streptomyces cuspidosporus*, has been the subject of investigation for its activity against fungi, bacteria, viruses, and several tumor systems. Other members of the pyrimidinylpropanamide family have also been investigated in the form of sulfoxides **1.11** and **1.12**.²⁵ The anti-bacterial properties of the β -lactam based Carpetimycin sulfoxide **1.13** have also been reported.²⁶ The ustiloxin cyclic peptides, isolated from the fungus *Ustilagoidea virens*, are known to exhibit antimetabolic properties which cause inhibition in growth of several human cancer lines; sulfoxide **1.14** and **1.15** have been found to be particularly potent against breast and liver cancer.^{27, 28}

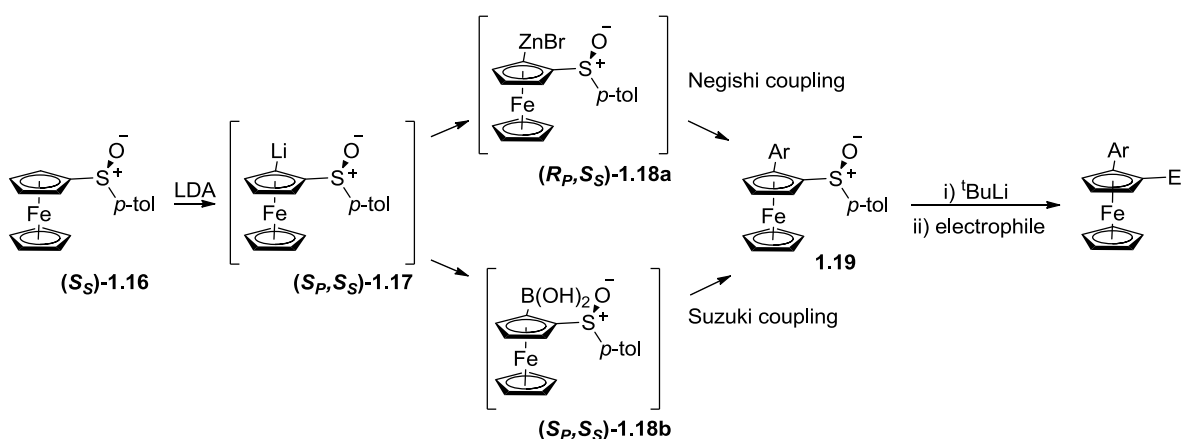


1.3 Applications of sulfoxides

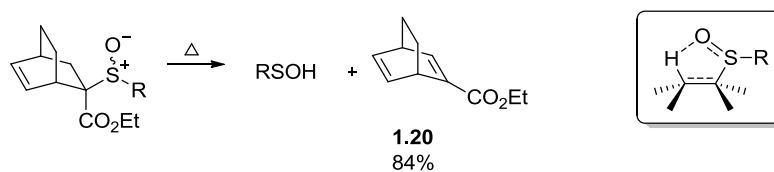
Sulfoxides are versatile starting materials for a wide range of synthetic transformations.^{5, 7} In addition, they can be used as chiral auxiliaries and ligands for use in asymmetric synthesis and have been called “one of the most efficient and versatile chiral controllers in C–C and C–X bond formation”.²⁹ The polarized S–O bond allows for co-ordination to both transition metals and Lewis acids, and the stable pyramidal configuration about sulfur gives rise to ordered and rigid transition state geometries. The pyramidal inversion barrier for a typical sulfoxide is between 35–43 kcal mol⁻¹ hence sulfinyl groups are configurationally stable at room temperature and generally remain so up to 200 °C.^{17, 30-32}

Chiral sulfoxides are often exploited for their ability to transfer stereochemical information in reactions sites that can be proximal or more distant within the reacting molecule.^{3, 6} The efficacy in employing sulfoxides for the purpose of stereochemical control can be attributed to two factors. Firstly the substituents on a sulfoxide sulfur, i.e. two different carbon ligands, a lone pair of electrons and an oxygen, provide a greatly contrasting steric and stereoelectronic environments in the diastereotopic faces of a reacting molecules.^{6, 33} Secondly, there is a great number of methods by which sulfoxides, particularly homochiral ones, may be obtained. The great success in developing these methods, particularly over the past two decades, has given rise to the development of sulfoxide mediated reactions which include Diels–Alder cycloadditions, asymmetric hydrogenations of ketones and olefins, Pd-catalyzed enantioselective allylic alkylations, and stereoselective radical allylations to name but a few.^{22, 34, 35} Unfortunately it is not possible to do justice to the extensive application that sulfoxides have in modern synthesis; instead a number of interesting highlights are presented here. For examination of this area in greater detail there are a number of excellent books and reviews that may be consulted, in addition to those texts already referenced herein.³⁶⁻⁵⁰

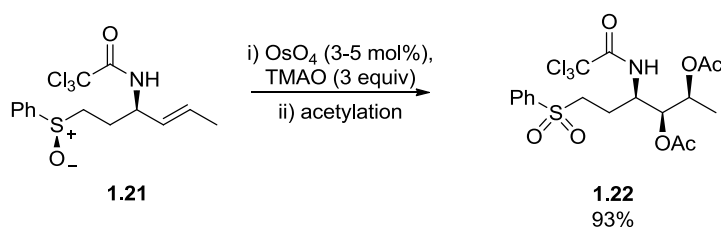
The sulfinyl group can act as an *o*-metalation group; when an optically pure sulfoxide species is used this reaction can occur in a diastereoselective manner, one such example was reported by Kagan and coworkers in the ortho-lithiation *p*-tolyl ferrocene species (*S_S*)-**1.16** which afforded sulfoxide (*S_P*,*S_S*)-**1.17** (Scheme 1.1).⁵¹ Subsequent lithium-zinc exchange with ZnCl₂ gave (*R_P*,*S_S*)-**1.18a** which then underwent a Negishi coupling to introduce an aryl group. Alternatively the aryl group could be introduced via Suzuki coupling with the boronic intermediate (*S_P*,*S_S*)-**1.18b**, also generated from the lithiated species (*S_P*,*S_S*)-**1.17**.



Sulfoxide species with a β -hydrogen are known to form olefins such as **1.20**, and a sulfenic acid by way of a syn-elimination type reaction.⁵²⁻⁵⁴ Under pyrolysis conditions the reaction proceeds in a stereocontrolled manner via a cyclic transition state, as shown in Scheme 1.2.⁵⁵

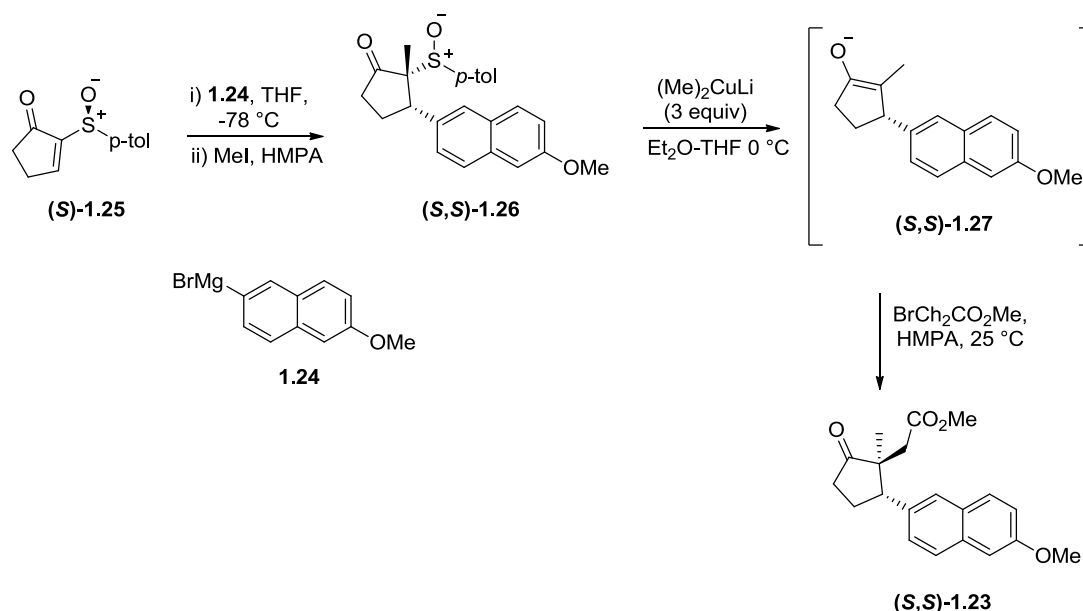


Hauser and coworkers reported the use of a remote sulfoxide group to guide a stereospecific hydroxylation in an acyclic system (Scheme 1.3).⁵⁶ The diastereomeric sulfoxide **1.21** was treated with osmium tetroxide in a catalytic amount (3-5 mol%) and trimethylamine *N*-oxide (TMAO) (3 equiv). Acetylation gave the diacetate sulfone **1.22** as the sole product. The stereoselectivity of the dihydroxylation was attributed to complexation between the osmium and the sulfinyl oxygen, with only a modest steric effect exerted by the chiral amide group.

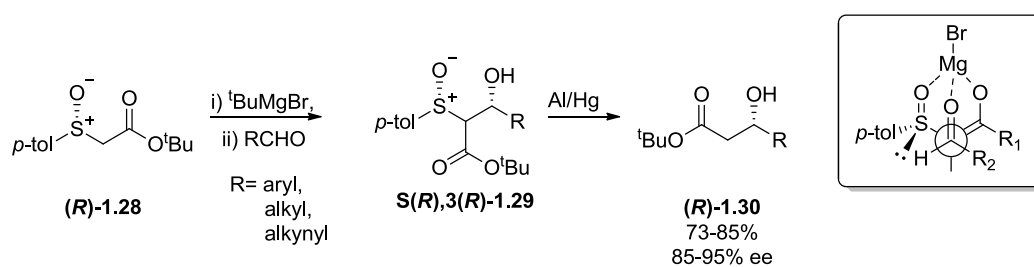


A sulfoxide directed asymmetric Michael addition was employed in the preparation of the 2,2,3-cyclopentanone (*S,S*)-**1.23** (Scheme 1.4).⁵⁷⁻⁵⁹ Addition of the naphthyl-Grignard reagent **1.24** to sulfoxide (*S*)-**1.25**, followed by *in situ* C-methylation gave (*S,S*)-**1.26** as a single

diastereomer. The α -sulfinylcyclopentanone (*S,S*)-**1.26** was converted into the enolate (*S,S*)-**1.27** via dimethylcopper lithium desulfurization. Alkylation of the enolate ion was found to proceed in a regio- and stereospecific manner, with the addition of bromoacetate affording the 9,11-secosteroid (*S,S*)-**1.23** with a yield of 89% from (*S*)-**1.25**

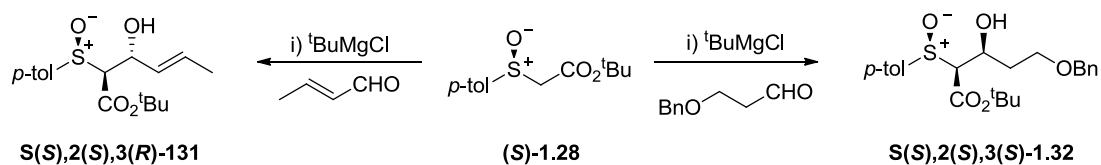


Sulfoxides can also be used to control the diastereofacial selectivity in aldol type reactions.^{60, 61} Solladié and coworkers reported an efficient synthesis of β -hydroxyacids based around the condensation of carbonyl compounds with *p*-tolyl sulfinyl acetates such as **1.28** (Scheme 1.5).



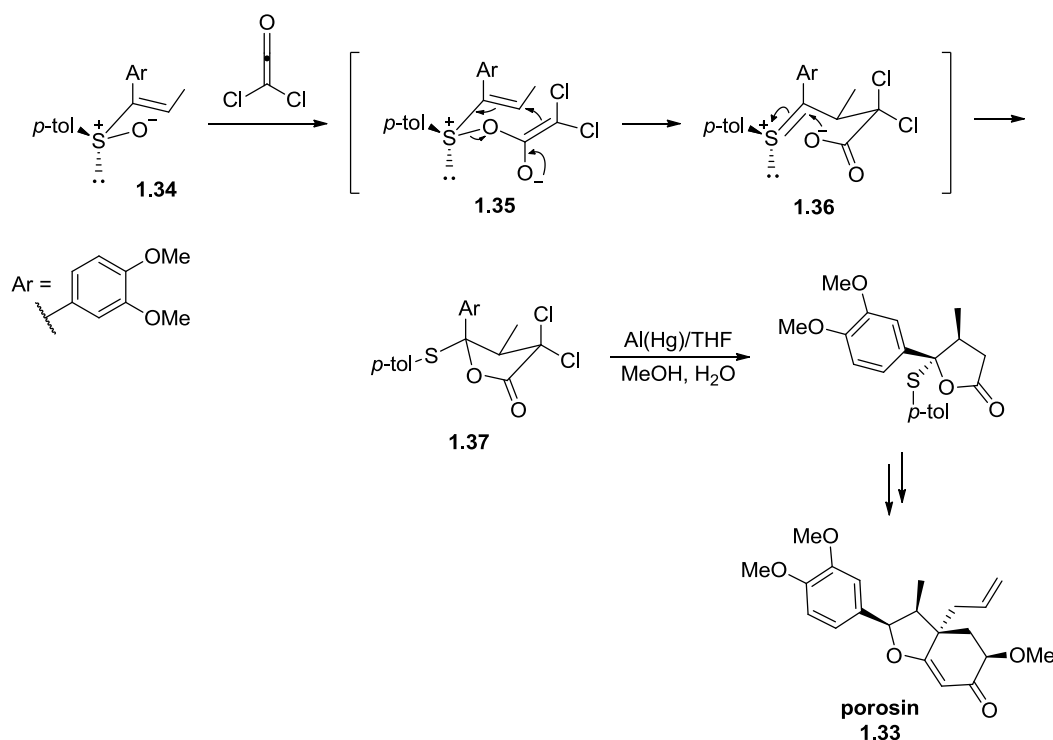
Diastereoselectivity was found to be high (85-95% ee) for the condensation reactions across a range of carbonyls. The success of the methodology was attributed to the use of a Grignard reagents, such as ^tBuMgBr, as the base which allowed for a chelation controlled transition state.⁶² An empirical rule was proposed relating the absolute configuration of the afforded β -hydroxyester to that of the parent sulfoxide. In subsequent studies an exception was noted in that the reactions of α,β -unsaturated carbonyls such as *trans* crotonaldehyde gave the

condensation product **1.31** with the opposite configuration for the hydroxyl group compared to the products, such as **1.32**, arising from the typical aldehydes (Scheme 1.6).⁶³



Scheme 1.6

In the synthesis of the neolignan porosin **1.33** a sulfoxide-directed lactonization was employed by Marino *et al.* (Scheme 1.7). This route provided efficient access to 3,4-disubstituted γ -butyrolactones and allowed for complete control over the relative and absolute stereochemistry at the lactone C-3 and C-4 positions.⁶⁴ A proposed mechanism for the lactonization step suggested acylation of the oxygen of sulfoxide **1.34** by the electrophilic ketene, generating the zwitterionic species **1.35**. A [3,3]-sigmatropic rearrangement would then give a Pummerer type intermediate **1.36** which, when trapped by the carboxylate anion, would produce the corresponding substituted lactone **1.37**. The successful application of this procedure saw the optically pure (3*R*,4*S*)-dichlorolactone **1.37** obtained in a yield of 76%.



Scheme 1.7

1.4 Synthesis of sulfoxides

The oxidative transformation from sulfide to sulfoxide affords a product with immense value and versatility in organic synthesis. Although the addition of a single oxygen atom may, at least on paper, seem incredibly simple, there are many aspects which one may wish to consider when approaching the selective synthesis of a particular sulfoxide. Considerations must be made with respects to the chemoselectivity of the oxidations process in order to avoid excessive production of unwanted sulfone. In addition, there is an increasing need for the use of environmentally friendly reagents and improved “atom efficiency”, particularly for syntheses carried out on an industrial scale.⁶⁵ The desire for the production of sulfoxide in stereoselective fashion brings about a further dimension of complexity; however there is an extensive library of techniques currently available to choose from.

It must be noted that one of the ways by which a target sulfoxide may be reached is through the transformation of the appending functional groups of a pre-existing sulfoxide. This, however, is beyond the scope of what can be covered here; instead we shall mainly focus of the generation of a sulfoxide species by ways of reactions that occur at the sulfur atom, such as oxidation or nucleophilic substitution, amongst others. The exception to this lies in the discussion of kinetic resolution of racemic sulfoxides (Section 1.4.2.1.2).

1.4.1 Racemic sulfoxides

When there is no requirement for control of the stereochemical outcome there are numerous methods that can be used for the oxidation of sulfides to sulfoxides.⁶⁶ Oxidizing agents applicable for this reaction include *m*CPBA, nitric acid, peracids, peresters, ozone, dinitrogen tetraoxide, *N*-halosuccinimide, 1-chlorobenzotriazole, diazobicyclo-[2,2,2]-octane bromine complex, selenium dioxide, manganese dioxide, chromic acid, ceric ammonium nitrate, oxone, and ϵ -phthalimidoperhexanoic acid (PPHA)⁶⁷⁻⁷⁰ Kowalski and coworkers have published a review covering S-oxidations using halogen derivatives such as molecular halogens, hyperchlorites, hypervalent iodine reagents and periodates.⁷¹ The same group has also reviewed method using hydrogen peroxide, giving consideration to the effects of solvents and range of metal, and non-metal based catalyst systems.⁷² The series of reviews by Rayner, and continued by Proctor, provide an overview of methods arising in the literature between 1994 and 2001.^{40, 41, 73-76}

In recent years advances have been made in the arena of metal based catalysts for use in sulfoxide synthesis. Novel catalyst systems comprising of Ta(V) or Nb(V) chlorides or ethoxides have also been investigated, with the use of an aqueous H₂O₂ oxidant.⁷⁷ An oxidation system has been reported that makes use of oxygen from the air with oxidation of aryl methyl sulfides to sulfoxides promoted by HNO₃ and FeBr₃.⁷⁸ A mild and chemoselective oxidation of sulfides and methyl cysteine containing peptides using Sc(OTf)₃ has also been published.⁷⁹ Using a more common metal for S-oxidation, a Ti(IV) system has been reported by Luchini *et al.* with a C₃-symmetric triphenolate amine ligand; the catalyst system was employed in loadings as low as 0.01 mol% for use with aqueous H₂O₂ as the oxidant.⁸⁰

Recent developments in metal free approaches to the synthesis of racemic sulfoxides include the use of organocatalysts such as thiourea dioxide, flavins and tetrazole amide derivatives.⁸¹⁻⁸⁴

A number of novel oxidizing agents have been reported such as the use of an urea-hydrogen peroxide adduct.⁸⁵ Oxaziridine-mediated and imine-catalyzed oxidations of sulfides have been included in a review by Adams *et al.*⁸⁶ A 2010 review by Stingl *et al.* covers many additional aspects of metal free sulfoxidation.⁸⁷

Investigations into developing more environmentally friendly oxidations have included the use of ultrasound in assisting sulfoxide synthesis, photooxidations and solvent free procedures.⁸⁸⁻⁹⁰

For environmentally friendly sulfide oxidations H₂O₂ is often the preferred oxidant. A longer reaction time is typically associated with this reagent, however a number of methods have been reported that overcome this problem such as the use of additives like poly(ethyleneglycol) dimethylether (PEGDME₅₀₀) or 1,3,5-triazo-2,4,6-triphosphorine-2,2,4,4,6,6-tetrachloride (TAPC) and the formation of oxidizing complexes such poly(N-vinylpyrrolidone)-H₂O₂ and poly(4-vinylpyridine)-H₂O₂.^{88, 91-94}

1.4.2 Chiral sulfoxides

In the synthesis of optically active sulfoxides there are four main approaches that may be considered, these are depicted in Figure 1.1. The first method involves the separation and isolation of each enantiomers of a racemic sulfoxide, or a sulfoxide of low enantiopurity. This resolution may be achieved through a physical method such as HPLC, or in the case of kinetic resolution through a chemical transformation. The second method involves the transformation of a diastereomerically pure sulfinate to a chiral sulfoxide through nucleophilic displacement with an organometallic based reagent. This reaction, pioneered by Andersen, typically proceeds with inversion of stereochemistry at sulfur.

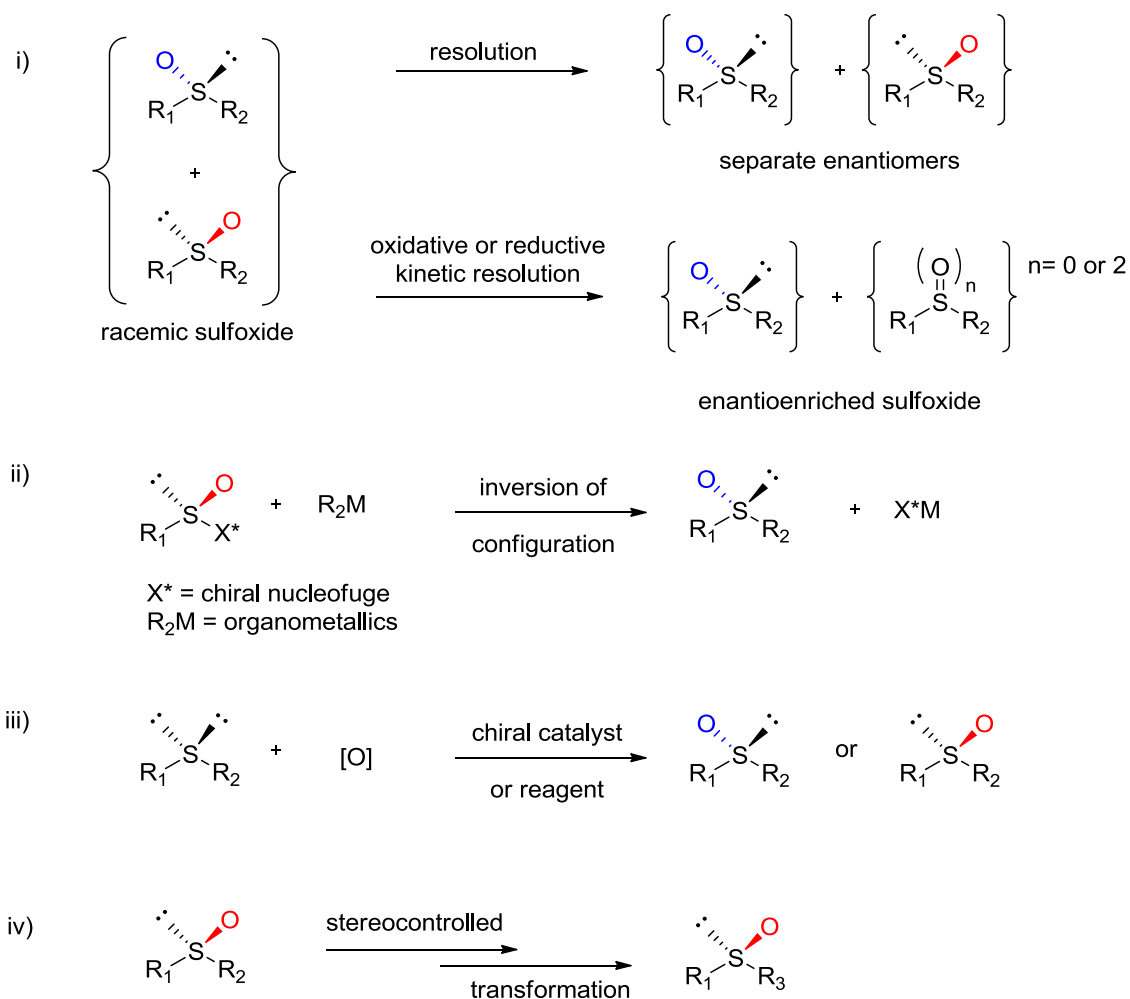


Figure 1.1

The third method involves the enantioselective oxidation of a prochiral sulfide and has become the most widely employed method for stereoselective synthesis of sulfoxides and can be separated into three categories: biological mediated oxidations, non-metal based oxidations, and metal-based oxidations. Biological and non-metal based methods of S-oxidation shall be discussed in the rest of this chapter, however in order to cover the extensive topic metal-based asymmetric synthesis of chiral sulfoxides has been given its own dedicated chapter.

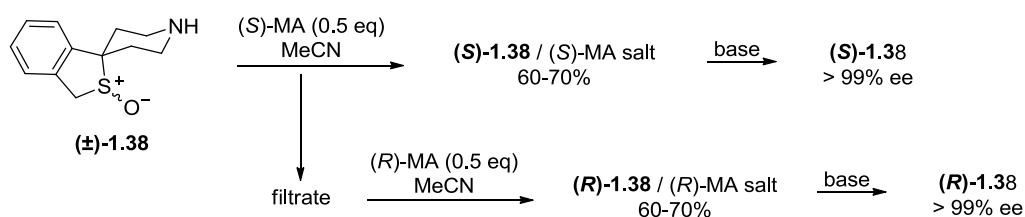
The fourth method involves the transformation of a pre-existing, optically pure sulfoxide under non-racemizing conditions; this route is greatly dependent on sourcing a suitable chiral sulfoxide from the chiral pool or prior synthesis for starting material therefore, with a small number of exceptions, particularly when discussion kinetic resolution of sulfoxides (Section 1.4.21.2), we shall limit discussion only to transformations that occur directly on sulfur, rather than further afield in the molecule.

1.4.2.1 Resolution of chiral sulfoxides

Resolution is the oldest synthetic method for the production of enantiomerically pure materials.⁹⁵ Several methods have been reported for the isolation of chiral sulfoxides, including classical resolution via diastereomers, chromatographic separation via the use of chiral stationary phases, and kinetic resolutions (both chemical and enzymic) amongst others. Despite inherent limitations (i.e. a maximum yield of only 50% of the desired enantiomer if starting from a racemic mixture), separation of enantiomers via resolution remains a popular technique in the pharmaceutical industry.⁹⁶ Where single enantiomer drugs are being assessed for *in vivo* testing for the first time, resolution allows for simple, rapid, and more cost efficient production of initial materials compared to the development of asymmetric synthesis method.^{15, 97}

1.4.2.1.1 Classical resolution

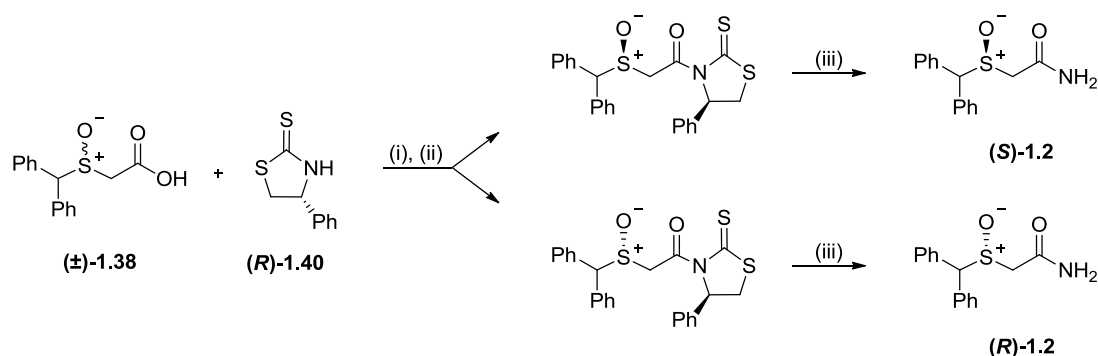
Many sulfoxide species have been successfully resolved using classical resolution techniques i.e. the preparation of diastereomers which allow for separation based upon differing physicochemical properties. In one of the earliest papers to address the structure and bonding of mixed sulfoxides (where $R_1 \neq R_2$), Harrison and coworkers described the resolution of racemic 4-aminophenyl *p*-tolyl sulfoxide by a process which involved the formation, recrystallization, and subsequent decomposition of diastereomeric camphorsulfonate salts.¹⁴ More recently, the enantiomers of sulfoxide (\pm)-**1.38** were resolved with mandelic acid (MA) in MeCN; both enantiomers were recovered in good yields (with respect to the resolving agent) and with excellent optical purity (> 99% ee) (Scheme 1.8).⁹⁸



Scheme 1.8

Prisinzano *et al.* reported the resolution of modafinic acid (\pm)-**1.39**, a carboxylic acid derivative of the psychostimulant Modafinil **1.2**, using fractional crystallization of the salts formed with the resolving agent α -methylbenzylamine.²⁰ The same group subsequently reported an alternative methodology whereby adducts were formed between modafinic acid (\pm)-**1.39** and a chiral thiazolidinethione auxiliary (*R*)-**1.40** (Scheme 1.9); this method allowed for separation of

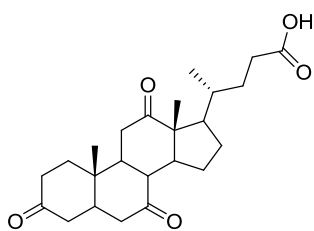
the diastereomeric products via column chromatography as opposed to the crystallizations employed previously.⁹⁹



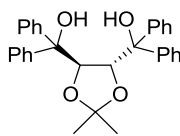
Scheme 1.9 Reagents and conditions: (i) DCC, DMAP, CH₂Cl₂; (ii) column chromatography; (iii) CHCl₃-MeOH-NH₄OH.

The formation of diastereomeric adducts has also been employed in the resolution of racemic aryl dichloromethyl sulfoxides, via reversible Aldol-type reactions with (–)-menthone.¹⁰⁰ The formation of complexes has also proved synthetically useful in the resolution of sulfoxides. The treatment of (+)- or (–)-*trans*-dichloro(ethylene)(α -methylbenzylamine)-platinum(II) with ethyl *p*-tolyl sulfoxide was reported to give rise to diastereomeric sulfoxide-amine-platinum complexes, via a slow displacement of ethylene, which were separable by crystallization.¹⁰¹

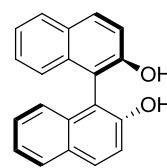
Resolution via host-guest complexation is also well known; one advantage of this method is that it is possible to resolve compounds which lack the acidic or basic functionalities required for classical resolutions involving the formation of diastereomeric salts. β -Cyclodextrins, which are natural oligosaccharides formed by seven glucose units and feature a hydrophobic cavity within a torus shaped molecule, have been employed in the direct resolution of a number of alkyl aryl and alkyl benzyl sulfoxides.¹⁰² Although the optical purities of the partially resolved sulfoxides were low (\geq 15% ee), they could be improved by recrystallization.¹⁰³ Dehydrocholic acid **1.41**, a bile acid derivative, has been successfully employed as a host molecule to form inclusion complexes with a range of aryl alkyl sulfoxides; guest sulfoxides were resolved with good to high optical purities (36-99% ee) in the final products.¹⁰⁴ Complexation of sulfoxides with chiral hosts such as the tartaric acid derivative **1.42** or (*R*)-BINOL (*R*)-**1.43** have also proved a simple and effective method for resolution.^{105, 106} Chiral host (2*R*,3*R*)-**1.42**, and its enantiomer were both reported to allow access to optically active alkyl pyridyl sulfoxides with very high enantiomeric excess (95-99.5% ee).¹⁰⁵ The use of diol (*R*)-**1.43** as a resolving agent for a number of aryl alkyl- and dialkyl sulfoxides gave sulfoxide products with either low (0-25% ee) or excellent enantiopurity (> 99.5% ee), revealing the importance of the sulfoxide molecular shape in the complexation process.¹⁰⁶



1.41



1.42



(R)-1.43

Separation of enantiomers based on classical resolution typically relies on the formation of stable diastereomers which can be isolated through crystallization or normal phase chromatography. Unfortunately these techniques cannot be applied universally; products may form oils, they may not be suitable for derivatization, or they may not be easily separable through crystallization or simple chromatography.

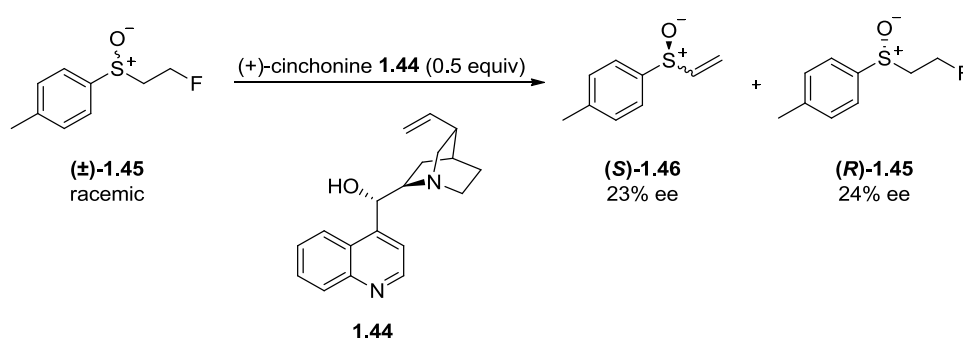
1.4.2.1.2 Kinetic resolution

Kinetic resolution occurs when two enantiomers of a racemate are subjected to a transformative process which occurs at different rates for each enantiomer. If the kinetic resolution is efficient, one enantiomer is converted to a new species while the other remains unchanged but enriched in optical purity.^{107, 108} Oxidative kinetic resolution of racemic sulfoxides is the most common type of this reaction reported for the attainment of chiral sulfoxides; reactions of this type are discussed in subsequent sections of this thesis, within the context of the oxidative methodology. There are, however, a number of other transformations which may afford chiral sulfoxides by way of kinetic resolution, such as reduction of racemic sulfoxides and modification to sulfoxide side chains.

Mikołajczyk and coworkers explored the preferential reduction of sulfoxide enantiomers by treating racemic methyl alkyl sulfoxides with *o*-ethyl phosphonothioic acid or *o*-¹propyl methylphosphonothioic acid.¹⁰⁹ Enantioselectivity of the reductions was low yielding sulfoxides with 6% ee at most. Optically active lithium aluminium hydride complexes were also employed for reduction kinetic resolution, but again only low optical purities were observed.¹¹⁰ Montanari *et al.* reported the selective reduction of mesityl *p*-tolyl sulfoxide in the presence of a chiral poly[*N*-(1-phenylethyl)iminoalane] tetramer.¹¹¹ A mixture of enantioenriched sulfoxide was obtained in 78% ee alongside the corresponding sulfide. Reductive kinetic resolution has been reported by a number of groups using DMSO reductases.^{112, 113} One example from Abo *et al.* used *Rhodobacter sphaeroides* f.s. *denitrificans*, isolated from the waste water of a tofu factory, in the reduction of the *S*-enantiomer of racemic methyl phenyl sulfoxide to the corresponding sulfide.¹¹⁴ The (*R*)-enantiomer of this sulfoxide

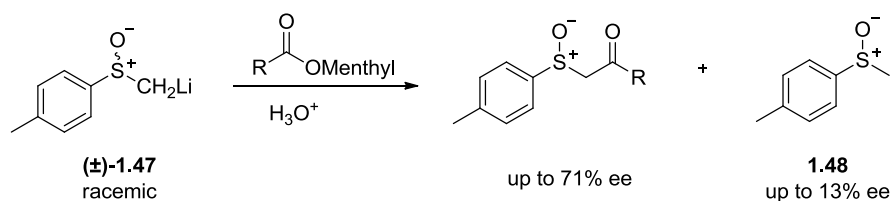
was obtained in optical purities between 79-97% ee; expansion of the substrate scope for enantioselective deoxygenation saw a range of racemic alky aryl- and diaryl-sulfoxides resolved to give recovered sulfoxides in up to > 99% ee.

Chemical transformations that occur beyond the sulfur atom of a sulfoxide are a common way to selectively transform one sulfoxide enantiomer during kinetic resolution. Naso *et al.* employed the chiral base (+)-cinchonine **1.44** to effect a selective elimination reaction, stereoselectively converting racemic β -halosulfoxides into enantioenriched vinyl sulfoxides (Scheme 1.10).¹¹⁵ Performing this reaction on *p*-tolyl β -fluoroethyl sulfoxide (\pm)-**1.45** gave vinyl sulfoxide (*S*)-**1.46** in 23% ee, with the unreacted sulfoxide recovered with 24% ee.



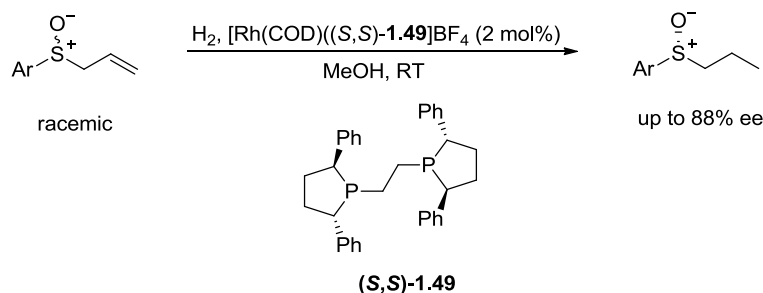
Scheme 1.10

Kunieda and coworkers obtained partially resolved β -ketosulfoxides with optical purities of up to 72% ee through the reaction of a menthyl ester with α -sulfinyl carbanions such as (\pm)-**1.47**; enantioenrichment was also observed in the sulfoxide **1.48** derived from unreacted starting material (up to 13% ee) (Scheme 1.11).



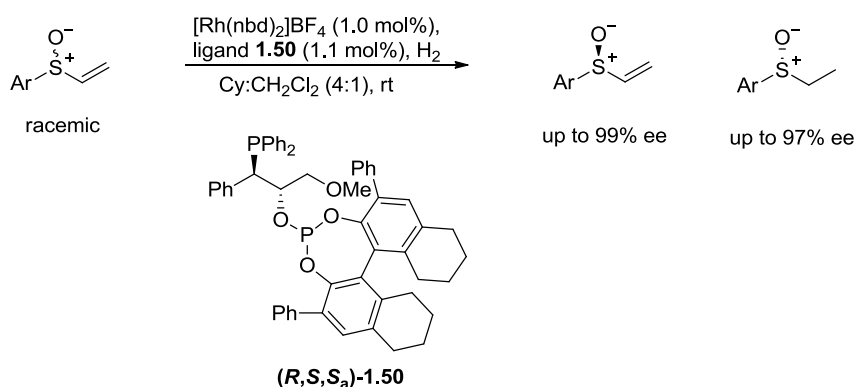
Scheme 1.11

The dynamic kinetic resolution of allylic sulfoxides was reported by Dornan and coworkers. By combining the Mislow [2,3]-sigmatropic rearrangement with catalytic asymmetric hydrogenation, sulfoxides with up to 88% ee were obtained, in yields between 53-84%. A rhodium based catalyst system was employed using the chiral diphosphine ligand (*S,S*)-**1.49** (Scheme 1.12).



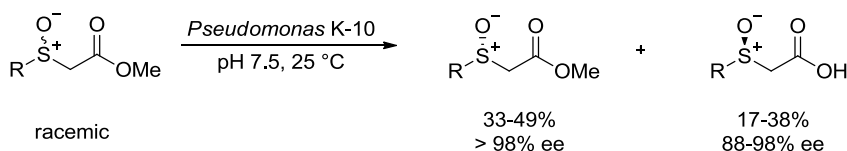
Scheme 1.12

Lao *et al.* reported their investigations into the hydrogenative kinetic resolution of vinyl sulfoxides; isolation of both recovered and reduced sulfoxide products, in excellent yields and optical purity, was achieved (Scheme.1.13).



Scheme 1.13

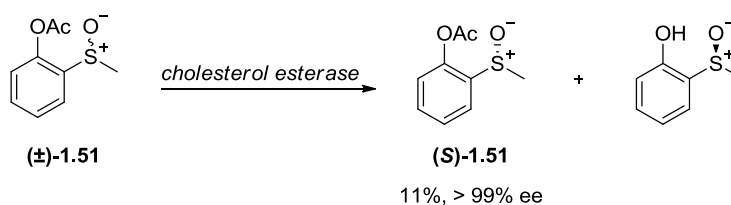
An enzymatic kinetic resolution was reported by Ohta and coworkers; hydrolysis of racemic sulfinyl acetates and propionate was carried out using *Corynebacterium equi* IF 3730 to afford the recovered chiral sulfoxides in optical purities of up to 90% ee and yields between 30-43% (of a possible 50%).¹¹⁶ Burgess and Henderson performed biocatalytic resolution of sulfinyl acetates using *Pseudomonas* K-10, affording unreacted sulfoxide acetates and corresponding acids with excellent enantiopurities (Scheme 1.14).¹¹⁷



Scheme 1.14

Enzyme catalyzed hydrolysis was also employed by Kwiatkowska *et al.* to produce enantiomerically enriched acetoxymethyl aryl sulfoxides through kinetic resolution.¹¹⁸ Serreqi *et al.* examined hydrolase-catalyzed kinetic resolution of sulfoxides by hydrolysis of pendant acetoxy groups.¹¹⁹ Hydrolase screening identified cholesterol esterase to be the most effective enzyme for enantioselectivity; from the racemic sulfoxide (\pm)-**1.51**, (*S*)-2-

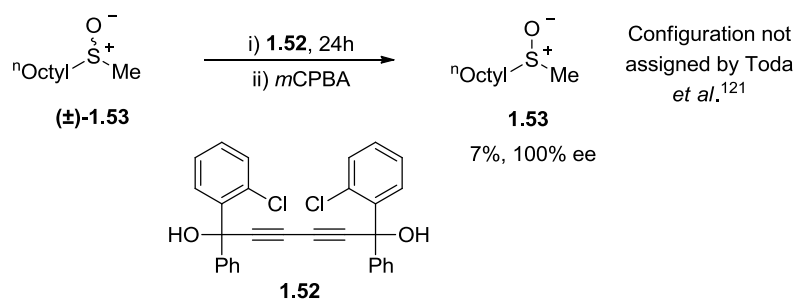
(methylsulfinyl)phenyl acetate (*S*)-**1.51** was obtained with > 99% ee, in a yield of 11% after one recrystallization (Scheme 1.15).



Scheme 1.15

Whole cells of *Rhodococcus sp.* ECU0066 were used to catalyze the resolution of racemic alkyl aryl sulfoxides.¹²⁰ Sulfoxides were recovered in high ee (up to > 99% ee) in good yields for the method employed (up to 45% yield).

A kinetic resolution in the solid state was reported by Toda *et al.* Racemic sulfoxides were oxidised in the presence of the optically active host compound (-)-1,6-di(*o*-chlorophenyl)-1,6-diphenylhexa-2,4-diyne-1,6-diol **1.52** (Scheme 1.16).¹²¹ Enantiopure methyl ⁿoctyl **1.53** was afforded through the combined process of enantioselective inclusion complexation and selective oxidation using *m*CPBA (Scheme 1.16).



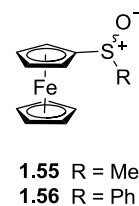
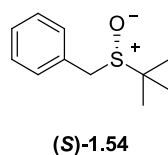
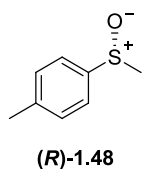
Scheme 1.16

An alternative method used to obtain optically active sulfoxides is through enantioselective chromatography via the use of a chiral stationary phase (CSP); chromatographic resolution of enantiomers is also a highly valuable, and widely employed, tool for analysis. For the resolution of sulfoxides via HPLC or LC there is a wide range of materials that have been successfully employed as CSPs. Some of the most commonly encountered are based upon functionalised silica coated with polysaccharides such as amylose or cellulose.¹²²⁻¹²⁴ These polysaccharide based CSPs include the commercially available Daicel columns: Chiralpak AD and AS, Chiralcel OD and OJ, which are sometimes referred to as the “golden four” due to their popularity and applicability.¹²⁵⁻¹²⁸ CSPs of this type are commonly employed for resolution of sulfoxide enantiomers via supercritical-fluid chromatography (SFC).¹²⁹⁻¹³¹ Pirkle type CSPs for

HPLC and LC are also commercially available; these include a π -acid based CSP containing the 3,5-dinitrobenzoyl derivative of 1,2-diaminocyclohexane (DACH-DNB).^{132, 133} Pirkle and coworkers also reported the use of (*R*)-*N*-(3,5-dinitrobenzoyl)phenylglycine bound to aminopropyl silica as a successful CSP for enantioselective LC of sulfoxides and *N*-substituted sulfoximines.¹³⁴ Nanoporous materials such as homochiral metal-organic frameworks have been applied as CSPs for HPLC.^{135, 136} Similarly, a recent publication reported the use a homochiral porous organic cage as a stationary phase for high resolution GC of a range of racemates, including sulfoxides.¹³⁷ Other chiral stationary phases employed for sulfoxide resolution include those based upon macrocyclic glycopeptides, and bovine serum albumin (BSA), immobilized to HPLC-silica.^{138, 139} Cyclodextrins have been employed as chiral selectors for sulfoxide enantioseparation using HPLC, GC, and capillary electrophoresis.¹⁴⁰⁻¹⁴²

1.4.2.1.3 Enantiomeric enrichment via achiral chromatography

Occasionally the isolation of enantiomerically enriched sulfoxides can be achieved through achiral gravity driven or flash chromatography due to the rare phenomenon of self-disproportionation of enantiomers (SDE).¹⁴³⁻¹⁴⁷ Kagan and coworkers described examples of atypical cases of fractionation of sulfoxide enantiomers by achiral flash chromatography.¹⁴⁸ Alerted by poor reproducibility of enantioselectivities during investigations of the asymmetric oxidation of methyl *p*-tolyl sulfide, it was found that the optical purity of the sulfoxide product (*R*)-**1.48** depended strongly on which fraction was analyzed. The possibility of partial racemisation was excluded after treating an enantiopure sample under the same conditions, with all fractions retaining the original 100% ee. Pollution by contaminant was also ruled out. Further investigation showed that starting from sulfoxide (*R*)-**1.48** (86% ee), enantioenrichment by during chromatography could be observed in the first fraction (99% ee, major enantiomer) with depletion occurring in the later fractions (73% ee, major enantiomer) (Table 1.1, entry 1). Similarly when starting from sulfoxide (*R*)-**1.48** with a lower initial optical purity (20% ee) the same trend was observed, with high initial ee values that decreased to give the lowest values in the last fractions (37% ee and 18% ee, respectively) (Table 1.1, entry 2). Increasing, or decreasing the amount of silica gel used did not improved the efficiency of enantiomeric enrichment (Table 1.1, entry 3 and 4, respectively). The splitting of the enantiomeric excess was less pronounced when alumina was employed as the stationary phase (Table 1.1, entry 5) and the use reverse phase silica was found to only affect the speed of elution, not the fractionation of sulfoxide ee (Table 1.1, entry 6).



Entry	Sulfoxide	% ee ^a	First fraction, % ee	Last fraction, % ee
1	<i>p</i> -Tol-S(O)-Me (1.48) ^b	86.0 (<i>R</i>)	99.5 (<i>R</i>)	73.5 (<i>R</i>)
2	<i>p</i> -Tol-S(O)-Me (1.48) ^b	20.0 (<i>R</i>)	37.0 (<i>R</i>)	18.0 (<i>R</i>)
3	<i>p</i> -Tol-S(O)-Me (1.48) ^{b,c}	85.5 (<i>R</i>)	93.0 (<i>R</i>)	72.0 (<i>R</i>)
4	<i>p</i> -Tol-S(O)-Me (1.48) ^{b,d}	85.5 (<i>R</i>)	89.5 (<i>R</i>)	80.0 (<i>R</i>)
5	<i>p</i> -Tol-S(O)-Me (1.48) ^{b,e}	86.0 (<i>R</i>)	91.0 (<i>R</i>)	80.5 (<i>R</i>)
6	<i>p</i> -Tol-S(O)-Me (1.48) ^{b,f}	91.0 (<i>R</i>)	99.5 (<i>R</i>)	73.0 (<i>R</i>)
7	Bn-S(O)- ^t Bu (1.54)	44.5 (<i>S</i>)	53.0 (<i>S</i>)	42.0 (<i>S</i>)
8	Fc-S(O)-Me (1.55) ^{g,h}	90.5 (<i>R</i>)	99.5 (<i>R</i>)	82.0 (<i>R</i>)
9	Fc-S(O)-Ph (1.56) ⁱ	65.0 (<i>R</i>)	79.0 (<i>S</i>)	94.0 (<i>R</i>)

Table 1.1 Chromatography performed using ~10 g silica gel/mmol sulfoxide with elution by EtOAc, unless stated otherwise. a) Initial sulfoxide % ee measured by HPLC on Chiralcel OD-H (Diacel); b) prepared by mixing of two enantiopure sulfoxides; c) 50 g silica gel/mmol sulfoxide; d) 4.5 g silica gel/mmol sulfoxide; e) flash chromatography on Al₂O₃; f) 20 g reverse phase silica gel/mmol sulfoxide; g) elution by 50% EtOAc–Et₂O; h) Fc = ferrocenyl; i) elution by 50% EtOAc–cyclohexane

Fractionation of enantiomeric excess during chromatography on silica was not unique to sulfoxide **1.48**, a similar trend was observed also for benzyl ^tbutyl sulfoxide **1.54**, methyl ferrocenyl sulfoxide **1.55** and phenyl ferrocenyl sulfoxide **1.56**. A change in the order of elution was observed with sulfoxide (*R*)-**1.56** (65% ee) where the minor (*S*)-enantiomer was afforded in the first fraction (79% ee (*S*)), whereas the major enantiomer was eluted with the highest ee towards the end (94% ee (*R*)). The enantiomeric modification was found not to be a general trend for all sulfoxides examined; no perturbation in optical purity was observed following chromatography of neither *p*-tolyl ferrocenyl sulfoxide nor ^tbutyl ferrocenyl sulfoxide. Further to the work of Kagan, only a small number of additional sulfoxides have been reported as showing a similar behaviour during achiral chromatography, including methyl ⁿpentyl sulfoxide and an important class of prazole based species which include the blockbuster drug Esomeprazole (*S*)-**1.1** (discussed further in chapter three).^{149, 150}

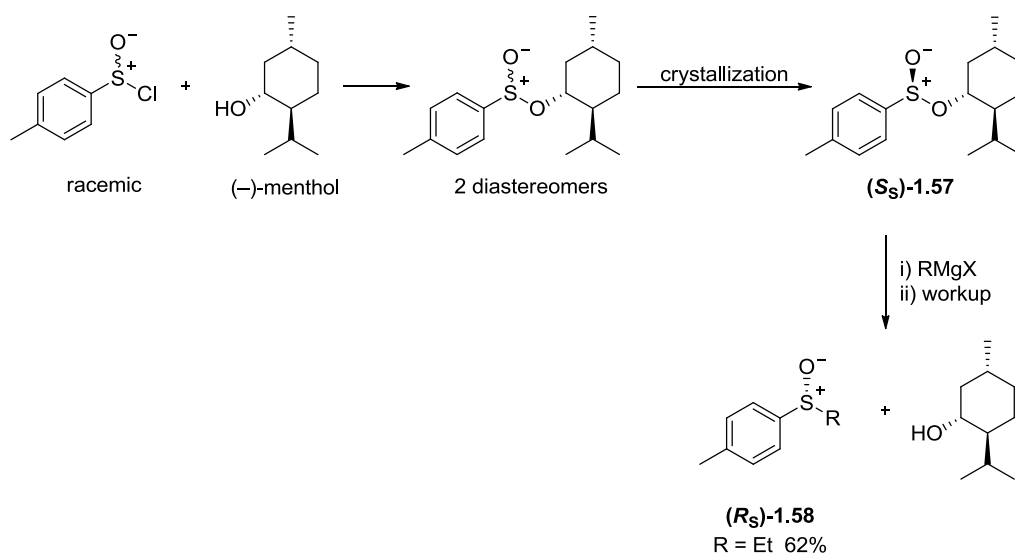
This remarkable physiochemical phenomenon of enantiomeric enrichment, or SDE, is thought to be attributed to intermolecular interactions, with auto-associations of the chiral species leading to formation of hetero- and/or homo- dimers.^{143, 151} These diastereomeric agglomerates may present with differing mobilities in the solution phase, or associate differently with the stationary phase, leading to fractionation of enantiomeric excesses. In order to avoid

complications arising from aggregation of this type, consideration must be made during workup and isolation stages, typically achieved by combining sulfoxide fractions prior to analysis.^{152, 153}

1.4.2.2 Synthesis of chiral sulfoxides via nucleophilic displacement at sulfur

1.4.2.2.1 The Andersen method

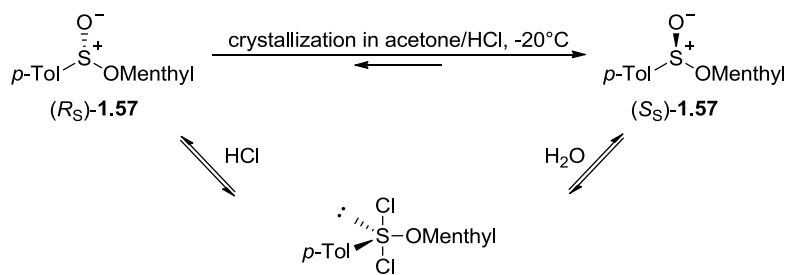
In 1962 a new method for the synthesis of sulfoxides with high optical purities was reported by Andersen *et al.* which involved the addition of an organomagnesium halide Grignard reagent to an optically active sulfinate ester (S_S)-**1.57**.¹⁵⁴ The resulting nucleophilic displacement of *O*-menthyl was found to proceed via an S_N2 mechanism with complete inversion of configuration at sulfur, affording (R_S)-ethyl *p*-tolyl sulfoxide **1.58** in a good yield (62%) (Scheme 1.17).¹⁵⁵⁻¹⁵⁷



Scheme 1.17

This methodology not only provided new access to enantiopure sulfoxides, which in turn could be used in further synthesis but, as a technique that could produce chiral sulfoxides in a stereospecific manner, it also provided important evidence for consideration in discussions, such as those by Mislow, concerning the assignment of absolute configuration of a number of sulfur containing species.^{4, 156-159} The Andersen method also circumvented many of the limitations in obtaining enantiopure sulfoxides found previously; there was no need for an acidic or basic handle for use in resolution by diastomeric salt formation, and this method gave sulfoxides with higher enantiopurity than those achieved through asymmetric sulfoxidation by optically active peracids which had been recently reported by Maccioni.^{14, 160} To achieve sulfoxide products with high ee using the Andersen method the preparation of the menthyl sulfinate precursor in high optical purity is necessary. Although both diastereomers of *p*-tolyl sulfinate

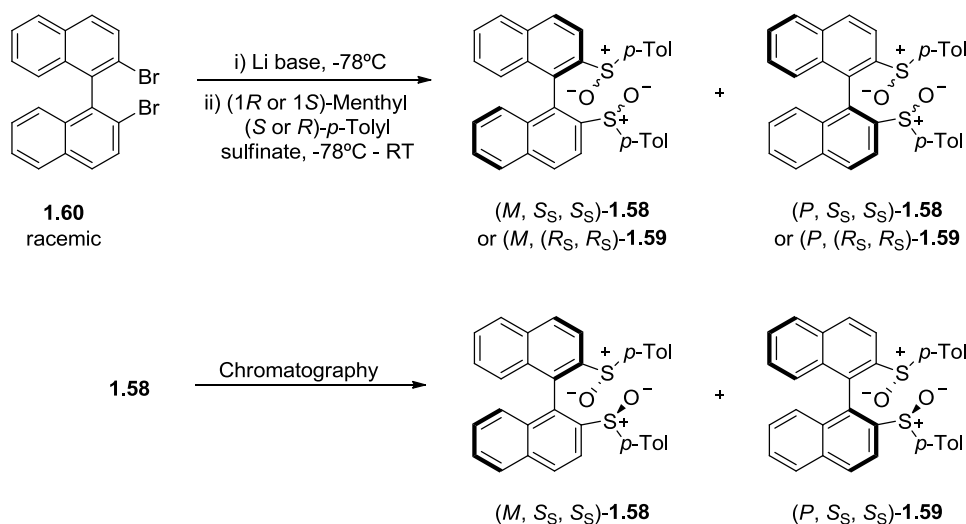
ester **1.55** are now commercially available it was previously necessary to perform repeated crystallizations to separate the less soluble isomer (*S_S*)-**1.57** from its oily epimer. Solladie and Mioskowski reported a method whereby interconversion of the sulfoxide epimers was promoted by acidic conditions and in combination with crystallization from acetone, the desired sulfinate ester precursor could be obtained in high yields (80-90%) (Scheme 1.18).¹⁶¹



Scheme 1.18

An alternative method for the preparation of a range of menthyl sulfinate esters was reported by Sharpless who described a one step procedure involving the *in situ* reduction of sulfonyl chlorides by trimethyl phosphites in the presence of triethylamine.¹⁶² In addition, the synthesis and/or application of crystalline menthyl sulfonates such as 1-naphthyl, 1-(2-naphthyl), 1-(2-OMe-naphthyl), 4-bromophenyl have been reported in the literature.^{155, 158, 163, 164} Alternative organometallic reagents have also been reported, with Harpp *et al.* disclosing the successful application of organocopper lithium reagents in place of the Grignard traditionally employed by the Andersen method.¹⁶⁵

Recently, Dorta *et al.* employed a classical Andersen approach in the synthesis of four bis-sulfoxide ligands for use in Rh-catalyzed asymmetric transformations.^{153, 154} The four stereoisomers of the 1,1'-binaphthalene-2,2'-diyl-bis(*p*-tolylsulfoxide) ligand (*p*-tol-BINASO **1.58** and **1.59**), were created in one-step reactions from racemic commercially available starting material **1.60** (scheme 1.12). Column chromatography separated the two atropisomers of the diastereomeric BINASO crude materials, and following the use of both epimers of the menthyl sulfinate ester four pure ligands were obtained in yields between 34-60% (Scheme 1.19).

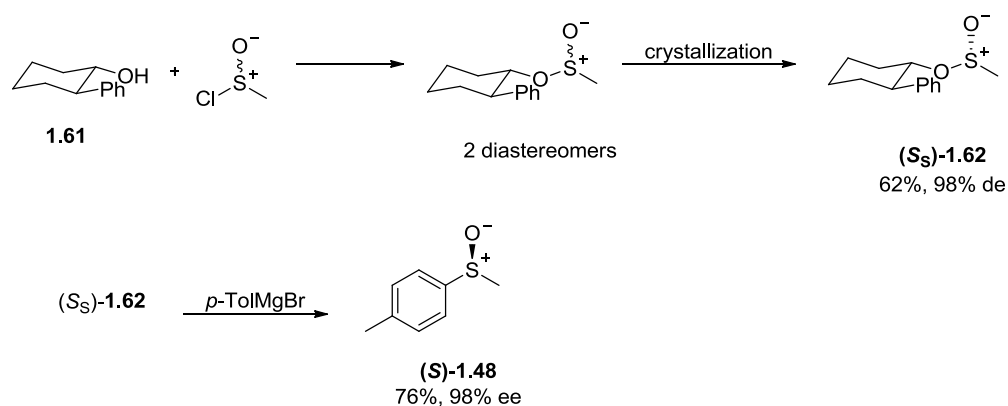


Scheme 1.19

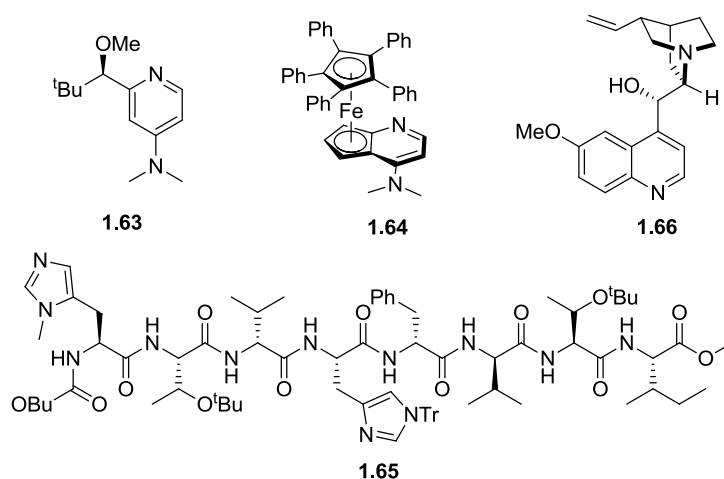
1.4.2.2.2 Alternative sulfinylating agents

The range of chiral sulfoxides that can be achieved by implementation of the Andersen methodology is generally restricted to alkyl aryl or diaryl sulfoxides due to the limited availability of appropriate menthyl sulfinates precursors. For example, the oily nature of menthyl methyl sulfinates results in diastereomers which are difficult to separate and are unsuitable for use in this way.¹⁶⁶ A solution to this problem lies in the replacement of menthyl with an alternative chiral alcohol, which allows for the formation of more easily separable sulfinates esters. Andersen *et al.* published a procedure wherein cholesterol was employed in place of menthol for the formation of the diastereomeric sulfinates esters precursors. Treatment of each epimer with a range of Grignard reagents afforded dialkyl sulfoxides; although yields were typically less than 50%, the optical purity of the sulfoxide products were high and generally in excess of 80% ee.

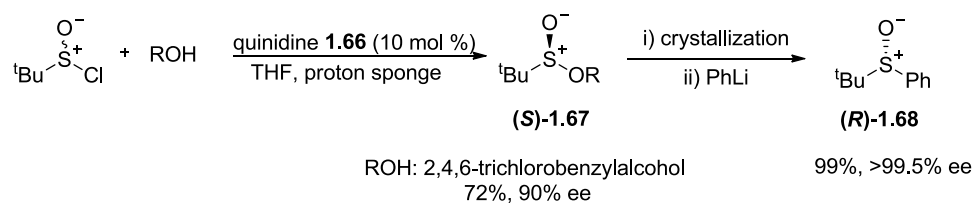
The use of *trans*-2-phenylcyclohexanol **1.61** for the production of enantiomerically enriched sulfinates ester was reported by Whitesell *et al.* Although more expensive than menthol, the chiral cyclohexanol auxiliary **1.61** allowed for production of sulfinates diastereomers that were readily separated by both chromatography and crystallization. The synthesis of sulfinates ester was observed to occur with some kinetic diastereoselectivity (up to 10:1), and with both isomers of the auxiliary available there was equal and ready access to the desired sulfinates ester, and chiral sulfoxide derived there from (Scheme 1.20).^{167, 168}



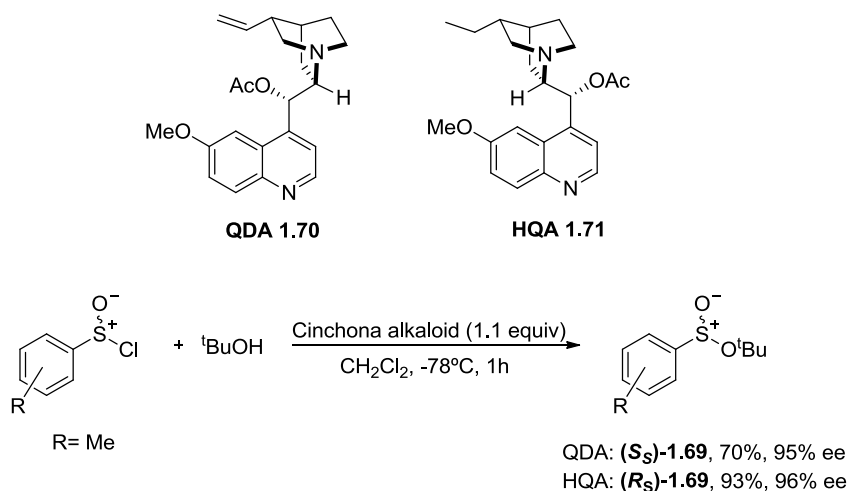
Ellman and coworkers evaluated a number of chiral acyl transfer catalysts for use in the preparation of sulfinate esters due to the similarities between sulfinyl and acyl transfer. Amongst them were the chiral (dimethylamino)pyridine derivative **1.63**, the more electron rich ferrocene-derived acyl transfer catalyst **1.64**, and the *N*-methylimidazole-containing peptide **1.65**.



Subsequent work featured the use of more commercially available and inexpensive cinchona alkaloids such as quinidine **1.66** in catalytic amounts to afford butylsulfinate ester **1.67**, and phenyl ^tbutyl-sulfoxide **1.68**, with excellent enantioselectivity (Scheme 1.21).

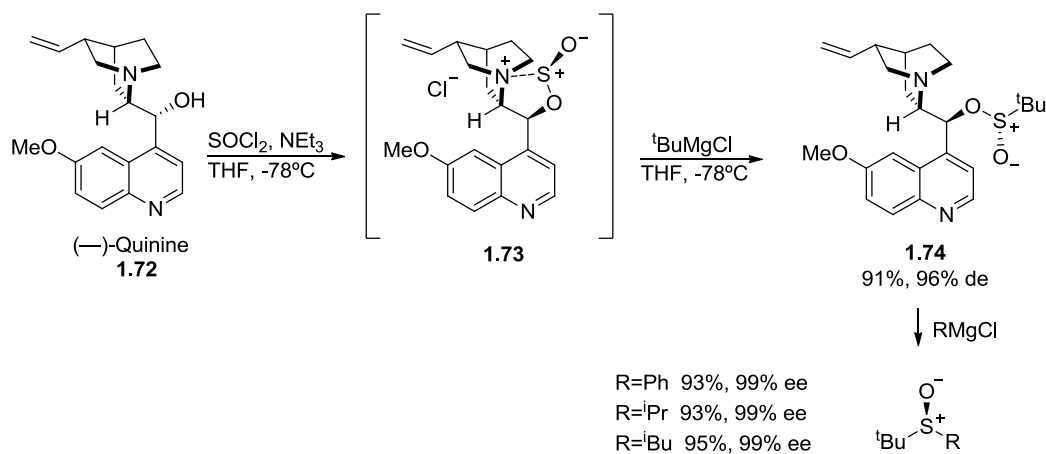


Toru *et al.* reported a novel approach centered around a cinchona alkaloid/sulfinyl chloride combination, prepared *in situ*, which was found to act as a sulfinylating agent on an achiral alcohol.¹⁶⁹ Aryl ^tbutyl sulfonates **1.69** were obtained in good yields (68-93%) with high enantioselectivity (83-99% ee); both enantiomers of the sulfonate esters could be obtained by using the alkaloid quinidine acetate (QDA **1.70**) to afford one isomer, and hydroquinine acetate (HQA **1.71**) to give the epimer (Scheme 1.22).



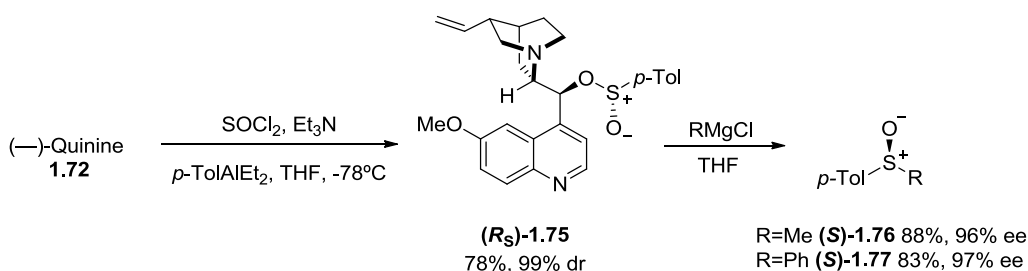
Scheme 1.22

A general sulfinylating process was reported by Senanayake *et al.* which allowed for the synthesis of sulfonate esters and their equivalent enantioenriched sulfoxides using the alkaloid quinine **1.72** and quinidine as chiral auxiliaries.¹⁷⁰ The reaction was presumed to proceed via formation of a pseudo five-membered ring oxathiazolidine **1.73**, featuring a noncovalent S-N bond, the displacement of which would be preferential over that of the S-O bond following addition of the ^tbutyl Grignard reagent (Scheme 1.23).



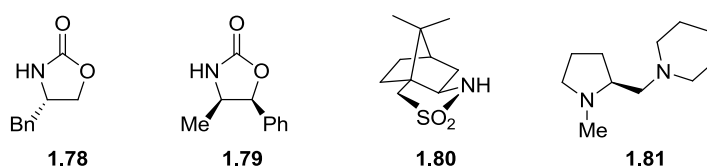
Scheme 1.23

When complex **1.73** was treated with *p*-tolylmagnesium chloride, only the formation of a racemic disulfoxide occurred. However, this was circumvented by employment of *p*-tolyl-diethylaluminum, prepared *in situ* from diethylaluminum chloride and *p*-tolylmagnesium bromide (Scheme 1.24).



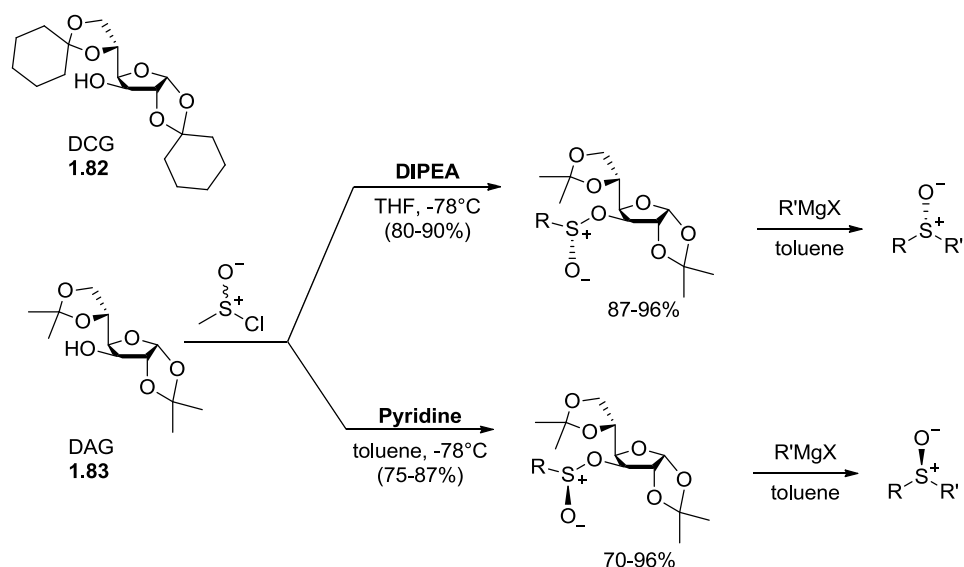
Scheme 1.24

The formation of diastereomeric sulfinamides also allows access to the formation of enantioenriched sulfoxides. Auxiliaries, such as the oxazolidinones **1.78** and **1.79** reported by Evans, and sultam **1.80** reported by Oppolzer formed intermediate sulfonamides diastereomers which were easily separable by crystallization, and from which a range of sulfoxides were produced with excellent enantiopurity (up to > 99% ee).^{171, 172} The oxazolidinones **1.78** and **1.79** were complimentary to each other as they afforded sulfoxides with opposite absolute configurations, and all three auxiliaries could be recovered and reused. Chiral diamine **1.81** was investigated by Toru *et al.* in the enantioselective synthesis of chiral sulfinates by the reaction of *p*-tolylsulfinyl chloride with achiral alcohols.¹⁷³



The application of carbohydrate auxiliaries for the preparation of diastereomeric sulfinate esters as precursors to chiral sulfoxides began with Ridley and Smal who, in 1981 reported the synthesis of a number of arenesulfinic esters of dicyclohexyl-D-glucofuranose (DCG, **1.82**).¹⁷⁴ A decade later, Fernández *et al.* reported an efficient synthesis of both enantiomers of various methylsulfoxides using diacetone-D-glucose (DAG, **1.83**) as the inducer of chirality (Scheme 1.25). Through the use of different amines it was possible to access either diastereomer of the sulfinate ester, with the utilization of diisopropylethylamine (DIPEA) giving the *S*- isomer and pyridine the *R*- epimer. With the configuration at sulfur conveniently predetermined treatment with a variety of Grignard reagents transformed the diastereomerically pure sulfinates into

enantiomerically pure alkyl- or aryl-methyl sulfoxides (> 99.5% ee) in good to high yields (37-90%) (Scheme 1.25).¹⁷⁵⁻¹⁷⁷



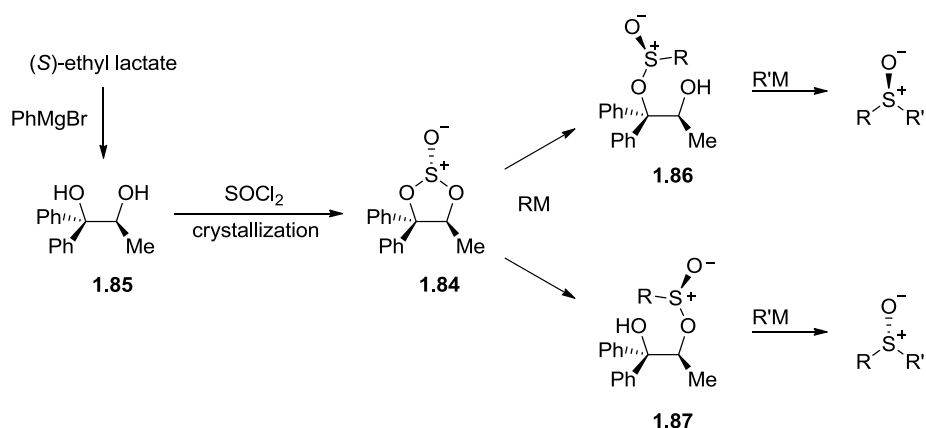
Scheme 1.25

Computational analysis of the DAG methodology suggested that the stereoselectivity and configurational outcome of the sulfinate ester synthesis was determined by firstly by a DKR mechanism of the sulfinyl chloride, and secondly by the bulkiness of the base used leading to differing pathways due to steric hindrance of the sulfinamides formed *in situ*.¹⁷⁸⁻¹⁸⁰ Subsequent improvements to the DAG methodology led to the development of a DMAP catalyzed process, which was found to enhance both the enantioselectivity and rate of reaction, and led to the formation of a range of sulfoxides and sulfinamides.¹⁸¹

1.4.2.2.3 Double nucleophilic displacement at sulfur

To create enantiomerically pure sulfoxides a strategy may be used whereby nucleophilic substitution occurs twice at sulfur. Here, the prochiral faces of thionyl chloride are differentiated through use of a bifunctional scaffold, which can be chiral diols or amino alcohols, to form diastereomeric sulfites or aminosulfites. The presence of two leaving groups in the molecule allows for two sequential reactions with organometallic reagents, affording the desired chiral sulfoxide. Kagan and coworkers investigated this approach and found it to be an efficient method for the synthesis of chiral sulfoxides, particularly ^tbutyl sulfoxides.¹⁸²⁻¹⁸⁴ Cyclic sulfite **1.84** was obtained as a mixture of diastereomers from the reaction of starting thionyl chloride and diol **1.85**, which in turn was produced easily in one step from (*S*)-ethyl lactate, a material which is inexpensive and readily available from the chiral pool.

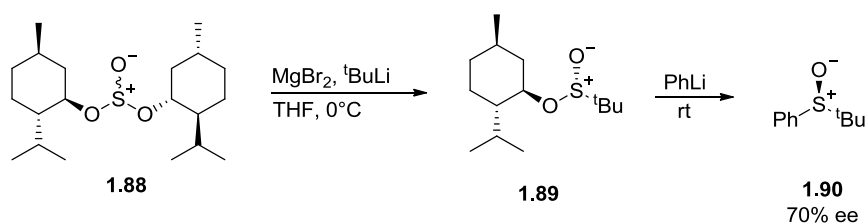
Crystallization of sulfite **1.84** was followed by the formation of monosubstituted sulfinates **1.86** or **1.87** following the addition of various Grignard reagents (Scheme 1.26).



Scheme 1.26

It was observed that when a hindered reagent, such as ^tBuMgBr or mesitylMgBr, was used (*S_S*)-sulfinate **1.87** was predominantly obtained; the less hindered MeMgI afforded an excess of (*R_S*)-sulfinate **1.86**. A range of chiral ^tbutyl sulfoxides were obtained using this approach in moderate to excellent yields (27-99%) and high enantiopurity (85-> 99.5% ee).

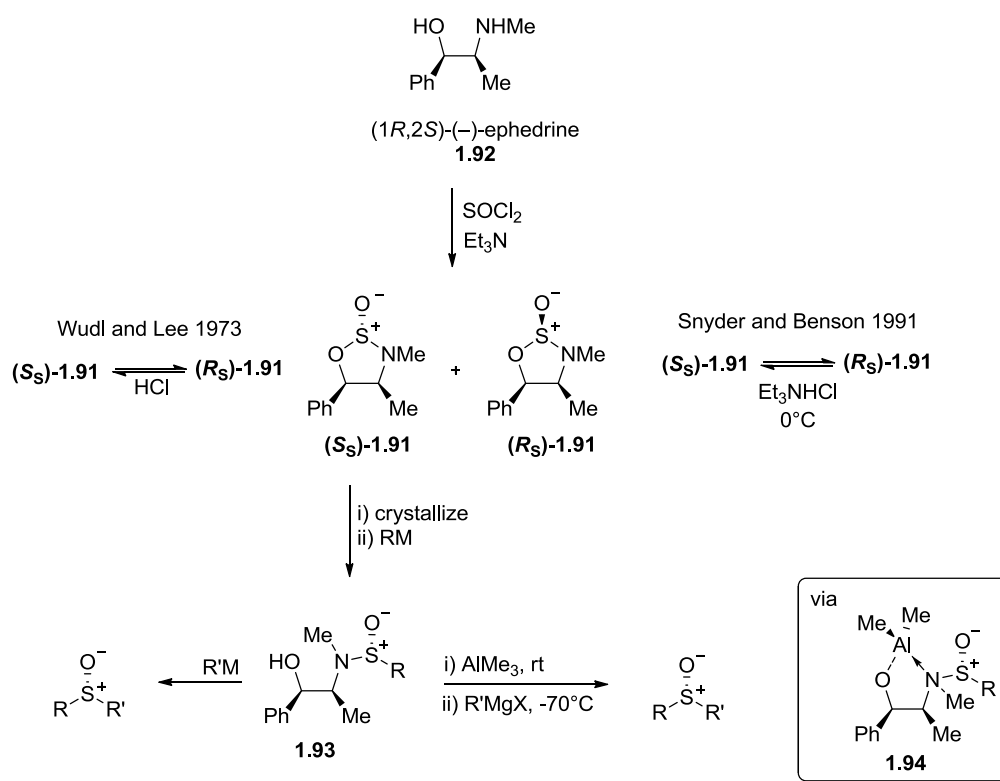
Kagan *et al.* also reported the use of cyclic sulfites derived from *C*₂-symmetric alcohols as precursors of sulfinates, where the diastereotopic oxygens of sulfite **1.88** had potential for differing reactivity towards attack by an achiral nucleophile.¹⁸⁴ From dimethyl sulfite **1.88**, menthyl ^tbutylsulfinate **1.89** was prepared by the reaction of 1,2-dibromoethane and Mg in THF, followed by addition of ^tBuLi (2 equiv). Sulfinate **1.89** was obtained in excellent yield (100%) as a mixture of diastereomers (70% de); transformation of **1.89** into (*S*)- phenyl ^tbutyl sulfoxide **1.90** (70% ee) by addition of PhLi (2.1 equiv) was achieved in a quantitative yield (Scheme 1.27). Cyclic sulfites were also explored by Vallée *et al.*, who found that *C*₂-symmetric sulfites formed from mannitol derivatives could be utilized in the synthesis of ^tbutylsulfinates.¹⁸⁵



Scheme 1.27

In 1972 Wudl and Lee reported the use of ephedrine as a chiral auxiliary in the pursuit of enantiomerically pure sulfoxides, thus pioneering the cyclic aminosulfite methodology (Scheme 1.28).¹⁸⁶ In subsequent work further application of the methodology and mechanistic detail was

discussed.¹⁸⁷ In this process 1,2,3-oxathiazolidine-*S*-oxide diastereomers (*S_S*)-**1.91** and (*R_S*)-**1.91** were obtained in a 72:28 ratio through reacting thionyl chloride with (–)-ephedrine **1.91** in the presence of the triethylamine. Crystallization allowed for diastereomerically pure (*S_S*)-**1.91** to be collected, and acid mediated equilibration allowed for further production of (*S_S*)-**1.91** from (*R_S*)-**1.91**. Treatment of optically pure (*S_S*)-**1.91** with alkyl or aryl lithium afforded hydroxysulfinamides **1.93** in good yield (60-90%) but only with an average of 50% ee at sulfur, with the low selectivity attributed to epimerization presumed to be due to a sulfinyl-transfer mechanism. Further transformation of the sulfonamides via reaction with organolithium reagents gave sulfoxides in good yield and high optical purity (70-75%, 85-86% ee); the use of MeMgBr produced optically pure methyl *p*-tolyl sulfoxide **1.48**, but only in 25% yield. This disparity was thought to be due to the difficulty in breaking the S-N bond, with racemisation potentially occurring.⁶



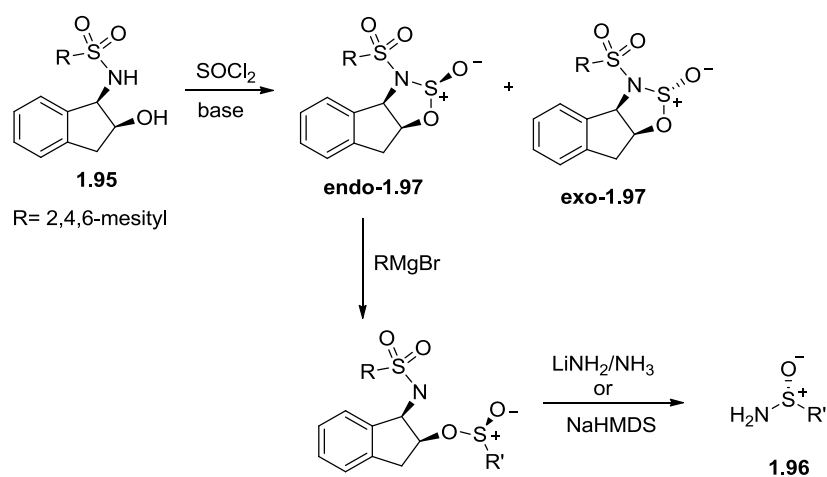
Scheme 1.28

By 1991 Snyder and Benson had developed a number of improvements to Wudl and Lee's aminosulfite methodology.¹⁸⁸ Firstly, by allowing the diastereomers **1.91** to equilibrate at 0 °C in the presence of triethylammonium diastereoselectivity was increased in favour of (*S_S*)-**1.91** to 80% which could then be isolated by crystallization in a 70% yield. Secondly, the transformation of **1.91** into sulfinamide **1.93** was carried out using various freshly prepared Grignard reagents in toluene, as opposed to organolithium reagents in THF used by Wudl *et al.*

Hydroxysulfinamides **1.93** were obtained in yields from 50 to 94%, and with diastereoselectivity ranging from 30 to > 99% ee (Scheme 1.28).

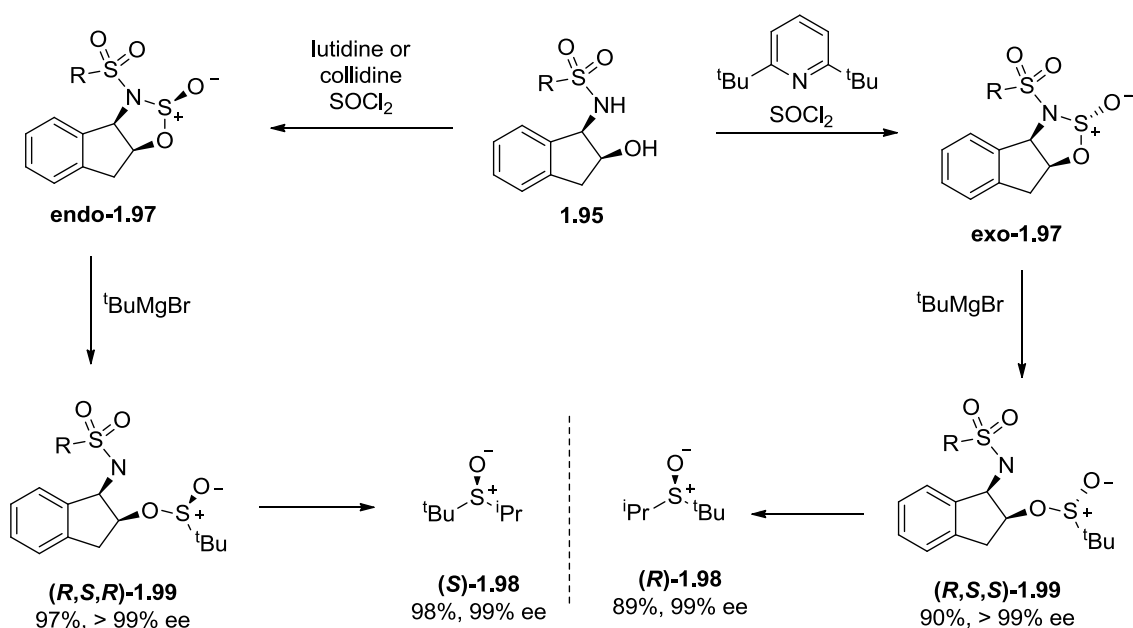
The choice of Grignards reagents over organolithiums was thought to avoid epimerization at sulfur during the first displacement step, and also prevented the formation of symmetric sulfoxides due to double displacement. Finally, for the second displacement step, it was found that addition of AlMe₃ to the intermediate sulfinamide prior to addition of the Grignard reagent gave the desired sulfoxides in good yields and excellent enantioselectivities (> 99% ee). The improvement in both yield and optical purity of the sulfoxide products was attributed to the formation of the dimethylaluminiumalkoxide complex **1.94**. With this approach, chiral alkyl aryl and dialkyl sulfoxides could be prepared, with access to both enantiomers by simply reversing the order of nucleophilic displacement or by using the commercially available (1*S*,2*R*)-(+)-ephedrine enantiomer as the chiral auxiliary. Despite the numerous improvements, this methodology still suffered limitations, for example it was not possible to produce and sulfinamide intermediate where R=Ph in an acceptable yield due to formation of diphenyl sulfoxides. No ^tbutyl sulfoxides could be produced either, due to the unreactive nature of the ^tbutyl sulfinamide, however these could easily be accessed via Kagan's cyclic sulfite methodology.

Further improvements to the aminosulfite methodology came from Senanayake *et al.* *N*-sulfonyl (1*R*,2*S*)-aminoindanol **1.95** was used as a chiral auxiliary in place of ephedrine.¹⁸⁹ The electron withdrawing group on nitrogen allowed for preferential cleavage of the N-S bond by an organometallic agent, reversing the selectivity of the initial nucleophilic displacement step (Scheme 1.29). This procedure was used by Senanayake *et al.* to generate a range of chiral sulfinamides **1.96** with excellent recovery of the chiral auxiliary. Production of the enantiopure endo **1.97** intermediate was achieved on kilogram scale.



Scheme 1.29

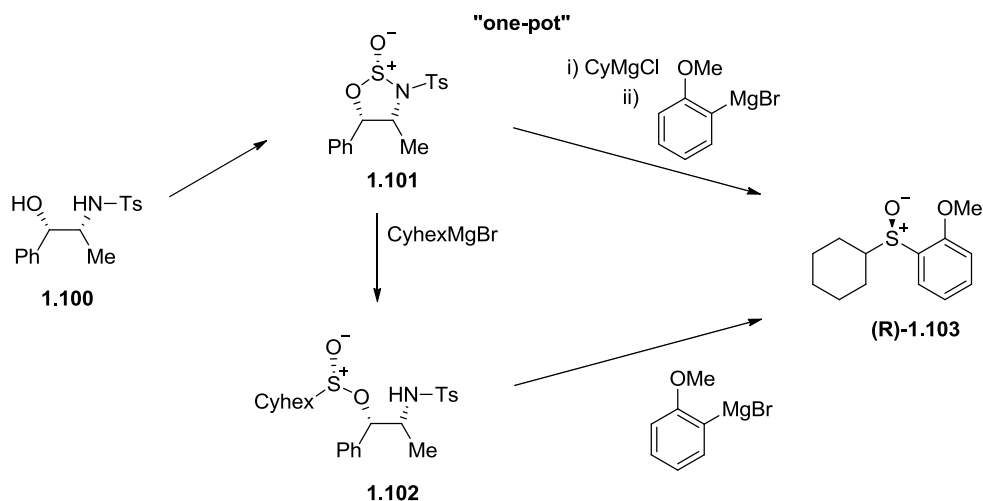
Soon after, Senanayake *et al.* reported the use of *cis*-aminoindanol **1.95** in the synthesis of optically active sulfoxides. It was demonstrated that simply changing the base could dramatically change the facial selectivity of the reaction between thionyl chloride and indanol **1.95** (Scheme 1.30).^{190, 191} (*S*)- and (*R*)-butyl isopropyl sulfoxide **1.98** were prepared via the sulfonates **1.99** using this procedure in good yield (98% and 89% respectively) with excellent enantioselectivity (99% ee for each epimer).



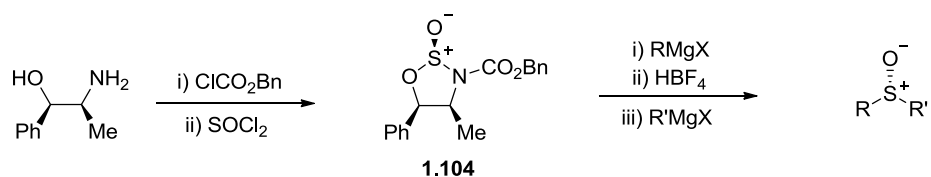
Scheme 1.30

Senanayake *et al.* also described their work in finding a less expensive alternative to *N*-sulfonyl (1*R*,2*S*)-aminoindanol **1.95**. Here, the readily available amino alcohol *N*-tosylnorephedrine **1.100** was used to prepare *N*-tosyl-1,2,3-oxathiazolidine-2-oxide **1.101**, from which chiral sulfoxides could be prepared in a one-pot synthesis; the auxiliary **1.100** could be easily

recovered and recycled from the final reaction mixture (Scheme 1.31). A wide range of optically active sulfoxides were furnished from this procedure in high yield (63-97%) and with excellent enantioselectivities (90-> 99% ee). The one-pot methodology was employed in the preparative-scale synthesis of (*R*)-methyl *p*-tolyl sulfoxide **1.48**, for use in the preparation of a drug intermediate without isolation of the sulfoxide during the process.¹⁹²



García Ruano *et al.* prepared enantiomerically enriched sulfoxides starting from norephedrine-derived *N*-benzyloxycarbonylsulfinamide **1.104**.¹⁹³ After a one-pot reaction of **1.104** with an organometallic reagent, then HBF₄, and then a final organometallic reagent, a variety of sulfoxides were obtained with optical purities typically greater than 93% ee, and yields between 50-78% (Scheme 1.32). A similar methodology to this was applied by Qin *et al.* in the synthesis of chiral sulfinamides.¹⁹⁴



1.4.2.3 Non-metal based oxidation of prochiral sulfides

1.4.2.3.1 Oxidations performed using a chiral oxidant

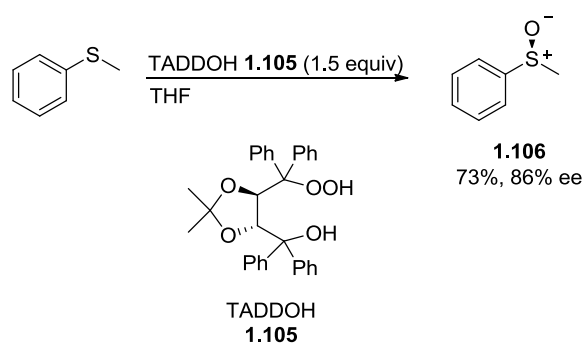
Peracids

Some of the earliest work in the field of asymmetric synthesis of chiral sulfoxides involved the use of peracids to oxidize prochiral sulfides. A number of research groups investigated a range

of peracids for this application; results however were generally poor, with reported enantioselectivities typically less than 10% ee.^{66, 157, 159, 160, 195-197}

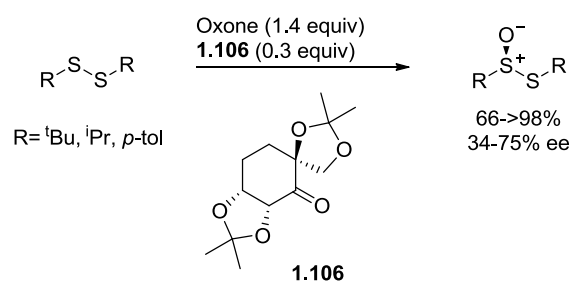
Chiral peroxides

In 2001 Aoki and Seebach investigated the use of the chiral hydroperoxy alcohol TADDOH **1.105**, a derivative of tetraaryl-1,3-dioxolane-4,5-dimethanol (TADDOL), in asymmetric sulfide oxidations (Scheme 1.33).¹⁹⁸ Using this reagent as the oxidant methyl phenyl sulfoxide was obtained as the (*S*)-enantiomer in a yield of 73% and enantioselectivity of 86% ee; some overoxidation to the sulfone was also observed.



Scheme 1.33

Colonna *et al.* reported a catalytic asymmetric sulfoxidation using a dioxirane generated *in situ* from potassium peroxymonosulfate (Oxone) and fructose derived ketone **1.106**. The product from monooxidation of di-^t-butyl disulfide was achieved to give the corresponding sulfoxide in 78% ee, with a yield of > 98% (Scheme 1.34).¹⁹⁹ Dieva *et al.* performed similar investigations using an *in situ* generated dioxirane producing benzyl methyl sulfoxide in a 46% yield, with low enantioselectivity (26% ee).²⁰⁰

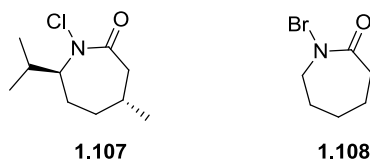


Scheme 1.34

Caprolactams

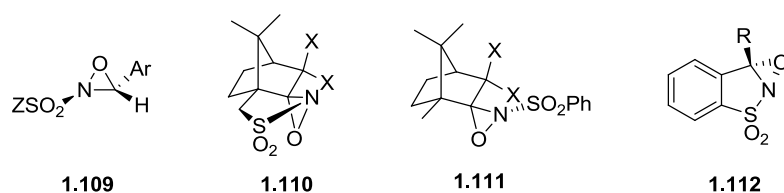
Sato *et al.* reported the enantioselective oxidation of sulfides using chiral halogenocaprolactam (+)-*N*-chloro-7-isopropyl-4-methyl-2-oxohexamethyleneimine **1.107**. (*R*)-Aryl alkyl sulfoxides

were obtained in very low ee (< 3% ee).²⁰¹ Previous work by Sato *et al.* had discussed the oxidation of sulfides by *N*-bromo- ϵ -caprolactam **1.108** in the presence of an optically active alcohol. Using this method, with (*R*)-menthol as the chiral alcohol, (*R*)-benzyl *p*-tolyl sulfoxide was produced in 56% ee but in low yield (4%).²⁰²

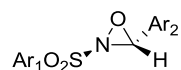


Oxaziridines

Oxaziridines are a class of heterocyclic compounds featuring a three-membered C-N-O ring which can act as aprotic, neutral oxidizing agents in a number of different reactions, one of which is sulfoxidation.²⁰³⁻²⁰⁵ Davies *et al.* conducted extensive research into oxaziridines, and developed a number of reagents that could be used for asymmetric sulfide oxidations, the four main types of which are shown below.^{205, 206}



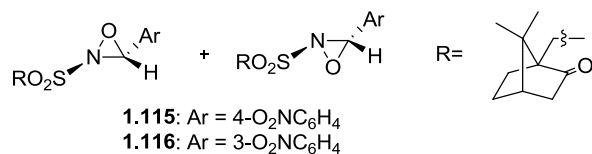
When *N*-sulfonyloxaziridines **1.109** were first reported in 1978 they represented a new class of oxaziridines as they were the first example of these compounds to have a substituent other than carbon or hydrogen attached to the nitrogen atom.²⁰⁵ The electrophilic oxygen was reported to be highly selective, oxidizing sulfides to sulfoxides with no overoxidation to sulfones.²⁰⁷ Using a stoichiometric amount of the oxaziridine oxidizing agents **1.113** and **1.114** sulfoxides were afforded in good to high yields. A catalytic version of this reaction was reported a number of years later.²⁰⁸



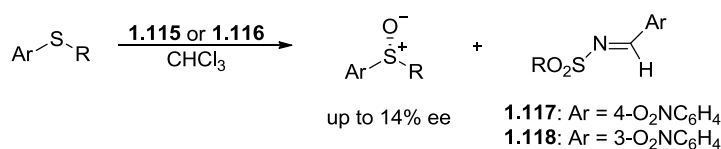
1.113: Ar₁ = Ar₂ = Ph
1.114: Ar₁ = 4-MeOC₆H₄, Ar₂ = Ph

The following year Davis and coworkers reported the development of an oxaziridine reagent capable of asymmetric induction during the sulfoxidation process.²⁰⁹ 2-[(–)-Camphor-10-

ylsulphonyl]-3-nitrophenyl) oxaziridines **1.115** and **1.116** were produced as a mixture of diastereomers; crystallizations of these gave **1.115** and **1.116** in 33% optical purity, and **1.115** in 68% optical purity.

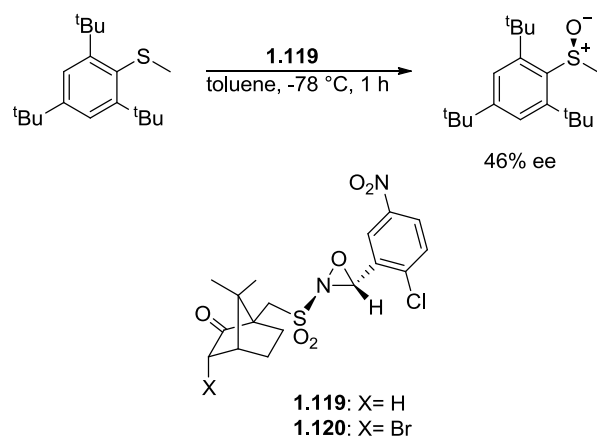


Oxidations performed on three sulfide substrates using the optically enriched oxaziridines gave sulfoxides with optical purities of up to 14% ee (Scheme 1.35); sulfonamides **1.117** and **1.118** could be recovered (> 90% yield) and recycled. Although enantioselectivities of these reactions were low, they represented values 1.3-2.0 times better than optical purities reported thus far using peroxy acids.²⁰⁹



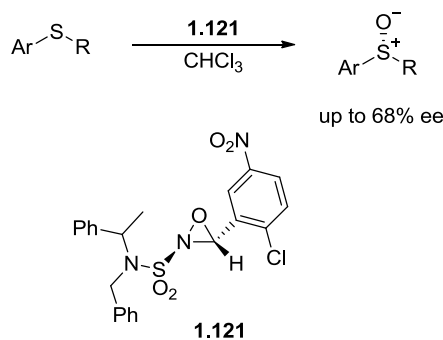
Scheme 1.35

The mechanism of oxygen transfer from oxaziridine was believed to be by nucleophilic attack by the sulfide substrate on the electrophilic oxaziridine oxygen. Asymmetric induction was believed to be made possible by the incorporation of the active site oxygen into a rigid chiral environment, with the enantioselectivity of the sulfoxidation reaction determined largely by the steric demands of both the sulfide substrate and the oxaziridine oxidizing agent.²¹⁰ The configuration of the oxaziridine's three-membered ring was thought to control the configuration of the sulfoxide product, leading Davis *et al.* to develop a model from which the stereochemical outcome of the reaction could be predicted. Improvements to the oxaziridine based oxidation led to increased enantioselectivity, by 1982 Davis and coworkers had greatly increased the optical purities of the sulfoxides, the best result being 46% ee, with the use of diastereomeric mixtures of oxaziridines such as **1.119** and **1.120** and their respective epimers (Scheme 1.36).²¹⁰ Davis *et al.* also reported a kinetic resolution of *p*-tolyl methyl sulfoxide using oxaziridines (*R,R*)-**1.120**, with the recovered sulfoxide isolated in up to 28% ee.²¹¹



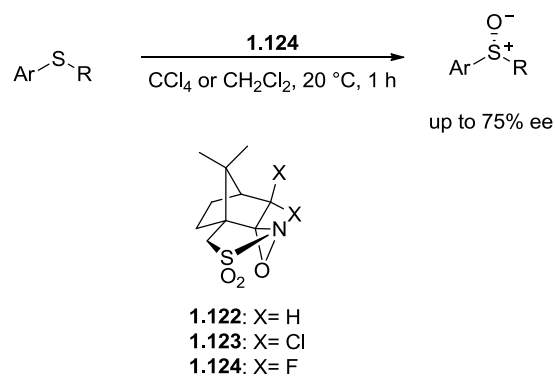
Scheme 1.36

Davis and coworkers reported the use of the chiral sulfamyloxaziridine **1.121**, which afforded *i*-propyl *p*-tolyl- and methyl 9-anthryl sulfoxides in 65 and 68% ee respectively, representing the highest optical purities reported for a chemical asymmetric sulfoxidation at that time (Scheme 1.37).²¹² The sulfamyloxaziridines offered numerous practical advantages over the sulfonyloxaziridines, including improved chromatographic stability, making them easier to purify, and greater ease in the structure could be varied. Further refinements to the sulfamyloxaziridine oxidizing agents saw (*S*)-alkyl aryl sulfoxides being produced in up to 91% ee; these results were comparable, and in some cases better than those being reported at that time by Kagan who employed a Ti-based modified Sharpless catalyst system.²¹³



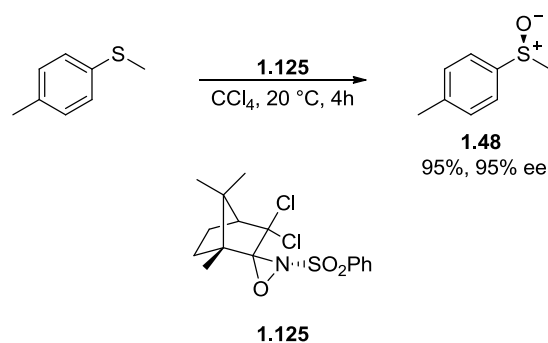
Scheme 1.37

Davis *et al.* also investigated the synthesis and properties of optically active (camphorsulfonyl)oxaziridines, such as **1.122-1.124**.²¹⁴ Although these oxaziridines were used in high optical purity, the enantioselectivity they displayed in sulfoxidations were inferior to those obtained using *N*-sulfamyloxaziridines. Methyl 9-anthryl- and ⁿbutyl *p*-tolyl- sulfoxide were both achieved in 75% ee using oxaziridines **1.124** (Scheme 1.38).²¹⁵



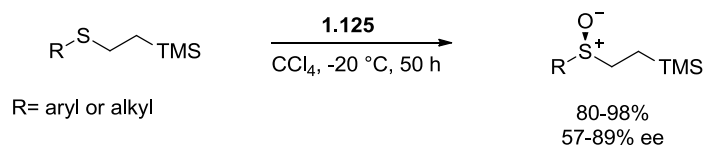
Scheme 1.38

A third class of oxaziridine was reported by Davis *et al.* in 1993. *N*-sulfonyloxaziridines, such as dichlorocamphorylsulfonyloxaziridine **1.125** were used in enantiomerically pure form, allowing access to sulfoxides in optical purities of 65 to > 95% ee (Scheme 1.39).^{216, 217} Oxaziridines such as these were also shown to be highly effective in the asymmetric synthesis of chiral selenoxides.²¹⁸



Scheme 1.39

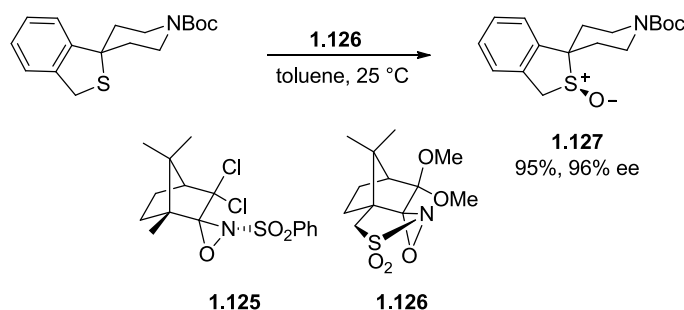
Oxaziridines **1.125** was employed by Schwan and Pippert for the oxidation of a number of aryl and alkyl 2-(trimethylsilyl)ethyl sulfides (Scheme 1.40).²¹⁹ The results from a number oxaziridine based oxidations were compared to those performed using various titanium based catalyst systems, and for four out a possible five sulfide substrates oxidized, the sulfoxides produced using the oxaziridine were higher in both yield and enantiopurity.



Scheme 1.40

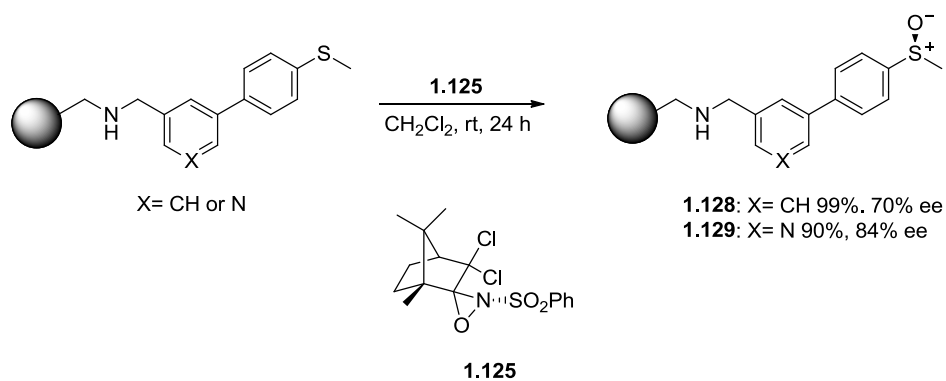
Nishi *et al.* reported the use of oxaziridines **1.125** and **1.126** for the asymmetric synthesis of (*S*)-**1.127**, a key intermediate for the synthesis of a biologically active sulfoxide.⁹⁸ A number of

metal based catalyst systems were also employed, and the results from which were compared with those from the oxaziridines. Both oxaziridines performed well, giving high yields and enantioselectivities; **1.126** gave the sulfoxide product in the highest optical and chemical yield of all the systems studied (95%, 96% ee) (Scheme 1.41).



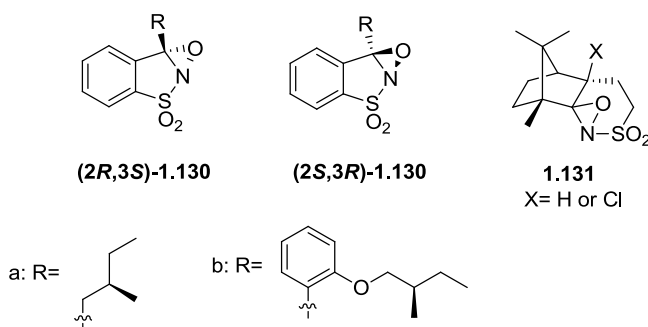
Scheme 1.41

Oxaziridine mediated oxidations on sulfides in the solid state were examined by Colombo *et al.*²²⁰ In the oxidation of two sulfides mounted on solid support resins, oxaziridine **1.125** outperformed the Ti-tartrate based catalyst systems of Kagan and Modena in regard to yield and enantioselectivity. Sulfoxides **1.128** and **1.129** were both obtained in high yield and enantioselectivities (Scheme 1.42).

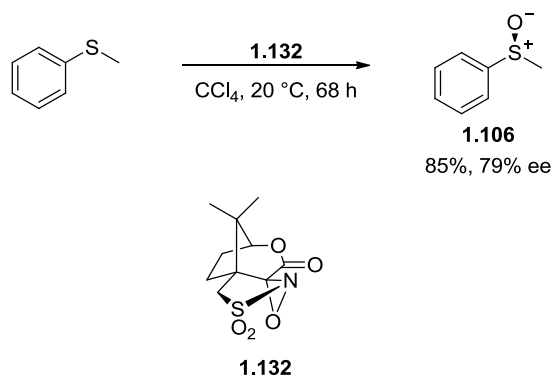


Scheme 1.42

Davis *et al.* also investigated sulfonyloxaziridines derived from benzothiazole, such as **1.130**, but found them to be less effective than oxaziridines reported previously, with the (2*S*,3*R*)-**1.130** isomer generally performing better than its epimer.²²¹ Using these oxaziridines methyl 9-anthryl- and ⁿbutyl *p*-tolyl sulfoxides were afforded in up to 53% and 19% ee, respectively. Davis and coworkers also investigated the preparation and utilization of exo-camphorylsulfonyloxaziridines such as **1.131**, however they were found to give sulfoxides with low optical purities (5-17% ee).²²²

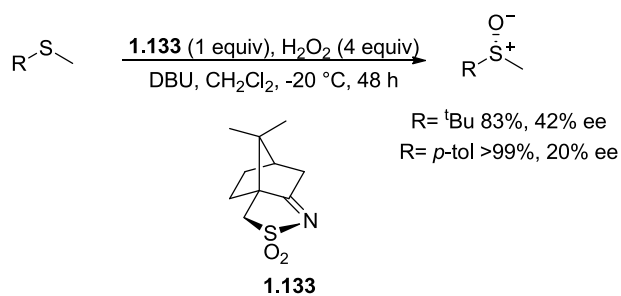


Meladinis *et al.* prepared a series of oxaziridines from 8-camphorsulfonic acid, including **1.132**, and applied them in asymmetric oxidations of prochiral sulfides. (*S*)-Methyl phenyl sulfoxide **1.106** was afforded in high yield and optical purity (Scheme 1.43).



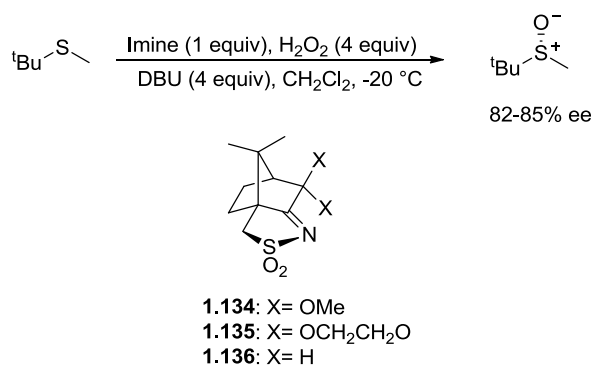
Scheme 1.43

Page *et al.* was the first to report the catalytic enantioselective oxidation of sulfides using an imine derived oxidizing agent that was generated *in situ*.²²³ This methodology involved the employment of an enantiomerically pure camphorsulfonylimine under basic conditions, with the generation of a highly oxidative species from H₂O₂ and the imine derivative. Oxidations were performed in the presence of an organic base, such as 1,8-diazabicyclo[5.4.0]undec-7-ene (DBU), which prevented any non-enantioselective oxidation of the sulfide substrate by the peroxide. Initial investigations of this system saw oxidations giving sulfoxides in moderate to high yields but modest enantioselectivities (Scheme 1.44).



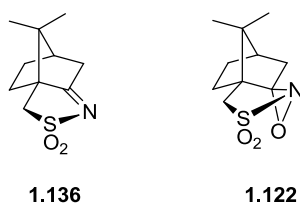
Scheme 1.44

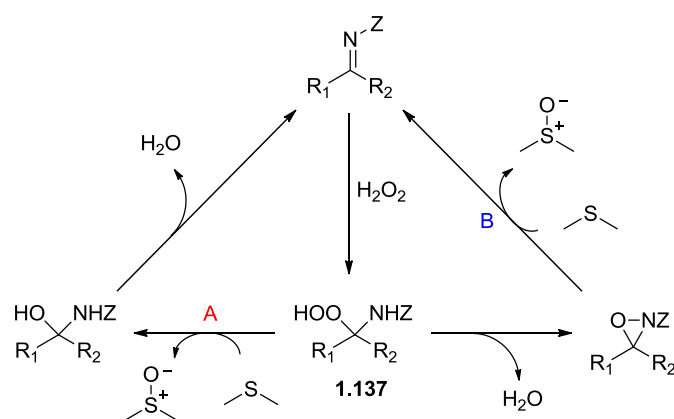
Further investigations by Page *et al.* found that the catalysts produced from H₂O₂ and imines **1.134** and **1.135** gave sulfoxide products with high enantioselectivity (82 and 85% ee, respectively) (Scheme 1.45).⁹



Scheme 1.45

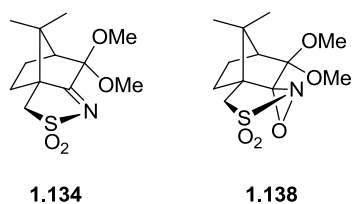
The sense of enantioselectivity observed using this system was initially observed to be the opposite of that obtained when using the oxaziridine **1.122** prepared from **1.136**. Page *et al.* surmised from this that the active oxidizing agent generated must be the α -hydroperoxyamine **1.137**, and that the sulfide oxidation must travel via pathway A, rather than via pathway B which involved oxidation by the *in situ* derived oxaziridines **1.122** (Scheme 1.46).^{9, 224}



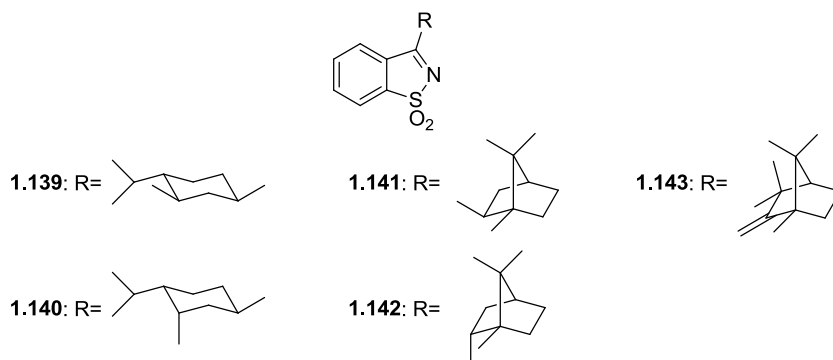


Scheme 1.46

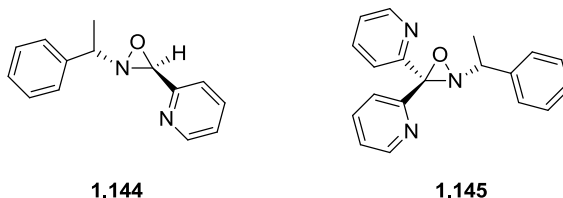
Subsequent studies compared the action of the catalyst system of imine **1.134** with that of the derived oxaziridine **1.138** and, in contrast to previous reports, found that they gave sulfoxides with the same sense of chirality, suggesting that they should have a similar reactive intermediate.^{225 224}



Like Davis *et al.* Page and coworkers explored benzisothiazole based structure for use in asymmetric sulfoxidation.²²⁶ The catalyst generated from H_2O_2 and imines **1.139-1.143** gave sulfoxides of low optical purities (up to 38% ee). Using the oxaziridine derived **1.143** oxidations were performed on a range of sulfides and dithianes, from which the monooxidation products of 2-phenyl-1,3-dithiane was afforded in 83% ee. Comparison of the enantioselectivity of the oxidations using the oxaziridine and those which used the imines showed a similar sense of asymmetric induction between the two methods.²²⁶

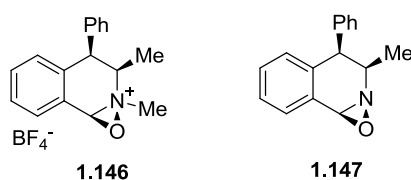


Schoumacker *et al.* reported a new and easily accessible chiral *N*-alkyloxaziridine such as **1.144** and **1.145**, which could be activated by protons or by a Lewis acid, specifically ZnCl₂. Alkyl aryl sulfoxides were generated in moderate to good optical and chemical yields through the use of 1.2 equivalents of both oxaziridine and ZnCl₂; the best result came from the oxidation of methyl naphthyl sulfide by oxaziridine **1.145** which gave the corresponding sulfoxide in 60% yield and 63% ee.

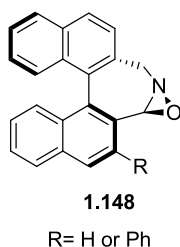


Oxaziridine salts

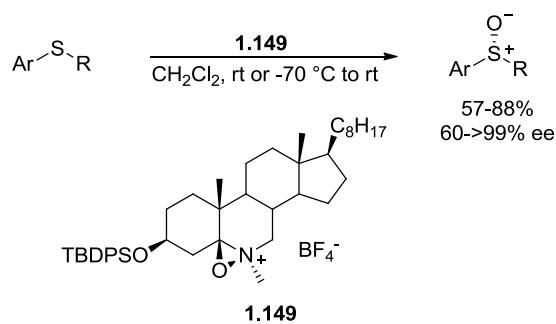
In 1988 Hanquet *et al.* reported the successful development of acid promoted oxygen transfer catalyst, allowing selective oxidation of sulfides to racemic sulfoxides.²²⁷ This system was later developed for asymmetric sulfoxidation. Chiral oxaziridinium salts were prepared from (1*S*,2*R*)-norephedrine and could be in a stoichiometric or substoichiometric amounts to effect oxidation of sulfides. Oxidation of methyl *p*-tolyl sulfide was performed by use of oxaziridinium **1.146**, or the neutral form **1.147**, affording the sulfoxide product in 32% and 43% ee, respectively.^{228, 229}



Hanquet *et al.* also developed *N*-alkyl binaphthyl derived oxaziridines, such as **1.148**, for use in acid promoted sulfoxidations of dialkyl or alkyl aryl sulfides.²³⁰ Good yields were achieved, with no formation of the sulfone overoxidation products observed. Enantioselectivities of between 20-88% ee were achieved, with the configuration of the sulfoxides dependent on the structure of the sulfide substrate. Enantiomerically pure imines, arising from oxygen transfer from the oxaziridine, could be recovered in yield up to 90%, and reused.



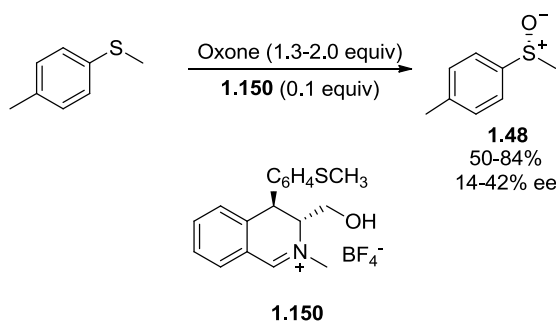
The novel oxaziridine salt **1.149**, derived from cholesterol was employed by Bohé *et al.* as an oxidizing agent in the enantioselective oxidation of sulfides with impressive results.²³¹ Sulfoxides were obtained in good yields and high optical purities, with (*R*)-methyl *p*-tolyl sulfoxide afforded in 88% yield and > 99% ee; (*R*)-benzimidazole sulfoxide was obtained also in high enantioselectivity (98% ee), but in a lower yield (57%) (Scheme 1.47).



Scheme 1.47

Isoquinolinium salts

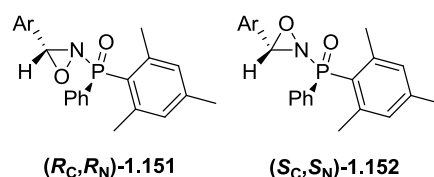
The isoquinolinium salt **1.150** was prepared by Rozwadowska *et al.* and applied in the enantioselective oxidation of methyl *p*-tolyl sulfide to the corresponding (*R*)-sulfoxide. Examining a range of reaction conditions, sulfoxide **1.48** was obtained in moderate to high yields and low to moderate optical purity (Scheme 1.48). The use of *m*CPBA as the oxidant lead to racemic sulfoxides, or products with very low enantiopurity.



Scheme 1.48

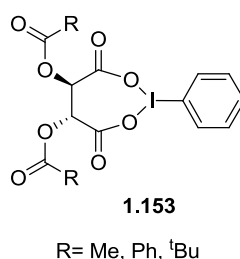
N-phosphinoyloxaziridines

Boyd *et al.* reported the use of *N*-phosphinoyloxaziridines **1.151** and **1.152** in the asymmetric oxidation of methyl *p*-tolyl sulfide and alkyl 9-anthryl sulfides.²³² Sulfoxides with moderate to high optical purities were obtained, with the (*S*)-ⁿbutyl 9-anthryl sulfoxide afforded by **1.152** with the highest enantioselectivity (70% ee). The configuration of the sulfoxide products was observed to be dependent on the oxaziridines configuration, with **1.151** giving (*R*)-sulfoxides, whilst **1.152** gave (*S*)-sulfoxides; the configuration at phosphorus was determined not to exert any influence on the enantioselectivity of the oxidation reactions.



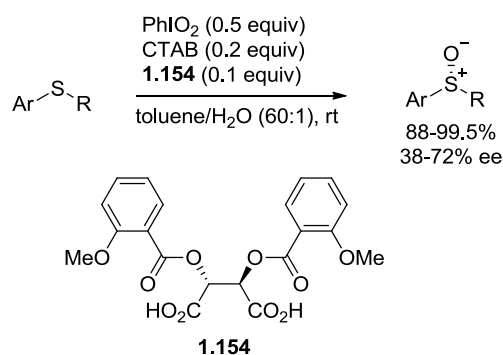
Hypervalent iodine compounds

The oxidation of sulfides by iodine, or iodine based compound has been known since the 1960s.²³³ Imamoto reported the application of the trivalent chiral iodine reagent **1.153**, generated by the reaction between iodosylbenzene with a derivative of L-tartaric anhydride, in the asymmetric oxidation of sulfides.²³⁴ Moderate enantioselectivity was observed for the oxidation of aryl methyl sulfides (up to 53% ee) but aliphatic sulfoxides were furnished in poor optical purities.



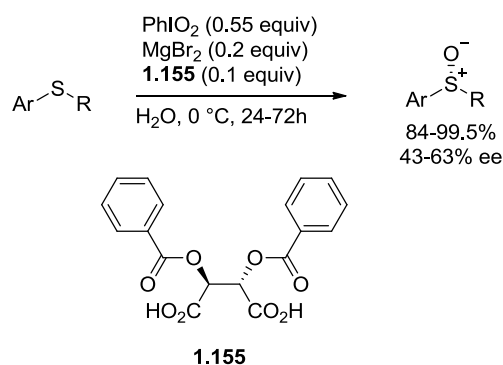
Tohma *et al.* employed the hypervalent iodine(V) reagent iodosylbenzene (PhIO_2) in a cationic reversed micellar system suitable for sulfide oxidations.²³⁵ Aryl alkyl (*S*)-sulfoxides were achieved in high yields and moderate to good enantioselectivities, with the addition of catalytic amounts of cetyltrimethylammonium bromide (CTAB) and the chiral tartaric acid **1.154** indispensable for enhancement of optical and chemical yields, the former especially for its ability to solubilize and activate PhIO_2 . Quideau and Ozanne-Beaudenon used similar conditions for the oxidation of methyl *p*-tolyl sulfide, using a stabilized version of 2-iodoxybenzoic acid (IBX) called SIBX, composed of IBX (49%), benzoic acid (22%), and

isophthalic acid (29%). Using **1.154** as the source of chirality, methyl *p*-tolyl sulfoxide was obtained in 81% yield, 50% ee (Scheme 1.49).²³⁶



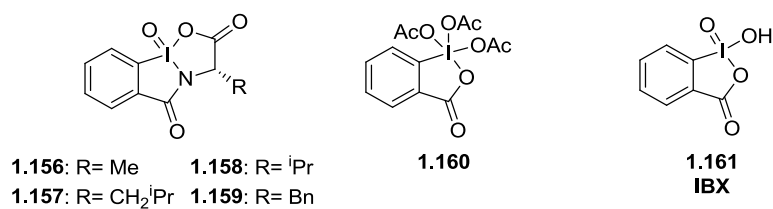
Scheme 1.49

Tohma *et al.* also developed a new catalytic enantioselective sulfoxidation that could be conducted in water using MgBr_2 and (+)-dibenzoyl-tartaric acid, both in substoichiometric amounts.²³⁷ (*R*)-Sulfoxides were obtained in high yield but moderate optical purities (Scheme 1.50), complementing the stereoselectivity of the catalyst system previously developed.

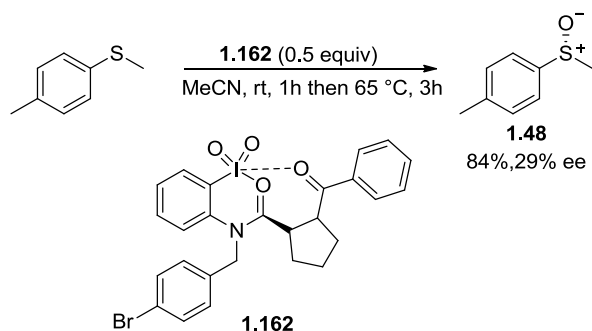


Scheme 1.50

Zhdankin *et al.* also developed a number of iodine based oxidizing agents for sulfoxidation reactions.^{238, 239} The novel amino acid derived benziodazole oxides **1.156-1.159** were amongst the first to be developed, and were analogous to the Dess-Martin periodinane (DMP) **1.160** and IBX **1.161**. Compounds **1.156-1.159** offered a better safety profile and greater solubility in non-polar organic solvents compared to oxidizing agents **1.160** and **1.161**, and could easily be prepared from commercially available precursors. Employment of the oxidizing agents **1.156-1.158** saw methyl phenyl sulfoxide achieved in high yield (90-92%) but low enantioselectivity (11-16% ee); the configuration of the afforded sulfoxide was not discussed.²⁴⁰



Zhdankin later developed a chiral pseudo-benziiodoxazine derivative prepared from (*S*)-proline. *N*-(2-Iodyl-phenyl)-aclyamide **1.162** was found to oxidize *p*-tolyl methyl sulfide to give sulfoxide **1.48** in high yield, but low enantioselectivity (Scheme 1.51).²⁴¹

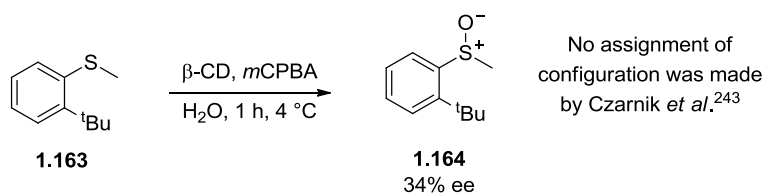


Scheme 1.51

1.4.2.3.2 Oxidations performed in presence of a chiral catalyst

Cyclodextrins

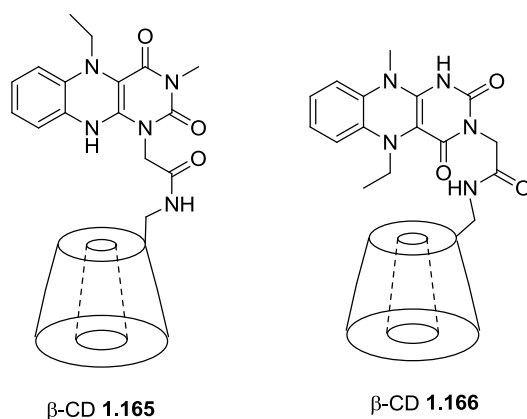
Cyclodextrins (CDs) are supramolecular cage molecules created from the enzymic degradation of starch.²⁴² These oligosaccharides are formed from 6, 7, or 8 glucose units (α -, β -, and γ -CD respectively) and feature a hydrophobic cavity that can encapsulate other molecules.^{102, 242} The use of cyclodextrins to mediate asymmetric sulfoxidations was first reported by Czarnik in 1984.²⁴³ Using *m*CPBA the oxidation of sulfide **1.163** was carried out in the presence of β -CD, giving sulfoxide **1.164** in 34% ee (Scheme 1.52), which at the time was comparable to the highest asymmetric induction reported for a chemical sulfoxidation reaction.²¹⁰ Drabowicz and Mikołajczyk also reported the synthesis of optical enriched sulfoxides using β -cyclodextrins, with H₂O₂ as the oxidant, achieving enantioselectivities up to 30% ee.²⁴⁴



No assignment of configuration was made by Czarnik *et al.*²⁴³

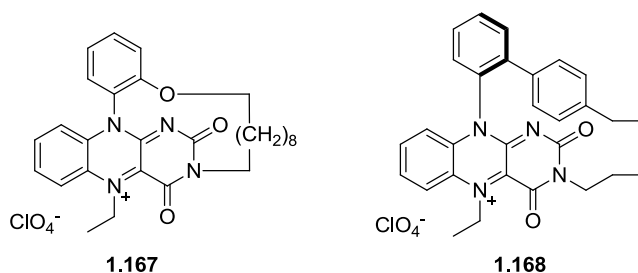
Scheme 1.52

Surendra investigated enantioselective sulfoxidations using *N*-bromosuccinimide in the presence of β -CD.²⁴⁵ Good chemical yields were obtained but asymmetric induction was poor (< 10% ee). Mojr *et al.* employed flavin-cyclodextrin conjugates such as **1.165** and **1.166** to catalyze sulfoxidations of methyl aryl sulfides with H₂O₂.^{246, 247} Catalyst loadings as low as 0.2 mol% were employed, with high conversions and modest to high enantioselectivities achieved (up to 80% ee).

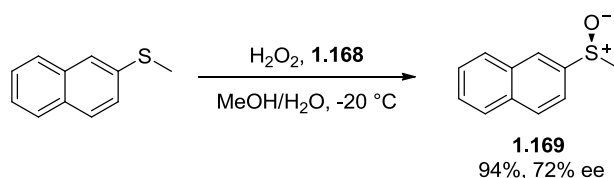


Flavins

A number of flavin-based species have been involved in asymmetric sulfoxidation reactions.²⁴⁸ In 1988, Toda reported flavin mediated synthesis of enantioenriched sulfoxides using the chiral flavin **1.167**, which acted as an asymmetric autorecycling oxygenation catalyst.²⁴⁹

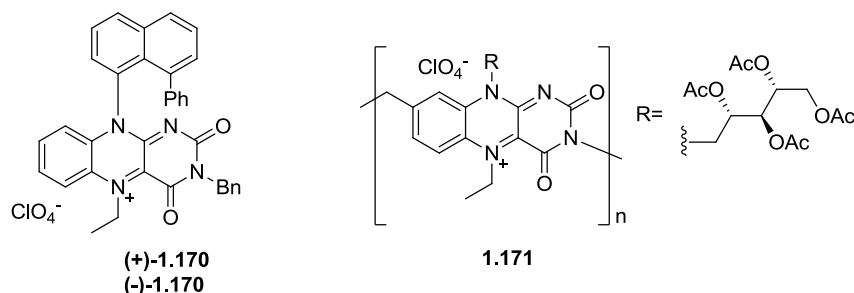


The catalyst was capable of performing up to eight turnovers, producing methyl aryl sulfoxides in modest to good enantioselectivities, the highest of which was 65% ee for (*R*)-methyl *p*-tolyl sulfoxide. A structurally related capped flavin **1.168** was prepared by Murahashi, which was used to prepare the naphthyl sulfoxide **1.169** in 72% ee (Scheme 1.53).²⁵⁰



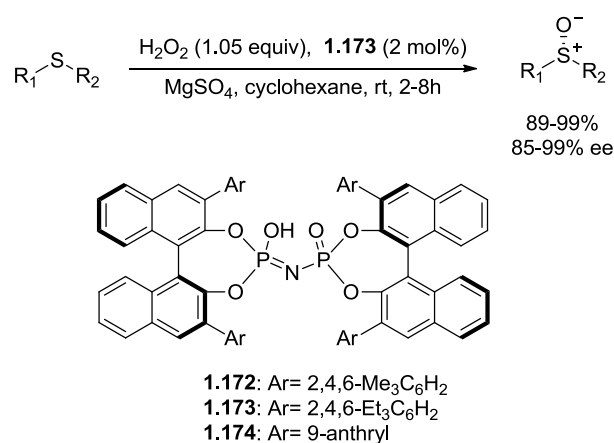
Scheme 1.53

More recently, Jurok *et al.* have reported their use of non bridged chiral flavinium salts **1.170** to mediate the oxidation of a range of sulfide substrates; methyl 2-naphthyl sulfoxide **1.169** was produced in 54% ee using this approach.^{251, 252} Yashima and coworkers prepared the novel optically active riboflavin polymer **1.171**, and used it to catalyze three model sulfide substrates. Methyl *p*-tolyl sulfoxide was obtained in 60% ee, representing the highest enantioselectivity reported for the catalyst; this result was most favourable compared to the monomeric flavin counterpart, which only achieved a maximum enantioselectivity of 30% ee.



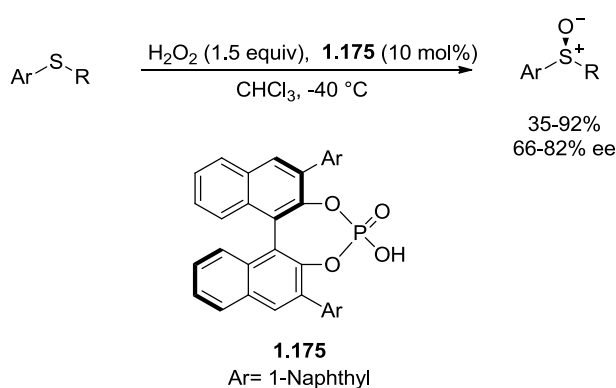
Chiral phosphoric acid derivatives

List and coworkers investigated a series of “confined” Brønsted acids for application in asymmetric sulfoxidations.²⁵³ The use of imidodiphosphoric acids catalysts **1.172-1.174** in the oxidation of thioanisole produced sulfoxides in optical purities up to 98% ee, in some cases in quantitative yields. The efficiency of the reaction was improved by the addition of MgSO_4 to removed water, shortening the reaction time from 24 h to 2. A variety of aryl alkyl and dialkyl sulfides were oxidized using this system, affording the sulfoxides in high yield and enantioselectivity (Scheme 1.54). The synthetic value of this approach was demonstrated by carrying out the key oxidation step in the asymmetric synthesis of Sulindac **1.3**, giving the target sulfoxide in 95% yield and 98% ee.



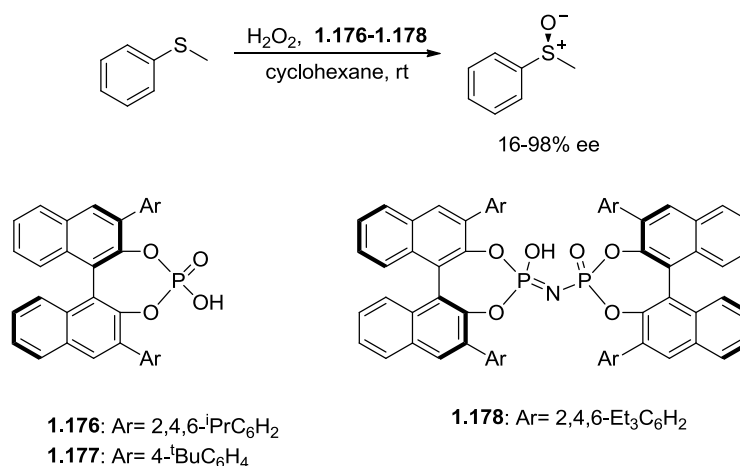
Scheme 1.54

Asymmetric sulfoxidations catalyzed by BINOL derived phosphoric acids were also reported by Liu *et al.*²⁵⁴ Through screening a range of BINOL derived catalysts **1.175** was found to be the most efficient in the oxidation of thioanisole, giving (*S*)-methyl phenyl sulfoxide in 65% yield, 78% ee. Oxidation of a range of sulfides gave the sulfoxides in modest to high yield and good to high enantioselectivity, with benzyl phenyl sulfoxide afforded in the highest optical purity (82% ee, 68% yield) (Scheme 1.55).



Scheme 1.55

Jindal and Sunoj reported oxidations of thioanisole performed in the presence of axial chiral BINOL derived phosphoric acid catalysts **1.176-1.178** (Scheme 1.55).²⁵⁵ The sulfoxide product obtained using catalysts **1.176** and **1.177** had enantiopurities of 16 and 56% ee respectively whereas excellent enantioselectivity was achieved using catalyst **1.178** (98% ee) (Scheme 1.56). Tsogoeva and coworkers examined similar BINOL based catalysts for use in the oxidation of thioanisole and *p*-nitro thioanisole.²⁵⁶ Enantioselectivities achieved were modest, with the highest achieved being 59% ee.



Scheme 1.56

Electrochemical asymmetric oxidation

In 1976 Firth and Miller reported their attempts at using modified chiral electrodes in order to perform enantioselective sulfide oxidations. The enantioselectivities from these early investigation of this method were poor (< 2% ee).²⁵⁷ In the decade following, Komori and Nonanka had greater success with electrochemical based sulfoxidations. Poly(L-valine) coated platinum electrodes were used to oxidize phenyl cyclohexyl sulfide, giving the sulfoxide with an optical purity of 54% ee and in a 31% yield.²⁵⁸ Subsequent work investigated a range of poly(amino acid) coated Pt/graphite electrodes and found poly(valine) to be the most effective at mediating this type of reactions. ^tButyl phenyl sulfoxide was produced using this method in high optical purity (93% ee), a result which compared favourably to those published by Kagan and Modena at the time.²⁵⁹

Solid state catalysis

Taghizadeh performed enantioselective sulfide oxidations using a solid state catalyst system in order to synthesis a library of sulfoxide-based Modafinil analogues.²⁶⁰ The catalyst system, comprising of functionalised silica-based mesoporous MCM-41 with chiral amino oxazoline, Cu(MeCN)₄ (10 mol%), and H₂O₂, was found to afford sulfoxides in enantioselectivities no greater than 37% ee.

1.4.2.3.3 Biological asymmetric sulfide oxidations

Biocatalysis provides an alternative to chemical synthesis for the production of enantiomerically enriched sulfoxides. It allows access to the target products in one step, often with high enantioselectivity.²⁶¹ There is little call for reactions to occur under high pressure, or temperature, and with water as a common solvent the reaction conditions are typically

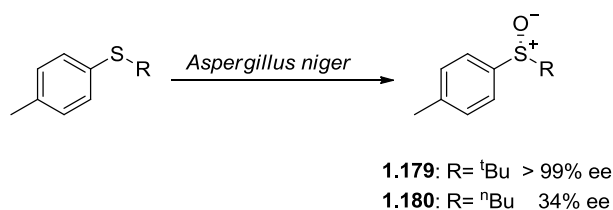
environmentally benign.^{4, 262} Biologically mediated sulfide oxidation can be carried out using whole cells or through isolated enzyme systems. A number of reviews with discussions on this topic have been published.^{4, 6, 66, 263, 264}

1.4.2.3.3.1 Oxidations using whole cells

The use of whole cells for asymmetric sulfoxidation avoids a number of problems associated with the isolation and use of complex enzyme systems.²² Whole microbial cells can be used in a resting state, or in an actively growing one.

Fungi

One of the earliest documentation of whole cell oxidation of a sulfide came from Wright *et al.* who, in 1954, reported the use of *Aspergillus niger* to convert biotin to the corresponding (–)-sulfoxide. In the decade following, Dodson and Tsuchiya successfully prepared benzyl phenyl sulfoxide in 18% ee by oxidation of the sulfide by fermentation with fungus *A. niger*.²⁶⁵ Boyd and coworkers reported the production of optically active sulfoxides through treatment of various sulfides under aerobic conditions with growing *A. niger*, or with the material obtained by extracting *A. niger* with acetone.²⁶⁶ Yields of the afforded sulfoxide were generally modest (up to 65%) with optical purities of 4-99.5% ee (Scheme 1.57). It was observed that sulfoxides with bulky side group were produced with greater enantioselectivity than those that were less sterically demanding (Scheme 1.56).



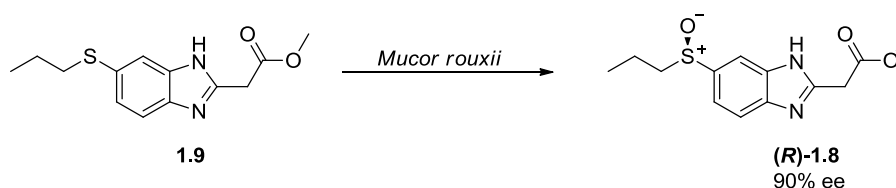
Scheme 1.57

Biocatalysts found in the fungus *Mortierella isabellina* ATCC 42613 were observed by Holland *et al.* to mediate the production of a variety of sulfoxide in very high enantiomeric excess.^{267, 268} This group also extensively reported investigations into the activity of the fungus *Helminthosporium* sp. NRRL 4671 toward asymmetric sulfoxidation.²⁶⁸⁻²⁷⁴ *Fusarium oxysporum* and *Helminthosporium* were employed in the enantioselective oxidation of five vinyl sulfides.²⁷⁵ Four sulfoxides were obtained in good to high optical purity (66-≥ 98% ee), with the biological oxidation of the sulfides giving better results with regard to

enantioselectivity than for oxidations carried out using an oxaziridine reagent or a Kagan type titanium based catalyst system.

Filamentous fungi *Botrytis cinerea*, *Eutypa lata*, and *Trichoderma viride* were employed to carry out a series of biooxidations of a series of substituted sulfides. Sulfoxides were produced with medium to high enantioselectivity, with the formation of (*R*)-enantiomers preferentially produced by *T. Viride* and *E. Lata*, whilst *B. cinerea* gave sulfoxides with the opposite sense of chirality.²⁷⁶ White rot basidiomycetes were found to promote oxidation of aromatic sulfides, producing sulfoxides with good optical purities and only minimal amounts of sulfone.²⁷⁷ Basidiomycetes, *Irpex lacteus*, *Pycnoporus sanguineus*, *Trichaptum byssogenum*, *Trametes rigida*, *Trametes versicolor* and *Trametes villosa*, all gave exceptionally high enantioselectivity (> 99% ee) in the oxidation of phenyl propyl sulfide.

Barth *et al.* employed fungi *Nigrospora sphaerica*, *Papulaspora immera* Hotson, and *Mucor rouxii* in the production of an enantiomerically enriched metabolite of the drug Albendazole **1.9** (Scheme 1.58). A study of the effects of pH on the fungi saw the sulfoxide (*R*)-**1.8** produced by *M. rouxii* in 90% ee after 96h of incubation at pH 5.²⁷⁸



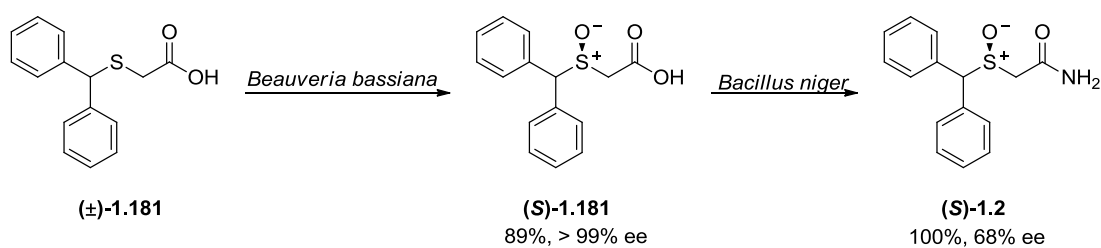
Scheme 1.58

Bacteria

The oxidation of antibiotics clindamycin and linomycin by *Streptomyces* in 1969 was the first evidence of bacterial cells being able to perform the biotransformation of converting sulfides to sulfoxides.^{279, 280} Adams *et al.* prepared a number of aryl alkyl sulfoxides using the commercially available topsoil bacterium *Pseudomonas frederiksbergensis*.²⁸¹ Sulfoxide with high enantiomeric excess were achieved (70-99% ee), including methyl *p*-tolyl sulfoxide which was produced in a quantitative yield and high optical purity (> 99% ee). Enantiopure ⁿbutyl phenyl sulfoxide was obtained by Ohta *et al.* using the bacteria *Corynebacterium equi* IFO 3730, alongside a variety of other alkyl and allyl aryl sulfoxides with high optical purities (75-99% ee).²⁸²⁻²⁸⁴ The bioconversion of alkyl aryl sulfides to give sulfoxides with up to 95% ee using *Gordonia terrae* IEGM 136 was reported by Kylosova *et al.*²⁸⁵ Cells of this bacterium were immobilized into a cryogel of polyvinyl alcohol, which reduced the biotransformation time from 144h to 12h, in comparison to using free cells. (*R*)-sulfoxides were produced using this

methodology, with high enantioselectivity (77-95% ee).²⁶² Kylosova *et al.* also reported their use of the bacterium *Rhodococcus rhodochrous* IEGM 66, which allowed access to enantiocomplementary (*S*)-sulfoxides in up to 89% ee.²⁸⁵

Chen and coworkers used the resting cells of *Pseudomonas monteilii* CCTCC M2013683, isolated from soil samples, to produce chiral sulfoxides, of (*R*)-configuration, in yield of 54-99% and enantioselectivities of 63-99%. (*R*)-Methyl phenyl sulfoxide was produced in high yield and optical purity (99%, 90% ee) using the ethane grown *Micrococcus sp.* M90C.²⁸⁶ The fungus *Beauveria bassiana* ATCC-7159 was used in the production of **1.181**, a key intermediate in the synthesis of Modafinil **1.2**. The (*S*)-sulfinyl carboxylic acid **1.181** was produced in enantiopure form and excellent yield 89%; subsequently the sulfoxide was subjected to transformation by the bacterium *Bacillus niger* to convert it to the final amide form, giving Modafinil **1.2** in 68% ee, in a quantitative yield (Scheme 1.59).²⁸⁷



Scheme 1.59

Algae

Microalgae have also proven valuable for their application in asymmetric sulfoxidation. Whole cells of *Chlorella sorokiniana* were used to oxidise a range of alkyl aryl and dialkyl sulfides, resulting in modest yields (up to 67% conversion) and moderate optical purities (up to 58% ee).²⁸⁸ The dialkyl sulfoxide products were found to be in the (*S*)-configurations, while the opposite enantiomer was favoured in the alkyl aryls oxidations.

Yeasts

Yeasts, such as *Saccharomyces cerevisiae* have been successfully used for the oxidation of sulfides to optically active sulfoxides. The low cost and abundance of these microbial species make them ideal for application in biotransformation.²⁸⁹ Beecher *et al.* reported that *S. cerevisiae* NCYC 73 and commercially available Allinsons yeast were both active for the oxidation of methyl phenyl- and methyl *p*-tolyl sulfide, but not for 'butyl methyl sulfide'.^{289, 290} Both strains of yeast produced the (*R*)-sulfoxide, complimenting the oxidations performed by Beecher *et al.* on the same sulfide substrates by one or more of the Baeyer Villiger

Monooxygenase (BMVO) enzymes present in *Pseudimonas putida* NCIMB 10007, which afforded sulfoxides in the (*S*)-configuration.²⁹¹

1.4.2.3.3.2 Oxidations using isolated enzymes

Peroxidases

The use of isolated enzymes to catalyze asymmetric sulfide oxidations has attracted considerable attention.²⁹²⁻²⁹⁵ Chloroperoxidase (CPO), from the marine fungus *Caldariomyces fumago*, is one of the most versatile of all the peroxidases, and is active towards asymmetric sulfoxidation.^{292, 296} Early applications of this enzyme gave poor results, as reported by Kobayashi *et al.* with the oxidation of thioanisole by H₂O₂ occurring to give the corresponding sulfoxide in just 13% ee.²⁹⁷ Subsequent research by Colonna and coworkers saw greater success; (*R*)-*p*-tolyl methyl sulfoxide was obtained in 83% ee using ^tbutyl hydrogen peroxide (TBHP), whereas oxidation by H₂O₂ resulted in a sulfoxide with an enantiopurity of 37% ee.^{42, 47} Using TBHP to test the generality of *C. fumago* oxidation, a series of alkyl aryl and dialkyl sulfides were examined. Sulfoxide yields ranging from 7-100% were achieved, with optical purities from 19-92% ee. It was determined that the enantioselectivity of the reaction was largely dictated by the steric demands of the sulfide substrate. Colonna *et al.* later showed the importance of experimental parameters, including the choice of oxidant, for the attainment of sulfoxides in high ee and demonstrated the optimized methodology with the oxidation of methyl 2-pyridyl sulfide, gaining the sulfoxide product in enantiopure form.²⁹⁸ Dialkyl sulfoxides were also produced with high conversion and in excellent enantioselectivities; these results were comparable to those reported at that time for the oxidation of dialkyl species by Kagan and Modena.²⁹⁹ Further optimization to the CPO sulfoxidation methodology was reported by Sheldon *et al.* who obtained excellent optical purities for sulfide oxidations carried out in ^tBuOH–water mixtures.^{294, 300} High enantioselectivities were reported by Vargas *et al.* for a series of β-carbonyl sulfoxides produced using CPO.³⁰¹

The first asymmetric electroenzymatic oxidation was carried out using electrochemically generated H₂O₂ and catalyzed by CPO from *C. fumago*. Using this method, thioanisole was oxidised to give the sulfoxide with 99% ee.³⁰² A biphasic system using supercritical carbon dioxide was employed as a reaction medium for CPO mediated sulfoxidation.³⁰³ Oxidations mediated by CPO using H₂O₂ took place in the aqueous phase, utilizing the oxidant generated *in situ* from H₂ and O₂ using a Pd-catalyst in the scCO₂ phase. Sulfoxides were achieved in high ee (up to 94% ee) albeit in modest yield (up to 34%). Hollmann *et al.* reported the light driven, *in situ* production of H₂O₂ to be used in CPO oxidations of sulfides, involving a flavine

photocatalyst and using EDTA as a sacrificial electron donor.³⁰⁴ Methyl phenyl sulfoxide was obtained in quantitative yield and 99% ee using this procedure; the use of formate in place of EDTA, in order to make the reaction less environmentally damaging, led to a decrease in enantioselectivity (78% ee). Nanobiocatalysts consisting of CPO-coated magnetic nanoparticles were utilized by Wang *et al.* to achieve the asymmetric oxidation of thioanisole to afford the (*R*)-sulfoxide with excellent enantioselectivity (99% ee).³⁰⁵

Lactoperoxidase was employed for asymmetric sulfoxidation reactions by Tuynman *et al.* The oxidation of thioanisole took place giving the (*R*)-sulfoxide in 85% yield and 80% ee.³⁰⁶ The performance of the enzyme was reported to improve when the oxidant was added continuously, rather than in discrete aliquots.

Studies by Colonna *et al.* using horse radish peroxidase (HRP) gave sulfoxides with optical purities of up to 68% ee. These results were later improved upon by Ozaki *et al.* with engineered biocatalysts, where one of the amino acids in the HRP enzyme, phenylalanine, was replaced with leucine.^{307, 308} This resulted in a major improvement in enzyme performance, with alkyl aryl sulfoxides afforded in > 90% ee in comparison to a maximum of 77% ee when using the native enzyme. A mutant enzyme produced by replacing phenylalanine with threonine gave poorer enantioselectivities, with 44% ee being the maximum achieved.

Myeloperoxidase (MPO) and manganese peroxidase (MnP) were examined by Tuynman for their application in sulfoxidation reactions.³⁰⁹ Oxidations of thioanisole that were performed using H₂O₂ catalyzed by MPO occurred with low enantioselectivity (23% ee at pH 5, 32% ee at pH 6) and gave the sulfoxide product as the (*R*)-enantiomer. Conversely, oxidations performed using MnP afforded the (*S*)-sulfoxide in low yields (18-36%) but with high enantioselectivity (91% ee at pH 5 and 87% ee at pH 7). *Coprinus cinereus* peroxidase was reported to catalyze the formation of (*S*)-methyl phenyl sulfoxide in 84% yield with 73% ee.³⁰⁶

Vanadium haloperoxidases have been well studied and are known to be highly active towards asymmetric sulfoxidation and kinetic resolution of racemic sulfoxides.^{310, 311} Vanadium bromoperoxidase (VBrPO) show great stability towards high temperature and the presence of organic cosolvents.^{312, 313} Andersson and Allenmark investigated the catalytic effect of VBrPO from the algae *Corallina officinalis* in the H₂O₂ oxidation of prochiral sulfides.^{314, 315} Their initial finding showed the preferential oxidation of a series of rigid, bicyclic sulfides to the (*S*)-enantiomer of the corresponding sulfoxides, which was in contrast to the enantioselectivity exhibited for the oxidations performed using CPO.³¹⁶ High activity was displayed by VBrPO, with 2,3-dihydrobenzo[*b*]thiophene oxidized quantitatively with 98% ee; substrates with a *cis*-

positioned carboxyl group were rapidly oxidized, with sulfoxide obtained with > 95% ee. Loss of enantioselectivity was observed in the presence of bromide ions, suggesting a competing reaction involving the oxidation of bromine. Wever *et al.* showed that haloperoxidases slowly mediated the oxidation of methyl and *p*-tolyl phenyl sulfide, as well as 4-methoxy thioanisole to the corresponding sulfoxides.³¹¹ VBrPO from brown seaweed *Ascophyllum nodosum* was used to obtain (*R*)-methyl phenyl sulfoxide in 88% ee. In contrast, when VBrPO from red seaweed *Corallina pilulifera* was employed the enantioselectivity was reversed, and (*S*)-methyl phenyl sulfoxide was afforded in 55% ee; CPO from *Curvularia inaequalis* employed for the same reaction gave only a racemic mixture.³¹¹

Monoxygenases

A number of Baeyer Villiger monooxygenases (BVMOs) have been to act as catalysts for asymmetric sulfide oxidations.³¹⁷⁻³²⁰ 4-Hydroxyacetophenone monooxygenase (HAPMO), a novel BVMO from *P. Fluorescens* ACB was found convert phenyl and benzyl sulfides to the corresponding (*S*)-sulfoxides with excellent optical purities (up to 99% ee) and conversions up to 97%; allyl and vinyl sulfoxide were obtained in conversions close to 70% with 98% ee. The high levels of optical purity was reported to be solely due to the asymmetric oxidation process, with no additional kinetic resolution of the afforded sulfoxides.³¹⁷ BVMO oxidations of heteroatom sulfides, using HAPMO, phenylacetone monooxygenase (PAMO), or a PAMO-mutant (M-PAMO) were reported by Gotor *et al.*³²⁰ HAPMO gave the best results, with excellent enantioselectivity (> 99% ee) but with great variation in conversions (11-99%). Borderwick *et al.* tested eight variants of *Yarrowia monooxygenase* for efficiency in sulfoxidation and found that optical purities of up to 99% ee were achievable for the oxidation of methyl *p*-tolyl sulfide and methyl phenyl sulfide.³¹⁸ Some variants however showed no reactivity towards the sulfides substrates at all. Recently, a BVMO has been successfully employed in the manufacture of a chiral sulfoxide drug intermediate on a kilogram scale.³¹⁹

Cyclohexanone monooxygenase (CMO) from *Acinetobacter* is another enzyme line that has been well studied with respect to enantioselective oxidation of sulfides³²¹⁻³²³ Colonna *et al.* studied the sulfoxidation of numerous alkyl aryl and alkyl sulfides and found that CMO produce a mixture of (*S*)- and (*R*)-sulfoxides in extremely high optical purities, with moderate to high yields.³²⁴ (*R*)-methyl phenyl sulfoxide was produced in 99% while using the same enzyme produced (*S*)-ethyl *p*-fluorophenyl in 93% ee. Subsequent studies extended the substrate scope to include sulfides with alkyl chains substituted with CN, Cl, vinyl, or hydroxyl groups. Optical purities of up to 99% ee were found, with yields of up to 95%.^{321, 325} From the results of oxidations of over 30 sulfide substrates Colonna and coworkers developed an active site model

to explain and predict the enantioselectivity of sulfoxidation reactions mediated by CMO from *Acinetobacter* NCIB 9871.³²²

A cytochrome P450 monooxygenase from *Rhodococcus sp.* ECU0066 was used by Zhang *et al.* for the oxidation of a range of aryl alkyl sulfides, producing (*S*)-sulfoxides with good to high enantiomeric excesses (64-99% ee).³²⁶ Subsequent investigations improved the methodology with the use of a biphasic organic-aqueous solvent system; (*S*)-phenyl methyl sulfoxide was achieved with 99% ee using this system which showed a marked improvement on the enantioselectivity of the single phase system which gave the sulfoxide in 60% ee.³²⁷

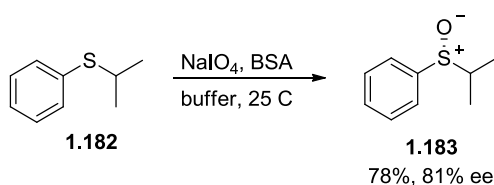
Studies by Brand *et al.* showed that naphthalene dioxygenase (NDO) from *Pseudomonas sp.* NCIB 9816-4 produced sulfoxides in the (*S*)-configuration from the asymmetric oxidation of aryl alkyl sulfides.³²⁸ In contrast, toluene dioxygenase (TDO) from *Pseudomonas putida* F1 produced sulfoxide of varying enantioselectivity and absolute configuration, which seemed to be dependent on the *p*-substituent on the aromatic ring system. This study showed that the dioxygenase component of NDO and TDO could function as sulfoxidases, whereas previously asymmetric sulfoxidations have only been inspected using intact cells of different bacteria expressing NDO and TDO. Extensive studies on NDO and TDO have also been reported by Boyd and coworkers, who employed *P. putida* UV4 and NCIMB 8859, producing sulfoxides in enantioselectivities of > 98% ee.³²⁸⁻³³²

Tyrosinase

Colonna and coworkers found that mushroom tyrosinase *Agaricus bisporus* was active in sulfoxidation reactions; with the use of a catechol as the reducing agent, the oxidation of thioanole was catalyzed by tyrosinase to give the (*R*)-sulfoxide with high ee (> 80% ee), albeit in low yield (< 20%). The low yield was believed to be due to the catechol competing with the sulfide in the oxidation reaction.^{333 334}

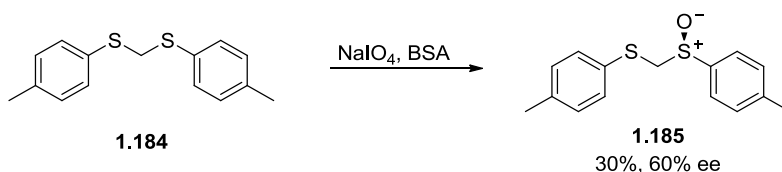
1.4.2.3.3 Oxidations in the presence of bovine serum albumin

Sugimoto reported the oxidation of aromatic sulfides performed by sodium metaperiodate in the presence of bovine serum albumin (BSA), a carrier protein in biological systems.³³⁵ Sulfoxides were obtained in good yield and high enantioselectivity, with the highest optical purity achieved for the oxidation of sulfide **1.182**, giving (*R*)-**1.183** in 81% ee (Scheme 1.60).



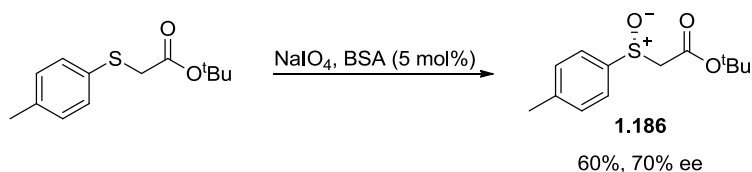
Scheme 1.60

Monooxidation of di-*p*-tolyl dithioacetal **1.184** was reported by Ogura; sodium periodate was used as the oxidant in the presence of BSA, with a two phase aqueous–organic solvent system in employment.³³⁶ The (*S*)-sulfoxide **1.185** was obtained in good ee but only modest yield (30%, 60% ee) (Scheme 1.561). Expansion of the substrate scope to include alkyl aryl sulfides saw *i*-propyl phenyl sulfoxide **1.183** produced with similar enantioselectivity (60% ee) but in greater yield (76%).



Scheme 1.61

Under similar conditions to those used by Sugimoto, Colonna *et al.* performed BSA catalyzed oxidations on a range of aryl alkyl sulfides featuring carbonyl groups on the alkyl chain. BSA was used in a catalytic amount (5 mol%) alongside two equivalents of the oxidant to furnish sulfoxides with enantioselectivities of up to 70% (Scheme 1.62). Interestingly, when H₂O₂ was used in place of NaIO₄ the (*S*)-enantiomer of ester **1.186** was obtained instead of the (*R*)-enantiomer previously given.



Scheme 1.62

Colonna and coworkers also reported on the oxidations of aryl alkyl sulfides using *in situ* generated dioxiranes, catalyzed by BSA. Sulfoxides were achieved in enantioselectivities up to 89% ee and with good yields.³³⁷ Subsequent oxidations of prochiral keto sulfide, where the carbonyl functional group served as the dioxirane precursor, gave (*S*)-sulfoxides in up to 84% ee.³³⁸

1.5 Summary

Sulfoxides are an important and useful functional group for many synthesis processes. Biologically active sulfoxides are found in a number of natural products and pharmaceuticals. As such a great deal of interest has been directed toward the development of new methods for the synthesis of sulfoxides, particularly those in high optical purity. Anyone wishing to pursue the asymmetric synthesis of a chosen sulfoxide would have a wide range of methods to do so by, each with its own inherent advantages and disadvantages.

Resolution of racemic enantiomers can be simple and rapid, but can also be wasteful and low yielding unless the undesired enantiomer can be reused or epimerized. Chromatographic methods can provide materials in high enantiopurity but are unsuitable on a larger scale and can be wasteful in terms of solvent use.

Alongside resolution techniques, there are a wide range of chemical methodologies for the synthesis of chiral sulfoxides. One of the most effective methods is enantioselective oxidation; in this chapter a variety of non-metal based processes have been presented. Biological oxidations are known to produce sulfoxides in excellent enantiopurity but can be highly substrate specific. Enantiomerically enriched sulfoxides have been successfully produced using chiral oxidants such as chiral hydroperoxides, oxaziridines and oxaziridinium salts, and hypervalent iodine compounds amongst others.

Catalytic methods, using non-metal based reagents have also been utilized for the synthesis of chiral sulfoxides. Cyclodextrins, flavins, and derivatives of phosphoric acid have been used in tandem with oxidants such as *m*CPBA and hydrogen peroxides to afford sulfoxides in high enantiopurity. Although these methods have proved useful in the formation of enantiomerically enriched sulfoxides, most require additional steps for the initial synthesis of the chiral oxidant or chiral catalyst.

Chiral auxiliaries have been employed to produce optically enriched sulfoxides for well over 50 years. This method build of the pioneering work of Andersen *et al.* and allows for separation of diastereomeric sulfinates and sulfinamides which can then be transformed to single enantiomer sulfoxides through reaction with various Grignard reagents. Despite the success of this method there is a reliance on the ability to create and separate the diastereomeric intermediates

Despite the great amount of interest in the production and utilization of sulfoxides, particularly over the past three decades, there still remain a number of challenges in this area. Many of the

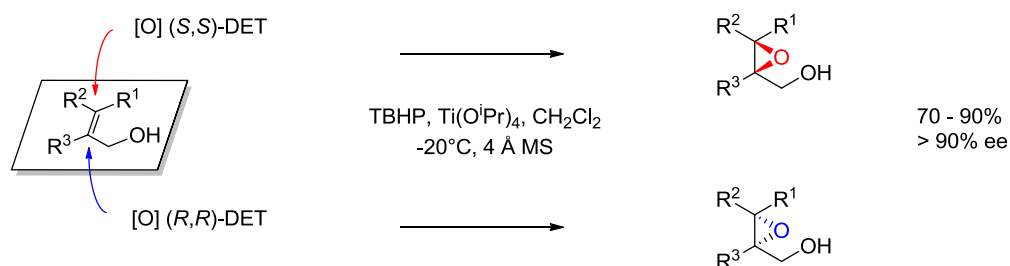
current methods employing non-metal based reagents require stoichiometric amounts of the auxiliary. It is likely that future developments in the synthesis of sulfoxides, particularly in the single enantiomer form, will look toward greener and more sustainable methodologies.

2 Introduction: Metal-catalyzed asymmetric sulfide oxidation

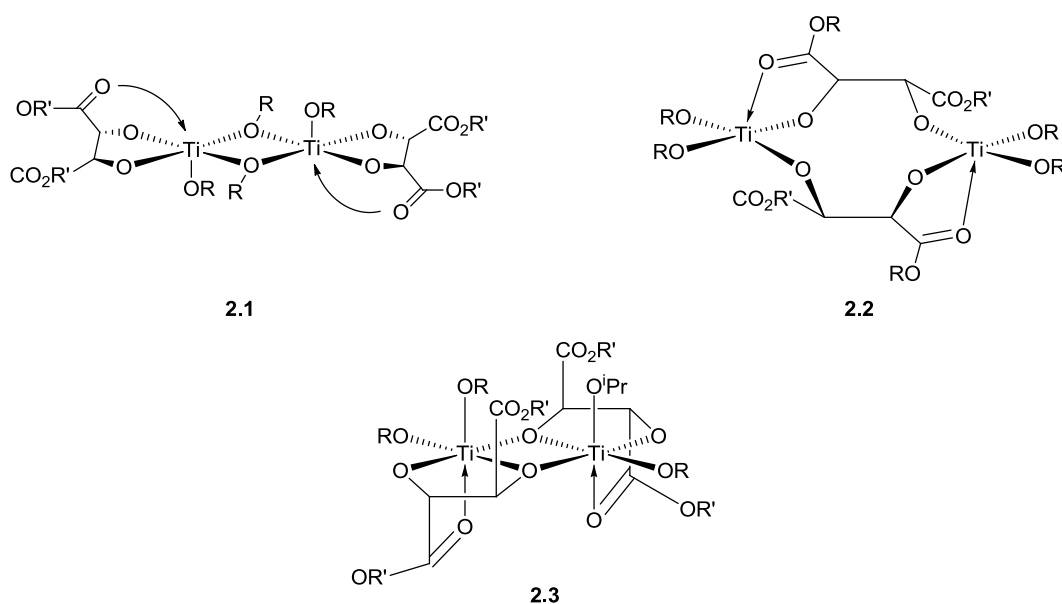
2.1 Titanium-catalyzed S-oxidations

Sharpless asymmetric epoxidation (SAE): The origin of Ti/tartrate mediated asymmetric sulfoxidation

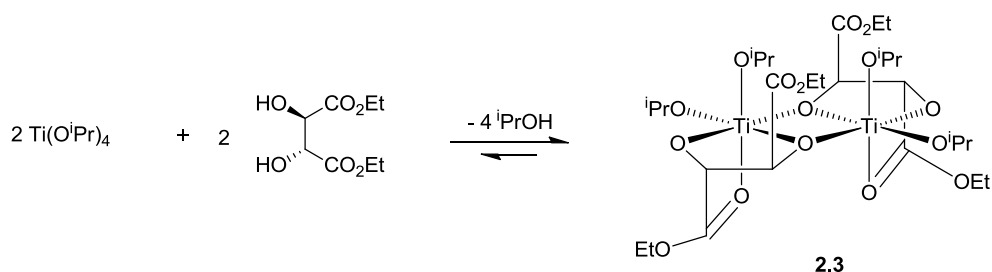
In 1980 a major breakthrough in the area of asymmetric oxidation occurred when Sharpless and Katsuki reported a new chiral epoxidation system.³³⁹⁻³⁴¹ A chiral titanium complex prepared from $\text{Ti}(\text{O}^i\text{Pr})_4$ and optically pure diethyl tartrate (DET) in a 1:1 ratio was employed to effect the asymmetric epoxidation of allylic alcohol using *t*-butyl hydroperoxide (TBHP). This system was found to give uniformly high asymmetric induction in a range of allylic alcohol substrates (> 90% ee), with consistent enantiofacial selectivity depending on the choice of (-)-(S,S)- or (+)-(R,R)-DET (Scheme 2.1).



For the epoxidation of less reactive substrates one equivalent of both $\text{Ti}(\text{O}^i\text{Pr})_4$ and tartrate were required to achieve reasonable reaction rates. However, for more reactive substrates substoichiometric amounts (e.g. 0.1 equiv) of both $\text{Ti}(\text{O}^i\text{Pr})_4$ and DET were sufficient. The use of anhydrous TBHP was an important requirement in order to achieve high enantiomeric purity, and was achieved by the use of molecular sieves.³⁴² The asymmetric epoxidation product of (*E*)- α -phenylcinnamyl alcohol was afforded in 99% ee. In contrast, the addition of one equivalent of water resulted in only 48% ee being obtained.³⁴² The mechanism of the SAE has been widely studied, particularly with respect to the structure of the active catalyst species.^{343, 344} Although an unexpected diversity in the binding modes of the tartrate ester ligands and titanium(IV) was observed, the dominant complex species arising from $\text{Ti}(\text{O}^i\text{Pr})_4$ and the dialkyl tartrate esters was shown to be $[\text{Ti}(\text{tartrate})(\text{OR})_2]_2$, for which a number of structures, such as **2.1-2.3**, were proposed. On the basis of solid state studies on similar binuclear vanadyl tartrate complexes structure **2.2**, with five-coordinate Ti atoms, was originally thought to be the correct Ti-tartrate structure.³⁴⁵ However, as a result of X-ray structure analysis of analogous Ti-tartramide species it was decided that conformation **2.3** was a truer representation of the active catalyst species.³⁴⁶⁻³⁴⁸

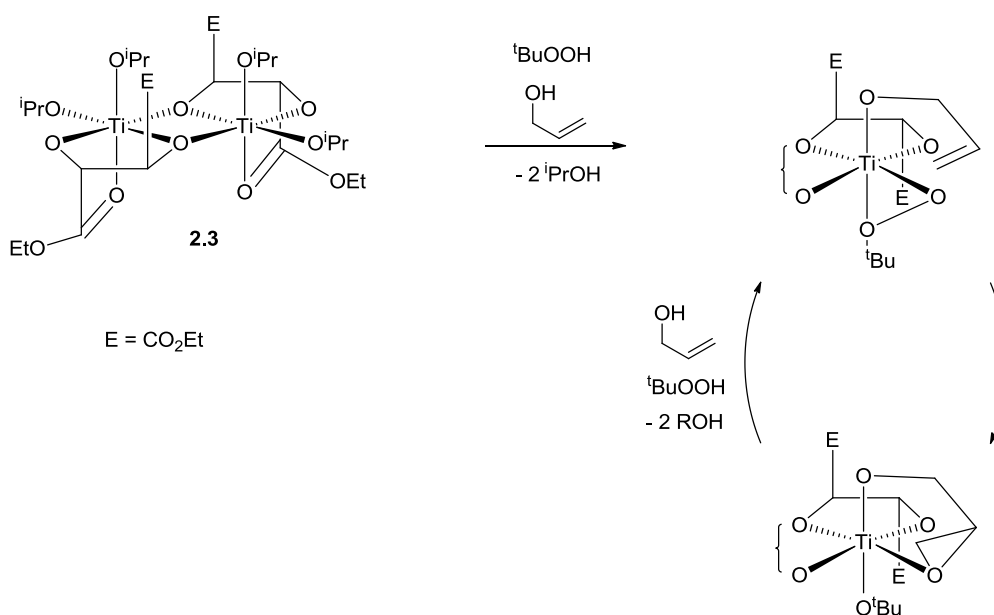


The $[\text{Ti}(\text{tartrate})(\text{OR})_2]_2$ catalyst species is formed via addition of the chiral tartrate resulting in the displacement of four molecules of ${}^i\text{PrOH}$ (Scheme 2.2). The bidentate tartrate diol has a higher binding constant for titanium in comparison to the individual isopropanol ligands; therefore the equilibrium of the reversible displacement reaction lies far to the right. The use of a 10 mol% excess of tartrate to Ti(IV) alkoxide is also important in promoting the desired reaction equilibrium and is vital in order to achieve the highest possible enantioselectivity.



Scheme 2.2

The oxidizing agent and allylic alcohol coordinate to the same Ti centre, displacing a further two ${}^i\text{PrOH}$ molecules, and forming the loaded catalyst. The hydroxyl group on the substrate provides a handle, directing the enantiofacial selectivity of the oxygen delivery to the lower face of the alkene as drawn (Scheme 2.3).^{349, 350}



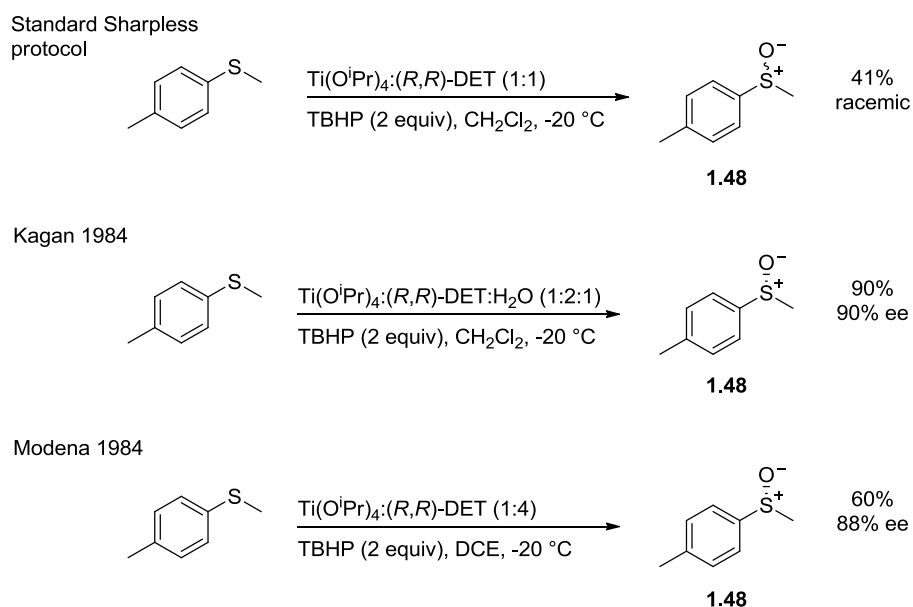
Scheme 2.3

The Kagan and the Modena Sulfoxidation Methodologies

Following the success of the SAE methodology, the application of chiral titanium(IV) tartrate complexes to the asymmetric oxidation of sulfides has been extensively studied.³⁴¹ In 1984 Kagan *et al.* reported that employment of the classical Sharpless reagent in the oxidation of methyl *p*-tolyl sulfide led to the racemic sulfoxide **1.48** (41%) and respective sulfone (17%); the addition of one equivalent of water dramatically increased the enantioselectivity of the sulfoxidation reaction to 84% ee; the use of a second equivalent of tartrate was found to further improve the optical purity of the afforded sulfoxide (90% ee) (Scheme 2.4).³⁴⁷ It was proposed that the addition of water to the classical Sharpless reagent (1:1 Ti(O^{*i*}Pr)₄:tartrate) induced a change in the structure of the active catalyst species. As titanium alcoholates are known to hydrolyze to give TiO₂ species, via the formation of Ti-OH, it was thought it was unlikely that water was acting as a ligand, instead the addition of water led to hydrolysis of a Ti-O^{*i*}Pr bond with formation of a μ -oxo bridge between dimers (Ti-O-Ti); the possible formation of oligomeric species containing multiple μ -oxo bridges was also hypothesized.^{347, 351 347}

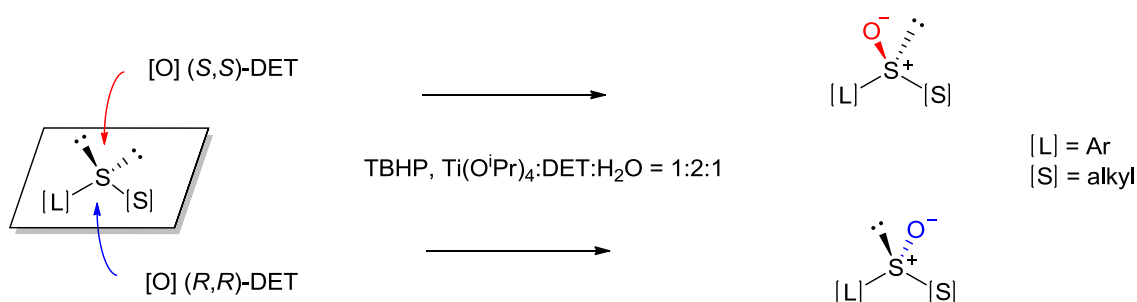
In the same year, the Modena group independently reported the use of 1:4 ratio of Ti(O^{*i*}Pr)₄:(*R,R*)-DET to obtain sulfoxides in satisfactory chemical yields (41-99%) and moderate to good enantioselectivity (14-88% ee) (Scheme 2.4).^{352, 353} Investigation of the Modena catalyst system by Kagan *et al.* revealed that under strictly anhydrous conditions a 1:4 ratio of Ti(O^{*i*}Pr)₄:(*R,R*)-DET afforded nearly racemic sulfoxides, which indicated the additional equivalents of tartrate employed by the Modena group may have inadvertently introduced water

to the system and it was proposed that both groups were in fact investigating the same 1:2:1 Ti(OⁱPr)₄:(*R,R*)-DET:H₂O composition in their sulfoxidation reactions.^{36, 354}



Scheme 2.4

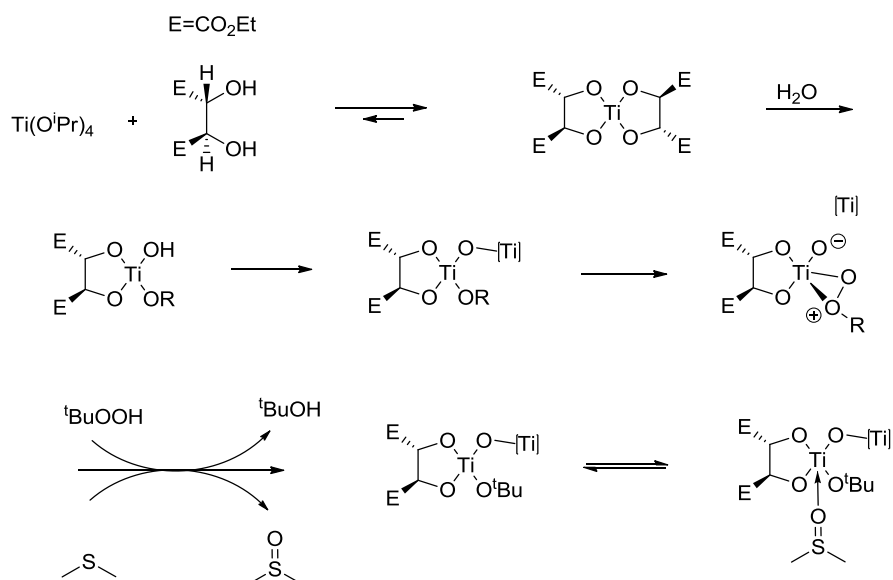
Subsequent studies by the Kagan group found their modified Sharpless reagent to be applicable in the asymmetric oxidation of a wide range of sulfides with consistent enantiofacial selectivity.^{47, 354} A relationship between the absolute configuration of the chiral tartrate and that of the product sulfoxide was established with the stereochemical outcome of such reactions attributed to the steric effects of the substituents on the sulfide (Scheme 2.5).



Scheme 2.5 [L] = large, [S] = small

A tentative mechanism for the asymmetric oxidation of sulfides with the water modified titanium reagent was proposed (Scheme 2.6) based on electron spectroscopy for chemical analysis (ESCA) studies on a solution of Ti(OⁱPr)₄ in isolation or with various other components of the catalyst system (DET, H₂O, TBHP). The ESCA studies revealed an immediate change in the coordination geometry of the Ti(OⁱPr)₄, which is tetrahedral, to an octahedral Ti species after

addition of DET; the octahedral structure of such a species may be accounted for by DET acting as a tridentate ligand similar to that shown in Figure 2.1. Vicinal titaniums, which may be expected from a Ti_2O_2 cores were not detected indicating an open or highly mobile complex structure.¹⁸³



Scheme 2.6 Note: possible coordination between ester groups and the titanium centre have been omitted for clarity

A transition state model for the asymmetric oxidation of methyl *p*-tolyl sulfide was proposed, consisting of a dimeric titanium-tartrate complex, proposing a bimetallic complex with the assumption that one tartrate acts as a tridentate ligand, and with the sulfide nucleophile attacking along the O-O bond of the coordinated peroxide (Figure 2.1).

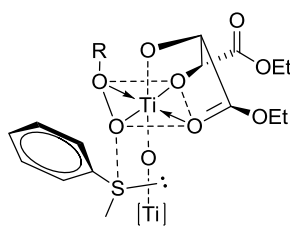
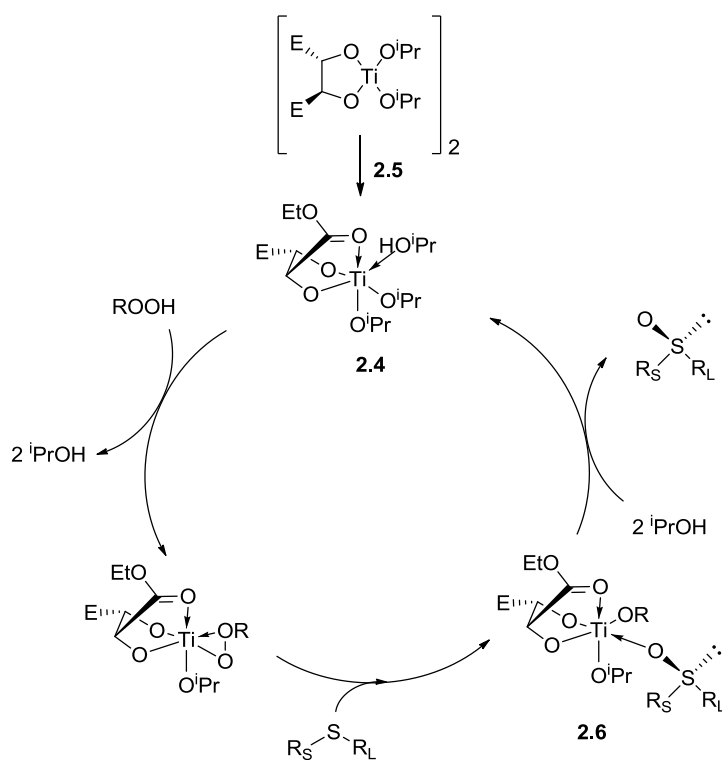


Figure 2.1

Attempts to apply the Kagan reagent in substoichiometric amounts, with respect to the sulfide substrate, yielded sulfoxides in poor optical purity which was attributed to the inhibitory effect of the product sulfoxide which are known to be good ligands for titanium alcoholates.³⁵¹ However, the use of cumene hydroperoxide (CHP) as the oxidant allowed the titanium-tartrate complex to be used in a reduced amount (20-50 mol%) without loss of enantioselectivity.³⁵⁵ A further reduction in catalyst loading, to 10 mol%, was achieved when $i\text{PrOH}$ was used in place

of water in the preparation of the Kagan Ti-tartrate complex, with the addition of molecular sieves, thought to regulate the amount of water present in the system. An optimized ratio of 1:4:4 of $\text{Ti}(\text{O}^i\text{Pr})_4:(R,R)\text{-DET}:\text{}^i\text{PrOH}$ with 4 Å MS led to the formation of methyl *p*-tolyl sulfoxide in 77% chemical yield and 96% ee. The application of a water and $^i\text{PrOH}$ free reagent comprising of $\text{Ti}(\text{O}^i\text{Pr})_4$ and $(R,R)\text{-DET}$ (1:2 equiv with respect to the substrate, 10 mol% catalyst loading) was found to afford the sulfoxide product with 7% ee.³⁵⁵ A modified catalytic cycle was proposed for the oxidation of sulfides with the new $^i\text{PrOH}$ modified Kagan reagent (Scheme 2.7).³⁵⁵ The active catalyst complex was proposed to be the monomeric titanium species **2.4**, formed from the dimeric species **2.5** in the presence of $^i\text{PrOH}$ (Scheme 2.7). The addition of $^i\text{PrOH}$ in the reaction mixture was believed to permit catalyst turnover by displacement of the sulfoxide in **2.6** to reform **2.4**, thus enabling the use of the modified Ti-tartrate reagent in substoichiometric amounts. This reaction mechanism however remains a matter of debate, as does the structure of the active catalyst species most likely due to the complex mixtures of equilibrating species involved.^{356, 357}

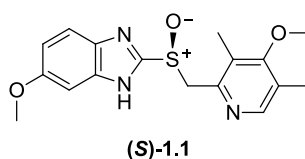


Scheme 2.7

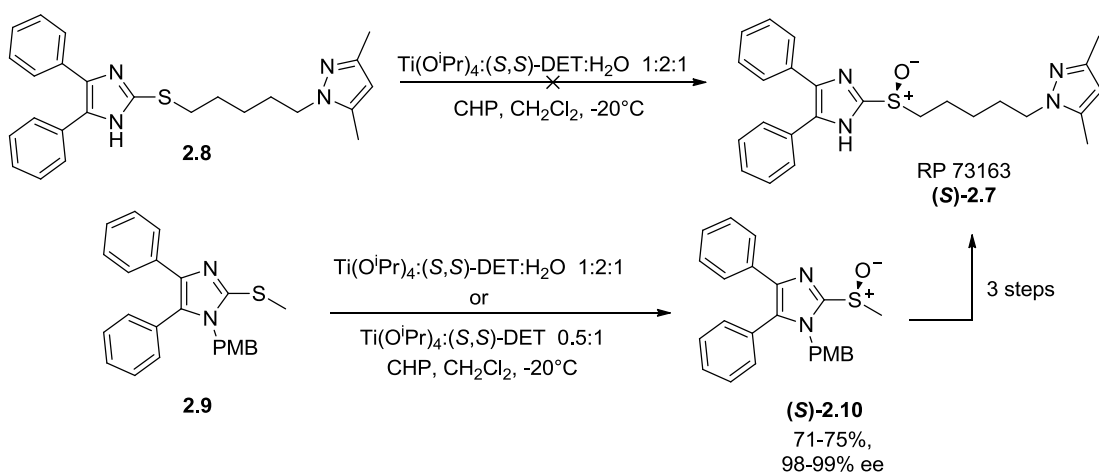
Applications of Titanium/Tartrate Catalyzed S-Oxidation

Titanium tartrate catalyst systems are a popular choice for the asymmetric oxidation of sulfides. The components of the system are inexpensive and readily available, with a range of alkyl tartrates to choose from and the option of either enantiomer of the ligand to enable to production of the sulfoxide isomer of choice. There is also the opportunity for fine tuning the system

through the variation of reagent ratios and/or the use of additives. This methodology is popular for the preparation of pharmaceutical ingredients, from discovery stage through to a multi kilogram scale. The blockbuster drug Esomeprazole (*S*)-**1.1** is prepared by a modified Kagan protocol developed by von Unge *et al.* using a catalyst system of $\text{Ti}(\text{O}^i\text{Pr})_4:(S,S)\text{-DET}:\text{H}_2\text{O}$ in ratios of 0.3:0.6:0.1 equiv with respect to sulfide. Cumene hydroperoxide (CHP) was employed as the oxidant; the base diisopropylethylamine (DIPEA) as an additive was found to be necessary for attainment of high enantioselectivity. This catalyst system and the synthesis of Esomeprazole (*S*)-**1.1** shall be discussed further in subsequent chapters.

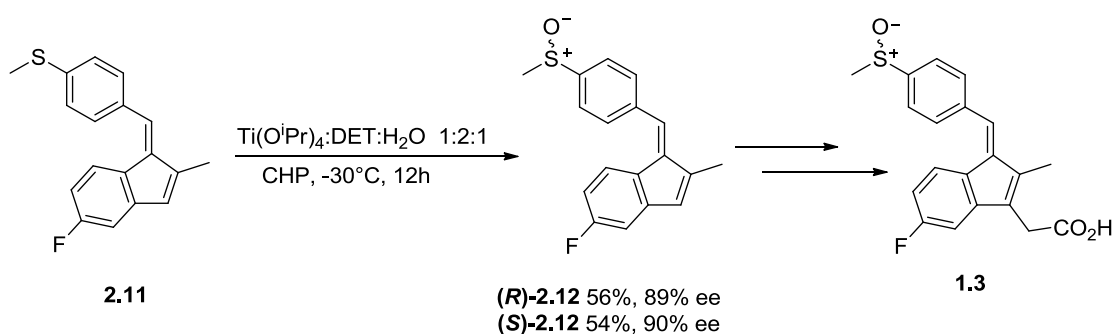


Kagan *et al.* used a titanium-tartrate catalyst system in the synthesis of RP73163 (*S*)-**2.7**, a metabolite of the potent ACAT inhibitor **2.8**; of the two possible sulfoxide enantiomers only the (*S*)-isomer was found to exhibit bioactivity hence the requirement for an asymmetric synthesis suitable for potential scale up.³⁵⁸ Direct oxidation of imidazole sulfide **2.8** using a stoichiometric amount of the catalyst system $\text{Ti}(\text{O}^i\text{Pr})_4:(S,S)\text{-DET}:\text{H}_2\text{O}$ (1:2:1 equiv with respect to the sulfide substrate) gave sulfoxide **2.7** in good yield but as a racemic mixture. An alternative route to (*S*)-**2.7** was found which involved asymmetric oxidation of the *p*-methoxy benzyl- (PMB) protected sulfide **2.9**, followed by transformation of sulfoxide (*S*)-**2.10**, exploiting the acidic nature of the protons α - to the newly formed sulfoxide centre (Scheme 2.8).



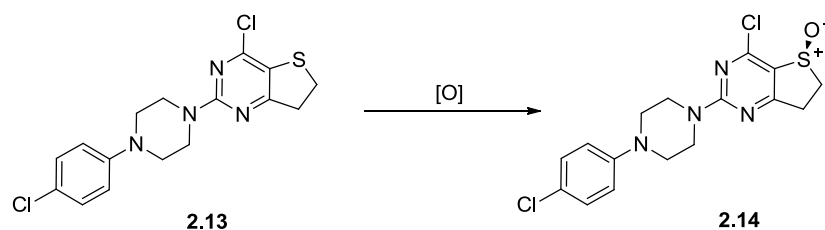
S-oxidation was found to proceed efficiently using the original catalyst conditions ($\text{Ti}(\text{O}^i\text{Pr})_4:(S,S)\text{-DET}:\text{H}_2\text{O}$ 1:2:1) to give sulfoxide (*S*)-**2.10** in 71% yield, with excellent enantiopurity (98-99% ee). In order to minimize the use of the (then) expensive unnatural (*S,S*)-form of the tartrate ligand the conditions were optimized and catalysis of the oxidation was achieved using modified, anhydrous conditions of 0.5 mol equiv of $\text{Ti}(\text{O}^i\text{Pr})_4$ and 1 mol equiv (*S,S*)-DET to afford the sulfoxide (*S*)-**2.10** in high ee (98-99% ee) and high yield (75%) after one recrystallization and requiring no chromatography. Subsequent reactions allowed target sulfoxide RP73163 (*S*)-**2.7** to be eventually achieved in > 99% ee. Having been successfully scaled up to a multikilogram scale, the synthesis of RP 73163 (*S*)-**2.7** represents one of the earliest examples of a large scale asymmetric sulfoxidation.

Sulindac **1.3** has been prepared in both enantiomeric forms by Maguire *et al.* using Kagan procedure.³⁵⁹ Asymmetric oxidation of sulfide **2.11** was carried out with CHP in the presence of $\text{Ti}(\text{O}^i\text{Pr})_4:\text{DET}:\text{H}_2\text{O}$ 1:2:1 at -30 °C for 12h. Using (*R,R*)- or (*S,S*)-DET as the chiral ligand afforded sulfoxide **2.12** in 89% and 90% ee respectively (yields 54-56%) (Scheme 2.9).



Scheme 2.9

Senanayake and coworkers screened a range of S-oxidation catalyst conditions as part of a program toward developing a scalable synthesis of dihydropyrimidines bearing chiral sulfoxide groups (Scheme 2.10).³⁶⁰ Methodologies developed by Kagan and by Modena were investigated (entries 1 and 2, Table 2), as well as those reported by von Unge for the asymmetric synthesis of blockbuster drug Esomeprazole (entry 3).¹²⁵ Of the Ti-tartrate catalyst systems examined, the Kagan protocol gave the target sulfoxide in excellent yield, with the highest enantioselectivity (73% ee).

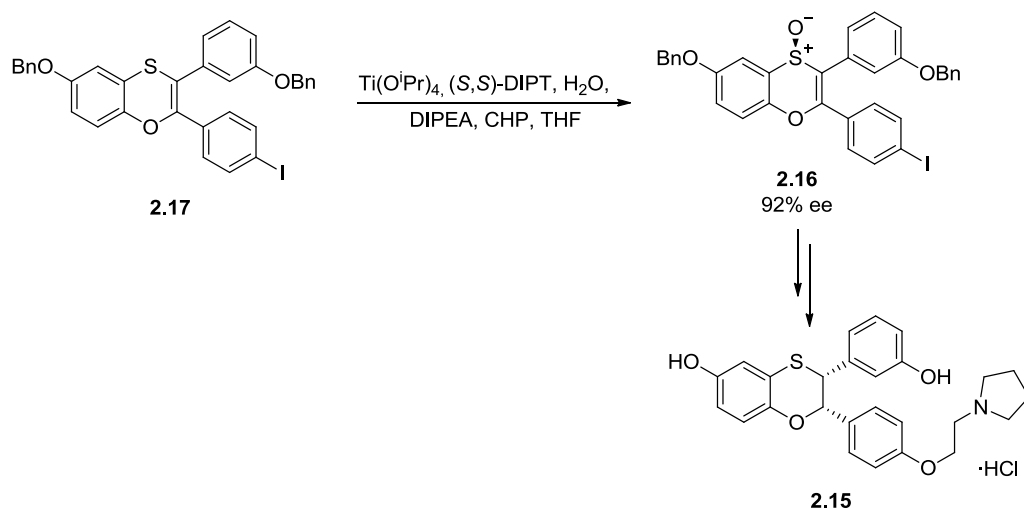


Scheme 2.10

entry	Ti(O ⁱ Pr) ₄ :(<i>S,S</i>)-DET / equiv	Additive (equiv)	CHP / equiv	solvent	<i>T</i> (°C) / time (h)	Isolated yield (%)	%ee (config)
1	1:2	H ₂ O (1)	2	CH ₂ Cl ₂	-20 / 24	99	73 (<i>S</i>)
2	1:4	-	2	CH ₂ Cl ₂	-20 / 24	99	31 (<i>S</i>)
3	0.3:0.6	H ₂ O (0.1) DIPEA (0.3)	1	toluene	35 / 24	90	1 (<i>S</i>)

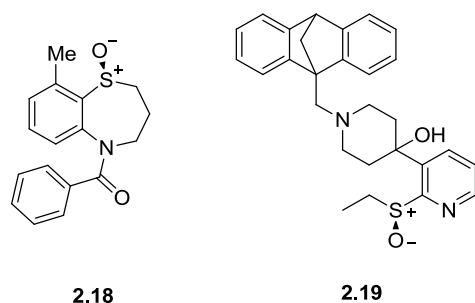
Table 2.1 DIPEA = diisopropylethylamine

The asymmetric synthesis of the selective estrogen receptor modulator **2.15**, with the stereoselective formation of key intermediate **2.16** was carried out via a modified Kagan oxidation of vinyl sulfide **2.17**.³⁶¹ Ligand screening showed that diisopropyl tartrate (DIPT) was best for induction of asymmetry with sulfoxide **2.16** afforded in 38% ee; this figure was significantly improved with further optimization, with great increase in ee values upon addition of diisopropylethylamine (DIPEA) to the catalyst mixture. The catalyst was used in a substoichiometric loading (15 mol%) with Ti(OⁱPr)₄:DIPT:H₂O:DIPEA ratios of 1:2:1:2. The order of addition of reagent held significant importance with respect to efficacy of the catalyst system, and reproducibility of the ee. Optimal conditions saw addition of Ti(OⁱPr)₄ to a solution of the tartrate ligand, DIPEA, and water in THF; aging of the catalyst system overnight was followed by addition of the sulfide **2.17**, and finally addition of CHP. This procedure was carried out on a multikilogram scale, with sulfoxide **2.16** formed in 92% ee; crystallization directly from the reaction mixture gave a product with an optical purity of 99% ee (86% yield) and avoided many difficulties typically encountered when dealing with titanium and tartrate ester residues in reactions of this type (Scheme 2.11).



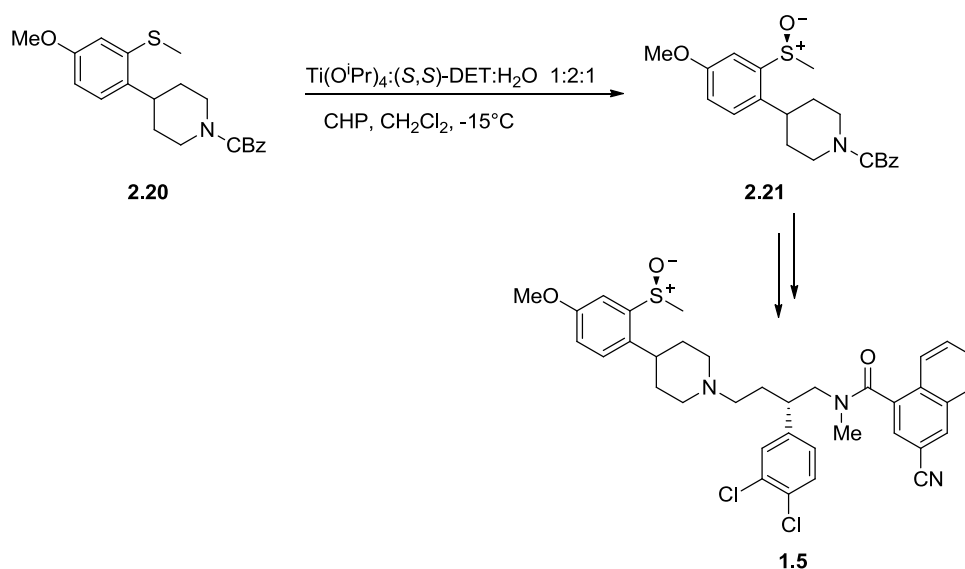
Scheme 2.11

A number of other biologically active sulfoxides have been synthesized using Kagan, or modified Kagan methodologies. Makino *et al.* recently published work on vasopressin receptors, detailing the optimization process leading to the synthesis of N-benzoyl-1,5-benzothiazepine sulfoxide **2.18**. High enantioselectivity was observed for catalyst loadings as low as 10%, with the benzothiazepine S-oxide derivative produced in 97% ee (94% yield).³⁶² The atypical antipsychotic agent **2.19**, which was in development for the treatment of schizophrenia, was required in > 99% ee, as the epimer was shown to have undesirable effects on the central nervous system.³⁶³ Hogan *et al.* reported their use of factorial design to examine 13 variables involved in the asymmetric oxidation process, and found increased sulfoxide ee was attained at lower charge ranges of DET and $\text{Ti}(\text{O}^i\text{Pr})_4$; improvement in the enantioselectivity was reported from 60% ee (discovery method) up to 92% ee following optimization of the catalyst system and reaction protocol, with a final achievement of > 99.5% ee (73% isolated yield) after sulfoxide crystallization.



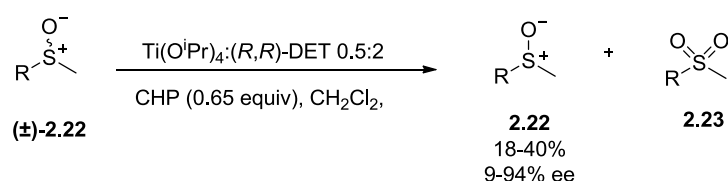
Asymmetric oxidation sulfide **2.20**, by Moseley and coworkers, formed part of the synthesis of the neurokinin antagonist ZD2249 **1.5**.³⁶⁴ Sulfoxide intermediate **2.21** was provided in 94% ee using Kagan's conditions (Scheme 2.12); the temperature of the reaction was a result of a compromise between enantioselectivity and reaction rate, and the almost stoichiometric use of

CHP (1.05 equiv) minimized the unacceptable production of the corresponding sulfone byproduct whilst allowing for an acceptable reaction time.



Scheme 2.12

The titanium/tartrate catalyst system has also been shown to be a useful tool in the kinetic resolution of racemic sulfoxides. Lattanzia *et al.* demonstrated that using the oxidative conditions reported by Modena, i.e. $\text{Ti(O}^i\text{Pr)}_4:(R,R)\text{-DET}$ (0.5:2 equiv) with CHP (0.65 equiv) as the oxidant, enantioselective oxidation of a racemic sulfoxides **2.22** to the sulfones **2.23** occurred, allowing for unreacted starting material to be recovered in enantioenriched form.³⁶⁵ Recovered sulfoxides were found to have ee values between 9-94% ee with low yields (18-40% - typical of a resolution process) (Scheme 2.13); the absolute configurations of the afforded enantioenriched sulfoxide were not disclosed.



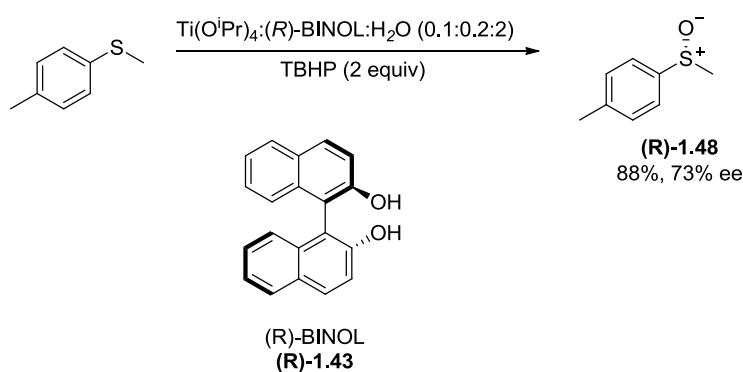
Scheme 2.13

Alternative Chiral Ligands for Use in Ti-Catalyzed S-Oxidations

In addition to research on titanium-tartrate type catalyst systems, many investigations have focused on the use of alternative chiral ligands for Ti-mediated asymmetric oxidations of sulfides.

Diols and related ligands

Uemura *et al.* reported the use of (*R*)-BINOL **1.43** as a catalyst ligand in the synthesis of chiral sulfoxides.³⁶⁶⁻³⁶⁸ Although enantiopure BINOL species had previously been found ineffective for employment in Sharpless asymmetric epoxidation reactions, initial publications on sulfoxidation reactions were more positive. Oxidations performed in the presence of catalyst species formed *in situ* from $\text{Ti}(\text{O}^i\text{Pr})_4$ and (*R*)-BINOL, in a 1:2 ratio, gave rise to methyl *p*-tolyl sulfoxide **1.48** in good enantioselectivity (73% ee) and high yield (88%) when a 10 mol% catalyst loading was used (Scheme 2.14).³⁶⁶ The presences of one equivalent of water (with respect to sulfide substrate) or more was found to be essential for attainment of high enantioselectivity of the reaction, and for extended catalyst turnover and lifespan.³⁶⁷

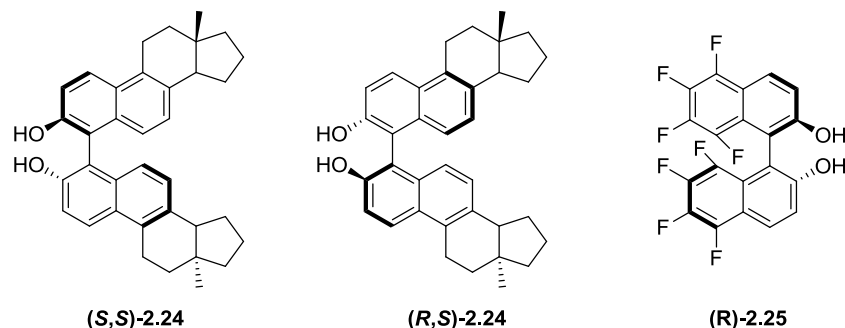


Scheme 2.14

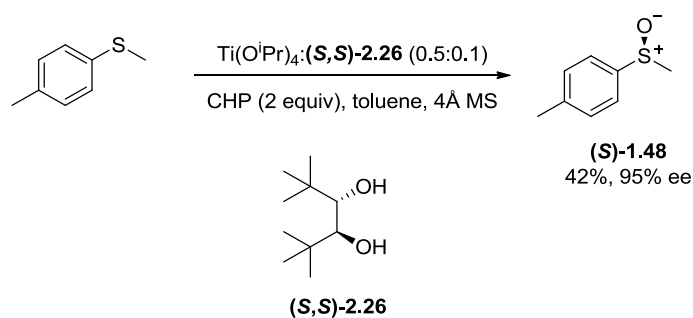
Subsequent optimization saw ee values of up to 96% achieved, using 2.5 mol% catalyst loading with TBHP as the oxidant, as it was proposed that the enantioselectivities were as a result of an initial asymmetric oxidation to the chiral sulfoxide (*ca* 50% ee) followed by kinetic resolution of the sulfoxide. Standalone kinetic resolution experiments saw methyl *p*-tolyl-, *p*-bromo-, and *p*-nitro-sulfoxides isolated in > 99% ee (24-26% yield).³⁶⁸

In addition to Uemura's work, a number of other groups have investigated sulfoxidation reactions catalyzed by titanium complexes of BINOL, or derivatives of BINOL.^{369, 370} Pescitelli *et al.* postulated $(\text{BINOLate})_6\text{Ti}_4(\text{OH})_4$ as the catalyst precursor species arising from Uemura's protocol of 1:0.5:10 BINOL/ $\text{Ti}(\text{O}^i\text{Pr})_4/\text{H}_2\text{O}$ mixture.³⁷¹ An immobilized chiral Ti-BINOL complex was employed by Sahoo and coworkers to obtain alkyl aryl sulfoxides in excellent ee (77-> 99% ee), and good yields (54-63%).³⁷² Bolm and Dabard demonstrated that the bissteroidal diols **2.24** could act as efficient ligand in asymmetric sulfoxidation, achieving (*S*)-sulfoxide **1.48** in 90% ee and 80% yield from a catalyst system with a Ti:ligand ratio of 1:2, in a 10 mol% catalyst loading.³⁷³ Martyn *et al.* investigated catalytic asymmetric sulfoxidation

using F₈BINOL **2.25** as the auxiliary in the chiral titanium catalyst, and found that the use of the fluorinated BINOL derivative gave better enantioselectivity than when BINOL was used, but also afforded sulfoxides with the opposite absolute configuration.^{374, 375}

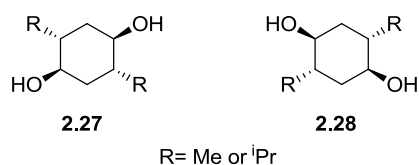


The chiral titanium complex produced from Ti(OⁱPr)₄ and optically active diol **2.26** was employed by Imamoto and Yamanoi to perform oxidation on methyl *p*-tolyl sulfide using TBHP at 20 °C.³⁷⁶ Initial results were disappointing, with only 10% ee observed (70% yield), but optimization of reaction conditions saw this increase to 95% ee, with a sulfide:Ti(OⁱPr)₄:**2.26** ratio of 10:5:1 used, CHP (2 equiv) employed as the oxidant and inclusion of 4 Å MS in the reaction mixture. This system was applied to the oxidation of a range of alkyl aryl sulfides, affording sulfoxides in modest to high yield (36-92%) and up to 95% ee (Scheme 2.15); significant production of the corresponding sulfone was also observed which the authors attributed to a kinetic resolution of sulfoxides following the initial oxidation process.

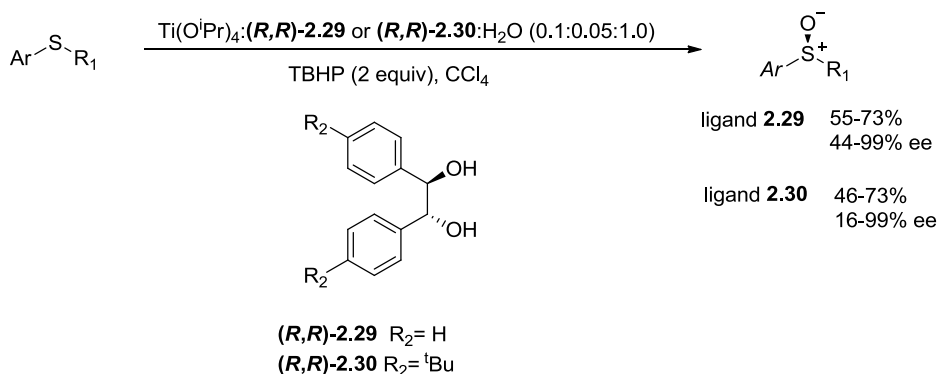


Scheme 2.15

Optically active diols **2.27** and **2.27** were used in the Ti-mediated synthesis of chiral alkyl aryls sulfoxides.³⁷⁷ High enantiopurities (up to 84% ee), with moderate yields (21-79%), were achieved in a range of sulfoxides through oxidations catalyzed by the chiral Ti-1,4-diol complexes formed *in situ*.

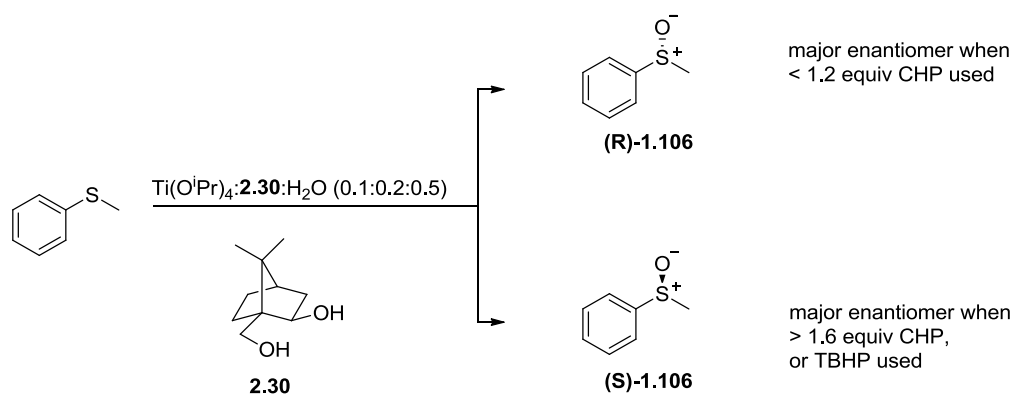


Rosini *et al.* examined the use of hydrobenzoin type ligands in Ti-mediated sulfoxidation reactions.³⁷⁸⁻³⁸⁰ Using ligand **2.29**, a range of aryl alkyl- and aryl benzyl sulfoxides were produced in good yields (55-74%) and moderate to high optical purities (22-99% ee). Subsequent work examined the use of a range of *p*-substituted hydrobenzoin species and found that the ^tBu-derivative **2.30** gave rise to (*S*)-*p*-tolyl methyl sulfoxide **1.48** with the highest enantioselectivity (90% ee), in high yield (70%) (Scheme 2.16). Capozzi and Cardellicchio also employed hydrobenzoin type diol ligands in catalytic asymmetric sulfoxidations, including the synthesis of chiral sulfoxide precursors to Sulindac **1.3**.³⁸¹⁻³⁸³



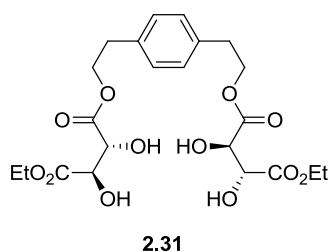
Scheme 2.16

Zeng *et al.* reported the use a 2,10-campanediol derived titanium complex catalyst in the asymmetric formation of sulfoxide **1.106**.³⁸⁴ When TBHP was used as the oxygen source the (*S*)-sulfoxide was always the predominant product; however the use of CHP gave varied results, depending on how much of the oxidant was employed. When less than 1.2 equiv of CHP was used, the (*R*)-sulfoxide was formed as the major enantiomer, conversely the (*S*)-sulfoxide was formed in excess when > 1.6 equiv of CHP was used (Scheme 2.17). The greatest enantioselectivity (99%, 11% yield) was observed when CHP (2 equiv) was used with a 10 mol% catalyst loading of Ti(OⁱPr)₄:**2.30**:H₂O (1:2:5). An accompanying kinetic resolution process alongside the asymmetric oxidation was indicated by increased sulfone production with longer reaction times, with similarly increasing ee values and reduction in sulfoxide yield.

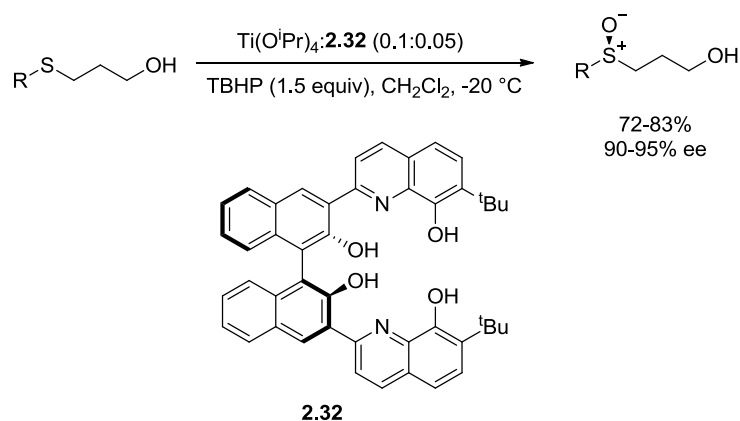


Scheme 2.17

The chiral tetradentate ligand **2.31** was created by Corey *et al.* which outperformed Kagan type oxidations for the asymmetric oxidation of a number of sulfides.³⁵⁶



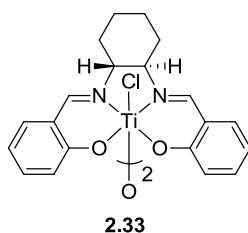
The 8-quinoline-based ligand **2.32**, developed by Bhadra *et al.*, formed part of a binuclear titanium catalyst that was reported to give high levels of stereoselectivity in sulfoxidations of γ -hydroxypropyl sulfides.³⁸⁵ Using a 10 mol% catalyst loading, with a $\text{Ti}(\text{O}^i\text{Pr})_4$:ligand ratio of 2:1, chiral γ -hydroxypropyl sulfoxide were obtained in high yield (72-83%) and high optical purities (90-95% ee) (Scheme 2.18).



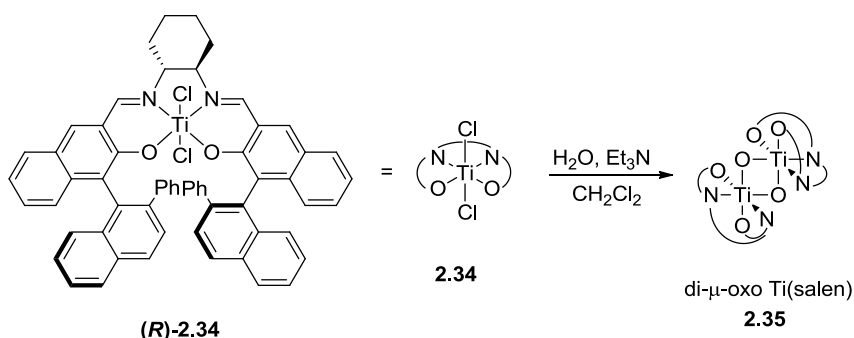
Scheme 2.18

Salen and Salan ligands

Numerous reports of the use of Ti-salen complexes in asymmetric sulfoxidation have been published.³⁸⁶⁻³⁸⁸ Fujita *et al.* reported the first Ti-salen based catalyst for asymmetric sulfoxidation.³⁸⁹ Using the binuclear *N,N'*-disalicylidene-(*R,R*)-1,2-cyclohexanediamine-titanium(IV) complex **2.33**, methyl phenyl sulfide was oxidized by trityl hydroperoxide (THP) with enantioselectivities up to 53% ee.



Katsuki and coworkers conducted extensive studies of new salen complexes for Ti-mediated sulfide oxidation, taking inspiration from a second generation (salen) manganese (III) complex developed within the group which performed well in oxidation of alkyl aryl sulfides.³⁹⁰⁻³⁹³ Application of (salen) titanium(IV) complex (*R*)-**2.34** (4 mol%) saw poor performance, giving an enantioselectivity of only 10 % ee for the oxidation of thioanisole. Complex **2.34** was converted to the corresponding di- μ -oxo (salen) titanium complex **2.35** (Scheme 2.19), which gave improved sulfoxidation enantioselectivity (76% ee); when oxidation was performed with a urea-hydrogen peroxide adduct (UHP) a considerably improved ee of 94% was achieved. The asymmetric sulfoxidation of a range of aryl sulfides was carried out using 2 mol% of complex **2.35**, with high yields (78-93%) and excellent enantiopurities (92-99% ee) obtained.

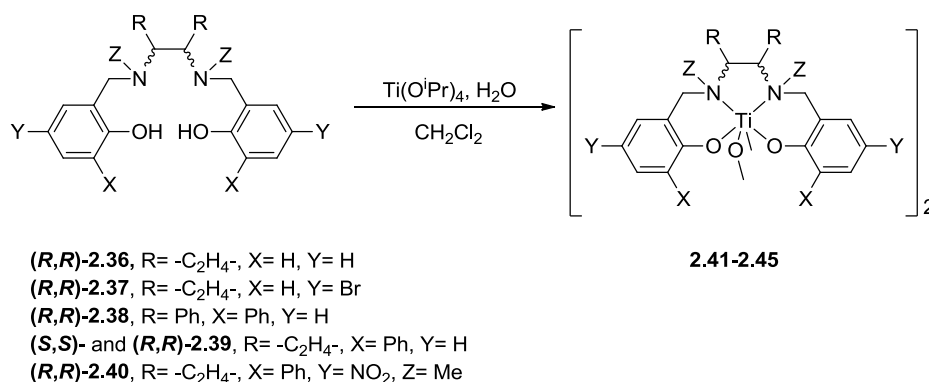


Scheme 2.19

Bryliakov and Talsi reported titanium-salan complexes capable of catalyzing stereoselective sulfoxidations with H_2O_2 , with accompanying kinetic resolution of the sulfoxides.^{29, 387, 394, 395}

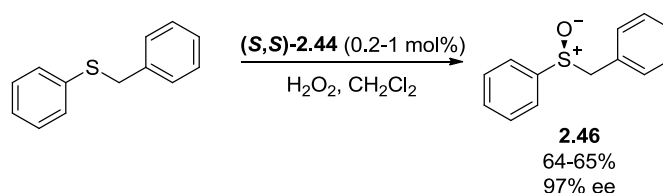
A number of tetradentate ligand were synthesized and the Ti-salan catalyst complexes formed *in situ* were evaluated for efficacy and enantioselectivity, using a catalyst loading of 2 mol% and a

slight excess of oxidant (1.1 equiv); optical purities of 43-64% ee were obtained, with sulfoxide yields of 63-68%.



Scheme 2.20

The corresponding di- μ -oxo titanium salen complexes **2.41-2.45** were prepared and evaluated for their use with a 1 mol% catalyst loading; oxidation of a range of alkyl aryl and alkyl benzyl sulfides proceeded with improved enantioselectivity, with the exception of **2.45**. Optimization of the system saw phenyl benzyl sulfoxide **2.46** produced in 97% ee (64-65% yield) using the preformed complex **2.44**, again with a significant amount of overoxidized product obtained (35% yield) (Scheme 2.21).

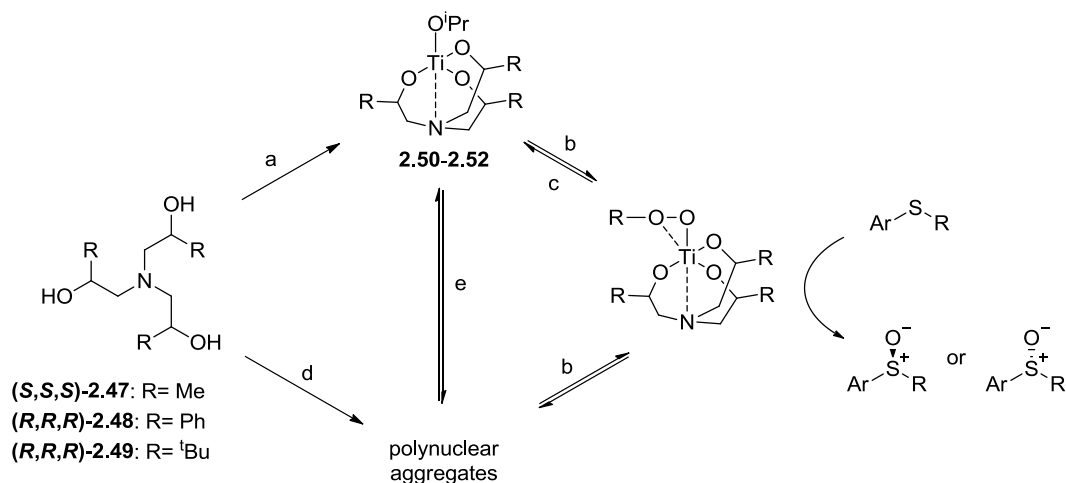


Scheme 2.21

Trialkanolamine ligands

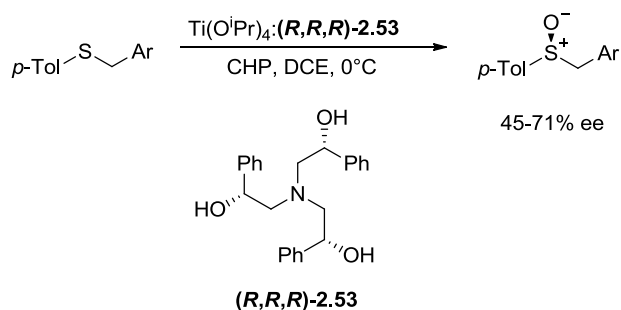
In 1994 Nugent and Harlow first documented the synthesis of complexes formed between Ti(OⁱPr)₄ and homochiral trialkanolamine ligands **2.47**.³⁹⁶ Complexes of this type were subsequently investigated for use in asymmetric sulfoxidation by Nugent, in collaborations with Modena *et al.*³⁹⁷⁻⁴⁰³ Initial studies examined the reactivity and enantioselectivity of catalyst complexes **2.50** and **2.51**, formed *in situ* from Ti(OⁱPr)₄ and enantiopure trialkanolamines **2.47** and **2.48** (Scheme 2.22). Claims made by the authors suggest the development of an effective catalyst capable of high turnover numbers (1-2 mol% catalyst loading) and enantiomeric excesses of afforded sulfoxides in the range of 40-84% ee, however these figures relate to only a small percentage of the results published; in general only moderate asymmetric induction was observed during the oxidation process (3-36% ee), with the highest enantioselectivity exhibited

when ligand **2.48** was employed, with CHP used as the oxidant. The optical purity of product sulfoxides was attributed to a combination of both an asymmetric oxidation process and kinetic resolution of the corresponding sulfoxide.



Scheme 2.22 Reagents and conditions: a) stoichiometric $\text{Ti}(\text{O}^i\text{Pr})_4$, CHCl_3 , 20 °C; b) oxidant (TBHP or CHP); c) $^i\text{PrOH}$; d) $\text{Ti}(\text{O}^i\text{Pr})_4$ (0.75 equiv.), CH_2Cl_2 , 20°C followed by solvent removal; e) excess of ligand

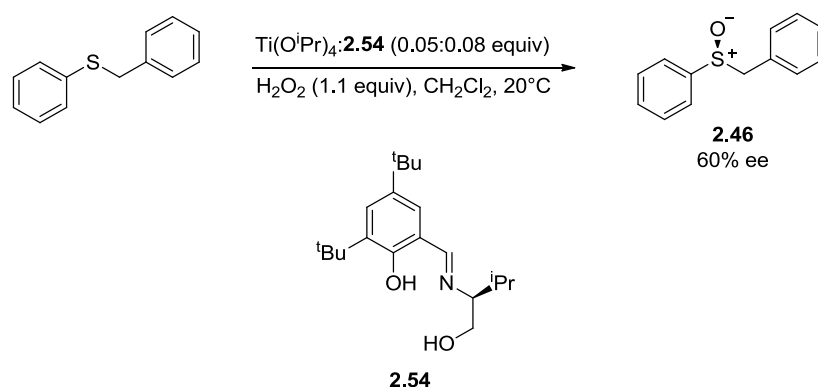
Numerous reports since then have discussed the structures of the various complexes involved, including the polynuclear aggregate obtained with a substoichiometric amount of $\text{Ti}(\text{O}^i\text{Pr})_4$ was added to the ligand, and the reaction mechanism of the titanium-trialkanolamine mediated sulfoxidations.^{398, 399} It was proposed that addition of cumyl hydroperoxide to complexes **2.50-2.52** afforded an active catalyst species with a biphilic nature, behaving as an electrophile towards sulfides while at the same time the kinetic resolution pathway saw a dominating nucleophilic behavior toward the oxidation of sulfoxides. Modena *et al.* have more recently reinvestigated the stereoselective oxidation of a range sulfides, catalyzed by the complex (*R,R,R*)-**2.53** (10 mol% catalyst loading), with modest to good enantioselectivities observed (45-71% ee) (Scheme 2.23).⁴⁰³



Scheme 2.23

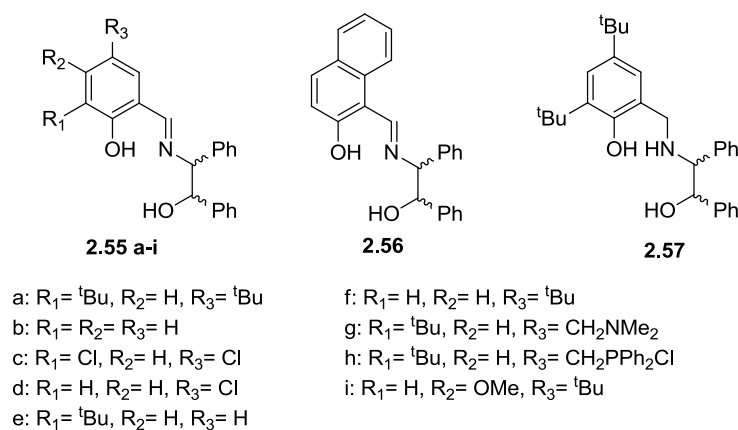
Schiff base ligands

Brylaikov and Talsi reported the use of tridentate Schiff base ligand, derived from chiral aminoalcohols, for use in titanium catalyzed sulfoxidation reactions.⁴⁰⁴ Screening of the ligands in the oxidation of benzyl phenyl sulfide showed that the best enantioselectivity was achieved through use of **2.54**, in a catalyst loading of 5 mol% with Ti(OiPr)₄:ligand ratio of 1:1.5. Sulfoxide (*S*)-**2.46** was afforded in modest enantiopurity (60% ee) (Scheme 2.24).



Scheme 2.24

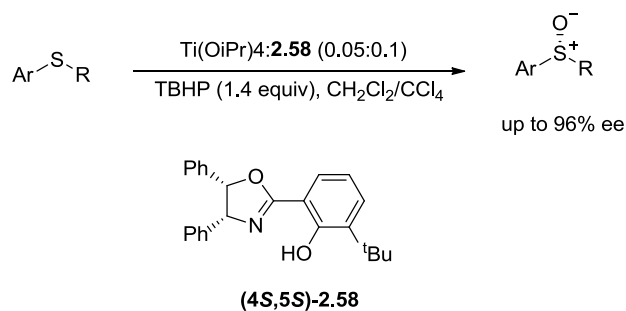
Bera *et al.* investigated a range of diphenyl Schiff bases (**2.55-2.57**) for use in the oxidation of thioanisole.⁴⁰⁵ A catalyst loading of 2.5 mol % was employed, with a Ti(O^{*i*}Pr)₄:ligand ratio of 1:1.2. Hydrogen peroxide (1.1 equiv) was used as the oxidant giving methyl *p*-tolyl sulfoxide **1.48** in moderate to high enantioselectivities (30-98% ee).



Miscellaneous ligands

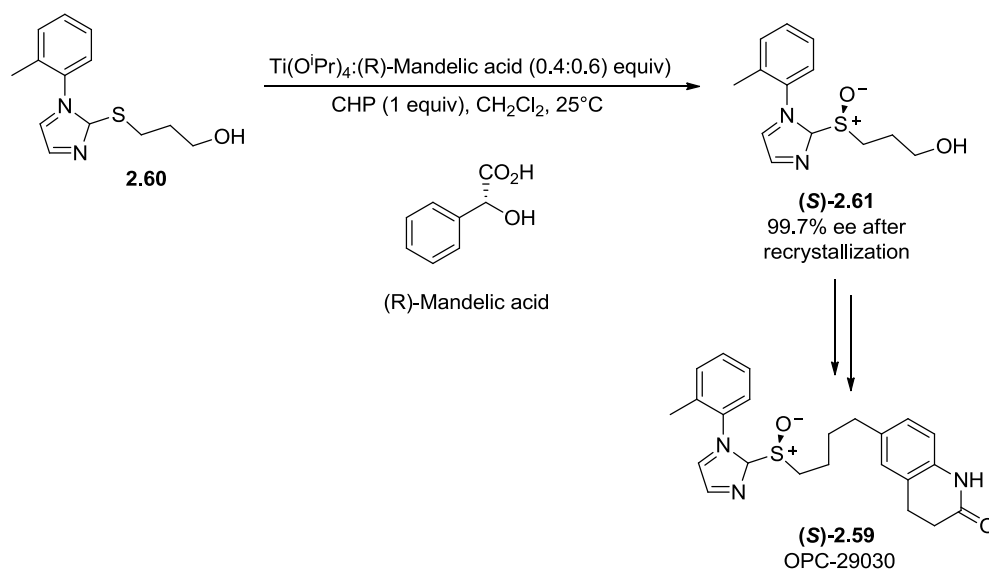
A range of oxazolines with diverse substituents were synthesized by Chen *et al.* and explored as chiral ligands in asymmetric sulfoxidation of a number of alkyl aryl sulfides.⁴⁰⁶ The highest ee value was achieved under optimized conditions using oxazoline **2.58**. Titanium isopropoxide and oxazoline were employed in ratios of 1:2 respectively, with a catalyst loading of 5 mol %.

The sulfoxide products were afforded in enantiopurities ranging from 21-96% ee, and in low yields (27-50%) (Scheme 2.25); high production of the over-oxidized sulfone products supports the authors proposal that the highest enantioselectivity observed was due to the concomitant processes of sulfide oxidation and kinetic resolution of the generated sulfoxide.



Scheme 2.25

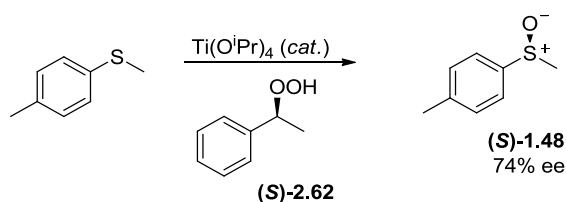
A practical method for the synthesis of platelet adhesion inhibitor OPC-29030 **2.59** was established utilizing the asymmetric oxidation of sulfide **2.60** to (*S*)-**2.61** employing a chiral titanium-mandelic acid complex catalyst system.⁴⁰⁷ Application of Kagan's sulfoxidation protocol to **2.60** gave sulfoxide (*S*)-**2.61** in only 54% ee (78% yield), although recrystallization could raise this figure to > 99.5% ee. Screening of Kagan type Ti-based catalyst systems were carried out, examining various mono-, bi-, and tridentate ligands in place of the usual tartrate esters. (*R*)-Mandelic acid was found to provide the best conditions for high enantioselectivity, and oxidative conditions of Ti(OiPr)₄:(*R*)-Mandelic acid:CHP (1:2:1 with respect to sulfide **2.60**) gave (*S*)-**2.61** in 74% yield, and 76% ee i.e. higher enantiopurity than the original Ti-tartrate system. The large scale synthesis of **2.59** was performed using the optimized conditions of Ti(OiPr)₄:(*R*)-Mandelic acid:CHP (0.4:0.6:1 equiv), which saw the production sulfoxide (*S*)-**2.61** in 99.7% ee (55% yield) after one recrystallization (Scheme 2.26).



Scheme 2.26

Titanium-Catalyzed S-Oxidations with Optically Active Peroxides

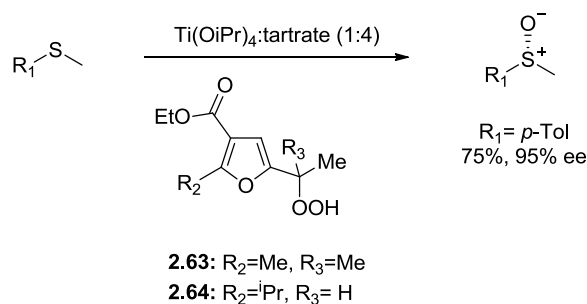
Although the majority of research on Ti-mediated synthesis of optically active sulfoxides has focused on the chiral ligand used, a number of groups have published work investigating the use of chiral peroxides in partnership with $\text{Ti}(\text{O}^i\text{Pr})_4$. Adams *et al.* reported the Ti-catalyzed asymmetric oxidation of alkyl aryl sulfides by optically active hydroperoxide **2.62** (> 99% ee).⁴⁰⁸ The oxygen transfer to methyl *p*-tolyl sulfide, from **(S)**-1-phenylethyl hydroperoxide **(S)-2.62**, gave sulfoxide **1.48** (74% ee) but with much overoxidation to the corresponding sulfone (Scheme 2.27); mechanistic studies showed that enantioselectivity arose from a combination of asymmetric induction in the oxidation and a kinetic resolution of the sulfoxide. Oxidation of further *p*-tolyl sulfides afforded sulfoxides in high ee (up to 80% ee) but once again higher optical purities came at the expense of greater sulfone production.



Scheme 2.27

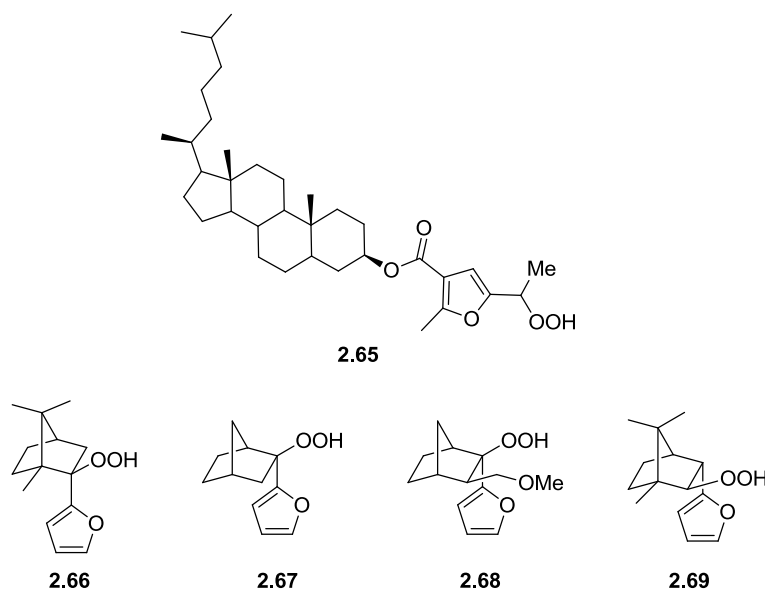
Lanttanzi, Scretti, and coworkers investigated the employment of furyl hydroperoxides as oxidants, gaining access to chiral sulfoxides through a modified Modena procedure.^{353, 409-417} Methyl aryl- and methyl alkyl-sulfides underwent asymmetric oxidation using tertiary furyl hydroperoxide **1.253** and $\text{Ti}(\text{O}^i\text{Pr})_4$:**(R,R)**-DET (in ratios 1:4 with respect to sulfide substrate), giving **(R)**-sulfoxides in good yields (53-79%) and enantioselectivities (74-91% ee). Secondary furyl hydroperoxides were employed in the oxidation of methyl *p*-tolyl sulfide, with two equiv

of chiral peroxide species **1.254**, and $\text{Ti}(\text{OiPr})_4:(R,R)\text{-DIPT}$ (1:4), giving sulfoxide **1.48** in excellent enantioselectivity (75% yield, 95% ee), with the observation that the asymmetric oxidation involved a kinetic resolution of the racemic hydroperoxide (Scheme 2.28). Kinetic resolution of $(\pm)\text{-1.48}$ using this system provided enantioenriched (*R*)-**1.48** in > 95% ee but only 38% yield.



Scheme 2.28

It was postulated that the attainment of chiral sulfoxides through Ti-catalyzed oxidation with furyl hydroperoxides such as **2.63** and **2.64** was achieved through enantioconvergent oxidation of sulfides and kinetic resolution of the sulfoxides.^{353, 413-416} Similar investigations were carried out using the steroidal peroxide species **2.65**, affording aryl alkyl sulfoxides in moderate to good yield (58-74%), and high optical purity (84-> 95% ee); hydroperoxide **2.65** allowed for reduced reaction times compared to **2.64**, but at the expense of product ee.⁴¹⁵



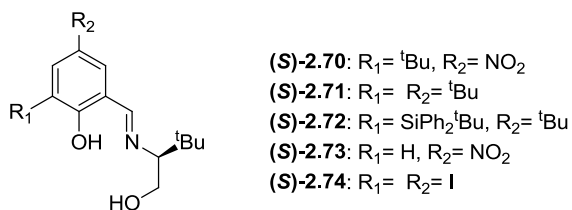
Various enantiopure camphor hydroperoxides (**2.66-2.69**) were synthesized by Lattanzi *et al.* for use in Ti-mediated asymmetric S-oxidation reactions.⁴¹⁸ In these investigations no additional chiral source, such as a tartrate, was deemed necessary; instead it was proposed that

asymmetric induction was brought about by steric interactions between the sulfide substrate and the camphor derived oxidant to result in the preferential formation of one sulfoxide enantiomer. An interesting feature of the work lies in the ability to regenerate the hydroperoxide; as the asymmetric oxidation occurs the peroxides were reduced to alcohols, these could then be recycled back to their corresponding peroxide using H₂O₂. Overall enantioselectivity of the S-oxidations performed using these peroxides in the presence of Ti(OⁱPr)₄ was only moderate; methyl *p*-methoxy-sulfoxide was obtained in 53% ee (yield 31%), representing the highest ee value achieved, with peroxide **2.67** as the oxygen source. Kinetic resolution of racemic sulfoxide (±)-**1.48** using **2.69** afforded enantioenriched (*R*)-**1.48** in only 34% ee and 27% yield. A review by Lattanzi and Scretti, describe these investigations in greater depth.⁴¹⁶

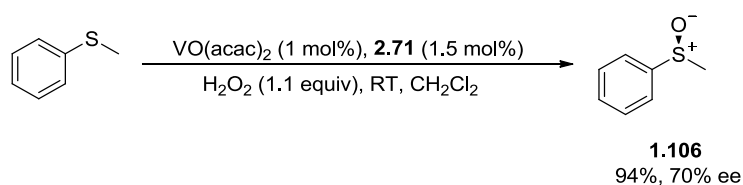
2.2 Vanadium-catalyzed S-oxidations

After titanium, vanadium is one of the most popular metals used in catalyst systems for asymmetric sulfoxidation reactions.⁴¹⁹⁻⁴²² Early investigations by Modena examined the mechanism of sulfide oxidation catalyzed by vanadyl acetylacetonates in the presences of optically active alcohols based solvents.⁴²³ Phenyl methyl- and *p*-tolyl methyl- sulfide were oxidized by TBHP, however asymmetric induction was low, with optical purities no greater than 10% ee achieved.

Vanadium catalyst with Schiff base type ligands have been widely researched and reported in the literature, with great diversity in structure and efficacy.⁴²⁴⁻⁴⁴¹ It is beyond the scope of this thesis to discuss this type of catalyst in great detail, however a general overview shall instead be provided. Imine based ligands **2.70-2.74** were employed by Bolm and coworkers who were the first to report high levels of enantioselectivity for vanadium mediated sulfoxidation reactions.⁴⁴²



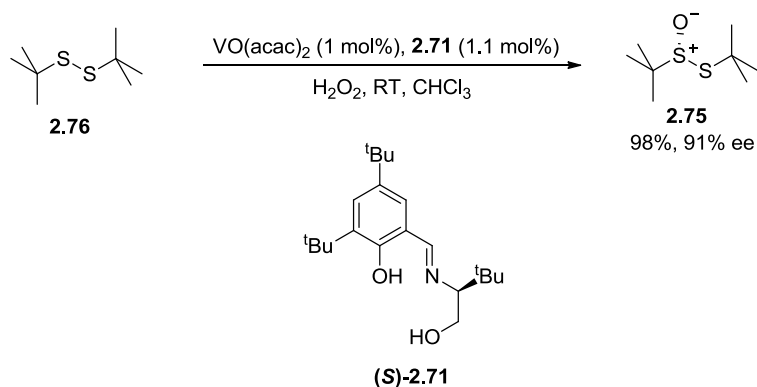
Oxidations were carried out using safe and inexpensive H₂O₂, and the vanadium-Schiff base catalyst system was reported to be simple to use, i.e. room temperature reaction conditions with exclusion of air and humidity unnecessary. The catalyst system was found to be highly efficient at concentrations as low as 0.01 mol% of the complex. Methyl phenyl sulfoxide **1.106** was obtained in 94% yield with 70% ee when ligand **2.71** was employed (Scheme 2.29).



Scheme 2.29

Very little over oxidation of sulfoxides to the sulfone products was observed suggesting the high enantioselectivities were as a result of the asymmetric oxidation process alone, without any associated kinetic resolution. Bolm *et al.* subsequently applied their methodology to the enantioselective oxidations of dithioacetals and dithioketals to give the corresponding monosulfoxides with ee values up to 85%.⁴⁴³

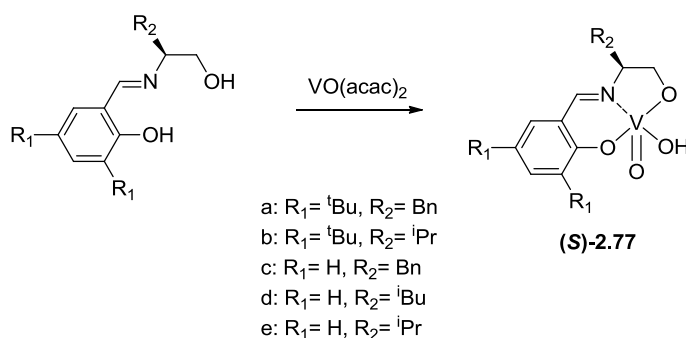
Ellman and coworkers employed the Bolm catalyst system for the preparation of synthetic intermediate **2.75** by way of the asymmetric oxidation of ^tbutyl disulfide **2.76**.⁴⁴⁴⁻⁴⁴⁶ Thiosulfinate **2.75** was achieved in excellent yield and enantioselectivity (98%, 91% ee) (Scheme 2.30). Subsequent optimization of this process allowed the reaction to be carried out successfully on a kilogram scale with only minor loss of enantioselectivity (86% ee).⁴⁴⁷



Scheme 2.30

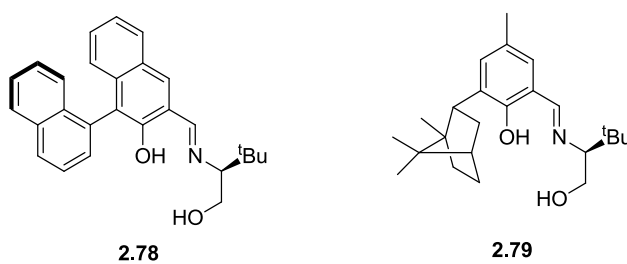
A tandem catalytic approach was used by Jackson *et al.* after examining asymmetric oxidations and kinetic resolutions using the 3,5-diido ligand (*S*)-**2.74**.⁴⁴⁸ (*R*)-methyl *p*-tolyl was obtained in 41% yield (out of a possible 50%) and 98% ee from kinetic resolution of the racemic sulfoxide carried out in chloroform at 0 °C; these conditions were subsequently used for asymmetric oxidations on a range of alkyl aryl sulfides. Enantioselectivities of up to > 99.5% ee were achieved, with the corresponding sulfones observed indicating that some kinetic resolution had taken place in addition to the oxidation process. Similar studies were carried out by Maguire and coworkers in the oxidation and kinetic resolution of benzyl aryl

sulfoxides, also using the 3,5-diido ligand (*S*)-**2.74**.^{449, 450} Zeng *et al.* reported their use of preformed chiral vanadium-Schiff base complexes **2.77 a-e**, and their application in asymmetric oxidation and accompanying kinetic resolution.^{430, 431} Enantioselectivities of up to 99% were achieved in the oxidation of methyl phenyl sulfide.

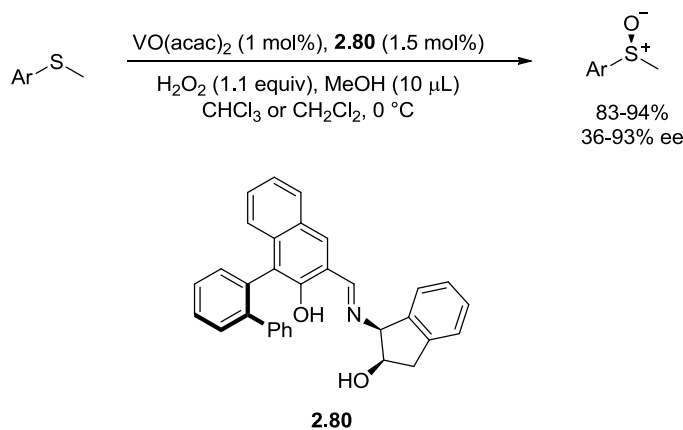


Scheme 2.31

Berkessel and Vetter examined a number of diastereomeric Schiff base ligands in order to determine the optimal conditions for the enantioselective oxidation of thioanisole and *o*-bromothioanisole.⁴⁵¹ Reactions were performed using a ratio of 1:1.5:100:110 of VO(acac)₂:ligand:substrate:H₂O₂. Using ligand **2.78**, methyl phenyl sulfoxide was obtained in 92% yield and 78% ee; ligand **2.79** afforded the same sulfoxide in similar yield (91%) but with slightly lower enantioselectivity (70% ee). The oxidation of *o*-bromothioanisole, when carried out using ligand **2.79**, afforded the corresponding sulfoxide in 78% ee and 97% yield.

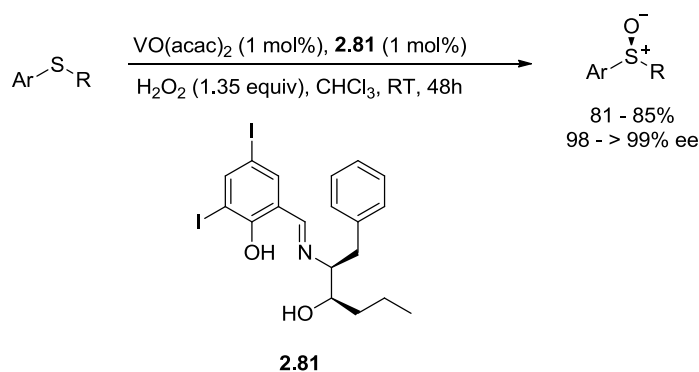


Katsuki *et al.* developed the ligand **2.80** for use in vanadium based enantioselective sulfoxidation. Oxidations carried out on a range of alkyl aryl sulfides using the chiral vanadium complex prepared *in situ* from VO(acac)₂ and ligand **2.80** afforded sulfoxides in high yields and moderate to high optical purities (Scheme 2.32). A small amount of methanol added to the reaction flask was found to be advantageous in regards to improving the enantioselectivity of the reaction due to the positive effect on the equilibration between peroxovanadium species.



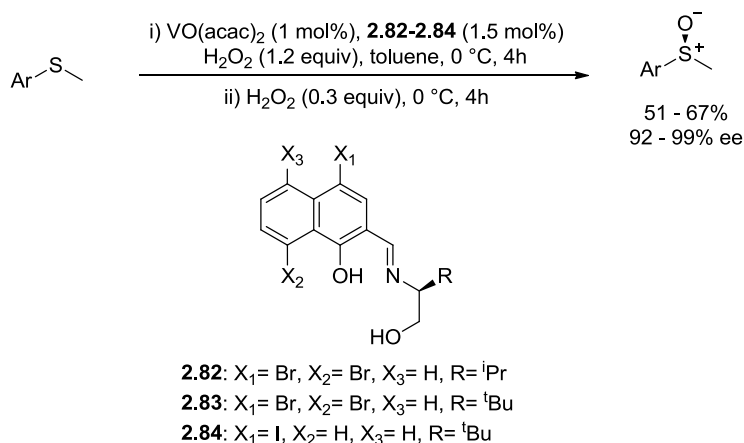
Scheme 2.32

Li *et al.* achieved excellent results from the asymmetric oxidations catalyzed by the vanadium-Schiff base complex featuring the diastereomeric ligand **2.81**, derived from a β -amino alcohol. High yields and exceptional enantioselectivity was observed for enantioselective synthesis of alkyl aryl sulfoxides (Scheme 2.33).



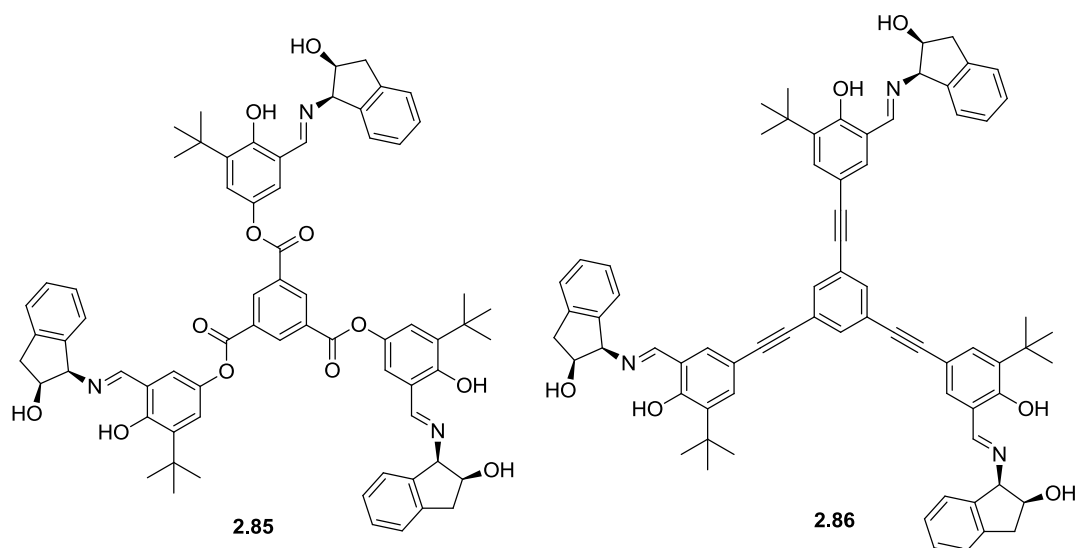
Scheme 2.33

High levels of asymmetric were also observed in the sulfoxide products reported by Wang *et al.* who disclosed the use of chiral Schiff bases derived from halogen functionalized hydroxynaphthaldehydes. A two step procedure was developed whereby an initial oxidation step was followed by further addition of oxidant to promoted oxidation of any remaining sulfide, and to effect kinetic resolution of the sulfoxide already formed. Ligand **2.82-2.84** were found to be the most effective, with enantioselectivities of 92 - 99% ee achieved, albeit with moderate yields (51-67%) (Scheme 2.34).



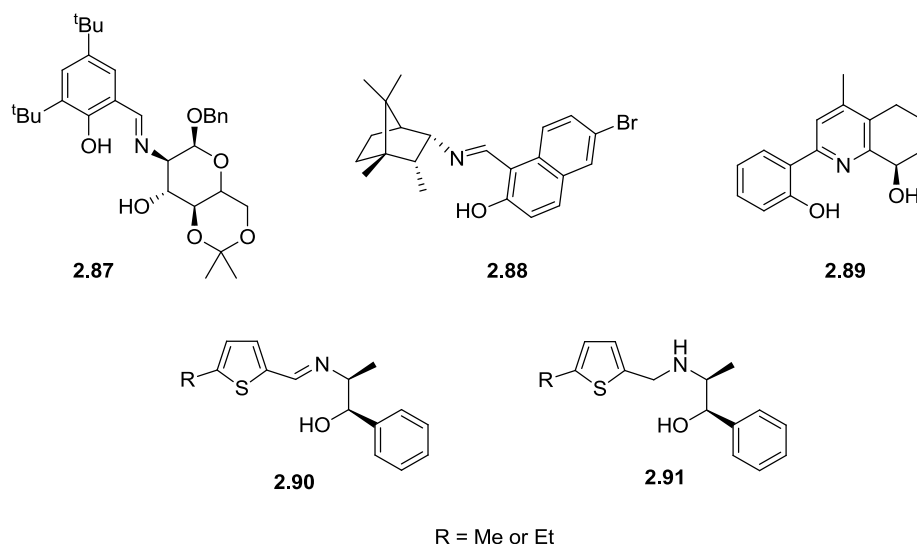
Scheme 2.34

Suresh *et al.* synthesized a series of trimeric variants of well known chiral vanadium-Schiff base catalysts. Examination of the catalytic activity showed that the C₃-symmetric ligands **2.85** and **2.86**, featuring a (1*R*,2*S*)-aminoindanol type Schiff base, were most effective in terms of activity and asymmetric induction.⁴⁵² The use of complexes formed *in situ* from **2.85** and VO(acac)₂ for asymmetric oxidation of various alkyl aryl and benzyl aryl sulfide afforded sulfoxides in moderate to high ee and high yields (54-86% ee and 82-98% yield). Ligand **2.86** performed equally well, affording sulfoxides in yields ranging from 81-94% with enantioselectivities between 67- 89% ee.



Ruffo and coworkers examined a series of Schiff bases with carbohydrate structures in vanadium mediated asymmetric sulfoxidation reactions.⁴⁵³ The catalyst system featuring ligand **2.87** was found to be the most efficacious in the oxidation of methyl phenyl sulfide, affording the corresponding sulfoxide in high yield (97%) but only modest enantioselectivity (60% ee). Chuo and coworkers examined twenty substitutionally and electronically diverse (1*R*)-camphor

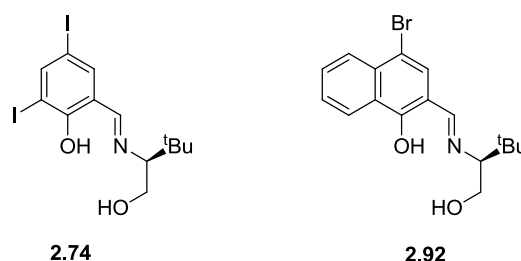
based Schiff base ligands; the vanadium complex with ligand **2.88** performed exceptionally well in the oxidation of ethyl 2-naphthyl sulfide at catalyst loadings of 1 mol%, affording the sulfoxide in excellent enantioselectivity and in good yield (> 99% ee, 72% yield).⁴⁵⁴ Various alkyl aryl sulfoxides were produced in high ee and good yields (85-97% ee, 60-74% yield) with the high levels of enantioselectivity attributed to a combination of asymmetric oxidation and subsequent kinetic resolution of the afforded sulfoxide.



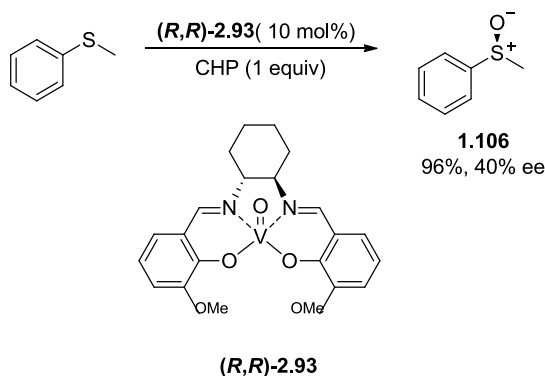
Liu *et al.* reported the synthesis and application of a rigid tetrahydroquinoline ligand **2.89**; asymmetric oxidations catalyzed by vanadium complexes featuring Liu gave sulfoxides in good to high yield (80-95%), with enantioselectivities up to 77% ee.⁴⁵⁵ Chiral norephedrine based β -amino alcohol based ligands were employed by Aydin.⁴⁵⁶ Schiff bases **2.90** and their reduced counterparts **2.91** were examined in vanadium mediated sulfide oxidations alongside their respective epimers. Sulfoxides were afforded with high optical purities (92-99% ee) in moderate to high yields (60-89%), with the observation that the reduced Schiff base ligands **2.91** gave sulfoxides lower enantioselectivities than ligand **2.90**.

Vanadium Schiff base complexes immobilized on mesoporous materials have been reported, although asymmetric induction for sulfoxidation reactions have generally been low (< 31% ee).^{440, 457} Barbarini *et al.* investigated polymer supported chiral Schiff base ligands, and reported sulfoxidation enantioselectivities of up to 61% ee. The most successful solid supported Schiff base ligands were developed by Jackson and coworkers.^{458, 459} Although initial studies from this group reported low enantioselectivities for sulfoxidation (11% ee being the highest), subsequent work focused on the rapid generation of libraries of simple chiral Schiff bases

mounted on Merrifield solid support resins. Ligand **2.74** and **2.92** were identified as the most effective, with optical purities of up to 97% ee achieved over a range of sulfoxides.

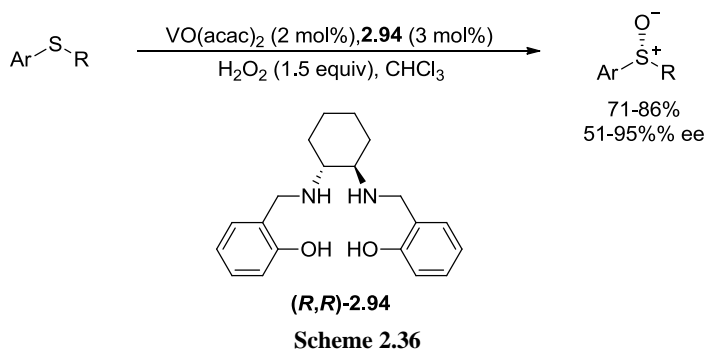


Salen type ligand have also been successfully applies in vanadium mediated sulfide oxidations. Fujita and coworkers were early pioneers of vanadium catalysts for sulfoxidation; (*R,R*)-**2.93** was used to catalyze the oxidation of methyl phenyl sulfide using a catalyst loading of 10 mol%, the corresponding sulfoxide was afforded in high yield (96%) but with only moderate enantioselectivity (40% ee) (Scheme 2.35). Subsequent studies by Fujita and coworkers examined oxovanadium(V) complexes with Schiff bases, derived from L-amino acids and salicylaldehyde, however the enantioselectivity of these catalyst systems were poor, providing sulfoxide with optical purities of up to a maximum of 14% ee.



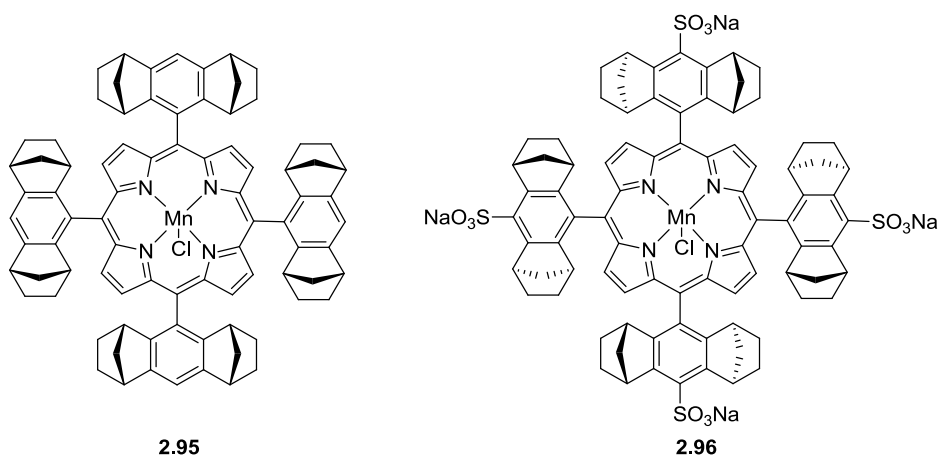
Scheme 2.35

High sulfoxide enantioselectivities were reported by Sun *et al.* with the use of vanadium-salen complex formed in situ from VO(acac)₂ and ligand **2.94**.¹⁵² Oxidation of a range of alkyl aryl and benzyl aryl sulfides afforded sulfoxides in high yields (71-86%) and moderate to high enantioselectivities (51-95% ee) (Scheme 2.36). Kinetic resolutions of a range of racemic sulfoxides using this catalyst system gave enantiomerically enriched sulfoxides with enantioselectivities ranging from 78-98% ee.

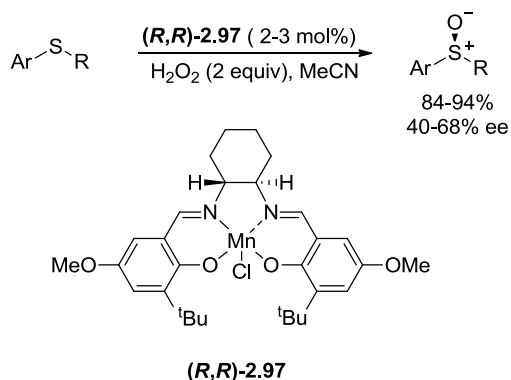


2.3 Manganese-catalyzed S-oxidations

One of the earliest reports of a manganese based catalyst for use in asymmetric sulfoxidation reactions came from Halterman *et al.* who carried out sulfide oxidations in the presence of the D_4 -symmetrical manganese-tetraphenylporphyrin complex **2.95**.⁴⁶⁰ Iodosylbenzene was employed as the oxidant, and with the use of a 0.25 mol% catalyst loading (with respect to sulfide) a range of sulfoxides were obtained in modest enantioselectivity (40-68% ee). Simmonneaux and coworkers used a similar manganese complex in their investigations into asymmetric sulfide oxidations using hydrogen peroxide, with sulfoxidation enantioselectivities of up to 80% ee achieved.⁴⁶¹ Complex **2.96** was employed in the enantioselective synthesis of Sulindac **1.3**, affording the target molecule in low ee (27% ee).

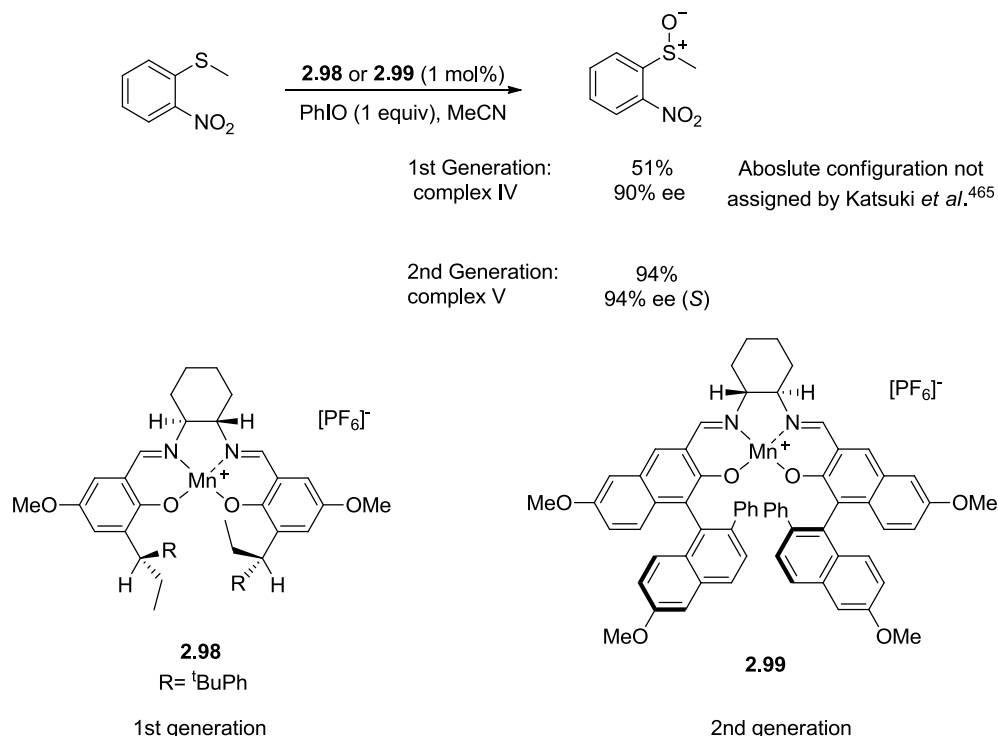


Jacobsen and coworkers reported their work on enantioselective sulfide oxidations, using chiral (salen)Mn(III)Cl complexes.⁴⁶² (**R,R**)-**2.97**, and its epimer were used in the production of a range of optically active sulfoxides with modest ee (up to 68% ee) in high yields (80-95%) (Scheme 2.37).



Scheme 2.37

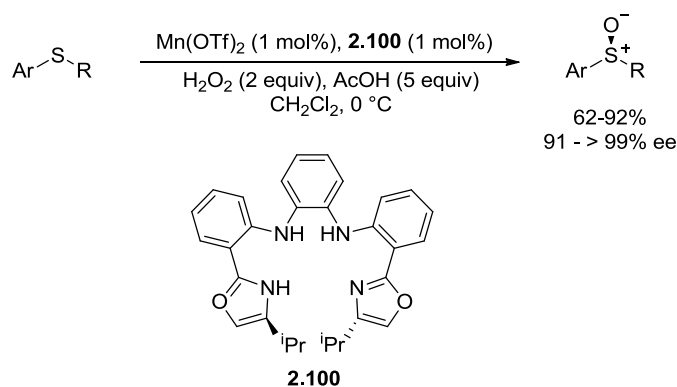
Katsuki *et al.* had greater success with their (salen)Mn(III)Cl complexes, with complex **2.98** affording methyl aryl sulfoxides with up to 90% ee and yields up to 76%.⁴⁶³⁻⁴⁶⁵ Subsequent work within the Katsuki group saw the development of the second generation Mn(salen) complex **2.99**, which exhibited improved enantioselectivity over complex **2.98** whilst retaining efficiency (Scheme 2.38). Sulfoxides with generally high optical purities (up to 96% ee) and good to high yields (up to 98%) were produced with complex **2.99**, using PhIO as the oxidant.^{466, 467} Performing the oxidations in the presence of 4-phenylpyridine *N*-oxide (4-PPNO) was found to increase enantioselectivity in a number of cases.



Scheme 2.38

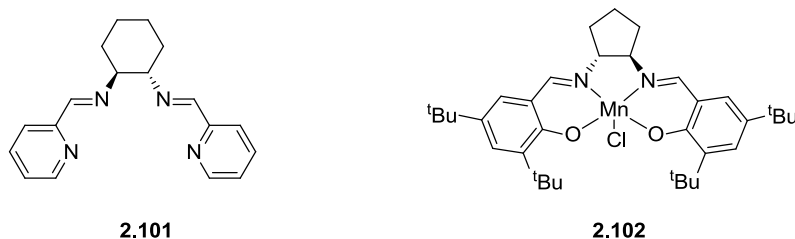
Dai *et al.* have used a porphyrin-inspired complex, formed *in situ* from Mn(OTf)₂ and ligand **2.100**, to catalyze a wide variety of sulfides oxidations by hydrogen peroxide. Optically active

alkyl aryl sulfoxides were produced in high yields (up to 92%) with excellent enantioselectivity (91 to > 99% ee) (Scheme 2.39).⁴⁶⁸ Further work has continued the development of this catalyst system, including recent adaptation for use under continuous-flow microreactor conditions, which enabled the direct scaling of enantioselective sulfoxidation reactions to a multi-gram scale, with the desired sulfoxide product afforded within 20 minutes.^{469, 470}

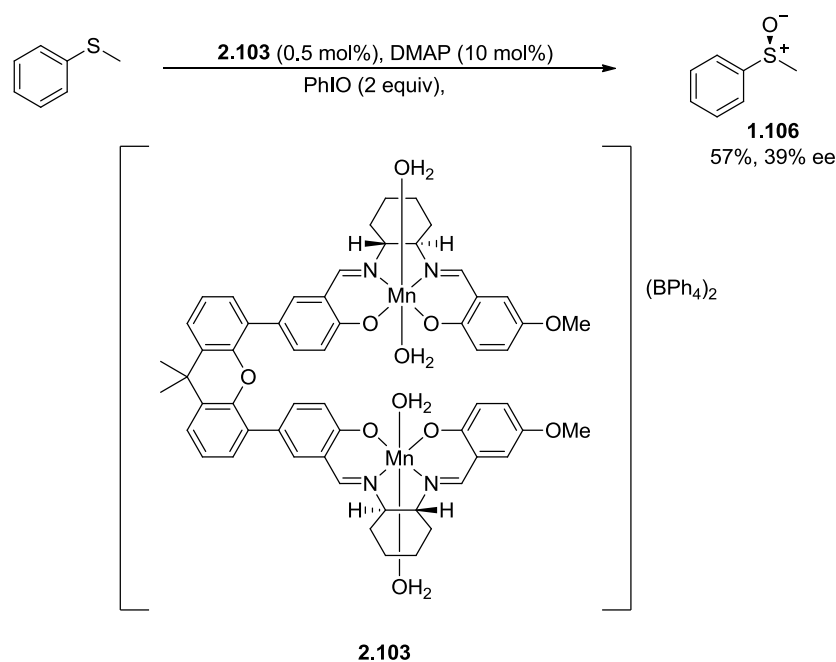


Scheme 2.39

Schoumacker *et al.* isolated a number of manganese(II) complexes from solutions of $\text{Mn}(\text{ClO}_4)_2$ or $\text{Mn}(\text{acac})_2$ and ligand **2.101** and evaluated their efficacy as catalyst in the oxidation of prochiral sulfides.⁴⁷¹ The alkyl aryl sulfoxides afforded from oxidation carried out in the presence of $[\text{Mn}(\mathbf{2.101})(\text{ClO}_4)_2]$ were found to have low optical purity (5-12% ee) with the (*S*)-enantiomer in excess. In contrast, when $[\text{Mn}(\mathbf{2.101})(\text{acac})_2]$ was employed (*R*)-sulfoxides were obtained, with moderate enantioselectivities (20-62% ee). Gao and coworkers reported the use of the chiral salen-manganese complexes **2.102** featuring a pyrrolidine backbone.⁴⁷² Optically active sulfoxides were obtained in low to modest ee (3-42% ee).



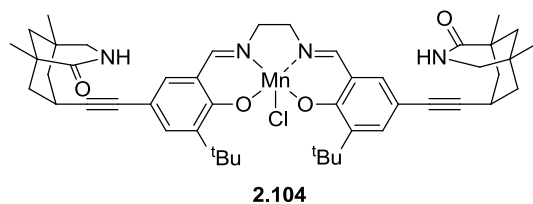
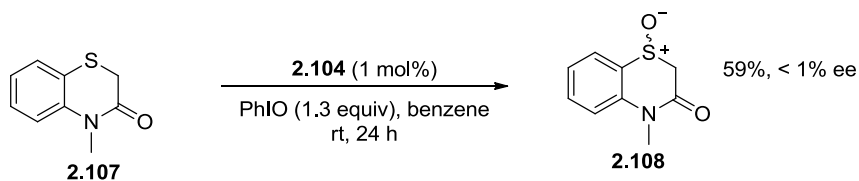
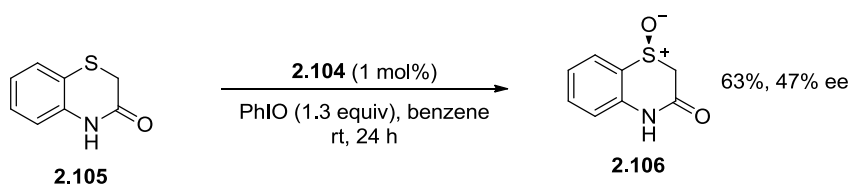
Hirotsu *et al.* prepared dimanganese(III) complexes of salen-type ligands anchored by 9,9-dimethylxanthene-4,5-diyl spacers and evaluated their abilities as catalyst for asymmetric sulfoxidation.⁴⁷³ Complex **2.103** afforded sulfoxides with the best enantioselectivities, ranging from 5-39% ee (Scheme 2.40). Performing the oxidations in the presence of 4-(dimethylamino)pyridine (DMAP) was found to enhance enantioselectivity.



Scheme 2.40

Mukaiyama *et al.* achieved the synthesis of optically active sulfoxides using pivaldehyde in the presence of a chiral β -oxo aldiminatomanganese(III) catalyst complex.^{474, 475} Alkyl aryl sulfoxides were produced in moderate to high yields (44-93%) and modest to good enantioselectivities (24-72% ee). Alcon and coworkers employed manganese complexes with tetradentate C_2 -symmetrical ligands encapsulated in zeolites; sulfoxidation proceeded with low asymmetric induction giving products with up to 27% ee.⁴⁷⁶ Zhang *et al.* used triply immobilized salen ligands for Mn-mediated sulfoxidation, achieving excellent results.⁴⁷⁷ Sulfoxides with enantioselectivities up to 92% ee were obtained.

Enantioselectivity due to hydrogen bonding was explored by Bach *et al.* with their use of a the chiral Mn(salen) complex **2.104**.⁴⁷⁸ The asymmetric oxidation of the sulfide containing lactam **2.105** proceeded smoothly, delivering the corresponding sulfoxide **2.106** with 47% ee, whereas oxidation of the *N*-methylated analogue **2.107** resulted in a racemic sulfoxide **2.108**, supporting the hypothesis of H-bonding driven stereoselectivity (Scheme 2.41). A range of cyclic sulfoxides were obtained using this catalyst system, with yields of 64-91% and enantioselectivities from 13 to 67% ee.



Scheme 2.41

2.4 Iron-catalyzed S-oxidations

In 1990 Groves and Viski reported the use of the chiral vaulted binaphthyl porphyrin **2.109** in a number of different Fe(III)-catalyzed asymmetric transformations, amongst them was the oxidation of prochiral sulfides.⁴⁷⁹ Alkyl aryl sulfoxides were produced via oxidation by iodosylbenzene in the presence of a 0.1 mol% catalyst loading of **2.109**-Fe(III)Cl, with high yields achieved (67-88%) but modest enantioselectivities (14-48% ee).

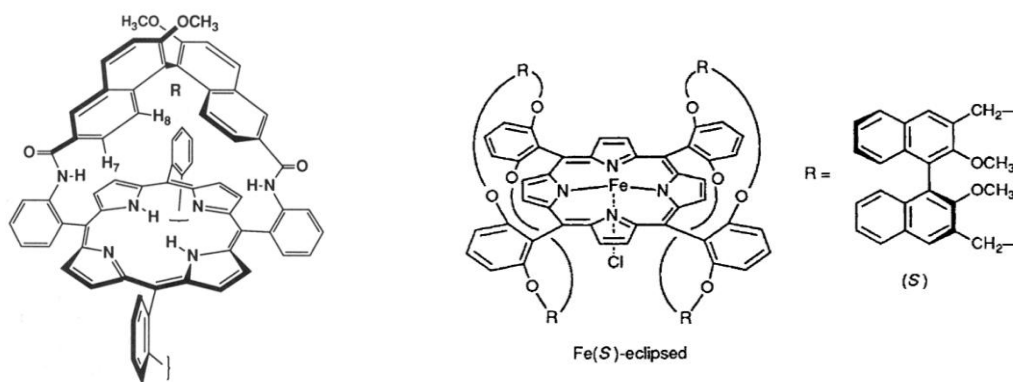
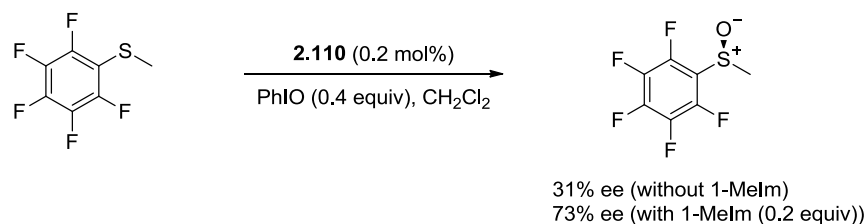


Figure 2.2 Left: Vaulted binaphthyl porphyrin **2.109**; image reproduced with permission from ref.⁴⁷⁹ Centre and right: C₂ symmetric "twin coronet" porphyrin catalyst **2.110**; image reproduced with permission from ref.⁴⁸⁰

Naruta *et al.* also reported modest enantioselectivities when using iron complexes of "twin coronet" porphyrin **2.110** to catalyze asymmetric sulfoxidations. Aryl sulfoxides were achieved in low ee (17-31% ee) (Scheme 2.42), however enantioselectivity was improved by the inclusion of 1-methylimidazole (1-MeIm) in the reaction mixture, which was believed to

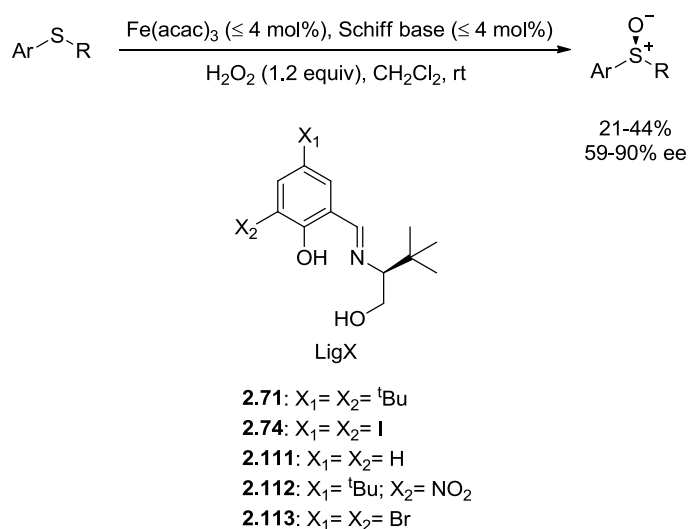
coordinated to the active metal centre and enhance the asymmetric induction by altering the porphyrin structure around iron and prevent catalyst decomposition.^{480, 481}



Scheme 2.42

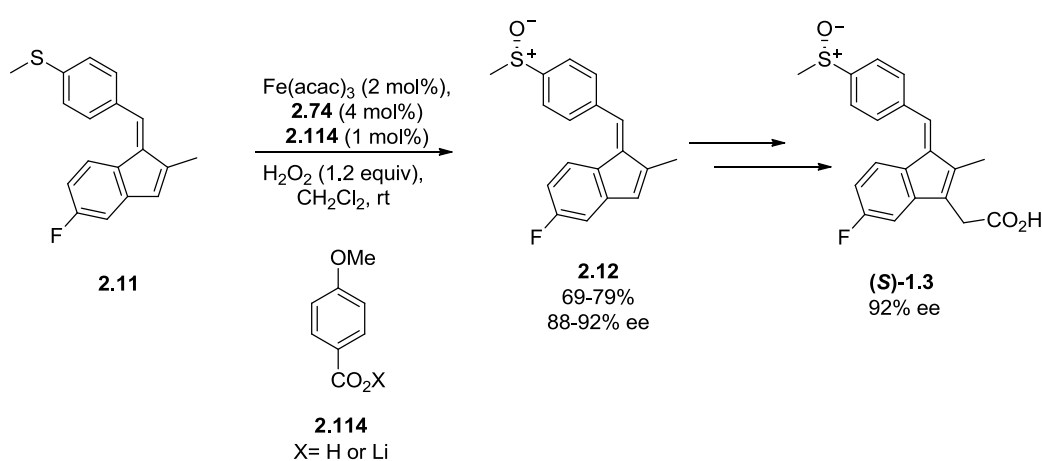
Iron porphyrin catalysts derived from the antipodes of a C₂-chiral 1,4-xylylene-strapped porphyrin were created by Inoue *et al.* and utilized in the asymmetric oxidation of a number of alkyl aryl sulfides.⁴⁸² Enantioselectivity was initially poor, with enantioselectivities between 0-36% obtained, however the addition of imidazole resulted in improved enantiomeric excesses of the afforded sulfoxides (18-71% ee).⁴⁸² Low optical purities (up to 40% ee) were also reported by Fontcave and coworkers following their investigation of sulfide oxidations catalyzed by the iron complex [Fe₂O(pb)₄(H₂O)₂](ClO₄)₄ (pb=(-)-4,5-pinene-2,2'-bipyridine).⁴⁸³

Tsogoeva *et al.* screened a range of iron(III) Schiff base complexes for use as catalyst in hydrogen peroxide oxidations of thioanisole. Results were modest, with enantioselectivities of up to 54% achieved.⁴³⁹ Bolm *et al.* were more successful in their endeavors to develop an iron based catalyst system for asymmetric sulfoxidation reactions.^{484, 485} A 2003 publication demonstrated the use of various iron complexes, formed *in situ* from [Fe(acac)₃] and Schiff bases **2.71**, **2.74**, and **2.111-2.113**, to allow access to optically active sulfoxides with up to 90% ee.⁴⁸⁶ The oxidations were carried out with simple conditions (stirring at RT in a capped vessel), and could be performed in the presence of air and moisture with no effect on enantioselectivity. Initial investigations revealed that ligand **2.113** performed best in the oxidation of thioanisole; expansion of the substrate scope saw oxidation of a number of alkyl aryl sulfoxides achieved in moderate to high ee (59-90% ee) but with only modest yields (21-44%) (Scheme 2.43). Little to no sulfone by product was observed indicating that high enantiopurities were achieved through asymmetric oxidation alone, without any additional kinetic resolution of the sulfoxides.



Scheme 2.43

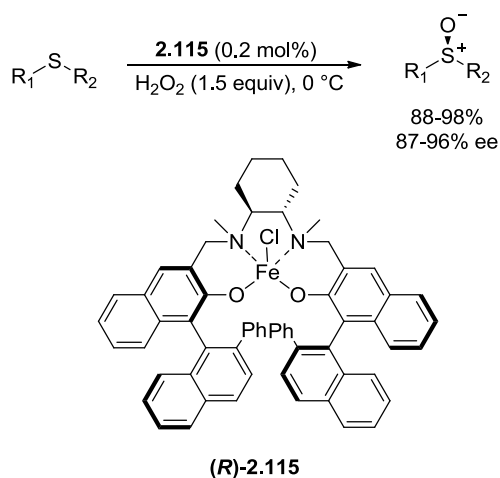
Subsequent work by Bolm and coworkers found that the addition of various carboxylic acids and their derivatives improved yields at no detriment to the enantioselectivity of the oxidations; enantioselectivities of up to 96% ee were reported, with improved yields (up to 78%).⁴⁸⁷ The asymmetric oxidation of key intermediates in the synthesis of Sulindac **1.3** was published using the Bolm Fe-catalyst system.⁴⁸⁸ Under the original 2003 oxidation protocol published by Bolm, the sulfoxide **2.12** was afforded in moderate enantioselectivity (58% ee, 53% yield); carrying out the oxidation in the presence of 4-methoxybenzoic acid, or its lithium derivative resulted in enhanced enantioselectivity (92% ee) and yield (71 or 69% respectively) (Scheme 2.44).



Scheme 2.44

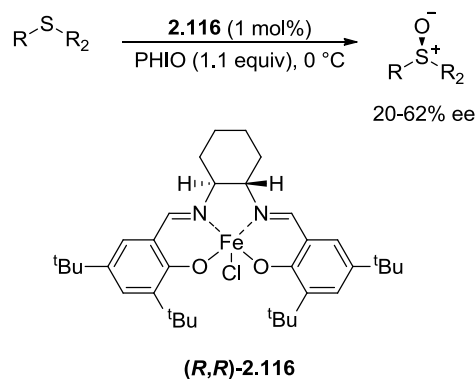
Katsuki and Egami reported a water compatible Fe(salan) catalyst system which carried out asymmetric sulfoxidations with high enantioselectivity and sulfoxide selectivity.^{489, 490} Fe(salan) **2.115** was used in a 0.2 mol % catalyst loading, with aq. H₂O₂ as the oxidant,

affording a range of methyl aryl- and methyl alkyl- sulfoxides in yields of 88-98% and enantiopurities of 87-96% ee (Scheme 2.45).



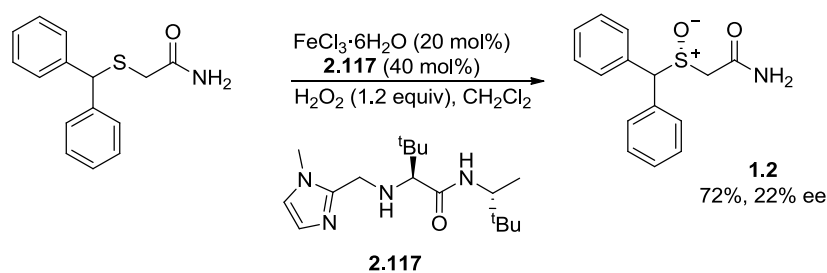
Scheme 2.45

An iodosylbenzene(salen)iron complex was identified by Bryliakov and Talsi as the active intermediate in a (salen)iron(III)-catalyzed asymmetric sulfide oxidation.^{491, 492} Modest enantioselectivities were reported with the use of complex **2.116** for a range of methyl aryl- and phenyl benzyl-sulfoxides (20-62% ee) (Scheme 2.46).



Scheme 2.46

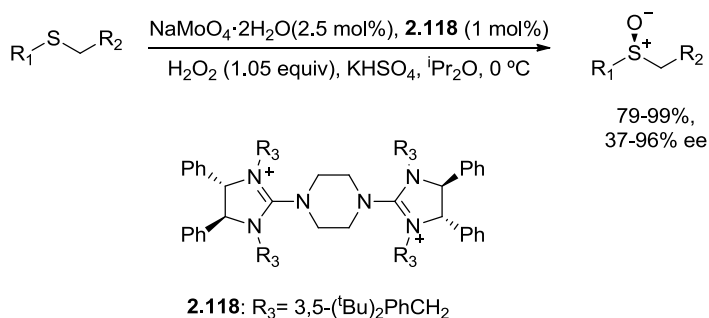
A dipeptide ligand was used as the source of chirality in the Fe-mediated synthesis of (*R*)-Modafinil **1.2** reported by Tsogoeva and coworkers.²⁵⁶ Using a relatively high catalyst loading of 20 mol% the biologically active sulfoxide was obtained in good yield (75%) but with only 22% ee (Scheme 2.47).



Scheme 2.47

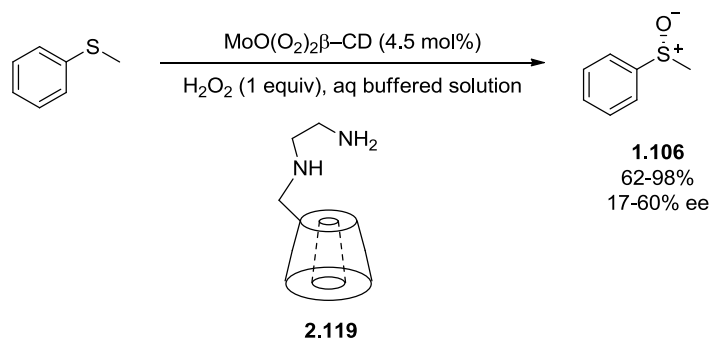
2.5 Molybdenum-catalyzed S-oxidations

Attempts at using molybdenum based catalyst systems with Schiff base type ligands have shown low asymmetric induction for sulfoxidation reactions, with enantioselectivities of < 17% ee reported.^{493, 494} Conversely, Tan and coworkers have produced excellent results employing a chiral bisguanidium dinuclear oxodiperoxomolybdosulfate ion pair catalyst for asymmetric sulfide oxidations.⁴⁹⁵ The ion pair catalyst [**2.118**]²⁺[μ-SO₄)Mo₂O₂(μ-O₂)₂(O₂)₂]²⁻, which was isolatable or generated *in situ*, enabled the production of sulfoxides with a wide range of structural characteristics to be obtained in high yields (79-99%), with ee values of 37-96% ee (Scheme 2.48).



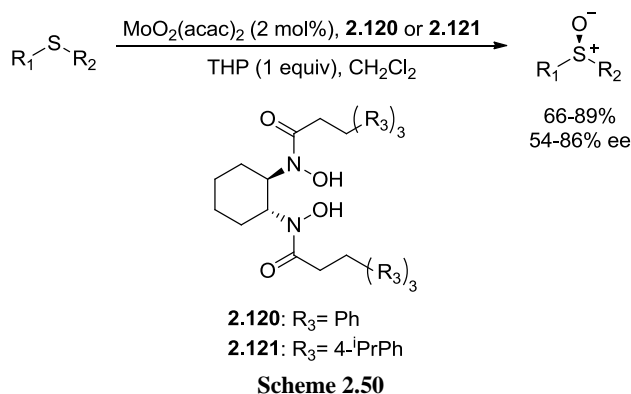
Scheme 2.48

Binchio *et al.* reported the enantioselective oxidation of thioanisole by hydrogen peroxide in the presence of a catalytic amount of Na₂MoO₄ and functionalised β-cyclodextrin (β-CD) based ligands such as **2.119**.⁴⁹⁶ The active oxidant oxodiperoxomolybdenum complex MoO(O₂)₂L (where L = **2.119**) was employed in a 4.5% catalyst loading, affording methyl phenyl sulfoxide in fair to good yields (62-98%) with enantioselectivities in the range of 17-60% ee (Scheme 2.49); no overoxidation to the corresponding sulfone was observed.

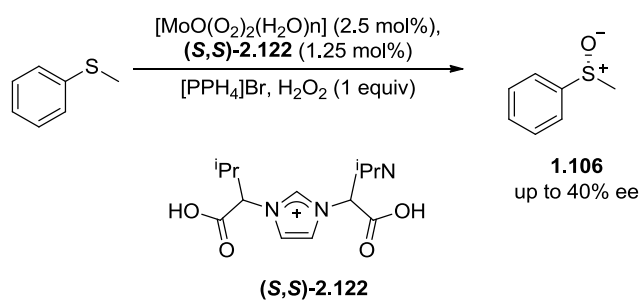


Scheme 2.49

A chiral bis hydroxamic acid (BHA)-molybdenum complex was employed by Yamamoto and coworkers to achieve the oxidation of sulfides and disulfides with yields up to 83% and optical purities of up to 86% ee.^{497, 498} Kinetic resolution of racemic methyl phenyl sulfoxide using BHA ligand **2.121** afforded the (*S*)-sulfoxide with 68-75% ee. A combination of asymmetric oxidation and kinetic resolution of the sulfoxide was performed using 1.5-1.75 equivalents of either CHP or THP giving enhanced enantioselectivity of the produced sulfoxides (92-99% ee) (Scheme 2.50).



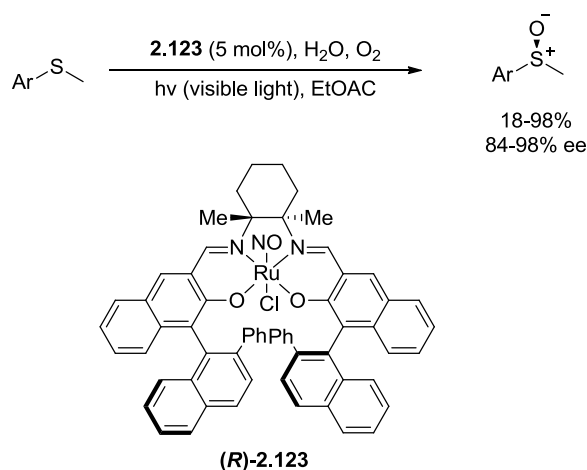
Galindo performed Mo-catalyzed asymmetric oxidations of prochiral sulfides with H_2O_2 in the presence of $[\text{MoO}(\text{O}_2)_2(\text{H}_2\text{O})_n]$ and the chiral imidazolium based carboxylate ligand **2.122**.⁴⁹⁹ Modest enantioselectivity was achieved in the oxidation of thioanisole (up to 42% ee at 93% conversion to sulfoxide) with the use of a 2.5 mol% catalyst loading and 1 equiv of H_2O_2 (Scheme 2.51); when 1.6 equiv of the oxidant was used optical purities up to 83% ee (40% yield) were achieved through concomitant asymmetric oxidation and oxidative kinetic resolution of the sulfoxide.



Scheme 2.51

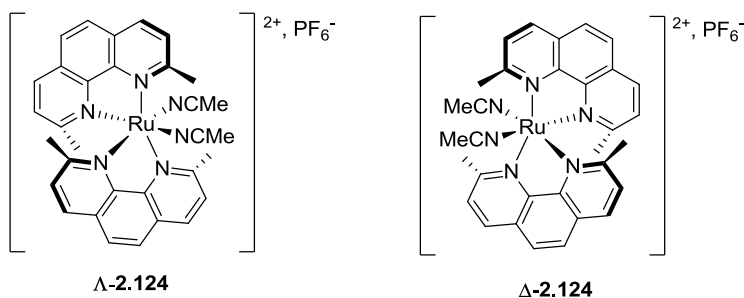
2.6 Ruthenium-catalyzed S-oxidations

Katsuki *et al.* employed the Ru-salen complex **2.123** for the aerobic sulfoxidation of methyl aryl sulfides under visible light irradiation.^{153, 393} Using a 5 mol% catalyst loading excellent enantioselectivities were achieved (84-98% ee), with yields from 18-98% (Scheme 2.52).

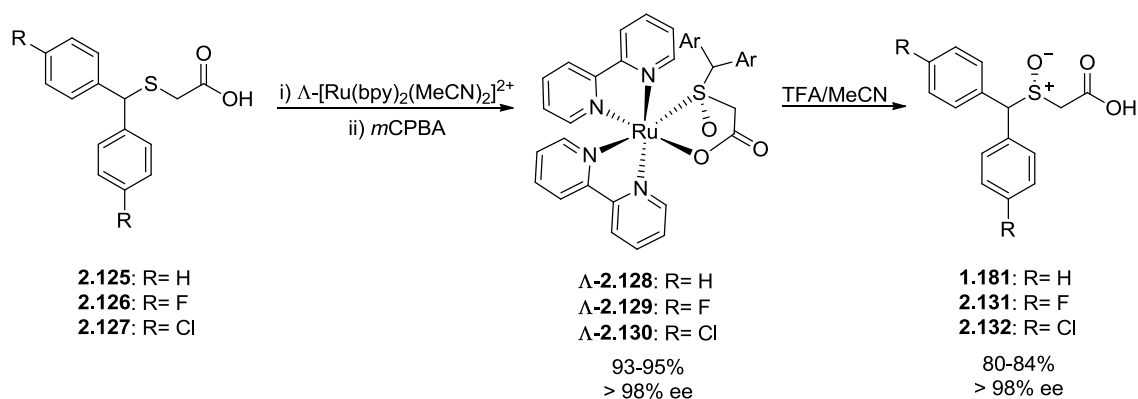


Scheme 2.52

Fontcave *et al.* reported the oxidation of several simple alkyl aryl sulfides using both the Λ - and Δ -enantiomers of the “chiral at metal” complexes *cis*- $[\text{Ru}(\text{dmp})_2(\text{MeCN})_2][\text{PF}_6]_2$ (dmp = 2,9-dimethyl-1,10-phenanthroline) **2.124**.⁵⁰⁰ Enantiomeric excesses of the afforded sulfoxides were poor, with a maximum ee of 18% achieved for methyl *p*-bromophenyl sulfoxide.



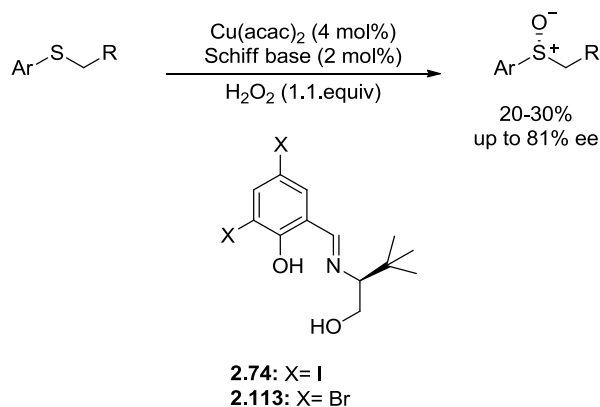
A “chiral at metal” Ru-complex was used by Li *et al.* for the synthesis of enantiopure Modafinil acid **1.181** and its analogues (**2.131** and **2.132**).⁵⁰¹ The use of both enantiomers of the Ru-complex allowed for both enantiomers of chiral Modafinil acids to be obtained in excellent ee (> 98% ee) and high yields (Scheme 2.53).



Scheme 2.53

2.7 Copper-catalyzed S-oxidations

Many attempts at designing an efficient copper based catalyst for asymmetric sulfoxidation reactions have met with little or no success.^{476, 502-505} Reports from the Maguire group however show that they are an exception, with initial studies employing a catalyst complex produced from copper(II)acetylacetonate (acac) and a Schiff base ligand providing sulfoxides with moderate ee (up to 81% ee), albeit in low yields (20-30%) (Scheme 2.54).^{30, 506} These results were in agreement with previous reports of low reactivity of copper towards sulfoxidation, and were indicative of catalyst inhibition, presumably through complexation of the sulfoxide to the metal centre.^{476, 505}

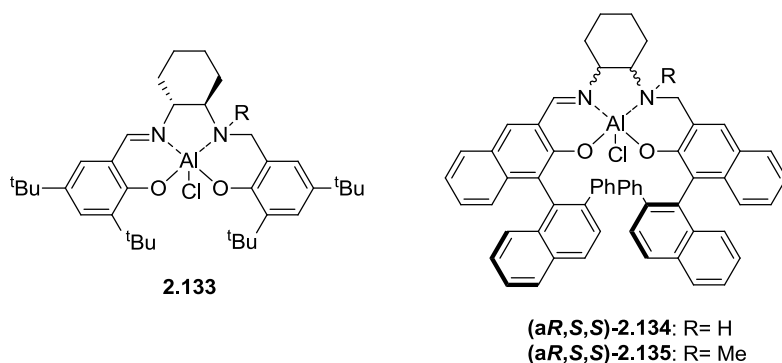


Scheme 2.54

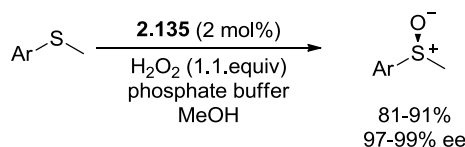
The Cu-mediated oxidation worked best for sterically hindered aryl benzyl sulfides, with little sulfone observed. Oxidations were performed on a number of sulfides with ligand **2.113** in the presence of additives such as dimethyl sulfoxide (DMSO), 4-methylmorpholine-*N*-oxide (NMO) or an ionic liquid which resulted in improvements in both yield and enantioselectivity for nearly all cases. Similar sulfoxidation protocols have been reported by Bolm *et al.* using vanadium or iron Schiff complexes, but interestingly the analogous copper based reactions afford the sulfoxide product with the opposite asymmetric induction. Maguire *et al.* later published work expanding upon their early investigation into Cu-mediated sulfoxidations, demonstrating the optimization of reaction conditions, the result of which gave improved yields whilst retaining good enantioselectivity.⁵⁰⁷ Inhibition of the catalyst by sulfoxide coordination was overcome by the use of a hexane–methanol mix as the solvent. It was determined that substrate steric effects were more significant than electronic effects when it came to the enantioselectivity of sulfide oxidation. In 2013 the group reported the best enantioselectivity so far for a sulfoxide produced using the Maguire catalyst system, 2-naphthyl benzyl sulfoxide was achieved in 97% ee, however the yield was only 32%.⁵⁰⁸

2.8 Aluminium-catalyzed S-oxidations

Katsuki *et al.* reported the development of water compatible aluminium (salalen) catalyst complexes for use in asymmetric sulfide oxidation reactions, with aqueous hydrogen peroxide as the oxidant.^{393, 422, 509, 510} Oxidation of thioanisole in the presence of Al(salalen) complex **2.133** was only moderately selective, poorly reproducible and afforded methyl phenyl sulfoxide in enantioselectivities ranging from 20-60% ee (40-60% yield). In contrast, complexes **2.134** and **2.135**, containing a binol based salalen ligand, performed better, with much higher levels of asymmetric induction and selectivity for sulfoxide production.



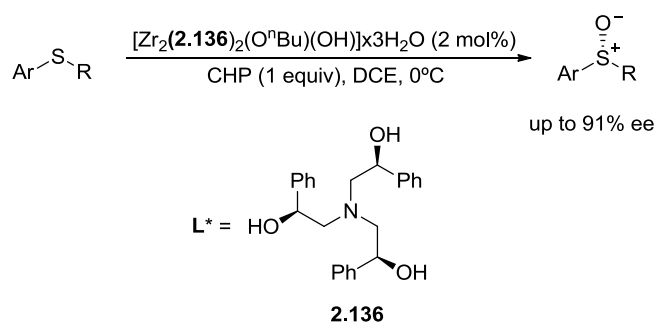
Using complex **2.135** (2 mol%) in MeOH, in the presence of a phosphate buffer, various alkyl aryl sulfoxide were obtained with excellent enantioselectivity and yield (97-99% ee, 81-91%) (Scheme 2.55). Oxidation of racemic methyl phenyl sulfoxide revealed that the (*R*)-enantiomer was preferentially oxidized to the sulfoxide, and it was concluded that a synergistic kinetic resolution process accompanied an initial asymmetric oxidation to allow the sulfoxide products to be obtained in such high optical purities.



2.9 Zirconium-catalyzed S-oxidations

In 1999 Modena and coworkers reported the use of polydentate ligand **2.136** in both Ti(IV)- and Zr(IV)- catalyst systems for asymmetric sulfoxidation using alkyl hydroperoxides.^{397, 402, 511} While the titanium based system was reported to be an effective catalyst with regard to high turnover numbers (1-2 mol% catalyst loading) and enantiomeric excesses of afforded sulfoxides in the range of 40-84% ee, it was reported that a partially hydrolyzed zirconium catalyst bearing the ligand **2.136** could perform equally well, if not better. Stereoselective sulfoxidations performed using the Zr-based system with low catalyst loadings (2 mol %) gave high enantioselectivity (80-91% ee), with the product sulfoxides afforded with opposite absolute configurations to those if the Ti-system had been used (Scheme 2.56). In addition, sulfinyl compounds with poor steric differentiation between substituents flanking sulfur, such as benzyl-, ^tbutyl-, ⁿbutyl-, or ⁱpropyl aryl sulfoxides, could be obtained with high enantioselectivities. One of the limitations of the Zr-based catalysis was high production of the over-oxidized to the sulfone products, which indicated that a second oxidative process was

occurring and that high ee values were as a result of both the asymmetric oxidation and a kinetic resolution, both leading to high amounts of the same sulfoxide enantiomer, albeit in low yield.

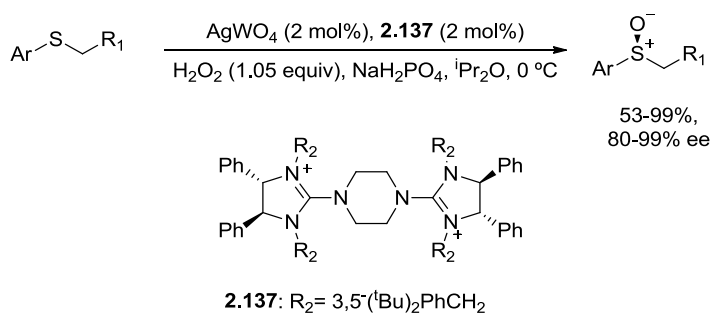


Scheme 2.56

2.10 Tungsten-catalyzed S-oxidations

Tan *et al.* reported a highly efficient system for enantioselective sulfoxidations using a catalytic amount of silver tungstate in the presence of a chiral dicationic bisguanidinium **2.137**.³⁶⁵

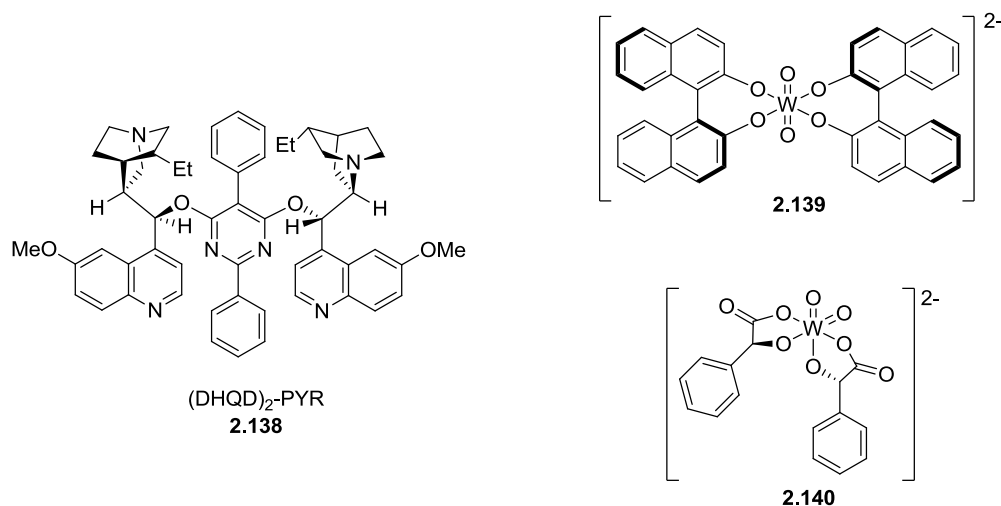
Using this system benzimidazole benzyl sulfoxide was obtained with 88% ee, in a yield of 83%; a number of other heterocyclic systems, such as benzothiazole, pyridine, and thiophene sulfoxides were produced, alongside various phenyl sulfoxides, in yields of 53-99% and high to excellent optical purities (80-99% ee) (Scheme 2.57).



Scheme 2.57

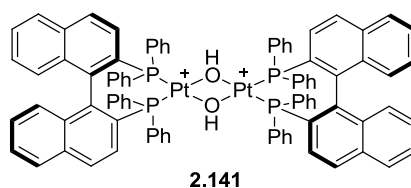
Thankur and Sudalai reported the application of a heterogeneous catalyst system based on WO_3 (5 mol%) and various chiral cinchona alkaloids (10 mol%), such as hydroquinidine-2,5-diphenyl-4,6-pyrimidinediyl diether [(DHQD)₂-PYR] **2.138**, in the asymmetric oxidation of aryl alkyl sulfides. Using 30% H_2O_2 (1.1 equiv) as the oxidant sulfoxides were isolated in good yields (62-90%) with up to 65% ee, representing the first successful application of a tungsten-catalyzed sulfoxidation system.⁵¹² WO_3 could be recovered and reused up to five times with no ill effect upon conversion and enantioselectivity of sulfoxide production. WO_3 -catalyzed kinetic resolutions of various racemic sulfoxides was also reported using (DHQD)₂-PYR **2.138**

as the ligand, affording optically active sulfoxides with 44-90% ee in yields between 25-44% along with the corresponding sulfones. Other tungsten based sulfoxidation processes have been reported, such as the ionic liquid-based system comprised of chiral anions **2.139** and **2.140**.⁵¹³



2.11 Platinum-catalyzed S-oxidations

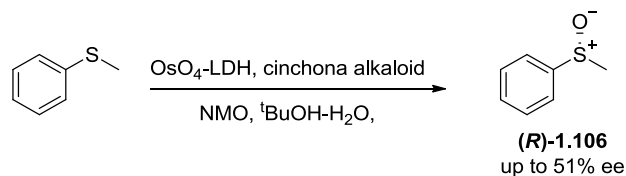
The stereoselective oxidation of prochiral aryl alkyl sulfides mediated by a chiral platinum diphosphine complex **2.141** was reported in 2005 by Scarso and Strukul.⁵¹⁴ A dimeric platinum complex $[(R)\text{-BINAP}]\text{Pt}(\mu\text{-OH})_2(\text{BF}_4)_3$ was used with low loading (1 mol%) at room temperature to activate 35% H_2O_2 towards sulfides in a water-surfactant solution. This system was reported to be the first to carry out an asymmetric catalytic oxidation performed in water. Chiral sulfoxides were afforded with optical purities ranging from moderate to good (22-88% ee), in good to high yields (63-99%) and with highly favourable sulfoxide/sulfone selectivity.



2.12 Osmium-catalyzed S-oxidations

An osmium catalyst supported on layered double hydroxides (LDH) was reported by Kantam *et al.*⁵¹⁵ Oxidations performed on methyl phenyl sulfide using *N*-methylmorpholine *N*-oxide (NMO) co-oxidant and a cinchona alkaloid as a chiral ligand afforded the sulfoxide **1.106** in good yields with moderate enantioselectivities (up to 51% ee) (Scheme 2.58). These oxidations

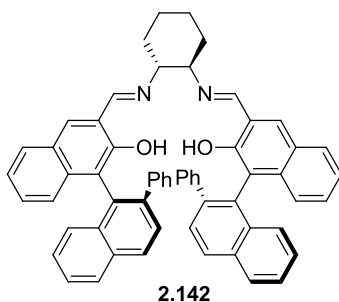
were performed using a catalyst loading of 1% and osmium:ligand ratios from 1:1 to 1:10. When (*R,R*)-diisopropyl tartrate and (*R,R*)-DET were employed as chiral ligand enantioselectivity was low (24% and 26% ee respectively). The authors included discussions on the effects of solvent, and the reusability of the LDH-OsO₄ catalyst which showed that although recovery of the catalyst was possible, it did not perform well when reused.



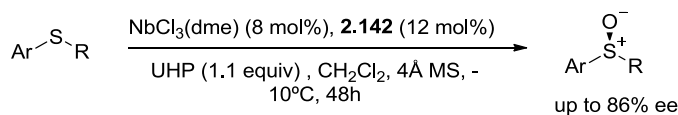
Scheme 2.58

2.13 Niobium-catalyzed S-oxidations

Katsuki and Miyazaki reported a niobium(salen) complex that was found to be an effective catalyst for sulfoxidation of various sulfides using urea-hydrogen peroxide (UHP) as the oxidant.³³⁹ The catalyst complex was created from niobium chloride dimethoxyethane (dme) [NbCl₃(dme)] and salen **2.142** which, following screening of a range of salen ligands and a Schiff base, was found to produce the greatest asymmetric induction during the oxidation of thioanisole. A 1:1 ratio of NbCl₃(dme):salen ligand was employed and using a catalyst loading of 5 mol% methyl phenyl sulfoxide **1.106** was afforded in 59% yield, with 68% ee.



Investigations of reaction time and temperature were discussed by the authors, as was the effect of the NbCl₃(dme):salen ratio on the optical purity of the afforded sulfoxides. Optimized catalyst conditions were then employed in the asymmetric oxidation of various sulfides, with the respective sulfoxides produced in good to high yields (58-94%), and with high optical purities (77-86% ee) (Scheme 2.59).

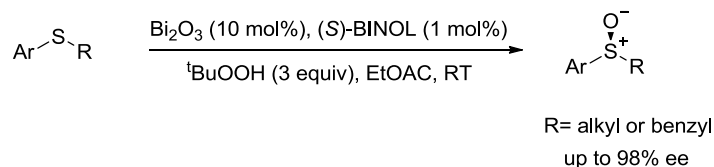


Scheme 2.59

Bolm and coworkers also investigate the use of niobium in a catalyst system for asymmetric sulfoxidation.³¹⁰ During investigation of vanadium based catalysts the oxidation of thioanisole was carried out with an analogous niobium based system, however, despite high yield (86%), poor enantioselectivity was observed (7% ee).

2.14 Bismuth-catalyzed S-oxidations

In 2012 the first asymmetric oxidation of sulfides by a bismuth based catalyst system was reported by Chakraborty and Malik.⁵¹⁶ Initial trials saw a range of Bi(III) compounds, such as Bi₂O₃, Bi(NO₃)₃·5H₂O, BiCl₃ and BiBr₃, screened for catalytic activity towards oxidation of sulfides by TBHP (70% in water, 3 equiv). The most efficacious catalyst in terms of sulfide to sulfoxide conversion was found to be Bi₂O₃ used in a loading of 10 mol%. (*S*)-BINOL was employed as the chiral ligand (1 mol%) and when the catalyst system was used against a various aryl alkyl- and aryl benzyl- sulfides, the afforded (*S*)-sulfoxides were isolated in both high yields (81-90%) and enantiopurities (78-98% ee) (Scheme 2.60); using this system no overoxidation to the respective sulfones was observed.



Scheme 2.60

2.15 Summary

Asymmetric sulfide oxidation using metal based catalyst is one of the most studied methods for the production of chiral sulfoxides. A number of biologically active sulfoxides such as Esomeprazole (*S*)-**1.1**, Modafinil **1.2**, Sulindac **1.3** have been produced in single enantiomer forms using this method.

One of the great advantages of this method is the versatility and range of catalyst systems available, with access to both enantiomers of the sulfoxide product made possible by the choice of the chiral ligand and its configuration. Alongside the choice of metal to base the catalyst

system on there is also great potential for modification of a catalyst with the choice of ligand, oxidant, and through the use of additives in the reaction mixture.

Great progress has been made in the area of metal catalyst sulfide oxidation since the groundbreaking work of Kagan in the 1980s. Titanium based catalyst systems remain one of the most popular choices, whilst Vanadium based catalysts developed by Bolm are also effective however many require a number of steps to produce the Schiff base or salen type ligands. There are limitations however to these methods; the titanium-tartrate catalyst system developed by Kagan suffers from poor catalyst turnover numbers, and so is wasteful when carried out at a larger scale. The use of vanadium catalysts is undesirable as it is believed to be hazardous to the environment.⁵¹⁷

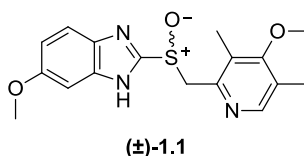
Manganese, aluminium, ruthenium, copper, iron, zirconium, niobium, and bismuth based systems amongst others have been reported as successful catalysts for asymmetric sulfoxidation. In addition to sulfoxidation reactions, numerous examples of oxidative kinetic resolution using metal based catalyst systems have also been discussed.

Future developments in this area are likely to be directed towards more sustainable methods, using environmentally friendly reagents and lower catalyst loadings. This last matter is particularly relevant in the application of Kagan type titanium tartrate catalyst systems; elucidation of the reaction mechanism and a greater understanding of the catalytic process involved would be a significant step towards improving the catalytic turnover and improving the efficiency of the asymmetric sulfoxidation reaction.

3 Introduction: Omeprazole and Esomeprazole

3.1 Omeprazole: A Proton Pump Inhibitor

Since its development in the late 1970s Omeprazole (Losec, Prilosec) (\pm)-**1.1** has become one of the world's best selling drugs, with over 800 million patients treated and peak annual sales exceeding \$6 billion.⁵¹⁸⁻⁵²⁰ The revenue generated from this single drug in 2000 was reported to be greater than the total cash intake from the top five grossing films up to that time (Jurassic Park, Titanic, Independence Day and two *Star Wars* movies), as well as the combined value of all the most well known paintings of the top ten-grossing artists (Picasso, Monet, Renoir, Degas, Cézanne, Chagall, Matisse, Pissaro, van Gogh, and Modigliani).¹⁶



Omeprazole belongs to a class of drugs named proton pump inhibitors (PPIs), which inhibit the molecular engine driving the generation of gastric acid secretion in the stomach.^{521, 522} Acid limiting drugs such as Omeprazole have been called “one of the most important advances in gastroenterology” and are part of the core treatments for the safe and effective management of gastric acid related diseases and injuries such as esophagitis, gastroesophageal reflux disease (GERD), peptic ulcer disease (PUD), and Zollinger-Ellison syndrome.⁵²³⁻⁵²⁵ Additional uses include prevention of non-steroidal anti-inflammatory drugs (NSAID) associated ulcers, and in combination with antibiotics are an integral part of eradication therapy for *Helicobacter pylori*.^{526, 527} Heartburn and acid reflux are the most common minor symptoms treatable by administration of drugs such as Omeprazole, with 25-40% of the population in industrialized countries reporting these symptoms weekly.^{528, 529} PPIs have had a dramatic impact on the occurrence of life threatening conditions, such as perforated ulcers, and have allowed management of gastric disease to change from a largely surgical path, to one that is now treatable by a family physician or GP.^{530, 531}

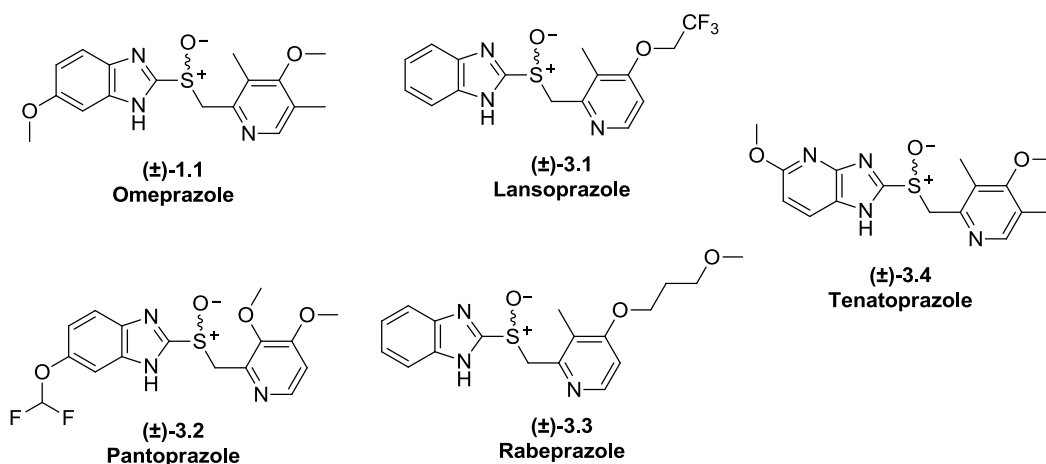
Omeprazole has an excellent safety profile and is prescribed to women during pregnancy and those breastfeeding, as well as infants under one, and children.^{532, 533} It is also on the WHO essential medicines lists for both adults and children.⁵³⁴ Given the extent to which Omeprazole has been prescribed it is a well established and well observed pharmaceutical. Long term PPI use has been investigated in regard to the effects of acid suppression and the resulting extended

pH increase in the gastric system, which may affect absorption of Fe, Ca, Mg, and vitamin B12 since their absorption in the body is facilitated by acid. There are conflicting reports, with some sources suggesting that this may lead to problems such as increased risks of fractures and risk of food sensitization; other reports indicate that long term PPI use is not problematic at all.^{526, 528, 535, 536} Omeprazole does however have its limitations such as a short plasma half life, which can lead to the reoccurrence of symptoms especially at night.⁵²⁶ Omeprazole has also been found to increase the bioavailability of certain drugs with acid dependent absorption, and is known to increase the plasma half life of diazepam.^{526, 530, 537, 538}

In addition to its activity as a gastric acid inhibitor, Omeprazole and the single enantiomer form Esomeprazole have been investigated for a number of additional uses such as a treatment for preeclampsia, smoke induced lung injury, and as an inhibitor of atrial fibrillation.⁵³⁹⁻⁵⁴¹ The antiprotozoal activity of Omeprazole has been considered with research conducted into its potential against the parasites *Trichomonas vaginalis*, *Giardia intestinalis*, *Entamoeba histolytica*, *Schistosoma mansoni*, and diseases such as Leishmaniasis.⁵⁴²⁻⁵⁴⁴ Omeprazole has also been investigated for its antioxidant properties, and has been a lead molecule for a number of drug discovery routes.⁵⁴⁵⁻⁵⁴⁷ There have also been reports of Omeprazole being used in the spectrophotometric determination of Ni(II) and the voltammetric determination of Cu.^{548, 549}

3.2 Development of Omeprazole

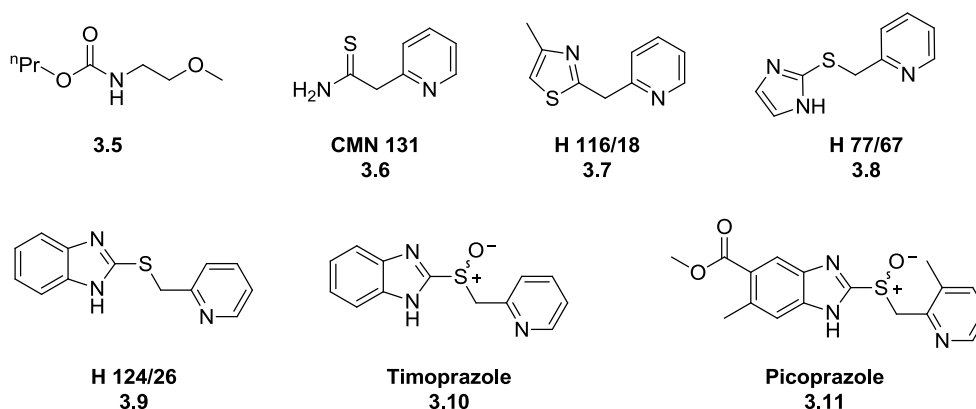
Omeprazole, developed by Astra Pharmaceuticals in Sweden (later to become AstraZeneca), was the first of its class of substituted benzimidazole compounds, specifically developed to target the H⁺, K⁺ -adenosine triphosphatase (ATPase) gastric acid pump. A number of other PPIs have been marketed by different companies, with Lansoprazole, Pantoprazole and Rabeprazole (**3.1-3.3**) featuring the same 2-pyridylmethylsulfinyl benzimidazole core structure; tenatoprazole **3.4** which features an imidazo-pyridine structure has been developed as a next generation PPI but not yet granted FDA approval.⁵⁵⁰ Although these drugs share a similar target and mechanism of action, the subtle differences between them affect the precise mechanism and location by which they inhibit the pump, resulting in slight clinical differences in their effectiveness.^{520, 551} Omeprazole **1.1** and Lansoprazole **3.1** are also marketed in their single enantiomer forms, Esomeprazole (*S*)-**1.1**, and Dexlansoprazole (*R*)-**3.1**.⁵⁵² The development and manufacturing of the single enantiomer form of Omeprazole shall be discussed further in subsequent sections.



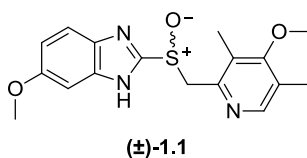
The inhibition of stomach acid production has long been a pharmaceutical target; the first drug recognized to inhibit gastric secretions was an extract of belladonna, the active agent of which was atropine- a potent but non selective muscarinic agent which inhibited the vagal stimulation of acid production.⁵³⁰ PPI predecessors such as Cimetadine and Ranitidine (Zantac) were the original blockbuster drugs, the former being the first drug ever to earn >\$1 billion in a year.^{521, 553} These drugs, developed in the late 70s and early 80s, acted as H₂-histamine receptor antagonists, mediating the basal rate of production of acid.^{530, 554} Despite their great success they suffered from a short duration of action and it was found that patients developed a tolerance toward them in as little as seven days, reducing the efficacy of these drugs by as much as 50%.⁵⁵⁵ H₂-histamine receptor blockers were quickly surpassed by PPIs upon the introduction of Omeprazole in Europe in 1988 and in the USA in 1990.^{518, 520, 526, 531}

The synthetic development of Omeprazole began in 1966, with research to find a gastric acid secretion blocker, initiated with the observation that some local anesthetics, such as Lidocaine, reduced acid production when given orally to man; this project ended in 1970 when compound **3.5**, which had been a highly effective antisecretory agent in rats, was found to have no effect in humans.⁵⁵⁶ From 1972 testing continued with the pyridylthioacetamide **3.6** (CMN131) as the lead compound, however hepatic toxicity issues due to the thioamide group saw this group replaced with other sulfur contained moieties to give compounds such as **3.7** and **3.8**. The latter of these two compounds was the starting point for investigations into compounds featuring two heterocyclic ring systems joined by a connecting chain from which compound **3.9** was generated and was found to exhibit very good antisecretory activity. After H 124/26 **3.9** was identified, it was discovered that it was already covered by a Hungarian patent which described the drug as a treatment for tuberculosis; the sulfoxide metabolite of **3.9** however was not covered and this metabolite, later to be name Timoprazole **3.10**, was found to be an even more

potent antisecretory agent than its parent sulfide.⁵³¹ Unfortunately both the sulfide and sulfoxide were found to be toxic, affecting the iodine recapture of the thyroid gland.⁵⁵³



A literature search showed that some substituted mercapto-benzimidazoles did not affect the thyroid, leading to the introduction of such substitutions to the Timoprazole structure. These substitutions eliminated the toxic effects without reducing the acid inhibition, and lead to the development of Picoprazole **3.11** in 1976.⁵⁵⁷ The following year, at a symposium on hydrogen ion transport George Sachs and coworkers presented data on the enzyme H^+ , K^+ -ATPase, newly discovered by Ganser and Forte, showing it to be the final step in a common pathway for all types of acid secretion.^{530, 554, 556, 558} These findings raised the idea that the benzimidazole agents could be inhibitors of the H^+ , K^+ -ATPase, and the biochemical and synthetic research was continued in parallel. Optimization of the substituted benzimidazole agents was carried out with the aim of finding a more potent agent than Picoprazole. It was found that increasing the pyridyl pKa through addition of electron donating substituents on the pyridine ring increased the potency of the drug as an acid inhibitor. The best analogue created was compound H 168/68, later to be named Omeprazole **1.1**.



The methoxy substituent on the benzimidazole ring was found to offer greater stability to the drug at neutral pH than for example, the benzimidazolyl substitution pattern of picoprazole **3.11**.⁵⁵⁷ It was found that the two methyl groups on the pyridine ring forced the methoxy group out of the plane of the ring, reducing the electron donating abilities and in turn the pKa; however this arrangement was found to be the most potent of all, giving *in vivo* activity higher than any other combination of methyl and methoxy substitution patterns.⁵⁵⁶ By 1980, after more

than a decade of research a compound had been developed that had the optimal safety and pharmacological profile, however Omeprazole presented a number of challenges with regard to shelf life and stability. A significant step toward solving these problems was the discovery that alkali salts of Omeprazole showed greater resistance to chemical instability and decomposition.⁵⁵⁷

3.3 Mechanism of Action

The parietal cells of the stomach secrete gastric acid in response to stimuli such as the sight, smell, taste, or thought of food, or the presence of food in the stomach or intestine. The result of such stimuli is the activation of histamine, acetylcholine, or gastrin receptors (the H₂, M₃, and CCK2 receptors respectively), located in the basolateral membrane of the parietal cell, which initiate signal transduction pathways that all result in the activation of the H⁺,K⁺-ATPase (Figure 3.1).⁵³¹ One of the great advantages of PPIs over other acid-inhibiting drugs lie in their mechanism of action; inhibition of the H⁺,K⁺-ATPase by Omeprazole will reduce acid secretion independently of how the secretion was stimulated. This is in contrast to pharmacological agents such as the H₂ receptor blockers Ranitidine and Cimetidine where their acid blocking effects can be overcome by food induced stimulation of acid production by acetylcholine or gastrin receptors.

Omeprazole, like other PPIs, is a prodrug which is converted to the active agent via an acid catalyzed rearrangement in the parietal cells of the stomach. Absorbed in the small bowel Omeprazole exists at physiological pH as a membrane permeable weak base, with a pKa of ~ 4 corresponding to the pyridine nitrogen.^{552, 556} It is transported to the parietal cells, of which there are over one billion of, where it selectively accumulates in the acidic secretory canaliculi which is the only space in the human body with a pH below 4.⁵³⁰ With secretion of gastric acid the extracellular lumen of the canaliculus achieved a pH as low as 1, resulting in a 1000-fold increase in concentration of Omeprazole compared to the plasma concentration.⁵⁵⁹ Omeprazole has a half life of approximately 2 minutes at pH 1 so rapidly undergoes activation by protonation and is converted to the achiral sulfenic acid and sulfenamide active forms, which are permanent cations making the molecules relatively membrane impermeable.⁵³⁰ These active forms are highly reactive and thiophilic and covalently bind to lumenally accessible cysteine residues on the H⁺,K⁺-ATPase irreversibly inhibiting acid secretion until replacement pumps can be created, which can take up to 36 hours.⁵⁶⁰ The covalent binding involved in the H⁺,K⁺-ATPase inhibition results in a duration of action that typically outlasts the plasma half life of Omeprazole.

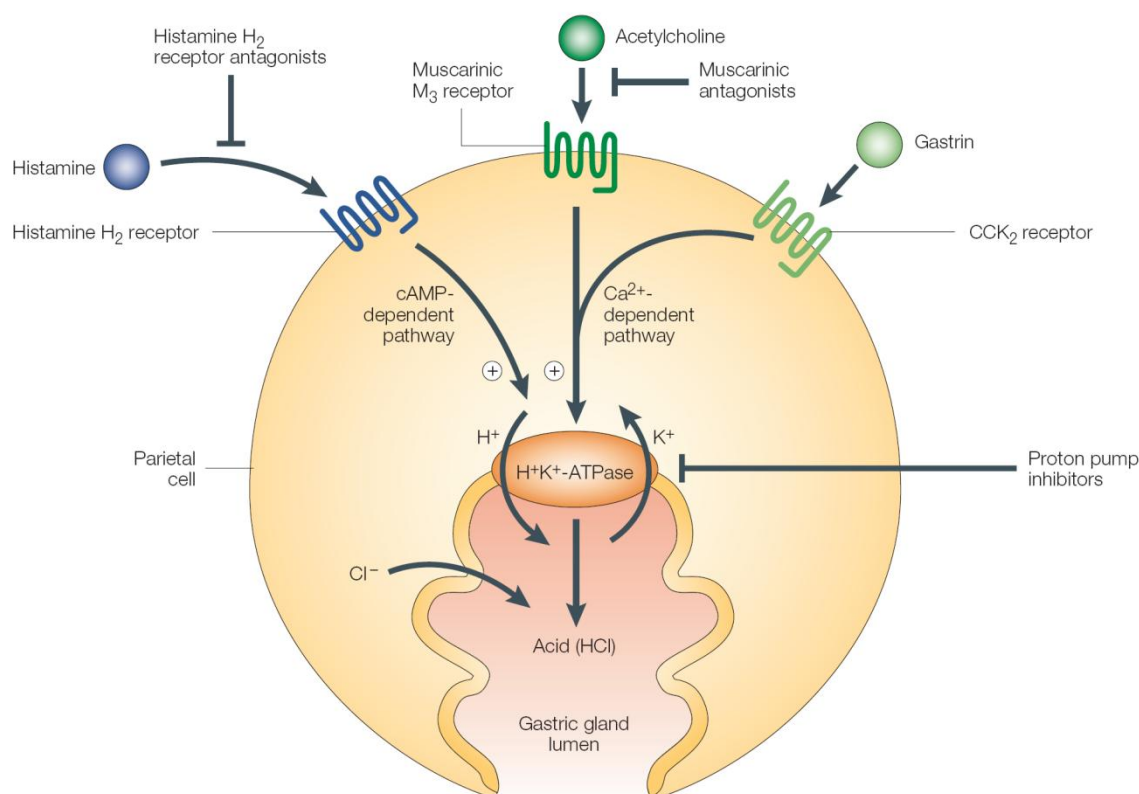


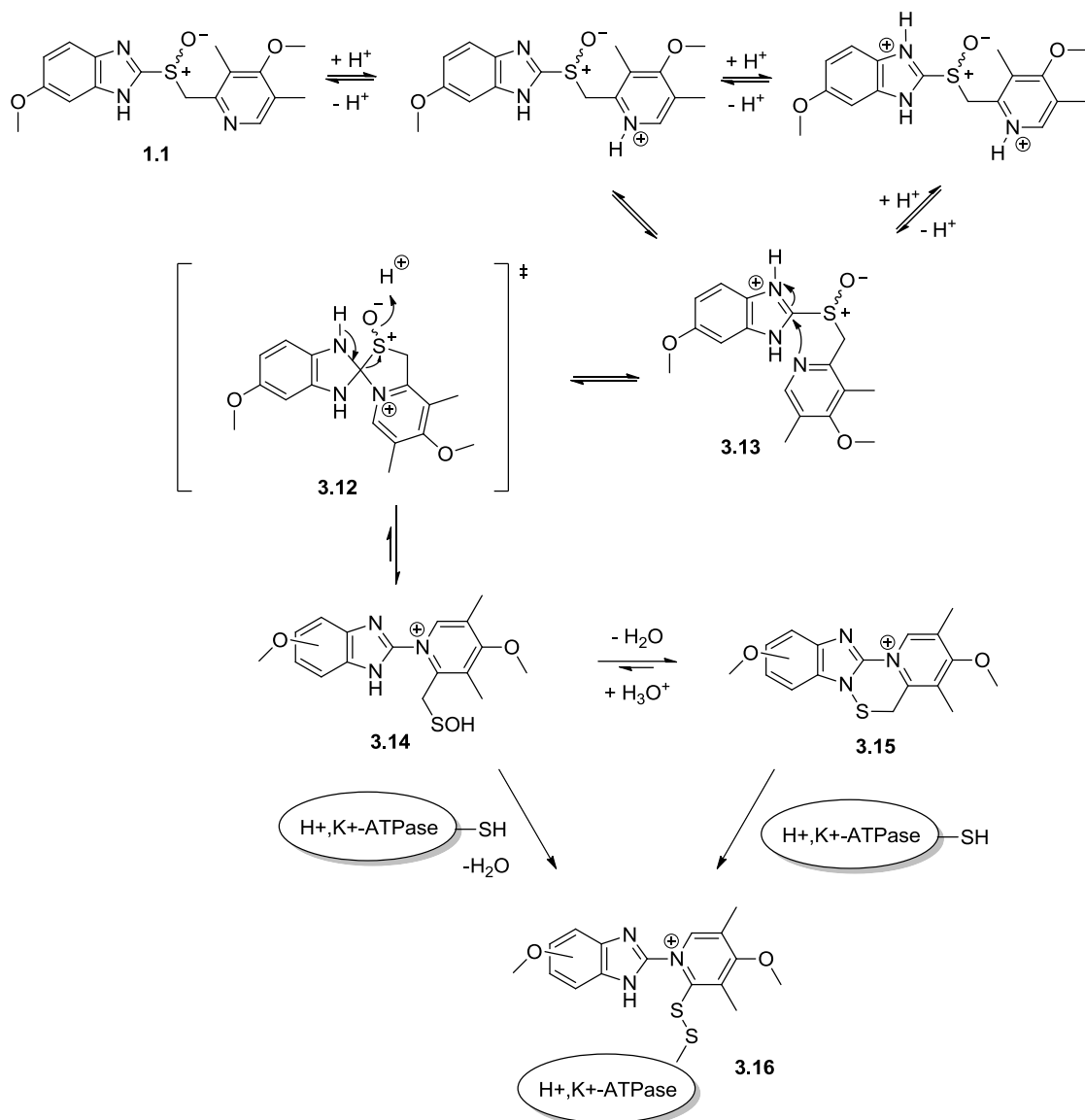
Figure 3.1 Representation of the parietal cell of the stomach; Image used with permission from ref⁵³¹

It is estimated that only 70% of proton pumps are inhibited at anytime as not all gastric acid pumps are active to produce the acid required to convert Omeprazole into its active form. It takes 26-96 hours for a steady state of acid inhibition to be achieved, and for long term relief from acid related symptoms the patient must take regular, that is at least daily, doses of the drug with pre-breakfast administration found to be most effective.^{552, 554}

As Omeprazole is acid labile, measures must be taken to protect it from exposure to the acidic environment of the stomach en route to the small bowel where the drug is absorbed into the bloodstream.⁵²⁶ There are a variety of delivery systems available which prevent absorption until an environmental pH greater than 5, such as enteric coated tablets, gelatin capsules, or coated granules which are supplied as powder for suspensions.^{520, 561} Some forms are packaged in combination with bicarbonate to provide pH neutralization, and some PPIs are available as IV preparations.^{520, 526}

The mechanism by which Omeprazole rearrangement occurs has been well studied.^{556, 560, 562-566} Under acid conditions Omeprazole is transformed to the spiro intermediate **3.12** which arises as a result nucleophilic attack of the pyridine nitrogen on the C2-position of the protonated benzimidazole **3.13** (Scheme 3.1). Aromatization to the sulfenic acid **3.14** is followed by dehydration to the tetracyclic sulfenamide **3.15** which reacts with the target enzyme and

deactivates it via formation of the disulfide complex **3.16**. Initially it was believed that the substituents on the pyridine ring were the main influence on the rate of reaction of conversion of Omeprazole and other PPIs to their active forms. Subsequent studies however showed that the reaction rate is influenced by the protonation of the benzimidazole and the nucleophilicity of the unprotonated pyridine.⁵⁶²



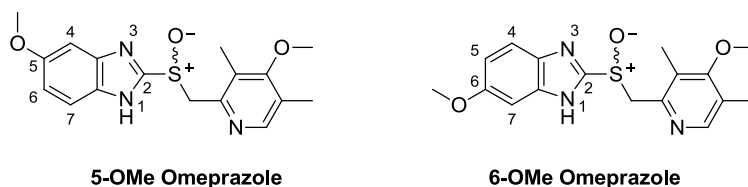
Scheme 3.1

3.4 Synthesis of Omeprazole

3.4.1 Structure and nomenclature of Omeprazole

Omeprazole can exist in two tautomeric forms, either the 5-methoxy or the 6-methoxy benzimidazole form.^{567, 568} Conventionally Omeprazole has been represented in the literature as the 5-methoxy isomer; however studies have shown that the 6-methoxy species may be the

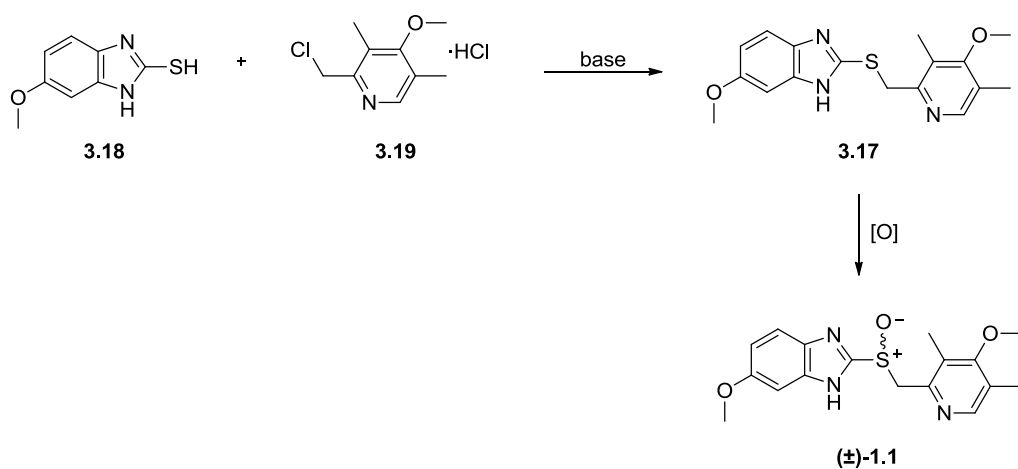
more common form in both the solid state and in solution.^{569, 570} Crystallographic data published on samples of racemic Omeprazole have clearly shown the 6-OMe form, however in more than one instance the molecule has been erroneously named as the 5-OMe benzimidazole.^{571, 572}



For the sake of accuracy, and in keeping with the solid state structures observed by the X-ray diffraction studies discussed in chapter 6, Omeprazole has been represented as the 6-OMe tautomer throughout this body of work, and by analogy this structural convention has continued for other methoxy benzimidazole contined species.

3.4.2 Synthesis of Omeprazole

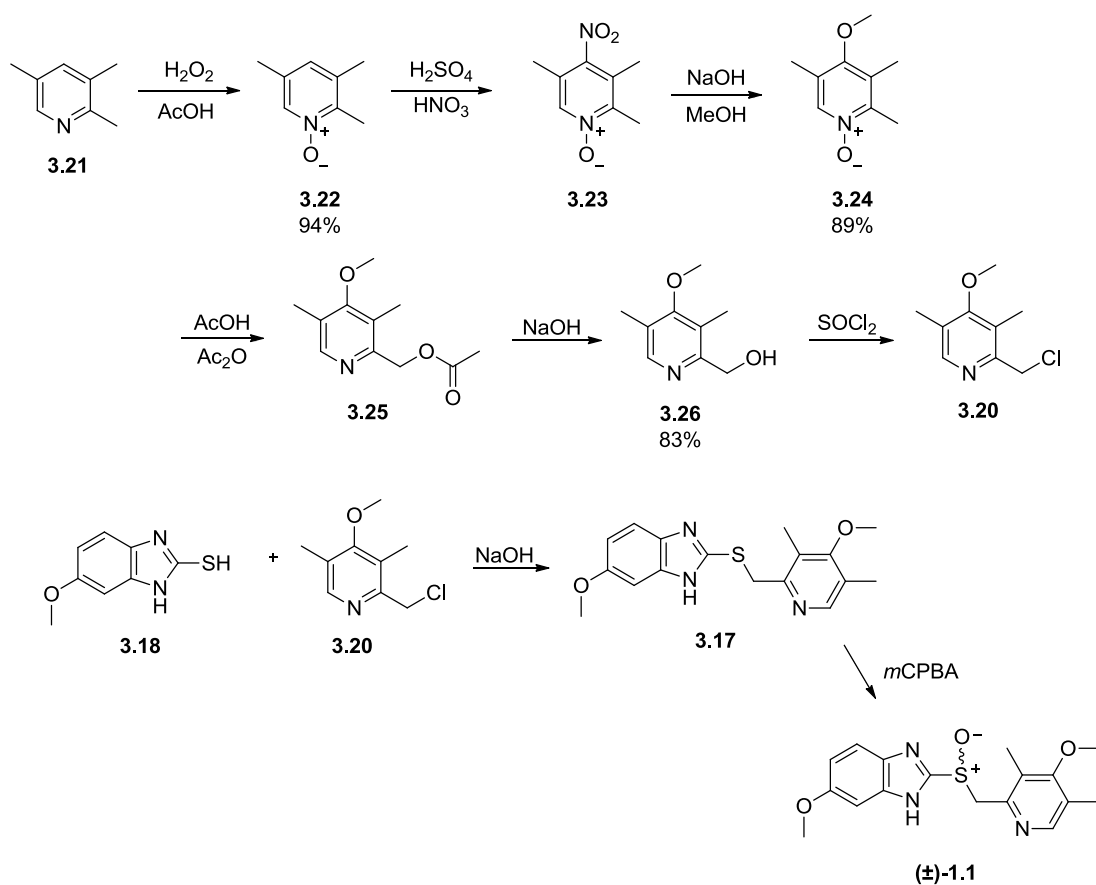
Omeprazole can be obtained through oxidation of the sulfide Pyrmetazole **3.17** which in turn is created through the reaction of benzimidazole thiol **3.18** and pyridine salt **3.19** in the presence of a base (Scheme 3.2).⁵⁷³ The thiol and the pyridine salt are commercially available to purchase in mutigram amounts, however that was not always the case leading to the development of a number of synthetic routes for the preparation of Omeprazole and its precursors.



Scheme 3.2

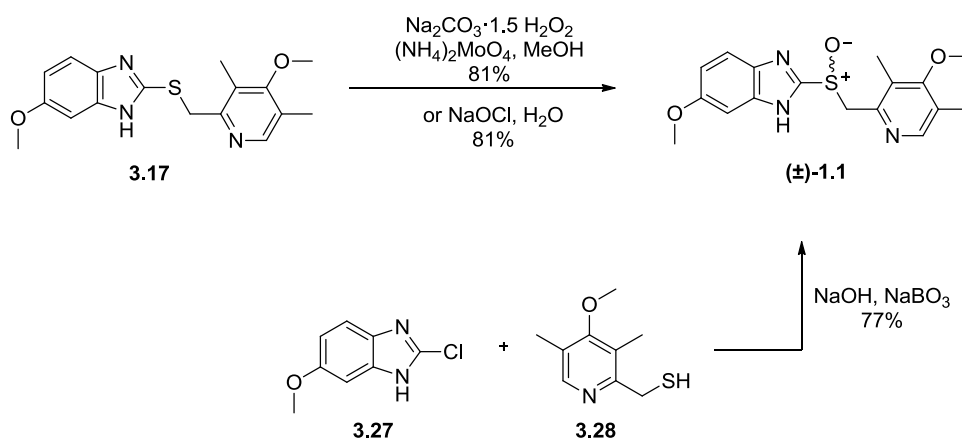
Branstrom *et al.*, who developed Omeprazole at Astra Pharmaceuticals, disclosed their method for the preparation of the tetrasubstituted pyridyl species **3.20** for use en route to Omeprazole

1.1 (Scheme 3.3).^{556, 574} Oxidation of trimethyl pyridine **3.21** was performed by hydrogen peroxide in acetic acid to give *N*-oxide **3.22**, followed by nitration giving the 4-nitro pyridine derivative **3.23**. Methoxy substitution of **3.23** displaced the nitro group to give the 4-methoxy pyridyl species **3.24** of which subsequent treatment with acetic anhydride gave the 2-pyridylmethyl acetate **3.25**.⁵⁷⁵ The corresponding alcohol derivative **3.26** was afforded through treatment of **3.25** with base, followed by reaction with thionyl chloride to displace the hydroxyl group with chloride giving the target pyridine **3.20**. Omeprazole **1.1** was obtained through reaction of thiol **3.18** with the pyridine **3.20** in the presence of NaOH; oxidation of Pymetazole sulfide with *m*CPBA gave **1.1** as a racemic mixture.⁵³



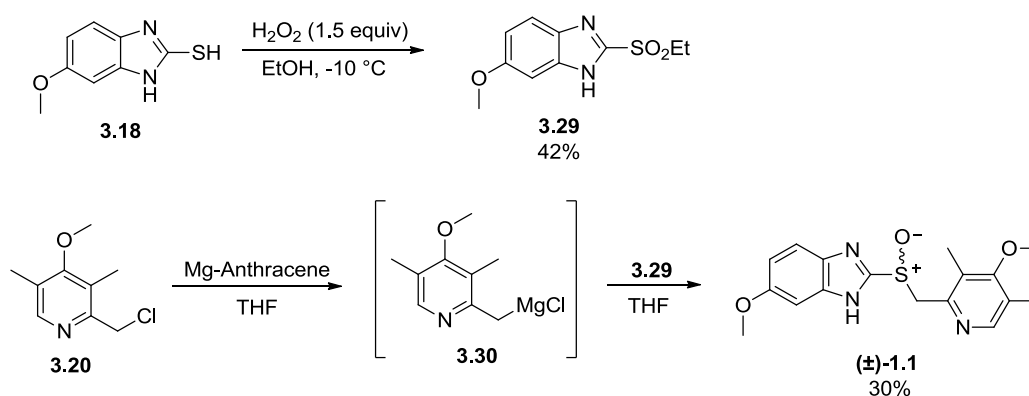
Scheme 3.3

Numerous patents have been granted for alternative methods for the synthesis of Omeprazole and its precursors; Al Badr gives an overview of ten of these patented synthetic routes in a book chapter dedicated to Omeprazole.⁵⁷⁶ Large scale oxidations from the pharmaceutical industry giving Omeprazole **1.1** from Pymetazole **3.17** have been reported which use inorganic oxidants such as sodium perborate, sodium hydrochlorite or sodium percarbonate in the presence of Mo catalysts (Scheme 3.4).⁹¹



Scheme 3.4

Bhalero and coworkers reported a novel synthetic route to Omeprazole **1.1**, via the formation of the benzimidazole ester **3.29** and subsequent *in situ* reaction with the pyridyl Grignard intermediate **3.30** (Scheme 3.5).⁵⁷⁷ Omeprazole was obtained in a yield of 30%.



Scheme 3.5

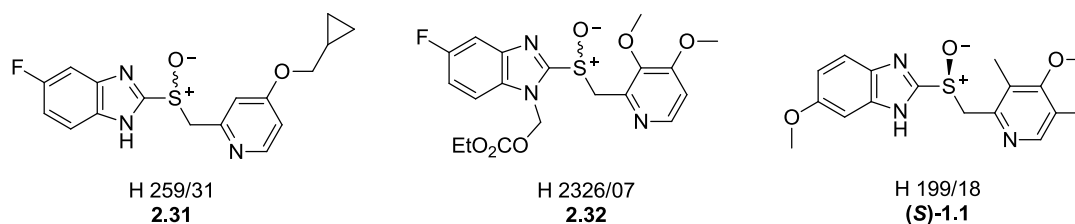
3.5 Esomeprazole: A single enantiomer proton pump inhibitor

3.5.1 Development of a new proton pump inhibitor

Following the global success of Omeprazole the development team at Astra began the hunt for a successor. Despite its excellent acid inhibitory ability Omeprazole was found not to be equally effective throughout the population, with some patients experiencing uncontrolled symptoms and requiring additional dosages to sufficiently control their acid production. By 1987 the search for the next proton pump inhibitor was underway, with the aim to find a compound which offered improved pharmacokinetics and metabolic profile, which would reduce interpatient variability with regard to acid control.⁵⁵⁷

A variety of analogues were produced based on the chemical and mechanistic knowledge gained from studying Omeprazole and its target enzyme, with over 30 scientists creating and screening hundreds of compounds. Only a small number of analogues were found to satisfy the preclinical goals from which four compounds, including sulfoxides H 259/31 **3.31** and H 326/07 **3.32**, were chosen for human testing after passing rigorous preclinical testing.

Assessment of the key parameters of pharmacokinetic properties, acid inhibition ability, and safety revealed that only one species proved superior to Omeprazole – H 199/18, the (*S*)-enantiomer of Omeprazole (*S*)-**1.1**, or Esomeprazole as it became known.



The finding that Esomeprazole performed better than its racemate Omeprazole was surprising for the development team. Given the knowledge that the mechanism of acid inhibition occurred via an achiral sulfenamide intermediate it was assumed that both enantiomers would have an identical effect. Supporting this theory were the findings from *in vitro* testing on isolated gastric glands which had shown identical dose-response curves for acid inhibition for both enantiomers. The possibility was raised however that the disparity in efficacy between the racemic Omeprazole and the single enantiomer form of the sulfoxide may be attributed to differences in metabolism; subsequent testing showed this hypothesis to be correct.⁵⁷⁸⁻⁵⁸²

Proton pump inhibitors, including Omeprazole, undergo hepatic metabolism via the cytochrome P450 system via the isoforms CYP2C19 and CYP3A4.^{559, 583} The CYP 2C19 enzyme metabolizes Omeprazole to the hydroxyl and 5-O desmethyl metabolites, while the CYP3A4 converts it to the sulfone^{559, 584} The two enantiomers undergo the same transformations but there are quantitative differences in the relative dependence on the two enzymes. Hydroxylation via CYP2C19 is responsible for 98% of the total intrinsic clearance of the *R*-enantiomer, but only for 70% of the *S*-enantiomer. In addition the CYP3A4 is responsible for 2% of clearance of the *R*-enantiomer, but 30% for Esomeprazole.^{580, 584-587} Metabolism by CYP3A4 occurs at a slower rate than by CYP2C19, and as a result Esomeprazole has a lower total intrinsic clearance than the *R*-enantiomer and its first-pass metabolism is decreased compared with the racemate, leading to higher plasma levels of the drug when Esomeprazole is used in the single enantiomer form.^{529, 557, 584, 585} As a result of the higher metabolic stability and improved bioavailability

afforded by Esomeprazole a more effective control of acid inhibition is achieved compared to the racemate at the same dosage.⁵⁸⁵⁻⁵⁸⁷

Testing of Esomeprazole also revealed improved performance towards interindividual variability compared with the racemate Omeprazole. Genetic polymorphism affects the metabolism of PPIs and therefore influences the extent of acid control between individuals. The CYP 2C19 enzyme is expressed polymorphically meaning that some individuals do not express this enzyme.^{41, 43} This leads to variation within the population with respect to how efficiently metabolism of Omeprazole occurs, with poor metabolizers making up 3% of the Caucasian population, and 15-20% in Asian populations.^{559, 583, 588} The pharmacokinetic differences for Esomeprazole compared to Omeprazole means that the significant difference in the relative dependence on CYP2C19 and CYP3A4 leads to a lower impact of the polymorphic metabolism *in vivo*. For the majority of the patient population (extensive metabolizers), the improved pharmacokinetics of Esomeprazole results in higher bioavailability, while for those considered poor metabolizers exposure is limited due to the greater involvement of the CYP3A4 enzyme in metabolizing the (*S*)-enantiomer. Overall the use of Esomeprazole was found to give a more consistent interpatient response in regards to acid inhibition.^{559, 583}

3.5.2 The Chiral Switch

In the pharmaceutical industry a chiral switch is defined as when a chiral drug that has previously been claimed, approved, and marketed as a racemate, or mixture of diastereomers, is subsequently redeveloped as a single enantiomer drug.⁵⁸⁹ The development of Esomeprazole is one of the most well known examples of a drug undergoing a “chiral switch”, and as well as being one of the most successful it may also be one of the most controversial.⁵⁹⁰⁻⁵⁹² The development of a single enantiomer form of a drug can offer a number of therapeutic advantages, such as reducing metabolic load on the body, increasing potency of a drug, and reducing side effects. This is particularly relevant when one enantiomer of a drug is ineffective or has adverse effects associated with it.^{587, 591, 593-595}

In the case of Esomeprazole there have been questions raised as to whether or not a single enantiomer form actually offers any significant advantage over the original racemate.^{590, 596, 592} One of the sources of doubt comes from publication of clinical trials which claim to show Esomeprazole superiority over Omeprazole and other PPIs but which compared non equivalent dosages of the drugs under inspection.⁵⁸² It is worth noting that the recommended daily dose of Esomeprazole is 40 mg, whilst that of Omeprazole is only 20 mg, leading some to suggest that the effectiveness of Esomeprazole is simply due to an increased dosage of the medication.^{597, 598}

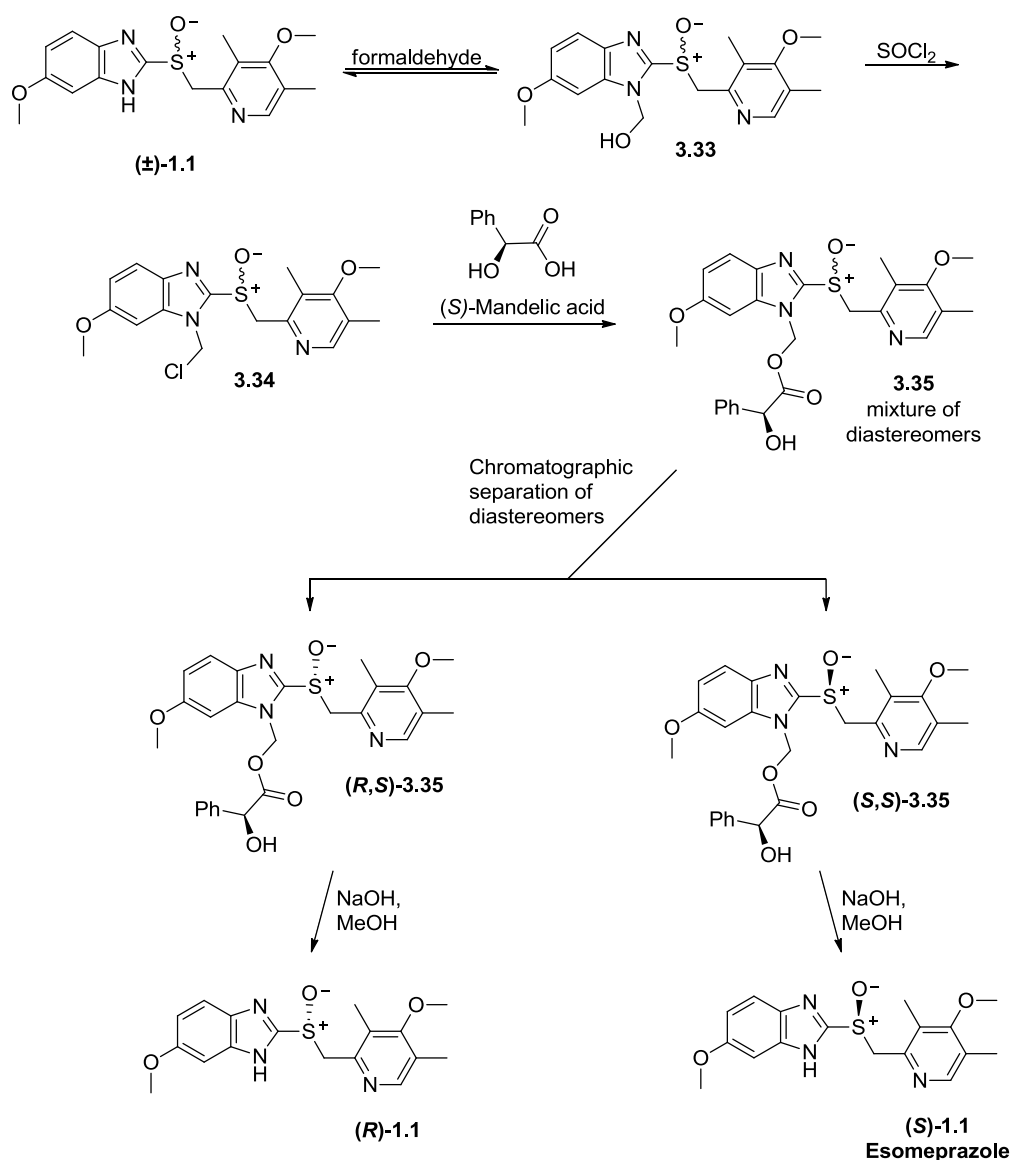
There are also those critics who suggest that chiral switches are simply one way of extending a patent franchise and to protect against competitions from generic racemates.^{591, 599} The development of single enantiomer drugs has also been criticized for placing an unfair financial burden on the patient, one which outweighs the therapeutic advantages of the single enantiomer drugs, for example Esomeprazole can cost up to 10 times as much as the racemic drug Omeprazole.⁵⁹⁰ Despite these criticisms, Esomeprazole has gone on to be a blockbuster drug in its own right, marketed in the form of the magnesium salt as Nexium, with peak global sales of \$8.1 billion in 2011.⁵⁸⁸

3.5.3 Asymmetric synthesis of Esomeprazole

3.5.3.1 Industrial Process Development of Esomeprazole

The preparations of the chiral sulfoxide Esomeprazole (*S*)-**1.1** typically involve asymmetric oxidation of Pymetazole **3.17**, or resolution of the derivatized racemate. Both of these methods were employed by Federsel and Larsson who have written about the process of developing Esomeprazole and how they successfully developed a method for synthesis of Esomeprazole from gram scale to multi ton per annum production.^{15, 519, 600} The first approach that was taken by Astra was resolution of racemic Omeprazole.

The identification of Esomeprazole as a potential successor to Omeprazole raised the issue of how to obtain sufficient amounts of the single enantiomer sulfoxide for *in vivo* testing. With unlimited access to an abundant amount of the racemic sulfoxide it was felt that it would be logical to pursue a resolution type procedure. Analytical and semi-preparative separation of the enantiomers of Omeprazole had been achieved on a milligram scale using chiral chromatography, but a larger scale resolution was required as 500 g of material had been requested for the first batch of the separated enantiomers.^{139, 601} Derivatization of Omeprazole for resolution was not straightforward due to its sensitivity towards acid, however a procedure was developed enabling the covalent attachment of a chiral handle prior to diastereomeric separation (Scheme 3.6). Racemic Omeprazole was reacted with formaldehyde to give **3.33** via substitution on the benzimidazole nitrogen with a hydroxymethyl group. Chloro-dehydroxylation by thionyl chloride to give compound **3.34** was followed by O-alkylation with (*S*)-mandelic acid to give a diastereomeric mixture of the esters **3.35**. Production of the mandeloyl derived esters was labour intensive, taking almost 300 man-hours over a period of 40 days. Starting from 40 kg of the racemic Omeprazole the three step procedure afforded 5.3 kg of the material in a purity of 93% pure, equating to a yield of approximately 9%.



Scheme 3.6

The next step was the separation of the derivatized diastereomers **3.35** by chromatography; this procedure was also labour and resource intensive, requiring 10 m³ of eluents for less than 1 kg of each enantiomer of the sulfoxide, and complicated by the necessity of a rapid work up of the collected fractions due to the potential for decomposition and racemisation of the Omeprazole derivatives. Nevertheless separation was achieved, giving a chromatographic yield of 65% for each diastereomer. Conversion under basic conditions gave around 900 g each of the target sulfoxide enantiomers, in optical purities of 96% ee, representing an overall yield of 4.5% based on 40 kg of the racemic starting material. The formation of the sodium salts not only improved the stability of the Omeprazole enantiomers but also converted the oily neutral forms into the crystalline solids of the salt form. Further loss of material during salt formation left just enough of each enantiomer to fulfil the original order of 500 g. Whilst the first attempt to scale up the

production of the Omeprazole enantiomers had achieved its original goal, another order was on its way but this time for 5 kg, ten times the amount that had just been produced.

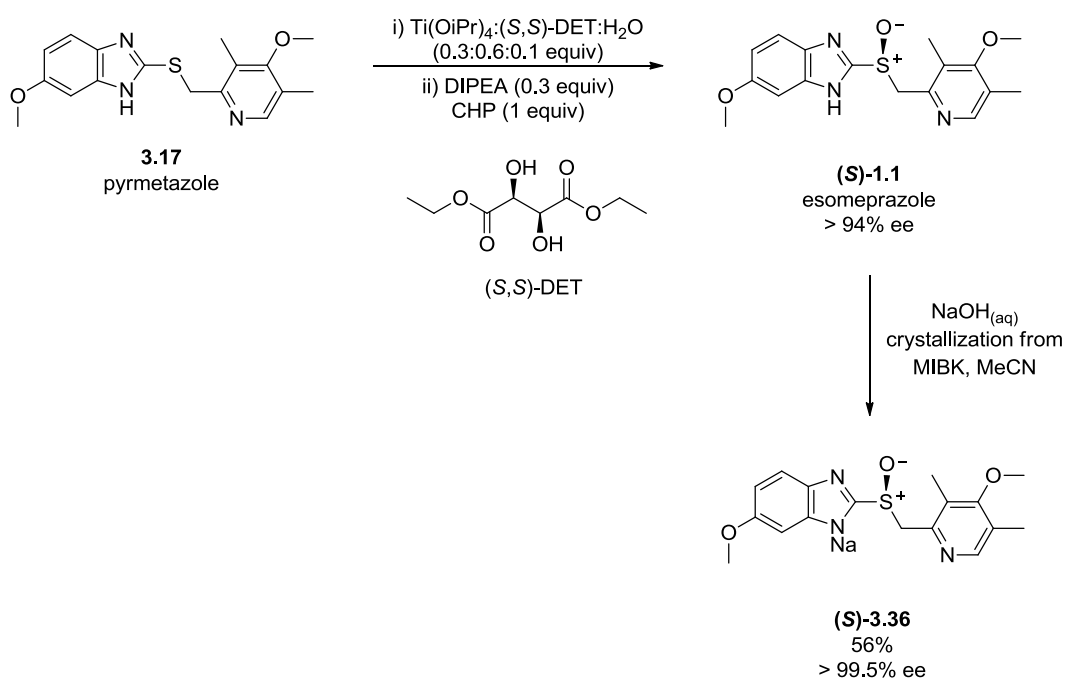
Optimization of the resolution strategy was able to greatly improve the yield for certain steps. For example, production of the chloromethyl species **3.34** was enhanced by isolation of the CH₂OH adduct **3.33** prior to chloro-dehydroxylation resulting in an increase in the yield of **3.34** to 60-70%. Improvements such as this however were not enough and other methodologies were considered for the large scale production of Esomeprazole. Biological strategies, such as kinetic resolution through bioreduction of racemic Omeprazole, or oxidation of the Omeprazole sulfide using various microorganisms were found to be workable but were not carried forward. New advances in the field of asymmetric sulfoxidation gave the best hope for the development of a new synthetic direction.

Asymmetric oxidation via the use of Davis oxaziridines was conducted, affording Esomeprazole (*S*)-**1.1** in 40% ee. As Omeprazole crystallizes as a racemate therefore it was possible to raise the optical purity of Esomeprazole to 94% ee by a crystallization process, leaving behind enantiomerically enriched Esomeprazole in the mother liquor. Despite the ability to obtain Esomeprazole in high enantiopurity this methodology was not feasible on a large scale due to the cost involved in the use of the oxidizing agents in stoichiometric amounts.

The titanium tartrate catalyst systems developed by Kagan for asymmetric sulfoxidation were tested but initial examination of the process gave disappointing results, affording the target sulfoxide in just 5% ee. It was soon discovered however that the addition of a base to the reaction mixture had a substantial impact upon improving the enantioselectivity of the catalyst system, allowing for the development of a successful methodology in which Esomeprazole could be produced in high enantiomeric purity on a large scale.

In 2000, ten years after the original patent on the procedure was filed, a paper was published by von Unge *et al.* which reported the asymmetric synthesis of Esomeprazole as developed by AstraZeneca.¹²⁵ Using cumene hydroperoxide (CHP) as the oxidant, the Omeprazole sulfide Pymetazole **3.17** was stereoselectively oxidized in the presence of a titanium-diethyl tartrate (DET) catalyst to give Esomeprazole (*S*)-**1.1** in over 94% ee; formation of the sodium salt (*S*)-**3.36** gave the sulfoxide in an enantiomeric excess of > 99.5% in a yield of 55% (Scheme 3.7). This protocol was employed on a multikilogram scale to produce 3.83 kg of sodium Esomeprazole (*S*)-**3.36**. This methodology was also employed for the enantioselective synthesis of seven Omeprazole analogues, with the optical purities of the obtained crude sulfoxides close

to or above 90% ee; the synthesis of the proton pump inhibitor Dexlansoprazole has also been reported using similar conditions⁶⁰²



Scheme 3.7

The attainment of Esomeprazole in high optical purity was achieved by three modifications to the original Kagan type oxidation protocol. Firstly, preparation of the catalyst, comprising of $\text{Ti}(\text{O}^i\text{Pr})_4$, (*S,S*)-DET and water was performed in the presence of the sulfide **3.17**, with care taken over the precise order of reagent addition. Secondly, aging of the catalyst was performed by allowing the components of the catalyst and the sulfide to be stirred at an elevated temperature to allow for equilibration of the catalyst complex. Thirdly, the oxidation was performed in the presence of the base *N,N*-diisopropylethylamine (DIPEA), also known as Hünig's base.¹²⁵

An optimized ratio of $\text{Ti}(\text{O}^i\text{Pr})_4:\text{DET}:\text{H}_2\text{O}$ of 0.3:0.6:0.1 equiv (with respect to sulfide substrate) was employed, equating to a catalyst loading of 30 mol%. Enantioselectivity in the oxidation process was observed when a catalyst loading of 4 mol% was used, with Esomeprazole obtained in 91% ee. It was, however reported that the use of catalyst loadings lower than 30 mol% had a detrimental effect on the reproducibility of the reaction enantioselectivity. The role of the base DIPEA in the reaction remains unclear, although it has been suggested that the inclusion of the base helped stabilize the acid sensitive sulfoxide product.²² von Unge and coworkers reported that using other bases, such as triethylamine and 4-methylmorpholine was possible but gave the product sulfoxide **1.1** with lower enantiopurity. When stronger bases, such as

1,8-diazabicyclo[5.4.0]undec-7-ene (DBU) were used the enantioselective of the reaction decreased dramatically, suggesting that the role of the base was more than just as an agent to abstract the benzimidazole NH proton. Additionally, it was observed that using a stronger base led to the predominant formation of the (*R*)-enantiomer of Omeprazole, despite the continued use of (*S,S*)-DET as the chirality source.¹²⁵ The importance of the benzimidazole NH in the sulfide substrate, with respect to the reaction enantioselectivity, was highlighted by the fact that sulfoxidation of *N*-alkylated benzimidazole species proceeded to give only racemic products. This was also the case for sulfide substrates lacking an imidazole or benzimidazole type group. From these findings it was hypothesized that the NH group of the benzimidazole and/or the base DIPEA may participate in the chiral titanium catalyst complex.

3.5.3.2 Alternative syntheses of Esomeprazole

A number of alternative strategies for the asymmetric synthesis of Esomeprazole have been published. These include metal and non metal based oxidations of the prochiral sulfide Pyrimetazole **3.17**, resolutions of the racemic sulfoxide Omeprazole **1.1**, and chromatographic separations.

3.5.3.2.1 Resolution of racemic Omeprazole

Chromatographic resolution

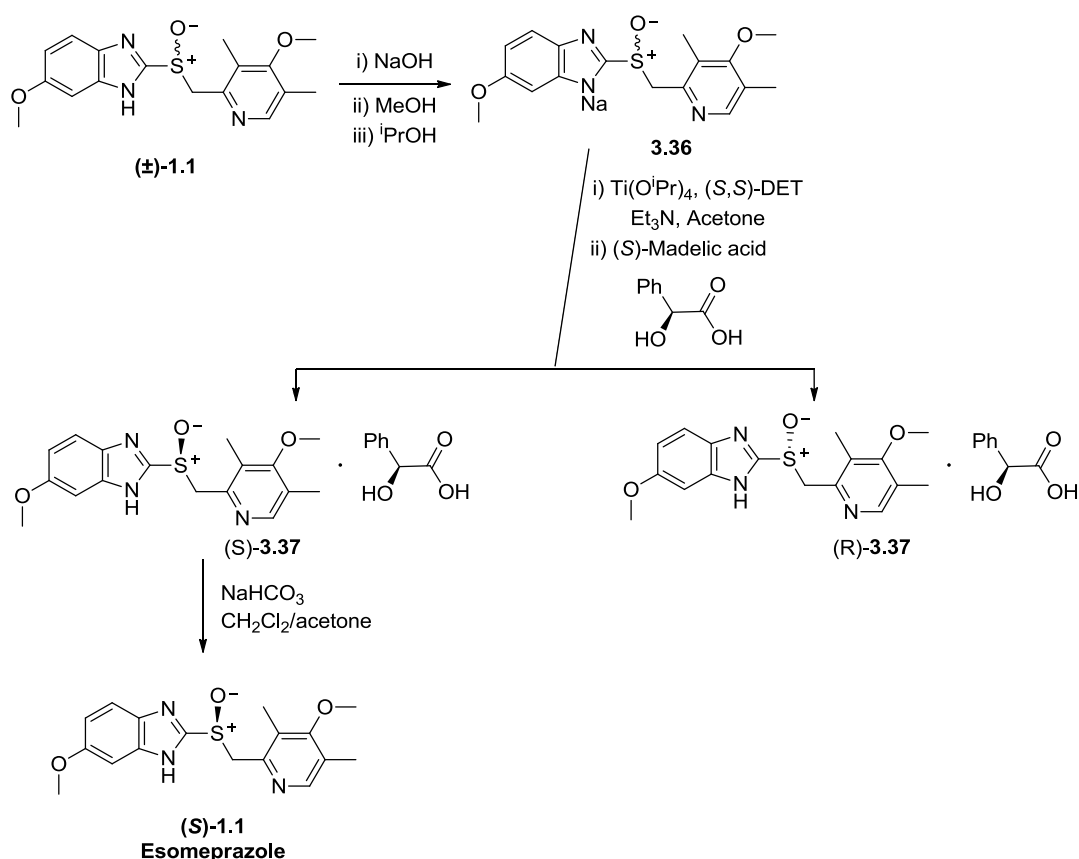
Esomeprazole (*S*)-**1.1** was resolved for the first time analytically in 1984 using an affinity chromatographic technique with immobilized bovine serum albumin.¹³⁹ In 1990 the semipreparative resolution of Omeprazole enantiomers was achieved on a trisphenylcarbamoylcellulose-based stationary phase.⁶⁰¹ Since that time there have been a number of reports published covering many aspects of the analytical separation of Omeprazole by HPLC methods.^{126, 127, 603-607} Supercritical fluid chromatography has been employed for the analytic, semipreparative and preparative resolution of Omeprazole enantiomers.^{130, 608-611}

The phenomenon of self-disproportionation of enantiomers (SDE) was observed for Omeprazole by Song *et al.*¹⁵⁰ It was observed that when non racemic mixtures of the sulfoxide were eluted under achiral column chromatography conditions, using a silica stationary phase, enrichment in the optical purity of the first fractions occurred, while depletion was observed in the final fractions. Across a range of solvents and solvent mixtures the differences in ee (Δee) between the first and the last were measured. Starting from a sample of Esomeprazole (76% ee) Δees of up to 39% were observed, with the largest effect seen when a 2:1 mixture of EtOAc–

CH₂Cl₂ was employed as the eluent; it was also observed that some decomposition occurred under these conditions. When racemic Omeprazole (0% ee) or pure Esomeprazole (100% ee) was examined no change in optical purity was observed between the first and last fraction when methyl isobutyl ketone was used as the solvent. It was proposed that the formation of heterochiral dimers of Omeprazole was the reason for the observed SDE during achiral gravity driven chromatography.

Classical resolution

Reddy *et al.* described the process for the separation of Esomeprazole from the racemic sulfoxide, affording (*S*)-**1.1** in an optical purity of > 99.5% ee (Scheme 3.8).⁶¹²⁻⁶¹⁴

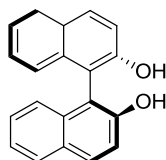


Scheme 3.8

Omeprazole **1.1** was treated with sodium hydroxide to afford the sodium salt **3.36**. Ti(OⁱPr)₄ and (*S,S*)-DET and triethylamine were added to a solution of **3.36**, followed by the addition of (*S*)-mandelic acid. The mandelic acid salt of Esomeprazole precipitate was collected and neutralized to give Esomeprazole (*S*)-**1.1** with an optical purity of > 99.5%.

Deng *et al.* reported the resolution of both enantiomers of Omeprazole via inclusion complexation with the chiral host BINOL **1.43**.⁵⁷¹ Recrystallisation of the inclusion complex

followed by separation of the species by column chromatography gave Esomeprazole (*S*)-**1.1** in 98% ee. Similarly using (*R*)-BINOL **1.43**, the (*R*)-enantiomer of Omeprazole was obtained in > 99% ee. Although it was not possible to grow crystals suitable for analysis of the inclusion complex by X-ray crystallography, IR analysis indicated the sulfinyl group did not contribute to the H-bonding within the inclusion complex

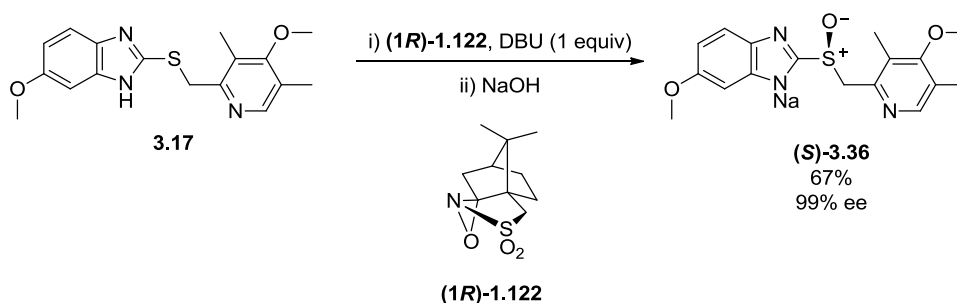


(*S*)-**1.43**

3.5.3.2.2 Non-metal based oxidations

Oxidations by oxaziridines and oxaziridinium salts

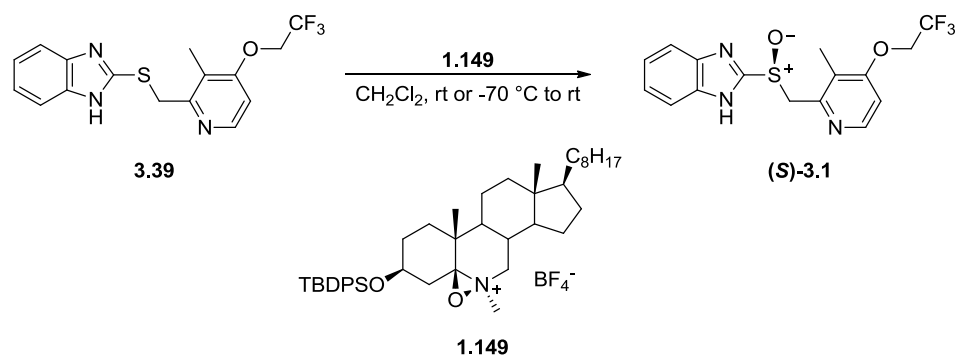
Esomeprazole-sodium (*S*)-**3.36** was obtained in 67% yield and 99% ee using a stoichiometric amount of (*1R*)-(-)-(10-camphorsulfonyl) oxaziridine (*1R*)-**1.122**, with the base DBU added to the reaction mixture to facilitate the reaction by activation of the prochiral sulfide **3.17** (Scheme 3.9).⁶¹⁵ The sodium salt was prepared directly from the crude material of the reaction. (*R*)-Rabeprazole (*R*)-**3.3** was prepared in a similar fashion, using the (*1S*)-enantiomer of the oxaziridine **1.122**; the target sulfoxide was afforded in 76% ee which was increased to 97% ee after transformation to the sodium salt. Delsarte *et al.* recently described a similar process which employed oxaziridine (*1R*-**1.122**) and the base DBU in the asymmetric synthesis of Esomeprazole.⁶¹⁶ The final product was the potassium salt of Esomeprazole (*S*)-**3.38** which was achieved in 80-85% and 75% ee.



Scheme 3.9

The asymmetric synthesis of the Esomeprazole analogue (*S*)-Lansoprazole from the sulfide **3.39** using the chiral oxaziridinium salt **1.149** was reported by del Bohé *et al.* Sulfoxide (*S*)-**3.1** was

afforded in 97% ee using a stoichiometric amount of the oxaziridinium oxidizing agent (Scheme 3.10).



Scheme 3.10

Biologically mediated synthesis of Esomeprazole

Babiak *et al.* reported the oxidation of Pyrimetazole **3.17** by the gram positive bacterium *Lysinibacillus* sp. B71, isolated from soil polluted with elemental sulfur. Esomeprazole obtained in enantiopure form, in a conversion of 77%.⁶¹⁷ A Baeyer-Villiger monooxygenase (BVMO) mediated oxidation affording Esomeprazole (S)-**1.1** has been reported, as has the production of the same sulfoxide from isolated and modified cyclohexane monooxygenases (CHMOs) from *Acinetobacter calcoaceticus* NCIMB9871.⁶¹⁸⁻⁶²⁰ Microbial oxidation of Rabeprazole sulfide by the mold *Cunninghamella echinulata* MK40 has been reported, with the (S)-sulfoxide afforded in > 99% ee.⁶²¹

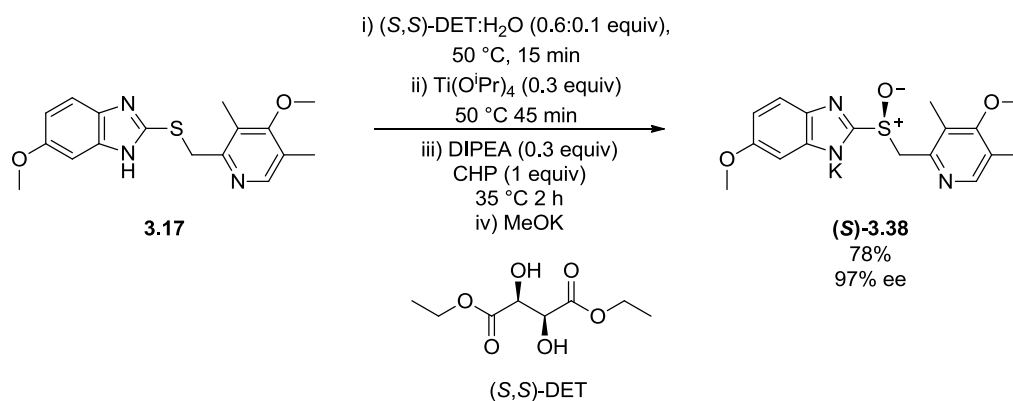
3.5.3.2.3 Metal based oxidations

Titanium mediated synthesis of Esomeprazole

Federsel *et al.* employed a modified von Unge protocol for the synthesis of Esomeprazole **1.1**, altering the order of addition of the reagents.⁶²² (S,S)-DET and water (0.6 and 0.1 equiv respectively) were added to sulfide **3.17** the mixture heated at 50 °C for a 15 min; subsequently $\text{Ti}(\text{O}^i\text{Pr})_4$ (0.3 equiv) was added and warming continued for a further 45 minutes. Following addition of DIPEA (0.3 equiv) and CHP (1.0 equiv) the temperature of the reaction mixture was adjusted to 35 °C, and stirring continued for 2 hours. Esomeprazole was obtained in the form of the potassium salt (S)-**3.38** (78% yield), with an optical purity of 97% ee (Scheme 3.11).

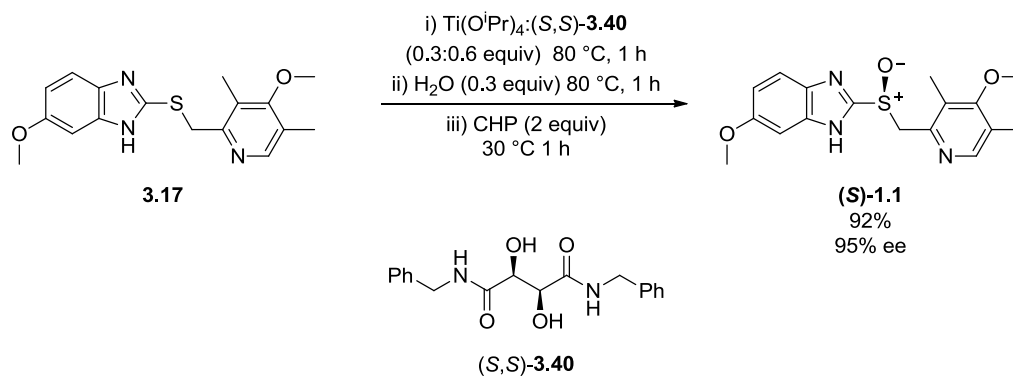
Follow up investigations described investigation of the catalyst active species via atmospheric pressure chemical ionization-mass spectrometry (APCI/MS), from which it was hypothesized that addition of water to the catalyst reaction mixture facilitated the formation of mononuclear

titanium species believed to be the active catalyst intermediates.⁶²³ NMR studies were also used to investigate the reactions, from which it was concluded that under catalytic conditions the amine DIPEA was able to coordinate to the titanium metal centre and dissociate the coordinated substrate, in this case an imidazole species.



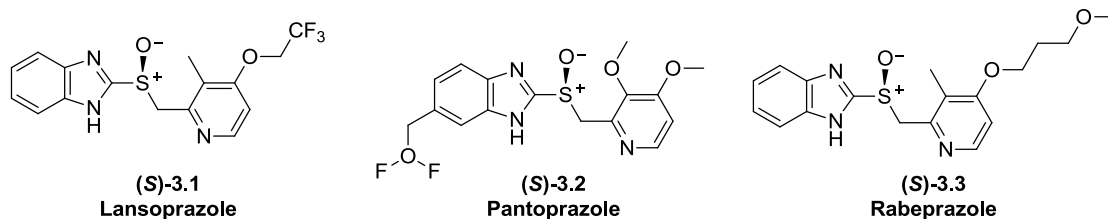
Scheme 3.11

Guoyong *et al.* used a tartramide as the chiral ligand in the Ti-mediated oxidation of Pymetazole **3.17** to give Esomeprazole (*S*)-**1.1** in high yield and enantioselectivity (92%, 95% ee) (Scheme 3.12).⁶²⁴ Ti(OⁱPr)₄ and the ligand **3.40** were added to a solution of the sulfide and heated for one hour, after which time water was added. With this methodology no additional base was required in order to achieve high enantioselectivity.

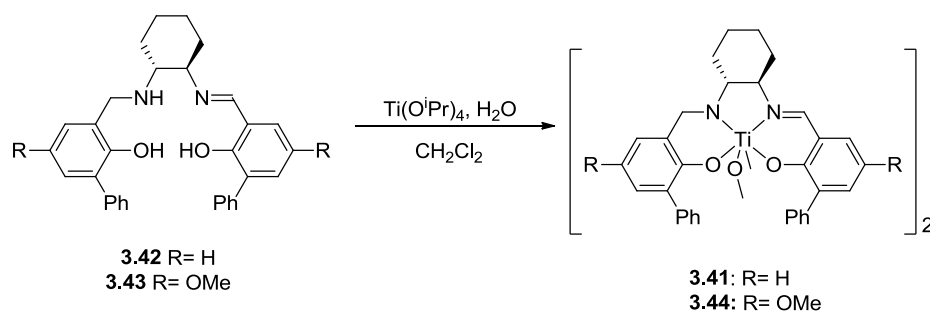


Scheme 3.12

The (*S*)-enantiomers of the PPIs Lansoprazole, Pantoprazole and rabeprazole (*S*)-**3.1-3.3** were all obtained in high yield and enantiopurity under this protocol (85-89%, 94-96% ee).

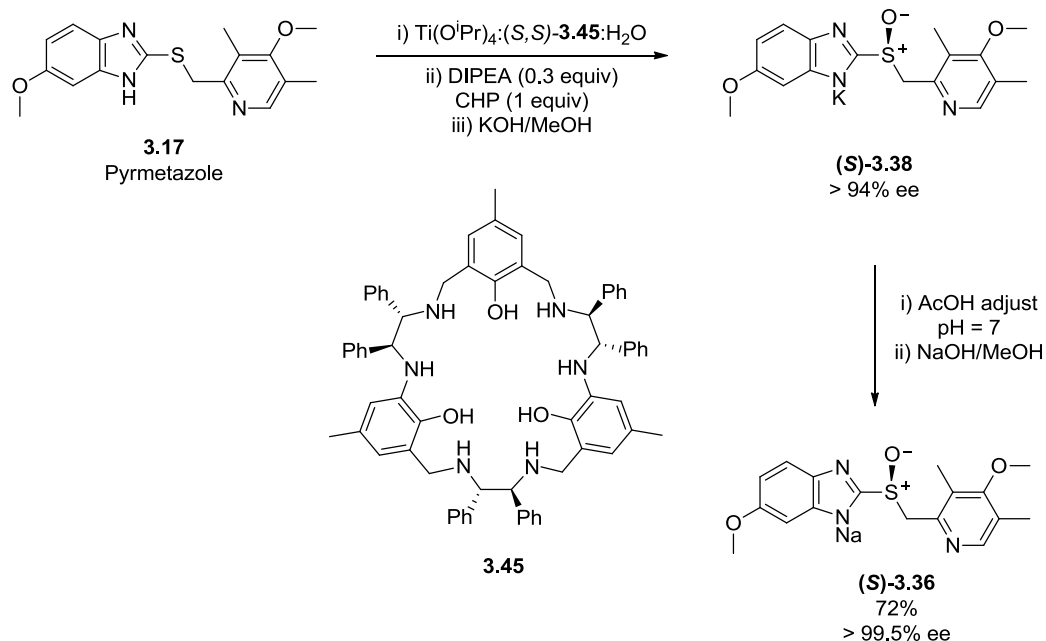


The asymmetric oxidation of Pymetazole **3.17** using the preformed titanium salalen complex **3.41**, prepared from $\text{Ti}(\text{O}^i\text{Pr})_4$ and ligand **3.42** (Scheme 3.13), was reported by Bryliakov and coworkers.^{387, 422, 625, 626} Despite the authors repeatedly discussing the synthesis of Esomeprazole (*S*)-**1.1** their results instead state that they obtained the (*R*)-enantiomer of Omeprazole. Nevertheless, the sulfoxide (*R*)-**1.1** was obtained in high yield and optical purity (96%, 96% ee) using a catalyst loading of 1%. It is presumed that using the opposite enantiomer of the chiral ligand would afford the (*S*)-enantiomer of the sulfoxide. Aqueous H_2O_2 (1.05 equiv) was employed as the oxidant, rendering it necessary for a two phase solvent system to be employed. (*R*)-Lansoprazole **3.1** was also obtained using this system, with the employment of the chiral ligand **3.43** to prepare the Ti-salalen complex **3.44**.



Scheme 3.13

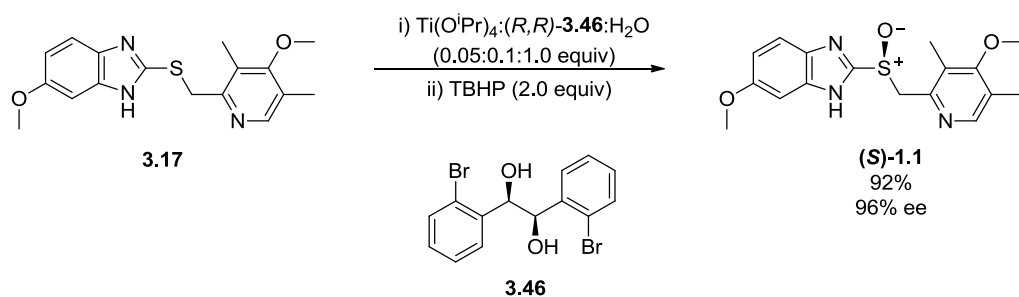
A titanium catalyst system formed *in situ* from $\text{Ti}(\text{O}^i\text{Pr})_4$ and the hexa-aza-triphenolic macrocycle ligand **3.45** was found to afford Esomeprazole as the sodium salt (*S*)-**3.36** in excellent enantioselectivity and high yield (72% yield, > 99.5% ee) (Scheme 3.14).⁶²⁷



Scheme 3.14

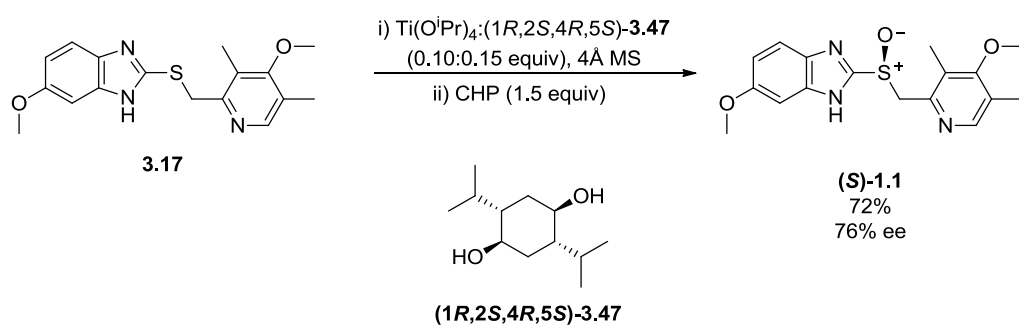
For this reaction $\text{Ti}(\text{O}^i\text{Pr})_4$ and water was added to a solution of macrocycle **3.45** in toluene then, after stirring for one hour at 25 °C, the sulfide substrate **3.17** was added followed by heating to 50 °C for a further 60 minutes. CHP (1.3 equiv) was employed as the oxidant and a base such as DIPEA was necessary for high enantioselectivity of the sulfoxidation reaction. A ratio of 1:2:2 for the ligand **3.45**: H_2O :DIPEA was established as optimal for the achievement of high sulfoxidation enantioselectivity. Examining the effect of catalyst loading on the reaction showed that the use of a $\text{Ti}(\text{O}^i\text{Pr})_4$:**3.45** ratio of 47:13 (mol%) gave Esomeprazole in excellent optical purity (> 99.5% ee), although a ratio of 66:13 also afforded the sulfoxide in high enantioselectivity (99% ee); it is unclear from the published data whether these figures relate to the sulfoxide product as the free base or as the final sodium salt form.

Jiang *et al.* developed a sulfoxidation procedure for the synthesis of Esomeprazole using the catalyst complex formed *in situ* from $\text{Ti}(\text{O}^i\text{Pr})_4$ and the hydrobenzoin type ligand **3.46**.⁶²⁸ In relative ratios of 1:2:10 $\text{Ti}(\text{O}^i\text{Pr})_4$:**3.46**: H_2O a catalyst loading of 5 mol% was employed, affording Esomeprazole (*S*)-**1.1** in high yield and enantiopurity (92%, 96% ee) (Scheme 3.15). The reaction was performed on a multigram scale and gave the sulfoxide in > 99% ee, obtained as the sodium salt (*S*)-**3.36** (70% yield). Using this catalyst system the (*S*)-enantiomers of the PPIs Lansoprazole, Pantoprazole and Rabeprazole (*S*)-**3.1-3.3** were also obtained in high yields and enantioselectivity (81-90%, 82-92% ee).



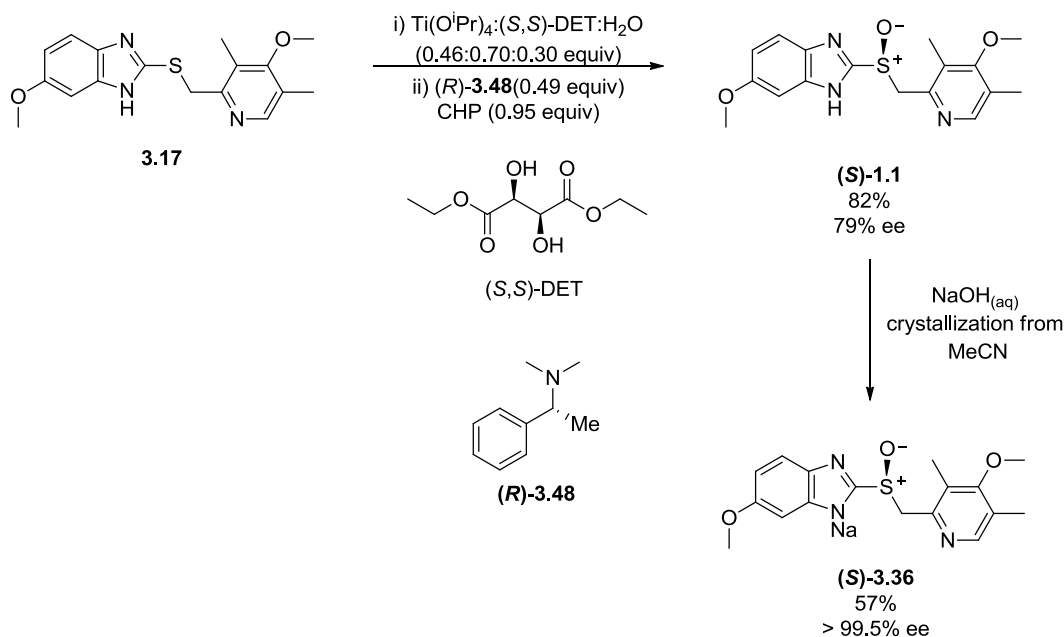
Scheme 3.15

Sun *et al.* employed the chiral diol **3.47** in the Ti-mediated asymmetric sulfoxidation of Pymetazole **3.17**.³⁷⁷ The catalyst complex was formed *in situ* from $\text{Ti}(\text{O}^i\text{Pr})_4$ and the diol, which were employed in a ratio of 0.10:0.15 (mol%) which equates to a catalyst loading of 10 mol%. Esomeprazole (*S*)-**1.1** was obtained in good yield and enantioselectivity (72%, 76% ee) (Scheme 3.16).



Scheme 3.16

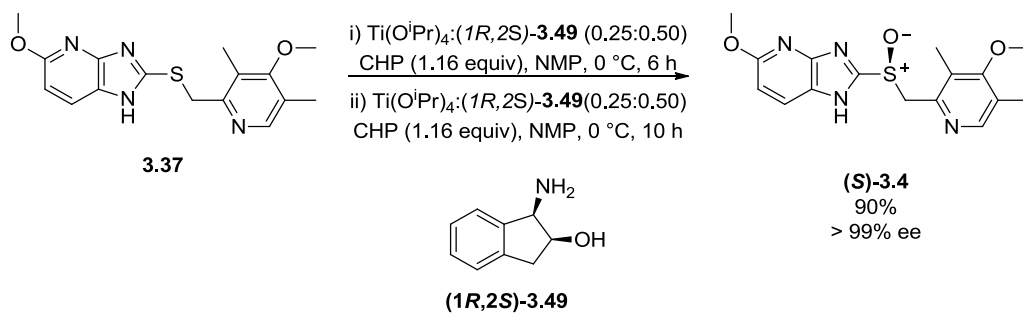
Khomenko and coworkers developed a method for the synthesis of Esomeprazole which mimicked the conditions used by von Unge *et al.* however instead of using DIPEA the chiral amine (*R*)-*N,N*-dimethyl-1-phenylethanamine was used instead.⁶²⁹ The catalyst complex formed *in situ* comprised of $\text{Ti}(\text{O}^i\text{Pr})_4$, (*S,S*)-DET and H_2O in a ratio of 46:70:30 (mol%), and was prepared in the presence of the sulfide **3.17**. Amine (*R*)-**3.48** (49 mol%) was added prior to addition of the oxidant CHP (0.95 equiv). Esomeprazole was obtained in 82% with an optical purity of 79% ee; conversion to the Na-salt (*S*)-**3.36** afforded the sulfoxide in 57% yields, with > 99.5% ee (Scheme 3.17).



Scheme 3.17

The use of the opposite enantiomer of the amine in an analogous procedure gave Esomeprazole (*S*)-**1.1** in similar yield but higher enantioselectivity (82%, 84% ee); transformation to the Na-salt (*S*)-**3.36** occurred giving an overall yield of 64% and optical purity of > 99.5% ee. It was proposed by the authors that the chiral amine acted as a second chiral ligand in the active catalyst complex as the change in absolute configuration of the amine had been observed to have an effect on the overall enantioselectivity of the reaction.

Kagan *et al.* examined the enantioselectivity of a range of asymmetric sulfoxidation reactions in order to identify the best procedure for the synthesis of Esomeprazole analogue (*S*)-Tenatoprazole (*S*)-**3.4**.⁶³⁰ Employment of Bolm's vanadium catalyzed asymmetric sulfoxidation method, using a catalyst complex formed from $\text{VO}(\text{acac})_2$ and a chiral Schiff base derivative saw (*S*)-Tenatoprazole (*S*)-**3.4** obtained in 80% ee, which was raised to 99% ee after two recrystallizations.⁴⁴² A tungsten mediated synthesis using a $(\text{WO})_3$ -cinchona alkaloid catalyst system, which had also been employed for the synthesis of (*S*)-Lansoprazole (*S*)-**3.1**, was also investigated in for the synthesis of (*S*)-Tenatoprazole, giving the sulfoxide (*S*)-**3.4** in good yield by only moderate enantioselectivity (75%, 41% ee).⁵¹² Under conditions similar to the von Unge Esomeprazole synthesis, including the use of the base DIPEA, the (*S*)-Tenatoprazole (*S*)-**3.4** was afforded in 63% ee and 73% yield. The best methodology found was a titanium mediated sulfoxidation which gave the target sulfoxide in the high yield and enantioselectivity (90%, > 99% ee) with $(1R,2S)\text{-cis}$ 1-amino-2-indanol $(1R,2S)\text{-3.49}$ used as the source of chirality (Scheme 3.18).

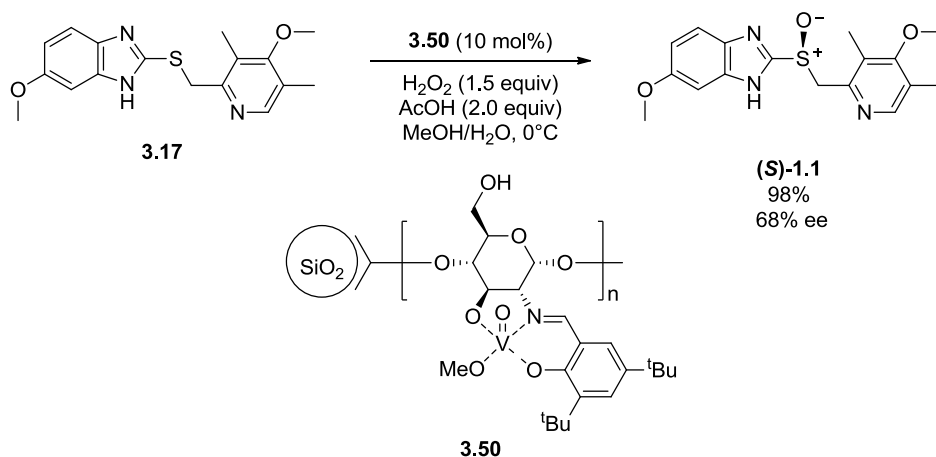


Scheme 3.18

A ratio of < 1:2 for $\text{Ti}(\text{O}^i\text{Pr})_4$:ligand was found to give the best results, and it was found that the addition of water to the reaction mixture had a deleterious effect on the chemical and optical yield of the sulfoxide. Ageing of the catalyst mixture was also found to be unfavourable. Other additives such as i -PrOH and DIPEA were found to have no effect upon the reaction outcome. The *cis* configuration of the β -amino alcohol was found to be crucial in ensuring a good enantiomeric outcome, and it was concluded that both the primary amine and hydroxyl group were important for good enantioselectivity. Curiously the reaction procedure sees the addition of the catalyst reagents and the oxidant carried out twice. $\text{Ti}(\text{O}^i\text{Pr})_4$ and the chiral ligand were added to the sulfide (in a ratio of 0.25:0.50 equiv) followed by 1.16 equiv of CHP. After stirring at 0 °C for 6 hours this process was repeated using the same amounts of each reagent. No explanation was included as to why the reaction was carried out in this manner.

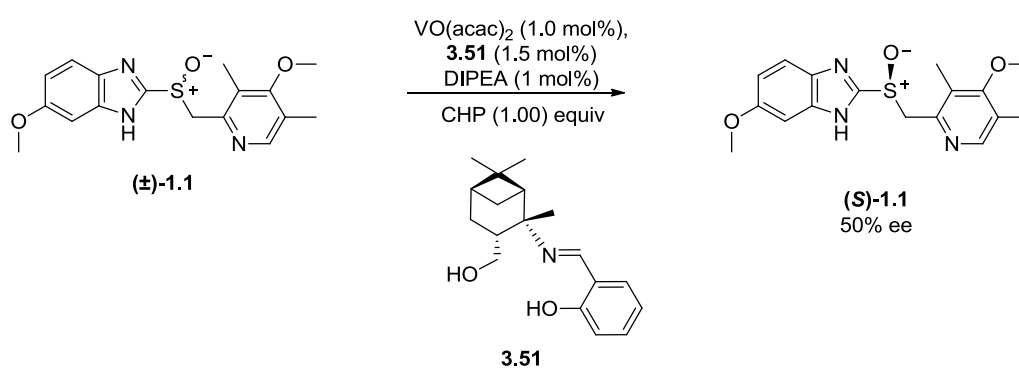
Vanadium mediated synthesis of Esomeprazole

The silica supported vanadium complex **3.50** was employed by Shen *et al.* as a heterogeneous catalyst for the asymmetric sulfoxidation of Pyrimetazole **3.17**.⁶³¹ Using H_2O_2 as the oxidant Esomeprazole (*S*)-**1.1** was obtained in high yield and good enantioselectivity (92%, 68% ee) (Scheme 3.19).



Scheme 3.19

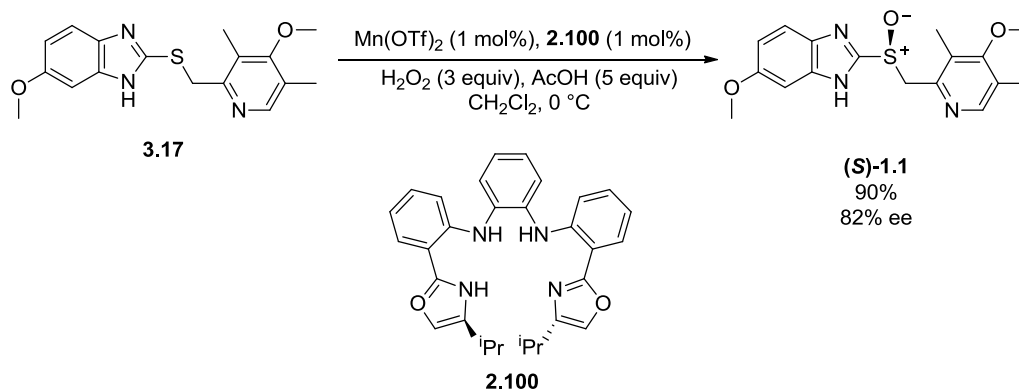
An oxidative kinetic resolution of racemic Omeprazole was reported by Khomento *et al.*⁶³² The active catalyst complex was formed *in situ* from VO(acac)₂ and the chiral ligand **3.51**; the base DIPEA was added to the catalyst complex solution prior to addition of the racemic sulfoxide which was then followed by addition of the oxidant (CHP, 1 equiv). A 1 mol% catalyst loading was employed, with a reagent ratio of 1.0:1.5:1.0 for VO(acac)₂:**3.51**:DIPEA. Enantioselective oxidation of the racemic sulfoxide gave Esomeprazole in 50% ee (Scheme 3.20). When DIPEA was excluded from the reaction mixture a complex mixture of products was obtained which was found to contain no sulfoxide. Using the catalyst system for the asymmetric oxidation of Pymetazole **3.17** gave Esomeprazole (*S*)-**1.1** in an optical yield of only 31% ee.



Scheme 3.20

Manganese mediated synthesis of Esomeprazole

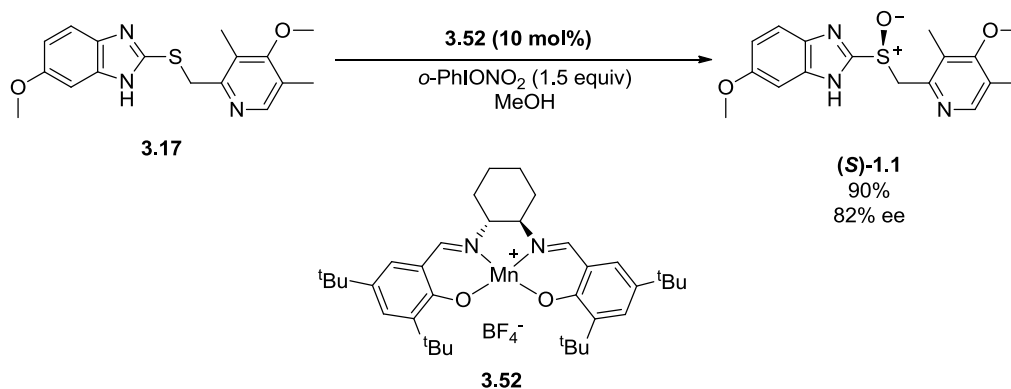
A gram scale asymmetric synthesis of Esomeprazole (*S*)-**1.1** was performed by Dai *et al.* using a porphyrin-inspired manganese catalyst complex which was formed *in situ* from Mn(OTf)₂ and the chiral ligand **2.100**.⁴⁶⁸ Esomeprazole (*S*)-**1.1** was obtained in a yield of 90% with an optical purity of 82% ee (Scheme 3.21).



Scheme 3.21

Kinetic resolution of the racemic sulfoxide Omeprazole (\pm)-**1.1** was also performed with this catalyst system; using 1 equiv of the oxidant and a catalyst loading of 1 mol%; Esomeprazole (*S*)-**1.1** was achieved in 89% ee, with a yield of 39%.

The synthesis of Esomeprazole was performed by Choi and coworkers using the manganese-salen catalyst complex **3.52** in a 10 mol% catalyst loading. The target sulfoxide was obtained in 70% ee with a yield of 59% (Scheme 3.22).⁶³³



Scheme 3.22

3.6 Summary

Omeprazole (\pm)-**1.1** is one of the most widely prescribed pharmaceuticals of all time. Used for the treatment of a number of stomach acid related conditions this drug is composed of a methylsulfinyl group flanked by a methoxy benzimidazole group on one side and a substituted pyridine on the other. Omeprazole (\pm)-**1.1** is a prodrug which is converted to the active form *in situ* and acts on the H⁺K⁺-ATPase pump which is the source of gastric secretions.

The single enantiomer drug Esomeprazole (*S*)-**1.1**, the (*S*)-enantiomer of Omeprazole (\pm)-**1.1**, was found to be superior to the original racemic sulfoxide in terms of efficacy and was found to reduce interpatient variability in acid inhibition. The synthetic approach to producing the chiral sulfoxide Esomeprazole (*S*)-**1.1** is typically via the enantioselective oxidation of the prochiral sulfide Pyrimetazole **3.17**, although procedures have also been reported for the isolation of Esomeprazole (*S*)-**1.1** via resolution of the racemic sulfoxide.

Oxidations have been reported which use biological agents and non-metal based reagents, such as oxaziridines. Metal based catalyst systems are a popular choice for the asymmetric synthesis of Esomeprazole (*S*)-**1.1**. Both vanadium and manganese based catalyst systems have been

reported to facilitate the oxidation of Pyrimetazole **3.17**, to give Esomeprazole in high enantioselectivity. Titanium based catalyst systems are the most commonly employed, with a range of different ligands explored, however relatively high catalyst loadings are required in order to obtain the target sulfoxide in high enantioselectivity.

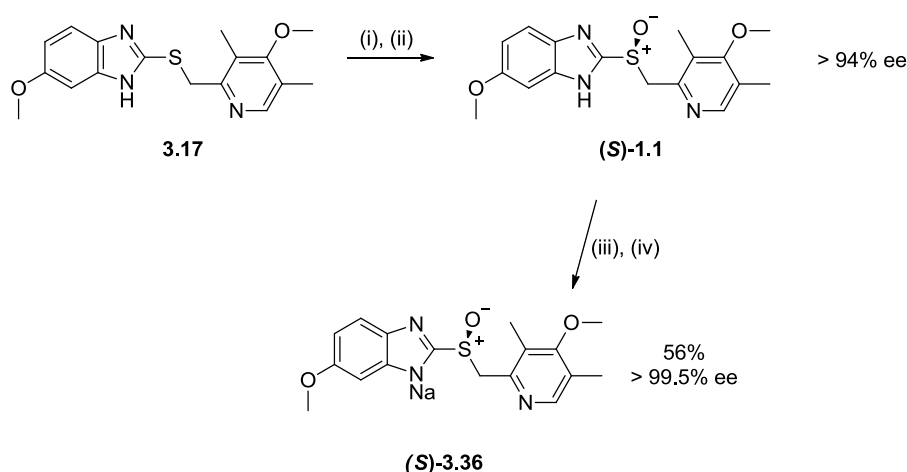
The development history of Omeprazole and Esomeprazole is described by Federsel, and Lindberg and Carlsson.^{15, 519, 556, 557, 600} Federsel provides insight into the processes involved in taking the production of the single enantiomer sulfoxide Esomeprazole (*S*)-**1.1** from mg scale to a multikilogram scale suitable for the industrial synthesis of the drug. The large scale synthesis, which was reported by von Unge *et al.*, employs a titanium-tartrate based catalyst system for the asymmetric oxidation of the Omeprazole sulfide Pyrimetazole **3.17** using the oxidant cumene hydroperoxide.¹²⁵ Catalyst equilibration and ageing steps, as well as the addition of the base DIPEA, are reported to be essential for the achievement of high enantioselectivity.

4 Results and Discussion: Asymmetric synthesis of Esomeprazole

4.1 Project aims

The asymmetric synthesis of the blockbuster drug Esomeprazole (**S**)-**1.1** is one of the great successes of the pharmaceutical industry (Scheme 4.1). Although a method has been developed which enables the asymmetric formation of Esomeprazole (**S**)-**1.1** in high optical purity, the high level of catalyst loading remains problematic. In the large scale synthesis, 2.35 kg of tartrate, 1.6 kg of $\text{Ti}(\text{O}^i\text{Pr})_4$, and 3.3 kg of oxidant (cumene hydroperoxide, CHP) are required in order to produce 3.83 kg of pure product.¹²⁵ Although the industrial process is likely to be more efficient there is still potential for improvement in terms of a reduction of catalyst loadings and simplification of the process. These modifications would not only lower costs in terms of starting materials but also reduce the amount of by-product waste, which may require specialist disposal considerations.

In addition to the low catalyst turnover, the process also affords the target sulfoxide in only moderate yields. For the two steps from sulfide **3.17** to sodium salt (**S**)-**3.36**, von Unge *et al.* report an overall yield of only 56% when using a 30 mol% catalyst loading (Scheme 4.1). In the same paper the authors report that upon completion of the S-oxidation reaction that the ratio of sulfoxide:sulfone in the crude material was 76:1 and that the conversion of the sulfide starting materials was 92%. It is apparent that a substantial amount of material is lost in the course of the workup procedure and/or during formation of the Na-salt.

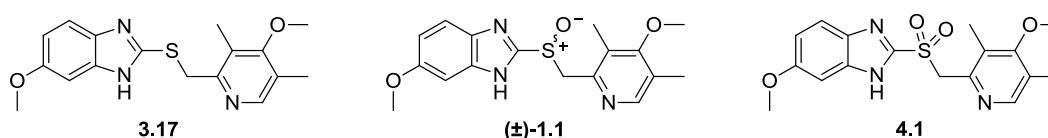


Scheme 4.1 Reagents and conditions: (i) $\text{Ti}(\text{O}^i\text{Pr})_4$:(S,S)-DET: H_2O (0.3:0.6:0.1 equiv relative to sulfide **3.17**), toluene, 54°C, 50 min; (ii) DIPEA:CHP (0.3:1), 30°C, 1h; (iii) NaOH (0.7), MIBK; (iv) crystallization from methyl isobutyl ketone and MeCN

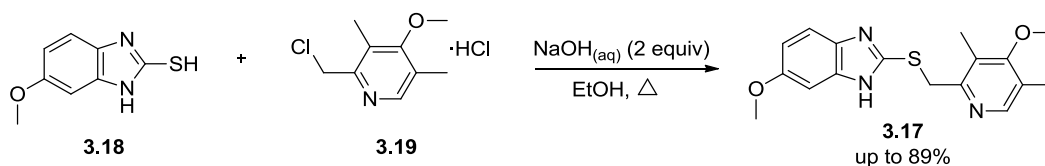
The primary objective of our studies was to gain insight into the Ti-tartrate mediated S-oxidation involved in the synthesis of Esomeprazole. It was our expectation that by studying the processes in detail we could achieve a greater understanding of some of the basic mechanistic features such as the effect of additives (e.g. water and amines), reaction times and temperatures and the effect of solvent choice, and to ascertain more information on the mechanism of asymmetric induction and identify the active catalyst species. In the course of this process we hoped to identify some of the limitations of the current methodology, and it was our long term goal to develop methods by which we could overcome these issues, potentially improving catalyst efficacy and/or developing a novel catalyst system.

4.2 Preparation of racemic Omeprazole and related compounds

To enable a detailed investigation into the Ti-mediated asymmetric synthesis of Esomeprazole (*S*)-**1.1** it was first necessary to prepare the sulfide precursor Pyrimetazole **3.17**, the racemic sulfoxide Omeprazole (\pm)-**1.1**, and the corresponding sulfone **4.1** in order to gather spectroscopic data on the different species, and in the case of the sulfide to produce materials for use in the asymmetric sulfoxidation reactions.

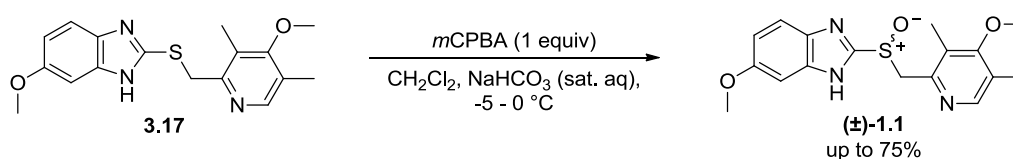


Thiol **3.18** and the pyridine salt **3.19** were reacted in the presence of two equiv of NaOH to give sulfide **3.17** in yields up to 89% (Scheme 4.2). This reaction was carried out on a scale of up to 30 g. The sulfide product was afforded as a colourless gum, which proved difficult to manipulate. Purification was achieved via column chromatography followed by trituration with diethyl ether which converted the material to a powder, allowing for greater ease of handling. The structure of Pyrimetazole **3.17** was confirmed by X-ray crystallography (discussed further in section 6.1).



Scheme 4.2

The racemic sulfoxide Omeprazole (\pm)-**1.1** was obtained via *m*CPBA oxidation of Pyrimetazole **3.17**. The use of a two phase solvent system was found to be necessary due to the sensitivity of the sulfoxide product to acid; using a system that had previously been employed within our research group one equiv of the oxidant was added dropwise to the sulfide in CH_2Cl_2 in the presence of NaHCO_3 (sat. aq.) which neutralised the benzoic acid by product of the sulfide oxidation.⁶⁹ This reaction was performed on a multigram scale, affording the sulfoxide product in conversions up to 97% from the sulfide (as measured by ^1H NMR analysis of the crude materials) in yields up to 75% (Scheme 4.3). The structure of the afforded sulfoxide was confirmed by X-ray crystallographic analysis. Over oxidation to the corresponding sulfone was minimized by slow addition of the oxidant under high dilution conditions.

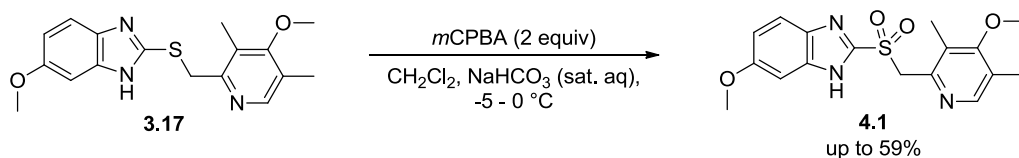


Scheme 4.3

Omeprazole was found to be challenging to work with and a great amount of time and effort was required to understand the properties of this compound in order to allow successful synthesis, isolation, and handling of the sulfoxide in both the racemic and single enantiomer form. Column chromatography was found not to be a viable method of purification due to the limited solubility of the racemic Omeprazole crude materials in the eluents which gave the best separation of the sulfide, sulfoxide and sulfone materials arising from the oxidation. Visible degradation of the sulfoxide was observed during attempts at column chromatography, with the colourless sulfoxide degrading to give materials purple in colour with an associated significant loss of material on the column. Purification of the crude racemic sulfoxide was eventually achieved through crystallization from CH_2Cl_2 by addition of diethyl ether which acted as an antisolvent.

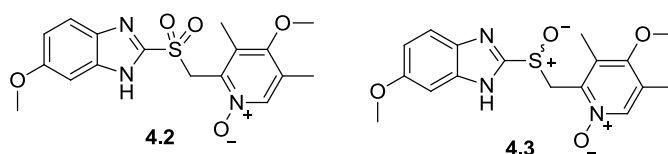
In addition to instability towards acidic conditions it is also known to be heat, light and moisture sensitive.⁶³⁴ When stored at rt for a number of weeks in a sealed glass container a significant change of colour was observed in the material, from colourless to light brown/purple. There was however very little difference found in the ^1H NMR spectra of the discoloured sulfoxide material compared to freshly produced Omeprazole, suggesting that the discolouration comes from the formation of a very small amount of highly coloured impurities; repurification of discoloured Omeprazole was achieved easily by dissolution in dichloromethane, treatment with activated charcoal and MgSO_4 followed by addition of diethyl ether to induce crystallization.

Synthesis of the Omeprazole sulfone was also carried out by oxidation of the sulfide **3.17** using *m*CPBA (2.0-2.5 equiv), again using the two phase solvent system of dichloromethane and NaHCO₃, affording the sulfone **4.1** in yields of up to 59% (Scheme 4.4).



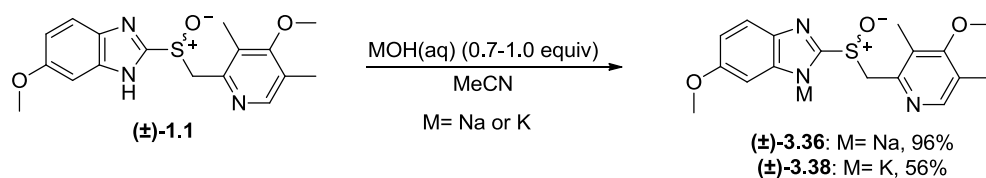
Scheme 4.4

The improved stability of the sulfone **4.1** compared to the sulfoxide **1.1** allowed for purification via column chromatography. Although recrystallization was possible it was found that any sulfone material recovered was in the form of the solvate of the recrystallization solvent; x-ray crystallography found the sulfone as the MeOH solvate. The *N*-oxide **4.2** was a common side product of this reaction, and could be easily identified by ¹H NMR by the characteristic singlet peak at 5.35 ppm corresponding to the CH₂ protons, compared to the sulfone which gave a singlet at 5.02 ppm for the same protons.⁶³⁵ The analogous sulfoxide *N*-oxide **4.3** was identified in crude materials from the synthesis of Omeprazole **1.1** by *m*CPBA oxidation but not isolated. The formation of this species occurred in amounts typically less than 2% of the sulfoxide yield and could be identified by ¹H NMR from a singlet occurring at 4.81 ppm corresponding the CH₂ protons.⁶³⁵



The alkali metal salts of Omeprazole are known to have increase stability compared to the neutral form.⁵⁵⁷ Sodium Omeprazole (±)-**3.36** was obtained via treatment of the racemic sulfoxide **1.1** with sodium hydroxide (0.7-1.0 equiv, ~ 50% w/w aqueous solution) (Scheme 4.5). Precipitation of the Omeprazole salt from MeCN was at times spontaneous, or could be induced by concentration of the solution under vacuum and/or seeding or scratching the flask. Crystallization could also be invoked by dropwise addition of the diethyl ether antisolvent. The potassium salt of Omeprazole was also synthesized using a similar methodology as the sodium salt is believed to produce crystals that are too small for analysis by single crystal X-ray diffraction (XRD).⁶³⁶ Crystals obtained of the K-salt (±)-**3.38** were found to be sufficient for

analysis by XRD; further discussion of the crystal structures of Omeprazole **1.1** and related species can be found in section 6.1.



Scheme 4.5

4.2.1 Spectroscopic and chromatographic analysis of Omeprazole and related compounds

^1H NMR spectroscopy was used to determine the level of oxidation of the products arising from the oxidation of sulfide Pyrimetazole **3.17**. Figure 4.1 shows the ^1H NMR spectra obtained using DMSO-d_6 whilst Figure 4.2 shows the spectra obtained using CDCl_3 .

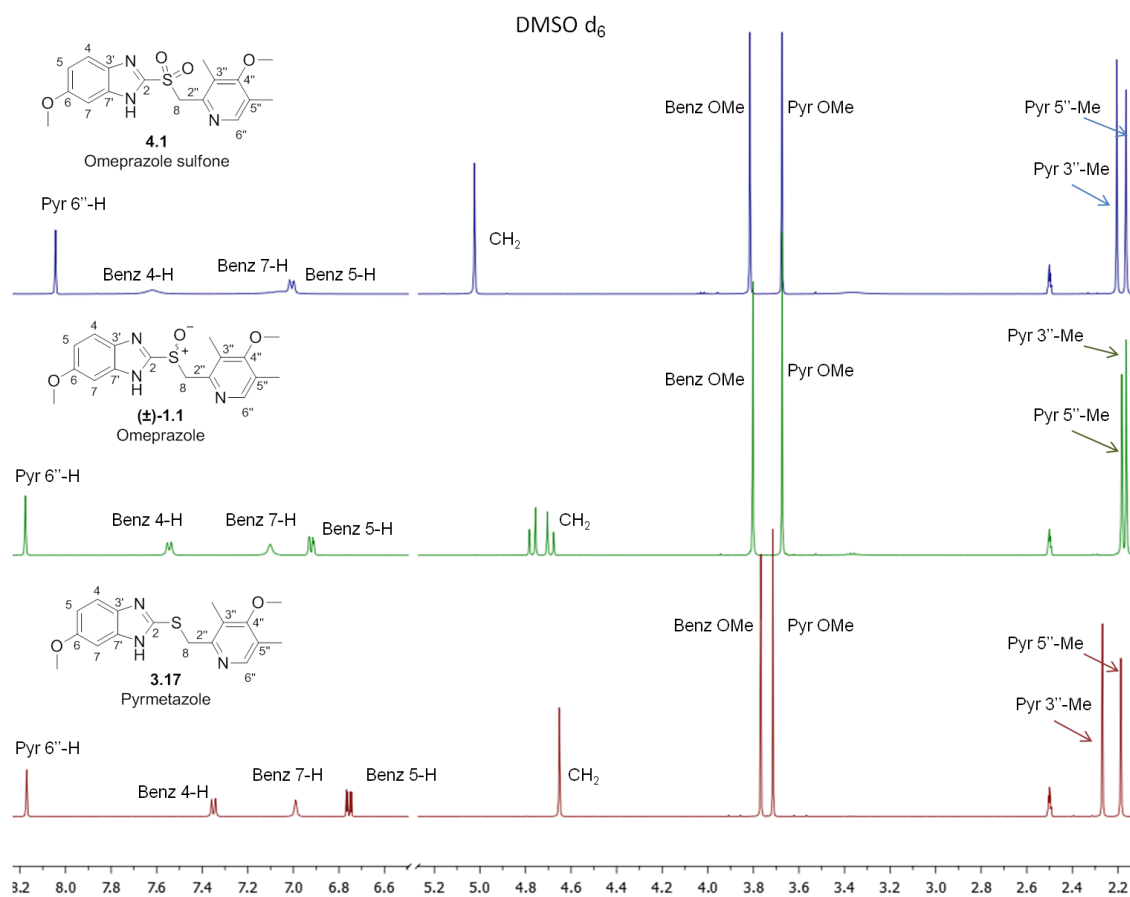


Figure 4.1 ^1H NMR spectra of Pyrimetazole **3.17**, Omeprazole **1.1**, and Omeprazole sulfone **4.1** in DMSO-d_6

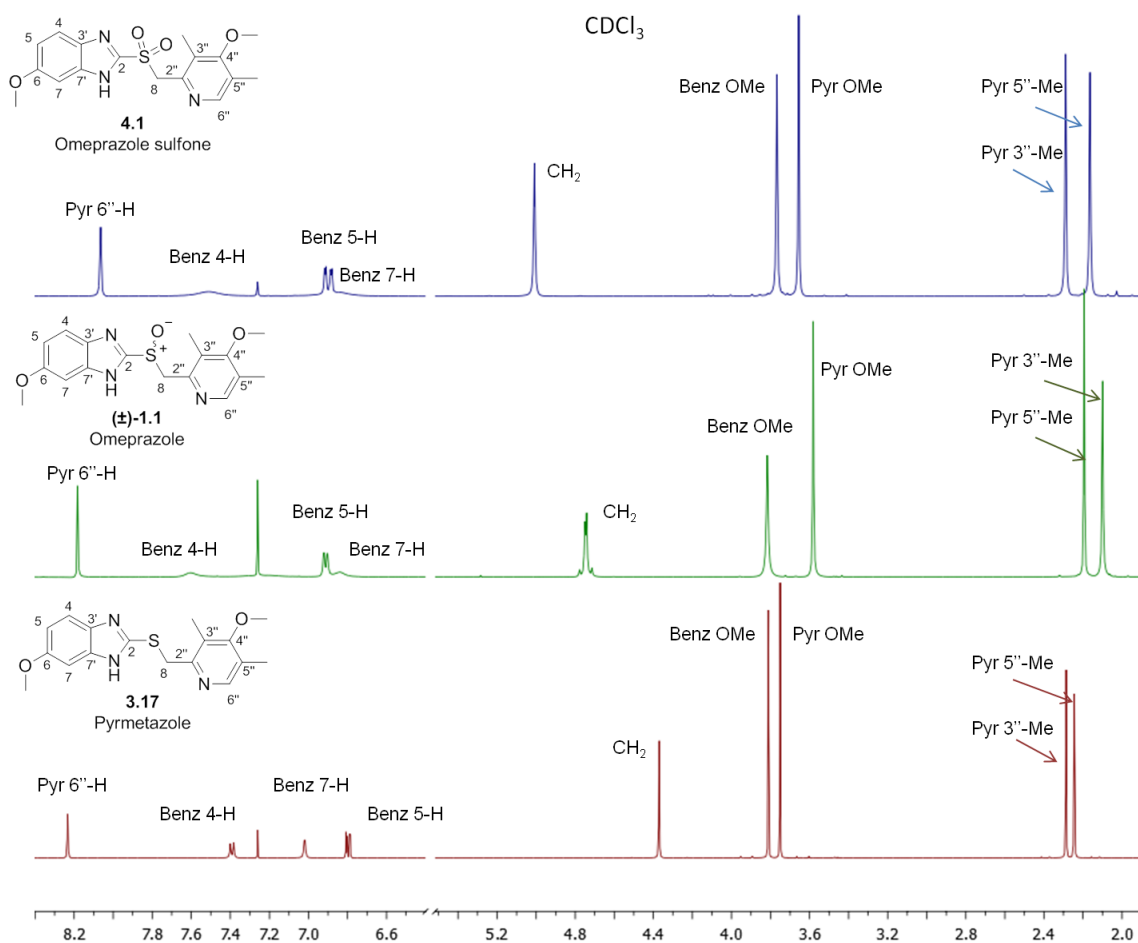


Figure 4.2 ¹H NMR spectra of Pyrimetazole **3.17**, Omeprazole **1.1**, and Omeprazole sulfone **4.1** in CDCl₃

Characteristic AB signals were observed for the diastereotopic CH₂ protons of the racemic sulfoxide **1.1** with DMSO-d₆ as the NMR solvent; when CDCl₃ was employed as the solvent the AB pattern of the diastereotopic protons was less pronounced. The methylene protons of the corresponding sulfone **4.1** and sulfide **3.17** were observed as singlets, with enhanced deshielding observed going from sulfide to sulfoxide to sulfone (Figures 4.1 and 4.2). The opposite effect was observed for the signal corresponding to the pyridine 6''-H, which was observed at a lower frequency for the sulfone **4.1** in comparison to the Omeprazole **1.1** and Pyrimetazole **3.17**.

Tautomerization of the benzimidazole heterocycle was observed as broadening of the aromatic proton signals, and was observed to a greater extent in samples using CDCl₃ as the NMR solvent. Tautomerism of Omeprazole will be discussed further in section 6.2. Interestingly the signal for the pyridyl 3''-Me was observed at a lower frequency than the 5''-Me for the sulfoxide, whereas for the sulfide or sulfone it is the 5''-Me protons which are observed further upfield. This may be due to the anisotropic effect of the S=O group on the protons of the

3''-Me group, or due to aggregation of the sulfoxide in solution, with the formation of heterochiral dimers altering the chemical shift of the pyridyl 3''-Me protons.^{637, 638}

The relative ratios of sulfide:sulfoxide:sulfone in a crude product could be determined from the signals of the CH₂ protons. These signals easily distinguished from each other in the ¹H NMR spectra when CDCl₃ was used as the solvent (Figure 4.2), however an overlap between the sulfide and sulfoxide CH₂ proton signals was found when DMSO-d₆ was used, which was often necessary for NMR comparison with compounds insoluble in CDCl₃. Where this was the case the relative ratios of the species could be determined by assessing each half of the sulfoxide AB signal separately and calculating the difference in peak integration arising from the overlapping sulfide signal (Figure 4.3).

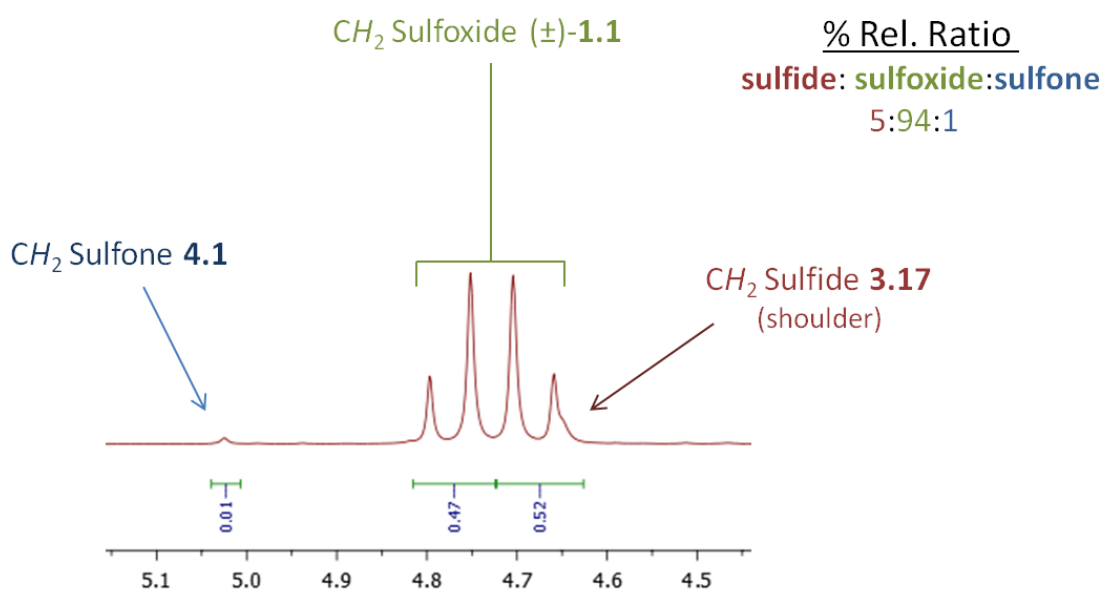


Figure 4.3 Partial ¹H NMR spectra of a mixture of Pyrimetazole 3.17, Omeprazole 1.1, and Omeprazole sulfone 4.1 in DMSO-d₆ illustrating how relative ratios of each species can be deduced from integration of characteristic proton signals

The formation of Na-Omeprazole 3.36 gave rise to a distinct change in the appearance of the CH₂ protons compared to the neutral sulfoxide 1.1 (Figure 4.4). An accompanying upfield shift was observed for the benzimidazole protons of the Na-salt 3.36.

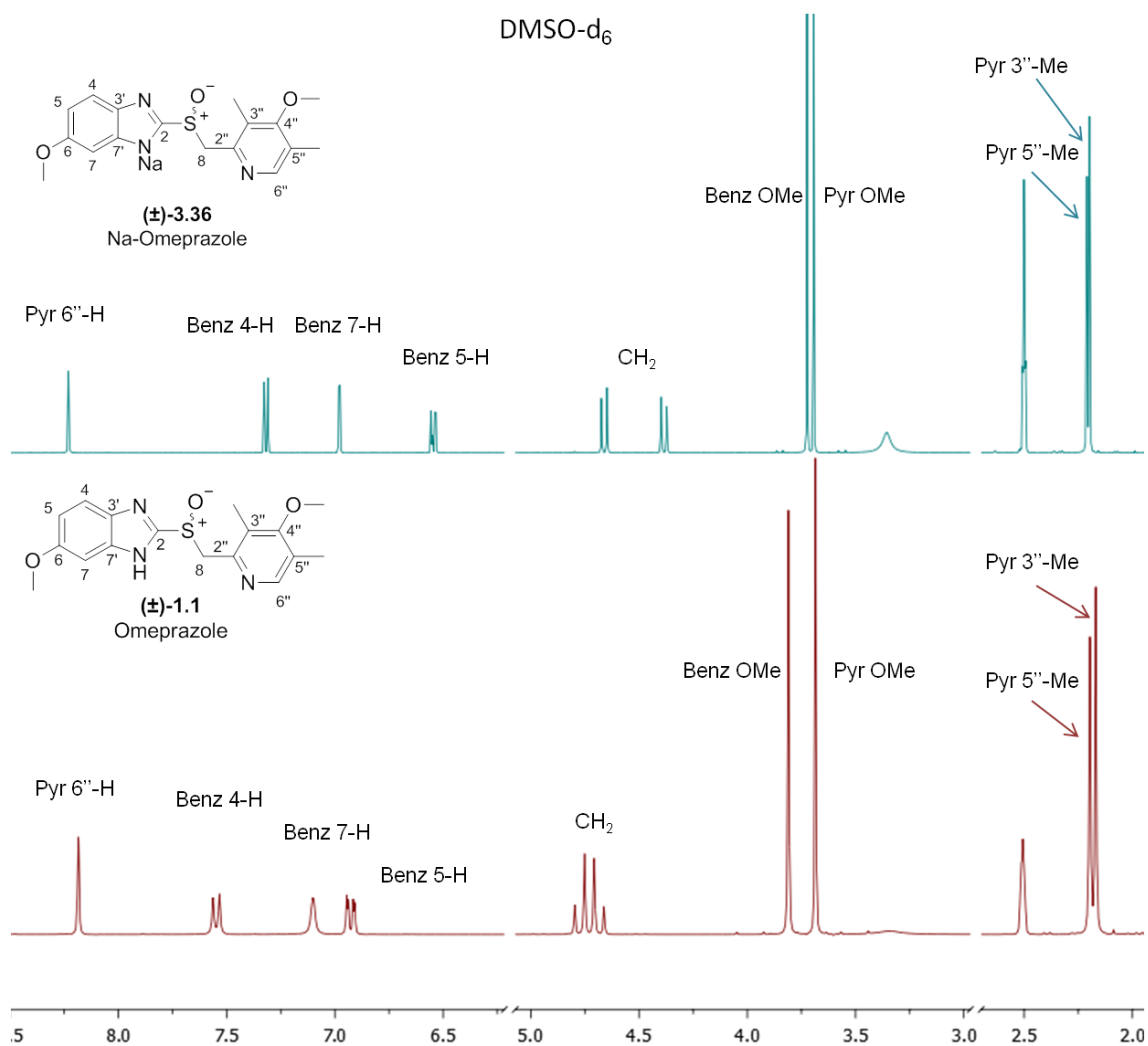


Figure 4.4 ¹H NMR spectra of Na-Omeprazole **3.36** and Omeprazole **1.1**, both in DMSO-d₆

It was often found that the CH₂ protons of Na-Omeprazole **3.36** were depleted or indeed absent from the ¹H NMR spectra; this phenomena was attributed to H/D exchange of the acidic protons with the NMR solvent (DMSO d₆), this shall be discussed further in section 6.3.

The enantiomeric purity of Esomeprazole (*S*)-**1.1** was determined by chiral HPLC, using a Chiracel OD-H column. The chromatographs for racemic Omeprazole (±)-**1.1** and enantioenriched Esomeprazole (*S*)-**1.1** (90% ee) are illustrated in Figure 4.5 and 4.6 respectively.

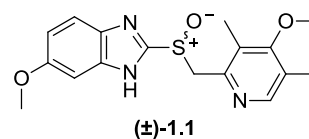
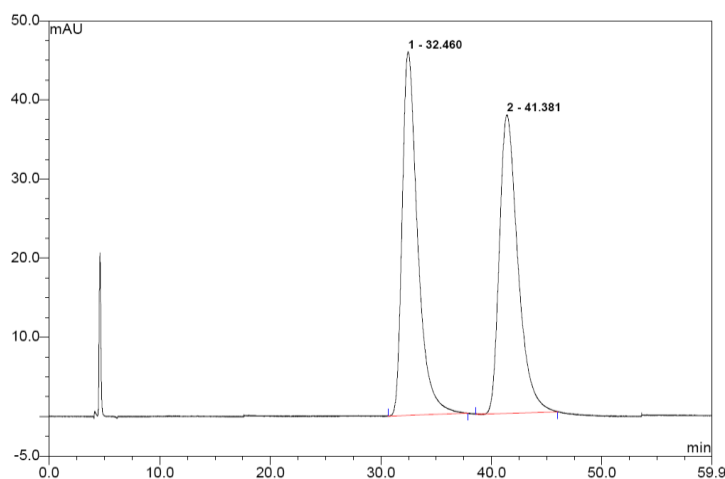


Figure 4.5 Chromatograph of racemic Omeprazole **1.1**; t_R ($S_{enantiomer}$) = 35.5 min, t_R ($R_{enantiomer}$) = 41.4 min
[Chiracel OD-H; flow rate 1.0 mL min⁻¹; 5% ethanol–hexane; 20 °C]

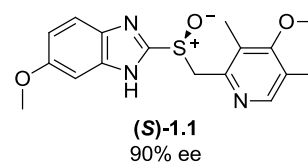
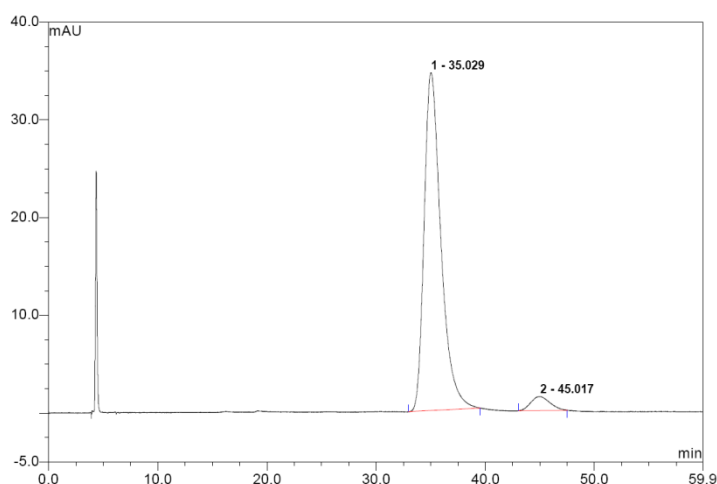


Figure 4.6 Chromatograph of Esomeprazole (**(S)**)-1.1 (90% ee); t_R (S_{major}) = 35.0 min, t_R (R_{minor}) = 45.0 min
[Chiracel OD-H; flow rate 1.0 mL min⁻¹; 5% ethanol–hexane; 20 °C]

The absolute configuration of the enantioenriched sulfoxide **1.1** was determined by comparison with the NMR data reported by Redondo *et al.* who used (*S*)-BINOL (**(S)**-1.43 as a chiral shift reagent for the determination of enantiomeric purity of Esomeprazole (**(S)**-1.1. As part of our work, enantiomerically pure tartrates, such as (*S,S*)-diethyl tartrate, (*S,S*)-diisopropyl tartrate and (*R,R*)-dimethyl tartrate, were identified as alternative, inexpensive chiral shift reagents for enantiomeric determination of sulfoxides such as Esomeprazole (**(S)**-1.1; this work is reported in chapter five.

4.2.2 ¹H NMR characterization of Omeprazole vs. Esomeprazole

During the course of this research it was observed that solutions of Omeprazole and Esomeprazole in CDCl₃ gave significantly different ¹H NMR spectra. As the enantiopurity of

the sulfoxide substrate **1.1** increased from 0% ee to 100% ee it was found that the pyridyl methoxy group showed a downfield shift of 0.08 ppm, whereas the benzimidazolyl methoxy group shifted upfield by less than 0.01 ppm (Figure 4.7). Similarly the 3''-Me group on the pyridine ring moved down field by 0.08 ppm as the enantiopurity of the sulfoxide increased from 0 to 100%, however the 5''-Me group was observed to be barely affected with a change of less than 0.01 ppm upfield.

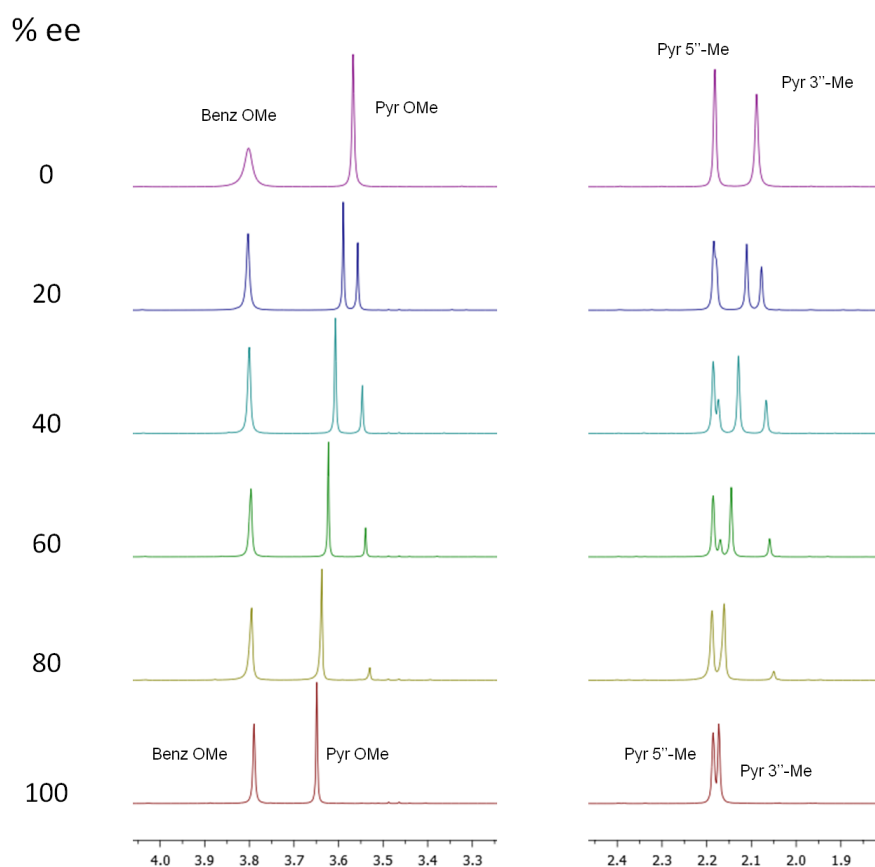
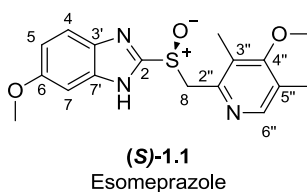


Figure 4.7 ^1H NMR (CDCl_3) of Esomeprazole from 0% ee to 100% ee

These findings are consistent with work reported by Albert *et al.* who investigated this phenomena through ^1H NMR monitoring of the online titration of the Omeprazole solutions from 100% (*R*)-enantiomer through to 100% (*S*)-enantiomer.⁶³⁷ In addition to the reported findings of Albert *et al.* we observed distinct changes to the appearance of the CH_2 protons and certain protons of the benzimidazole group. With increasing % ee of the sulfoxide solution the CH_2 group coalesces to give a singlet at 4.80 ppm, in contrast to the characteristic AB system

observed for the racemic sample of the sulfoxide (Figure 4.8). In addition, the chemical shifts of the broad signals corresponding to the benzimidazole 4-H and 7-H protons are also observed to change, with the Benz 7-H proton undergoing a downfield shift of up to 0.15 ppm as the optical purity of the sulfoxide was increased.

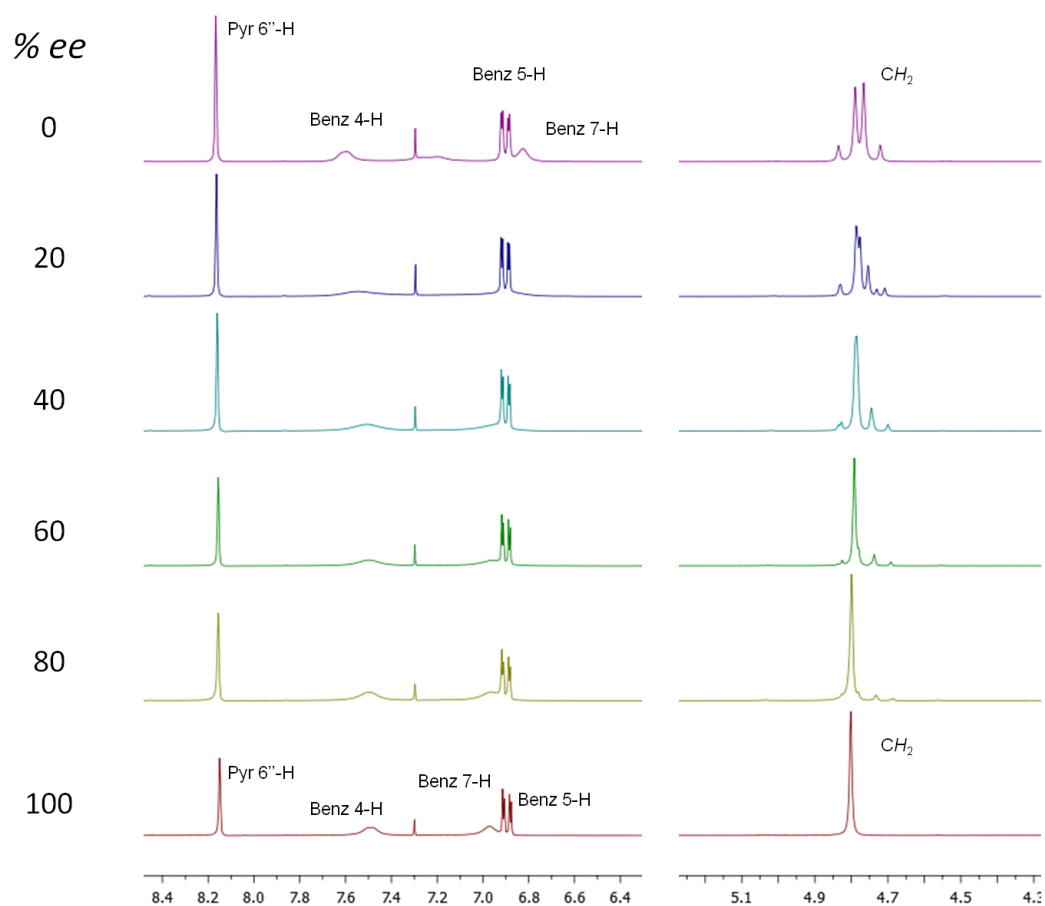


Figure 4.8 ^1H NMR (CDCl_3) of Esomeprazole from 0% ee to 100% ee

Albert and coworkers proposed that the origin of the differences in chemical shifts observed for racemic Omeprazole compared to the single enantiomer form (either (*R*)- or (*S*)- enantiomer) may be due to the formation of heterochiral dimers in solution, such as that shown in Figure 4.10. Dimerization takes place over the SO-H-N bonds generating a 10 membered chair conformation with π - π stacking of the heterocyclic rings stabilizing the structure. In an aggregation of this type the methoxy and 3''-Me group of the pyridine ring would be subject to the ring current effects, whereas the benzimidazole methoxy group, and the pyridyl 5''-Me would be less affected. This proposed structure is identical to that reported for the crystal structure of racemic Omeprazole in the solid state, and the crystal structure obtained from XRD analysis of Omeprazole obtained during this work (Figure 4.9).⁵⁷² Further discussion of the solid state structure of Omeprazole and related compounds can be found in section 6.1.

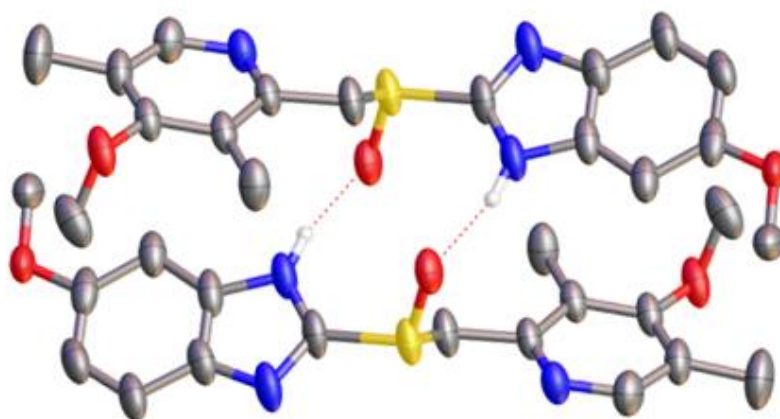


Figure 4.9 Crystal structure of Omeprazole showing the structure of the heterochiral dimer; displacement of ellipsoids are at the 50% probability level and hydrogen atoms are omitted for clarity

Comparison of the structures of the heterochiral dimer and the two possible homochiral dimers of omeprazole reveals the importance of the orientation of the sulfinyl group with respect to the formation of hydrogen bonds. Whereas the heterochiral dimer is able to form two hydrogen bonding between the sulfoxide molecules, in the homochiral dimers the orientation of the sulfinyl groups allows for only one H-bond to form, thus reducing the stability of the overall intermolecular interactions.

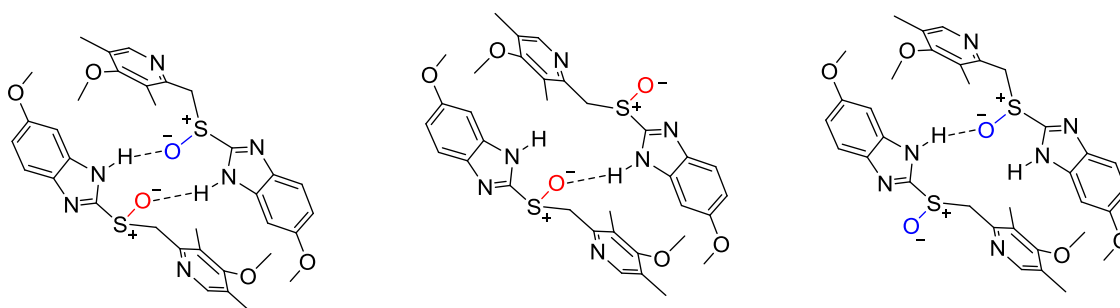


Figure 4.10 Heterochiral (left) and homochiral dimers (centre and right) of Omeprazole 1.1

4.3 The Asymmetric synthesis of Esomeprazole

Early attempts to study the titanium tartrate mediated asymmetric synthesis of Esomeprazole (*S*)-**1.1** gave disappointing results. Using a scaled down version of the literature procedure published by von Unge *et al.* the target sulfoxide was afforded in low optical and chemical yields, with poor reproducibility.¹²⁵ In addition isolation and purification of the reaction products was extremely difficult. The work up procedure involved quenching of the reaction using aqueous ammonium hydroxide, separation of the phases, then acidification of the aqueous

phase and extraction of the sulfoxide; during the quenching process large amounts of insoluble titanium salts were produced which made separation of the phases extremely difficult. Attempts to remove the titanium dioxide via filtration through a number of different media did not work, and on occasion was found to exacerbate the problem. Although ^1H NMR analysis of the crude products indicated the presence of the desired sulfoxide, large amounts of tartrate and cumyl alcohol were also identified. Unfortunately it was believed that purification via column chromatography was not feasible for Esomeprazole (*S*)-**1.1** as attempts at chromatography of the racemic sulfoxide had led to decomposition of the material on the column. Chiral HPLC analysis performed on the crude materials showed the presence of many unidentifiable species, suggested that decomposition of the sulfoxide was occurring during, or prior to HPLC analysis.

Although the synthesis, isolation, and subsequent handling of Esomeprazole were initially found to be more difficult than anticipated, through greater understanding of the properties of Omeprazole and Esomeprazole many of these issues were eventually resolved. Improvements were made to the work up procedure which allowed for greater ease in isolating the target sulfoxide; quenching of the reaction, by addition of aqueous ammonium hydroxide, was followed by vigorous stirring of the mixture, after which the mixture was allowed to settle. This process improved the efficiency in the removal of the insoluble titanium dioxide, achieved via filtration through a pad of Celite, and as a result allowed for better subsequent phase separation. The crude materials afforded from this work up process were found to contain less tartrate material, presumably due to hydrolysis during the extended quenching process.

In contrast to the racemic sulfoxide Omeprazole, which was obtained as fine colourless crystalline platelets, Esomeprazole (*S*)-**1.1** was obtained as a colourless oil that dried to a glassy foam under vacuum. The enantioenriched sulfoxide was found to be more soluble in a range of solvents compared to the racemate, and this improved solubility allowed for column chromatography to be used for purification as the sulfoxide material was able to pass through the stationary phase at a more rapid pace. The contrast between the physical forms of the racemic sulfoxide and enantioenriched Esomeprazole is in agreement with the models proposed in Figure 4.9, with the formation of heterochiral dimers held together by two hydrogen bonds leading to a crystalline product for racemic Omeprazole, whereas the enantioenriched sulfoxide, unable to form such stable dimers was obtained in the form of a glassy oil with greater solubility properties compared to the racemate.

Esomeprazole (*S*)-**1.1** is known to undergo self-disproportionation of enantiomers during chromatography, where the process of achiral gravity driven or flash chromatography can cause aggregation of enantiomers and lead to fractionation of the enantiomerically enriched sulfoxide

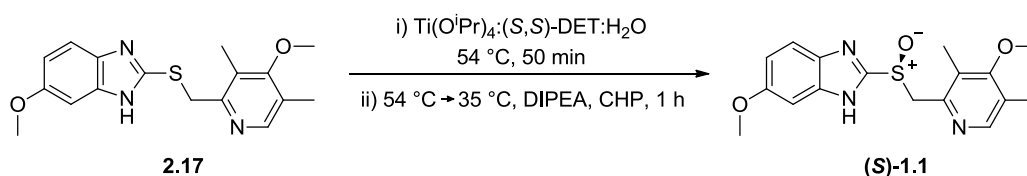
which for Esomeprazole would be observed as enrichment of ee in early fractions, and depletion of ee in later ones.¹⁵⁰ In order to avoid errors in determining the enantioselective outcome of the Ti-mediated asymmetric sulfoxidation process chromatography of the sulfoxide products was conducted with care to combine all fractions of the sulfoxide prior to chiral HPLC or ¹H NMR analysis for the determination of enantioselective excess.

Optimization of the chiral HPLC conditions was the most critical factor in allowing investigation into the asymmetric synthesis of Esomeprazole (*S*)-**1.1**. Reevaluation of the HPLC conditions used previously revealed that the poor results previously encountered with respect to enantioselectivity and reproducibility were not due to the reaction itself, but were an artifact of the HPLC conditions, in particular the use of a reversed phase column and the solvent system required for separation on that column, which were causing decomposition of the sulfoxide during analysis. Using a normal phased column for chiral HPLC allowed for the use of a solvent system and conditions under which no sulfoxide decomposition was observed during analysis and thankfully accurate measurement of product ee was achieved. In addition to withstanding the modified HPLC conditions, sulfoxide (*S*)-**1.1** was actually found to be more robust than previously assumed, with degradation occurring over a much longer time period, and to a lesser extent than previously thought; this extended to the crude reaction materials which had not yet been subjected to purification. ¹H NMR of these crude materials showed very little degradation after 10 days, whereas previously it was thought possible that decomposition may have been occurring, in a much shorter time frame, before HPLC analysis could be performed on the samples. Esomeprazole material acquired following column chromatography could be stored in a sealed glass container at rt for a number of days with very little degradation observed by ¹H NMR or by any observable change in colour typically associated with decomposition of this sulfoxide.

An additional factor that aided in the analysis of products afforded by the Ti-mediated synthesis of Esomeprazole (*S*)-**1.1** was the development of a new NMR method for the measurement of enantiomeric excess (discussed in chapter five). It was found the chiral tartrates, such as the (*S,S*)-diethyl tartrate (DET) employed in the asymmetric oxidation reaction as a ligand, could be used as a chiral shift reagents for Esomeprazole. The ability to use ¹H NMR for the determination of enantiomeric excess greatly increased the speed and simplicity of % ee determination, with the convenience of an inexpensive chiral shift reagent that was readily at hand having already been used as a ligand in the asymmetric oxidation process.

The synthesis of Esomeprazole was achieved following a smaller scale version of the literature procedure; Ti(O^{*i*}Pr)₄, (*S,S*)-(DET), and water were added to a suspension or solution of the

sulfide **3.17**; employing a 30 mol% catalyst loading equated to the use of $\text{Ti}(\text{O}^i\text{Pr})_4:(S,S)\text{-DET}:\text{H}_2\text{O}$ in a ratio of 0.3:0.6:0.1 equiv. with respect to the sulfide substrate. After heating the mixture at 54 °C for 45 minutes it was allowed to cool to 35 °C whereupon diisopropylethylamine (DIPEA) (0.3 equiv.) and cumene hydroperoxide (CHP, 80% in cumene) (1.0 equiv.) were added and the mixture stirred for one hour. As mentioned previously quenching of the reaction was achieved by addition of aqueous ammonium hydroxide, phases separation followed by acidification and extraction of the aqueous phase; whereas methyl isobutyl ketone was employed in the workup procedure reported in the literature we used dichloromethane which aided the separation of phases during the extraction processes. Column chromatography was employed for purification of the crude materials to give Esomeprazole (*S*)-**1.1** (Scheme 4.6 and Table 4.1).



Scheme 4.6

entry	Catalyst loading / mol %	solvent	Recovered S:SO:SO ₂ / % ^a	Isolated yield / %	Ee / % ^b	Sulfoxide configuration
1	30	toluene	0:90:10	30	93	(<i>S</i>)
2	4	toluene	0:97:3	56	88	(<i>S</i>)
3	1	toluene	3:94:3	0 ^d	72 ^{e, f}	(<i>S</i>)
4	30	toluene	0:99:1	64 ^g	>99.5	(<i>S</i>)
5	30	CHCl ₃	0:95:5	71	93	(<i>S</i>)
6	30	CHCl ₃	0:93:7	62	91	(<i>S</i>)
7	30	CHCl ₃	10:88:2 ^h	48	92	(<i>S</i>)
8	4	CHCl ₃	0:96:4	58	88	(<i>S</i>)
9	1	CHCl ₃	4:92:4	20	14 ^f	(<i>S</i>)
10	30 ⁱ	CHCl ₃	12:72:16	10	84 ^f	(<i>S</i>)
11	30 ^j	CHCl ₃	33:54:13	7	82 ^f	(<i>R</i>)

Table 4.1 a) ratio of sulfide, sulfoxide and sulfone present in crude material as determined by ¹H NMR; b) % ee determination performed on sulfoxide following column chromatography; c) proposed configuration based on ¹H NMR experiments using (*S*)-BINOL as a chiral shift reagent according to ref 639; d) material lost during purification; e) % ee determined by ¹H NMR using (*S,S*)-DET as a chiral shift reagent; f) % ee from the crude sulfoxide; g) obtained as the Na-salt (*S*)-**3.36**; h) reaction quenched using NaHCO₃; i) (*S,S*)-DIPT used as the chiral ligand; j) (*R,R*)-DMT used as the chiral ligand.

During development of the industrial scale process used by AstraZeneca it was found that the oxidation ran well in a broad range of solvents including EtOAc, methyl isobutyl ketone and toluene.¹⁵ The latter solvent was employed for the asymmetric oxidation for the large scale synthesis of Esomeprazole (*S*)-**1.1**; the industrial preparation of the Pymetazole **3.17** afforded the sulfide precursor as a toluene solution, therefore conducting the asymmetric sulfoxidation in the same solvent allowed the first process to be fed directly into the next. In order to replicate the process described by von Unge *et al.* we also employed toluene as a solvent.¹²⁵ Although the sulfide starting material was found not to be fully soluble in toluene, once the catalyst reagents were added a homogenous mixture was obtained. Titanium catalyzed oxidation were performed using catalyst loadings of 30 and 4 mol%, affording Esomeprazole (*S*)-**1.1** in 93 and 88% ee respectively (Table 4.1, entries 1 and 2), in close agreement with the reported results for this reaction of over 94% ee (30 mol% loading) and 91% ee (4 mol% loading). Reducing the catalyst loading to 1 mol% resulted in production of Esomeprazole with decreased enantioselectivity (72% ee, Table 4.1, entry 3). Yields of the reactions performed in toluene were moderate to low, although the literature procedure reports only a 56% yield of the sulfoxide after conversion to the sodium salt (*S*)-**3.36**. Analysis of the crude materials by ¹H NMR indicated high conversions to the sulfoxide. Some overoxidation to the Omeprazole sulfone **4.1** was observed, with the greatest amount (10%) afforded from use of a 30 mol% catalyst loading of the titanium catalyst. When the reaction was carried out using a catalyst loading of 1 mol% an increased amount of unreacted sulfide starting material was recovered in the crude material in addition to a small amount of sulfone (Table 4.1, entry 3). Isolation of the product sulfoxide in enantiopure form and moderate yield was achieved by the formation of as the Na-salt (*S*)-**3.36** from the crude material following the work up procedure (Table 4.1, entry 4).

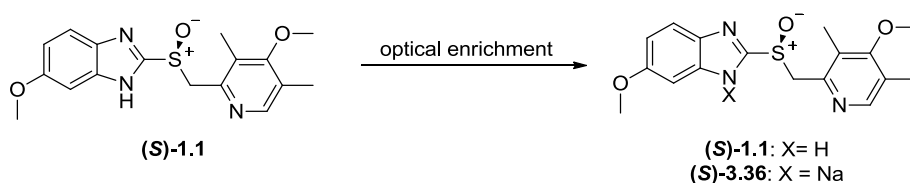
Chloroform was employed as an alternative solvent for the asymmetric synthesis of Esomeprazole (*S*)-**1.1** as chlorinated solvents are known to be suitable solvents in metal-catalyzed asymmetric sulfoxidation reactions.⁶⁴⁰ Additionally, sulfide **3.17** was found to be fully soluble in this solvent, in contrast to the use of toluene in which it formed a suspension. The use of catalyst loadings of 30 and 4 mol% gave Esomeprazole (*S*)-**1.1** in high enantioselectivity (93 and 88% ee respectively) in good to high yields (Table 4.1, entries 5 and 8) which for the 30 mol% catalyst loading reaction yielded the sulfoxide product in an amount twice that of the analogous reaction performed in toluene. Using a 1 mol% loading in CHCl₃ resulted in a greatly reduced enantioselectivity compared to the reaction in toluene (Table 4.1, entries 9 and 3). Reproducibility of the reaction was tested (Table 4.1, entries 5 and 6) with repetition of the oxidation performed using a 30 mol% catalyst loading; although comparable results were achieved for the enantiopurity of the afforded sulfoxide a disparity was observed in

the yield which may be related to loss of material during the workup procedure. Using sat. aq. NaHCO_3 during the quenching stage of the work up procedure dramatically change the profile of products found in the crude materials suggesting a change in the species being carried through the work up procedure; the optical purity of the sulfoxide product was not affected (Table 4.1, entry 7).

Alternative tartrates to (*S,S*)-DET were examined as chiral ligands. Reactions where (*S,S*)-diisopropyl tartrate (DIPT) and (*R,R*)-dimethyl tartrate (DMT) were employed were found to afford Esomeprazole (*S*)-**1.1** in good enantioselectivity but very low yields (Table 4.1, entries 10 and 11). A distinct colour change in the reaction mixture, from pale yellow to dark purple, was observed during the reaction which suggested possible decomposition of the sulfoxide which was reflected in the ratios of the species recovered. Using a tartrate of the opposite chirality gave the (*R*)-sulfoxide (determined by ^1H NMR using (*R,R*)-DMT as a chiral shift reagent)

4.4 Enhancement of optical purity by crystallization

The enhancement of the optical purity of Esomeprazole (*S*)-**1.1** by crystallization was examined. Formation of the Na-salt (*S*)-**3.36** using 1 equiv. of $\text{NaOH}_{(\text{aq})}$ afforded the salt (*S*)-**3.36** in yields of 64–65% and was found to give enantiopure sulfoxide from (*S*)-**1.1** with an enantiopurity of 91 or 93% ee (Table 4.1, method A). Method B exploited the fact that Omeprazole is known to crystallize as the racemate; a solution of Esomeprazole (*S*)-**1.1** (80% ee) in dichloromethane was treated with diethyl ether, with dropwise addition, to initiate the formation of the Omeprazole racemate. Removal of the racemic material left behind an optically enriched solution of Esomeprazole with 98% ee, and a yield of 78%. Interestingly it was found that precipitation of the Omeprazole racemate occurred from a simple solution of Esomeprazole in acetonitrile (Table 4.2, method C). Esomeprazole (80% ee) in acetonitrile was stirred for 10 minutes at rt, after which time racemic Omeprazole crystallized out of solution and was removed by filtration; removal of solvent from the filtrate gave enantiomerically enriched Esomeprazole (97% ee, 79%).



Scheme 4.7

Esomeprazole ee / %	Product ee / %	Sulfoxide product	Yield / %	Method
91	> 99.5	(<i>S</i>)- 3.36	65	A
93	> 99.5	(<i>S</i>)- 3.36	64	A
80	98	(<i>S</i>)- 1.1	78	B
80	97	(<i>S</i>)- 1.1	79	C

Table 4.2 Method A: Optical enrichment via formation and preferential crystallization of (*S*)-3.36** via addition of 1 equiv of aq. NaOH to sulfoxide **1.1**; Method B: Formation and removal of the crystalline Omeprazole racemate, leaving behind optically enriched Esomeprazole (*S*)-**1.1** in solution via addition of Et₂O antisolvent to a solution of Esomeprazole in CH₂Cl₂; Method C: Formation and removal of the crystalline Omeprazole racemate from a solution in MeCN, leaving behind optically enriched Esomeprazole (*S*)-**1.1** in solution**

Isolation of Esomeprazole as the Na-salt (*S*)-**3.36** using method A allows for the sulfoxide product to be obtained in exceedingly high optical purity; in addition, formation of the product in the form of the Na-salt is known to confer greater stability to the sulfoxide species, however this process suffers from loss of material with yields of 64-65% obtained in this work, and a yield of 55% reported in the literature.^{125, 557} While methods B and C afford both Esomeprazole in high ee and yield it is yet to be discovered whether or not these methods could be employed as part of the work up process following a Ti-mediated sulfoxidation reaction, and it may be that the presence of other species in the crude material such as residual tartrate or cumyl alcohol may prevent adequate crystallization of the racemate out of solution that is needed in order to leave optically enriched material behind following filtration. Modification and/or simplification of the procedure required to isolate Esomeprazole (*S*)-**1.1** in high yield and ee following asymmetric sulfoxidation is one area of great interest going forward, testing these methods may provide a fruitful line of enquiry to follow.

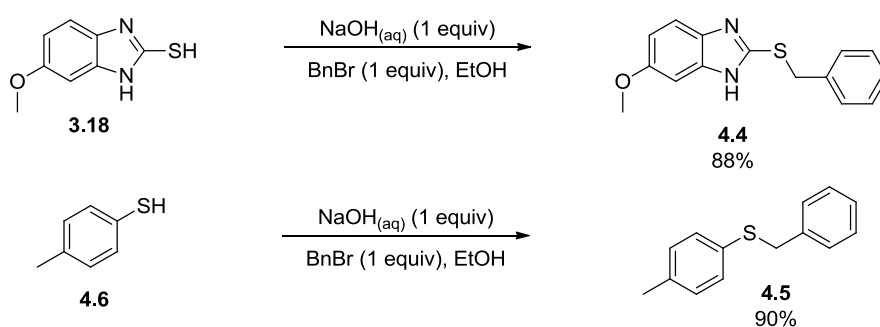
4.5 Synthesis of sulfides, sulfoxides, and sulfones analogous to the Omeprazole series

To further the study of the Ti-mediated synthesis of Esomeprazole we synthesized a range of sulfides featuring structural similarities to Pyrimetazole **3.17**, in order to understand how the heterocyclic motifs affected outcome of the asymmetric oxidations. Seenivasaperumal *et al.* have reported on the importance of the benzimidazole NH with respect to its stereodirecting influence in Ti-tartrate mediated sulfoxidation reactions; in a similar manner we wanted to examine whether or not the pyridyl functional group contributed to the stereoselectivity of the asymmetric oxidation. Additionally the synthesis and subsequent oxidation of Pyrimetazole-like sulfides would allow for examination of various properties of the Omeprazole analogues but

without the possibility of rearrangement that occurs when both the benzimidazole and pyridine rings are present in a sulfinyl compound such as Omeprazole.

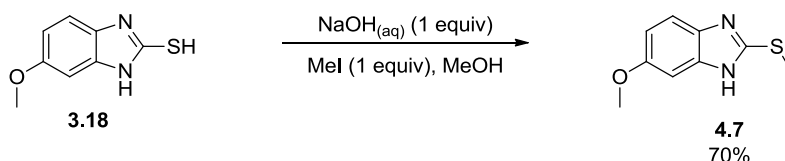
4.5.1 Synthesis of sulfides

Sulfides **4.4** and **4.5** were synthesized by *in situ* formation of the sodium thiolates of thiol **3.18** or *p*-tolyl thiol **4.6** followed by addition of benzyl bromide (Scheme 4.8). Purification of sulfide **4.4** was achieved by recrystallisation of the crude materials from ethyl acetate with hexane used as an anti solvent. Sulfide **4.5** required purification by column chromatography prior to recrystallisation from aqueous ethanol. Both sulfides were obtained in high yield.



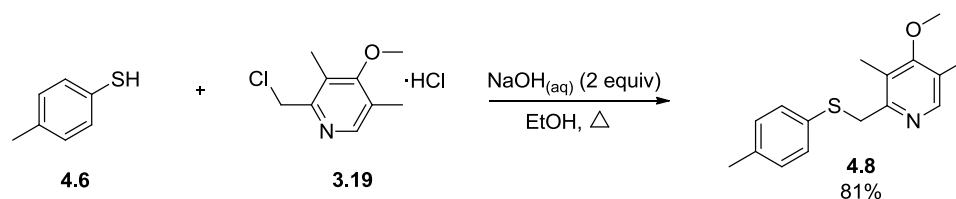
Scheme 4.8

Sulfide **4.7** was prepared via methylation of 6(5)-methoxy-benzimidazole thiol **3.18** according to the procedure reported by Sachs *et al.* (Scheme 4.9). Sulfide **4.7** was afforded in a yield of 70% following recrystallisation from chloroform with hexane used as an antisolvent; the structure of this sulfide (as the 6-OMe tautomer) in the solid state was confirmed by X-ray diffraction analysis on a suitable crystal of sulfide **4.7**.



Scheme 4.9

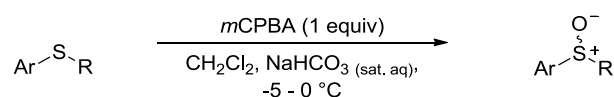
Sulfide **4.8** was obtained in 81% yield from *p*-tolyl thiol **4.6** and the pyridine salt **3.19** using a process analogous to that employed for the synthesis of Pyrimetazole sulfide **3.17** (Scheme 4.10). Column chromatography followed by recrystallisation was used for the purification of sulfide **4.8**. Sulfides **4.4**, **4.5** and **4.8** were all produced in up to 100 mmol scale reactions and sulfide **4.7** was produced on a 50 mmol scale.



Scheme 4.10

4.5.2 Synthesis of racemic sulfoxides

Following the process used for the synthesis of Omeprazole (\pm)-**1.1** a range of racemic sulfoxides were prepared from sulfides **4.4-4.8** (Scheme 4.11). The synthesis of methyl *p*-tolyl sulfoxide **1.48** was also undertaken, using methyl *p*-tolyl sulfide **4.9** purchased from Sigma Aldrich. A two phase solvent system of dichloromethane and sat. aq. NaHCO_3 was employed in order to minimize the benzoic acid byproduct of the oxidation reaction and avoid any potential decomposition of sulfoxide products under acidic conditions.



Scheme 4.11

Sulfide	Ar	R	Sulfoxide	Yield / %
4.4			4.9	78
4.5			4.10	91
4.6		Me	4.11	70
4.7			4.12	96
4.8		Me	1.48	91

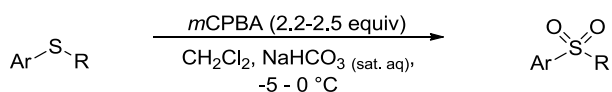
Table 4.3

Racemic sulfoxides **4.9-4.12**, and **1.48** were obtained in high to excellent yields following column chromatography and crystallization or trituration (Table 4.1). The structures of **4.10**, **4.11**, and **4.12** were confirmed by single crystal X-ray diffraction. The synthesis of each

sulfoxide was carried out on a multigram scale, and in contrast to Omeprazole (\pm)-**1.1** all sulfoxides were found to be stable at rt indefinitely.

4.5.3 Synthesis of sulfones

In order to provide reference material for use in analyzing the products of Ti-mediated sulfoxidation reactions samples of sulfones were prepared by oxidation of sulfides **4.4–4.8** using 2.2-2.5 equivalents of *m*CPBA (Scheme 4.12). A two phase solvent system of dichloromethane and sat. aq. NaHCO₃ was employed to neutralize the benzoic acid byproduct of the oxidation. Purification was achieved by column chromatography of the crude sulfones, followed by recrystallization with the exception of sulfone **4.17** where chromatography was followed by trituration to afford a colourless amorphous solid. Sulfones **4.13–4.17** were obtained in moderate to high yields (Table 4.4). Single X-ray diffraction confirmed the structure of sulfone **4.13**.



Scheme 4.12

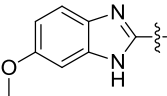
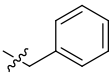
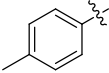
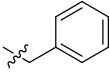
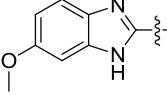
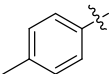
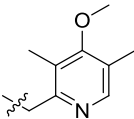
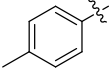
Sulfide	Ar	R	Sulfone	Yield / %
4.4			4.13	79
4.5			4.14	40
4.6		Me	4.15	70
4.7			4.16	55
4.8		Me	4.17	40

Table 4.4

As with the synthesis of Omeprazole **1.1** and the corresponding sulfone **4.1** it was possible to identify the level of sulfide oxidation in the synthesis of sulfoxides **4.9–4.12**, and **1.48**, and sulfones **4.13–4.17** by the use of ¹H NMR spectroscopy. For sulfoxides **4.9**, **4.10**, and **4.12** characteristic signals were observed at 4.58, 4.12, and 4.27 ppm respectively which correspond

to the diastereotopic CH₂ adjacent to the sulfinyl group. Oxidation to the sulfones resulted in the enhanced deshielding of the CH₂ protons of compounds **4.13**, **4.14**, and **4.16** which were observed as singlets at 4.94, 4.62 and 4.71 ppm respectively.

For the oxidation products of sulfides **4.6** and **4.8**, which do not contain diastereotopic CH₂ groups, the protons signals from the methyl adjacent to the sulfinyl group are sufficient to identify to level of oxidation due to the deshielding that is observed going from sulfide to sulfoxide, and the on to the overoxidized sulfone. For example, oxidation of sulfide **4.6** afforded either the sulfoxide **4.11** or sulfone **4.15**; the SOCH₃ protons signals for these species were observed at 2.67, 3.08 and 3.46 ppm respectively and are sufficiently separated to allow for identification and quantification if each of these components were present in a crude product mixture (Figure 4.10). A similar trend is observed for the methyl groups in the ¹H NMR spectra of sulfide **4.8** and the corresponding sulfoxides **1.48** and sulfone **4.17**, again allowing for identification and quantification of the species in a crude product mixture.

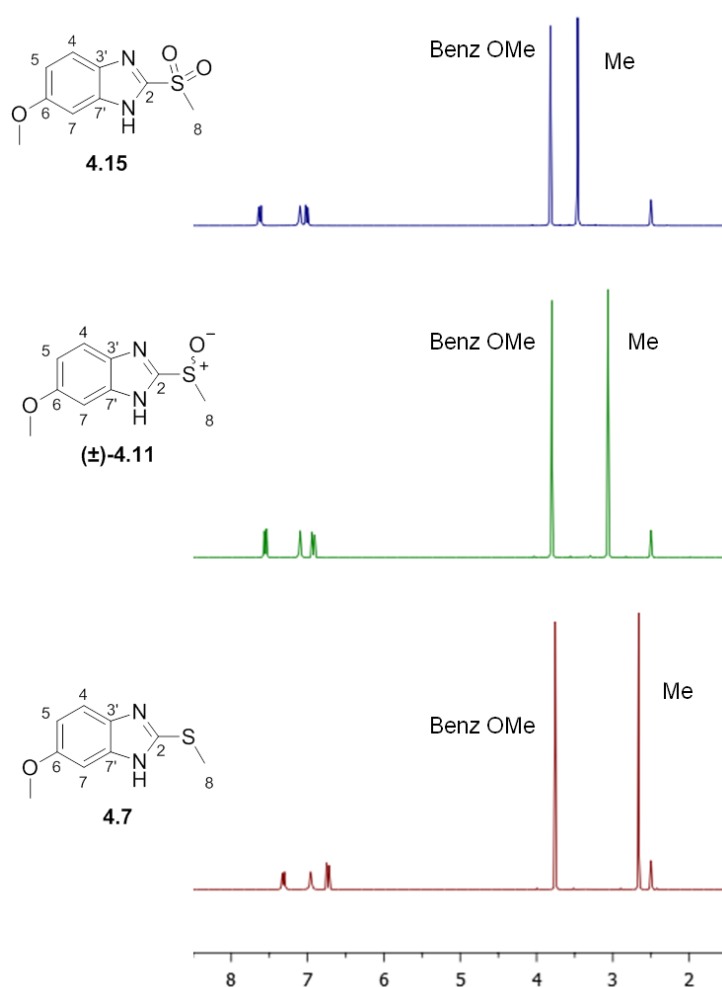
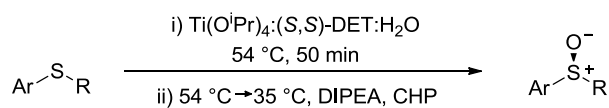


Figure 4.11 ¹H NMR (DMSO-d₆) spectra of sulfide **4.6**, racemic sulfoxide **4.11** and sulfone **4.15**

4.6 Titanium mediated asymmetric synthesis of chiral sulfoxides

The titanium tartrate mediated asymmetric oxidation of sulfides **4.4-4.8** was performed following the procedure employed for the asymmetric synthesis of Esomeprazole (*S*)-**1.1** (Scheme 4.13). Reactions were performed in toluene using a 30 mol% catalyst loading with catalyst equilibration and ageing performed in the presence of the sulfide substrates; following the addition of the oxidant (CHP) the reaction mixtures were stirred at 35 °C for the time specified in Table 4.5.



Scheme 4.13

Sulfide	Ar	R	Sulfoxide	time / h	S:SO:SO ₂ / % ^a	Yield / % ^b	Ee / % ^b
3.17			1.1	1	0:95:5	32	95
4.4			4.9	4	0:68:32	29	95
4.5			4.10	2	15:65:20	40 (24) ^c	16 (19) ^c
4.6		Me	4.11	4	0:85:15	60	95
4.7			4.12	2	3:85:12	60 (40) ^c	20 (27) ^c
4.8		Me	1.48	2	7:70:23	63	6

Table 4.5 a) from the crude reaction products; b) after purification via column chromatography; c) following recrystallization

For sulfoxides **4.9** and **4.11**, which feature the benzimidazole heterocycle the reaction was quenched with aqueous ammonium chloride and was followed by an acid/base extraction process

in order to isolate the crude product, analogous to the process employed for the isolation of Esomeprazole (*S*)-**1.1**. For the remaining sulfoxides the quenching of the reaction was achieved using water, and the crude product was obtained through separation and extraction of the phases. The absolute configuration of sulfoxides **1.48** and **4.10** are both presumed to be (*S*)-enantiomer based on HPLC analysis and comparison of the order of elution with literature sources.^{449, 507} Based on the precedent set by the absolute configuration of these sulfoxides and the synthesis Esomeprazole (*S*)-**1.1** it was presumed that sulfoxides **4.9**, **4.10** and **4.12** were also afforded with the (*S*)-enantiomer as the major product. Determination of the enantiomeric excess of all sulfoxides was performed following column chromatography where all fractions containing sulfoxide material were combined prior to HPLC analysis in order to avoid any enhancement of ee via self disproportion of enantiomers, as discussed in sections 1.4.2.1.3.

Sulfoxides were afforded in high enantiomeric excess (95% ee) from asymmetric oxidation of the sulfides containing a benzimidazole heterocycle, whilst low enantioselectivity was observed in the absence of this structural feature. This finding was in agreement with those of Seenivasaperumal *et al.* who reported the importance of the benzimidazole NH group for high enantioselectivity in the asymmetric synthesis of heterocyclic sulfoxides. It is unlikely that the pyridine nitrogen contributes to stereodirection in the oxidation process as indicated by the low optical purity of the product afforded from the Ti-mediated sulfoxidation of sulfide **4.7**. Overall the yields of the asymmetric oxidations were low to moderate, which may be due to the difficulties associated with work up procedure and removal of the insoluble titanium dioxide. From ¹H NMR analysis of the crude products of the reactions it was found that significant overoxidation occurred, with the sulfone side product accounting for up to 32% of the species present in the crude products, in contrast to the synthesis of Esomeprazole (*S*)-**1.1** which saw the formation of the sulfone **4.1** accounting for 5% of the crude material. In addition, in the synthesis of the *p*-tolyl sulfoxides **4.10**, **4.12**, and **1.48** unreacted starting materials were recovered in the crude materials which may be due to the use of a different work up procedure to sulfoxides **1.1**, **4.9**, and **4.11**, or due to differing interaction with the active catalyst species in the absence of a stereodirecting handle such as the benzimidazole NH leading to reduced efficacy of the oxidation process.

4.7 Improving the understanding of the Ti-tartrate asymmetric S-oxidation reaction: NMR studies of the catalyst components

The asymmetric synthesis of Esomeprazole (*S*)-**1.1** is carried out using a high catalyst loading of 30 mol%, which reflects the poor efficiency and low catalyst turnover of this system in

sulfoxidation processes. Unfortunately using a lower catalyst loading increases the inefficiency of the reaction and is reported to be associated with loss of reproducibility, an important factor in the industrial scale production of pharmaceuticals. In order to understand the relationship between catalyst loading and reaction enantioselectivity NMR studies were performed with the aim to develop a model for the *in situ* formation of the catalytically active Ti-complex.

4.7.1 NMR studies of the catalyst components: $\text{Ti}(\text{O}i\text{Pr})_4$ + Pyrimetazole sulfide

During the asymmetric synthesis of Esomeprazole (*S*)-**1.1**, via the oxidation of Pyrimetazole **3.17**, the titanium based catalyst is formed *in situ* with importance placed on the order of addition of the reagents; $\text{Ti}(\text{O}i\text{Pr})_4$ is added to a solution or suspension of sulfide **3.17**, followed by addition of the chiral tartrate ligand and water. For the attainment of high enantioselectivity it is then necessary to perform the equilibration and ageing of the catalyst in the presence of the sulfide. In order to develop a model of the processes occurring during these steps we first investigated the interactions between the sulfide substrate and $\text{Ti}(\text{O}i\text{Pr})_4$ in solution.

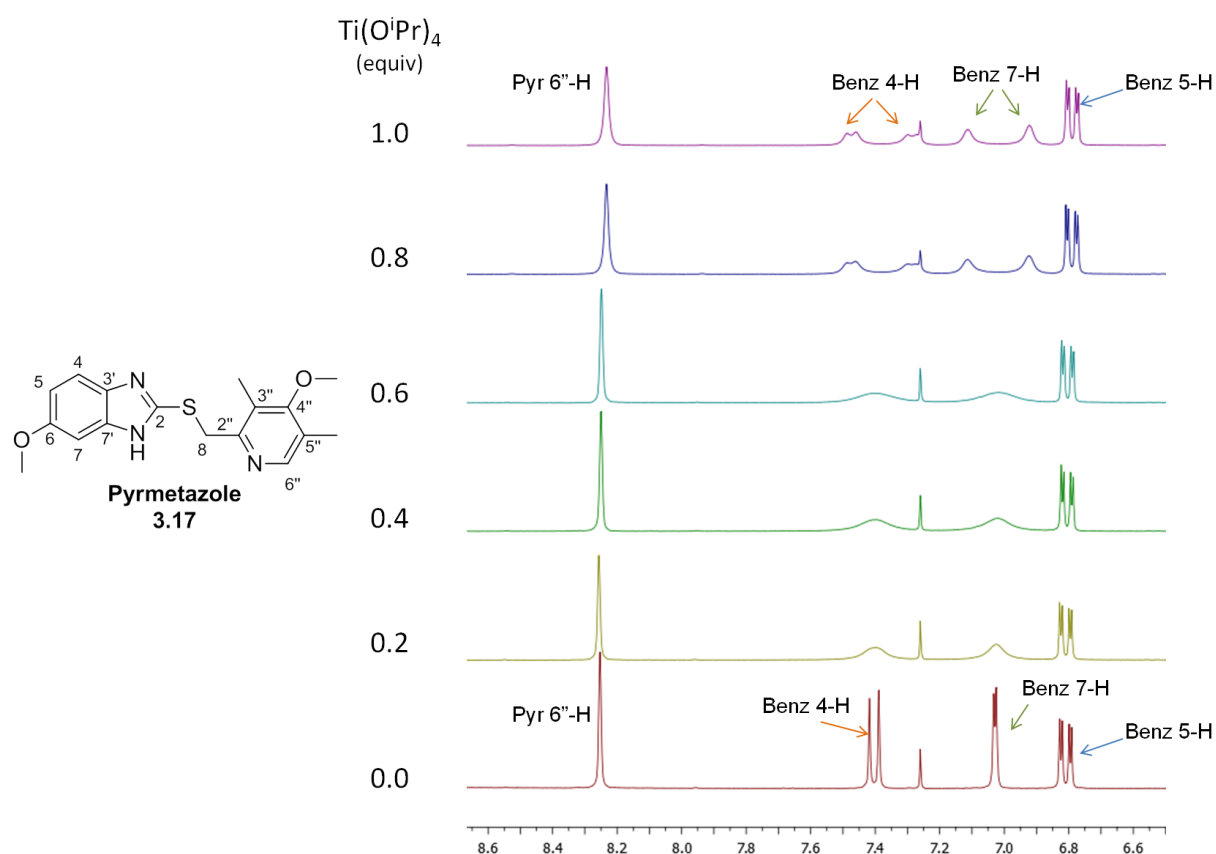
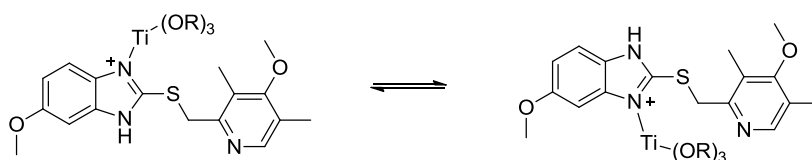


Figure 4.12 Partial ^1H NMR spectra of Pyrimetazole sulfide **3.17** in CDCl_3 with the addition of varying amounts of $\text{Ti}(\text{O}i\text{Pr})_4$ added

^1H NMR characterization performed on solutions comprised of Pyrimetazole **3.17** and $\text{Ti}(\text{O}^i\text{Pr})_4$ in ratios of 1:0 to 1:1 equiv respectively (Figure 4.12). Interestingly it was observed that addition of $\text{Ti}(\text{O}^i\text{Pr})_4$ induced a broadening of the benzimidazole 4-H and 7-H proton signals, and at ratios of sulfide: $\text{Ti}(\text{O}^i\text{Pr})_4$ above 1:0.8 these signals split. The broadening of the signals attributed to the 4-H and 7-H protons, both of which are adjacent to the imidazole ring, implies the occurrence of exchange induced by the presence of the titanium reagent, with coordination of the benzimidazole to the metal centre resulting in two different tautomeric complexes (Scheme 4.14). Further discussion of the effects of annular tautomerism of compound such as Pyrimetazole **3.17** may be found in section 6.2. The formation of coordination complexes such as these is consistent with the observed structural requirements for the induction of high sulfoxidation enantioselectivity i.e. the need for a (benz)imidazole group in the sulfide substrate.



Scheme 4.14

It is also possible that the broadening effect may arise from $\text{Ti}(\text{O}^i\text{Pr})_4$ acting as a desiccant, removing residual water from the CDCl_3 NMR solvent; when no $\text{Ti}(\text{O}^i\text{Pr})_4$ is present the small amount of water in the solvent may be enough to allow for prototropic tautomerization to occur for the benzimidazole ring of the sulfide, the result of which is that the benzimidazole 4-H and 7-H are seen on the NMR timescale as averages of the two possible isomeric forms. The reduction in water that may occur with the addition of increasing amounts of $\text{Ti}(\text{O}^i\text{Pr})_4$ may result in slowing the prototropic exchange sufficiently to allow for the benzimidazole 4-H and 7-H protons to be seen in their two different tautomeric environments according to the 5-OMe or the 6-OMe isomers.

4.7.2 NMR studies of the catalyst components: $\text{Ti}(\text{O}^i\text{Pr})_4$

4.7.2.1 $\text{Ti}(\text{O}^i\text{Pr})_4$ concentration studies

During the ^1H NMR investigation of solutions of $\text{Ti}(\text{O}^i\text{Pr})_4$ and Pyrimetazole sulfide **3.17** it was found that $\text{Ti}(\text{O}^i\text{Pr})_4$ by itself displayed some notable concentration dependent behavior in solution, with large amounts of isopropyl alcohol liberated from the metal complex at low concentrations. We examined the concentration dependent behavior of $\text{Ti}(\text{O}^i\text{Pr})_4$ in solution further in order to determine the possible effects this may have on catalyst formation and turnover during asymmetric sulfoxidation. ^1H NMR characterization was performed on

solutions of $\text{Ti}(\text{O}^i\text{Pr})_4$ over a concentration range of $0.01\text{-}0.3\text{ mol L}^{-1}$, simulating the conditions which may be associated with the use of differing catalyst loadings in a fixed volume of reaction solvent. Solutions in both CDCl_3 and Tol-d_8 were assessed, with integration values of the methine proton signals of the bound isopropoxide ligand (4.91 ppm CDCl_3 , 4.54 ppm Tol-d_8) and $^i\text{PrOH}$ (4.04 ppm CDCl_3 , 3.68 ppm Tol-d_8) used to determine the relative quantities of $\text{Ti}(\text{O}^i\text{Pr})_4$ and free IPA in solution (Table 4.6). For the solutions of $\text{Ti}(\text{O}^i\text{Pr})_4$ in CDCl_3 , characterization was performed after 2h at room temperature in order to allow the equilibrium to be achieved, mimicking the catalyst ageing step in the Esomeprazole process. Samples prepared using Tol-d_8 as the solvent were also analyzed after a 2 hour period at rt. The ^1H NMR spectra of $\text{Ti}(\text{O}^i\text{Pr})_4$ in CDCl_3 at different concentrations is shown in Figure 4.13.

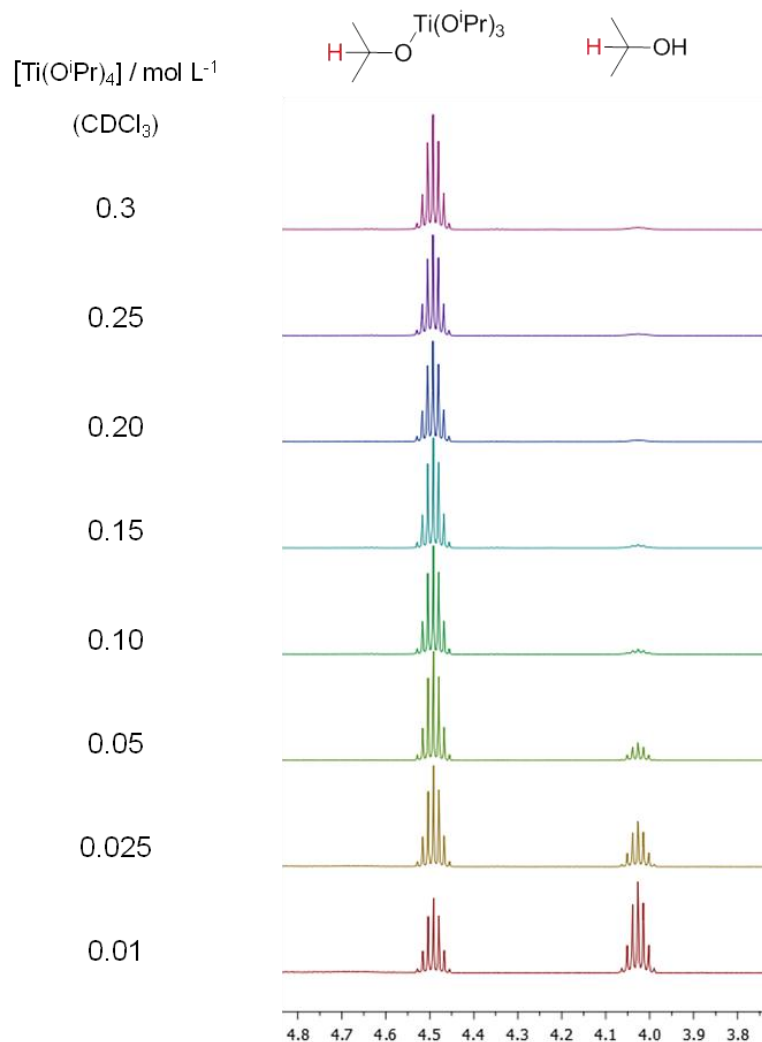


Figure 4.13 ^1H NMR spectra of $\text{Ti}(\text{O}^i\text{Pr})_4$ at varying concentrations in CDCl_3

[Ti(O ⁱ Pr) ₄] / mol L ⁻¹	CDCl ₃		Toluene d ₈	
	% bound alkoxide	% free alcohol	% bound alkoxide	% free alcohol
0.30	95	5	93	7
0.25	95	5	93	7
0.20	95	5	92	8
0.15	93	7	90	10
0.10	91	9	90	10
0.05	81	19	76	24
0.025	65	35	61	39
0.01	40	60	35	65

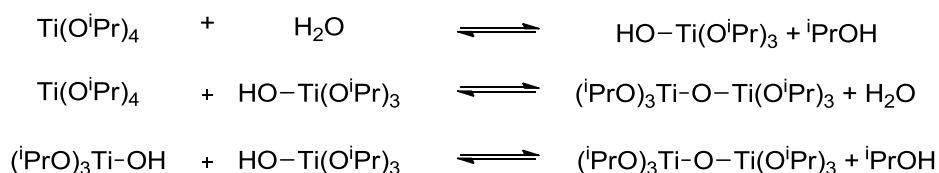
Table 4.6 % based on integration of methane proton peaks of the bound alkoxide of Ti(OⁱPr)₄ and the of the free alcohol ⁱPrOH observed by ¹H NMR for solutions of Ti(OⁱPr)₄ in CDCl₃ or Tol-d₈

At the highest concentration examined in both solvents, 0.30 M, the predominant species in solution was the Ti-alkoxide, accounting for 93-95 % of the total methine signals, with only small amounts of ⁱPrOH observed (5-7 %) (Table 4.6). When the Ti(OⁱPr)₄ concentration was varied, the ratio of bound alkoxide:free alcohol was found to change, with disproportionately high levels of alcohol observed at lower concentrations, accompanied by a depletion in Ti(OⁱPr)₄. The increase in ⁱPrOH content for samples of low Ti(OⁱPr)₄ concentration indicated that there must be a source of protons to allow formation of the alcohol from the alkoxide. Ti(OⁱPr)₄ was purchased as a 97% solution, it is presumed that the reagent is 97% Ti(OⁱPr)₄ in ⁱPrOH, and was used with no prior treatment in order to mimic the process for the synthesis of Esomeprazole reported by von Unge which details no special measurements taken such as the requirement for anhydrous conditions.¹²⁵

A number of theories have been considered to explain why such a disproportionately high amount of free alcohol is observed in solutions of low concentrations (i.e. < 0.1M Ti(OⁱPr)₄). Aggregation of the metal-alkoxide species, to form dimers, trimers and oligomers of higher molecular complexities with multiple μ-oxo bridging groups, would be expected to be accompanied by the liberation of ⁱPrOH from the displacement of alkoxide ligands. A number of Ti-alkoxides have been reported to display concentration dependent variations in molecular weight. Barraclough *et al.* found that for the normal alkoxides in dioxane, as the concentration was increased, the molecular weight increased, with no limiting value of increased molecular complexity up to the measured concentration of 0.5M.⁶⁴¹ This type of concentration dependent behavior is likely to result in detection of relatively high amounts of free alcohol and decreased alkoxide signals at higher concentrations, in contrast with the observed behavior of Ti(OⁱPr)₄.

Furthermore, $\text{Ti}(\text{O}^i\text{Pr})_4$ was been reported by Bradley *et al.* as showing an average molecular association of 1.4 (in refluxing benzene), with a subsequent value of 1.1 (± 0.01) reported over a decade later for a range of concentrations from 3.39×10^{-3} to 16.29×10^{-3} M.⁶⁴² Amyloxide, secondary and tertiary alkoxides of titanium are reported to be typically monomeric due to effective shielding of the metal core by the bulky substituents, which prevent aggregation.⁶⁴³⁻⁶⁴⁶ Molecular weight determinations performed by Sharpless and coworkers confirmed the monomeric nature of $\text{Ti}(\text{O}^i\text{Pr})_4$, measuring a degree of association equal to 1 for a 0.22M solution in CH_2Cl_2 .⁶⁴⁷ It is therefore unlikely that the observed behavior of $\text{Ti}(\text{O}^i\text{Pr})_4$ is due to aggregation of the metal alkoxide under the different concentration conditions. For further clarification of this, analogous studies may be carried out on Ti-alkoxides which are known to vary in molecular complexity with concentration and the results compared with those discussed here.

The formation of dimeric species is known to occur in the presence of water. Hydrolysis of the Ti-alkoxide bonds, to form Ti-OH and liberate $^i\text{PrOH}$, may enable the formation of dimeric complexes through the relief of the steric shielding around the metal centre, thus allowing subsequent attack on the electropositive Ti (Scheme 4.15).^{351, 648}



Scheme 4.15

$\text{Ti}(\text{O}^i\text{Pr})_4$ is known to undergo hydrolysis in the presence of water in quantities as low as 0.3 H_2O molecules per Ti atom. The addition of dilute solutions of H_2O (3% w/w) in $^i\text{PrOH}$ to the isopropoxide was reported to give a solid with a molecular composition corresponding to $\text{TiO}_2(\text{O}^i\text{Pr})_6$.⁶⁴⁸ The formation of complex such this would result in a bound alkoxide:free alcohol ratio of 3:1, compared an assumed ratio of 4:0 for $\text{Ti}(\text{O}^i\text{Pr})_4$, and may account for the unexpectedly high proportions of free alcohol at lower concentrations.

The impact of solution concentration on the observed alkoxide:alcohol ratios was most significant below 0.1 M, where the relative ratios of bound alkoxide:free alcohol dropped from 81:19 (0.05 M) to 40:60 (0.01 M) (CDCl_3). A similar trend was observed in Tol- d_8 . From these findings it is clear that at lower $\text{Ti}(\text{O}^i\text{Pr})_4$ concentrations, $^i\text{PrOH}$ is liberated at the expense of the parent Ti-alkoxide (Figure 4.14)

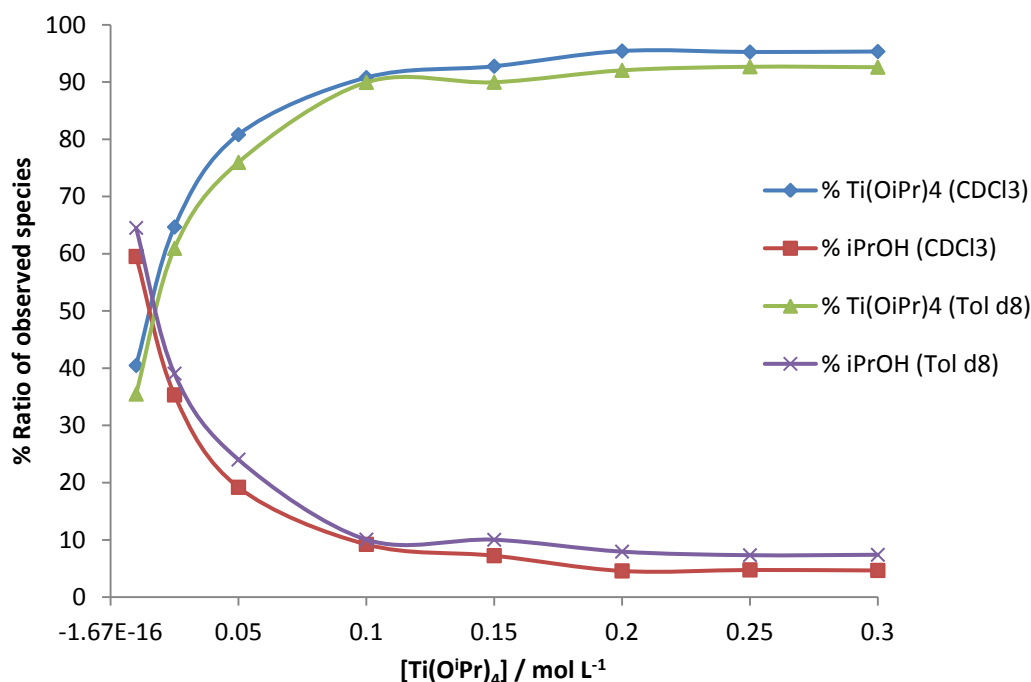


Figure 4.14 Percentage ratio of methine protons of bound alkoxide and free alcohol observed by ¹H NMR in solutions of Ti(OiPr)₄ against solution concentration.

Quantification of the species in solution was based on three assumptions: i) excluding solvent, only Ti(OⁱPr)₄ and ⁱPrOH were present in solution, ii) the Ti-alkoxide complex was monomeric, and iii) four alkoxide methine protons equate to one Ti(OⁱPr)₄ molecule, giving a 0.25:1 stoichiometry for the protons assigned as bound alkoxide and free alcohol. The calculated quantities of Ti(OⁱPr)₄ and ⁱPrOH are given in Table 4.7.

[Ti(O ⁱ Pr) ₄] / mol L ⁻¹	CDCl ₃				Toluene d ₈			
	% bound alkoxide	% free alcohol	Ti(O ⁱ Pr) ₄ / μmol ^a	ⁱ PrOH / μmol ^a	% bound alkoxide	% free alcohol	Ti(O ⁱ Pr) ₄ / μmol ^a	ⁱ PrOH / μmol ^a
0.30	95	5	214	45	93	7	209	63
0.25	95	5	178	38	93	7	174	53
0.20	95	5	143	30	92	8	138	48
0.15	93	7	105	32	90	10	101	45
0.10	91	9	68	27	90	10	68	30
0.05	81	19	30	29	76	24	29	36
0.025	65	35	12	26	61	39	11	29
0.01	40	60	3	18	35	65	3	20

Table 4.7 Percentage ratio of methine protons observed for bound isopropoxide ligand and free alcohol, ⁱPrOH, in solutions of Ti(OⁱPr)₄ determined from integrals of methine proton peaks observed by ¹H NMR; assuming monomeric, tetra-coordinated Ti-alkoxide, giving a 1:4 alkoxide:free alcohol stoichiometry

Figure 4.15 illustrates the relationship between amount of $\text{Ti}(\text{O}^i\text{Pr})_4$ and $^i\text{PrOH}$ in CDCl_3 ; the results for samples prepared in Tol-d_8 were found to be in close approximation. In contrast to the trend observed for $\text{Ti}(\text{O}^i\text{Pr})_4$ which shows a steady, linear increase, the effect of increasing concentrations appears to have a less significant effect on the amount of free alcohol in solution. While there is a $200 \times$ difference in the molar quantity of $\text{Ti}(\text{O}^i\text{Pr})_4$ between high and low concentrations (0.01-0.3M) only a threefold difference in the amount of free alcohol across the concentration range was observed. This observation may be indicative of $\text{Ti}(\text{O}^i\text{Pr})_4$ acting as a scavenger for water in the deuterated solvents. As the amount of free alcohol observed in samples of a constant volume (and therefore constant water content) does not appear to vary as significantly as $\text{Ti}(\text{O}^i\text{Pr})_4$ bound alkoxide quantity, it may be that the traces of water present are a limiting reagent in the formation of alternative Ti-complexes.

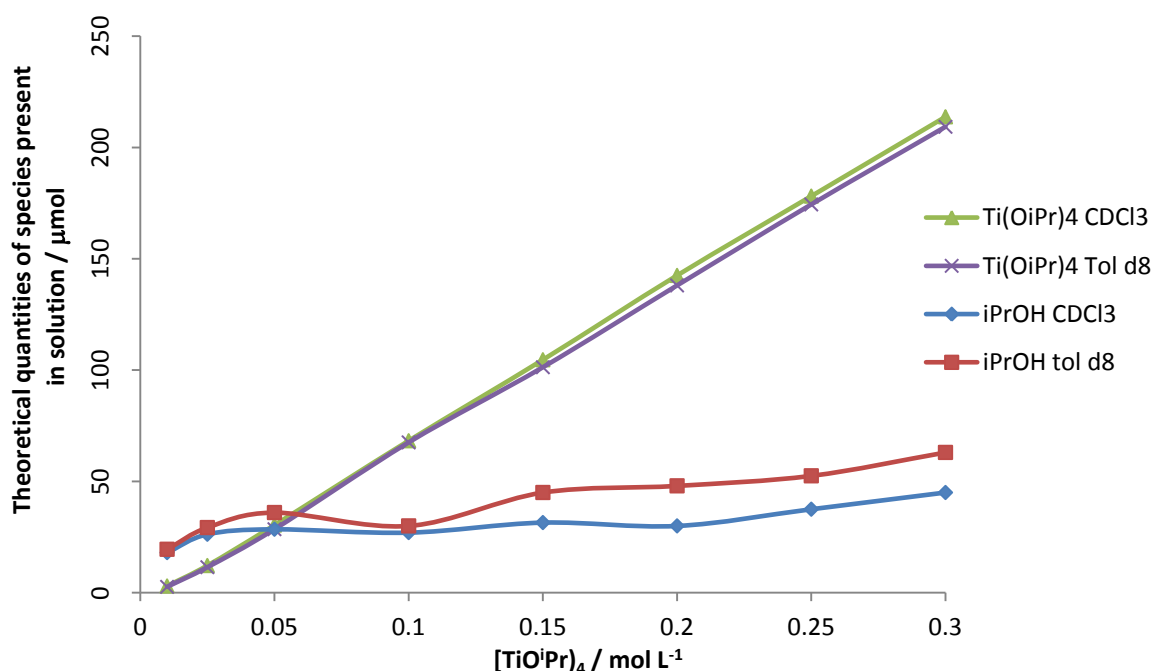


Figure 4.15 Calculated quantities of $\text{Ti}(\text{O}^i\text{Pr})_4$ and $^i\text{PrOH}$ (μmol) for solutions of different $[\text{Ti}(\text{O}^i\text{Pr})_4]$

Although only small relative quantities of water are required for the hydrolysis of $\text{Ti}(\text{O}^i\text{Pr})_4$, the amount of water present in the prepared NMR samples is believed to be too low to have a significant effect. In addition the formation of solid material was not observed. Karl Fischer titrations were carried out on solvents that had been treated under similar conditions to those used for the NMR studies; CDCl_3 was passed through a plug of alumina and stored over 4 \AA MS, while Tol-d_8 was taken straight from a newly opened bottle with no additional drying steps. The water content of CDCl_3 and Tol-d_8 was found to be 1.9 ppm and 50 ppm respectively. In NMR samples containing 0.75 mL of the deuterated solvents the water content of the solvent alone would be $18 \times 10^{-3} \mu\text{mol H}_2\text{O}$ in CDCl_3 and $353 \times 10^{-3} \mu\text{mol H}_2\text{O}$ in Tol-d_8 . These

quantities of water may be too small to cause the liberation of *i*PrOH on the scale observed here, suggesting that additional reactions may be occurring, or that there are additional sources of water causing these effects, such as incompletely dried glassware or if the prepared solutions were hygroscopic in nature.

Further investigation of the effect of water on the alkoxide:alcohol ratio could be conducted using solvents with varying water content. As the amount of free alcohol observed in samples of a constant volume (and therefore constant water content) does not appear to vary as significantly as $\text{Ti}(\text{O}^i\text{Pr})_4$, it may be that the traces of water present are a limiting reagent in the formation of alternative Ti-complexes. An analogous study would therefore be performed whereby the concentration of $\text{Ti}(\text{O}^i\text{Pr})_4$ is varied through the use of different solvent volumes, which should provide varying levels of moisture.

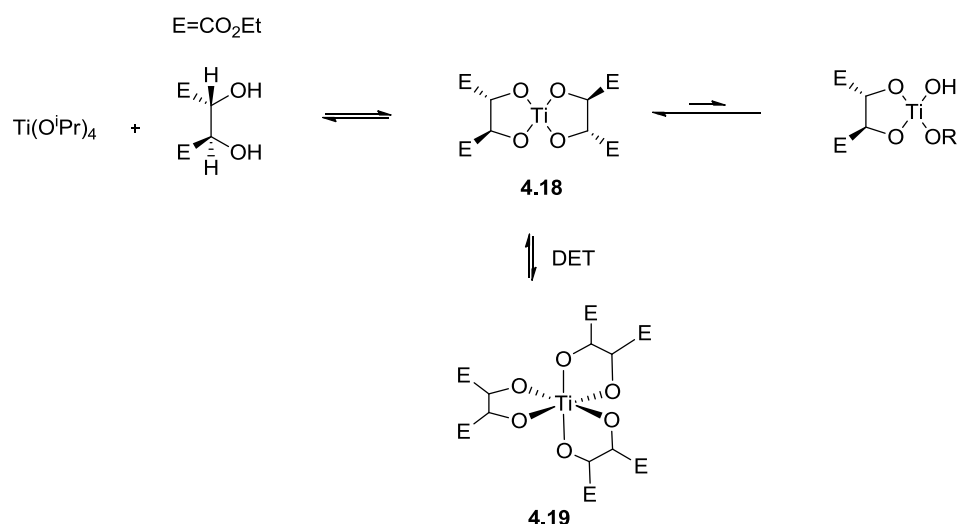
4.7.2.2 Implications for the Ti-mediated synthesis of Esomeprazole

Although further work is required to understand the apparent concentration dependent behavior of $\text{Ti}(\text{O}^i\text{Pr})_4$, there are clear implication for the *in situ* formation of the active catalyst species based on these findings. Kagan *et al.* reported that, in the absence of water, a ¹PrOH modified reagent (1:2:4 or 1:4:4 $\text{Ti}(\text{O}^i\text{Pr})_4$:DET:¹PrOH) could be employed in the asymmetric oxidation of *p*-tolyl methyl sulfide, affording the sulfoxide in high ee (83 and 93% ee respectively). Higher proportions of ¹PrOH were found to be detrimental to the enantioselectivity and strict regulation of reaction conditions were required to maintain high enantiomeric excess of the sulfoxide product.³⁵⁵ The undesired presence of ¹PrOH at low reagent concentrations, in addition to water, may decrease efficiency of the catalyst system, due to competition for coordination sites on the metal centre. It has been proposed that the inclusion of ¹PrOH in the catalyst system aids catalyst turnover by displacement of the sulfoxide product from the active catalyst complex, it is likely therefore that the amount of this alcohol in the catalyst system requires careful regulation in order to achieve maximum efficacy.

If lowering of the catalyst loading was to be achieved by way of decreasing the quantities of the catalyst precursors added to solution then the *in situ* formation of the active catalyst may be compromised. The relatively low amounts of $\text{Ti}(\text{O}^i\text{Pr})_4$ observed in solutions of low concentrations may result in perturbations of the optimized catalyst reagent stoichiometry. In the AstraZeneca procedures described by von Unge *et al.*, the synthesis of (*S*)-**1.1** using a 30 mol% catalyst loading was performed using an initial $\text{Ti}(\text{O}^i\text{Pr})_4$ concentration of 0.224 M (in toluene), whereas for the lower catalyst loading reaction (4 mol%), it was 0.042 M suggesting that the differences in enantioselectivity may partly be attributed to a variation in reagent

concentration. From the results of the NMR studies performed in Tol- d_8 it can be estimated from Figure 4.12 that by lowering the $Ti(O^iPr)_4$ concentration from 0.224 M to 0.042 M, the alkoxide:free alcohol ratio would change from 92:8 to 72:28, resulting in a significant difference in the amount of $Ti(O^iPr)_4$ and iPrOH present in the reaction mixture.

Subsequently other reagents present in the catalyst preparation/ageing step would effectively be present in an excess to the optimized ratio, and therefore may alter the efficacy of an active catalyst species. A reduction in the amount of $Ti(O^iPr)_4$, due to concentration dependent behavior, may contribute to a poor formation or destruction (e.g. through hydrolysis in the presence of excess water) of the active catalyst species, thus effectively lowering the catalyst loading. Disturbance in the reaction equilibria may occur, with preferential formation of potentially inactive or competing catalysts species such as **4.18**. The formation of coordinatively saturated complexes such as **4.19** would reduce or prevent catalytic turnover (Scheme 4.16).



Scheme 4.16 Preferential formation of an undesired Ti-complex due to an excess of DET with respect to $Ti(O^iPr)_4$

4.7.3 NMR studies of the catalyst components: $Ti(OiPr)_4 + DET + H_2O$

Further NMR studies were conducted investigating the combination of $Ti(O^iPr)_4$ and DET, with and without the presence of water (Figure 4.16). With the addition of water a complex mixture of signals occurring between 3.8-5.6 ppm was observed. The peaks at 4.32 and 4.55 ppm are due an excess of DET in solution, however the appearance of signals at higher chemical shifts

may be indicative of the formation of low concentrations of complexes between DET and titanium, formed only in the presence of the water.

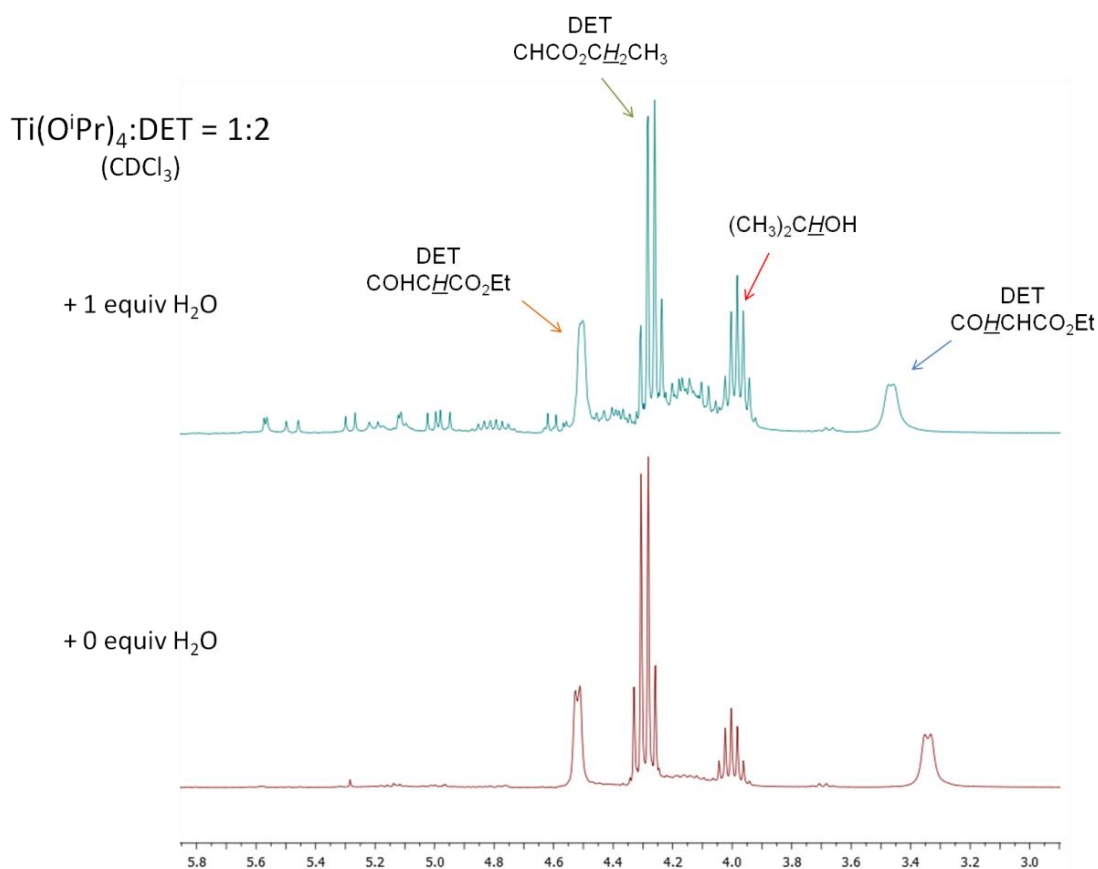


Figure 4.16 Partial ^1H NMR (CDCl_3) spectra of $\text{Ti}(\text{O}^i\text{Pr})_4$ and diethyl tartrate (DET) in a 1:2 ratio with and without the addition of 1 equiv of H_2O

The sulfoxidation catalyst reagents employed by Kagan, Modena and von Unge were examined by NMR (Figure 4.17).^{125, 347, 352} Once again, in addition to signals attributed to an excess of DET in solution, the formation of a complex mixture of species was observed. Although further investigation is required to gain more information of the Ti-based complexes formed between these reagents it can be seen that the Modena catalyst system of 1:4:0 $\text{Ti}(\text{O}^i\text{Pr})_4$:DET: H_2O produces a mixture of components almost identical to that formed by the Kagan system which features the addition of less tartrate but one equivalent of water. It has been proposed that the addition of 4 equivalents of the hygroscopic tartrate in the Modena sulfoxidation system inadvertently introduces water into the catalyst mixture, and that the active catalysts investigated by Kagan and Modena were in fact the same 1:2:1 $\text{Ti}(\text{O}^i\text{Pr})_4$:DET: H_2O .^{36, 354} Comparison of the ^1H NMR spectra of the Kagan and Modena reagents supports this hypothesis.

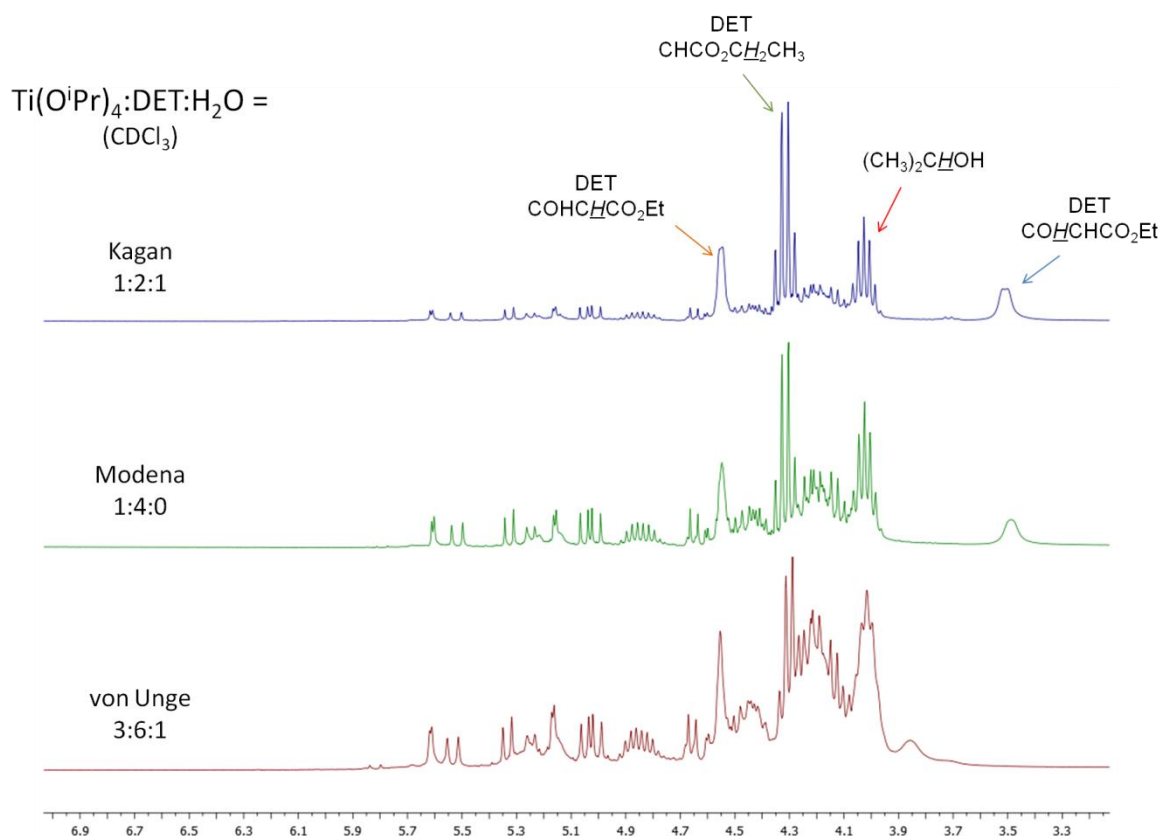


Figure 4.17 Partial ^1H NMR (CDCl_3) spectra of the Kagan, Modena, and von Unge catalyst systems comprising of $\text{Ti}(\text{O}^i\text{Pr})_4$, diethyl tartrate (DET), and H_2O in various ratios

4.8 Conclusions and future direction

In pursuing investigations into the Ti-mediated asymmetric synthesis of Esomeprazole a number of unexpected challenges were faced, and thankfully most were overcome. Esomeprazole and Omeprazole proved to be demanding compounds to synthesize and manipulate; as well as decomposing under acidic conditions, they also are known to be sensitive to light, moisture, and heat. Racemic Omeprazole was found to be unsuitable for purification by column chromatography due to poor solubility and decomposition on the column, and the workup procedure for the Ti-based sulfoxidation process was difficult and precarious. Early attempts to quantify the enantioselectivity of products from the asymmetric sulfoxidation by chiral chromatography saw the decomposition of materials on the column, which had also been observed when during purification of Omeprazole by column chromatography. The possibility was also raised that the sulfoxide was too unstable, and decomposition was occurring prior to analysis. Through time and experience, however, we found suitable ways to isolate and analyze these sulfoxides. Synthetic methodologies were developed for the production and isolation of Pyrimetazole **3.17**, the sulfide precursor to Esomeprazole (*S*)-**1.1**, Omeprazole (\pm)-**1.1** the

racemic form of the sulfoxide, and the corresponding sulfone **4.1**, all of which were achieved in good to high yield.

Using a titanium-tartrate based catalyst system, developed by Kagan and subsequently modified by von Unge *et al.* the synthesis of Esomeprazole (*S*)-**1.1** was achieved in good yields (up to 71%) and high enantioselectivity (up to 93% ee); conversion of the sulfoxide product to the Na-salt resulted in optical enrichment allowing for Na-Esomeprazole (*S*)-**3.36** to be isolated in near optically pure form (> 99.5% ee). The asymmetric sulfoxidation process was performed on a range of structurally diverse sulfides, some of which featured the heterocyclic motifs found in Esomeprazole. It was found that the presence of the benzimidazole NH group was of great importance with respect to the stereoselectivity of the reaction, and that species without a benzimidazole ring were afforded in low ee. Although further work is required to gain the desired insight into the processes involved in the Ti-mediated asymmetric synthesis of Esomeprazole (*S*)-**1.1**, in carrying out the work that is laid out here a great amount of worthy information was gathered on these compounds which would be of benefit to anyone continuing this vein of research.

Omeprazole and Esomeprazole were found to exhibit differences in their physical and spectroscopic characteristics, arising from heterochiral dimer formation of the racemic sulfoxide. Importantly, it was realized that while Omeprazole (\pm)-**1.1** required purification via crystallization and crystallized as the racemate, Esomeprazole (*S*)-**1.1** however, was found to exist as an oil that would dry to a glassy solid under vacuum, and most importantly could withstand chromatography due to increase solubility over the racemic sulfoxide.

With the knowledge gained during this body of work there are a number of paths that could be followed in its continuation. It would be highly desirable to improve efficacy of the Ti-mediated sulfoxidation, particularly with respect to the synthesis of Esomeprazole. Alterations to the reaction process might involve the pre-formation of the active catalyst species. Alternatively one may wish to investigate the importance of catalyst loading during the different stages of the reactions, during the catalyst aging step or during the oxidation. If it was found that a high catalyst loading was more important during the catalyst preparation and ageing step then the addition of further amounts of sulfide following catalyst ageing would result in the oxidation stage, and overall reaction occurring at an effectively lower catalyst loading. Simplification and/or improvements made to the work up procedure for the Ti-tartrate based sulfoxidation reaction may allow for greater recovery of material, and therefore greater reaction economy. Further analysis of the conditions that afford Esomeprazole or Na-Esomeprazole in

high enantiopurity and higher yields may also allow for improvements in the reaction methodology.

In this work we have identified that the concentration at which the catalyst reagents are used may have importance with respect to why lower catalyst loadings lead to a reduction in enantioselectivity. Performing the asymmetric synthesis of Esomeprazole at varying concentrations may provide greater information on this matter. Further studies could be performed using NMR, and other analytical means, to gather information on the nature of the active catalyst species, investigating the aspects of the sulfoxidation reaction protocol such as the importance placed on the order of addition of catalyst components, or on the role played by water, or additives such as DIPEA.

Modifications to the current methodology may also be of interest to study, such as the application of a range of more structurally diverse chiral tartrates, or tartramide, based ligands. Future work may look at developing alternative methodologies for the asymmetric synthesis of Esomeprazole (*S*)-**1.1**, and may begin by assessing processes that are currently available for the asymmetric oxidation of sulfides, but have not yet been applied or adapted for use in the oxidation of Pyrimetazole. Alternatively, it may be possible to adapt the current Ti-tartrate based oxidation process for the production of alternative chiral sulfoxide, though modification of the current protocol.

5 Evaluation of chiral tartrates for use as chiral solvating agents

5.1.1 NMR spectroscopy as a tool for quantitative stereochemical analysis

With the development of new methodologies in the field of asymmetric synthesis it is important to also develop new strategies for the measurement of enantiomeric purity. Despite its relative low sensitivity compared to other techniques such as chiral HPLC or GC, NMR spectroscopy is nonetheless an attractive option by which enantiomeric excess determination can be achieved quickly and simply.¹⁰² The measurement of enantiomeric purity of a chosen solute can be achieved in a number of ways.⁶⁴⁹⁻⁶⁵² A recent development in the utility of NMR for enantiodiscrimination is the use of chiral liquid crystals (CLC) as a solvent or as an orientating medium.⁶⁵³⁻⁶⁵⁸ Here the induction of a magnetic field orientates the CLC and in doing so has an aligning effect upon the enantiomeric solute. The orientation of the solute is different between the two enantiomeric forms, thus all other sensitive NMR interactions, such as chemical shift anisotropies and dipolar coupling, are also different. As this technique is based on shape recognition it is applicable to substrates such as chiral alkanes which lack a functional group required for derivitisation or complexation.⁶⁵⁹ Unfortunately this technique is still in its infancy and has been reported to suffer from poor sensitivity to chirality.⁶⁶⁰ The requirement of specialized reagents in the CLCs is also limiting in the widespread application thus far.

A more classic approach is with the use of chiral derivitisation agents (CDAs). These reagents are used prior to NMR analysis to form covalent bonds to the molecules of the mixture of enantiomers under investigation, thus producing diastereomers measurable under NMR conditions.⁶⁶¹ In a simple achiral medium it is not possible to distinguish enantiomers by NMR as the resonances of enantiotopic nuclei are isochronous. In contrast, diastereomeric species are distinguishable due to the anisochronous nature of certain diastereomeric nuclei. The magnetic nonequivalence arising from this is reflected in the chemical shifts of the related stereogenic centers. With sufficient resolution of the appropriate signals, this phenomenon, which was first noted by Cram over half a century ago, gives the relative ratios of diastereomers present by simple measurement of the signal integration values.⁶⁵¹ There are a wide range of CDAs available, such as the acids developed by Mosher **5.1**, and Mislow **5.2**, camphanic acid **5.3**, and the diamine **5.4** (Figure 5.1).^{651, 662-665} As a covalent bond forming reaction must take place it is important to select the appropriate CDA with respect to the functional groups available within the sample under investigation. Great care must also be taken to ensure racemisation or kinetic resolution does not occur during the preparation of the derivatized materials in order to render accurate results from the subsequent spectroscopic analysis.

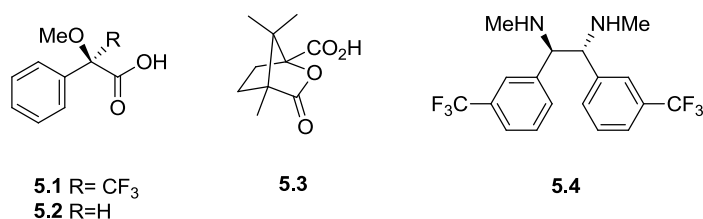


Figure 5.1

A third method, and the one which shall be the focus from here on in, is the use of chiral solvating agents, also referred to as chiral shift agents (CSAs). These reagents are used to form diastereomeric association complexes in solution which produce different chemical shifts. Additionally, the association constants of the complexes may differ in the formation of complexes between the CSA and the two enantiomers under scrutiny, giving rise to different time averaged solvation environments, contributing to the recognition of individual chiral species.^{666, 667} Hydrogen bonds, van der Waals forces and π - π interactions are often reported as the driving forces behind the formation of complexes in solution.⁶³⁹ There have been a wide range of CSAs reported in the literature. Host-guest interactions between cyclodextrins (CDs) or crown ethers and chiral substrates are well known.^{649, 668} Derivatised CDs were found to be appropriate for enantiopurity determination of Selegiline **5.5**, an anti-Parkinson's drug for which only the (*R*)- enantiomer is active, and analogous phenylamines **5.6** and **5.7** (Figure 5.2). Functionalised crown ether **5.8** was shown to display enantiodiscrimination towards *cis*-aminoindanol, with the crown cavity acting as a host towards ammonium salts which formed upon reaction of the carboxylic groups and the amine of the substrate.^{669, 670}

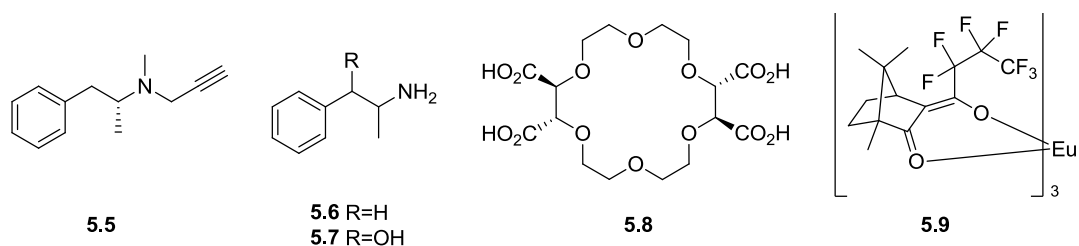


Figure 5.2

Lanthanides shift reagents, such as Eu(hfc)₃ (hfc = heptafluoropropylhydroxymethylene)-(+)-camphorate) **5.9**, are widely used and commercially available. Lewis-acid type complexation between the studied solute and the paramagnetic metal core of the shift reagent give rise to strong shielding or deshielding effects observed in the spectra of the solute.⁶⁷¹ In addition there can be changes in chemical shift arising from interactions such as transfer of electron spin density (contact shift) or by the magnetic effect of unpaired electron magnetic moment (pseudo contact shift).⁶⁷²⁻⁶⁷⁶ Shift reagents of this kind usually require their gradual addition in small

amounts to the sample under scrutiny in order to achieve sufficient resolution. One disadvantage to CSAs of this type is that signal line broadening, often due to proton-electron dipolar relaxation, can occur. These reagents are also relatively expensive; Sigma-Aldrich currently quotes prices of £56-166 per g for $\text{Eu}(\text{hfc})_3$ and £23-151 per g for $\text{Eu}(\text{fod})_3$.^{677, 678}

Simple, small chiral molecules are often effective as CSAs. Chiral aryltrifluoromethylcarbinols, such **5.10** and **5.11**, developed by Pirkle *et al.* are widely used, commercially available, simple to employ and in contrast to lanthanide type reagents do not suffer from line broadening.^{679 680} The asymmetric synthesis of the antitumor alkaloid (+)-Crispine A **5.12**, and the determination of enantiopurity by ^1H NMR was recently reported, with (+)-(*R*)-*t*-butylphenylphosphinothioic **5.13** successfully employed as a CSA.⁶⁸¹ The phosphinothioic acid **5.13** however, is not commercially available; for their own research on the synthesis of the chiral alkaloid **5.12**, Yuste *et al.* reported that, due to limitations in the exportation of certain phosphorus compounds in their country (Mexico), the synthesis of the acid was not a viable option. Instead they employed (*S*)-1,1'-binaphthyl-2,2'-diol ((*S*)-BINOL) **1.43** as a CSA, reporting that the use of five equivalents of the diol gave sufficient enantioresolution for accurate and reliable measurement of alkaloid enantiopurity.⁶⁸² The cost of reagents such as can vary dramatically, for example 1 g of Pirkle's alcohol **5.11** currently costs over £500 per g whereas (*S*)-BINOL **1.43** is available for £13-33 per g.^{683, 684}

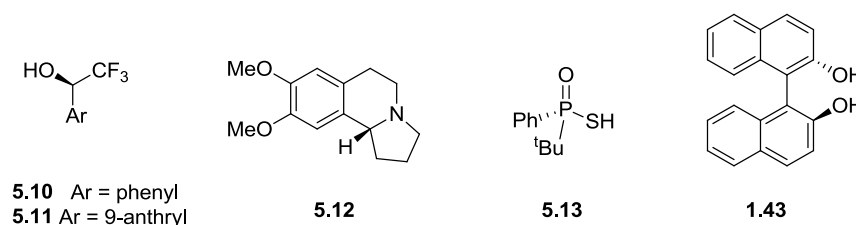


Figure 5.3

5.1.2 CSA for the enantiodiscrimination of chiral sulfoxides

There is a wide choice of CSA available for the enantiodetermination of chiral sulfoxides, including lanthanide- and macrocyclic- based reagents.^{637, 685-688} The larger aromatic group of alcohol **5.11**, compared with **5.10**, give a chiral shift agent with greatly increased shielding ability, with the 9-anthryl species giving up to 5 times greater chemical shift nonequivalence in comparison to phenyl analogue.⁶⁸⁹ The benzamide reagent **5.14**, developed by Kagan *et al.* was reported to successfully resolve all four enantiomers in samples of Mesoridazine **5.15**, a sulfoxide metabolite of the antipsychotic drug Thioridazine, thus allowing for the quantification of the diastereomeric ratios (Figure 5.4). The enantio-recognition of reagents such as Pirkle's

alcohols and Kagan's amide is attributed to the H-bonding interactions between the sulfinyl group of the chiral solutes and the OH- and NH-groups of the respective CSAs.⁶⁹⁰

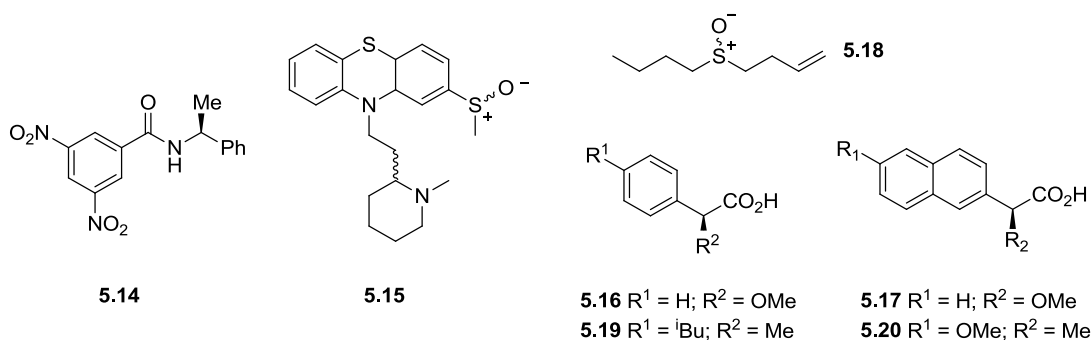


Figure 5.4

(*S*)- α -Methoxyphenyl and (*S*)- α -methoxy-2-naphthyl acetic acids ((*S*)-MPA **5.16** and (*S*)-NMA **5.17** respectively) were reported to be good CSAs for dialkyl sulfoxide species such as **5.18**.⁶⁹¹ The success of the methodology was attributed to the fact that these reagents were more acidic than those of Pirkle and Kagan, allowing for complexation with the basic sulfinyl oxygen of the target substrates at more dilute concentrations. In subsequent studies on dialkyl sulfoxide **5.18** (*S*)-Ibuprofen **5.19** and (*S*)-Naproxen **5.20** were employed because of their structural similarity to MPA and NMA, and greatly reduced price.⁶⁹²

5.2 NMR enantiodiscrimination of Omeprazole, Esomeprazole, and related PPIs

Whilst there are numerous papers on HPLC methods for the determination of enantiomeric purity of Esomeprazole and analogous PPIs, reports of using NMR as a tool are very limited. This is not surprising given the challenges present when handling these sulfoxides; water soluble or acid based CSAs are unsuitable due to the poor solubility and stability of Esomeprazole in neutral or acidic conditions, and a lack of appropriate functionalities means that the use of derivitisation agents is very limited.

Cyclodextrins have been employed as CSAs for the sodium salts of Omeprazole and neutral forms in D₂O, and (*S*)-BINOL **1.43** for use with the neutral forms of the sulfoxides.^{102, 639, 693} Both BINOL and cyclodextrins have been reported in their application for their role in the production of Esomeprazole, the former as a chiral ligand in the Ti-mediated S-oxidation, and both CDs and BINOL in resolution of enantiomers via the formation of inclusion complexes.^{571,}

628, 694-696

More recently Wenzel *et al.* examined 32 different compounds and assessed their use as NMR chiral solvating agents for the determination of enantiopurity of 16 analytes, including Omeprazole.⁶⁹⁷ Five compounds were found to effect full enantiodifferentiation in the ¹H NMR of Omeprazole, these included Pirkle's alcohol **5.10**, BINOL **1.53**, quinine **1.72**, valine **5.21**, and the dinitro- species **5.22**, a CSA named "Whelk-O" developed within the author's laboratories (Figure 5.5). A further four compounds were reported to induced partial enantiodifferentiation when employed as a CSA with Omeprazole **1.1**.

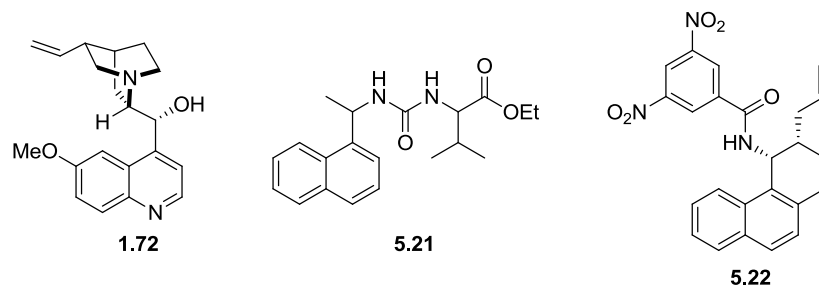


Figure 5.5

5.3 Chiral tartrates as CSA for ee determination in Esomeprazole

We became interested in identifying alternative methods for the determination of enantiopurity of Esomeprazole. Struggles to isolate and purify Esomeprazole had prevented the use of polarimetry. Early results from use of chiral HPLC had led us to believe that the substrate was far too unstable for chromatographic analysis. However upon switching from a reverse-phase HPLC column to a normal-phase one we found that not to be the case. Although satisfactory HPLC methods were subsequently developed for the analysis of Esomeprazole and its salts, this method was sensitive to the presence of other species, such as the sulfide **3.17** and sulfone **4.1**, causing overlapping of signals which affected the accurate measurement of enantiopurity. We decided to look to NMR for an alternative method for measure enantiopurity. Preliminary investigations were carried out using $\text{Eu}(\text{hfc})_3$ and Kagan's benzamide **5.14**, however neither of these were found to give satisfactory NMR spectra suitable for the purpose of measuring enantiomeric excess.

5.3.1 (*S*)-BINOL vs. (*S,S*)-DET as chiral shift agents

The procedure reported by Redondo *et al.*, for the use of (*S*)-BINOL **1.43** as a CSA was followed on a sample of Omeprazole. A 40 mM solution of Omeprazole in CDCl_3 was combined with 1 equivalent of (*S*)-BINOL and a 32 scan 1D ¹H NMR spectra obtained. The enantiodiscriminating effect of the CSA was evident; splitting of the proton signals was

observed for the pyr 6''-H and pyr methyl groups of Omeprazole (\pm)-**1.1**, in accordance with the literature.⁶³⁹ Sample preparation was easy and quantification of enantiopurity was achieved within minutes, as opposed to hours in the case of HPLC. The use of BINOL was however found to have some distinct limitations. Changes in solution concentration and/or NMR experiment run time resulted in overlapping of signals in the aromatic region, limiting the ability to use the pyr 6''-H signals for measurement of the enantiomer ratio (Figure 5.6).

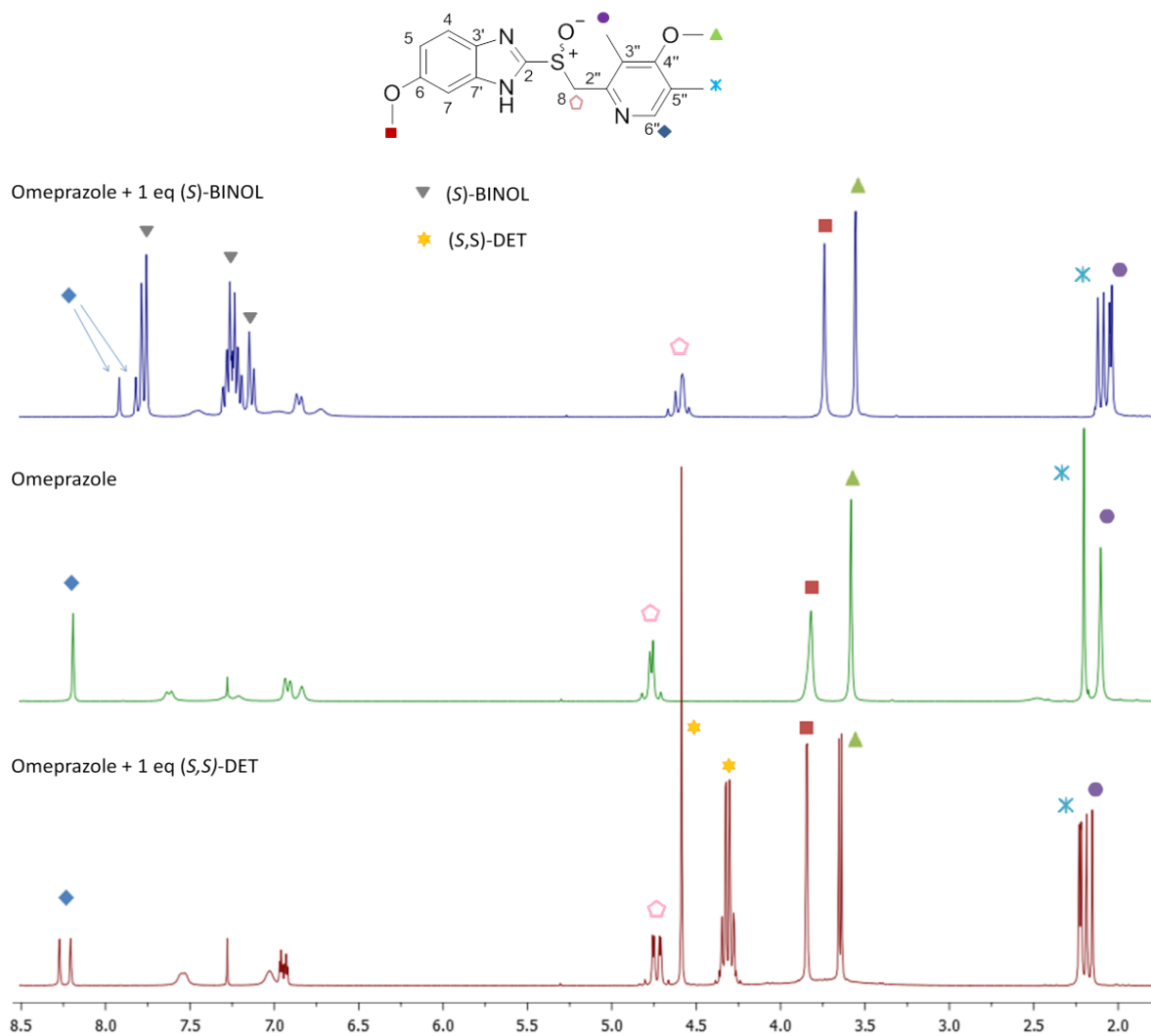


Figure 5.6 ^1H NMR in CDCl_3 : (top) 1:1 (*S*)-BINOL:Omeprazole; (middle) Omeprazole only; (bottom) 1:1 (*S,S*)-DET:Omeprazole.

The dual functionality of BINOL as a CSA and a chiral ligand in the asymmetric synthesis of Esomeprazole gave the inspiration to try (*S,S*)-diethyl tartrate (DET), the reagent we had previously employed as a chiral ligand, as a CSA. In the discussion that follows $\Delta\delta$ and $\Delta\Delta\delta$ shall both be used to describe and quantify the effects observed in the NMR spectra of a specific substance following complexation in solution; $\Delta\delta$ refers to an observed change in the chemical

shift for a specific resonance of a substance and $\Delta\Delta\delta$ is used to quantify the extent of induced magnetic nonequivalence ($\Delta\Delta\delta = |\delta_R - \delta_S|$) of specific signals pertaining to that species.¹⁰²

One equivalent of (*S,S*)-DET in a CDCl₃ solution of racemic Omeprazole gave excellent enantiodiscrimination (Figure 5.6). Magnetic nonequivalence was observed in the form of signal splitting for nearly all protons with the exception of the benz 4- and 7-H which appeared broadened due to tautomerization; quantification of the induced nonequivalence for each of the proton signals is shown in Figure 5.7. In contrast to when BINOL was employed as the CSA, none of the signals from DET were observed to overlap with those of Omeprazole, which was greatly preferable (Figure. 5.6).

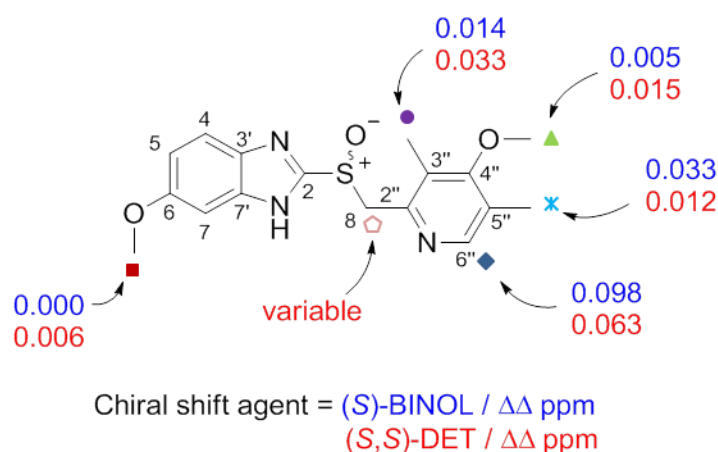


Figure 5.7

5.3.2 Choice of NMR solvent

It was found that the anisochrony between diastereomeric pairs was best observed in hydrophobic deuterated solvents such as DCM-d₂, CDCl₃, toluene-d₈, and benzene-d₆ (Figure 5.8). Due to poor substrate solubility the latter two solvents may be considered poorly suited for this role, however they did afford well resolved spectra with large $\Delta\Delta\delta$ values observed for pyr 6''-H which may be beneficial for measurement of sulfoxide enantiopurity.

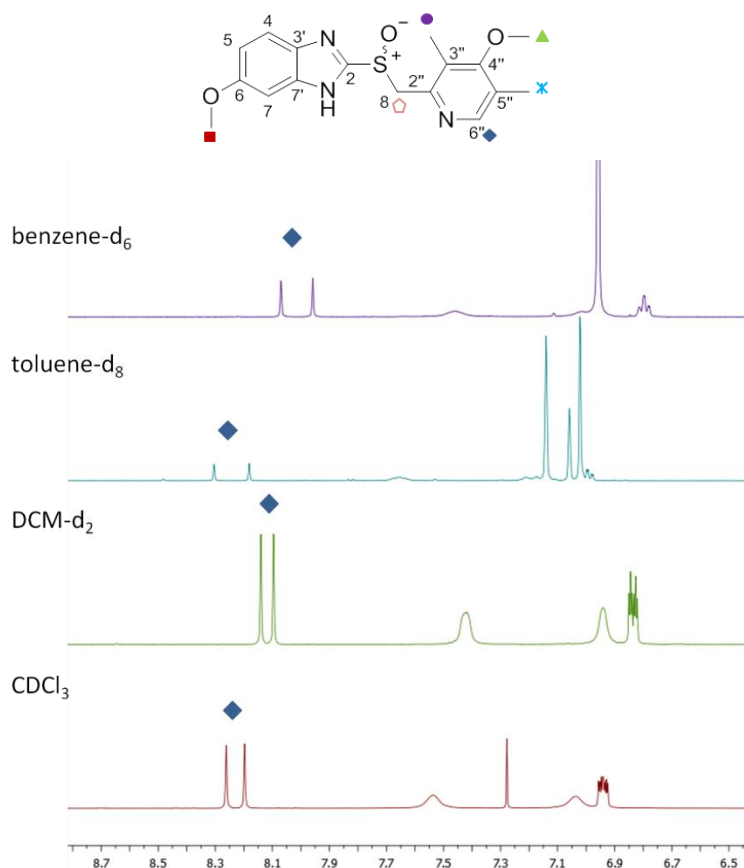


Figure 5.8 ^1H NMR spectra of Omeprazole and DET (1:1) in various solvents

When hydrophilic solvents, such as CD_3OD and DMSO-d_6 , were employed no splitting of resonances for Omeprazole were observed; when acetone-d_6 was used only a very small splitting of the pyr OMe and the Me signals were seen (Table 5.1). It is likely that such water miscible solvents disrupt the hydrogen bonding interactions necessary for the formation of diastereomeric host-guest complexes, whereas the hydrophobic solvents may assist the complex formation via solvophobic effects. Conveniently the pretreatment of CDCl_3 prior to use, such as drying with molecular sieves or passing through a plug of alumina to remove water and DCl , was found to be unnecessary.

Solvent	$\Delta\Delta\delta$ (ppm)						
	pyr 6''-H	CH_2 (d)	CH_2 (u)	benz OMe	pyr OMe	5''-Me	3''-Me
benzene- d_6	0.112	0.008	0.027	0.006	0.011	0.008	0.011
toluene- d_8	0.123	0.005	0.024	0.005	0.007	0.022	0.011
DCM-d_2	0.044	singlet	singlet	0.004	0.012	0.009	0.025
CDCl_3	0.064	0.009	0.007	0.006	0.015	0.012	0.033
acetone- d_6	-	-	-	-	0.004	0.006	0.016

Table 5.5.1 (d) = downfield signal, (u) = upfield signal, refers to the position of the individual proton signals of the CH_2 group

In DCM-d₂, the CH₂ protons of Omeprazole were seen as two singlets but for the other hydrophobic solvents two distinct proton environments could be seen, with different $\Delta\Delta\delta$ values observed for each of the CH₂ protons. In benzene and toluene the sulfoxide CH₂ was weak relative to other Omeprazole signals, these solvents did however provided excellent separation between the signals for the pyr 3''- and 5''-Me, in contrast to the chlorinated solvents. In the spectra of samples in CDCl₃ and DCM-d₂, nonequivalence could be seen for the tartrate CH₂ protons ($\Delta\Delta\delta$ 0.004 ppm in either solvent). When either benzene-d₆ or toluene-d₈ was used a much larger splitting of the tartrate CH₂ was seen, with the higher $\Delta\Delta\delta$ resulting in a complex signal, shown in (Figure 5.9); no other signals of the tartrate CSA showed evidence of magnetic nonequivalence in any of the solvents examined.

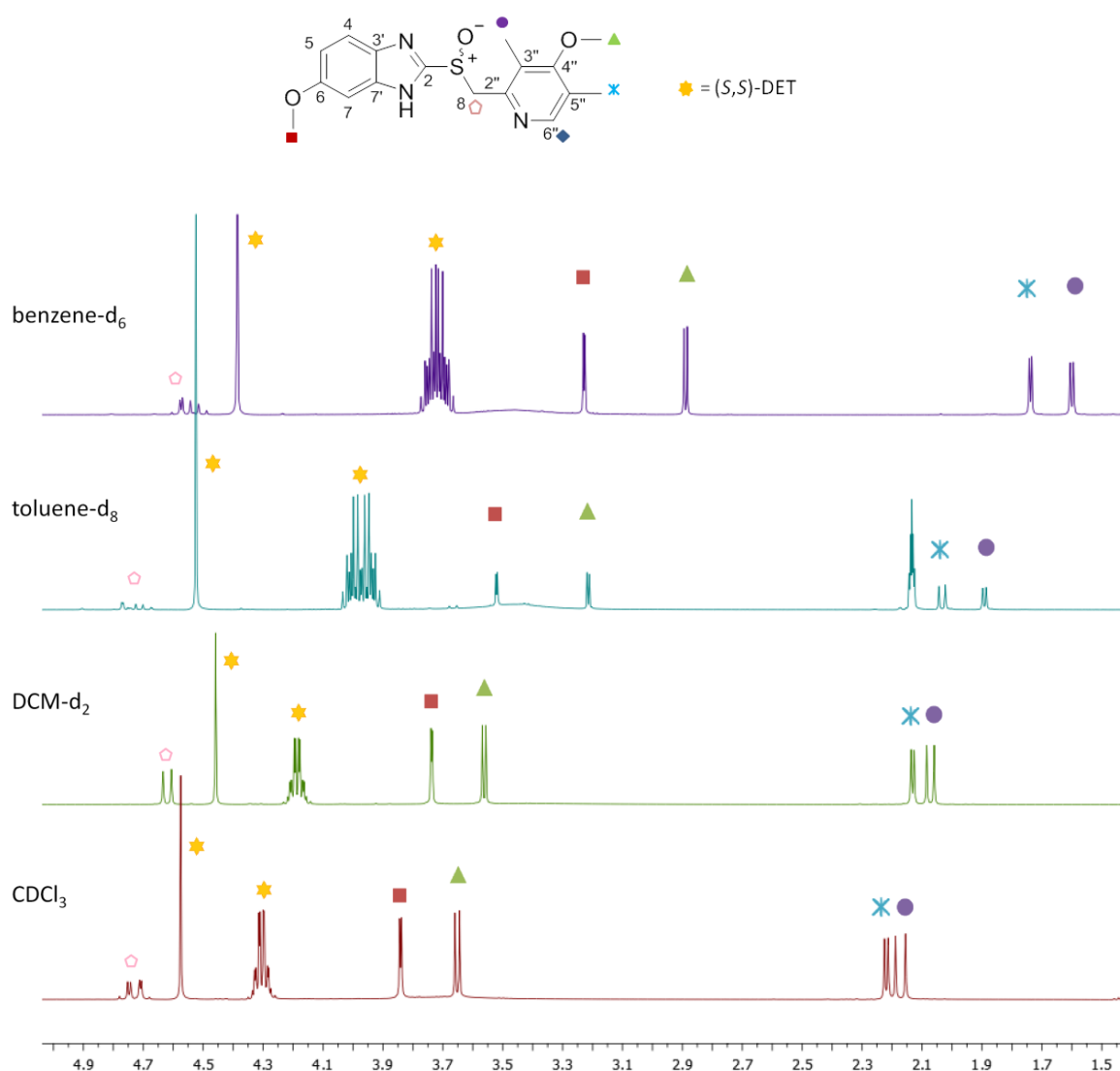
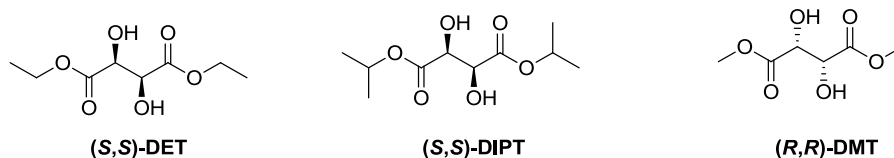


Figure 5.9 ¹H NMR spectra of Omeprazole and DET (1:1) in various solvents

5.3.3 Host-guest ratio

Next we investigated how much chiral tartrate was required to achieve enantioresolution in a sample of racemic Omeprazole. In addition to DET, (*S,S*)-diisopropyl (DIPT), and (*R,R*)-dimethyl tartrate (DMT) were also examined.



It was found that substoichiometric amounts of all three tartrates were sufficient to achieve enantiodifferentiation between the two sulfoxide enantiomers of Omeprazole. When using a 500 MHz spectrometer the addition of only 0.2 equivalents of DET or DIPT was sufficient to achieve baseline separation of the pyr 6''-H peaks of the two enantiomers. If a lower field strength spectrometer i.e. 300 MHz was employed the amount of DET required to resolve the pyr 6''-H resonances of Omeprazole rose to one equivalent. With the 300 MHz instrument we found that 0.5 equivalents of DMT was required for the total separation of the diagnostic pyr 6''-H peaks; it may be assumed that this amount would decrease with the use of a higher frequency instrument.

Samples of racemic Omeprazole in CDCl₃ were treated with increasing amounts of DET and the ¹H NMR spectra obtained (Figure 5.10). No information concerning the enantiodiscriminatory effects of DET as a CSA could be gained from the benzimidazole protons, observed between 6.8-7.70 ppm, due to signal broadening. With increasing amount of DET however the benzimidazole 4- and 7-H signals become more resolved, and a downfield field shift was observed for the benz 4-H, from 6.85 ppm (for Omeprazole) to 7.10 ppm in the presence of five equivalents of DET. The magnetic nonequivalence induced by the addition of the CSA was calculated for diagnostic proton resonances and plotted against the amount of tartrate employed relative to Omeprazole. With increasing amount of the tartrate applied to the substrate, an increase in signal separation was observed relating to a shift in the complexation equilibrium toward the associated species. The effect of complexation was least observed in the methoxy group of the benzimidazole, with $\Delta\Delta\delta$ of only 0.007 ppm after five equivalents of DET. As this group appears to be the least affected this may indicate that it is the furthest away from any site(s) of binding in the association complex. The benzimidazole NH proton signal was not observed in solutions with greater than 0.5 equivalents of tartrate added, however the information that may be gleaned from this observation alone is limited as the NH proton was

found to be highly exchangeable even in the absence of a CSA. The CH₂ signals were also not suitable as the resolution of these protons was found to vary quite significantly; it is thought that this is related to sample concentration, NMR spectrometer frequency and molecular aggregation.

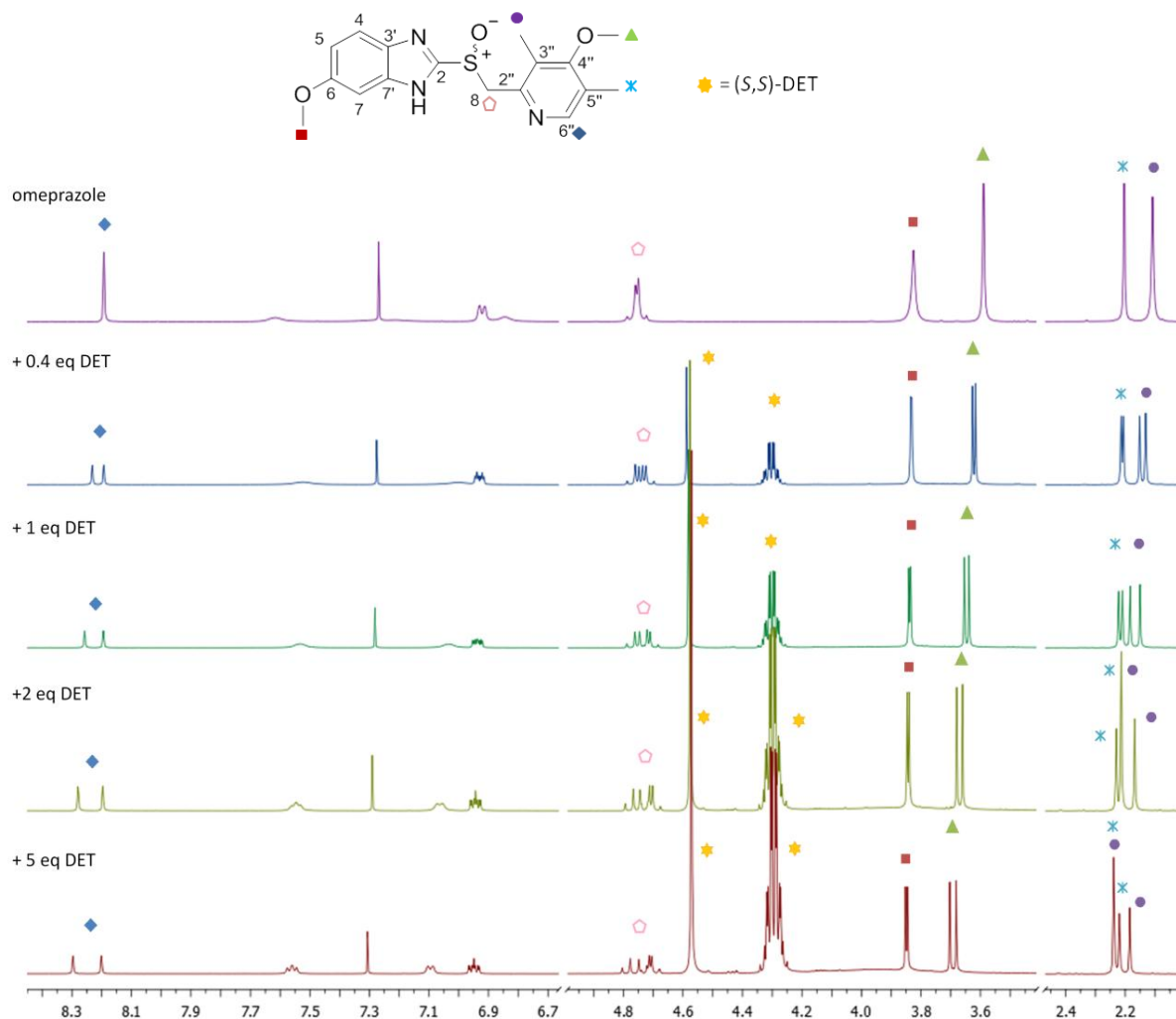


Figure 5.10 ¹H NMR spectra of omeprazole in CDCl₃ in the presence of (S,S)-DET; Top to bottom: 0 equiv DET, 0.4 equiv DET, 1 equiv DET, 2equiv DET and 5equiv DET.

The greatest extent of signal splitting was observed in signals of the pyr 6''-H and 3''-Me protons. Out of all of the proton environment around the pyridine system, these protons are in the closest proximity to the sulfinyl group as illustrated by the presence of cross peaks between these groups and the CH₂ protons in the NOESY spectra of Omeprazole. The high $\Delta\Delta\delta$ values may indicate the involvement of nearby sulfinyl group in complexation with the CSA. The pyridine 5''-Me and methoxy groups are affected very similarly by the increasing addition of the tartrate CSA, and are perturbed to a far lesser extent than the other signals from the pyridine moiety.

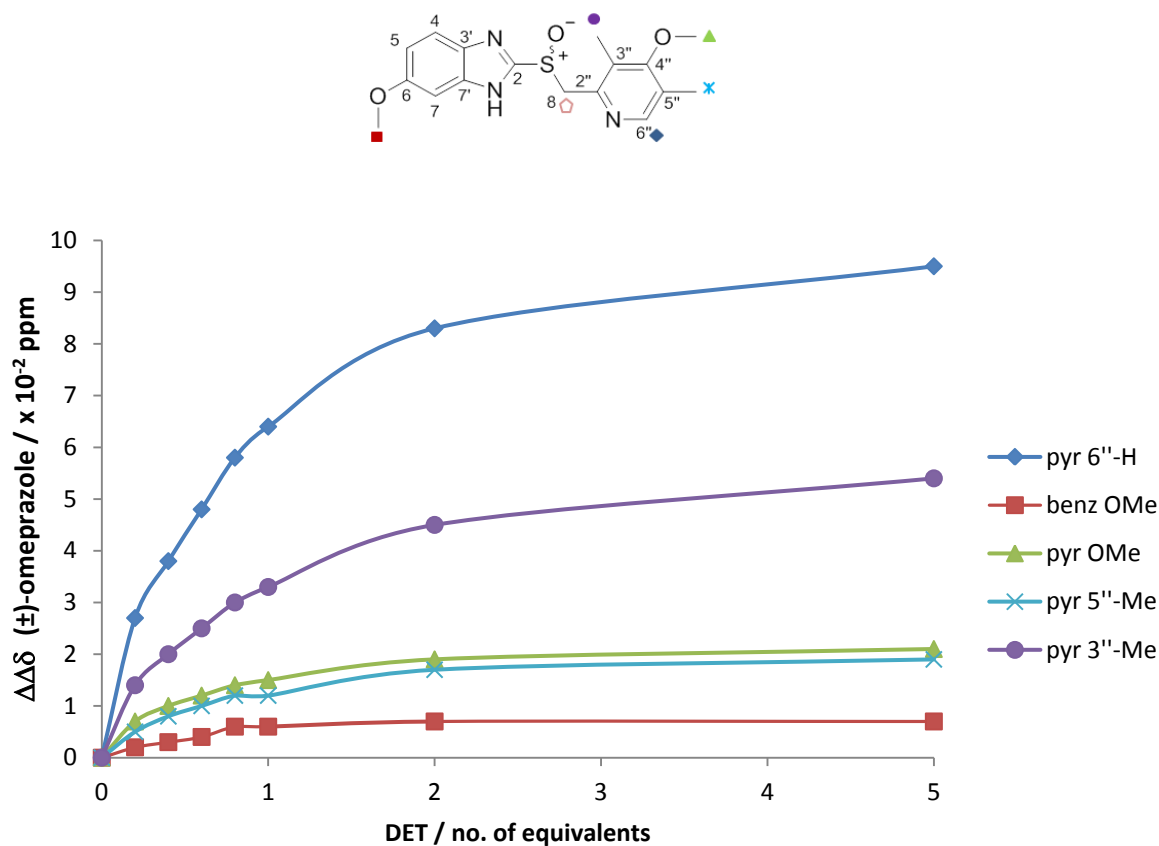


Figure 5.11 $\Delta\Delta\delta$ (ppm) of nonequivalent proton signals observed in spectra of Omeprazole + DET (CDCl_3) against no. of equivalents DET

The effects of adding (*S,S*)-DIPT and (*R,R*)-DMT to racemic Omeprazole were also examined in the same fashion (Figures 5.11 and 5.12 respectively). The extent of splitting in the resonances of the substrate followed the same trend as for DET, with the pyr 6''-H protons affected the most, followed by the pyr 3''-Me group. When DMT was employed no significant splitting of the benzimidazole OMe protons was observed; when DIPT was used no splitting of the pyr 5''-Me protons was found. Interestingly, while the non equivalence observed for the pyr 6''-H signal was distinctly affected by changing the tartrate, very little difference in $\Delta\Delta\delta$ ppm was seen in the signals of other groups. The use of two equivalents of tartrate to Omeprazole produced a nonequivalence of between $\Delta\Delta\delta$ 4.5 and 4.6 in the signal for pyr 3''-Me regardless of which tartrate was employed. In contrast the splitting of the pyr 6''-H peak was found to increase from DMT < DET < DIPT ($\Delta\Delta\delta$ 6.4 < 8.3 < 9.0 respectively). This may be indicative of a correlation between the size of the CSA and the extent of induced nonequivalence, with the tartrate with the larger steric bulk giving rise to greater splitting observed for the specified peak.

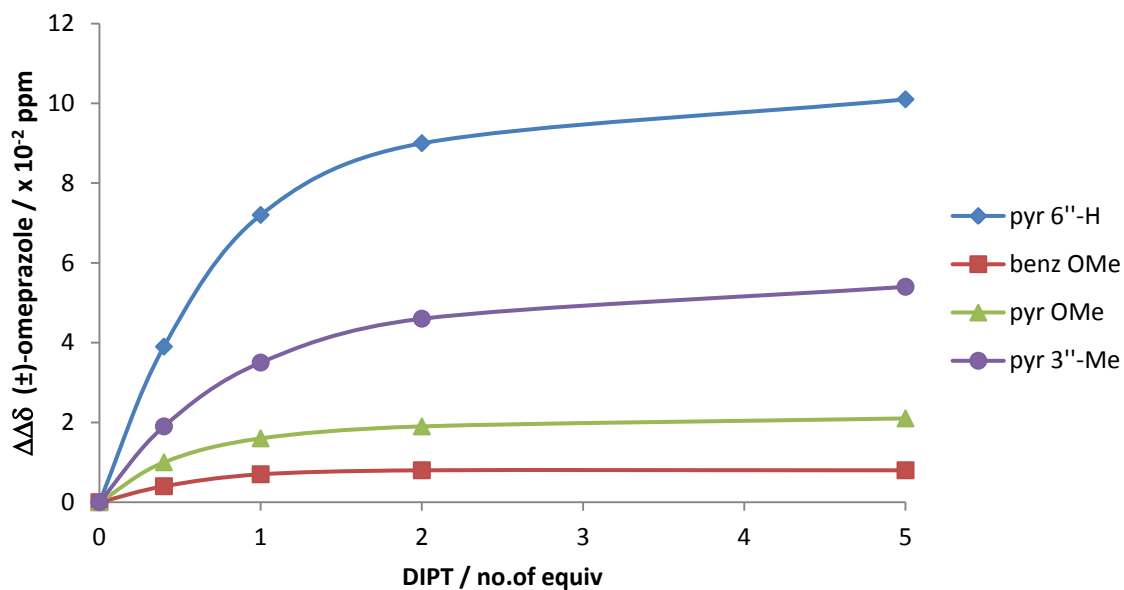
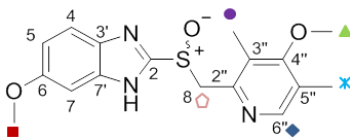


Figure 5.12 $\Delta\Delta\delta$ (ppm) of nonequivalent proton signals observed in spectra of Omeprazole + DIPT (CDCl_3) against no. of equivalents DIPT

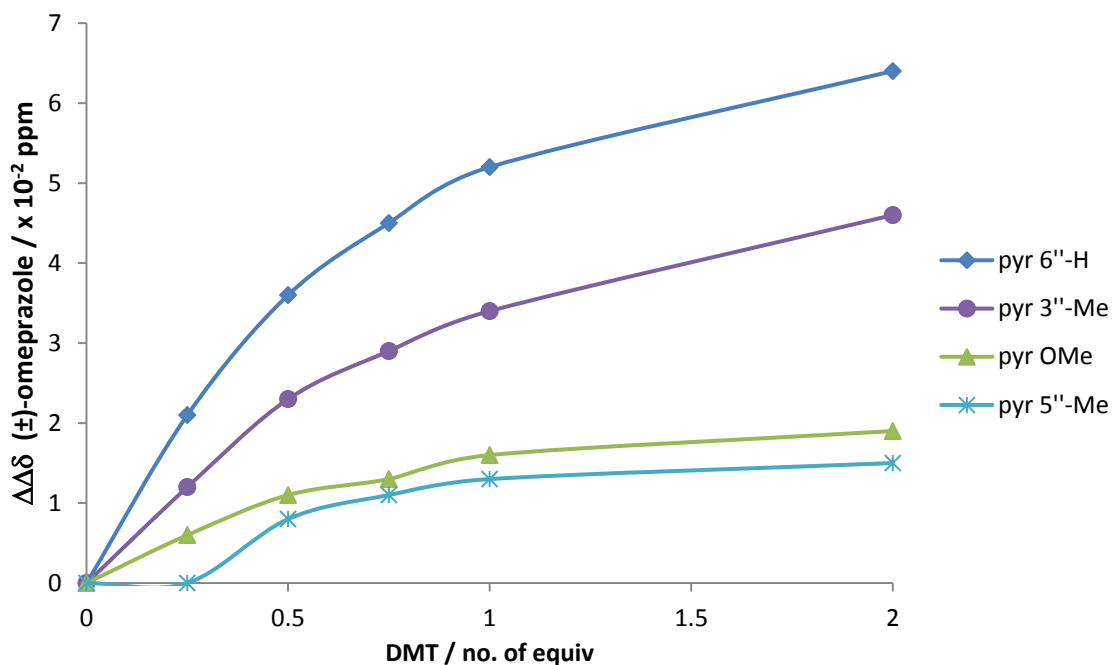


Figure 5.13 $\Delta\Delta\delta$ (ppm) of nonequivalent proton signals observed in spectra of Omeprazole + DMT (CDCl_3) against no. of equivalents DMT

In addition to the nonequivalence induced in many of the proton signals of racemic Omeprazole, notable changes in chemical shifts were also observed upon complexation with DET, DIPT and

DMT. Table 5.2 shows the observed changes in chemical shift for the affected resonances of Omeprazole induced by the addition of 1 equivalent of tartrate; where peak splitting was induced by addition of the tartrate CSA two values are reported, one for each of the nonequivalent proton signals. Complexation with DMT was found to cause the smallest change in the Omeprazole chemical shifts; the effects of DIPT were only marginally greater than those observed when DET was used. The protons of the pyridine group of Omeprazole were all observed to undergo a downfield shift with addition of the tartrate CSAs. The most significant deshielding was observed for the benz 7-H proton (with DET and DIPT), giving a strong indication that in addition to the sulfinyl group, the benzimidazole NH may also be involved in hydrogen bonding interactions with the tartrate CSAs. The tartrates each had a similar shielding effect of the chemical shift of the CH₂ protons.

Assignment	+ (<i>S,S</i>)-DET $\Delta\delta$ / ppm	+ (<i>S,S</i>)-DIPT $\Delta\delta$ / ppm	+ (<i>R,R</i>)-DMT $\Delta\delta$ / ppm
pyr 3''-Me	0.10	0.10	0.09
	0.12	0.13	0.11
pyr 5''-Me	0.03	0.03	0.03
	0.04	0.04	–
pyr OMe	0.08	0.08	0.07
	0.09	0.09	0.08
benz OMe	0.03	0.03	0.03
	0.04	0.04	–
CH ₂ upfield	-0.04	-0.04	-0.03
CH ₂ downfield	-0.06	-0.06	-0.06
benz 4-H	-0.07	-0.07	0.01
benz 5-H	0.03	0.03	0.03
benz 7-H	0.20	0.21	0.10
pyr 6''-H	0.03	0.04	0.03
	0.09	0.10	0.07

Table 5.2 Changes in ¹H chemical shift ($\Delta\delta$ (ppm)) of Omeprazole observed following complexation with 1 equivalent of tartrate

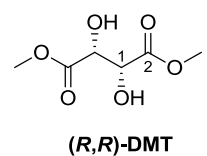
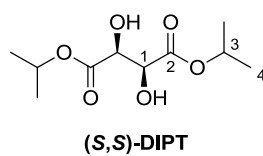
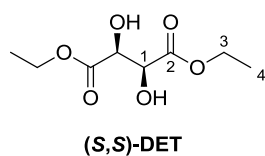
The effects of the tartrate CSAs on the ¹³C chemical shifts of Omeprazole are shown in Table 5.3. Carbon signals from the benzimidazole group offered limited information due to signal broadening and are excluded. Signals assigned to the pyridine and the CH₂ groups were seen further downfield when diastereomeric complexes with the CSAs were formed, with the exception of the pyr C2'' signal which moved upfield. Two peaks were found for many of the

carbon signals ($\Delta\Delta\delta$ values shown in Table 5.3) with appreciable nonequivalence observed for the CH_2 carbon induced by the enantiodiscrimination agents.

Assignment	+ (<i>S,S</i>)-DET		+ (<i>S,S</i>)-DIPT		+ (<i>R,R</i>)-DMT	
	$\Delta\delta$ / ppm	$\Delta\Delta\delta$ / ppm	$\Delta\delta$ / ppm	$\Delta\Delta\delta$ / ppm	$\Delta\delta$ / ppm	$\Delta\Delta\delta$ / ppm
pyr 3''-Me	0.1	0.02	0.1	0.03	0.1	0.02
pyr 5''-Me	0.1	0.02	0.1	0.02	0.1	0.02
pyr OMe	0.2	0.02	0.2	0.02	0.2	–
CH_2	0.1 and 0.3	0.23	0.1 and 0.4	0.23	0.1 and 0.3	0.18
pyr C5''	0.3	0.08	0.2	0.09	0.3	0.05
pyr C3''	0.2	0.07	0.1 and 0.2	0.09	0.2	0.05
pyr C2''	-0.3	0.04	-0.3	0.04	-0.3	0.04
pyr C6''	0.0 and 0.1	0.13	-0.1 and 0.1	0.17	0.0 and 0.1	0.09
pyr C4''	0.1	0.04	0.1	0.03	0.1	0.04

Table 5.3 Changes in ^{13}C chemical shift ($\Delta\delta$ (ppm)), and signal nonequivalence ($\Delta\Delta\delta$ (ppm)) of Omeprazole observed following complexation with one equivalent of tartrate

The changes seen in the chemical shifts of the tartrate CSAs upon interaction with Omeprazole were minimal (Table 5.4). For DMT no change in chemical shift was observed for the methyl groups. Complexation with Omeprazole gave rise to a deshielding effect observed for the 1-H protons of all three tartrates; deshielding was also observed in the ^{13}C signals of C1 and C2 for all tartrates. The alkyl protons of DET and DIPT underwent an upfield shift, which may be attributed to magnetic anisotropy of the heteroaromatic groups of the sulfoxide.

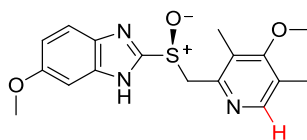


Tartrate	¹ H Assignment	¹ H Δδ (ppm)	¹³ C Assignment	¹³ C Δδ (ppm)
DET	4-H	-0.01	C4	0.1
	3-H	-0.01	C3	0.0
	1-H	0.03	C1	0.1
			C2	0.1
DIPT	4-H	-0.01	C4	0.0
	3-H	-0.01	C3	-0.1
	1-H	0.02	C1	0.2
			C2	0.1
DMT	3-H	0.00	C3	0.0
	1-H	0.03	C1	0.2
			C2	0.2

Table 5.4 Changes in ¹H and ¹³C chemical shift (Δδ (ppm)) of tartrates DET, DIPT, and DMT observed following complexation with one equivalent of Omeprazole.

5.3.4 Determination of enantiomeric excess

The efficacy of the diethyl- and dimethyl tartrates in the role of chiral shift reagents for enantiodetermination by NMR was assessed by comparing the results of chiral HPLC and NMR analysis of Esomeprazole samples across a range of % optical purities. A range of sulfoxide:tartrate ratios were examined, from 0.25 equivalents of tartrate up to five equivalents, with CDCl₃ used as the solvent. The pyr 6"-H was used to measure the ratio of diastereomeric complexes formed with the chiral tartrates in solution (Figure 4.14). The agreement between the two methods was found to be very good; the greatest variation between HPLC and NMR was found to be only 1% ee for both DET and DMT (Table 5.5).



(S)-1.1

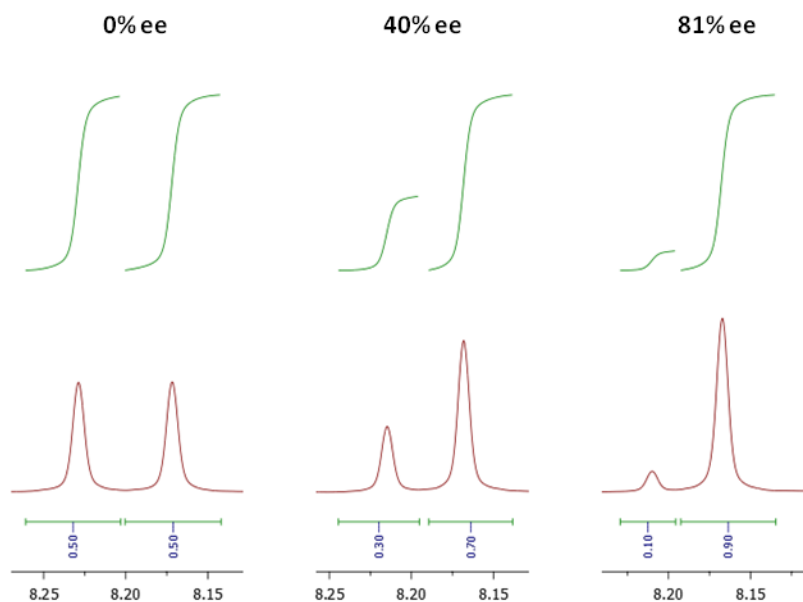


Figure 5.14

Tartrate CSA	% ee (NMR)	% ee (HPLC)
DET (one equiv)	0	0
	20	20
	40	40
	53	54
	60	60
	81	81
	100	100
DMT (one equiv)	0	0
	22	21
	40	41
	50	50
	62	63
	81	81
	100	100

Table 5.5 Comparison of enantiomeric excesses determined by ^1H NMR using tartrate based chiral shift reagent and by chiral HPLC

When (*S,S*)-DET or (*R,R*)-DMT were used as the CSA one equivalent of the tartrate was required to get baseline resolution of the diagnostic pyr 6"-H proton for sulfoxides across the whole ee range (Figure 5.15). The resolution of nonequivalent peaks was easily improved by further addition of the appropriate tartrate.

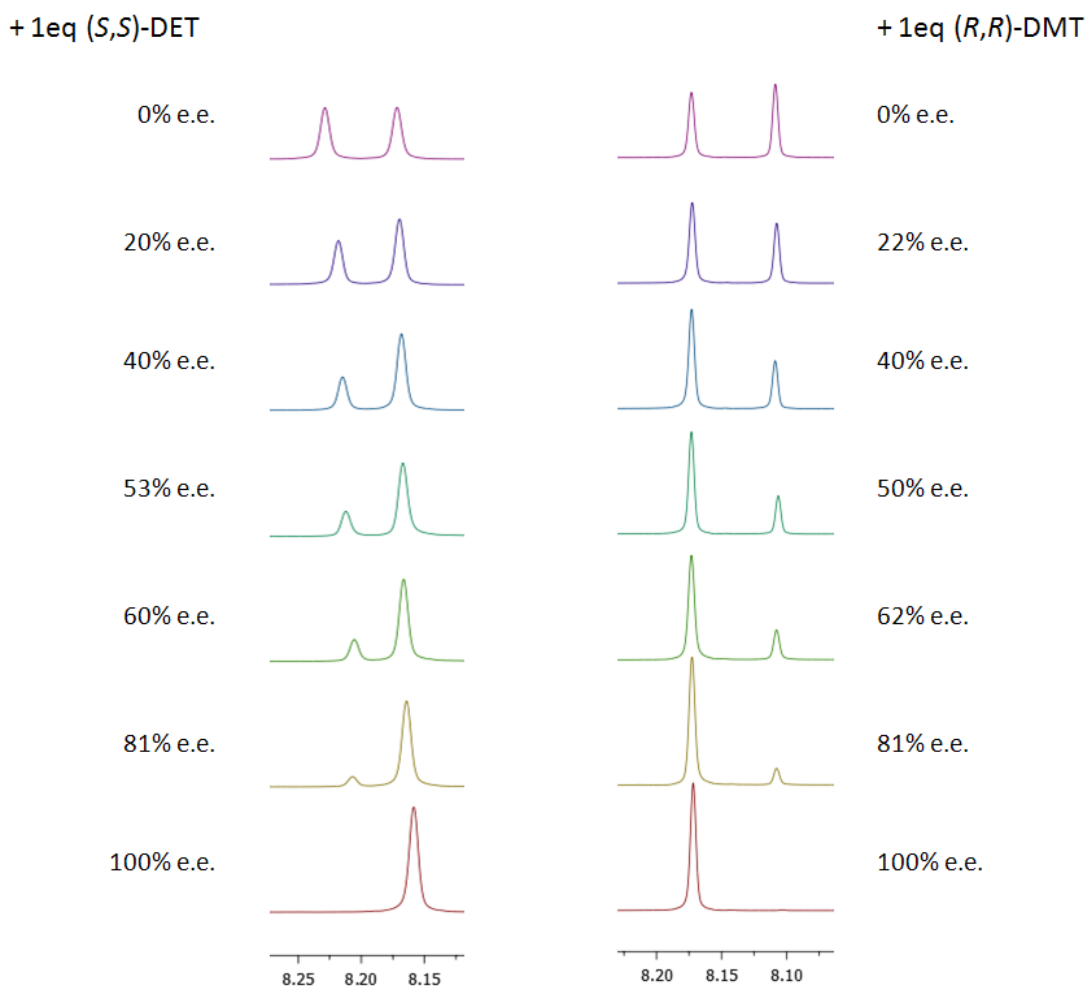


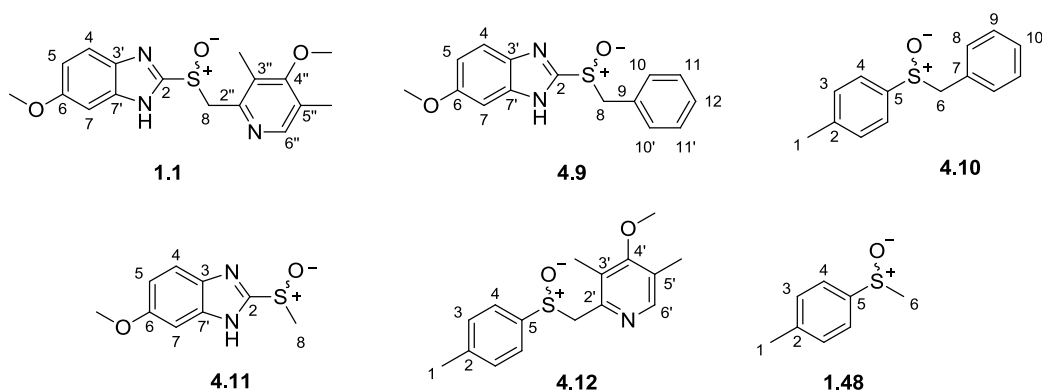
Figure 5.15 Comparison of the ^1H NMR obtained from Esomeprazole of varying enantiopurity with the addition of chiral shift reagents (*S,S*)-DET or (*R,R*)-DMT

As mentioned previously, the use of chiral HPLC for the determination of Esomeprazole enantiopurity required prior purification of the sulfoxide, either by column chromatography or via formation of the Na-salt **3.36**. One important advantage that was found with using NMR was that no prior purification was required for such analysis. With all three tartrates it was possible to measure the ratio of sulfoxide enantiomers from the materials obtained from the extraction process of the asymmetric S-oxidation process, which typically contained other compounds such as the sulfide starting material and/or sulfone byproduct.

When using the tartrates as CSAs with the Omeprazole and Esomeprazole it was observed that a distinct colour change took place, with the colourless sulfoxide solutions changing to a dark purple over a number of hours. This change in appearance is typically observed when Omeprazole undergoes degradation reactions to produce highly coloured product. In order to assess if any significant degradation of the sulfoxide was taking place in the presence of the tartrates ^1H NMR analysis was carried out on solutions containing stoichiometric amounts of DET and Esomeprazole, with sulfoxide enantiomeric excess of 94 and 88%. ^1H NMR spectra obtained 24h after sample preparation showed evidence of degradation in the form of trace impurities now present on the base line; by comparison with the NMR spectra acquired less than 10 min after sample preparation it was possible to estimate that for each of the two samples over 90% of the original sulfoxide material remained after 24h. The enantiodiscrimination of the tartrate CSA was still in effect with little to no change in sulfoxide % ee, suggesting that under these conditions the rates of decomposition are equal for both enantiomers.

5.4 Contrasting enantiodiscriminatory action of CSAs: DET vs. BINOL.

The effects of (*S,S*)-DET and (*S*)-BINOL on a broad range of sulfoxides were compared with the addition of one equivalent of either chiral shift agent to solutions of the racemic sulfoxide **4.9-4.11** and **1.48** in CDCl_3 (Table 5.6). The two chiral shift reagents were found to have very different effects on the sulfoxides examined. With DET significant splitting of peaks was only seen in spectra of Omeprazole and sulfoxide **4.11**. In contrast, enantiodiscrimination was observed for every sulfoxide with BINOL. For Omeprazole the pyr 6''-H protons had a nonequivalence of $\Delta\Delta\delta$ 0.098 and 0.095 with (*S*)-BINOL and DET respectively. The only other incidence of a splitting of such magnitude ($\Delta\Delta\delta$ 0.077) was seen for the analogues pyr 6''-H proton of sulfoxide **4.12** with BINOL as the CSA.



Sulfoxide	Assignment	(S)-BINOL	(S,S)-DET
		$\Delta\Delta\delta$ (ppm)	$\Delta\Delta\delta$ (ppm)
Omeprazole (\pm)-1.1	pyr 3''-Me	0.014	0.047
	pyr 5''-Me	0.033	0.019
	pyr OMe	0.005	0.020
	benz OMe	–	0.007
	CH ₂ (u)	–	0.008
	CH ₂ (d)	–	0.015
	pyr 6''-H	0.098	0.094
(\pm)-4.9	benz OMe ^a	0.011	–
	CH ₂ (u)	0.010	–
	CH ₂ (d)	0.022	–
(\pm)-4.10	CH ₂ (u)	0.007	–
	CH ₂ (d)	0.013	–
(\pm)-4.11	SMe	0.018	0.008
(\pm)-4.12	pyr 3''-Me	0.011	0.005
	pyr 5''-Me	0.022	–
	CH ₂ (u)	0.054	–
	CH ₂ (d)	0.021	–
	pyr 6''-H	0.077	–
(\pm)-1.48	SMe	0.011	–

Table 5.5.6 ^a downfield tautomeric signal; (u) upfield CH₂ proton; (d) downfield CH₂ proton

For sulfoxides **4.9**, **4.11** and **1.48** the enantiorecognition of the CSAs was not sufficient, either in terms of magnitude or resolution of NMR signals, for practical measurement of % ee with one equivalent of either DET or BINOL. Complexation of sulfoxides **4.10** and **4.12** with

(*S*)-BINOL resulted in well resolved splitting of the CH₂ proton (Figure 5.16). Although some nonequivalence was observed for analogous protons in other sulfoxide spectra only for sulfoxide **4.12** and **4.10** was the effect so distinct.

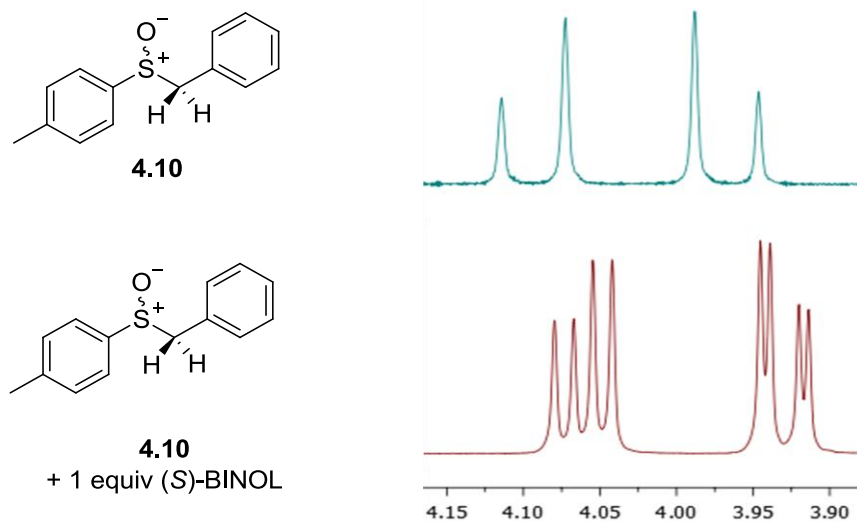


Figure 5.16

BINOL and DET were found to induce contrasting nonequivalence in the pyr methyl signals of Omeprazole. With DET as the CSA, a greater $\Delta\Delta\delta$ was observed for the pyr 3''-Me than the 5''-Me (0.047 and 0.019 ppm respectively). This was reversed however when BINOL was employed, with observed $\Delta\Delta\delta$ of 0.012 (pyr 3''-Me) and 0.028 ppm (pyr 5''-Me). (*S,S*)-DET was also found to exert an effect upon the methoxy group protons of both the benzimidazole and the pyridine groups of Omeprazole; in contrast BINOL showed no significant splitting of either OMe signal. It is possible that the contrasting chiral recognition displayed for Omeprazole with DET and BINOL arises from different modes of complexation. Toda *et al.* reported that chiral host molecules such as BINOL worked in a similar manner to shift reagents such as Pirkles alcohols, with hydrogen bonding between the sulfinyl oxygen of a guest sulfoxide and the host alcohol (Figure 5.17). Studies of the X-ray structure of (-)-methyl *m*-tolyl sulfoxide and (*S*)-BINOL showed the appropriate orientation of the naphthyl group of (BINOL) to account for the shielding of the methyl group observed in the NMR spectra.⁶⁹⁸ It may be assumed that sulfoxides such as Omeprazole interact with BINOL in a similar fashion, with the size disparity of the groups either side of the sulfinyl group matching those of the proposed model.

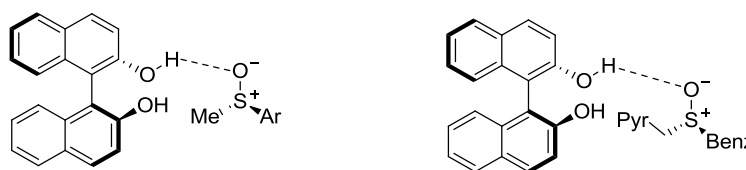


Figure 5.17

The contrasting effects of the dialkyl tartrate CSAs, in terms of the groups in which nonequivalence is induced and with respect to the shielding/deshielding observed in the NMR spectra of Omeprazole indicate that there may be additional interactions in the host-guest complexes. One possibility is the involvement of the pyridyl nitrogen, in addition to the sulfinyl group and benzimidazole NH, in hydrogen-bonding interactions with the tartrate CSA, (Figure 5.18). However, given that sulfoxide **4.12** shows minimal splitting with DET it is unlikely that interaction with the pyridine nitrogen alone in combination with hydrogen bonding interactions of the sulfinyl group is responsible for the induced nonequivalence observed.

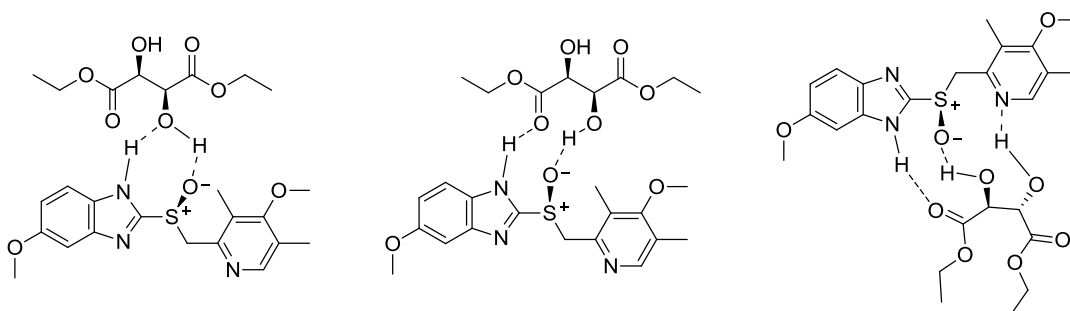
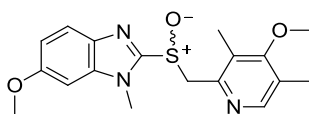


Figure 5.18

When the NMe derivative of Omeprazole **5.22** was treated with a tartrate based CSA no enantiodiscrimination was observed by NMR, highlighting the importance of the NH functionality in the formation of diastereomeric complexes with the tartrates such as DET. The greater length of the tartrate CSAs backbone, in comparison with BINOL, may account for the splitting in signals observed for groups on the periphery of the sulfoxide such as the benz- and pyr-OMe protons.



5.22

To further investigate the nature of the interactions between the tartrate CSAs and Omeprazole, attempts were made to grow co-crystallize Omeprazole with DMT, the only crystalline tartrate of the three examined. Unfortunately this was not successful, with only the racemic sulfoxide obtained in crystal form, as determined by X-ray analysis. It was interesting however that with the addition of one equivalent of DMT, crystallization of Omeprazole by the optimized method (diethyl ether anti solvent added to concentrated solution of sulfoxide in dichloromethane) gave the sulfoxide product in a more crystalline form than the powders typically obtained. Future

optimization of the crystallization process may allow for the growth of co-crystals between Omeprazole or Esomeprazole and various tartrates.

5.5 Conclusions and future directions

(*S,S*)-Diethyl tartrate is a common chiral ligand in the synthesis of Esomeprazole via Ti-mediated asymmetric oxidation; we have shown that it can have a second application in the quantification of enantiopurity by NMR. (*S,S*)-Diethyl tartrate was shown to have excellent enantioselectivity towards the enantiomers of Omeprazole, but limited applicability towards other sulfoxides examined here. It is likely that tartrate CSA such as DET, DIPT, and DMT would, however, be applicable for other analogous PPIs such as Rabeprazole **3.3** which share a common structural benzimidazole-pyridine framework with Omeprazole. Although other CSAs such as (*S*)-BINOL have been reported for this specific application, the diethyl, diisopropyl, and dimethyl tartrates examined here are better suited as they have little or no overlap with proton signals of the sulfoxide substrate, enabling easier analysis of spectra, and subsequently better measurement of sulfoxide enantiopurity. The 2016 paper from Wenzel *et al.* identified a number of compounds that enabled partial or total enantiodifferentiation in the ¹H NMR spectra of Omeprazole but again these CSA give rise to numerous additional proton signals, some of which overlap with those of the sulfoxide under examination.

The tartrates DET, DIPT, and DMT are inexpensive, non toxic and widely available in both their natural and unnatural enantiomeric forms. Sample preparation for NMR analysis was quick and simple; the liquid tartrates DET and DIPT could be injected directly into an NMR tube, and if necessary the separation of the sulfoxide from the CSA could be simply achieved by column chromatography. One of the only disadvantages of this method comes from the high viscosity of DET and DIPT, meaning that it can be difficult to use in μL quantities. However, the enantiodiscriminatory effects of the tartrates increase as the ratio of tartrate to sulfoxide increases so the only limitation to the overuse of tartrate comes from the relative intensities of guest/host signal peaks in the NMR spectra. The tartrates examined here were highly suitable for use with sensitive substrates such as Esomeprazole. In samples of Omeprazole and tartrate changes in colour were observed, from colourless to purple, which is typically associated with decomposition of the sulfoxide. Analysis by NMR showed that although after 24 h some decomposition had occurred, there was sufficient time for collection of extensive spectroscopic data. Similar issues would be expected with other shift reagents, especially those which are more acidic in nature such as (*S*)-Binol **1.43**.

Comparison of chiral HPLC and NMR methods showed good agreement in the optical purities measured for a range of Esomeprazole samples. It was also found that with the tartrate CSAs it was possible to measure the enantiopurity of Esomeprazole in the presence of common impurities such as sulfide **3.17** and sulfone **4.1**, which is greatly advantageous over the chiral HPLC method. Further investigation may give insight into the structural aspects of complexes formed between sulfoxides such as Omeprazole and the tartrates examined here. More information on the stoichiometry of the sulfoxide:tartrate complex may be gained through investigations using the Continuous Variation Method i.e. construction of a Job plot.^{699, 700} It is possible that sulfoxides with similar heterocyclic motifs, such as imidazole rings, may also be suitable substrates for tartrates CSAs. Examination of the enantiodiscrimination abilities of tartrates on alternative substrates may give insight into the diastereomeric complexes formed in solution. The variation in spectra arising from the use of the different hydrophobic NMR solvents may prove useful in optimizing % ee measurement and further consideration of the nature of the enantiodiscriminating abilities of the tartrates examined here. In addition, investigations of tartramides and alternative tartrates, such as diaryl tartrates may prove fruitful in terms of understanding the nature of host-guest interactions between CSAs of this type and sulfoxides. Investigations may although reveal further compounds which can be used for enantiomeric determination of sulfoxides such as Esomeprazole (*S*)-**1.1**; the tartaric acid derivative **1.42** is known to resolve pyridyl sulfoxides through host-guest complexation and would be an interesting candidate for exploring its abilities to act as a CSA toward Omeprazole.¹⁰⁵ The X-ray crystallographic structure of the complex between **1.42** and ethyl pyridyl sulfoxide showed hydrogen bonds between the sulfinyl group and the hydroxyl group of **1.42**, with no involvement of the pyridine heterocyclic (Figure 5.19); formation of analogous host:guest complexes with Omeprazole and Esomeprazole may also prove enlightening.

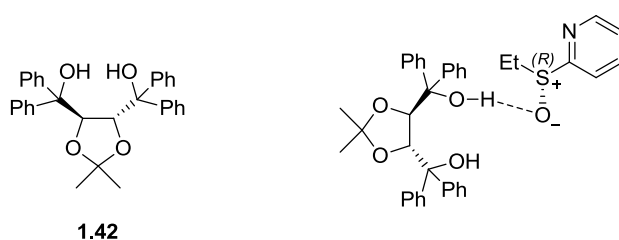
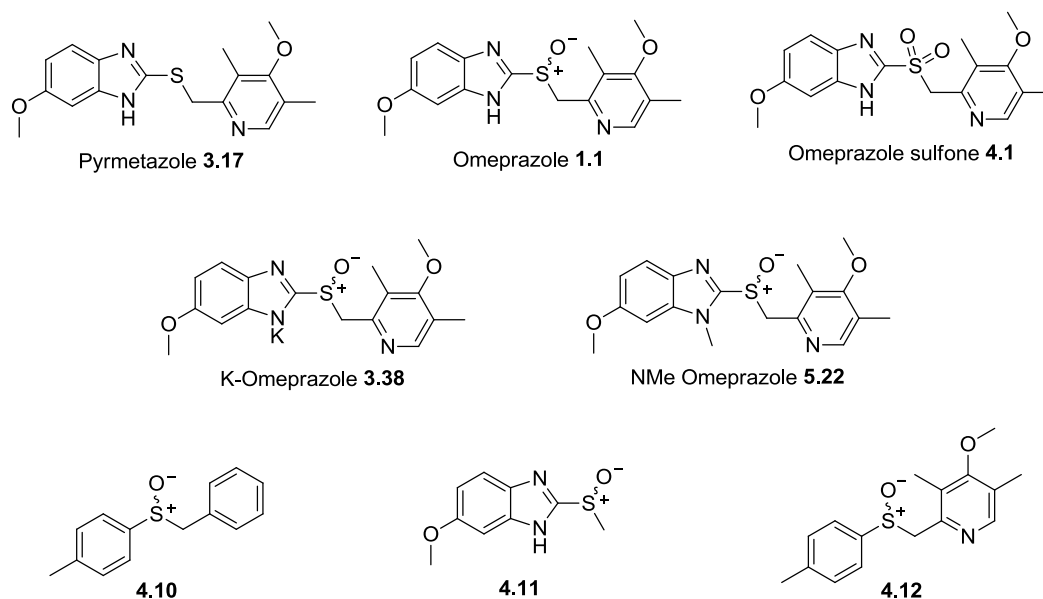


Figure 5.19

6 Studies on the structure and reactivity of Omeprazole and related compounds

6.1 X-ray crystallography of Omeprazole and related compounds

X-ray characterization was performed for a variety of compounds in the Omeprazole family: Omeprazole **1.1**, the sulfide Pyrimetazole **3.17**, Omeprazole sulfone **4.1**, the potassium salt of Omeprazole **3.38**, and NMe Omeprazole **5.22**. In addition characterization was also performed on the sulfoxides **4.10-4.12**. Of these compounds only the crystal structures of Omeprazole **1.1** and sulfoxide **4.10** have been previously deposited in the Cambridge Crystallographic Data Centre (CCDC), the crystal structures for the remaining compounds are thus far unreported.^{567, 571, 572, 701, 702} X-ray diffraction (XRD) analysis was kindly performed by Dr Chris Pask, of the University of Leeds Department of Chemistry, who also assisted in the analysis of the crystallographic structures and packing of these compounds.



6.1.1 X-ray structures of the Omeprazole family

X-ray characterization for Omeprazole **1.1**

Materials suitable for XRD analysis were grown by slow evaporation from an acetone solution, or from addition of Et₂O to a solution in CDCl₃. Crystals were obtained as colourless platelets which were cut down for the X-ray analysis. Omeprazole **1.1** crystallizes in a triclinical cell and was solved in the *P*-1 space group, with one molecule in the asymmetric unit (Figure 6.1). The

crystal structure obtained for Omeprazole was found to be in excellent agreement with the previously published data.⁵⁷² Tautomeric disorder was exhibited by the compound; disorder of the benzimidazole ring could not be adequately modeled which is in line with the previous publication.⁵⁶⁷ The ratio of tautomers (derived from refinement of the site occupancy factors) was 15:85 5-OMe:6-OMe, matching one of the tautomeric polymorphic crystal forms of Omeprazole reported by Desiraju and Bhatt.⁵⁶⁷

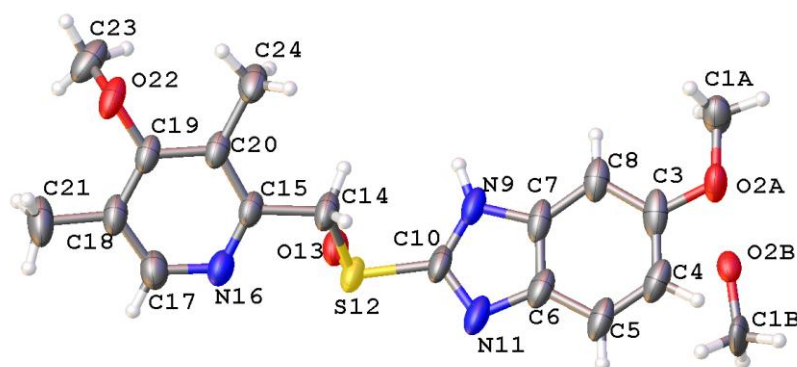


Figure 6.1 Crystal structure of Omeprazole 1.1. Displacement ellipsoids are at 50% probability level and hydrogen atoms are omitted for clarity

Assessment of the intermolecular interactions was conducted taking only the main tautomer (6-OMe Omeprazole) into consideration. Omeprazole **1.1** adopts an extended form with the pyridine ring almost coplanar to the benzimidazole; in addition the methylsulfinyl group adopting a *trans* conformation. In the solid state the racemic sulfoxide **1.1** forms heterochiral dimers, with two centrosymmetrically related molecules connected by intermolecular H-bonding between the benzimidazole NH and the sulfinyl oxygen, with N9H...O13 and H...O13 distances of 2.759(3) Å and 1.87(4) Å respectively (Figure 6.2).

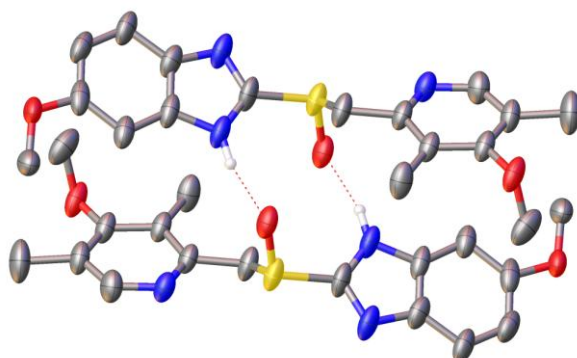


Figure 6.2 Heterochiral dimer formed through H-bonding between molecules of Omeprazole 1.1

The dimers of Omeprazole formed through H-bonding pack together through π - π interactions, with a stacking distance of 3.647(2) Å between benzimidazole rings (Figure 6.3)

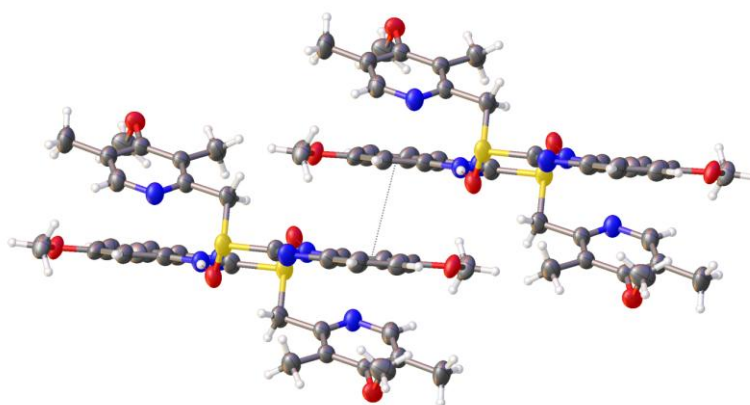


Figure 6.3 π -Stacking interactions between dimers of Omeprazole 1.1

The formation of heterochiral dimers in the solid state is consistent with the experimental observations made for Omeprazole, mentioned previously in chapter 4. Omeprazole was found to exhibit different physical properties to the single enantiomer form Esomeprazole, with the racemic sulfoxide being less soluble than the optically pure isomer which can be attributed to the formation of stable heterochiral dimers in the solid state, with two H-bonding interactions between molecules. In contrast if analogous homochiral dimers were to form, for example for Esomeprazole, fewer H-bonding interactions are possible due to the orientation of the sulfinyl groups which leads to dimers with less favourable intermolecular interactions holding them together (Figure 6.4).

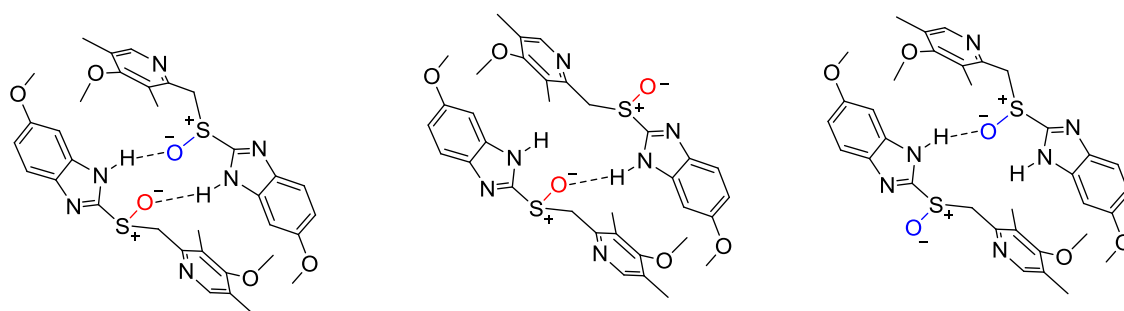


Figure 6.4 Heterochiral (left) and homochiral dimers (centre and right) of Omeprazole 1.1

Crystallization of Omeprazole as a racemate was found to be advantageous with respect to enhancing the enantiopurity of Esomeprazole afforded by the titanium-mediated asymmetric sulfoxidation reactions. Precipitation of racemic Omeprazole could be induced from materials of high sulfoxide ee ($> 80\%$ ee) with the sulfoxide remaining in solution being enhanced in ee. The process was achieved by addition of an antisolvent to a solution in CH_2Cl_2 , or by stirring a solution in MeCN. Using this method Esomeprazole was obtained in $> 97\%$ ee from starting materials of 80% ee.

X-ray characterization for Pyrimetazole sulfide **3.17**

Colourless crystals of Pyrimetazole **3.17** suitable for XRD were obtained by slow evaporation from a solution in CDCl_3 over a period of several days. This sulfide crystallized in an orthorhombic cell and structural solution was performed in the space group $P2_12_12_1$ with one molecule in the asymmetric unit (Figure 6.5).

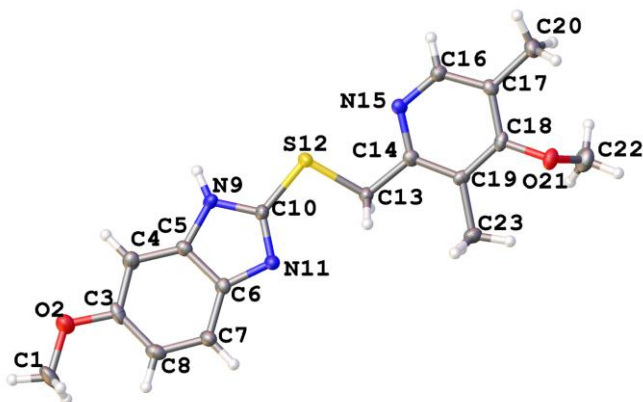


Figure 6.5 Crystal structure of Pyrimetazole **3.17**. Displacement ellipsoids are at 50% probability level and hydrogen atoms are omitted for clarity

Pairs of sulfide molecules are held together by H-bonding interactions between the thioether group and the benzimidazole NH (N9H...S12 3.371(2) Å, H...N 2.692(3) Å) and the benzimidazole NH and pyridyl N (N9H...N15 2.937(3) Å, H...N 2.142(4) Å) (Figure 6.6). The dimers of the sulfide **3.17** form a double strand type structure along the crystallographic a axis (Figure 6.7).

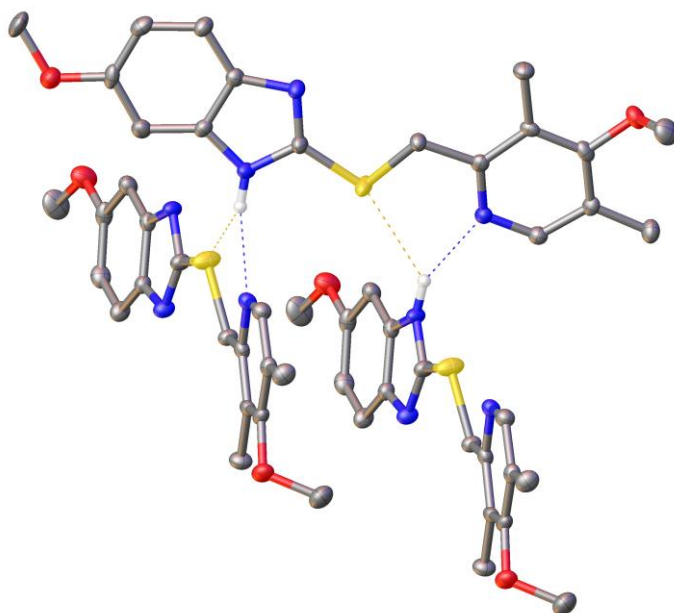


Figure 6.6 Intermolecular H-bonding between molecules of Pyrimetazole sulfide **3.17**

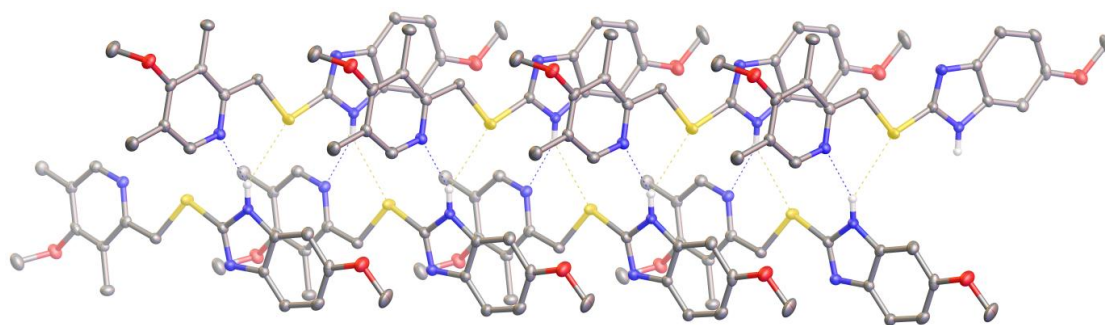


Figure 6.7 Double strand structure formed by Pyrmetazole 3.17

X-ray characterization for Omeprazole sulfone 4.1

Crystals of the sulfone **4.1** suitable for XRD was obtained in the form of the solvate by slow evaporation from a solution in MeOD over a period of several days. Crystals were obtained as colourless cubes which were cut down for the X-ray experiment. Omeprazole sulfone **4.1** crystallized in a triclinical cell and was solved in the *P*-1 space group, with one molecule of MeOD in the asymmetric unit.

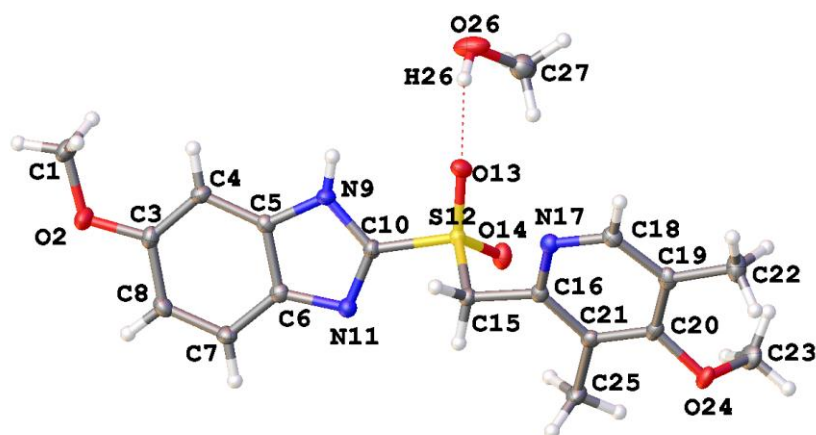


Figure 6.8 Crystal structure of the Omeprazole sulfone 4.1, obtained as the MeOD solvate. Displacement ellipsoids are at 50% probability level and hydrogen atoms are omitted for clarity

The solvate of the sulfone **4.1** exists as tetramers comprising of two molecules of the sulfone plus two solvent molecules connected through H-bonding interactions (N17H...O26 2.766(2) Å, H...O26 1.97(2) Å, and O26H...O13 2.746(18) Å, H...O13 2.00(3) Å) (Figure 6.8). No significant π - π stacking is observed between the tetramers of sulfone **4.1** (Figure 6.9 and 6.10).

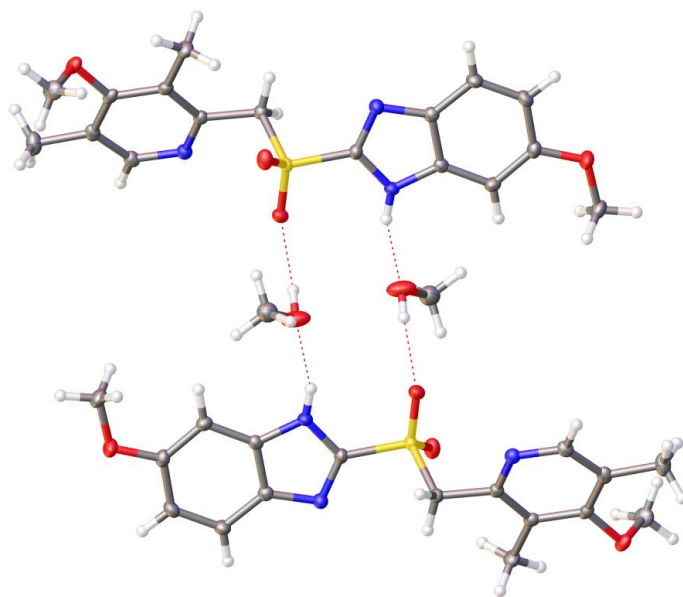


Figure 6.9 Tetramer formed between molecules of Omeprazole sulfone 4.1 and MeOD

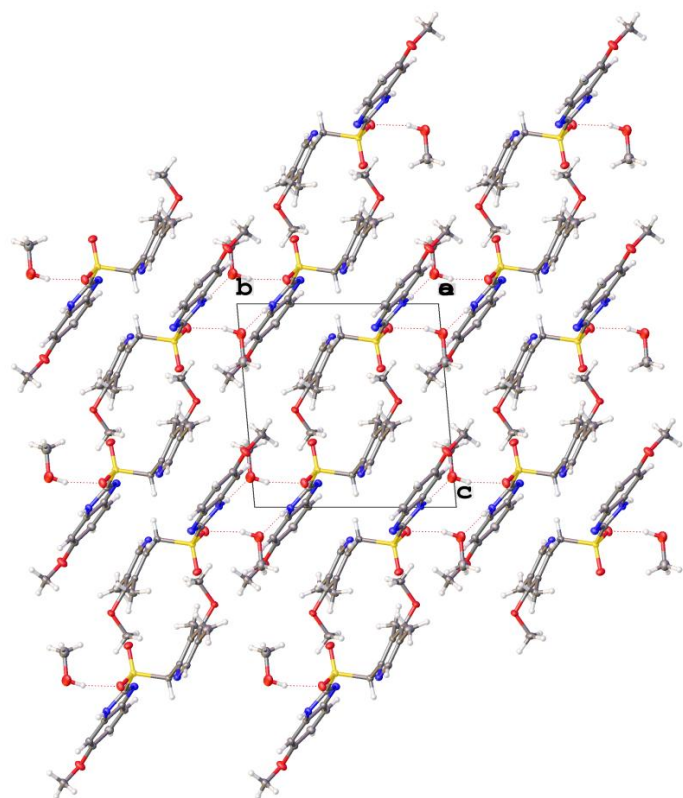


Figure 6.10 Packing diagram of Omeprazole sulfone 4.1 as the MeOD solvate

X-ray characterization for K-Omeprazole 3.38

Colourless platelets of K-omeprazole **3.38** were obtained through addition of Et₂O to a solution in MeOH. The compound crystallized as a one dimensional polymeric chain with one “unit” in the asymmetric unit (Figure 6.11).

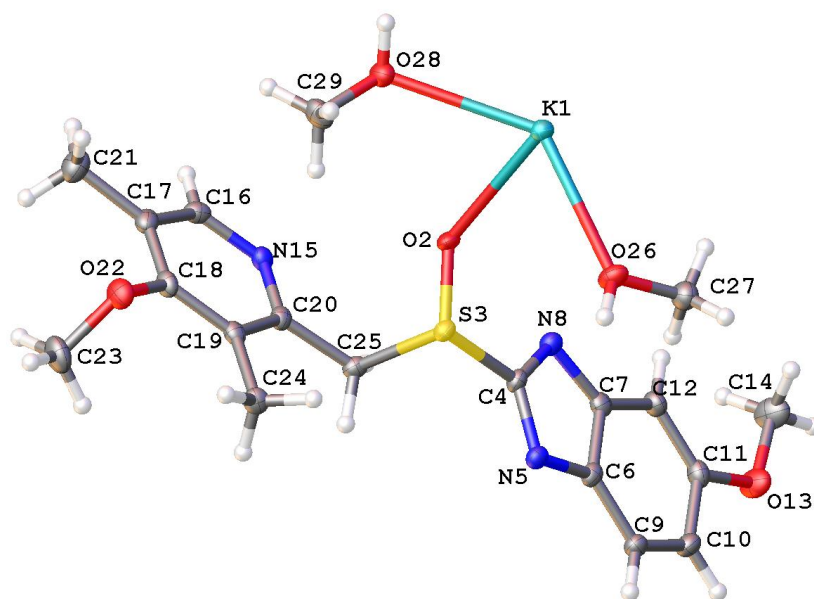


Figure 6.11 Crystal structure of the potassium salt of Omeprazole 3.38. Displacement ellipsoids are at 50% probability level and hydrogen atoms are omitted for clarity

Each potassium ion is bridged by the oxygen of the sulfoxide group, one MeOH molecule, and the N15 of the pyridyl ring to form a one dimensional chain along the crystallographic *b* axis (Figures 6.12 and 6.13)

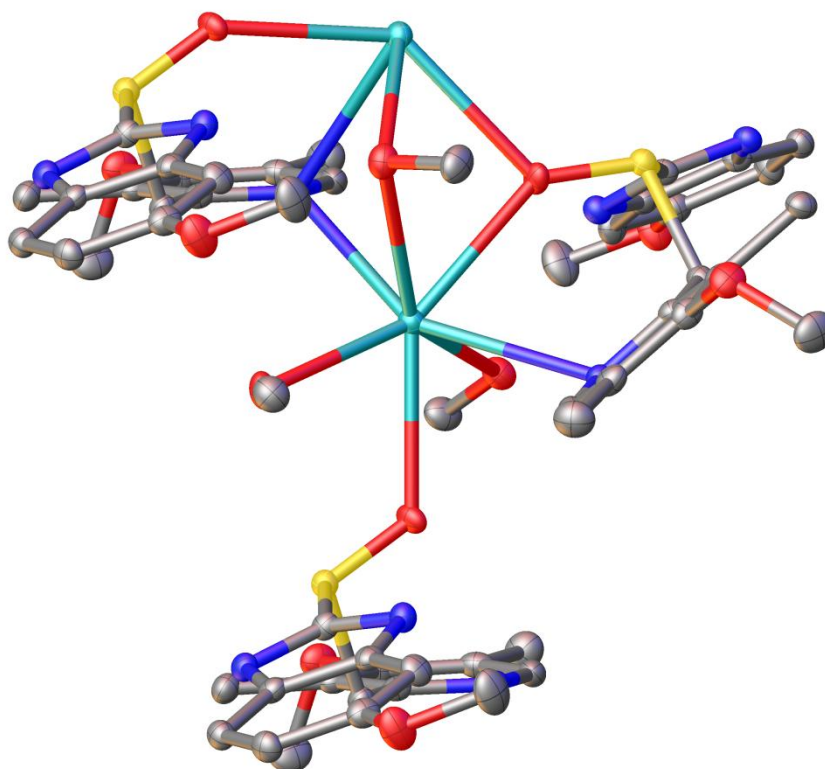


Figure 6.12 Crystal structure of the potassium salt of Omeprazole 3.38 showing the bridging interactions of the pyridine N, MeOH, and the sulfinyl group with the K atom. Displacement ellipsoids are at 50% probability level and hydrogen atoms are omitted for clarity. Note: not all bonds to the K atoms are shown

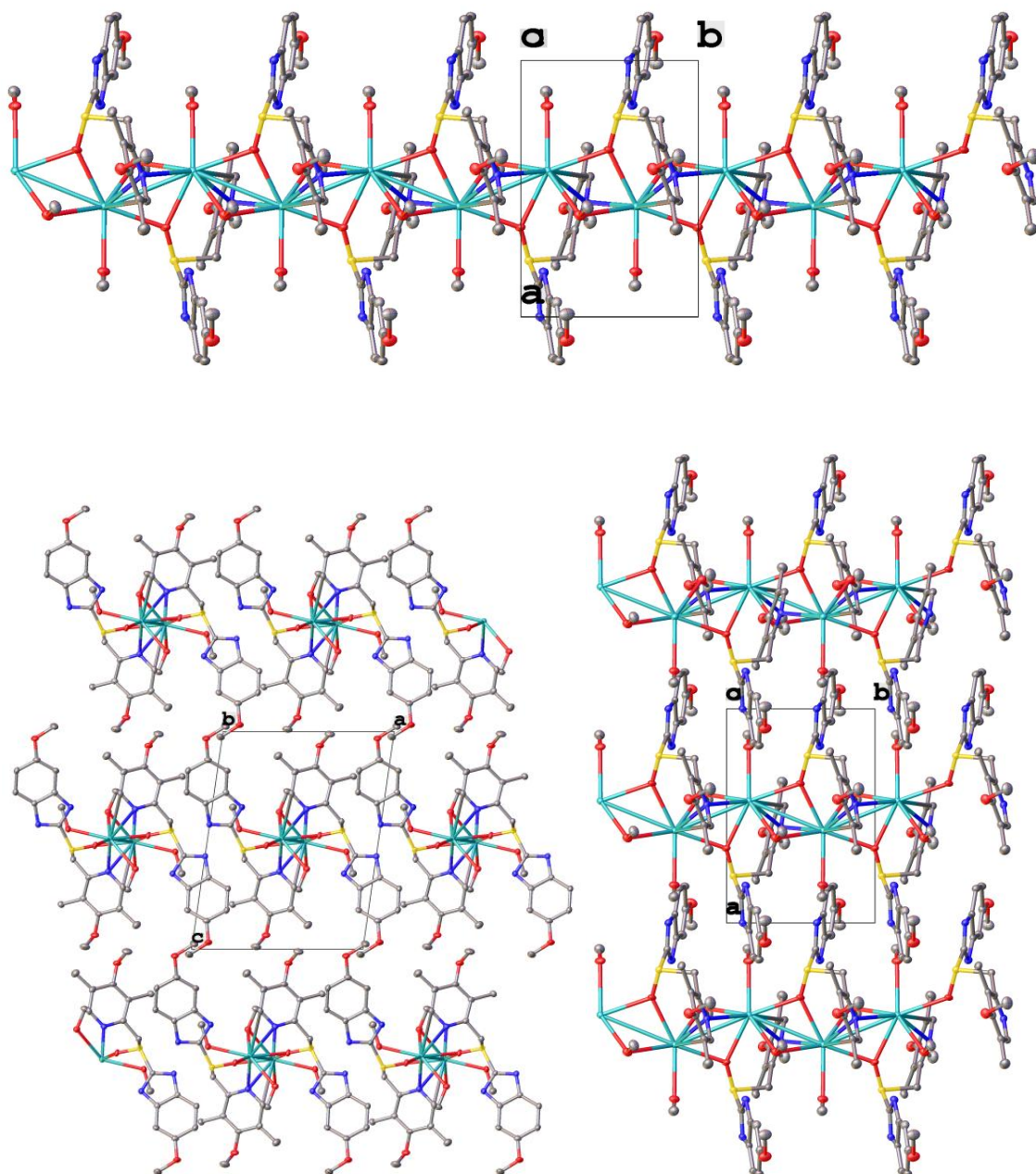


Figure 6.13 Top: Series of K...O, N, K interactions forming a 1D chain along the crystallographic *b* axis of K-Omeprazole 3.38 (viewed down the *a* axis); **Bottom:** packing diagram of K-Omeprazole as viewed down the *b* axis (left) and *c* axis (right)

Each potassium atom is eight coordinate, including the metal-metal bond, with K-K interaction distances of 3.9554(5) (Figure 6.13). Two distances were measured for between the K atom and the 2 sulfinyl group coordinated to it, K1...O2 ($\times 2$) 2.732(2) and 2.664(3). No interaction between the metal and the benzimidazole group is found, but three interactions of the metal with the sulfoxide occurs via the pyridine N15 (K1...N15 2.938(3) and 2.916(3) $\times 2$) (Figure 6.14).

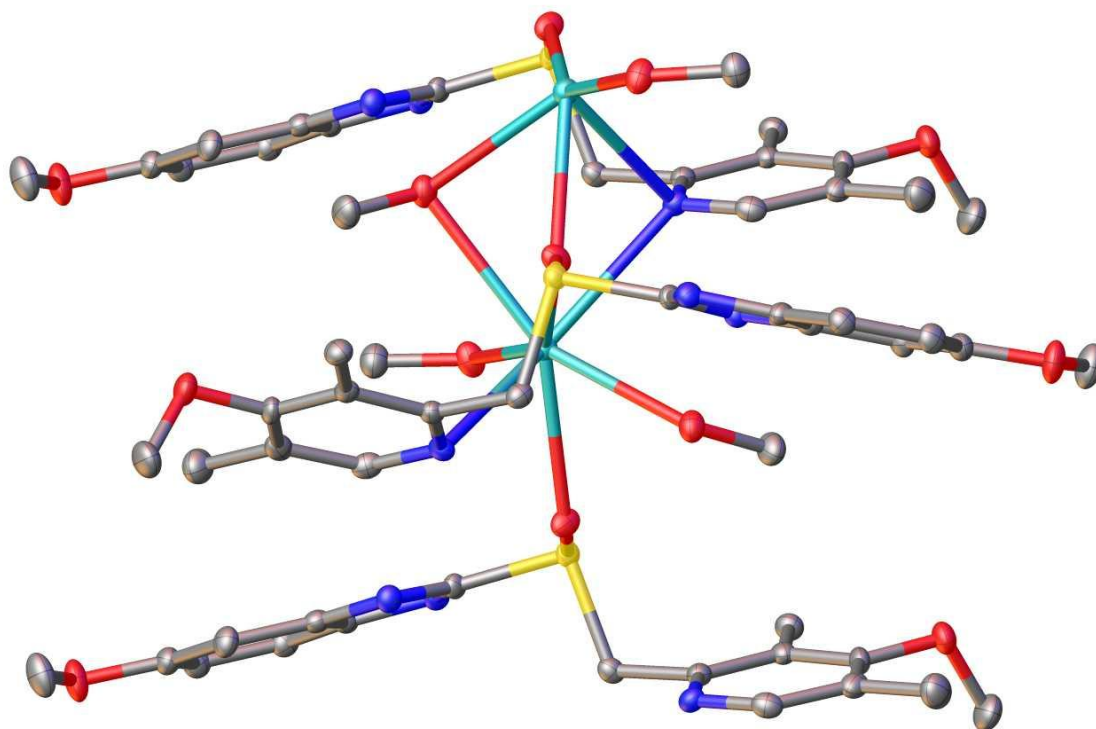


Figure 6.14 Crystal structure of the potassium salt of Omeprazole 3.38 showing three pyridine N to K atom interactions

Although the potassium salt of Omeprazole forms a complex structure in the solid state, the fact that the sulfoxide crystallizes in a form other than the heterochiral dimers seen for just Omeprazole suggests that crystallization of this salt could be used to improve the optical yield of asymmetric reactions producing Esomeprazole in a process similar to that employed in this body of work with the formation of the Na-salt of Esomeprazole.

X-ray characterization for NMe Omeprazole 5.22

Crystals of *N*-methylated derivative of Omeprazole **5.22** were obtained through addition of Et₂O to a solution in CH₂Cl₂. The compound crystallized as colourless plates, in a triclinic cell and was solved in the *P*-1 space group, with one molecule in the asymmetric unit (Figure 6.15) This compound exhibited isomeric disorder; disorder of the benzimidazole ring could not be adequately models in line with the previous publications.⁵⁶⁷ Disorder in the molecule was observed around the position of the methoxy group on the benzimidazole ring. The minor isomer (8%) has been ignored in the discussion of the packing

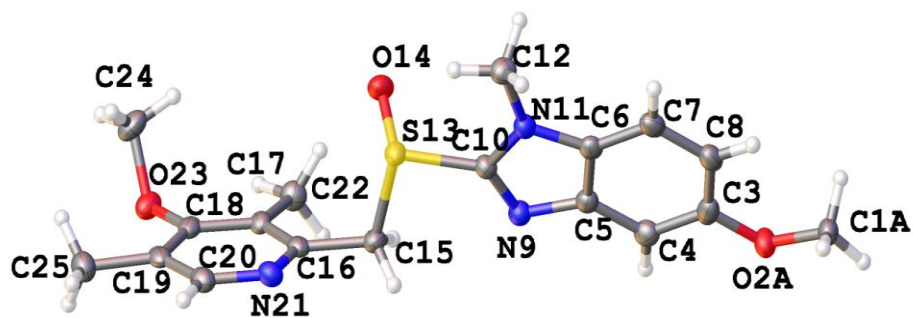


Figure 6.15 Crystal structure of NMe Omeprazole 5.22. Displacement ellipsoids are at 50% probability level and hydrogen atoms are omitted for clarity

No intra- or intermolecular hydrogen bonding is observed, however π - π stacking is observed between benzimidazole rings (centroid-centroid distance 3.593 Å) (Figure 6.16).

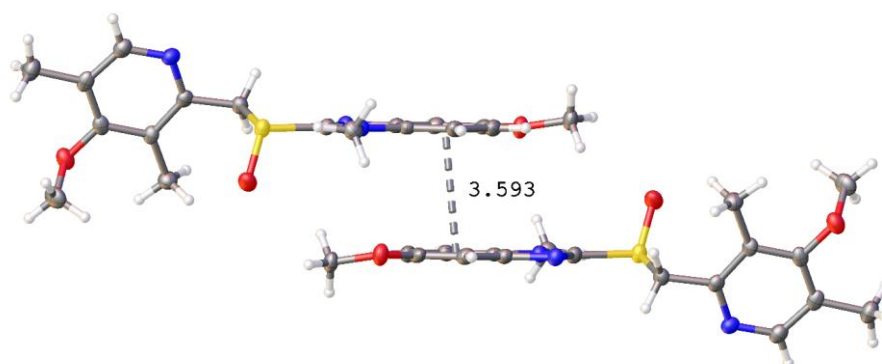


Figure 6.16 π - π Stacking between molecules of NMe Omeprazole 5.22

As a result of the intermolecular stacking between the benzimidazole rings the molecules pack as head-to-toe pairs along the crystallographic a axis (Figure 6.17)

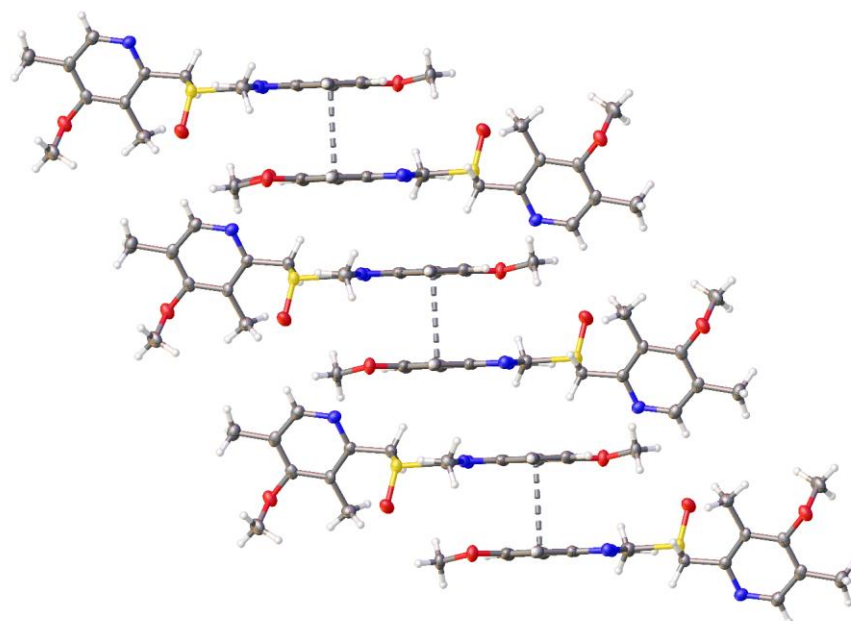
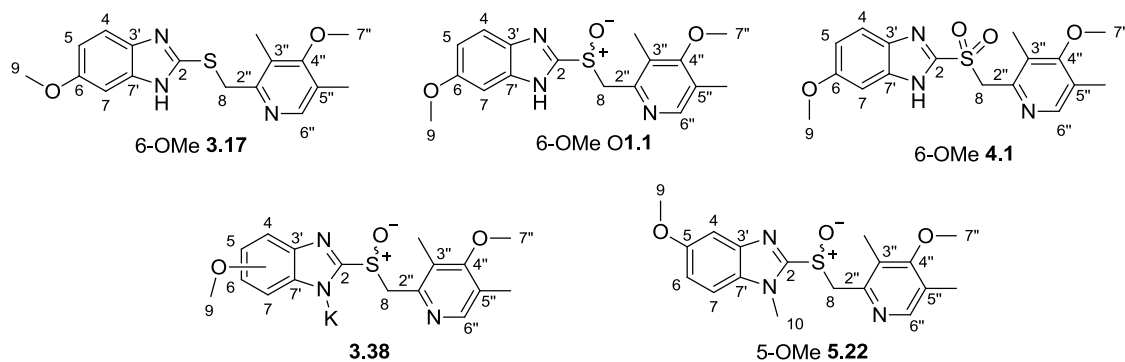


Figure 6.17 Packing of head-to-tail pairs along crystallographic a-axis.

6.1.2 Structural analysis of the Omeprazole family



Selected bond lengths for the compounds belonging to the Omeprazole family are shown in Table 6.1. Sulfoxides **1.1**, **3.38**, and **5.22** have S-O bond distances ranging from 1.494(2) Å to 1.506(2) Å which are consistent with the average bond length reported for sulfoxides (1.497(13)).⁷⁰³ Shorter S-O bond lengths were found for the sulfone **4.1**. The shortest C2-S bond was found for the sulfide **3.17** (1.744(3) Å) where as the potassium salt of Omeprazole **3.38** and the *N*-methylated derivative **5.22** contained the longest bonds of this type (1.797(3) and 1.794(3) Å respectively). Similar distances of the S-C8 bond were found for the sulfide **3.17** and sulfoxide **1.1**, with the shortest bond of this type featured in the sulfone **4.1**. All compounds were found to have a similar C8-C2'' distance (1.499(4) to 1.509(2) Å) with the exception of Omeprazole which was longer (1.522(4) Å).

Bond	Distance / Å				
	sulfide 3.17	Omeprazole 1.1	Sulfone 4.1	K- Omeprazole 3.38	NMe- Omeprazole 5.22
S-O	-	1.506(2)	1.4440(12) 1.4338(11)	1.502(3)	1.494(2)
C2-S	1.744(3)	1.776(3)	1.7628(15)	1.797(3)	1.794(3)
S-C8	1.800(3)	1.800(3)	1.7831(15)	1.833(4)	1.812(3)
C8- C2"	1.506(4)	1.522(4)	1.509(2)	1.504(5)	1.499(4)
N1-C2	1.359(4)	1.352(4)	1.361(2)	1.336(4)	1.370(4)
N3-C2	1.312(3)	1.322(4)	1.312(2)	1.334(4)	1.314(4)
N1-C9	-	-	-	-	1.456(4)

Table 6.1 Selected bond lengths (Å) for the series of compounds belonging to the Omeprazole family

Bonds	Angle / °				
	sulfide 3.17	Omeprazole 1.1	Sulfone 4.1	K-Omeprazole 3.38	NMe- Omeprazole 5.22
C2-S-O	-	107.11(14)	105.73(7) 109.73(7)	107.74(15)	107.23(14)
O-S-C8	-	105.52(15)	109.85(7) 108.89(7)	104.98(15)	107.36(14)
O-S-O	-	-	118.51(7)		-
C2-S-C8	99.62(13)	96.55(14)	103.00(7)	94.99(15)	96.82(13)
S-C8-C2"	109.34(34)	109.5(2)	109.97(10)	111.1(2)	107.1(2)
N1-C2-N3	114.4(2)	115.2(3)	115.28(13)	119.6(3)	115.2(3)
N1-C2-S	117.49(19)	125.2(2)	121.31(11)	122.2(3)	119.5(2)
N3-C2-S	114.4(2)	119.5(3)	123.41(12)	118.1(2)	125.3(2)

Table 6.2 Selected bond angles (°) for the series of compounds belonging to the Omeprazole family

Similar C2-S-O bond angles were found for all compounds of this series, while the O-S-C8 bond angle was found to range from 104.98(15)° to 109.85(7)° with the greatest angle observed in the sulfone **4.1** (Table 6.2). The C2-S-C8 angles for all five compounds were smaller, ranging from 94.99(15)° for the K-salt **3.38** to 103.00(7)° for the sulfone **4.1**. Torsion angles with magnitudes ranging from 163.37(19)° to 179.76(10)° were found for this series of compounds for the C2-S-C8-C2" backbone of these compounds joining the two aromatic ring

systems. The pyridyl OMe group was found to be almost perpendicular to the plane of the adjacent ring for each of these compounds, with C7''-O-C4''-C5'' torsion angles ranging from 87.77(17)° to 96.8(3)° in magnitudes. In contrast, for all of these compounds the OMe group of the benzimidazole ring system was generally found to be almost coplanar with the adjacent ring, with the exception of the NMe sulfoxide where the benz OMe group was at an angle of 11.5(4)° out of the plane of the benzimidazole ring.

Bonds	Torsion Angle / °				
	Sulfide 3.17	Omeprazole 1.1	Sulfone 4.1	K-Omeprazole 3.38	NMe- Omeprazole 5.22
N1-C2-S-O	-	49.7(3)	5.68(14) -123.21(13)	-14.2(3)	87.5(3)
O-S-C8-C2''	-	71.5(3)	-67.48(12) 63.81(12)	-53.4(3)	-74.5(2)
C2-S-C8-C2''	-169.37(19)	-178.7(2)	-179.76(10)	-163.3(3)	175.0(2)
N1-C2-S-C8	-165.4(2)	-58.8(3)	120.96(13)	93.3(3)	-161.9(2)
N3-C2-S-C8	18.2(3)	123.8(3)	-58.64(14)	-87.1(3)	18.7(3)
S-C8-C2''-N1''	-12.5(3)	31.9(4)	83.19(14)	97.9(3)	-80.4(3)
C7''-O-C4''-C5''	96.8(3)	-90.2(4)	-87.77(17)	96.6(4)	95.2(3)
C9-O-C6-C5	2.6(4)	177.2(3)	177.31(14)	3.6(6)	-
C9-O-C5-C6	-	-	-	-	11.5(4)

Table 6.3 Selected torsion angles (°) for the series of compounds belonging to the Omeprazole family

Compound	Dihedral angle between aromatic rings / °
Sulfide 3.17	11.76(10)
Omeprazole 1.1	29.57(9)
Omeprazole sulfone 2.99	24.61(5)
K-Omeprazole 3.38	21.36(11)
NMe Omeprazole 5.22	74.51(9)

Table 6.4 Dihedral angle measure between the planes of the two aromatic rings of the compounds belonging to Omeprazole family

The dihedral angles between the planes of the two aromatic rings of these compounds were measured using Olex2 (Table 6.4).⁷⁰⁴ The N-methyl sulfoxide **5.22** featured the greatest dihedral angle at 74.51(9)° while the smallest angle was observed for the sulfide **3.17** (11.76(10)°).

6.1.3 X-ray structures of selected racemic sulfoxides

X-ray characterization for benzyl *p*-tolyl sulfoxide 4.10

Colourless fragments of sulfoxide **4.10** suitable for XRD were obtained through evaporation of a solution in CDCl_3 over a period of a number of days which afforded colourless needles which were cut to size for the X-ray experiment. The compound crystallized in an orthorhombic cell and was solved in the $P2_12_12_1$ space group, with one molecule in the asymmetric unit (Figures 6.18 and 6.19). No intermolecular H-bonds or π - π stacking was observed in this structure and it was in good agreement with the structure previously reported in the literature.⁷⁰¹

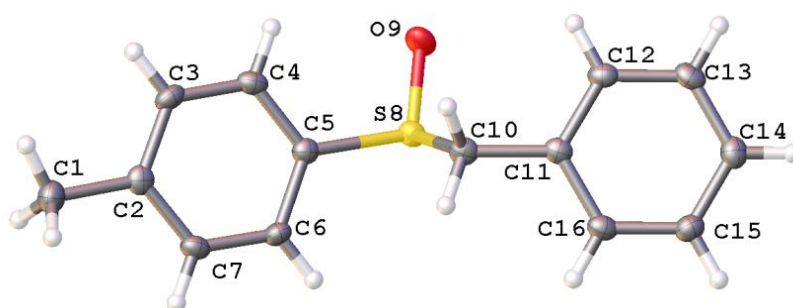


Figure 6.18 Crystal structure of sulfoxide 4.10. Displacement ellipsoids are at 50% probability level and hydrogen atoms are omitted for clarity

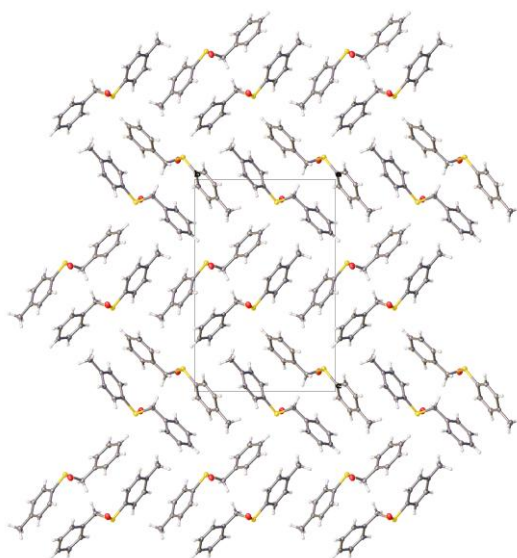


Figure 6.19 Packing viewed down crystallographic *a* axis

X-ray characterization for methyl 6(5)-OMe benzimidazole sulfoxide 4.11

Crystals suitable for XRD were obtained through slow addition of hexane to a solution in EtOAc. The sulfoxide **4.11** crystallized as colourless needles. The compound crystallized in a monoclinic cell and was solved in the $P2_1/c$ space group, with two molecules in the asymmetric

unit (Figure 6.17). The asymmetric unit contains two crystallographically independent molecules, which are bound through an intermolecular hydrogen bond (NH...O 2.721(5) Å, H...O 1.866(5) Å).

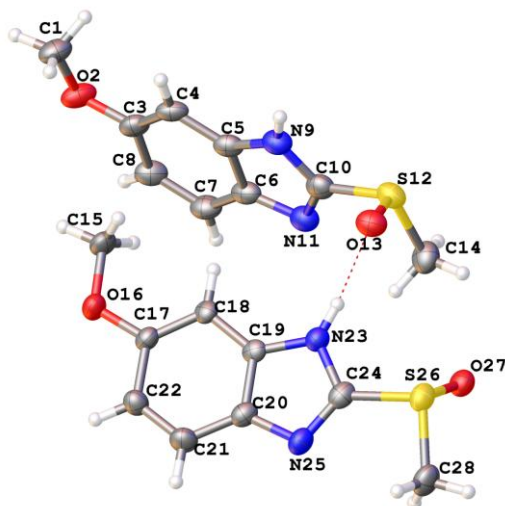


Figure 6.20 Crystal structure of the methyl benzimidazole sulfoxide 4.11. Displacement ellipsoids are at 50% probability level and hydrogen atoms are omitted for clarity

The H-bond interactions extend to form chains of molecules along the crystallographic *a* axis (Figure 6.20). These chains then pack in an alternating fashion (Figure 6.21 and 6.22)

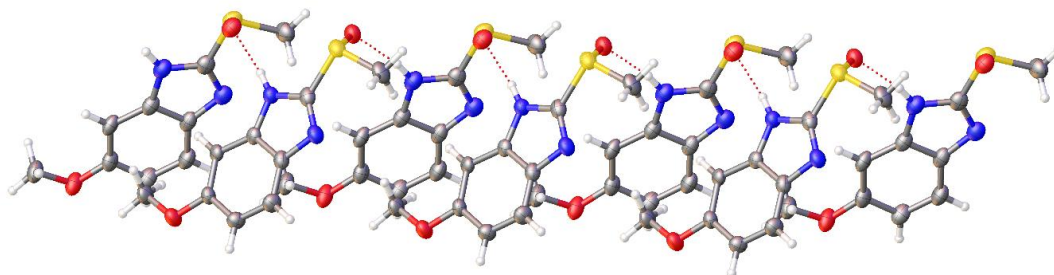


Figure 6.21 Hydrogen-bond interactions leading to chains of molecules along *a* axis.

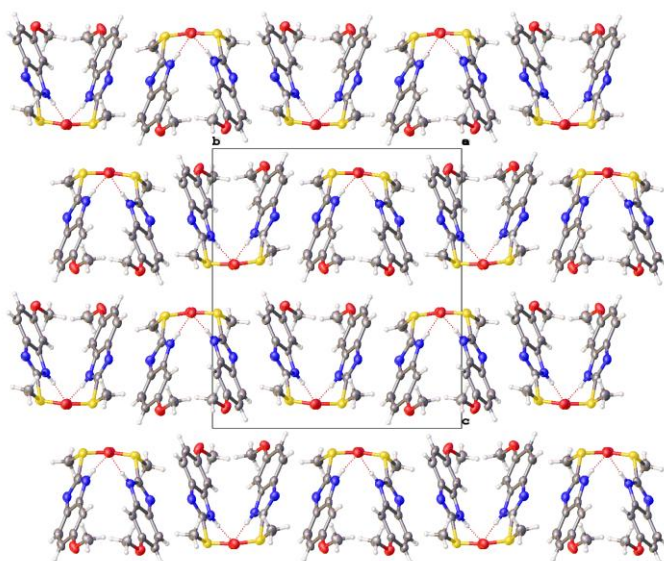


Figure 6.22 Packing arrangement of chains viewed down the crystallographic *a* axis.

X-ray characterization for pyridyl *p*-tolyl sulfoxide 4.12

Colourless fragments of sulfoxide **4.12** suitable for XRD were obtained through evaporation of a solution in CDCl_3 over a period of a number of days which afforded colourless needles which were cut to size for the X-ray experiment. The compound crystallized in a monoclinic cell and was solved in the $P2_1/c$ space group, with one molecule in the asymmetric unit (Figure 6.23). Disorder of the molecule was observed around the tolyl group. Only the major component (70%) is shown in the figures.

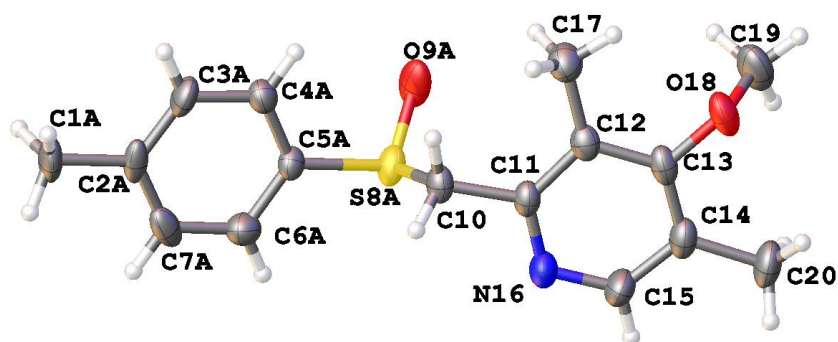


Figure 6.23 Crystal structure of the sulfoxide 4.12. Displacement ellipsoids are at 50% probability level and hydrogen atoms are omitted for clarity

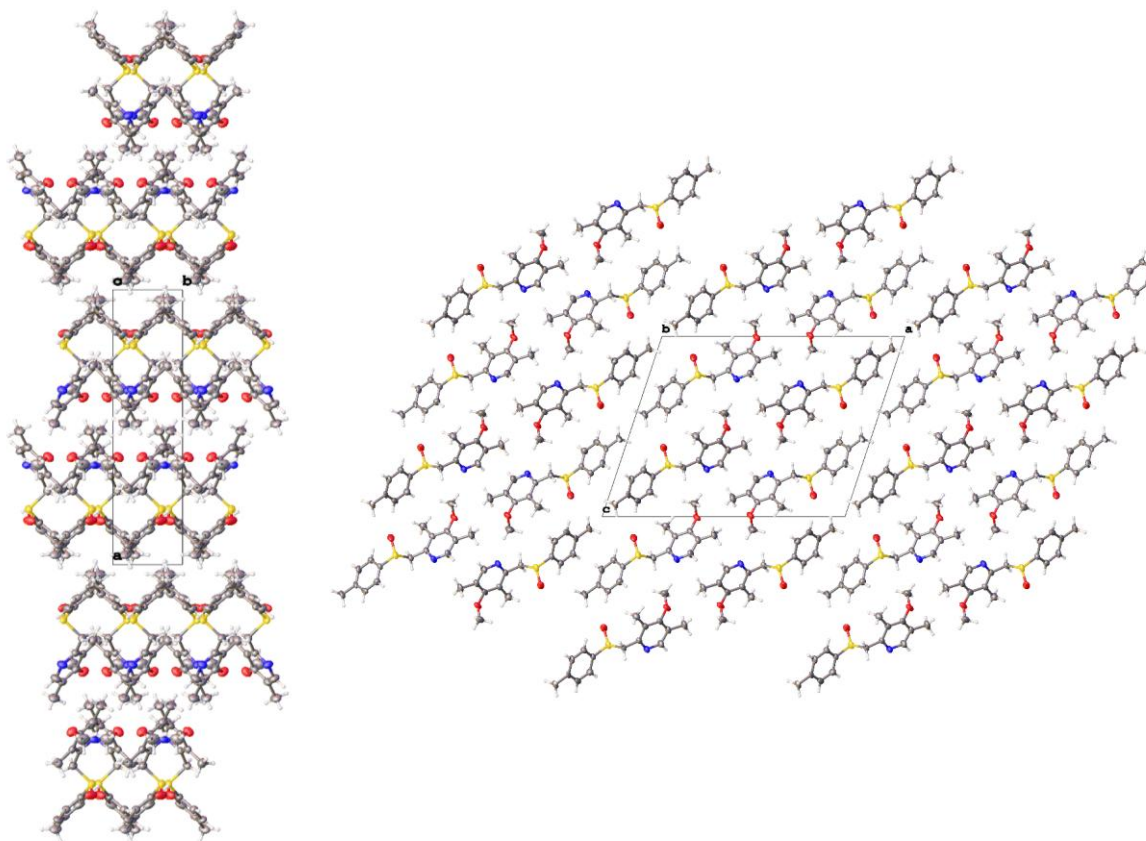
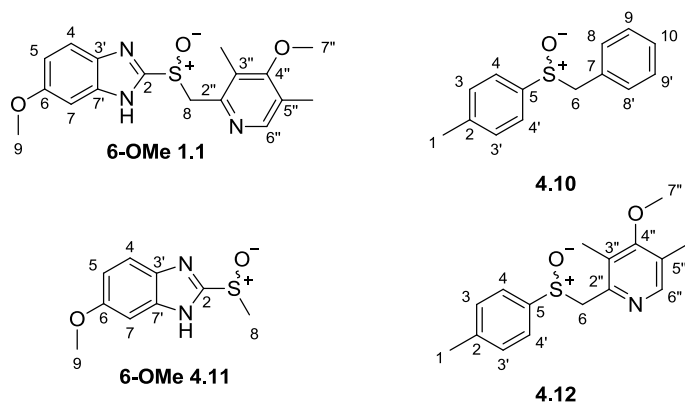


Figure 6.24 Packing of sulfoxide **4.12** viewed along the crystallographic *c* axis (left) and *b* axis (right)

No classical H-bonding or π - π stacking was observed for this structure. Figure 6.24 shows the molecules packed in layers along the crystallographic *c* axis and along the *b* axis.

6.1.4 Structural analysis of racemic sulfoxides



Selected bond lengths for the racemic sulfoxides **1.1** and **4.10-4.12** are reported in Table 6.5. Similar S-O distances were observed for each sulfoxide, from 1.490(3) Å to 1.506(4) Å. The shortest C2-S distance was found for Omeprazole **1.1** (1.790(4) Å), whilst the alkyl aryl

sulfoxide **4.11** had a bond length of 1.784(5) Å for the S-C8 bond, which was shorter than that of Omeprazole or the equivalent S-C6 bond of sulfoxides **4.10** and **4.12**.

	Omeprazole 1.1	6-OMe 4.11	4.10		4.12	
Bond	Distance / Å	Distance / Å	Equivalent bond	Distance / Å	Equivalent bond	Distance / Å
S-O	1.506(2)	1.506(4)	S-O	1.4965(12)	S-O	1.490(3)
C2-S	1.776(3)	1.790(4)	C5-S	1.7931(18)	C5-S	1.792(3)
S-C8	1.800(3)	1.784(5)	S-C6	1.8254(17)	S-C6	1.825(2)
C8-Pyr C2"	1.522(4)	-	C6-C7	1.502(2)	C6-Pyr C2"	1.506(2)
N1-C2	1.352(4)	1.366(6)	-	-	-	-
N3-C2	1.322(4)	1.304(6)	-	-	-	-

Table 6.5 Selected bond lengths (Å) for the sulfoxides **4.10-4.12** and Omeprazole **1.1**

Selected bond angles for sulfoxides **4.10-4.12**, and Omeprazole **1.1** are shown in Table 6.6.

The angles around the sulfoxide group i.e. C2-S-O, and O-S-C8/C6 for these racemic sulfoxides were found to range from 105.44(14)° to 108.53(17)°, and for each sulfoxide, with the exception of the methyl benzimidazole sulfoxide **4.11**, the C2-S-O angle is greater in magnitude than the O-S-C8/C6 angle. For each of sulfoxides the C2-S-C8 and equivalent C5-S-C6 bond angle is in close approximation with each other (96.55(14) to 97.5(2)°.

	Omeprazole 1.1	6-OMe 4.11	4.10		4.12	
Bonds	Angle / °	Angle / °	Equivalent bond	Angle / °	Equivalent bond	Angle / °
C2-S-O	107.11(14)	105.76(19)	C5-S-O	107.55(8)	C5-S-O	108.53(17)
O-S-C8	105.52(15)	107.5(2)	O-S-C6	106.86(8)	O-S-C6	105.44(14)
C2-S-C8	96.55(14)	97.5(2)	C5-S-C6	96.88(8)	C5-S-C6	97.32(11)
S-C8-C2"	109.5(2)	-	S-C8-C7	110.30(11)	S-C6-C2"	109.32(13)
N1-C2-N3	115.2(3)	114.7(4)	-	-	-	-
N1-C2-S	125.2(2)	118.7(3)	-	-	-	-
N3-C2-S	119.5(3)	126.5(4)	-	-	-	-

Table 6.6 Selected bond angles (°) for the sulfoxides **4.10-4.12** and Omeprazole **1.1**

For the four compounds of Omeprazole **1.1** and the sulfoxides **4.10-4.12** there is great variation on the N1-C2-S-O for the benzimidazole sulfoxides and equivalent C4'-C5-S-O bond in the p-

tolyl sulfoxides, ie the sulfinyl S-O and the plane of aromatic group on its left hand side as illustrated above (Table 6.7). These angles range from 49.7(3)° to 171.40(13)°. In contrast the torsion angles between the right hand of the sulfoxide molecules and the sulfinyl group shows less variation in magnitudes, with O-S-C8-C2" and the equivalent O-S-C6-C7/C2" torsion angles of 71.5(3)° to -75.79(13)°. As found previously for Omeprazole **1.1** the benzimidazole OMe group of sulfoxide **4.11** lies at a nearly coplanar angle to the plane of the adjacent aromatic ring (174.5(4)° for the angle C9-O-C6-C5) , whereas the pyridyl OMe group of sulfoxide **4.12** sits perpendicular to the plane of the pyridine ring (82.9(2)° for the angle C7"-O-C4"-C5")

Bonds	Omeprazole 1.1	6-OMe 4.11	4.10		4.12	
	Torsion Angle / °	Torsion Angle / °	Equivalent bonds	Torsion Angle / °	Equivalent bonds	Torsion Angle / °
N1-C2-S-O	49.7(3)	69.4(4)	C4'-C5-S-O	171.40(13)	C4'-C5-S-O	148.0(3)
O-S-C8-C2"	71.5(3)	-	O-S-C6-C7	-75.79(13)	O-S-C6-C2"	-74.99(18)
C2-S-C8-C2"	-178.7(2)	-	C5-S-C6-C7	173.47(13)	C5-S-C6-C2"	173.42(19)
N1-C2-S-C8	-58.8(3)	-180.0(4)	C4-C5-S-C6	102.97(15)	C4-C5-S-C6	77.9(3)
N3-C2-S-C8	123.8(3)	-0.5(5)	C4'-C5-S-C6	-78.45(14)	C4'-C5-S-C6	-103.0(3)
S-C8-C2"-N1"	31.9(4)	-	S-C6-C7-C8'	-102.24(16)	S-C6-C2"-N1"	-73.43(18)
C9-O-C6-C5	177.2(3)	174.5(4)	-	-	-	-
C7"-O-C4"-C5"	-90.2(4)	-	-	-	C7"-O-C4"-C5"	82.9(2)

Table 6.7 Selected torsion angles (°) for the sulfoxides **4.10-4.12** and Omeprazole **1.1**

Using Olex2 the dihedral angles between the planes of the aromatic rings were measured for sulfoxides **4.12** and **4.10** (Table 6.8), with the smallest angle found for the pyridyl *p*-tolyl sulfoxide **4.12** (11.22(6)°) whilst the greatest dihedral angle was observed in Omeprazole **1.1** (29.57(9)°).

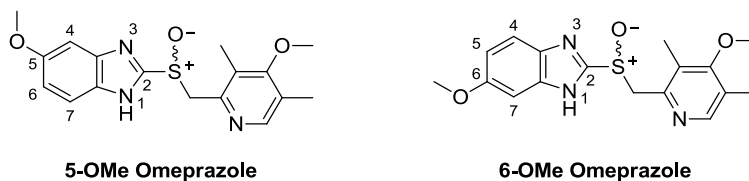
Compound	Dihedral angle between aromatic rings /°
Omeprazole 1.1	29.57(9)
4.10	14.07(14)
4.12	11.22(6)

Table 6.8 Dihedral angles between the planes of the two aromatic rings of sulfoxides **1.1**, **4.10** and **4.12**

6.2 Tautomerism of Omeprazole and related compounds

6.2.1 Prototropic exchange of Omeprazole and related species

In addition the optical isomerism of sulfoxides such as Esomeprazole (*S*)-**1.1**, prototropic tautomerism of the benzimidazole ring system gives rise to another aspect of structural diversity whereby the methoxy group can be found at either the 5- or the 6- position relative to the NH of this heterocyclic group.^{567, 568}



Of the two tautomeric forms Omeprazole has shown to exist more commonly as the 6-Ome isomer in both the solid state and in solution.^{569, 570} Conventionally, however, Omeprazole has been represented in the literature as the 5-Ome tautomer, most likely as a result of a number of naming errors in the literature, the most notable of which is found in one of the earliest reports on the crystal structure of Omeprazole, which despite discussing and illustrating the sulfoxide as the 6-Ome form, named the molecule as the 5-Ome benzimidazole in the title of the paper.^{571, 572} For the sake of accuracy, and in keeping with the observed structures discussed in the previous section, Omeprazole and all related methoxy benzimidazole species have been depicted in this thesis as the 6-Ome tautomers.

The annular tautomerism of Omeprazole is a fast process the result of which is that only averaged signals are observed by NMR (¹H, ¹³C) at room temperature.⁷⁰⁵ In DMSO-d₆ the averaged aromatic proton signals from the benzimidazole group of Omeprazole **1.1**, and its sulfide precursor Pymetazole **3.17**, are observed as sharp peaks with well resolved splitting (Figure 6.25). In accordance with the observation of only one set of proton signals in the presence of two possible tautomers this indicates that the prototropic exchange is so rapid that it effectively results in magnetic equivalence of the 7-H proton of the 5-Ome tautomer and 4-H proton of the 6-Ome tautomer, and *vice versa*. In contrast, broadening of the benzimidazole 4-H and 7-H signals was observed for Omeprazole sulfone **4.1** in DMSO-d₆, indicating slower prototropic exchange for this compound compared to the sulfide **3.17** or sulfoxide **1.1** in this solvent. Similarly, when CDCl₃ was employed as the NMR solvent for these compounds the averaged signals for benzimidazole protons of the sulfide **3.17** were sharp and well resolved while those of the sulfone **4.1** were broadened for the 4-H and 7-H protons; however in CDCl₃ broadening of these proton signals was also observed for Omeprazole **1.1**.

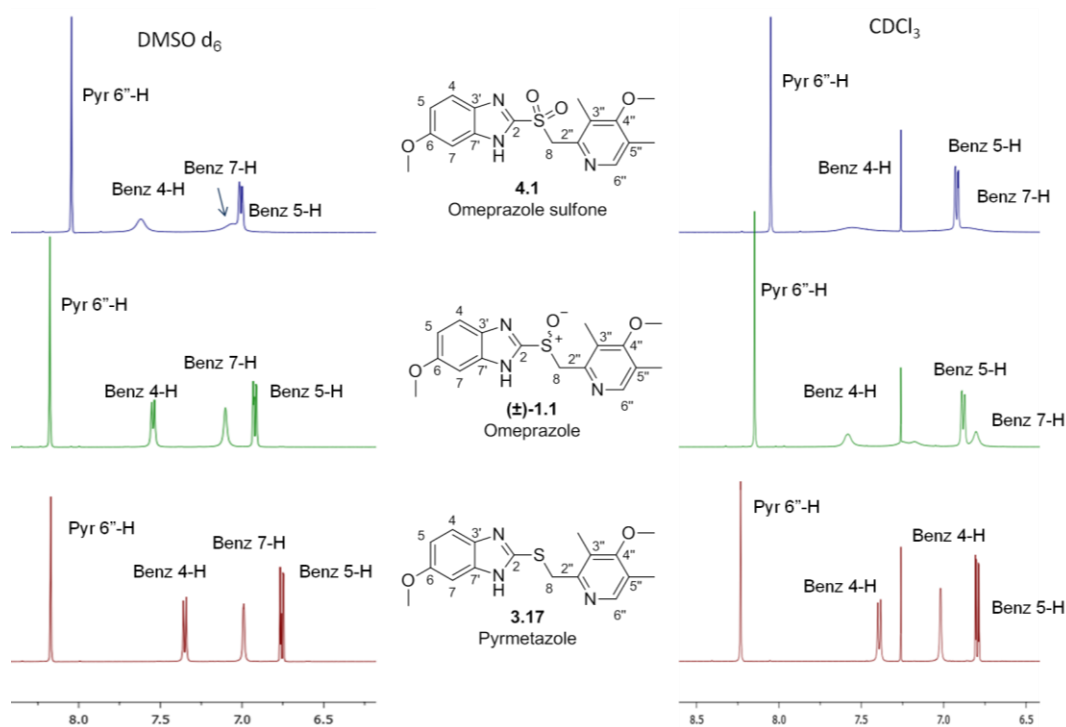


Figure 6.25 Partial ^1H NMR spectra of Pyrimetazole 3.17, Omeprazole 1.1, and Omeprazole sulfone 4.1 in DMSO-d_6 or CDCl_3

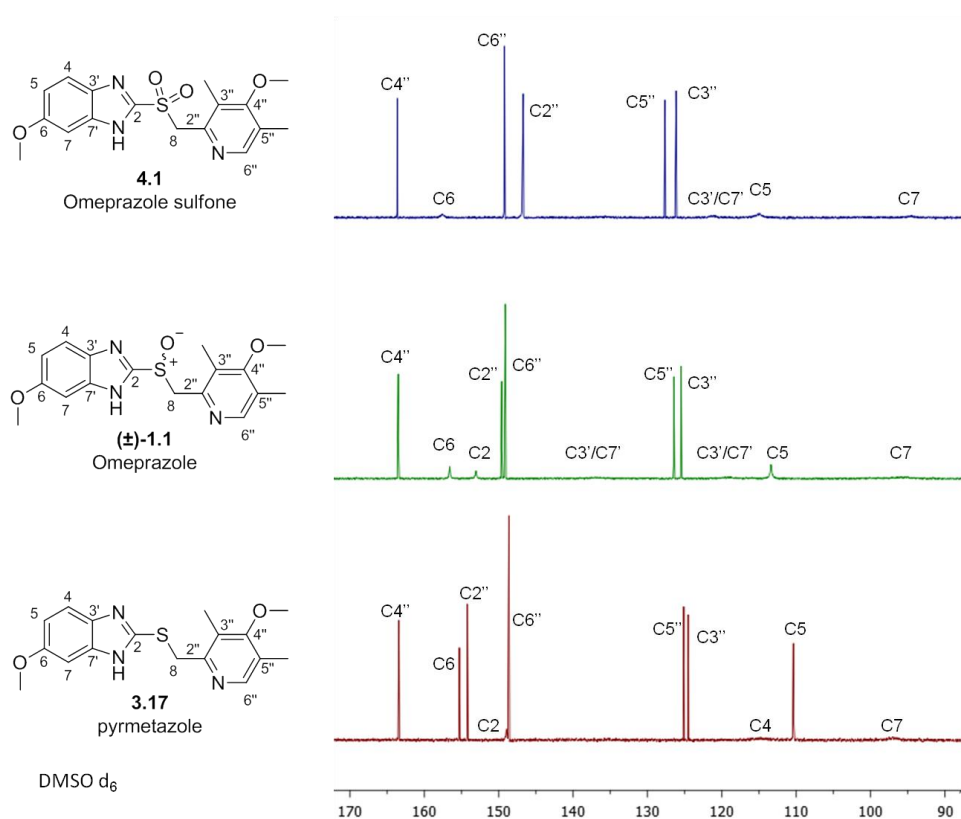


Figure 6.26 Partial ^{13}C NMR spectra of sulfide 3.17, Omeprazole 1.1, and sulfone 4.1 in DMSO-d_6 . Using ^{13}C NMR on sulfide 3.17, sulfoxide 1.1, and sulfone 4.1 revealed the tautomerism of these compounds in the form of partial or missing signals attributed to the carbons of the

benzimidazole ring system (Figure 6.26). This effect was observed when either DMSO or CDCl_3 were employed as the NMR solvent. In contrast, all 17 carbon signals can be seen in the ^{13}C NMR of Na-Omeprazole (Figure 6.27).

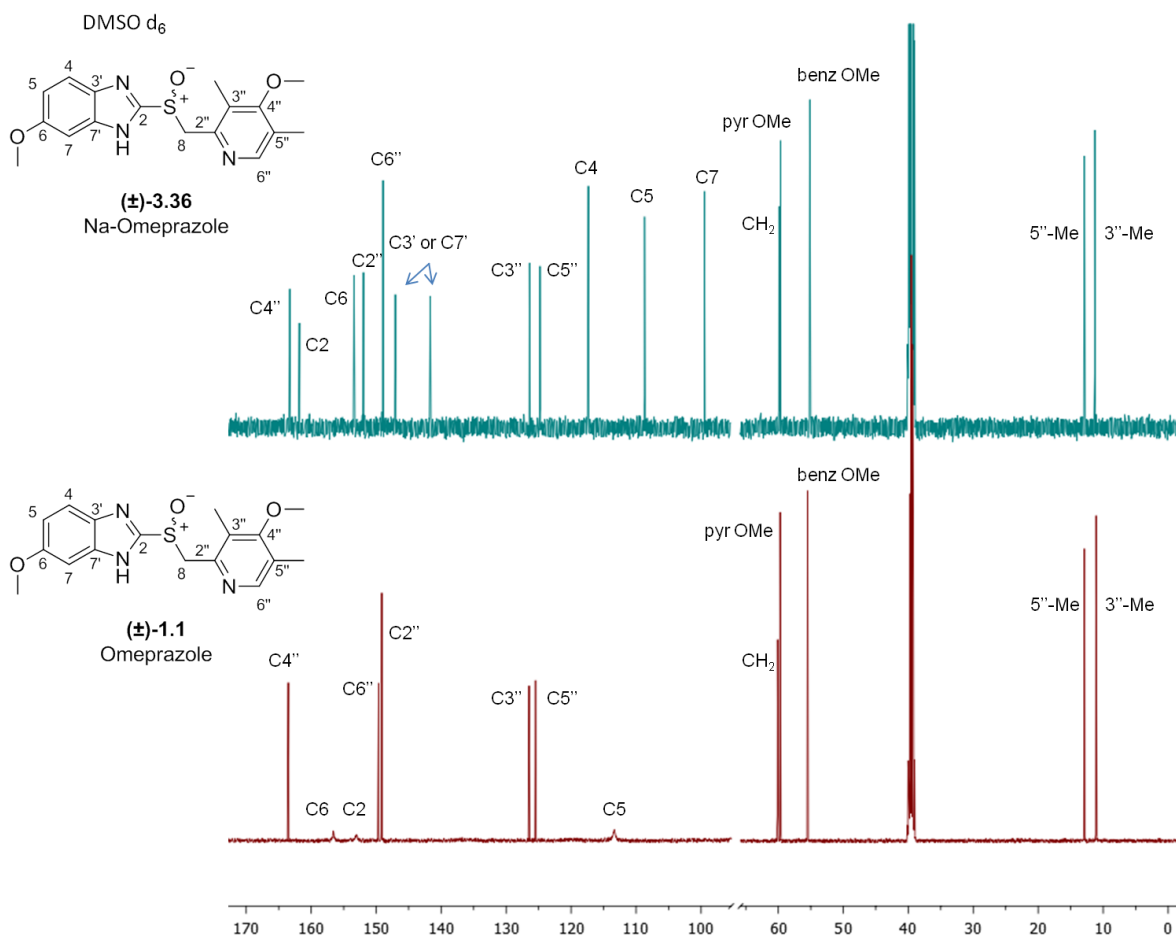


Figure 6.27 ^{13}C NMR spectra of Omeprazole 1.1, and Na-Omeprazole 3.36 in DMSO-d_6

The ^1H NMR of Omeprazole in CDCl_3 was conducted at 279, 300, and 323K (Figure 6.28). At low temperature the prototropic exchange was sufficiently slowed allowing for observation of the two tautomers of Omeprazole.

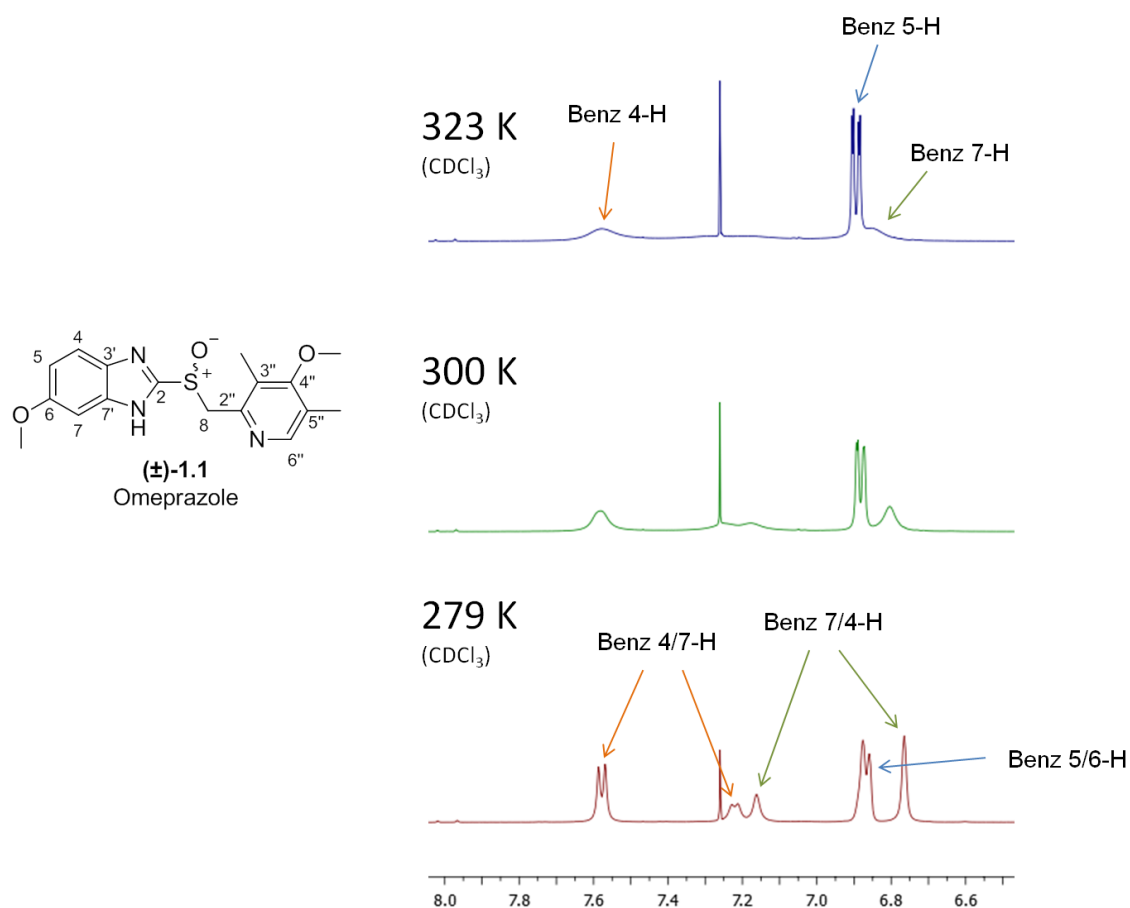
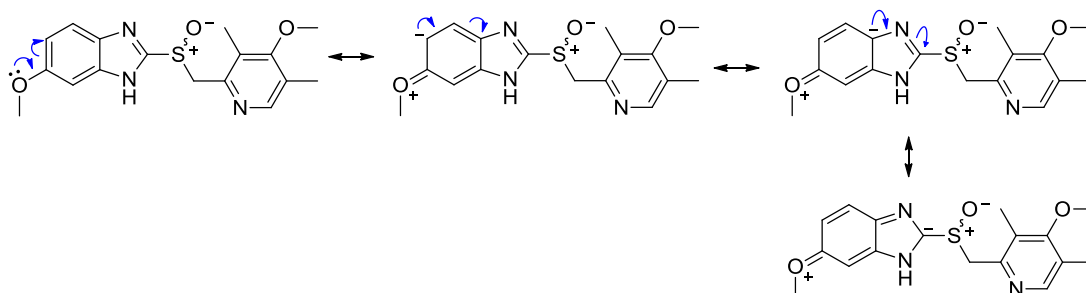


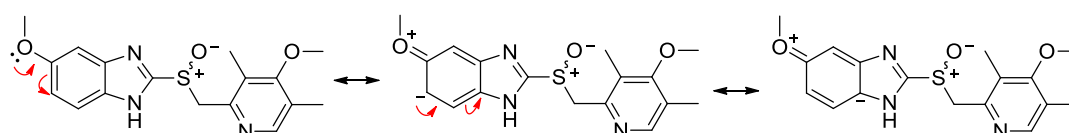
Figure 6.28 Partial ¹H NMR (CDCl₃) of Omeprazole 1.1 at low temperature, room temperature, and high temperature

Integration of the benzimidazole proton signals revealed the ratio of the two tautomers to be 70:30, although it was not possible to identify whether the 5-OMe or 6-OMe tautomer was present in the greatest quantity it is likely that the 6-OMe tautomer predominates. This is due to the electronic effects of the methoxy group on the benzimidazole ring system, where the positioning of the OMe group on C6 offers greater delocalization of the methoxy lone pair across the imidazole ring, with the potential of further conjugation with the sulfinyl group. In contrast when the methoxy group is at the 5-position there is less opportunity for delocalization and therefore less contribution to stability via conjugation (Scheme 6.1)

6-OMe Omeprazole



5-OMe Omeprazole



Scheme 6.1 Delocalization of the OMe lone pair across the benzimidazole ring system with greater resonance offered by having the OMe group at the 6-position, compared to having the OMe group at the 5-position

Annular tautomerism was also observed in a number of other benzimidazole species investigated as part of these studies (Figure 6.29). Of these compounds the sulfoxides **4.9** and **4.11** were notable as the ratios of their tautomers were measurable in CDCl_3 at room temperature.

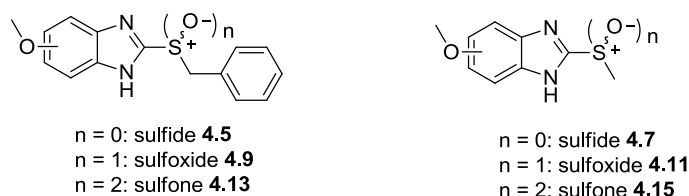


Figure 6.29 Methoxy benzimidazole species featuring annular tautomerism

For the benzyl benzimidazole sulfoxide **4.9** when CDCl_3 was employed as the NMR solvent the signals attributed to the benzimidazole NH and the OMe group were each observed as two peaks, one for each tautomer (Figure 6.30). Measurement of the integrals of the OMe group, with peaks from the two tautomers occurring at 3.89 and 3.82 ppm gave the ratio of tautomers to be 37:63. Similarly for the methyl benzimidazole sulfoxide **4.11** it was possible to measure a ratio of tautomers of 62:38 from the doublets occurring at 7.65 and 7.46 ppm respectively (Figure 6.31). Although further characterization would be required to correctly identify which tautomers are responsible for these NMR signals it is to be expected that for both sulfoxide **4.9** and **4.11** that the 6-OMe isomer be the most prevalent, as is the case for Omeprazole **1.1**.

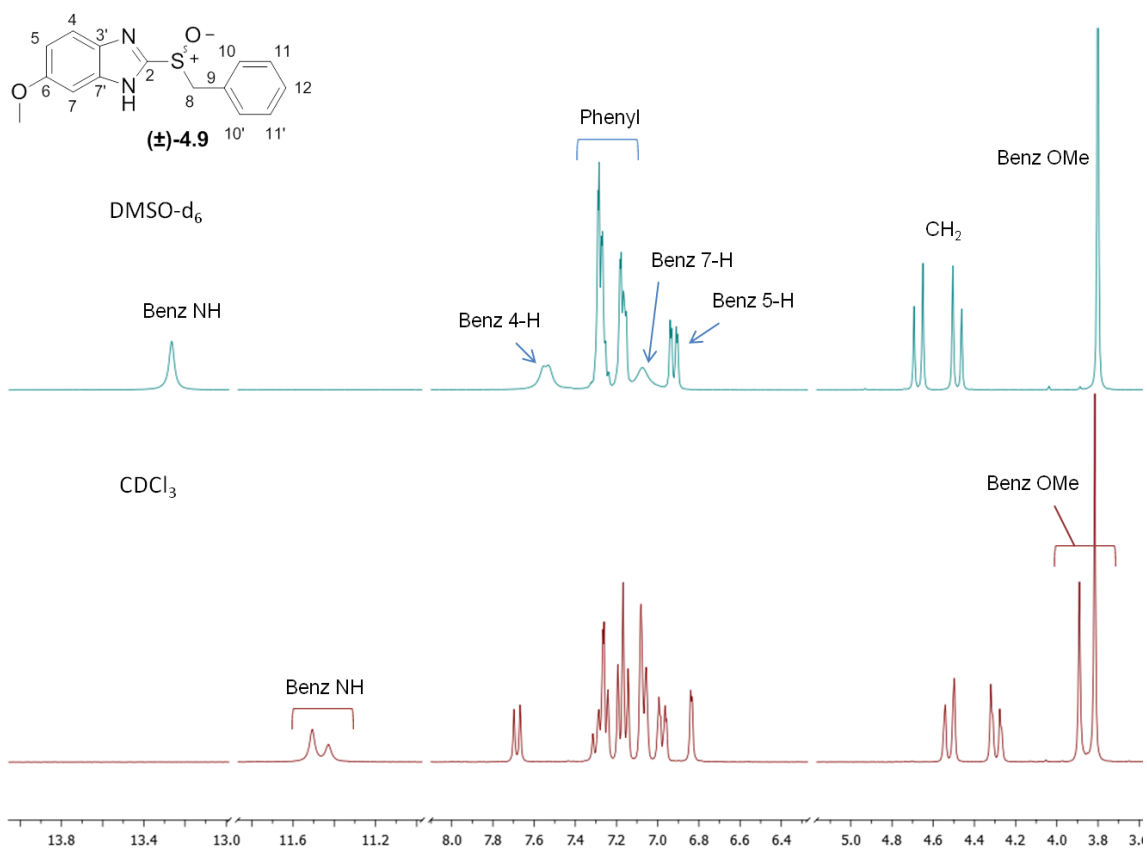


Figure 6.30 Partial ^1H NMR of benzyl benzimidazole sulfoxide **4.9** in DMSO- d_6 (top) and CDCl_3 (bottom)

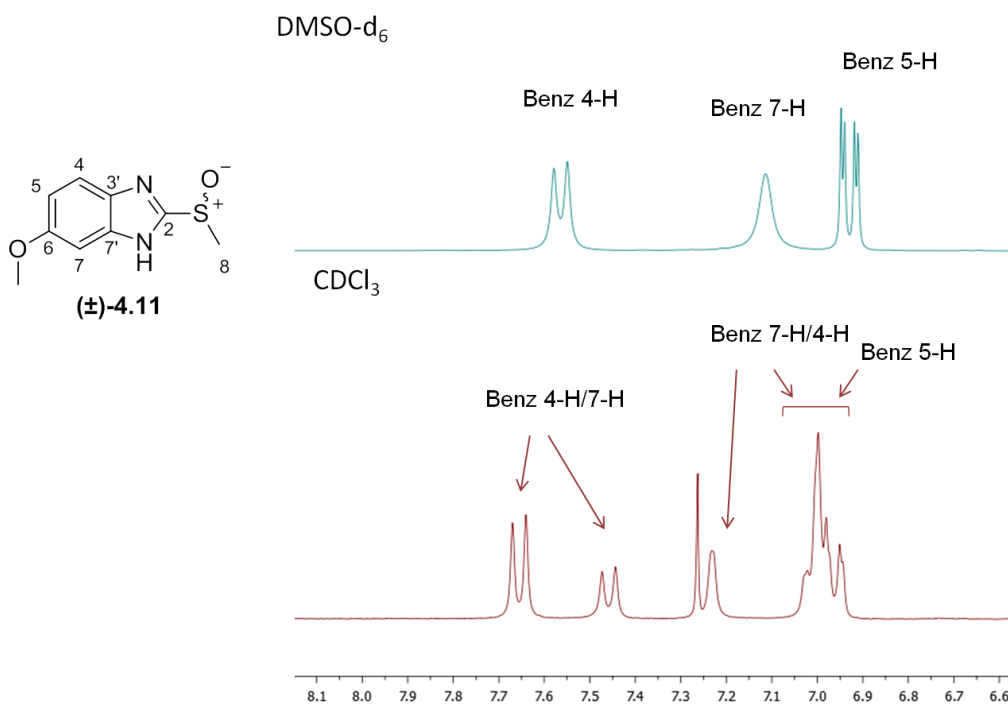
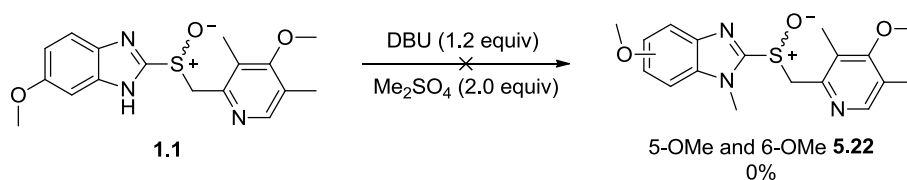


Figure 6.31 Partial ^1H NMR of methyl benzimidazole sulfoxide **4.11** in DMSO- d_6 (top) and CDCl_3 (bottom)

In contrast to the NMR spectra of Omeprazole **1.1** which showed broadened aromatic signals in CDCl₃, sulfoxide **4.9** was found to exhibit broadening of the aromatic signals attributed to the benzimidazole 4-H and 7-H when DMSO-d₆ was employed as the solvent, with the use of CDCl₃ leading to spectra with sharp, well defined peaks. For both sulfoxide **4.9** and **4.11** full assignment of the ¹³C NMR was not possible with the use of either DMSO-d₆ or CDCl₃ as the NMR solvent. For the benzyl benzimidazole sulfoxide **4.9** the carbon signals for both tautomers could be seen with either solvent, however these carbon signals were very weak leading to difficulties in assigning their identities. In addition neither proton spectra from using DMSO-d₆ or CDCl₃ could be used for 2D NMR analysis due to broadening of the aromatic peaks with the former solvent, and the splitting of the NH and OMe peak due to the two tautomers present with the use of the latter solvent. Similarly full assignment of the ¹³C NMR spectra of sulfoxide **4.11** was not possible due to broadening of signals in ¹³C NMR (in the case of DMSO-d₆), or due to the presence of observable tautomers in the ¹H NMR (in the case of CDCl₃), both of which prevented analysis by 2D NMR.

6.2.2 Synthesis and characterization of derivatized Omeprazole and related species

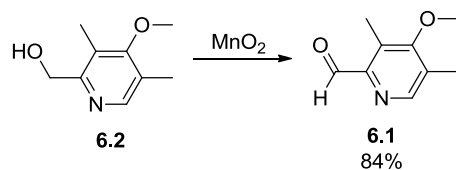
To further our studies on the tautomerism of species such as Omeprazole we investigated the synthesis of various derivatized methoxy benzimidazoles. Using a procedure reported by Shin *et al.* for the *N*-methylation of benzimidazoles Omeprazole **1.1** was treated with 1,8-diazabicyclo-[5.4.0]undec-7-ene (DBU, 1.2 equiv) and dimethyl sulfate (2.0 equiv), with the aim of producing the NMe sulfoxides **5.22** (Scheme 6.2).⁵⁶² The reaction was unsuccessful in yielding the desired target, instead a complex mixture of species was found in the crude materials.



Scheme 6.2

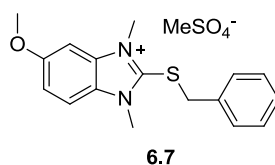
Column chromatography of the crude materials isolated the pyridyl aldehyde **6.1** the identification of which was supported by independent synthesis of this aldehyde by oxidation of the pyridyl alcohol **6.2** by MnO₂ (Scheme 6.3).⁷⁰⁶ The presence of aldehyde **6.1** in the crude materials in addition to the isolation of materials containing only the benzimidazole ring system

of Omeprazole suggested degradation of the sulfoxide starting materials, effectively cleaving the two halves of the molecule.

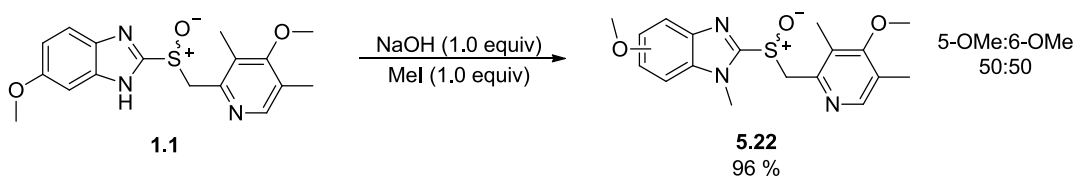


Scheme 6.3

Attempted *N*-methylation of sulfides **3.17**, **4.5**, and **4.7** using this method was also unsuccessful, with none of the desired methylated benzimidazole species isolated. For the derivitization of the benzyl benzimidazole sulfide **4.5** the isolated product was the dimethylated methyl sulfate salt **6.7**, the structure of which was confirmed by XRD.



An alternative method was found which allowed for greater success in the synthesis of *N*-methylated benzimidazole sulfides, and NMe-Omeprazole **5.22**.^{707, 708} Omeprazole **1.1** was treated with aqueous NaOH followed by methyl iodide (1.0 equiv) followed by heating at 40 °C for 1 h (Scheme 6.4). This reaction protocol was found to be highly efficient, producing only the desired methylated sulfoxide **5.22**, with no formation of side products or evidence of sulfoxide decomposition.



Scheme 6.4

The ratio of isomers produced from this reaction was found to be 50:50, with assignment of the proton signals for each of the 5-OMe and 6-OMe isomers possible through NOESY NMR with DMSO-*d*₆ as the NMR solvent (Figure 6.32). Through the process of preferential crystallization it was possible to enrich the afforded mixture of methylated sulfoxides in favour of the 6-OMe isomer. To achieve this the *N*-methylated sulfoxides **5.22** (50:50 5-OMe:6-OMe) were dissolved in the minimum amount of dichloromethane followed by slow addition of diethyl

ether to induce precipitation which was collected via filtration. ^1H NMR analysis of the solid material revealed a ratio of 18:82 in favour of the 6-OMe tautomer, with the use of correlation NMR to confirm the identity of the two tautomers.

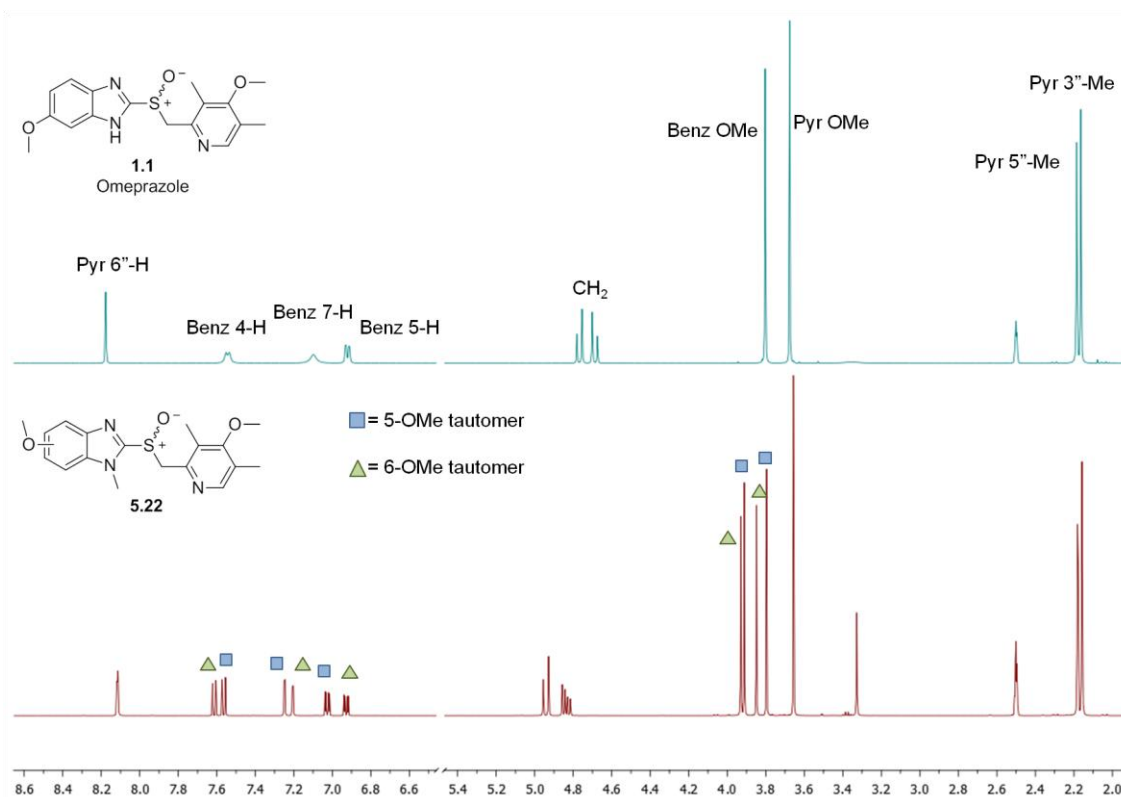
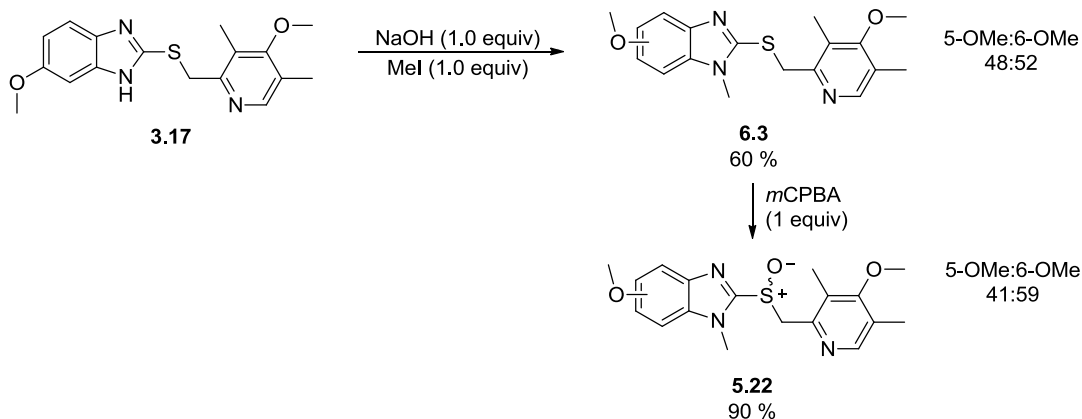


Figure 6.32 ^1H NMR of Omeprazole **1.1** (top) and *N*-methylated Omeprazole **5.22**, obtained as a 1:1 mixture of 5-OMe:6-OMe tautomers

An alternative method for the synthesis of *N*Me-Omeprazole **5.22** was investigated via the oxidation of the methylated sulfide **6.3** (Scheme 6.5). *N*-methylated Pyrmetazole **6.3** was produced in a yield of 60% by the treatment of the sulfide **3.17** with NaOH and methyl iodide; following purification by column chromatography and trituration the ratio of sulfide isomers was 48:52 5-OMe:6-OMe, as determined by ^1H NMR in DMSO- d_6 . Full characterization of each of the 5-OMe and 6-OMe isomers was achieved with the aid of 2D correlation NMR. Oxidation of the *N*-methylated sulfide **6.3** using *m*CPBA gave *N*Me-Omeprazole **5.22** as a mix of 5-OMe and 6-OMe isomers in a yield of over 90% following column chromatography, with the ratio of isomers found by ^1H NMR in DMSO- d_6 to be 41:59 (5-OMe:6-OMe). Subsequent recrystallization afforded the *N*-methylated sulfoxide in a yield of 32%; the recrystallized material **5.22** was found by ^1H NMR to be enriched in the 6-OMe isomer with a ratio of 13:87 5-OMe:6-OMe.



Scheme 6.5

Of the two methods employed in the synthesis of NMe-Omeprazole **5.22** oxidation of the methylated sulfide was the less favourable as isolation of the derivatized sulfoxide required chromatography and crystallization which incurred significant loss in material, whereas methylation of the sulfoxide produced NMe-Omeprazole in high yield with no need for further purification.

6.3 Selective deuteration of Na-Omeprazole and related compounds

Deuterium incorporation on carbon centers has chemical relevance in a number of areas such as investigations of reaction mechanisms or of metabolic pathways, or in the use of deuterated materials as reference standards e.g. for application in mass spectrometry.⁷⁰⁹ In addition, there is growing interest in assessing the pharmacokinetics of deuterated pharmaceutical bioisosteres, which may reveal superior properties with respect to toxicity or metabolic stability, allowing for new opportunities to increased efficacy of drug therapies.

During the course of our studies on Omeprazole, and related species, we encountered an unexpected observation in that the CH₂ group of Na-Omeprazole **3.36** underwent H/D exchange in DMSO-d₆. Leading on from this finding the selective deuteration of the methylene group was investigated for a number of other compounds using ¹H NMR in MeOD and D₂O under a range of pH conditions, with the aim of gaining insight in the relative acidio-basic properties of compounds in question.

6.3.1 Deuteration of Na-Omeprazole in an aprotic solvent

For NMR analysis of small organic molecules DMSO-d₆ is a common solvent. Classified as a “dipolar aprotic solvent”, it is generally not expected that DMSO-d₆ could promote deuteration of solute molecules due to its inherent chemical stability even under acidic or basic conditions.

However, during the course of these studies it was observed that on occasion the CH₂ signal of the sodium salts of Omeprazole (\pm)-**3.36** and Esomeprazole (*S*)-**3.36** was depleted or indeed absent from the ¹H NMR spectra when DMSO-d₆ was employed as the solvent. This effect was attributed to H/D exchange of the weakly acidic methylene protons. The selective deuteration of the sodium salts of Omeprazole, and related proton pump inhibitors such as Pantoprazole **3.2** and Rabeprazole **3.3**, was also observed and recently reported on by Redondo *et al.*⁷⁰⁹

Figure 6.33 shows the ¹H NMR spectra of Na-Omeprazole (\pm)-**3.36**, showing the methylene resonances of the protonated and partially deuterated species, and the absence of the CH₂ signals for the fully deuterated form of the Na-salt. In addition, on the occasions when ¹H NMR characterisation showed the full deuteration of the methylene protons the absences of the corresponding CH₂ carbon signal at 59.9 ppm was also noted (Figure 6.34). The H/D exchange of the methylene protons with the deuterated solvent was found to be a fast process, often taking no longer than the time required to prepared and run the NMR sample.

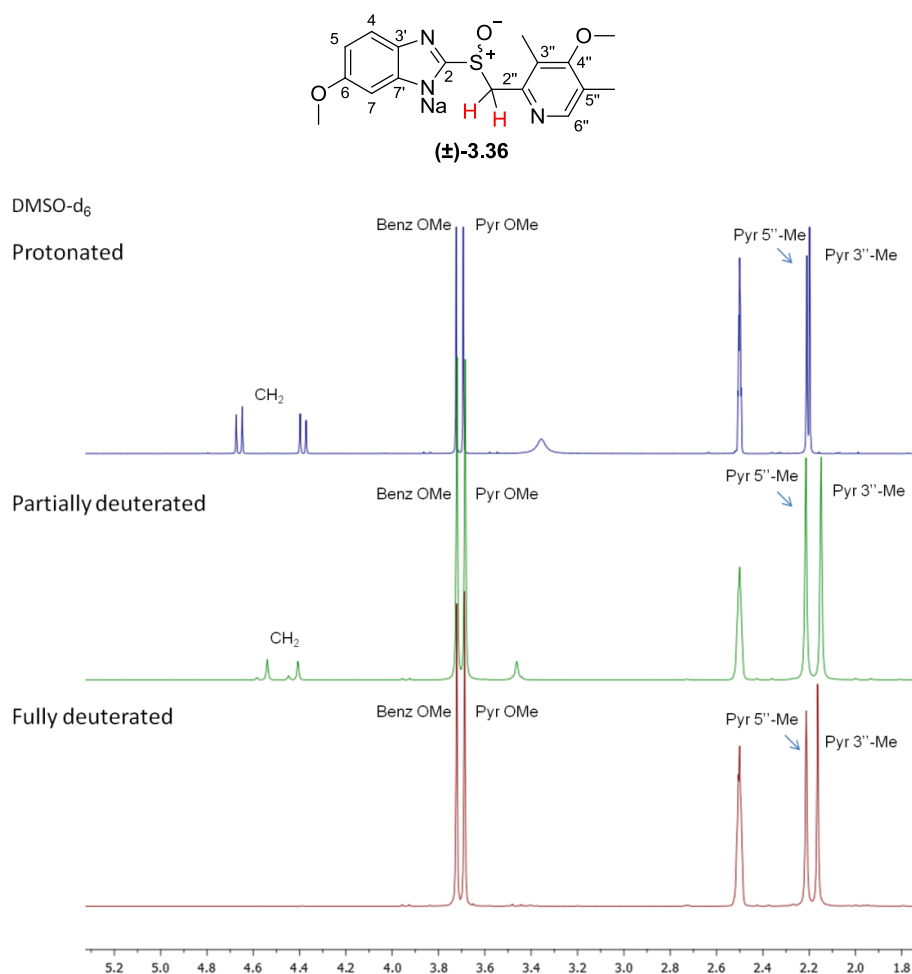


Figure 6.33 ¹H NMR (DMSO-d₆) spectra of the protonated, partially deuterated and fully deuterated forms of Na-Omeprazole (\pm)-**3.36**

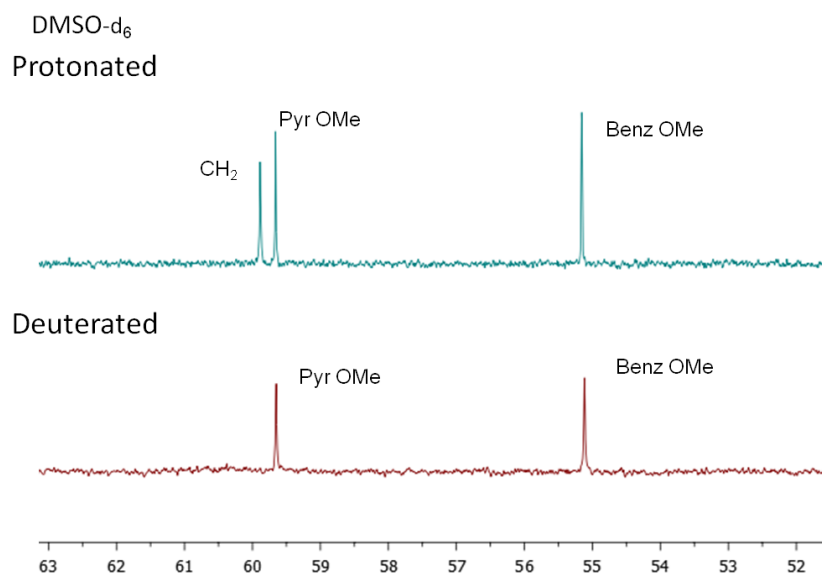
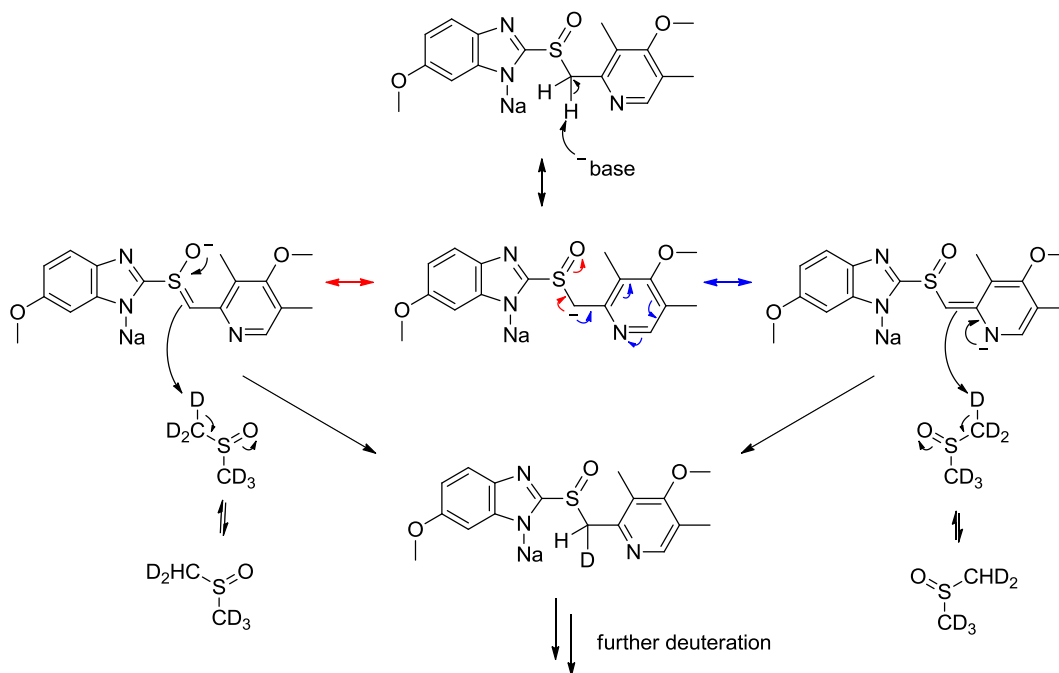


Figure 6.34 ^{13}C NMR (DMSO-d₆) spectra showing the absence of the CH₂ carbon peak for the deuterated form of Na-Omeprazole (\pm)-3.36

The protons of the CH₂SO group are weakly acidic as the negative charge created by deprotonation can be stabilized via delocalization. The mechanism of this remains a matter of debate but it is likely to occur via the 3s and 3p orbitals of sulfur, with some contribution to stabilization from the electronegative effects of the oxygen atom.^{710, 711} In PPIs such as Omeprazole there is also the possibility of delocalization into the adjacent pyridine ring (Scheme 6.6).

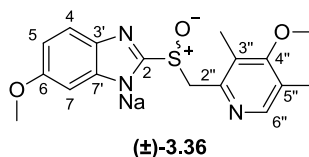


Scheme 6.6

The sodium salt of Omeprazole is a basic compound and it is possible that the pH of a solution may be sufficiently high enough to trigger the H/D exchange via removal of the methylene protons. Although measurements have not been conducted in DMSO- d_6 , aqueous solutions of Na-Omeprazole (40 mM concentration) have been shown to have a pH of 10.4, which may be sufficient to instigate the deuteration of the sulfoxide via a small population of deprotonated molecules. Alternatively, Redondo has shown that catalytic amounts of aqueous NaOH (5 μ L) in DMSO- d_6 is sufficient to effect deuteration in solution; in addition it was reported that the deuteration process was reversible, with addition of the deuterated sample to an excess of non deuterated DMSO resulting in restoration of the protonated solute molecule.⁷⁰⁹

In addition to the depletion of the CH₂ proton signals, deuteration of Na-Omeprazole **3.36** to give Na-Omeprazole- d_2 in DMSO- d_6 was accompanied by a shift in a number of proton ¹H NMR signals which may be the result of long-range isotopic effects (Table 6.10). Although Redondo *et al.* discuss this effect for the deuteration of Na-Omeprazole in MeOD or D₂O they make no mention of it occurring in DMSO- d_6 .

The most significant effect was observed for the pyridyl 3''-methyl group, which underwent a downfield shift of 35 ppb with complete deuteration of the methylene protons (Figure 6.35). For Na-Omeprazole- d_2 the aromatic benzimidazole protons and the pyridyl 6''-H were all observed at higher chemical shifts (10-19 Δ ppb) compared to the spectra of the native Omeprazole salt. The changes in chemical shifts that arise following the exchange of H for D, as seen in the ¹H NMR spectra of Na-omeprazole and Na-Omeprazole- d_2 , are believed to arise due to the resulting changes in the rotational and vibrational state of the molecule.⁷¹²



Proton	Na-omeprazole / ppm	Na-omeprazole-d ₂ / ppm	Δ ppb in DMSO-d ₆
Pyr 3''-Me	2.198	2.163	-35
Pyr 5''-Me	2.210	2.213	3
Pyr Ome	3.693	3.687	-6
Benz Ome	3.724	3.721	-3
CH ₂ downfield	4.385	-	-
CH ₂ upfield	4.661	-	-
Benz 5-H	6.545	6.555	10
Benz 4-H	7.318	7.336	18
Benz 7-H	6.979	6.998	19
Pyr 6''-H	8.230	8.242	12

Table 6.9 Deuterium isotope effects (Δ ppb) on ¹H NMR chemical shift of the proton signals of Na-Omeprazole

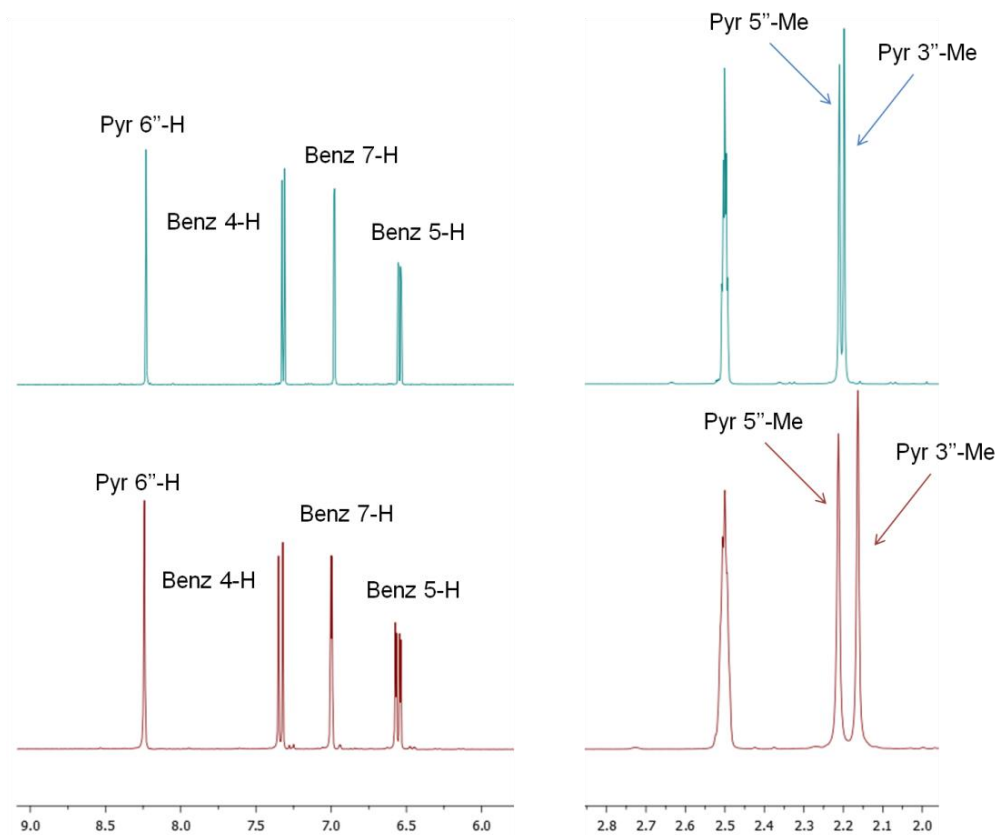


Figure 6.35 ¹H NMR (DMSO-d₆) spectra of Na-Omeprazole (top) and Na-Omeprazole-d₂ (bottom) showing the differences due to deuterium isotopic effects. Please note the scale of the X and Y axes differ between the two images

6.3.2 Deuteration of Na-Omeprazole and related compounds in protic solvents

The selective deuteration of Na-Omeprazole has also been observed to occur in protic solvents such as D₂O (Figure 6.36) and MeOD (Figure 6.37).

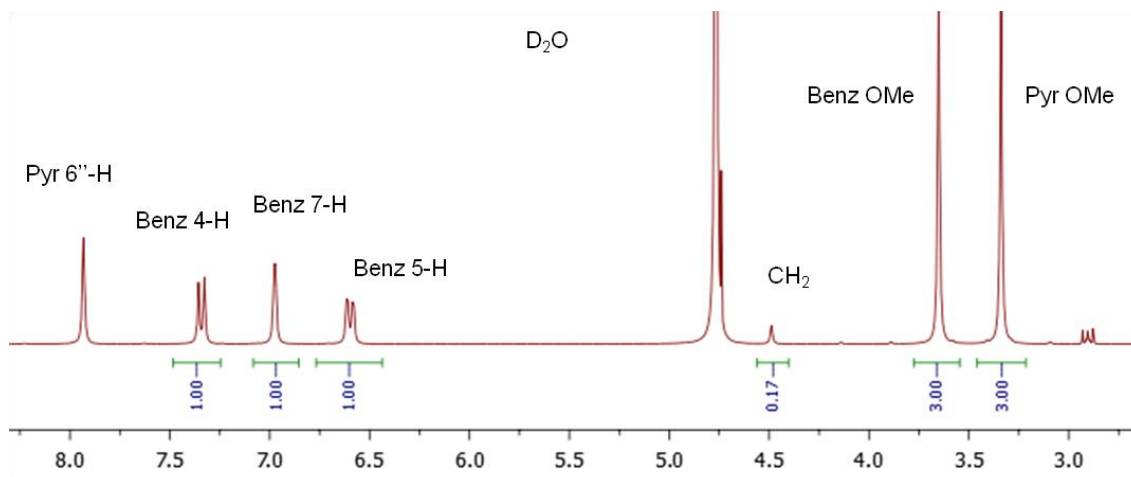


Figure 6.36 ¹H NMR (D₂O) of Na-omeprazole 3.36 showing partial deuteration of the CH₂ group

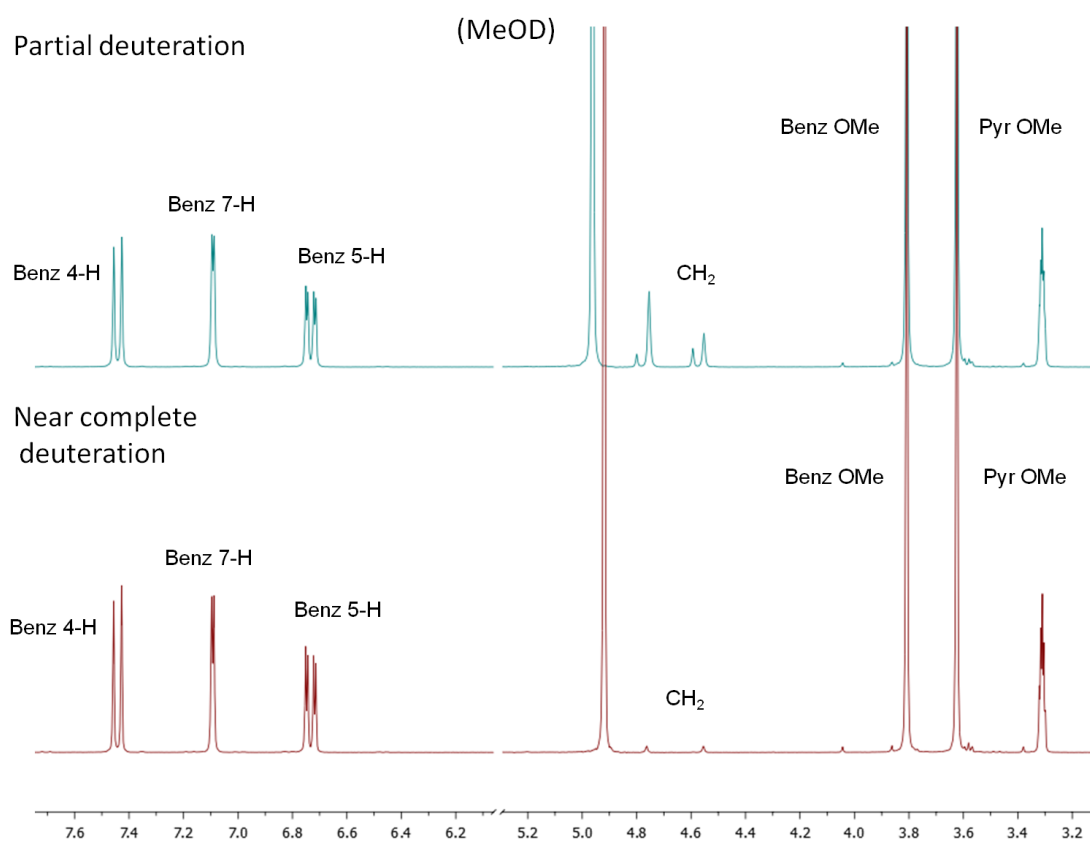
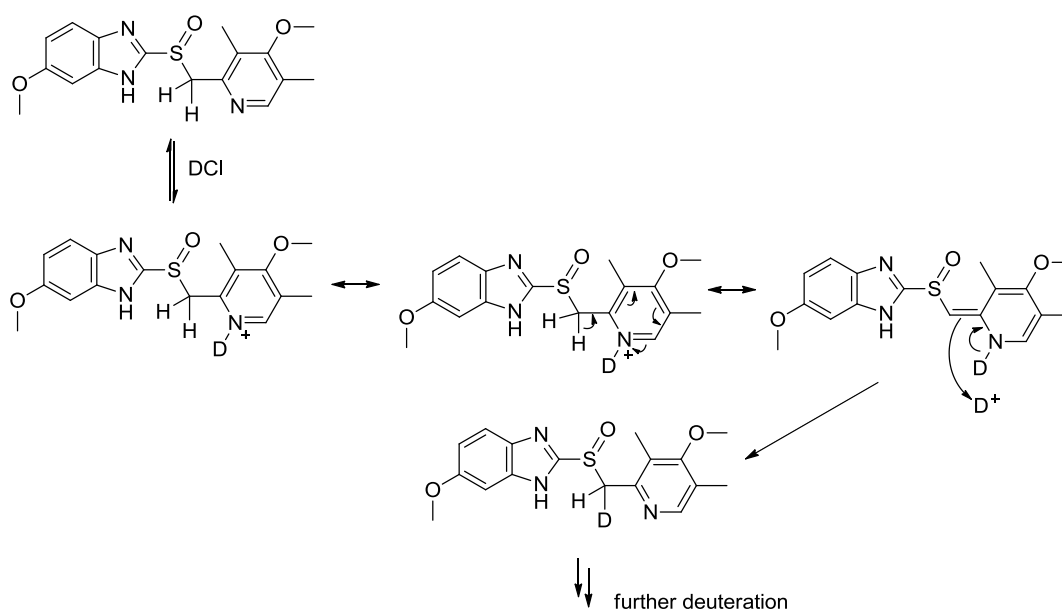


Figure 6.37 ¹H NMR (MeOD) of Na-omeprazole 3.36 showing partial deuteration and near complete of the CH₂ group

When MeOD was employed as the NMR solvent stereoselective exchange was observed, with the depletion of the two doublets from the diastereotopic methylene protons occurring at different rates which may indicate stereoselective H/D exchange of the methylene protons in agreement with the reported findings of Redondo *et al.*⁷⁰⁹

In continuation of our examination of selective deuteration in sulfoxides we looked at a variety of other compounds related to Na-Omeprazole, starting with Omeprazole **1.1** in the neutral, free base form. NMR spectra were collected from samples across a range of pH conditions in order to examine the possibility of acid promoted deuteration, which may occur via the mechanism shown in Scheme 6.7.



Scheme 6.7 Proposed mechanism for acid promoted deuteration of the CH₂SO group of Omeprazole **1.1** in a protic NMR solvent

Unlike the sodium salt **3.36**, Omeprazole **1.1** is insoluble in D₂O; however with the addition of one equivalent of NaOD a fully homogenous solution was formed which produced a ¹H NMR spectrum where the methylene signals were completely absent indicating complete H/D exchange. Under acidic conditions, i.e. with the addition of one equivalent of DCl, decomposition/rearrangement of Omeprazole was observed, with a complex mixture of products shown by NMR. In MeOD under neutral conditions the ¹H NMR spectra of Omeprazole showed no depletion of the CH₂ protons; with the addition of one equivalent of NaOD almost complete deuteration was observed for the methylene group. Typically under acidic conditions Omeprazole was found to decompose rapidly, however it was possible through swift characterization to collect the characterization data for Omeprazole deuterated with DCl (1 equiv) prior to the commencement of rearrangement (Figure 6.38).

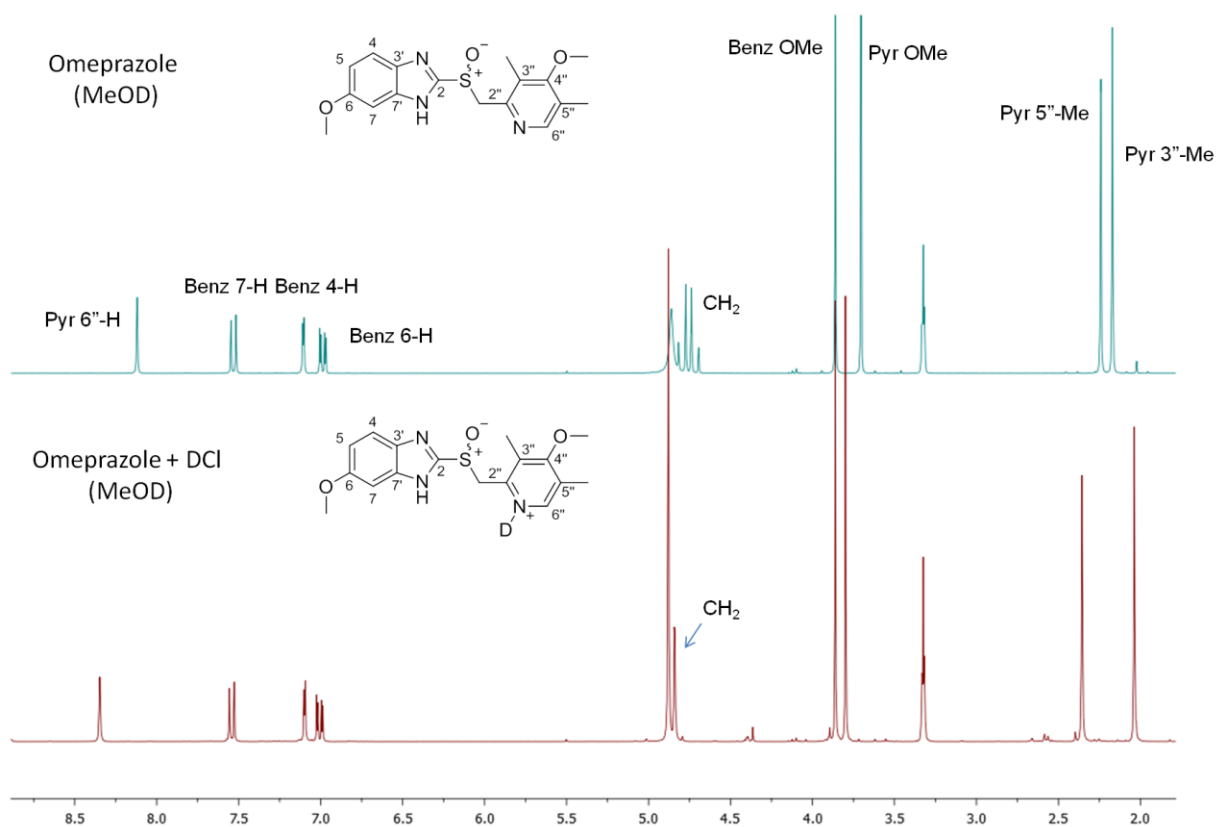
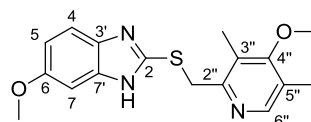


Figure 6.38 ^1H NMR spectra (MeOD) of Omeprazole **1.1** under neutral conditions (top) and with addition of one equiv of DCl (bottom)

It was found that acidification of Omeprazole in MeOD resulted in deuteration on the pyridine ring, indicated by the significant changes in the chemical shifts of the pyridyl protons signals but not of those for the benzimidazole ring. Coalescence of the CH_2 signal gave a singlet at 4.76 ppm with little apparent depletion of the methylene protons due to H/D exchange however accurate determination of this was not possible due to the proximity of the solvent peak.

Pyrimetazole **3.17**, the sulfide precursor to Omeprazole, was examined next (Fig 6.39). Under basic and neutral conditions in MeOD no deuteration of methylene protons was observed, however with the addition of one or two equivalents of DCl depletion of the CH_2 proton signals was seen. In addition the methylene signal under these conditions was observed to have split into a fine doublet, with unequal depletion observed between the two peaks, possible indicating selective deuteration between the two protons at this position. Interestingly when five equivalents of DCl were added to the sulfide integration of the signal for the methylene protons showed no deuteration had occurred. It may be possible that deuteration of both the benzimidazole and pyridine prevents H/D exchange. When D_2O was employed as the NMR solvent no deuteration was observed at the methylene position Pyrimetazole **3.17** under basic or acidic conditions.



Pyrimetazole 3.17

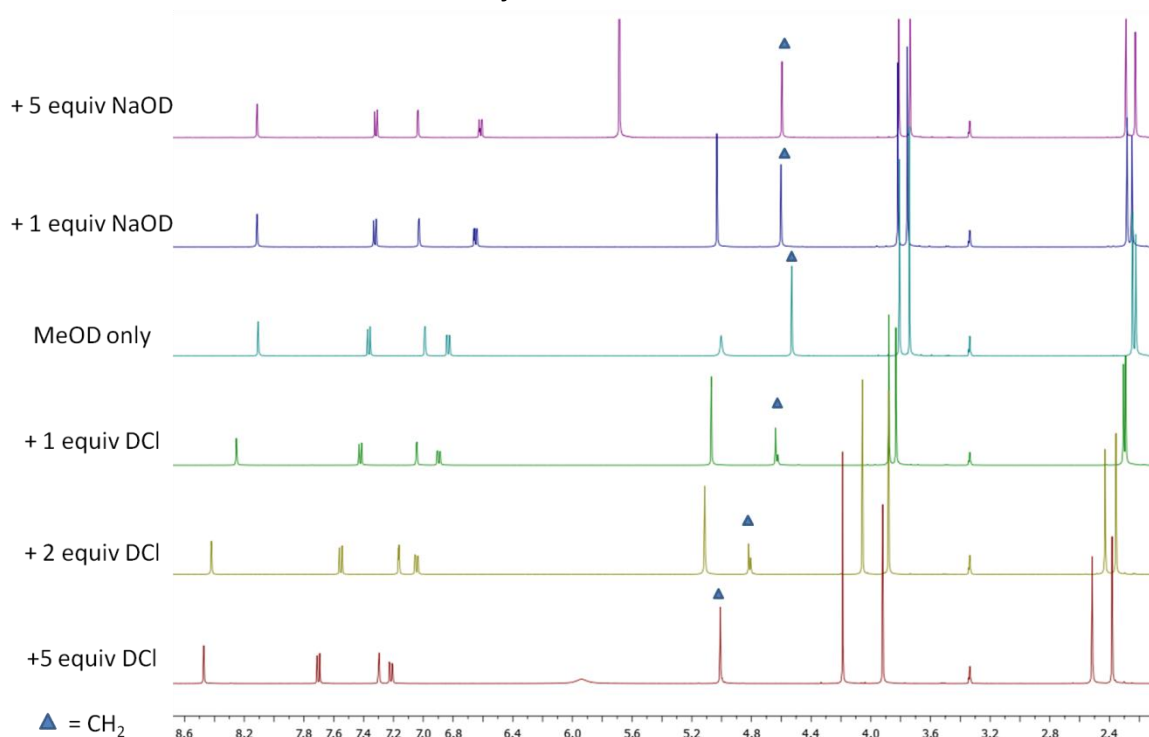


Figure 6.39 ^1H NMR (MeOD) spectra of Pyrimetazole sulfide 3.17 across a range of pH conditions; the signals for the CH_2 are indicated by ▲

NMR investigation of Omeprazole sulfone **4.1** under basic conditions in MeOD was not possible due to poor solubility of the substrate, however under neutral and acidic conditions full H/D exchange of the methylene group was observed (Figure 6.40). In D_2O the same result was found for both basic and acidic solutions of the sulfone, although poor solubility prevented characterization in neutral D_2O .

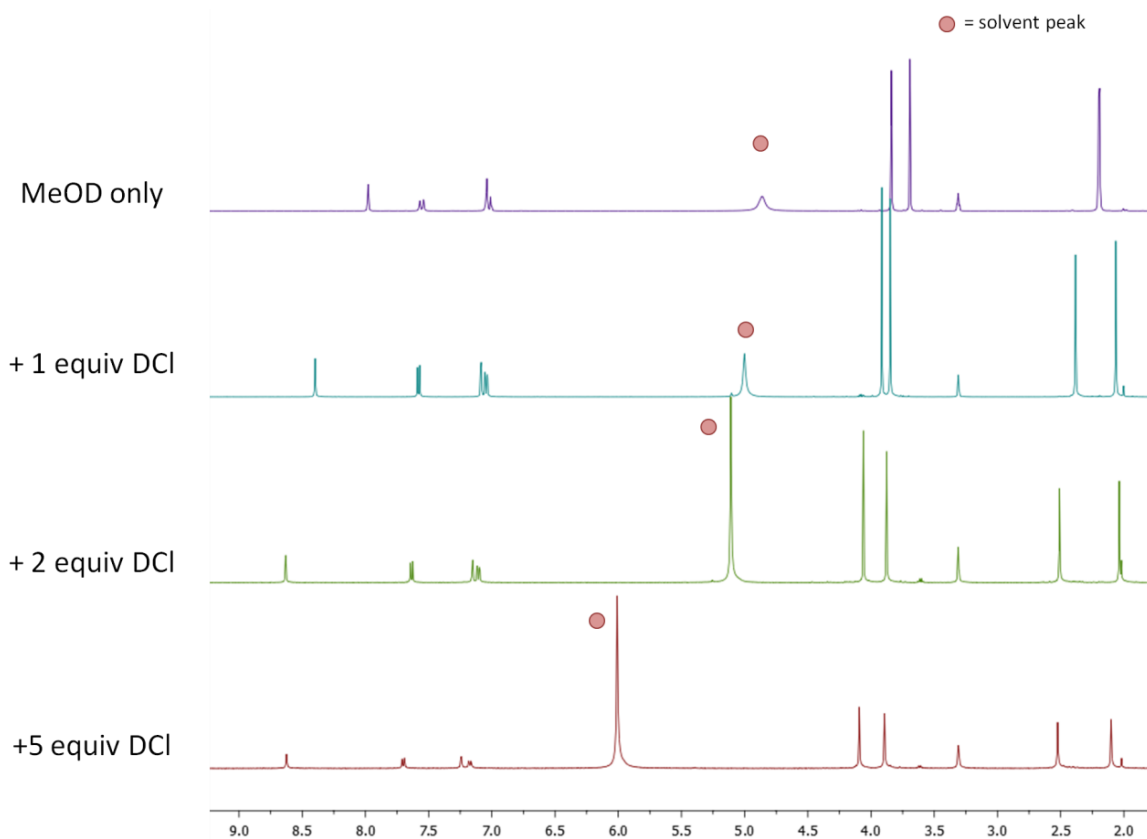
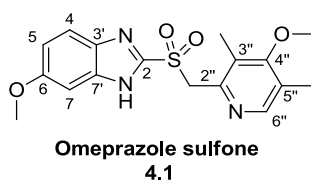


Figure 6.40 ^1H NMR (MeOD) spectra of Omeprazole sulfone **4.1** under neutral and acidic conditions; no CH_2 group observed under any conditions

^1H NMR investigations of the benzyl benzimidazole sulfoxide **4.9** and the *p*-tolyl pyridyl sulfoxide **4.12** were also performed, using MeOD as the NMR solvent (Figures 6.41 and 6.42 respectively). Under basic conditions both sulfoxides were observed to have undergone depletion of the methylene signals. For sulfoxide **4.9** partial H/D exchange was seen with the addition of one equivalent of NaOD, and near complete deuteration observed with the addition of an excess of base (five equiv). Similarly full exchange of the CH_2 protons was observed for sulfoxide **4.12** with an excess of base, and also with the stoichiometric addition of NaOD, in keeping with the increase acidity of the methylene protons of sulfoxide **4.12** over those of sulfoxide **4.9**.

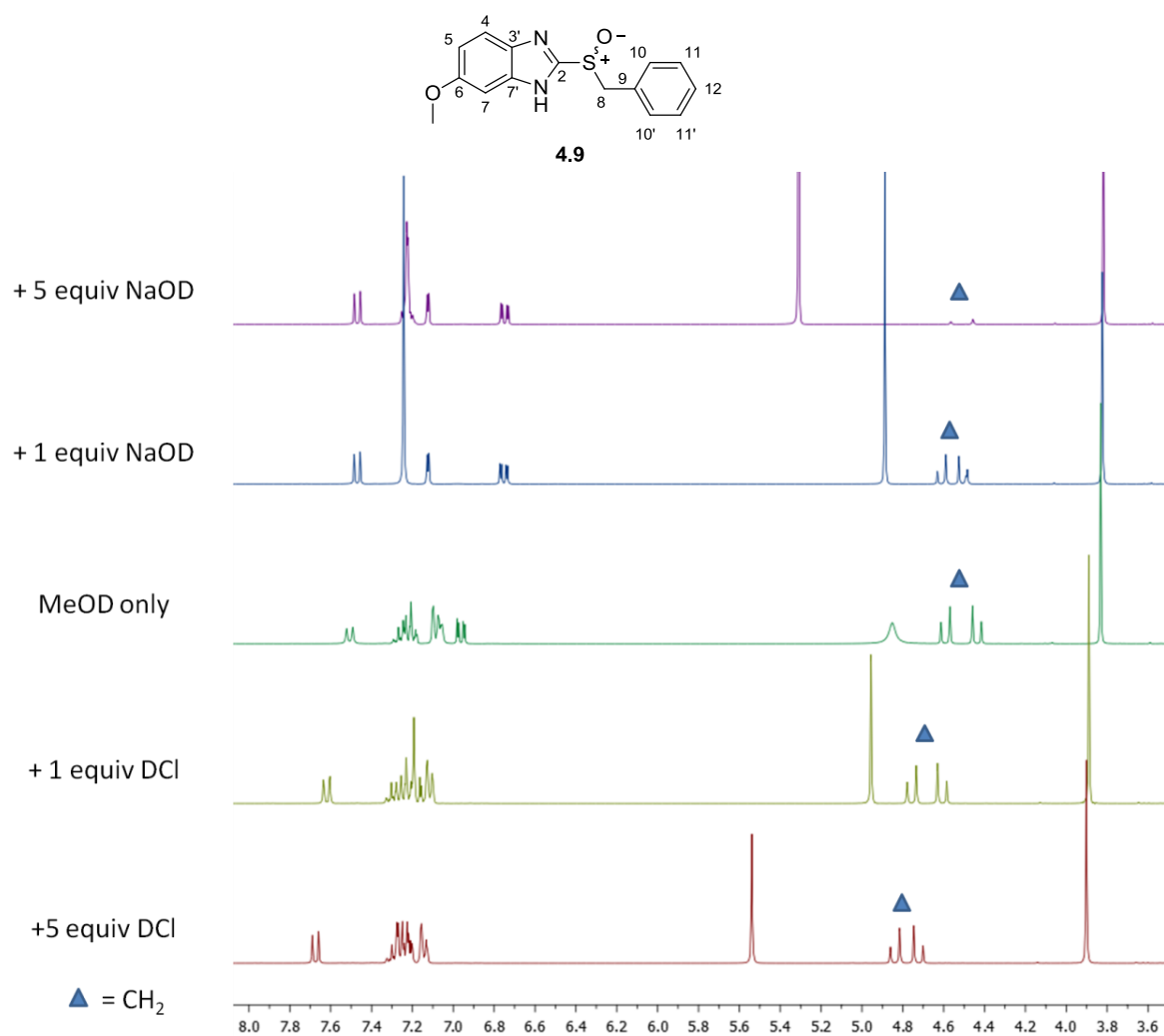


Figure 6.41 ¹H NMR (MeOD) spectra of sulfoxide **4.9** across a range of pH conditions; the signals for the CH₂ are indicated by ▲

While no deuteration of the methylene group was observed under neutral or acidic conditions for sulfoxide **4.9**, with the addition of one equivalent of DCl sulfoxide **4.12** produced an NMR spectrum where the resonances attributed to the CH₂ protons were depleted, and had collapsed in upon itself, no longer appearing as the characteristic AB system (Figure 6.42).

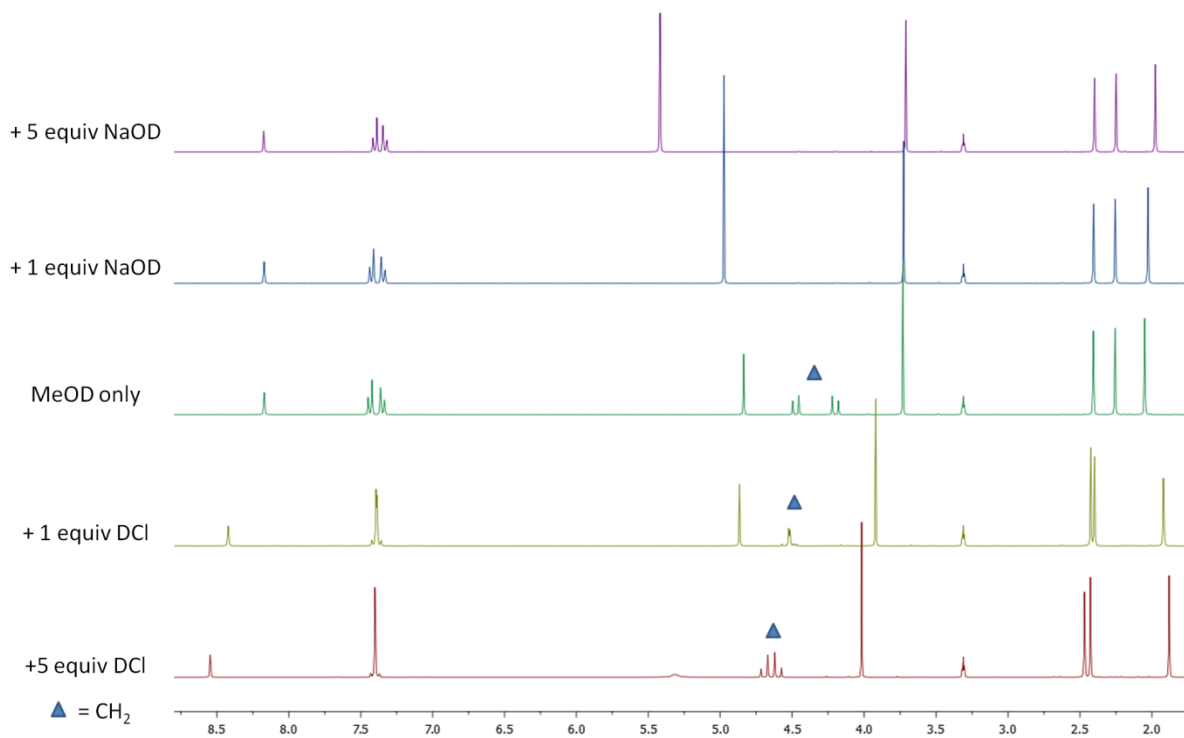
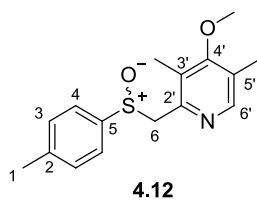
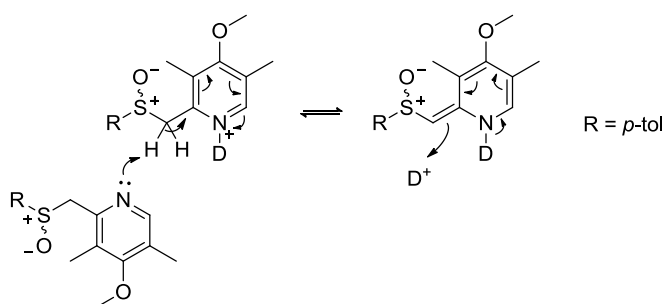


Figure 6.42 ¹H NMR (MeOD) spectra of sulfoxide **4.12** across a range of pH conditions; the signals for the CH₂ are indicated by ▲

Similar to the observed behavior of the sulfide Pyrimetazole **3.17**, when an excess of acid was employed no deuteration was observed for sulfoxide **4.12**, this may suggest that both the pyridine and pyridinium salt are required to be present for exchange to take place (Scheme 6.8).



Scheme 6.8

6.4 Conclusion and Future direction

The examination of the properties of Omeprazole and related compounds in this chapter has revealed a great diversity in the physical and chemical nature of the species produced as part of

this body of work. Through the use of X-ray crystallography the solid state structures and intermolecular interactions of compounds including and related to Omeprazole were uncovered. Omeprazole itself was found to crystallize as the racemate, forming heterochiral dimers held together with H-bonding interactions. The ability of Omeprazole, but not Esomeprazole, to form a structure of this type account for the contrasting physical properties of Omeprazole and Esomeprazole with respect to crystallinity and solubility. The formation of heterochiral dimers of Omeprazole can also be exploited to enhance the optical purity of Esomeprazole by formation and removal of racemic materials from solution. In contrast to the dimers formed by Omeprazole **1.1**, the sulfide Pyrimetazole **3.17** formed a double strand type structure with both the benzimidazole and pyridyl N atoms interacting with the thioether sulfur atom. The sulfone of Omeprazole **4.1** was found as a tetramer, formed between two molecules of the sulfone and two molecules of solvent. Although it was not possible to form crystals of the Na-salt of Omeprazole, the K-salt **3.38** was found to crystallize in a complex structure, with polymeric chains formed from bridging interactions between the sulfinyl group, solvent molecules, the potassium atom, and the pyridyl nitrogen. The benzyl benzimidazole sulfoxide **4.11** was found to form dimers, with H-bonding interactions between the benzimidazole and sulfinyl group, whereas both sulfoxide **4.10** and **4.12** did not display any H-bonding interactions or π - π stacking in their solid state packing. For completeness, it would be desirable to grow and analyze crystals of the benzyl benzimidazole sulfoxide **4.9** and compare and contrast the structure with the sulfoxides already examined. Further studies would also endeavor to grow suitable crystals for XRD analysis of the single enantiomer forms of the sulfoxides and examine any possible differences in their solid state structure in comparison with their racemic forms.

The annular tautomerism of various methoxy benzimidazole compounds, including Omeprazole, was investigated by ^1H and ^{13}C NMR. For many of the substituted benzimidazole species featured in this thesis the spectra obtained by ^1H NMR contained broadened signals in the aromatic region, and for ^{13}C NMR appeared to be missing many of the signals from the benzimidazole group, both of these effects can be attributed to the prototropic tautomerism of this aromatic group. In contrast, the NMR spectra collected for the Na-salt of Omeprazole **3.36** featured sharp proton signals and a full complement of peaks in the ^{13}C NMR. The benzyl benzimidazole sulfoxide **4.9** and the methyl benzimidazole sulfoxide **4.11** were both found to show evidence of their two tautomeric forms at room temperature in CDCl_3 , from which a relative ratio of tautomeric isomers could be measured. Further characterization may allow identification of which tautomer is most prevalent in solution for both of these two sulfoxides. The effect of varying the temperature at which the NMR of Omeprazole was performed was examined briefly, with broad signals for the benzimidazole 4-H and 7-H seen at high temperature, due to rapid tautomeric exchange, whereas at low temperature the exchange was

slowed sufficiently to be able to observe these protons in their different environments for the two tautomeric isomers. Further investigation of this matter would examine a range of NMR solvents in order to be able to access a wider range of temperatures to conduct the NMR experiments. In addition, further characterization, including possible 2D correlation NMR experiments would be conducted at low temperature to assist in assigning the tautomeric signals to the correct isomer. The synthesis and full NMR characterization of *N*-methylated Pyrmetazole **6.3**, and *N*-methylated Omeprazole **5.22** was achieved. It was found that it was possible to produce material enriched in the 6-OMe isomer of NMe Omeprazole **5.22** by antisolvent induced crystallization of a 50:50 mix of isomers. Future studies into the annular tautomerism of compounds such as Omeprazole may involve computational studies such as molecular modeling to uncover more information about the relative energies of the tautomeric forms of the benzimidazole species investigated here.

The selective deuteration of Na-Omeprazole and Na-Esomeprazole was unexpectedly encountered during the course of these studies, observed by ¹H NMR as the depletion or indeed absences of the CH₂ protons. This effect was attributed to H/D exchange with the deuterated solvent, DMSO-d₆, and was found to occur within minutes, within the time required for the NMR sample to be prepared and run. The selective deuteration of the methylene group of Na-Omeprazole was also observed to occur in the protic solvents MeOD and D₂O, with possible stereoselective H/D exchange observed in the former NMR solvent. Both Pyrmetazole sulfide **3.17** and Omeprazole sulfone **4.1** underwent deuteration, with H/D exchange of the sulfide occurring in 1 or 2 equivalents of DCl in MeOD, whereas the exchange occurred to a much greater extent for the more acidic methylene protons of the sulfone, with no CH₂ protons observed for this species, due to complete deuteration, in MeOD and D₂O in acidic, basic and neutral conditions. The benzyl benzimidazole sulfoxide **4.9** underwent H/D exchange in basic conditions, while the pyridyl *p*-tolyl sulfoxide **4.12** showed evidence of complete deuteration with the addition of NaOD, and partial deuteration with a stoichiometric amount of DCl. With the addition of an excess of acid, both Pyrmetazole and sulfoxide **4.12** appeared resistant to H/D exchange, suggesting that the pyridine and pyridinium salt needs to be present for the mechanism of exchange to occur. Further examination of the selective deuteration would investigate the time required for these transformations to occur, possibly with the use of substoichiometric amounts of acid and base, which may provide information on the relative reactivities of the methylene groups of the various compounds examined. The reversibility of the H/D exchange could also be investigated.

7 Appendix

The X-ray diffraction data for the compounds discussed in section 6.1 has been included on the accompanying disk. Alternatively, for the electronic version of this thesis this data may be found at the end of the document.

8 Experimental

8.1 General Experimental

All reagents were obtained commercially and used directly without further purification, unless stated otherwise. All solvents were distilled before use or obtained dry from commercial suppliers. Solvents were removed under reduced pressure using a diaphragm pump with a Buchi rotary evaporator. Additional traces of solvent were removed by drying under high vacuum at 0.25 mmHg using a rotary oil pump. Flash silica chromatography was performed using silica gel (230-400 mesh) supplied by E.M. Merck. Thin layer chromatography (TLC) was performed using Merck aluminium TLC sheets (silica gel 60 F₂₅₄). Visualisation of the TLC plates was carried out using a UV lamp (245 nm) or by dipping in KMnO₄ followed by exposure to heat. Melting point determination was carried out on a Reichert Hot Stage apparatus and are reported uncorrected. Elemental analysis was carried out using a Carlo Ebra 1108 Elemental Analyzer. Determination of halogen and sulfur were carried out using the Schoniger Oxygen Flask combustion method followed by the relevant titration for the particular halogen. LCMS analysis was performed using a Bruker HCT open access system consisting of a Bruker HCT Ultra mass spectrometer and an Agilent Technologies 1200 series HPLC under acid free conditions with positive ion electrospray ionization.

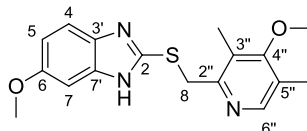
Nuclear magnetic resonance (NMR) spectra were recorded for ¹H at 300 or 500 MHz, and ¹³C at 75 or 125 MHz on a Bruker DPX300 FT spectrometer or Bruker Avance 500 spectrometer both of which utilize an internal deuterium lock. Coupling constants are given in Hertz (Hz). Chemical shifts were recorded downfield from tetramethylsilane (TMS) defined as 0 in parts per million (ppm) or by residual proton signals from the deuterated solvents were used as references [chloroform (¹H 7.26 ppm, ¹³C 77.1 ppm), DMSO-d₆ (¹H 2.50 ppm, ¹³C 39.5 ppm), MeOD (¹H 3.31 ppm, ¹³C 49.0 ppm)]. When D₂O was employed as the NMR solvent, the reference peak ($\delta = 0$) was the methyl signal of the sodium salt of 3-(trimethylsilyl)propane-1-sulfonic acid; a sealed capillary tube containing a solution of the reference material in D₂O (2 % w/w) was added to each NMR tube.⁷¹³ In reporting ¹H and ¹³C NMR data the following abbreviations will be used; s = singlet, d = doublet, t = triplet, q = quartet, m = multiplet. Proton and carbon assignment has been based on HMQC, HMBC, and NOESY spectra analysis where appropriate. Mass spectra (HRMS) was recorded in house using a Micromass GCT Premier, using electron impact ionisation (EI) or a Bruker Daltonics microTOF, using electron spray ionisation (ESI). Infrared (IR) spectra were recorded on a Perkin Elmer Spectrum One FT-IR spectrometer, as solid samples unless stated otherwise. Vibrational frequencies are reported in wavenumbers (cm⁻¹). Chiral HPLC was carried out using an Agilent 1290 Infinity employing Chiralcel AD-H

or OD-H columns as stated, with column dimensions of 250 mm × 4.6 mm and 5 μm particle sizes. Solvent system, flow rate and operating temperature are stated for each chiral species analyzed.

Single crystal X-ray diffraction data were collected on an Agilent (Rigaku) SuperNova X-ray diffractometer equipped with an Atlas CCD detector using monochromated Mo-Kα ($\lambda = 0.7107 \text{ \AA}$) or Cu-Kα ($\lambda = 1.5418 \text{ \AA}$) radiation. Samples were mounted on a nylon loop under inert oil and cooled to 120 K using an Oxford Cryosystem low temperature device.⁷¹⁴ The full dataset was collected and processed using CrysAlisPro.⁷¹⁵ Structural solution was achieved using direct methods (SHELXS) or charge-flipping methods (Superflip) and the model refined by full matrix least squares on F2 using SHELXL-973 interfaced through Olex2.^{704, 716, 717} Molecular graphics, editing of CIFs and construction of data tables were achieved using Olex2. Unless otherwise stated, hydrogen atoms were placed using idealized geometric positions (with free rotation for methyl groups), allowed to move in a “riding model” along with the atoms to which they were attached, and refined isotropically.

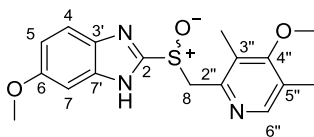
8.2 Synthetic Protocols

6(5)-Methoxy-2-[[[(4-methoxy-3,5-dimethyl-2-pyridinyl)methyl]thio]-1*H*-benzimidazole (Pyrimetazole) **3.17**⁷¹⁸



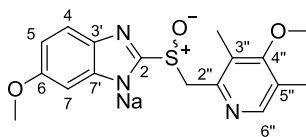
A solution of NaOH (4.00 g, 100 mmol) in H₂O (20 mL) was added to a suspension of 2-(chloromethyl)-3,5-dimethyl-4-methoxypyridine hydrochloride **3.19** (22.2 g, 100 mmol) and 5-methoxy-1*H*-benzimidazole-2-thiol **3.18** (18.0 g, 100 mmol) in EtOH (100 mL). The mixture was heated at reflux for 15 min then a solution of NaOH (4.00 g, 100 mmol) in H₂O (20 mL) was added and heating continued for 3h. The mixture was allowed to cool to rt followed by the addition of H₂O (50 mL) and CH₂Cl₂ (100 mL). The phases were separated and the aqueous phase extracted with CH₂Cl₂ (3 × 100 mL), the organic materials were combined, dried (MgSO₄), filtered and the solvent removed *in vacuo*. Column chromatography (eluting with EtOAc) gave sulfide **3.17** as a viscous gum which was triturated with Et₂O to afford the title compound **3.17** (29.3 g, 89.0 mmol, 89%) as a colourless amorphous powder; **m.p.** 112.1-113.8 °C (Et₂O); **R_f** 0.58 (5% MeOH–EtOAc); ¹H NMR (DMSO-d₆, 500 MHz): δ 2.19 (3H, s, pyr 5''-Me), 2.27 (3H, s, pyr 3''-Me), 3.71 (3H, s, pyr OMe), 3.77 (3H, s, benz OMe), 4.65 (2H, s, CH₂), 6.76 (1H, dd, *J* 8.7 and 2.4, benz 5-H), 6.99 (1H, br s, benz 7-H), 7.35 (1H, d, *J* 8.7, benz 4-H), 8.17 (1H, pyr 6''-H), 12.45 (1H, br s, NH, exchangeable); ¹³C NMR (DMSO-d₆, 125 MHz): δ 10.9 (pyr 3''-Me), 12.9 (pyr 5''-Me), 36.5 (CH₂), 55.4 (benz OMe), 59.8 (pyr OMe), 96.0 (br benz C7), 110.4 (benz C5), 113.0 (br benz C4), 124.5 (pyr C3''), 125.1 (pyr C5''), 148.6 (pyr C6''), 148.9 (benz C2), 154.2 (pyr C2''), 155.3 (benz C6), 163.4 (Pyr C4''); ¹H NMR (CDCl₃ 500 MHz): δ 2.25 (3H, s, 5''-Me), 2.30 (3H, s, 3''-Me), 3.76 (3H, s, pyr OMe), 3.82 (3H, s, benz OMe), 4.38 (2H, s, CH₂), 6.81 (1H, dd, *J* 8.7 and 2.4, benz 5-H), 7.03 (1H, br s, benz 7-H), 7.40 (1H, d, *J* 8.7, benz 4-H), 8.24 (1H, pyr 6''-H); ¹³C NMR (CDCl₃, 125 MHz): δ 11.3 (pyr 3''-Me), 13.4 (pyr 5''-Me), 35.5 (CH₂), 56.0 (benz OMe), 60.1 (pyr OMe), 97.8 (br benz C7), 111.2 (benz C5), 114.9 (br benz C4), 125.5 (pyr C3''), 126.2 (pyr C5''), 134.4 (benz C3' or C7'), 140.0 (benz C3' or C7'), 148.5 (pyr C6''), 150.7 (benz C2), 155.8 (pyr C2''), 156.0 (benz C6), 165.1 (Pyr C4''), NMR data in accordance with the literature;⁷¹⁸ **v_{max}/cm⁻¹ (solid)** 3071, 2959, 1635, 1594, 1567, 1635, 1435, 1308, 1261, 1155, 1078 ; **m/z (ESI)** (Found MH⁺, 330.1283, C₁₇H₁₉N₃O₂S requires *MH* 330.1271); **Anal. Calcd.** for C₁₇H₁₉N₃O₂S (%): C, 62.0; H, 5.80; N, 12.8; **Found:** C, 61.9; H, 5.90; N, 13.0.

(±)-6(5)-Methoxy-2-[[[4-methoxy-3,5-dimethyl-2-pyridinyl)methyl]sulfinyl]-1*H*-benzimidazole (±)-Omeprazole (±)-**1.1**^{576, 719, 720}



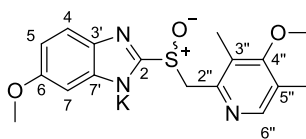
Saturated aqueous NaHCO₃ (100 mL) was added to a solution of Pymetazole **3.17** (8.24 g, 25.0 mmol) in CH₂Cl₂ (100 mL) and the mixture cooled to 0 °C. A solution of *m*CPBA (75% *m*CPBA, 5.60 g, 25.0 mmol) in CH₂Cl₂ (90 mL) and MeOH (10 mL) was added dropwise and the reaction stirred vigorously for 3h. The reaction was quenched by addition of saturated aqueous Na₂S₂O₃ (50 mL), the phases were separated and the aqueous layer extracted with CH₂Cl₂ (3 × 50 mL). The combined organic extracts were washed with brine (25 mL), treated with charcoal and MgSO₄, filtered and the volume reduced *in vacuo* to approximately 20 mL. Et₂O was added slowly to induce precipitation. The precipitate was collected by vacuum filtration and washed with Et₂O to give the title compound (±)-**1.1** (6.48 g, 18.8 mmol, 75%) as colourless microcrystals; **m.p.** decomp > 135 °C (CH₂Cl₂– Et₂O) (lit. decomp > 135 °C);⁷¹⁹ **R_f** 0.46 (5% MeOH–EtOAc); **¹H NMR** (DMSO-*d*₆, 500 MHz): δ 2.16 (3H, s, pyr 3''-Me), 2.18 (3H, s, pyr 5''-Me), 3.67 (3H, s, pyr OMe), 3.80 (3H, s, benz OMe), 4.69 and 4.77 (2H, AB-system, *J* 13.5, CH₂), 6.92 (1H, dd, *J* 8.9 and 2.4, benz 5-H), 7.10 (1H, br s, benz 7-H), 7.54 (1H, d, *J* 8.9, benz 4-H), 8.18 (1H, pyr 6''-H), 13.42 (1H, br s, NH, exchangeable) **NMR** data in accordance with the literature;^{576, 720} **¹³C NMR** (DMSO-*d*₆, 125 MHz): δ 11.1 (pyr 3''-Me), 12.9 (pyr 5''-Me), 55.5 (benz OMe), 59.7 (pyr OMe), 60.1 (CH₂), 95.6 (br benz C7), 113.4 (br benz C5), 119.3, 125.5 (pyr C5''), 126.5 (pyr C3''), 136.5, 149.2 (pyr C6''), 149.6 (pyr C2''), 153.1 (benz C2), 156.6 (benz C5), 163.5 (pyr C4'') **¹H NMR** (CDCl₃ 500 MHz): δ 2.06 (3H, s, pyr 3''-Me), 2.19 (3H, s, pyr 5''-Me), 3.57 (3H, s, pyr OMe), 3.81 (3H, s, benz OMe), 4.75 and 4.80 (2H, 2 d, *J* 13.7, CH₂), 6.83 (1H, br s, benz 7-H), 6.91 (1H, dd, *J* 8.9 and 2.1, benz 5-H), 7.61 (1H, br s, benz 4-H), 8.17 (1H, pyr 6''-H), 12.64 (1H, br s, NH, exchangeable); **¹³C NMR** (CDCl₃, 125 MHz): δ 11.5 (pyr 3''-Me), 13.3 (pyr 5''-Me), 55.9 (benz OMe), 59.8 (pyr OMe), 60.7 (CH₂), 95.1 (benz C7), 102.0 (benz C3' or C7'), 113.5 (benz C5), 120.9 (benz C4), 126.3 (pyr C5''), 127.0 (pyr C3''), 135.6 (benz C3' or C7'), 149.0 (pyr C2''), 149.8 (pyr C6''), 151.1 (benz C2), 157.9 (benz C6), 164.5 (pyr C4''); **v_{max}/cm⁻¹ (solid)**: 3056, 2943, 2901, 1626, 1585, 1509, 1401, 1310, 1154, 1074;^{576, 721} **m/z (ESI)** (Found MH⁺, 346.1230 C₁₇H₁₉N₃O₃S requires *MH* 346.1220); **Anal. Calcd.** for C₁₇H₁₉N₃O₃S (%): C, 59.1; H, 5.55; N, 12.2; **Found**: C, 59.4; H, 5.60; N, 12.0.

(±)-6(5)-Methoxy-2-[[4-methoxy-3,5-dimethyl-2-pyridinyl)methyl]sulfinyl]-1H-benzimidazole sodium ((±)-Na Omeprazole) (±)-3.36



A solution of NaOH (0.200 g, 5.00 mmol) in H₂O (0.25 mL) was added to a suspension of Omeprazole (±)-**1.1** (1.73 g, 5.00 mmol) and MeCN (10 mL) and the resulting solution stirred at room temperature. After 1h the solution was concentrated to approximately half volume *in vacuo* and precipitation of the salt was induced by dropwise addition of Et₂O. The precipitate was collected by filtration and washed with Et₂O to give the title compound (±)-**3.36** (1.76 g, 4.80 mmol, 96%) as a colourless powder; **m.p.** > 240 °C (MeCN); **¹H NMR** (DMSO-d₆, 500 MHz): δ 2.20 (3H, s, pyr 3''-Me), 2.21 (3H, s, pyr 5''-Me), 3.69 (3H, s, pyr OMe), 3.72 (3H, s, benz OMe), 4.38 and 4.66 (2H, AB-system, *J* 12.9, CH₂, exchangeable), 6.54 (1H, dd, *J* 8.6 and 2.5, benz 5-H), 6.98 (1H, d, *J* 2.5, benz 7-H), 7.32 (1H, *J* 8.6, benz 4-H), 8.23 (1H, pyr 6''-H); **¹³C NMR** (DMSO-d₆, 125 MHz): δ 11.3 (3''-Me), 12.9 (5''-Me), 55.2 (benz OMe), 59.7 (pyr OMe), 59.9 (CH₂), 99.5 (benz C7), 108.7 (benz C5), 117.4 (benz C4), 124.8 (pyr C5''), 126.4 (pyr C3''), 141.7 (benz C3' or C7'), 147.1 (benz C3' or C7'), 149.0 (pyr C6''), 152.0 (pyr C2''), 153.4 (benz 6C), 161.8 (benz C2), 163.3 (pyr C4''), NMR data in accordance with that reported in the literature for the (*S*)-enantiomer of this compound;^{125, 628} **m/z (ESI)** (Found MH⁺, 368.1044 C₁₇H₁₈N₃NaO₃S requires *MH* 368.1039).

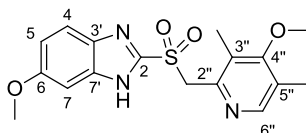
(±)-6(5)-Methoxy-2-[[4-methoxy-3,5-dimethyl-2-pyridinyl)methyl]sulfinyl]-1H-benzimidazole potassium ((±)-K Omeprazole) (±)-3.38⁶²³



Omeprazole (±)-**1.1** (1.18 g, 3.40 mmol) and MeCN (20 mL) were added to a solution of KOH (0.190 g, 3.40 mmol) in H₂O (0.19 mL) and the solution stirred at rt. After 1h the solution was concentrated to approximately half volume *in vacuo* and precipitation of the salt induced by dropwise addition of Et₂O. The precipitate was collected by filtration and recrystallised from MeOH–Et₂O give the title compound (±)-**3.38** (0.720 g, 1.90 mmol, 56%) as a colourless powder; **m.p.** decomp > 130 °C (MeOH–Et₂O); **¹H NMR** (DMSO-d₆, 300 MHz): δ 2.20 (3H, s, pyr 3''-Me), 2.21 (3H, s, pyr 5''-Me), 3.69 (3H, s, pyr OMe), 3.72 (3H, s, benz OMe), 4.38 and 4.75 (2H, 2 × d, *J* 12.8, CH₂), 6.54 (1H, dd, *J* 8.6 and 2.5, benz 5-H), 6.98 (1H, d, *J* 2.5, benz 7-H), 7.32 (1H, *J* 8.6, benz 4-H), 8.23 (1H, pyr 6''-H); **¹³C NMR** (DMSO-d₆, 75 MHz): δ 11.3

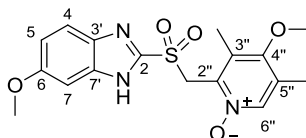
(3''-Me), 12.9 (5''-Me), 55.2 (benz OMe), 59.7 (pyr OMe), 59.9 (CH₂), 99.5 (benz 7C), 108.7 (benz 5C), 117.4 (benz 4C), 124.8 (pyr C5''), 126.4 (pyr C3''), 141.7 (benz C3' or C7'), 147.1 (benz C3' or C7'), 149.0 (pyr C6''), 152.0 (pyr C2''), 153.4 (benz 6C), 161.8 (benz C2), 163.3 (pyr C4''), NMR data in accordance with that reported in the literature for the (*S*)-enantiomer of this compound;⁶²³ **m/z (ESI)** (Found MH⁺, 368.1044 C₁₇H₁₈N₃NaO₃S requires *MH* 368.1039).

6(5)-Methoxy-2-[[[(4-methoxy-3,5-dimethyl-2-pyridinyl)methyl]sulfonyl]-1*H*-benzimidazole (Omeprazole sulfone) 4.1



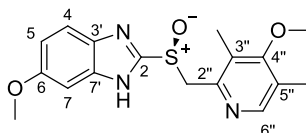
Saturated aqueous NaHCO₃ (50 mL) was added to a solution of Pyrimetazole **3.17** (3.29 g, 10.0 mmol) in CH₂Cl₂ (50 mL) and the mixture cooled to 0 °C. A solution of *m*CPBA (75% *m*CPBA, 5.60 g, 25.0 mmol) in CH₂Cl₂ (45 mL) and MeOH (5 mL) was added dropwise and the reaction stirred vigorously for 3h. The reaction was quenched by addition of saturated aqueous Na₂S₂O₃ (50 mL). The phases were separated and the aqueous layer extracted with CH₂Cl₂ (3 × 25 mL), the combined organic extracts were washed with brine (20 mL), dried (MgSO₄), filtered and the solvent removed *in vacuo*. EtOAc (30 mL) was added to the crude materials and the insoluble *N*-oxide byproduct removed by filtration. The filtrate was concentrated *in vacuo* and subjected to column chromatography (eluting with EtOAc) to afford the title compound (2.13 g, 5.90 mmol, 59%) as a colourless viscous gum which dried as a solid foam under vacuum. **m.p.** 98.6-100.7 °C (from CH₂Cl₂); **R_f** 0.55 (5% MeOH–EtOAc); **¹H NMR** (DMSO-*d*₆, 500 MHz): δ 2.16 (3H, s, pyr 5''-Me), 2.20 (3H, s, pyr 3''-Me), 3.67 (3H, s, pyr OMe), 3.82 (3H, s, benz OMe), 5.02 (2H, s, CH₂), 7.01 (1H, dd, *J* 8.9 and 1.6, benz 5-H), 7.05 (1H, br s, benz 7-H), 7.61 (1H, br s, benz 4-H), 8.04 (1H, pyr 6''-H), 13.59 (1H, br s, NH exchangeable); **¹³C NMR** (DMSO-*d*₆, 125 MHz): δ 11.3 (pyr 3''-Me), 12.9 (pyr 5''-Me), 55.5 (benz OMe), 59.7 (pyr OMe), 60.6 (CH₂), 94.6, 115.0 (br, benz C5), 121.4 (br C3' or C7'), 126.2 (pyr C3''), 127.7 (pyr C5''), 135.7 (br C3' or C7'), 146.7 (pyr C2''), 149.3 (pyr C6''), 157.6 (benz C6), 163.7 (pyr C4''); **¹H NMR** (CDCl₃ 500 MHz): δ 2.16 (3H, s, pyr 5''-Me), 2.29 (3H, s, pyr 3''-Me), 3.66(3H, s, pyr OMe), 3.79 (3H, s, benz OMe), 5.00 (2H, s, CH₂), 6.88 (1H, br s, benz 7-H), 6.93 (1H, dd, *J* 9.0 and 2.3, benz 5-H), 7.56 (1H, br s, benz 4-H), 8.06 (1H, pyr 6''-H), 12.16 (1H, br s, NH exchangeable); **¹³C NMR** (CDCl₃, 125 MHz): δ 11.9 (pyr 3''-Me), 13.4 (pyr 5''-Me), 55.7 (benz OMe), 60.0(pyr OMe), 60.8 (CH₂), 94.2, 101.9, 115.2, 122.1, 127.3 (pyr C5''), 128.9 (pyr C3''), 134.9, 137.6, 146.1(pyr C2''), 149.4 (pyr C6''), 158.9 (benz C6), 165.0 (pyr C4''); **m/z (ESI)** (Found MH⁺, 362.1175 C₁₇H₁₉N₃O₄S requires *MH* 362.1169)

6(5)-Methoxy-2-[[[(4-methoxy-3,5-dimethyl-2-pyridinyl)methyl]sulfonyl]-1H-benzimidazole N-Oxide 4.2⁶³⁵



The title compound 4.2 was isolated during the purification procedure in the synthesis of Omeprazole sulfone **4.1**; **m.p.** 205.4-205.9 °C (from EtOAc) (Lit. m.p. 206 - 207 °C);⁶³⁵ **¹H NMR** (DMSO-*d*₆, 500 MHz): δ 2.16 (3H, s, pyr 5''-Me), 2.20 (3H, s, pyr 3''-Me), 3.70 (3H, s, pyr OMe), 3.82 (3H, s, benz OMe), 5.33 (2H, s, CH₂), 7.00 (1H, d, *J* 9.0, benz 5-H), 7.06 (1H, br s, benz 7-H), 7.59 (1H, br s, benz 4-H), 8.06 (1H, pyr 6''-H), 13.69 (1H, br s, NH exchangeable), NMR data in accordance with the literature data;⁶³⁵ **m/z (ESI)** (Found MH⁺, 378.1129 C₁₇H₂₀N₃O₅S requires *MH* 378.1112)

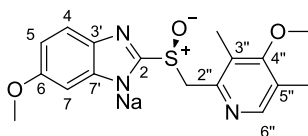
(S)-6(5)-Methoxy-2-[[[(4-methoxy-3,5-dimethyl-2-pyridinyl)methyl]sulfinyl]-1H-benzimidazole ((S)-Esomeprazole) (S)-1.1⁶²⁸



Ti(O^{*i*}Pr)₄ (444 μL, 0.43 g, 1.50 mmol), (*S,S*)-DET (513 μL, 0.62 g, 3.00 mmol) and H₂O (9.0 μL, 9.01 mg, 0.50 mmol) were added to a suspension of Pyrimetazole **3.17** (1.65 g, 5.00 mmol) in toluene (7.5 mL) and the mixture heated at 54 °C for 50 min. The solution was cooled to 30 °C and DIPEA (261 μL, 0.19 g, 1.5 mmol) was added, followed by addition of CHP (80% in cumene, 924 μL, 0.76 g, 5.00 mmol). After 1 h the reaction was quenched by addition of aqueous NH₄OH (12.5% NH₃, 10 mL) and the mixture stirred vigorously for 30 min then allowed to sit for 45 min. The reaction mixture was filtered through a pad of Celite and the Celite pad washed with aqueous NH₄OH (12.5% NH₃, 3 × 50 mL) and CH₂Cl₂ (4 × 50 mL). The phases of the filtrate were separated and the organic phase extracted with aqueous NH₄OH (12.5% NH₃, 3 × 25 mL). CH₂Cl₂ (50 mL) was added to the combined aqueous extracts and AcOH added with caution until a pH of ~ 8 was achieved. The phases were separated and the aqueous phase extracted with CH₂Cl₂ (3 × 25 mL). The combined organic extracts were washed with saturated aqueous NaHCO₃ (20 mL), then brine (25 mL), dried (MgSO₄), filtered and the solvent removed *in vacuo*. Column chromatography (eluting with 5% MeOH-EtOAc) gave the title compound (S)-1.1 (0.52 g, 1.50 mmol, 30%, 96% ee) as a colourless oil which dried as a glassy foam under vacuum; **m.p.** decomp > 125 °C (MeOH-Et₂O); **R_f** 0.46 (5% MeOH-EtOAc); **¹H NMR** (DMSO-*d*₆, 300 MHz): δ 2.16 (3H, s,

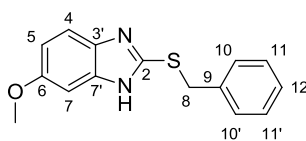
Me 8), 2.19 (3H, s, Me 7), 3.68 (3H, s, pyr OMe), 3.80 (3H, s, benz OMe), 4.67 and 4.76 (2H, AB-system, J 13.5, CH₂), 6.92 (1H, dd, J 8.9 and 2.4, benz 5-H), 7.09 (1H, br s, benz 7-H), 7.54 (1H, d, J 8.9, benz 4-H), 8.18 (1H, pyr 6''-H), 13.41 (1H, br s, NH, exchangeable); ¹³C NMR (DMSO-d₆, 75 MHz): δ 11.1 (pyr 3''-Me), 12.9 (pyr 5''-Me), 55.5 (benz OMe), 59.7 (pyr OMe), 60.1 (CH₂), 125.5 (pyr C3''), 126.5 (pyr C5''), 149.1 (pyr C6''), 149.6 (pyr C2''), 153.0 (benz C2), 156.6 (benz C6), 163.5 (pyr C4'') not all carbon signals observed due to annular tautomerism of the benzimidazole system, NMR data in accordance with the literature;⁶²⁸ ¹H NMR (CDCl₃, 300 MHz): δ 2.17 (3H, s, pyr 3''-Me), 2.19 (3H, s, pyr 5''-Me), 3.64 (3H, s, pyr OMe), 3.75 (3H, s, benz OMe), 4.79 (2H, s, CH₂), 6.90 (1H, br s, benz 7-H), 6.97 (1H, dd, J 8.9 and 2.1, benz 5-H), 7.49 (1H, br s, benz 4-H), 8.15 (1H, pyr 6''-H); **m/z (ESI)** (Found MH⁺, 346.1234 C₁₇H₁₉N₃O₃S requires MH 346.1220; **HPLC**: t_R (S_{major}) = 32.5 min, t_R (R_{minor}) = 41.9 min [Chiracel OD-H; flow rate 1.0 mL min⁻¹; 5% EtOH –hexane; 20 °C]

(S)-6(5)-Methoxy-2-[[4-methoxy-3,5-dimethyl-2-pyridinyl)methyl]sulfinyl]-1H-benzimidazole sodium ((S)-Na Esomeprazole) (S)-3.36^{125, 628}



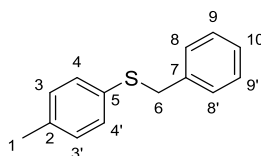
esomeprazole (S)-1.1 (0.31 g, 0.90 mmol) and MeCN (5 mL) were added to a solution of NaOH (36.0 mg, 0.90 mmol) in H₂O (40 μL) and the solution stirred at rt for 1h. The resulting precipitate was collected by filtration and washed with Et₂O to give the title compound (S)-3.36 (0.22 g, 0.60 mmol, 65%, > 99.5% ee) as a colourless powder; **m.p.** > 160 °C (decomp) (from MeCN–Et₂O); ¹H NMR (DMSO-d₆, 300 MHz): δ 2.20 (3H, s, pyr 3''-Me), 2.21 (3H, s, pyr 5''-Me), 3.69 (3H, s, pyr OMe), 3.72 (3H, s, benz OMe), 4.38 and 4.66 (2H, AB-system, J 12.9, CH₂), 6.54 (1H, dd, J 8.6 and 2.5, benz 5-H), 6.98 (1H, d, J 2.5, benz 7-H), 7.32 (1H, J 8.6, benz 4-H), 8.23 (1H, pyr 6''-H); ¹³C NMR (DMSO-d₆, 75 MHz): δ 11.3 (3''-Me), 12.9 (5''-Me), 55.2 (benz OMe), 59.7 (pyr OMe), 59.9 (CH₂), 99.5 (benz 7C), 108.7 (benz 5C), 117.4 (benz 4C), 124.8 (pyr C5''), 126.4 (pyr C3''), 141.7 (benz C3'or C7'), 147.1 (benz C3'or C7'), 149.0 (pyr C6''), 152.0 (pyr C2''), 153.4 (benz 6C), 161.8 (benz C2), 163.3 (pyr C4''), NMR data in accordance with the literature;^{125, 628} **m/z (ESI)** (Found MH⁺, 368.1045 C₁₇H₁₈N₃NaO₃S requires MH 368.1039); **HPLC**: t_R (S_{major}) = 38.2 min [Chiracel OD-H; flow rate 1.0 mL min⁻¹; 5% EtOH –hexane; 20 °C]

6(5)-Methoxy-2-[(phenylmethyl)thio]-1H-benzimidazole 4.4



A solution of NaOH (4.00 g, 100 mmol) in H₂O (20 mL) was added to a solution of 6(5)-methoxy-1H-benzimidazole-2-thiol **3.18** (18.0 g, 100 mmol) in EtOH (100 mL). Benzyl bromide (11.9 mL, 17.1 g, 100 mmol) was added and the reaction heated at reflux for 2h. The mixture was allowed to cool to rt followed by the addition of H₂O (50 mL) and CH₂Cl₂ (100 mL). The phases were separated and the aqueous phase extracted with CH₂Cl₂ (3 × 100 mL). The combined organic materials were washed with brine (50 mL), dried (MgSO₄), filtered and the solvent removed *in vacuo*. Recrystallization from EtOAc–hexane gave the title compound **4.4** (25.3 g, 88.0 mmol, 88%) as a colourless powder; **m.p.** 114.2-115.3 °C (from EtOAc–hexane); **R_f** 0.36 (50% EtOAc–hexane); **¹H NMR** (DMSO-d₆, 300 MHz): δ 3.77 (3H, s, OMe), 4.58 (2H, s, CH₂), 6.80 (1H, dd, *J* 8.7 and 2.4, benz 5-H), 7.02 (1H, d, *J* 2.4, benz 7-H), 7.21-7.32 (3H, m, phenyl 12-H and 11/11'-H), 7.39 (1H, d, *J* 8.7, benz 4-H), 7.41-7.46 (2H, m, phenyl 10/10'-H), 12.47 (1H, br s, NH, exchangeable); **¹³C NMR** (DMSO-d₆, 125 MHz): δ 35.6 (CH₂), 55.5 (OMe), 96.9 (benz C7), 111.0 (benz C5), 114.7 (benz C4), 127.3 (phenyl C12), 128.5 (phenyl C10/10'), 128.8 (phenyl C11/11'), 133.8 (C3' or C7'), 137.6 (phenyl C9), 139.1 (C3' or C7'), 148.5 (benz C2), 155.6 (benz C6); **v_{max}/cm⁻¹ (solid)** 3059, 2951, 2628, 1633, 1451, 1433, 1401, 1159, 1030, 987; **m/z (ESI)** (Found MH⁺, 271.0905 C₁₅H₁₄N₂OS requires *MH* 271.0900); **Anal. Calcd.** for C₁₅H₁₄N₂OS (%): C, 66.6; H, 5.20; N, 10.4; **Found:** C, 66.5; H, 5.20; N, 10.4;

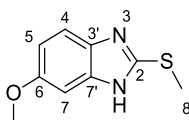
1-Methyl-4-[(phenylmethyl)thio]-benzene 4.5^{722, 723}



A solution of NaOH (4.00 g, 100 mmol) in H₂O (20 mL) was added to a solution of 4-methylbenzene-1-thiol **4.6** (12.4 g, 100 mmol) in EtOH (100 mL). Benzyl bromide (11.9 mL, 17.1 g, 100 mmol) was added and the reaction heated at reflux for 2h. The mixture was allowed to cool to rt followed by the addition of H₂O (25 mL) and CH₂Cl₂ (20 mL). The phases were separated and the aqueous phase extracted with CH₂Cl₂ (3 × 20 mL). The combined organic materials were washed with brine (50 mL), dried (MgSO₄), filtered and the solvent removed *in vacuo*. Column chromatography (eluting with hexane) followed by recrystallization from aqueous EtOH gave the title compound **4.5** (19.3 g, 90.0 mmol, 90%) as a colourless crystalline

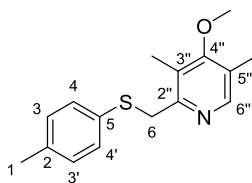
solid; **m.p.** 39.7-41.5 °C (aq EtOH) (lit. 45-46 °C from Pet. Ether 60-80);⁷²³ **R_f** 0.90 (50% EtOAc–hexane); **¹H NMR** (DMSO-d₆, 500 MHz): δ 2.24 (3H, s, tol Me), 4.17 (2H, s, CH₂), 7.09 (2H, d, *J* 8.2, H-3/3'), 7.23 (2H, d, *J* 8.2, H-4/4'), 7.20-7.25 (1H, m, phenyl H-10), 7.26-7.30 (2H, m, phenyl H-9/9'), 7.30-7.34 (2H, m, phenyl H-8/8'); **¹³C NMR** (DMSO-d₆, 125 MHz): δ 20.5 (tol Me), 37.4 (CH₂), 126.9 (phenyl C10), 128.2 (phenyl C9/9'), 128.7 (phenyl C8/8'), 129.1 (tol C4/4'), 129.5 (tol C3/3'), 132.3 (tol C5), 135.5 (tol C2), 137.7 (phenyl C7); **¹H NMR** (CDCl₃, 300 MHz): δ 2.21 (3H, s, tol Me), 3.98 (2H, s, CH₂), 6.97 (2H, d, *J* 9.0, tolyl), 7.11-7.23 (7H, m, phenyl and tolyl); **¹³C NMR** (CDCl₃, 75 MHz): 21.2 (tol Me), 39.9 (CH₂), 128.2, 128.5, 129.0, 129.7, 130.8, 132.6, 136.7, 137.9, NMR data in accordance with the literature.⁷²²

6(5)-Methoxy-2-methylthio-1*H*-benzimidazole **4.7**^{562, 724}



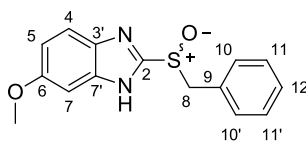
A solution of NaOH (2.00g, 50.0 mmol) in H₂O (50 mL) was added to a suspension of 6(5)-methoxy-1*H*-benzimidazole-2-thiol **3.18** (9.00 g, 50.0 mmol) in MeOH (50 mL). The solution was cooled to 0 °C and MeI (3.11 mL, 7.10 g, 50.0 mmol) was added dropwise. The reaction mixture was stirred at room temperature for 2 h and then concentrated to approximately half volume *in vacuo*. Saturated aqueous NaHCO₃ (30 mL) was added and the suspensions stirred at 0 °C for 2 h. The crude sulfide was collected by filtration, washed with H₂O (2 × 50mL) and dried *in vacuo*. Recrystallization from CHCl₃–hexane gave the title compound **4.7** (6.70 g, 35.0 mmol, 70%) as colourless needles; **m.p.** 141.8-143.1 °C (from CHCl₃–hexane) (lit. 125-128 °C from aq EtOH); **R_f** 0.54 (EtOAc); **¹H NMR** (DMSO-d₆, 300 MHz): δ 2.67 (3H, s, SMe), 3.76 (3H, s, benz OMe), 6.74 (1H, dd, *J* 8.7 and 2.4, benz 5-H), 6.96 (1H, d, *J* 2.4 benz 7-H), 7.33 (1H, d, *J* 8.7, benz 4-H), 12.38 (1H, br s, benz-NH, exchangeable); **¹³C NMR** (DMSO-d₆, 75 MHz): δ 13.9 (SMe), 55.4 (benz OMe), 97.1 (benz C7), 110.0 (benz C5), 114.4 (benz C4), 134.8 (benz C3' or C7'), 140.0 (benz C3' or C7'), 150.4 (benz C2), 155.1 (benz C6), NMR data in accordance with the literature;⁷²⁴ **v_{max}/cm⁻¹(solid)** 3046, 2997, 2951, 2929, 2878, 2827, 1633, 1594, 1388, 1265, 1153, 1030; **m/z (ESI)** (Found MH⁺, 195.0588 C₉H₁₀N₂OS requires *MH* 195.0587); **Anal. Calcd.** for C₉H₁₀N₂OS (%): C, 55.7; H, 5.20; N, 14.4; **Found:** C, 55.6; H, 5.25; N, 14.7.

4-Methoxy-3,5-dimethyl-2-[(4-methylphenyl)sulfanyl]methylpyridine **4.8**



A solution of NaOH (4.00 g, 100 mmol) in H₂O (20 mL) was added to a suspension of 2-(chloromethyl)-3,5-dimethyl-4-methoxypyridine hydrochloride **3.19** (22.2 g, 100 mmol) and *p*-tolyl thiol **4.6** (12.4 g, 100 mmol) in EtOH (100 mL) and the mixture heated at reflux for 15 min. A solution of NaOH (4.00 g, 100 mmol) in H₂O (20 mL) was added and heating continued for 3h. The mixture was allowed to cool to rt followed by the addition of H₂O (20 mL) and CH₂Cl₂ (500 mL). The phases were separated and the aqueous phase extracted with CH₂Cl₂ (3 × 200 mL), the organic materials were combined, dried (MgSO₄), filtered and the solvent removed *in vacuo*. Column chromatography (eluting with 0-15% EtOAc–hexane) followed by recrystallization from hexane gave the title compound **4.8** (22.2 g, 81.1 mmol, 81%) as a colourless crystalline solid; **m.p.** 48.5-49.7 °C (hexane); **R_f** 0.60 (EtOAc); **¹H NMR** (DMSO-d₆, 500 MHz): δ 2.16 (3H, s, 5''-Me), 2.20 (3H, s, 3''-Me), 2.25 (3H, s, tol Me), 3.69 (3H, s, pyr OMe), 4.24 (2H, s, CH₂), 7.10 (2H, d, *J* 8.1, tol 3/3'-H) 7.28 (2H, d, *J* 8.1, tol 4/4'-H) 8.12 (1H, s, pyr 6''-H); **¹³C NMR** (DMSO-d₆, 125 MHz): δ 10.9 (pyr 3''-Me), 12.8 (pyr 5''-Me), 20.5 (tol Me), 38.5 (CH₂), 59.6 (pyr OMe), 124.6 (pyr C3''), 124.8 (pyr C5''), 129.3 (tol C4/4'), 129.5 (tol C3/3'), 132.6 (tol C5), 135.5 (tol C2), 148.5 (pyr C6''), 155.1 (pyr C2''), 163.4 (Pyr C4''); **m/z** (**ESI**) (Found MH⁺, 296.1083 C₁₆H₁₉NOS requires *MH* 296.1080); Found: C, 70.1; H, 7.00; N, 5.1; S, 11.7; C₁₆H₁₉NOS requires C, 70.3; H, 7.00; N, 5.1; S, 11.5%

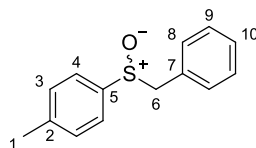
(±)-6(5)-Methoxy-2-[(phenylmethyl)sulfinyl]-1*H*-benzimidazole **4.9**



Saturated aqueous NaHCO₃ (50 mL) was added to a solution of sulfide **4.4** (6.76 g, 25.0 mmol) in CH₂Cl₂ (50 mL) and the mixture cooled to 0 °C. A solution of *m*CPBA (75% *m*CPBA, 5.60 g, 25.0 mmol) in CH₂Cl₂ (45 mL) and MeOH (5 mL) was added dropwise and the reaction stirred vigorously for 3.5h. The reaction was quenched by addition of saturated aqueous Na₂S₂O₃ (50 mL), the phases were separated and the aqueous layer extracted with CH₂Cl₂ (3 × 50 mL). The combined organic extracts were washed with brine (25 mL), dried (MgSO₄), filtered and the solvent removed *in vacuo*. Column chromatography (eluting with 1:1 EtOAc–CH₂Cl₂) followed by recrystallization from EtOAc–hexane gave the title compound (±)-**4.9** (5.57 g, 19.5 mmol, 78%) as colourless needles; **m.p.** 136.3-137.5 °C (from

EtOAc–hexane); R_f 0.42 (EtOAc); $^1\text{H NMR}$ (DMSO- d_6 , 300 MHz): δ 3.80 (3H, s, benz OMe), 4.48 and 4.67 (2H, AB-system, J 12.8, CH_2), 6.92 (1H, dd, J 8.9 and 2.4, benz 5-H), 7.07 (1H, br s, benz 7-H), 7.11-7.22 (2H, m, phenyl-H), 7.23-7.35 (3H, m, phenyl-H), 7.54 (1H, s, J 8.9, benz 4-H), 13.26 (1H, br s, NH exchangeable); $^{13}\text{C NMR}$ (DMSO- d_6 , 75 MHz) mixture of two tautomers: δ 55.5 (OMe), 59.5 (CH_2), 94.6 (br, benz C7), 101.5 br, 112.9 (br, benz C5), 114.3 br, 120.4 (br, benz C4), 128.2, 128.4 (phenyl), 129.9, 130.4 (phenyl), 136.4 br, 137.6 br, 144.1 br, 151.9 br, 153.3 br, 156.0 br, 156.9 br, extra carbon signals observed due to annular tautomerism of the benzimidazole system; $^1\text{H NMR}$ (CDCl_3 , 500 MHz) mixture of tautomers A:B in a ratio of 37:63: δ 3.82 and 3.89 (3H, s, OMe, tautomers B and A respectively), 4.30 and 4.52 (2H, AB-system, J 13.2, CH_2), 6.77-7.75 (8H, m, phenyl and benz H), 11.43 and 11.5 (1H, br s, NH, exchangeable, tautomers A and B respectively); $\nu_{\text{max}}/\text{cm}^{-1}$ (solid) 2996, 2919, 1629, 1405, 1206, 1153, 1050, 1025; m/z (ESI) (Found MH^+ , 287.0853 $\text{C}_{15}\text{H}_{14}\text{N}_2\text{O}_2\text{S}$ requires MH 287.0849); **Anal. Calcd.** for $\text{C}_{15}\text{H}_{14}\text{N}_2\text{O}_2\text{S}$ (%): C, 63.0; H, 4.95; N, 9.8; **Found:** C, 62.8; H, 4.90; N, 9.6.

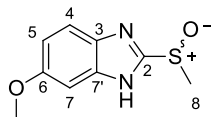
(±)-1-Methyl-4-[(phenylmethyl)sulfinyl]-benzene 4.10⁷²⁵



Saturated aqueous NaHCO_3 (60 mL) was added to a solution of sulfide **4.5** (6.83 g, 25.0 mmol) in CH_2Cl_2 (100 mL) and the mixture cooled to 0 °C. A solution of *m*CPBA (70% *m*CPBA, 6.16 g, 25 mmol) in CH_2Cl_2 (100 mL) and MeOH (10 mL) was added dropwise and the reaction stirred vigorously for 1h. The reaction was quenched by addition of saturated aqueous $\text{Na}_2\text{S}_2\text{O}_3$ (50 mL), the phases were separated and the aqueous layer extracted with CH_2Cl_2 (3 × 50 mL). The combined organic extracts were washed with brine (25 mL), dried (MgSO_4), filtered and the solvent removed *in vacuo*. Column chromatography (eluting with 50-100% EtOAc-hexane) followed by recrystallization from CHCl_3 –hexane gave the title compound (±)-**4.10** (5.21 g, 22.6 mmol, 91%) as a colourless needles. **m.p.** 134.2-135.7 °C (CHCl_3 –hexane) (lit 139-140 °C);⁷²⁵ R_f 0.36 (50% EtOAc–hexane); $^1\text{H NMR}$ (DMSO- d_6 , 500 MHz): δ 2.36 (3H, s, tol Me), 4.04 and 4.20 (2H, AB-system, J 12.7, CH_2), 7.07-7.13 (2H, m, phenyl 8/8'-H), 7.24-7.30 (3H, m, phenyl 9/9'-H and 10-H), 7.32 (2H, d, J 8.4, tol 3/3'-H), 7.41 (2H, d, J 8.4, tol 4/4'-H); $^{13}\text{C NMR}$ (DMSO- d_6 , 125 MHz): δ 20.9 (tol Me), 61.8 (CH_2), 124.3 (C4/4'), 127.7 (phenyl C10), 128.1 (phenyl C9/9'), 129.4 (tol C3/3'), 130.3 (phenyl C8/8'), 130.5 (phenyl C7), 140.3 (tol C5), 140.7 (tol C2); $^1\text{H NMR}$ (CDCl_3 , 300 MHz): δ 2.40 (3H, s, tol Me), 4.03 (2H, AB-system J 12.5, CH_2), 7.00 (2H, dd, J 7.4 and 1.8, tolyl), 7.19-7.37 (7H, m, tolyl and phenyl),

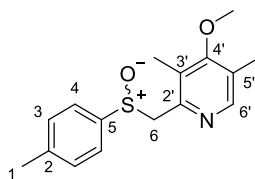
NMR data in accordance with the literature data;⁷²⁵ **m/z (ESI)** (Found MH^+ 231.0842, $C_{14}H_{14}OS$ requires MH 231.0838).

(±)-6(5)-Methoxy-2-(methylsulfinyl)-1H-Benzimidazole 4.11⁵⁶²



Saturated aqueous $NaHCO_3$ (60 mL) was added to a solution of sulfide **4.7** (7.77 g, 40.0 mmol) in CH_2Cl_2 (60 mL) and the mixture cooled to 0 °C. A solution of *m*CPBA (75% *m*CPBA, 9.20 g, 40 mmol) in CH_2Cl_2 (96 mL) and MeOH (4 mL) was added dropwise and the reaction stirred vigorously for 3h. The reaction was quenched by addition of saturated aqueous $Na_2S_2O_3$ (50 mL), the phases were separated and the aqueous layer extracted with CH_2Cl_2 (3×50 mL). The combined organic extracts were washed with brine (25 mL), dried ($MgSO_4$), filtered and the solvent remove *in vacuo*. Column chromatography (eluting with 1:1 EtOAc–hexane) followed by recrystallization from EtOAc–hexane gave the title compound (±)-**4.11** (5.85 g, 27.8 mmol, 70%) as a colourless powder; **m.p.** 97.6-98.9 °C (from EtOAc–hexane); **R_f** 0.14 (50% EtOAc–hexane); **¹H NMR** ($DMSO-d_6$, 300 MHz): δ 3.08 (3H, s, SMe), 3.80 (3H, s, benz OMe), 6.93 (1H, dd, *J* 8.9 and 2.4, benz 5-H), 7.11 (1H, br s, benz 7-H), 7.56 (1H, br d, *J* 8.9, benz 4-H), (13.42 (1H, br s, NH exchangeable); **¹³C NMR** ($DMSO-d_6$, 75 MHz): δ 40.3 (SMe), 55.5 (benz OMe), 95.3 (br, benz C7) 113.5 (benz C5), 120.0 (br, benz C4) 136.3 br, 154.2, 156.7, not all carbon signals observed due to annular tautomerism of the benzimidazole system; **¹H NMR** ($CDCl_3$, 300 MHz) mixture of tautomers A:B in a ratio of 38:62: δ 3.17 (3H, s, SMe), 3.86 (3H, s, benz OMe), 6.98 (m, benz 5-H and benz 7-H tautomer B), 7.11 (br s, benz 7-H, tautomer A), 7.46 and 7.65 (1H, $2 \times d$, *J* 8.8, benz 4-H, tautomers B and A respectively), 12.01 (1H, br s, NH exchangeable), NMR data in accordance with the literature;⁵⁶² **ν_{max}/cm^{-1} (solid)** 2966, 2884, 2769, 2591, 1621, 14.3, 1302, 1202, 1153, 1011; **m/z (ESI)** (Found MH^+ , 211.0535 $C_9H_{10}N_2O_2S$ requires MH 211.0535); **Anal. Calcd.** for $C_9H_{10}N_2O_2S$ (%): C, 51.4; H, 4.80; N, 13.3; **Found:** C, 54.4; H, 4.80; N, 13.3.

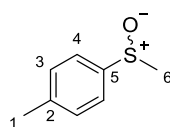
(±)-4-Methoxy-3,5-dimethyl-2-[(4-methylphenyl)sulfinyl]methyl}pyridine 4.12



Saturated aqueous $NaHCO_3$ (60 mL) was added to a solution of sulfide **4.8** (6.83 g, 25.0 mmol) in CH_2Cl_2 (100 mL) and the mixture cooled to 0 °C. A solution of *m*CPBA (70% *m*CPBA, 6.16

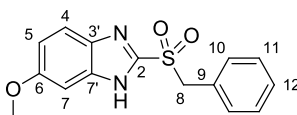
g, 25 mmol) in CH₂Cl₂ (100 mL) and MeOH (10 mL) was added dropwise and the reaction stirred vigorously for 1h. The reaction was quenched by addition of saturated aqueous Na₂S₂O₃ (50 mL), the phases were separated and the aqueous layer extracted with CH₂Cl₂ (3 × 50 mL). The combined organic extracts were washed with brine (25 mL), dried (MgSO₄), filtered and the solvent remove *in vacuo*. Column chromatography (eluting with EtOAc) followed by recrystallization from CH₂Cl₂–hexane gave the title compound (±)-**4.12** (6.93 g, 24.0 mmol, 96%) as a colourless needles; **m.p.** 90.3-91.9 °C (CH₂Cl₂–hexane); **R_f** 0.14 (EtOAc); **¹H NMR** (DMSO-d₆, 500 MHz): δ 2.02 (3H, s, 3''-Me), 2.19 (3H, s, 5''-Me), 2.36 (3H, s, tol Me), 3.66 (3H, s, pyr OMe), 4.17 and 4.36 (2H, AB-system, *J* 12.8, CH₂), 7.33 (2H, d, *J* 8.2, tol 3/3'-H), 7.44 (2H, d, *J* 8.3, tol 4/4'-H), 8.20 (1H, s, pyr 6''-H); **¹³C NMR** (DMSO-d₆, 125 MHz): δ 11.1 (pyr 3''-Me), 12.9 (pyr 5''-Me), 20.9 (tol Me), 59.6 (pyr OMe), 62.8 (CH₂), 124.1 (tol C4/4'), 125.2 (pyr C5''), 126.5 (pyr C3''), 129.6 (tol C3/3'), 141.0 (tol C2), 141.1 (tol C5), 149.0 (pyr C6''), 150.1 (Pyr C2''), 163.4 (Pyr C4''); **m/z (ESI)** (Found MH⁺, 290.1219 C₁₆H₁₉NO₂S requires *MH* 296.1209); **Anal. Calcd.** for C₁₆H₁₉NO₂S (%): C, 66.4; H, 6.60; N, 4.8; **Found:** C, 66.2; H, 6.90; N, 4.7.

(±)-**1-Methyl-4-(methylsulfinyl)-benzene 1.48**⁷²⁰



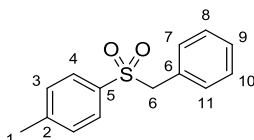
Saturated aqueous NaHCO₃ (60 mL) was added to a solution of *p*-tolyl sulfide (6.72 mL, 6.92 g, 50.0 mmol) was dissolved in CH₂Cl₂ (75 mL) and the mixture cooled to 0 °C. A solution of *m*CPBA (70% *m*CPBA, 12.3 g, 50.0 mmol) in CH₂Cl₂ (75 mL) and MeOH (5 mL) was added dropwise and the reaction stirred vigorously for 2.5h. The reaction was quenched by addition of saturated aqueous Na₂S₂O₃ (50 mL), the phases were separated and the aqueous layer extracted with CH₂Cl₂ (3 × 25 mL). The combined organic extracts were washed with brine (15 mL), dried (MgSO₄), filtered and the solvent remove *in vacuo*. Column chromatography (eluting with 30-100% EtOAc–hexane) gave a colourless oil which was triturated with cold hexane to afford the title compound (±)-**1.48** (7.05 g, 46.0 mmol, 91%) as a colourless waxy solid; **m.p.** 39.0-40.2 °C (hexane) (lit. 39.0-40.0)⁷²⁰; **R_f** 0.08 (50% EtOAc–hexane); **¹H NMR** (DMSO-d₆, 500 MHz): δ 2.36 (3H, s, tol Me), 2.69 (3H, s, Me), 7.37 (2H, d, *J* 8.1, tol 3/3'-H), 7.57 (2H, d, *J* 8.3, tol 4/4'-H); **¹³C NMR** (DMSO-d₆, 75 MHz): δ 20.8 (tol Me), 43.3 (SMe), 123.5 (tol C4/4'), 129.7 (tol C3/3'), 140.5 (tol C2), 143.2 (tol C5); **¹H NMR** (CDCl₃ 300 MHz): δ 2.41 (3H, s, tol Me), 2.70 (3H, s, Me), 7.33 (2H, d, *J* 8.1, tol 3/3'-H), 7.54 (2H, d, *J* 8.3, tol 4/4'-H), NMR data in accordance with the literature;⁷²⁰ **m/z (ESI)** (Found MH⁺, 155.0524 C₈H₁₀OS requires *MH* 155.0525).

6(5)-Methoxy-2-[(phenylmethyl)sulfonyl]-1H-benzimidazole 4.13



Saturated aqueous NaHCO_3 (50 mL) was added to a solution of sulfide **4.4** (1.08 g, 4.0 mmol) in CH_2Cl_2 (50 mL) and the mixture cooled to 0 °C. A solution of *m*CPBA (75% *m*CPBA, 2.24 g, 10.0 mmol) in CH_2Cl_2 (40 mL) was added dropwise and the reaction stirred vigorously for 3h. The reaction was quenched by addition of saturated aqueous $\text{Na}_2\text{S}_2\text{O}_3$ (50 mL), the phases separated and the aqueous layer extracted with CH_2Cl_2 (3 × 50 mL). The combined organic extracts were washed with brine (25 mL), dried (MgSO_4), filtered and the solvent removed *in vacuo*. Purification by column chromatography (eluting with 50% EtOAc–hexane) gave the title compound **4.13** (0.95 g, 3.20 mmol, 79%) as a colourless powder; **m.p.** 219.7-220.2 °C (from EtOAc–hexane); **R_f** 0.40 (50% EtOAc–hexane); **¹H NMR** (DMSO-d_6 , 500 MHz): δ 3.81 (3H, s, OMe), 4.94 (2H, s, CH_2), 7.02 (1H, dd, *J* 8.9 and 1.9, benz 5-H), 7.06 (1H, br s, benz 7-H), 7.18-7.37 (5H, m, phenyl), 7.39 (1H, d, *J* 8.7, benz 4-H), 7.41-7.46 (2H, m, phenyl 10/10'-H), 12.47 (1H, br s, NH, exchangeable); **¹³C NMR** (DMSO-d_6 , 75 MHz): δ 55.5 (OMe), 60.0 (CH_2), 94.9 br, 115.2 (br, benz 5-H), 120.9 br, 127.4 br, 128.4 (phenyl), 128.7 (phenyl), 131.0 (phenyl), 135.8 br, 146.6 br, 154.3 br, 157.6 (br benz), not all carbon signals observed due to annular tautomerism of the benzimidazole system; **m/z (ESI)** (Found MH^+ , 303.0804 $\text{C}_{15}\text{H}_{14}\text{N}_2\text{O}_3\text{S}$ requires *MH* 303.0798).

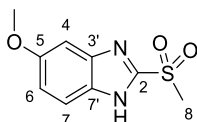
1-Methyl-4-[(phenylmethyl)sulfonyl]-benzene 4.14⁷²⁶



Saturated aqueous NaHCO_3 (50 mL) was added to a solution of sulfide **4.5** (1.07g, 5.0 mmol) in CH_2Cl_2 (20 mL) and the mixture cooled to 0 °C. A solution of *m*CPBA (70% *m*CPBA, 2.71 g, 11.1 mmol) in CH_2Cl_2 (40 mL) was added dropwise and the reaction stirred vigorously for 3h. The reaction was quenched by addition of saturated aqueous $\text{Na}_2\text{S}_2\text{O}_3$ (30 mL), the phases were separated and the aqueous layer extracted with CH_2Cl_2 (3 × 50 mL). The combined organic extracts were washed with brine (25 mL), dried (MgSO_4), filtered and the solvent removed *in vacuo*. Purification by column chromatography (eluting with 40% EtOAc–hexane) followed by recrystallization from CHCl_3 –hexane gave the title compound **4.14** (0.48 g, 2.77 mmol, 40%) as colourless needles; **m.p.** 139.3-140.6 °C (CHCl_3 –hexane) (lit. 144.0 °C from ether);⁷²⁶ **R_f** 0.22 (40% EtOAc–hexane); **¹H NMR** (DMSO-d_6 , 500 MHz): δ 2.38 (3H, s, tol Me), 4.62 (2H, s, CH_2), 7.12-7.18 (2H, m, phenyl 8/8'-H), 7.25-7.33 (3H, m, phenyl 9/9'-H and 10-H), 7.37 (2H,

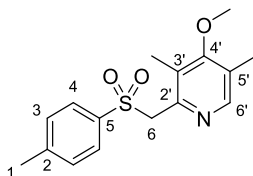
d, J 8.4, tol H-3/3'-H), 7.59 (2H, d, J 8.4, tol H-4/4'-H); ^{13}C NMR (DMSO- d_6 , 125 MHz): δ 21.0 (tol Me), 60.8 (CH_2), 128.0 (tol C4/4'), 128.2 (phenyl C9/9'), 128.2 (phenyl C10), 128.8 (phenyl C7), 129.5 (tol C3/3'), 130.9 (phenyl C8/8'), 135.6 (tol C2), 144.2 (tol C5); ^1H NMR (CDCl_3 300 MHz): δ 2.33 (3H, s, tol Me). 4.21 (2H, s, CH_2), 7.01 (2H, dd J 7.8 and 1.2, tolyl), 7.11-7.28 (5H, m, phenyl), 7.42 (2H, dd J 7.8, tolyl), NMR data in accordance with the literature;⁷²⁶ **m/z (ESI)** (Found MH^+ 247.0787, $\text{C}_{14}\text{H}_{14}\text{O}_2\text{S}$ requires 247.0787);

6(5)-Methoxy-2-(methylsulfonyl)-1H-benzimidazole 4.15



Saturated aqueous NaHCO_3 (20 mL) was added to a solution of sulfide **4.7** (2.91 g, 15.0 mmol) in CH_2Cl_2 (20 mL) and the mixture cooled to 0 °C. A solution of *m*CPBA (70% *m*CPBA, 9.25 g, 37.5 mmol) in CH_2Cl_2 (38 mL) and MeOH (2 mL) was added dropwise and the reaction stirred vigorously for 3h. The reaction was quenched by addition of saturated aqueous $\text{Na}_2\text{S}_2\text{O}_3$ (30 mL), the phases were separated and the aqueous layer extracted with CH_2Cl_2 (3×50 mL). The combined organic extracts were washed with brine (25 mL), dried (MgSO_4), filtered and the solvent remove *in vacuo*. Purification by column chromatography (eluting with 5% MeOH–EtOAc) followed by recrystallization from EtOAc–hexane gave the title compound **4.15** (5.85 g, 27.8 mmol, 70%) as a colourless powder; **m.p.** 131.6-134.2 °C (from EtOAc–hexane); **R_f** 0.22 (5% MeOH–EtOAc) ^1H NMR (DMSO- d_6 , 300 MHz): δ 3.46 (3H, s, Me), 3.82 (3H, s, OMe), 7.01 (1H, dd, J 8.9 and 2.3, benz 5-H), 7.10 (1H, br s, benz 7-H), 7.62 (1H, d, J 8.9, benz 4-H), 13.75 (1H, br s, benz-NH); ^{13}C NMR (DMSO- d_6 , 75 MHz): δ 42.6 (SMe) 55.6 (OMe), 96.6 (br, benz C7), 115.5, (benz C5), 119.2 (br, benz), 137.3 (br, benz), 148.3 (benz), 157.5 (benz), not all carbon signals observed due to annular tautomerism of the benzimidazole system; **m/z (ESI)** (Found MH^+ , 227.0491 $\text{C}_9\text{H}_{10}\text{N}_2\text{O}_3\text{S}$ requires *MH* 227.0485); **Anal. Calcd.** for $\text{C}_9\text{H}_{10}\text{N}_2\text{O}_3\text{S}$ (%): C, 47.8; H, 4.45; N, 12.4; **Found:** C, 47.8; H, 4.50; N, 12.7.

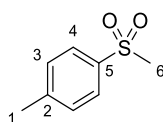
4-Methoxy-3,5-dimethyl-2-([(4-methylphenyl)sulfonyl]methyl)pyridine 4.16



Saturated aqueous NaHCO_3 (50 mL) was added to a solution of sulfide **4.8** (1.37g, 5.00 mmol) in CH_2Cl_2 (20 mL) and the mixture cooled to 0 °C. A solution of *m*CPBA (70% *m*CPBA, 2.71 g, 11.1 mmol) in CH_2Cl_2 (40 mL) was added dropwise and the reaction stirred vigorously for

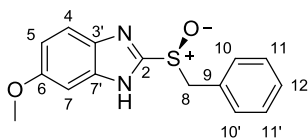
3h. The reaction was quenched by addition of saturated aqueous $\text{Na}_2\text{S}_2\text{O}_3$ (30 mL), the phases were separated and the aqueous layer extracted with CH_2Cl_2 (3×50 mL). The combined organic extracts were washed with brine (25 mL), dried (MgSO_4), filtered and the solvent removed *in vacuo*. Purification by column chromatography (eluting with 80-100% EtOAc–hexane) gave the title compound **4.16** (0.84 g, 2.77 mmol, 55%) as a colourless platelets; **m.p.** 89.7-91.4 °C (CHCl_3 -hexane); **R_f** 0.40 (EtOAc); **¹H NMR** (DMSO- d_6 , 500 MHz): δ 2.12 (3H, s, 3''-Me), 2.17 (3H, s, 5''-Me), 2.38 (3H, s, tol Me), 3.67 (3H, s, pyr OMe), 4.71 (2H, s, CH_2), 7.37 (2H, d, J 8.1, tol 3/3'-H), 7.56 (2H, d, J 8.1, tol 4/4'-H), 8.08 (1H, s, pyr 6''-H); **¹³C NMR** (DMSO- d_6 , 125 MHz): δ 11.3 (pyr 3''-Me), 12.9 (pyr 5''-Me), 21.0 (tol), 59.7 (pyr OMe), 61.5 (CH_2), 125.9 (pyr C5''), 127.5 (pyr C3''), 128.0 (tol C4/4'), 129.6 (tol C3/3'), 136.4 (tol C5), 144.3 (tol C2), 147.6 (Pyr C2''), 149.0 (pyr C6''), 163.6 (pyr C4''); **m/z (ESI)** (Found MH^+ , 306.1170 $\text{C}_{16}\text{H}_{19}\text{NO}_3\text{S}$ requires MH 306.1158).

1-Methyl-4-(methylsulfonyl)-benzene **4.17**⁷²⁰



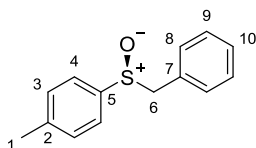
Saturated aqueous NaHCO_3 (50 mL) was added to a solution of *p*-tolyl sulfide (0.67 mL, 0.69 g, 5.00 mmol) dissolved in CH_2Cl_2 and the mixture cooled to 0°C. A solution of *m*CPBA (70% *m*CPBA, 2.71 g, 11.1 mmol) in CH_2Cl_2 (40 mL) was added dropwise and the reaction stirred vigorously for 3h. The reaction was quenched by addition of saturated aqueous $\text{Na}_2\text{S}_2\text{O}_3$ (25 mL), the phases were separated and the aqueous layer extracted with CH_2Cl_2 (3×20 mL). The combined organic extracts were washed with brine (25 mL), dried (MgSO_4), filtered and the solvent removed *in vacuo*. Purification by column chromatography (eluting with 50-100% EtOAc–hexane) followed by recrystallization from aqueous EtOH gave the title compound **4.17** (0.48 g, 2.77 mmol, 40%) as colourless platelets; **m.p.** 82.3-82.9 °C (aq EtOH) (lit. 82.0-85.0);⁷²⁰ **R_f** 0.67 (EtOAc); **¹H NMR** (DMSO- d_6 , 500 MHz): δ 2.40 (3H, s, tol Me), 3.17 (3H, s, Me), 7.44 (2H, d, J 8.4, tol 3/3'-H), 7.81 (2H, d, J 8.4, tol 4/4'-H); **¹³C NMR** (DMSO- d_6 , 125 MHz): δ 20.8 (tol Me), 43.7 (SMe), 126.9 (tol C4/4'), 129.8 (tol C3/3'), 138.1 (tol C2), 144.00 (tol C5); (CDCl_3 300 MHz): δ 2.44 (3H, s, tol Me), 3.02 (3H, s, Me), 7.35 (2H, d, J 8.1, tol 3/3'-H), 7.81(2H, d, J 8.3, tol 4/4'-H); **¹H NMR** (CDCl_3 , 300 MHz): δ 2.38 (3H, s, tol Me), 2.96 (3H, s, SMe), 7.29 (2H, d, J 8.2, tolyl), 7.75 (2H, d, J 8.2, tolyl); **¹³C NMR** (CDCl_3 , 75 MHz): δ 21.6 (tol Me), 44.6 (SMe), 127.4 (tolyl), 130.0 (tolyl), 137.8 (tolyl), 144.8 (tolyl) NMR data in accordance with the Lit. data⁷²⁰

(S)-6(S)-Methoxy-2-[(phenylmethyl)sulfinyl]-1H-benzimidazole (S)-4.9



Ti(OⁱPr)₄ (444 μL, 0.43 g, 1.50 mmol), (*S,S*)-DET (513 μL, 0.62 g, 3.00 mmol) and H₂O (9.0 μL, 9.01 mg, 0.50 mmol) were added to a suspension of sulfide **4.4** (1.35 g, 5.00 mmol) in toluene (7.5 mL) and the mixture heated at 54 °C for 50 min. The reaction mixture was cooled to 30 °C and DIPEA (261 μL, 0.19 g, 1.5 mmol) was added, followed by CHP (80% in cumene, 924 μL, 0.76 g, 5.00 mmol). The reaction mixture was stirred at 30°C and followed by TLC. After 4 h no sulfide starting material was observed by TLC and the reaction was quenched by addition of aqueous NH₄OH (12.5% NH₃, 10 mL). The mixture was stirred vigorously for 30 min then allowed to sit for 45 min. The reaction mixture was filtered through a pad of Celite and the Celite pad washed with aqueous NH₄OH (12.5% NH₃, 3 × 50 mL) and CH₂Cl₂ (4 × 50 mL). The phases of the filtrate were separated and the organic phase extracted with aqueous NH₄OH (12.5% NH₃, 3 × 25 mL). CH₂Cl₂ (50 mL) was added to the combined aqueous extracts and AcOH added with caution until a pH of ~ 8 was achieved. The phases were separated and the aqueous phase extracted with CH₂Cl₂ (3 × 25 mL). The combined organic extracts were washed with saturated aqueous NaHCO₃ (20 mL), then brine (25 mL), dried (MgSO₄), filtered and the solvent removed *in vacuo*. Column chromatography (eluting with 50% EtOAc–CH₂Cl₂) gave the title compound (*S*)-**4.9** (0.29 g, 0.85 mmol, 17%, 95% ee) as a colourless gum; *R*_f 0.42 (EtOAc); ¹H NMR (DMSO-d₆, 300 MHz): δ 3.80 (3H, s, benz OMe), 4.48 and 4.67 (2H, AB-system, *J* 12.8, CH₂), 6.92 (1H, dd, *J* 8.9 and 2.4, benz 5-H), 7.07 (1H, br s, benz 7-H), 7.11-7.22 (2H, m, phenyl-H), 7.23-7.35 (3H, m, phenyl-H), 7.54 (1H, s, *J* 8.9, benz 4-H), 13.26 (1H, br s, NH exchangeable); ¹³C NMR (DMSO-d₆, 75 MHz): δ 55.5 (OMe), 59.5 (CH₂), 128.1, 128.4 (phenyl), 129.9, 130.4 (phenyl), not all carbon signals observed due to annular tautomerism of the benzimidazole system; *m/z* (ESI) (Found MH⁺, 368.1045 C₁₇H₁₈N₃NaO₃S requires *MH* 368.1039); HPLC: *t*_R (*R*_{minor}) = 55.7 min, *t*_R (*S*_{major}) = 61.9 min, [Chiracel OD-H; flow rate 1.0 mL min⁻¹; 5% IPA–hexane; 20 °C]

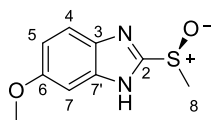
(S)-1-Methyl-4-[(phenylmethyl)sulfinyl]-benzene (S)-4.10⁴⁴⁹



Ti(OⁱPr)₄ (444 μL, 0.43 g, 1.50 mmol), (*S,S*)-DET (513 μL, 0.62 g, 3.00 mmol) and H₂O (9.0 μL, 9.01 mg, 0.50 mmol) were added to a suspension of sulfide **4.5** (1.07 g, 5.00 mmol) in

toluene (7.5 mL) and the mixture heated at 54 °C for 50 min. The reaction mixture was cooled to 30 °C and DIPEA (261 μL, 0.19 g, 1.5 mmol) was added, followed by CHP (80% in cumene, 924 μL, 0.76 g, 5.00 mmol). After 2 h stirring at 30 °C the reaction was quenched by addition of H₂O (10 mL). The mixture was stirred vigorously for 30 min then allowed to sit for 45 min. The reaction mixture was filtered through a pad of Celite and the Celite pad washed with H₂O (2 × 50 mL) and CH₂Cl₂ (4 × 50 mL). The phases of the filtrate were separated and the aqueous phase extracted with CH₂Cl₂ (3 × 50 mL). The combined organic extracted were washed with brine (25 mL), dried (MgSO₄), filtered and the solvent removed *in vacuo*. Column chromatography (eluting with 0-50% EtOAc–hexane) gave the title compound (*S*)-**4.10** (0.46 g, 40%, 16% ee) as colourless crystalline solid. Recrystallization from CH₂Cl₂–hexane afforded the sulfoxide (*S*)-**4.10** as colourless needles (0.28 g, 1.2 mmol, 24%, 19% ee); **m.p.** 133.7-135.0 °C (CHCl₃–hexane) (lit. 165.3.7-165.80 °C);⁴⁴⁹ **R_f** 0.36 (50% EtOAc–hexane); **¹H NMR** (DMSO-d₆, 300 MHz): δ 2.36 (3H, s, tol Me), 4.04 and 4.20 (2H, 2 × d, *J* 12.7 CH₂), 7.07-7.13 (2H, m, phenyl 8/8'-H), 7.24-7.30 (3H, m, phenyl 9/9'-H and 10-H), 7.32 (2H, d, *J* 8.4, tol 3/3'-H), 7.41 (2H, d, *J* 8.4, tol 4/4'-H); **¹³C NMR** (DMSO-d₆, 75 MHz): δ 20.9 (tol Me), 61.8 (CH₂), 124.3 (C4/4'), 127.7 (phenyl C10), 128.1 (phenyl C9/9'), 129.4 (tol C3/3'), 130.3 (phenyl C8/8'), 130.5 (phenyl C7), 140.3 (tol C5), 140.7 (tol C2), NMR data not comparable to the literature due to the use of a different solvent (CDCl₃)⁴⁴⁹ but is comparable to the data previously described here for the racemic sulfoxide; **m/z (ESI)** (Found MH⁺ 231.0842, C₁₄H₁₄OS requires *MH* 231.0838); **HPLC**: *t_R* (*R_{minor}*) = 25.0 min), (*S_{major}*) *t_R* = 30.6 min, [Chiracel OD-H; flow rate 1.0 mL min⁻¹; 5% IPA–hexane; 20 °C]

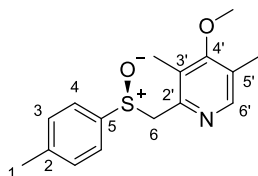
(*S*)-6(5)-Methoxy-2-(methylsulfinyl)-1H-benzimidazole (*S*)-4.11⁶²³



Ti(O^{*i*}Pr)₄ (444 μL, 0.43 g, 1.50 mmol), (*S,S*)-DET (513 μL, 0.62 g, 3.00 mmol) and H₂O (9.0 μL, 9.01 mg, 0.50 mmol) were added to a suspension of sulfide **4.7** (1.35 g, 5.00 mmol) in toluene (7.5 mL) and the mixture heated at 54 °C for 50 min. The reaction mixture was cooled to 30 °C and DIPEA (261 μL, 0.19 g, 1.5 mmol) was added, followed by CHP (80% in cumene, 924 μL, 0.76 g, 5.00 mmol). After 4 h stirring at 30 °C the reaction was quenched by addition of aqueous NH₄OH (12.5% NH₃, 10 mL). The mixture was stirred vigorously for 30 min then allowed to sit for 45 min. The reaction mixture was filtered through a pad of Celite and the Celite pad washed with aqueous NH₄OH (12.5% NH₃, 3 × 50 mL) and CH₂Cl₂ (4 × 50 mL). The phases of the filtrate were separated and the organic phased extracted with

aqueous NH_4OH (12.5% NH_3 , 3×25 mL). CH_2Cl_2 (50 mL) was added to the combined aqueous extracts and AcOH added with caution until a pH of ~ 8 was achieved. The phases were separated and the aqueous phase extracted with CH_2Cl_2 (3×25 mL). The combined organic extracts were washed with saturated aqueous NaHCO_3 (20 mL), then brine (25 mL), dried (MgSO_4), filtered and the solvent removed *in vacuo*. Column chromatography (eluting with 50% EtOAc– CH_2Cl_2) gave the title compound **4.11** (0.63 g, 30.0 mmol, 60%, 95% ee) as a colourless gum; R_f 0.14 (50% EtOAc–hexane); $^1\text{H NMR}$ (DMSO-d_6 , 300 MHz): δ 3.06 (3H, s, SMe), 3.80 (3H, s, benz OMe), 6.92 (1H, dd, J 8.9 and 2.3, benz 5-H), 7.10 (1H, br s, J 2.3, benz 7-H), 7.55 (1H, d, J 8.9, benz 4-H), (13.36 (1H, br s, NH exchangeable); $^{13}\text{C NMR}$ (DMSO-d_6 , 75 MHz): δ 40.2 (SMe), 55.5 (benz OMe), 113.4 (benz), 154.2 (benz), 156.7 (benz), not all carbon signals observed due to annular tautomerism of the benzimidazole system, NMR data not comparable to the literature due to the use of a different solvent (MeOD)⁶²³ but is comparable to the data previously described here for the racemic sulfoxide (\pm)-**4.11**; m/z (ESI) (Found MH^+ , 211.0534 $\text{C}_9\text{H}_{10}\text{N}_2\text{O}_2\text{S}$ requires MH 211.0535); HPLC: t_R (R_{minor}) = 55.7 min, t_R (S_{major}) = 61.9 min, [Chiracel AD-H; flow rate 0.5 mL min^{-1} ; 5% IPA–hexane; 20 °C]

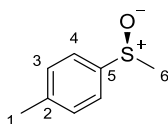
(S)-4-Methoxy-3,5-dimethyl-2-([(4-methylphenyl)sulfinyl]methyl)pyridine (S)-4.12



$\text{Ti}(\text{O}^i\text{Pr})_4$ (444 μL , 0.43 g, 1.50 mmol), (*S,S*)-DET (513 μL , 0.62 g, 3.00 mmol) and H_2O (9.0 μL , 9.01 mg, 0.50 mmol) were added to a suspension of sulfide **4.8** (1.37 g, 5.00 mmol) in toluene (7.5 mL) and the mixture heated at 54 °C for 50 min. The reaction mixture was cooled to 30 °C and DIPEA (261 μL , 0.19 g, 1.5 mmol) was added, followed by CHP (80% in cumene, 924 μL , 0.76 g, 5.00 mmol). After 2 h stirring at 30 °C the reaction was quenched by addition of H_2O (10 mL). The mixture was stirred vigorously for 30 min then allowed to sit for 45 min. The reaction mixture was filtered through a pad of Celite and the Celite pad washed with H_2O (2×50 mL) and CH_2Cl_2 (4×50 mL). The phases of the filtrate were separated and the aqueous phase extracted with CH_2Cl_2 (3×50 mL). The combined organic extracts were washed with brine (25 mL), dried (MgSO_4), filtered, and the solvent removed *in vacuo*. Column chromatography (eluting with 0-2.5% MeOH–EtOAc) gave the title compound (*S*)-**4.12** (0.87 g, 30.0 mmol, 60%, 20% ee) as colourless crystalline solid. Recrystallization from CH_2Cl_2 –hexane afforded the sulfoxide (*S*)-**4.12** as colourless needles (0.58 g, 40%, 27% ee);

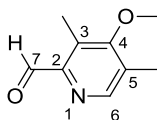
m.p. 90.3-91.9 °C (CH₂Cl₂–hexane); **R_f** 0.14 (EtOAc); **¹H NMR** (DMSO-d₆, 300 MHz): δ 2.02 (3H, s, 3''-Me), 2.19 (3H, s, 5''-Me), 2.36 (3H, s, tol Me), 3.66 (3H, s, pyr OMe), 4.17 and 4.36 (2H, AB-system, *J* 12.8, CH₂), 7.33 (2H, d, *J* 8.2, tol 3/3'-H), 7.44 (2H, d, *J* 8.3, tol 4/4'-H) 8.20 (1H, s, pyr 6''-H); **¹³C NMR** (DMSO-d₆, 125 MHz): δ 11.1 (pyr 3''-Me), 12.9 (pyr 5''-Me), 20.9 (tol Me), 59.6 (pyr OMe), 62.8 (CH₂), 124.1 (tol C4/4'), 125.2 (pyr C5''), 126.5 (pyr C3''), 129.6 (tol C3/3'), 141.0 (tol C2), 141.1 (tol C5), 149.0 (pyr C6''), 150.1 (Pyr C2''), 163.4 (Pyr C4''); **m/z (ESI)** (Found MH⁺, 290.1211 C₁₆H₁₉NO₂S requires *MH* 296.1209); **HPLC**: *t_R* (*S_{major}*) = 24.6 min, *t_R* (*R_{minor}*) = 30.3 min, [Chiracel OD-H; flow rate 1.0 mL min⁻¹; 5% IPA–hexane; 20 °C]

(S)-1-Methyl-4-(methylsulfinyl)-benzene (S)-1.48^{153, 727}



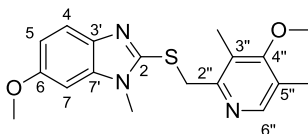
Ti(O^{*i*}Pr)₄ (444 μL, 0.43 g, 1.50 mmol), (*S,S*)-DET (513 μL, 0.62 g, 3.00 mmol) and H₂O (9.0 μL, 9.01 mg, 0.50 mmol) were added to a suspension of *p*-tolyl sulfide (1.07 g, 5.00 mmol) in toluene (7.5 mL) and the mixture heated at 54 °C for 50 min. The reaction mixture was cooled to 30 °C and DIPEA (261 μL, 0.19 g, 1.5 mmol) was added, followed by CHP (80% in cumene, 924 μL, 0.76 g, 5.00 mmol). After 2 h stirring at 30 °C the reaction was quenched by addition of H₂O (10 mL). The mixture was stirred vigorously for 30 min then allowed to sit for 45 min. The reaction mixture was filtered through a pad of Celite and the Celite pad washed with H₂O (2 × 50 mL) and CH₂Cl₂ (4 × 50 mL). The phases of the filtrate were separated and the aqueous phase extracted with CH₂Cl₂ (3 × 50 mL). The combined organic extracted were washed with brine (25 mL), dried (MgSO₄), filtered and the solvent removed *in vacuo*. Column chromatography (eluting with 50-100% EtOAc–hexane) gave the title compound (*S*)-**1.48** (0.49 g, 3.15 mmol, 63%, 6% ee) as colourless waxy solid; **m.p.** 40.2-41.2 °C (hexane) (lit. 74.5-75.5);⁷²⁷ **R_f** 0.08 (50% EtOAc–hexane); **¹H NMR** (DMSO-d₆, 300 MHz): δ 2.36 (3H, s, tol Me), 2.69 (3H, s, SMe), 7.37 (2H, d, *J* 8.1, tol 3/3'-H), 7.57 (2H, d, *J* 8.3, tol 4/4'-H); **¹³C NMR** (DMSO-d₆, 125 MHz): δ 20.8 (tol Me), 43.3 (SMe), 123.5 (tol C4/4'), 129.7 (tol C3/3'), 140.5 (tol C2), 143.2 (tol C5) NMR data not comparable to the literature due to the use of a different solvent (CDCl₃)¹⁵³ but is comparable to the data previously described here for the racemic sulfoxide; **m/z (ESI)** (Found MH⁺, 155.0524 C₈H₁₀OS requires *MH* 155.0525); **HPLC**: *t_R* (*R_{minor}*) = 26.5 min, (*S_{major}*) *t_R* = 29.4 min [Chiracel OD-H; flow rate 0.5 mL min⁻¹; 5% EtOH–hexane; 20 °C]

4-Methoxy-3,5-dimethylpyridine-2-carboxaldehyde **6.1**⁷⁰⁶



To a stirred solution of 3,5-dimethyl-2-hydroxymethyl-4-methoxypyridine (0.330 g, 2.00 mmol) in CHCl_3 (25 mL) was added activated MnO_2 (2.65 g, 30 mmol, 15 equiv). The resulting mixture was stirred at rt for 19 h and then was filtered through a pad of Celite and the pad washed with CHCl_3 (3×15 mL). The organic materials were combined and the solvent removed *in vacuo* to give the title compound **6.1** (0.282 g, 1.70 mmol, 85%) as a yellow oil; R_f 0.48 (50% EtOAc–hexane); $^1\text{H NMR}$ (CDCl_3 , 500 MHz): δ 2.35 (3H, s, pyr 5-Me), 2.56 (3H, s, pyr 3-Me), 3.81 (3H, s, pyr OMe), 8.45 (1H, s, pyr 6''-H), 10.13 (1H, s, 7-H); $^{13}\text{C NMR}$ (CDCl_3 , 125MHz): δ 10.5 (pyr 3-Me), 13.8 (pyr 5-Me), 60.1 (pyr OMe), 129.3 (pyr C3), 130.5 (pyr C5), 150.2 (pyr C2), 150.4 (pyr C6), 164.8 (pyr C4), 195.0 (C7) NMR data in accordance with the literature data.⁷⁰⁶

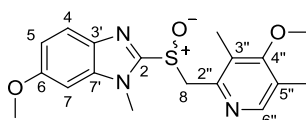
6(5)-Methoxy-2-[[[(4-methoxy-3,5-dimethyl-2-pyridinyl)methyl]thio]-1-methyl-1H-benzimidazole (NMe Pyrimetazole) **6.3**



Pyrimetazole **3.17** (6.56 g, 20.0 mmol) was suspended in a solution of NaOH (0.80 g, 20 mmol) in H_2O (0.8 mL). MeI (1.2 mL, 2.69 g 20 mmol) was added whereupon the mixture became homogenous, and the mixture stirred at 40 °C for 1 h. The reaction mixture was allowed to cool to rt and then diluted with H_2O (10 mL) and CHCl_3 (10 mL). The phases were separated and the aqueous layer extracted with CHCl_3 (3×10 mL). The combined organic materials were washed with brine (20 mL), dried (MgSO_4), filtered, and the solvent removed *in vacuo*. Column chromatography (eluting with 0.0–2.5 % MeOH– CHCl_3) followed by trituration with Et_2O gave the title product **6.3** as a colourless amorphous powder (4.09 g, 12.0 mmol, 60%) as mixture of tautomers in the ratio of 48:52 5-OMe:6-OMe; **m.p.** 105.2–106.9 °C (from Et_2O); R_f 0.22 (CHCl_3); $^1\text{H NMR}$ (DMSO-d_6 , 500 MHz): 5-OMe isomer: δ 2.19 (3H, s, pyr 5''-Me), 2.26 (3H, s, pyr 3''-Me), 3.62 (3H, s, NMe), 3.72 (3H, s, pyr OMe), 3.78 (3H, s, benz OMe), 4.68 (2H, s, CH_2), 6.82 (1H, dd, J 8.7 and 2.4, benz 6-H), 7.14 (1H, d, J 2.4, benz 4-H), 7.34 (1H, d, J 8.7, benz 7-H), 8.17 (1H, s, pyr 6''-H); 6-OMe isomer: δ 2.19 (3H, s, pyr 5''-Me), 2.25 (3H, s, pyr 3''-Me), 3.62 (3H, s, NMe), 3.71 (3H, s, pyr OMe), 3.81 (3H, s, benz OMe), 4.64 (2H, s, CH_2), 6.78 (1H, dd, J 8.7 and 2.4, benz 5-H), 7.06 (1H, d, J 2.4, benz 7-H), 7.45 (1H, d, J 8.7, benz 4-H), 8.17 (1H, s, pyr 6''-H); $^{13}\text{C NMR}$ (DMSO-d_6 , 125 MHz): 5-OMe isomer: δ 10.8 (pyr

3''-Me), 12.9 (pyr 5''-Me), 29.9 (NMe), 37.3 (CH₂), 55.6 (benz 6-OMe), 59.8 (pyr OMe), 93.5 (benz C7), 110.7 (benz C5), 118.1 (benz C4), 124.5 (pyr C3''), 125.1 (pyr C5''), 137.3 (benz C), 143.6 (benz C), 148.7 (pyr C6''), 149.5 (benz C2), 153.9 (pyr C2''), 155.6 (benz C6), 163.4 (pyr C4''); 6-OMe isomer: δ 10.8 (pyr 3''-Me), 12.9 (pyr 5''-Me), 29.8 (NMe), 37.2 (CH₂), 55.4 (benz 5-OMe), 59.8 (pyr OMe), 100.8 (benz C4), 109.7 (benz C7), 110.4 (benz C6), 124.5 (pyr C3''), 125.1 (pyr C5''), 131.3 (benz C), 143.6 (benz C), 148.7 (pyr C6''), 151.1 (benz C2), 153.9 (pyr C2''), 155.4 (benz C5), 163.4 (pyr C4''); **m/z (ESI)** (Found MH⁺, 344.1441. C₁₈H₂₁N₃O₂S requires *MH* 344.1427)

(±)-6(5)-Methoxy-2-[[4-methoxy-3,5-dimethyl-2-pyridinyl)methyl]sulfinyl]-1-methyl-1H-benzimidazole ((±)-NMe Omeprazole) 5.22^{562, 708}



Method A: methylation of Omeprazole **1.1**^{562, 708}

Omeprazole (±)-**1.1** (10.4 g, 30.0 mmol) was suspended in a solution of NaOH (1.20 g, 30 mmol) in H₂O (5 mL) and MeCN 5 mL. MeI (1.87 mL, 4.26 g 30 mmol) was added and the mixture stirred at 40 °C for 1 h. The reaction mixture was allowed to cool to rt and then diluted with H₂O (20 mL) and CHCl₃ (20 mL). The phases were separated and the aqueous layer extracted with CHCl₃ (3 × 30 mL). The combined organic materials were washed with brine (20 mL), dried (MgSO₄), filtered, and the solvent removed *in vacuo* to give the title compound **5.22** as a 50:50 mixture of 5-OMe:6-OMe tautomers (10.3 g, 28.7 mmol, 93%) as a colourless viscous gum that dried as a glassy foam under vacuum. No further purification was required. **m.p.** 112.8-114.2 °C (Et₂O); **R_f** 0.32 (5% MeOH–EtOAc); **¹H NMR** (DMSO-d₆, 500 MHz): two isomers 5-OMe:6-OMe 5-OMe isomer: δ 2.16 (3H, s, pyr 5''-Me), 2.18 (3H, s, pyr Me), 3.66 (3H, s, pyr Me), 3.80 (3H, s, benz OMe), 3.91 (3H, s, NMe), 4.84 and 4.94 (2H, 2×d, *J* 13.8, CH₂), 7.02 (1H, dd, *J* 8.9 and 2.4, benz 6-H), 7.25 (1H, d, *J* 2.4, benz 4-H), 7.56 (1H, d, *J* 8.9, benz 7-H), 8.11 (1H, s, pyr 6''-H); 6-OMe isomer: δ 2.16 (3H, s, pyr 5''-Me), 2.18 (3H, s, pyr 3''-Me), 3.66 (3H, s, pyr OMe), 3.85 (3H, s, benz OMe), 3.93 (3H, s, NMe), 4.82 and 4.94 (2H, 2×d, *J* 13.7, CH₂), 6.93 (1H, dd, *J* 8.9 and 2.4, benz 5-H), 7.21 (1H, d, *J* 2.4, benz 7-H), 7.61 (1H, d, *J* 8.9, benz 4-H), 8.12 (1H, s, pyr 6''-H); **¹³C NMR** (DMSO-d₆, 125 MHz): 5-OMe isomer: δ 11.0 (pyr 3''-Me), 12.8 (pyr 5''-Me), 30.4 (NMe), 55.5 (benz 5-OMe), 58.4 (CH₂), 59.7 (pyr OMe), 101.7 (benz C4), 111.4 (benz C7), 114.7 (benz C6), 125.4 (pyr C3''), 126.1 (pyr C5''), 130.9 (benz C3' or C7'), 142.3 (benz C3' or C7'), 148.9 (pyr C6''), 150.1 (pyr C2''), 152.5 (benz C2), 156.3 (benz C5), 163.3 (pyr C4''); 6-OMe isomer: δ 11.0 (pyr 3''-Me), 12.8

(pyr 5''-Me), 30.4 (NMe), 55.7 (benz 6-OMe), 58.4 (CH₂), 59.7 (pyr OMe), 93.4 (benz C7), 113.4 (benz C5), 120.8 (benz 4H), 125.4 (pyr C3''), 126.1 (pyr C5''), 135.9 (benz C3' or C7'), 137.1 (benz C3' or C7'), 148.9 (pyr C6''), 150.1 (pyr C2''), 151.4 (benz C2), 157.3 (benz C6), 163.3 (pyr C4''); ¹H NMR (CDCl₃, 500 MHz): mixture of tautomers A:B ratio 50:50: δ 2.20 (3H, s, pyr 5''-Me), 2.26 and 2.27 (3H, s, pyr 3''-Me), 3.68 and 3.69 (3H, s), 3.85 and 3.86 (3H, s), 3.93 and 3.94 (3H, s), 4.93 (2 H, m, CH₂), tautomer A: 6.78 (d, *J* 2.4), 6.96 (dd, *J* 8.9 and 2.4), 7.66 (d, *J* 8.9), tautomer B: 7.02 (1H, dd, *J* 8.9 and 2.4), 7.25 (d, *J* 2.4), 7.28 (d, *J* 8.9), 8.11 (1H s, pyr 6''-H) NMR data in accordance with the literature;⁵⁶² **m/z (ESI)** (Found MH⁺, 360.1384 C₁₈H₂₁N₃O₃S requires *MH* 360.1376)

Method B: oxidation of NMe Pymetazole **6.3**

Saturated aqueous NaHCO₃ (10 mL) was added to a solution of NMe Pymetazole **6.3** (0.69 g, 2.00 mmol) in CH₂Cl₂ (10 mL) and the mixture cooled to 0 °C. A solution of *m*CPBA (75% *m*CPBA, 0.46 g, 2.00 mmol) in CH₂Cl₂ (90 mL) was added dropwise and the reaction stirred vigorously for 2h. The reaction was quenched by addition of saturated aqueous Na₂S₂O₃ (20 mL), the phases were separated and the aqueous layer extracted with CH₂Cl₂ (3 × 10 mL). The combined organic extracts were washed with brine (10 mL), dried with MgSO₄, filtered and the solvent removed *in vacuo*. Column chromatography (eluting with 2.5-5.0 % MeOH–EtOAc) gave the title compound (±)-**5.22** as a mixture of tautomers in the ratio of 41:59 5-OMe:6-OMe. Recrystallization was achieved by addition of the minimum amount of CH₂Cl₂ followed by dropwise addition of Et₂O to induce precipitation. The precipitate was collected by vacuum filtration and washed with Et₂O to give the title compound (±)-**5.22** as colourless microcrystals (0.24 g, 0.66 mmol, 32%) as mixture of tautomers in the ratio of 13:87 5-OMe:6-OMe. NMR characterization data as stated above.

8.3 NMR studies

^1H NMR studies of the catalyst components (chapter 4)

^1H NMR studies were conducted using NMR tubes that had been dried under vacuum for 24h. Glassware in which sample were prepared were dried in an oven for 24h; prior to use they were stoppered and removed from the oven and allowed to cool. CDCl_3 was dried using 4Å molecular sieves and was passed through a plug of alumina immediately prior to use. All solutions were filtered through a plug of cotton wool prior to NMR analysis. Although samples were not prepared under strictly anhydrous conditions, exposure to environmental moisture was minimized by preparation under a blanket of nitrogen and rapid analysis in addition to the use of dried glassware and Parafilm sealed NMR tubes.

NMR studies of the catalyst components: $\text{Ti}(\text{O}^i\text{Pr})_4$ + Pyrimetazole sulfide **3.17 (section 4.7.1)**

Pyrimetazole sulfide **3.17** (32.9 mg, 0.10 mmol) was dissolved in CDCl_3 (0.75 mL) which had been passed through alumina to remove residual water. The solution was transferred to the NMR tube and $\text{Ti}(\text{O}^i\text{Pr})_4$ was added according to the quantities given in Table 8.1. The tubes were sealed using Parafilm and the contents mixed for 30 s. Characterization by ^1H NMR was performed within 10 min of preparation for each sample.

$\text{Ti}(\text{O}^i\text{Pr})_4$ / equiv	$\text{Ti}(\text{O}^i\text{Pr})_4$ / mmol	$\text{Ti}(\text{O}^i\text{Pr})_4$ / μL
0.2	0.02	5.9
0.4	0.04	11.8
0.6	0.06	17.8
0.8	0.08	23.7
1.0	0.1	29.6

Table 8.1 Volumes of $\text{Ti}(\text{O}^i\text{Pr})_4$ employed in sample preparation for NMR studies on the interaction of sulfide **3.17** and $\text{Ti}(\text{O}^i\text{Pr})_4$

NMR studies of the catalyst components: $\text{Ti}(\text{O}^i\text{Pr})_4$ concentration studies (section 4.7.2.1)

Solutions of $\text{Ti}(\text{O}^i\text{Pr})_4$ in CDCl_3 and Tol-d_8 were prepared in accordance with the quantities given in Table 8.2 using 0.75 mL of solvent. The tubes were sealed using Parafilm and the contents mixed for 30 s. Characterization by ^1H NMR was performed within 10 min of preparation for each sample.

$[\text{Ti}(\text{O}^i\text{Pr})_4] / \text{mol L}^{-1}$	$\text{Ti}(\text{O}^i\text{Pr})_4 / \text{mmol}$	$\text{Ti}(\text{O}^i\text{Pr})_4 / \mu\text{L}$
0.30	0.23	66.6
0.25	0.19	55.5
0.20	0.15	44.4
0.15	0.11	33.3
0.10	0.08	22.2
0.05	0.04	11.1
0.025	0.02	5.6
0.01	0.01	2.2

Table 8.2 Volumes of $\text{Ti}(\text{O}^i\text{Pr})_4$ employed in sample preparation for NMR studies on the effects of concentration

NMR studies of the catalyst components: $\text{Ti}(\text{O}^i\text{Pr})_4 + \text{DET} + \text{H}_2\text{O}$ (section 4.7.3)

Ti(OⁱPr)₄: DET:H₂O = 1:2:0

$\text{Ti}(\text{O}^i\text{Pr})_4$ (29.6 μL , 0.1 mmol) and DET (34.3 μL , 0.2 mmol) were added to CDCl_3 (1.0 mL) in an NMR tube. The tube was sealed using Parafilm and the contents mixed for 30 s. Characterization by ^1H NMR was performed within 10 min of preparation

Ti(OⁱPr)₄: DET:H₂O = 1:2:1

$\text{Ti}(\text{O}^i\text{Pr})_4$ (59.2 μL , 0.2 mmol), DET (68.5 μL , 0.4 mmol), and H_2O (3.6 μL , 0.2 mmol) were added to CDCl_3 (2.0 mL); the solution was thoroughly mixed and 1.0 mL removed for analysis. The tube was sealed using Parafilm and the contents mixed for 30 s. Characterization by ^1H NMR was performed within 10 min of preparation

Ti(OⁱPr)₄: DET:H₂O = 1:4:0

$\text{Ti}(\text{O}^i\text{Pr})_4$ (29.6 μL , 0.1 mmol) and DET (68.5 μL , 0.4 mmol) were added to CDCl_3 (1.0 mL) in an NMR tube. The tube was sealed using Parafilm and the contents mixed for 30 s. Characterization by ^1H NMR was performed within 10 min of preparation

Ti(OⁱPr)₄: DET:H₂O = 3:6:1

$\text{Ti}(\text{O}^i\text{Pr})_4$ (88.8 μL , 0.3 mmol), DET (102.8 μL , 0.6 mmol), and H_2O (1.8 μL , 0.1 mmol) were added to CDCl_3 (3.0 mL); the solution was thoroughly mixed and 1.0 mL removed for analysis. The tube was sealed using Parafilm and the contents mixed for 30 s. Characterization by ^1H NMR was performed within 10 min of preparation

Evaluation of chiral tartrates for use as chiral shift reagents (chapter 5)

(S)-BINOL vs. (S,S)-DET as chiral shift reagents (section 5.3.1)

(S)-BINOL (11.4 mg, 0.04 mmol) was added to a solution of Omeprazole (\pm)-**1.1** (13.8 mg, 0.04 mmol) in CDCl₃ (0.75 mL). The solution was mixed and passed through a plug of cotton wool into an NMR tube. Characterization by ¹H NMR was performed within 10 min of preparation

(S,S)-DET (8.24 mg, 6.8 μ L, 0.04 mmol) was added to a solution of Omeprazole (\pm)-**1.1** (13.8 mg, 0.04 mmol) in CDCl₃ (0.75 mL). The solution was mixed and passed through a plug of cotton wool into an NMR tube. Characterization by ¹H NMR was performed within 10 min of preparation

Choice of NMR solvent (section 5.3.2)

Solutions of Omeprazole (\pm)-**1.1** (17.3 mg, 0.05 mmol) and (S,S)-DET (10.3 mg, 8.6 μ L, 0.05 mmol) were prepared in 0.75 mL in the following solvents: acetone-d₆, benzene-d₆, CDCl₃, DCM-d₂, D₂O, DMSO-d₆, MeOD, and Tol-d₈. The solutions were mixed and passed through a plug of cotton wool into an NMR tube.

Host-guest ratio (section 5.3.3)

Solutions of Omeprazole (\pm)-**1.1** (34.5 mg, 0.1 mmol) and (S,S)-DET or (S,S)-DIPT were prepared in CDCl₃ (1.0 mL) according to the quantities of the tartrates given in Table 8.3. The solutions were mixed and passed through a plug of cotton wool into an NMR tube.

equiv of tartrate	(S,S)-DET / mL	(S,S)-DIPT / μ L
0.2	3.4	-
0.4	6.8	8.4
0.6	10.3	-
0.8	13.7	-
1.0	17.1	21.0
2.0	34.2	41.9
5.0	85.6	104.9

Table 8.3 Quantities of DET or DIPT employed in order to investigate the Host-guest ratios

(R,R)-DMT was added to solution of Omeprazole (\pm)-**1.1** (34.5 mg, 0.1 mmol) according to the quantities given in Table 8.4. The solutions were mixed and passed through a plug of cotton wool into an NMR tube.

equiv of tartrate	(<i>R,R</i>)-DMT / mg
0.25	4.45
0.50	8.91
0.75	13.36
1.00	17.81
2.00	35.63

Table 8.4 Quantities of DMT employed in order to investigate the Host-guest ratios

Determination of enantiomeric excess (section 5.3.4)

(S,S)-DET as the chiral shift reagent

Samples of Esomeprazole (*S*)-**1.1** of varying % ee were prepared by mixing the appropriate amounts of racemic Omeprazole with Esomeprazole of high optical purity (> 99.5% ee, obtained through neutralization of the Na-salt of Esomeprazole). Solutions were prepared using 103.6 mg (0.3 mmol) of the sulfoxide mixtures in 0.8 mL of CDCl₃. 0.1 mL of each solution was removed for analysis by HPLC; chiral HPLC showed these mixtures to have enantiomeric purities of 0, 20, 40, 54, 60, 81, and > 99.5% ee. (*S,S*)-DET was added to the remainder of the sulfoxide solutions according to the quantities given in Table 8.5

equiv of tartrate	(<i>S,S</i>)-DET / μ L
0.25	11.2
0.50	22.5
0.75	33.7
1.00	44.9
2.00	89.8
5.00	224.6

Table 8.5 Quantities of DET used with solutions of Esomeprazole of varying ee to compare with ee determination performed by chiral HPLC

(R,R)-DMT as the chiral shift reagent

Samples of Esomeprazole (*S*)-**1.1** of varying % ee were prepared by mixing the appropriate amounts of racemic Omeprazole with Esomeprazole of high optical purity (> 99.5% ee, obtained through neutralization of the Na-salt of Esomeprazole); chiral HPLC showed these mixtures to have enantiomeric purities of 0, 21, 41, 50, 63, 81, and > 99.5% ee. Solutions were prepared using 69.1 mg (0.20 mmol) of the sulfoxide mixtures in 0.7 mL of CDCl₃. (*R,R*)-DMT was added to the sulfoxide solutions according to the quantities given in Table 8.6

equiv of tartrate	(<i>R,R</i>)-DMT / mg
0.25	8.91
0.50	17.81
0.75	26.72
1.00	35.63
2.00	71.26

Table 8.6 Quantities of DMT used with solutions of Esomeprazole of varying ee to compare with ee determination performed by chiral HPLC

Selective deuteration of Omeprazole and related compounds (chapter 6)

Deuteration of Na-Omeprazole in aprotic, and protic solvents (section 6.3.1 and 6.3.2)

Solutions of Na-Omeprazole **3.36** were typically prepared using 40.0 mg of the Omeprazole salt dissolved in 0.75 mL of DMSO- d_6 , MeOD, or D_2O . All solutions for NMR analysis were mixed thoroughly and passed through a plug of cotton wool to remove any solid material.

Deuteration of Omeprazole and related compounds in protic solvents (section 6.3.2)

Solutions were prepared using 0.2 mmol of each of the following compounds suspended or dissolved in 0.8 mL of D_2O or MeOD: Omeprazole **1.1** (69.1 mg), Pyrimetazole sulfide **3.17** (65.9 mg), Omeprazole sulfone **4.1** (72.3 mg), sulfoxide **4.9** (57.3 mg), and sulfoxide **4.12** (57.9 mg). NaOD (14.24 M in D_2O) or DCl (11.68 M in D_2O) was added in accordance with the quantities given in Table 8.7. All solutions for NMR analysis were mixed thoroughly and passed through a plug of cotton wool to remove any solid material.

equiv	mmol	DCl / μL	NaOD / μL
0	0.0	0.0	0.0
1	0.20	17.1	14.00
2	0.40	34.2	28.1
3	0.60	51.4	42.1
4	0.80	68.5	56.2
5	1.00	85.6	70.2

Table 8.7 Quantities of DCl or NaOD added to Omeprazole **1.1** in D_2O or MeOD to prepared samples for ^1H NMR analysis across a range of pH condition

References

1. Patai, S.; Rappoport, Z.; Stirling, C., *The Chemistry of Sulphones and Sulphoxides*. John Wiley & Sons, Ltd: 1988;
2. Bolm, C.; Muñiz, K.; Hildebrand, J. P., *Comprehensive asymmetric catalysis*, Ed. Eric N. Jacobsen, A. P., Hisashi Yamamoto, Springer, Berlin, London, **1999**, Vol. 2, p 697.
3. Trost, B. M.; Rao, M., *Angew. Chem., Int. Ed.*, **2015**, *54*, 5026-5043.
4. Wojaczyńska, E.; Wojaczyński, J., *Chem. Rev.*, **2010**, *110*, 4303-4356.
5. Carreno, M. C., *Chem. Rev.*, **1995**, *95*, 1717-1760.
6. Fernández, I.; Khair, N., *Chem. Rev.*, **2003**, *103*, 3651-3706.
7. Sipos, G.; Drinkel, E. E.; Dorta, R., *Chem. Soc. Rev.*, **2015**, *44*, 3834-3860.
8. Otocka, S.; Kwiatkowska, M.; Madalińska, L.; Kielbasiński, P., *Chem. Rev.*, **2017**, *117*, 4147-4181.
9. Page, P. C. B.; Heer, J. P.; Bethell, D.; Collington, E. W.; Andrews, D. M., *Synlett*, **1995**, *1995*, 773-775.
10. Agarwal, K. C., *Med. Res. Rev.*, **1996**, *16*, 111-24.
11. Schaumann, E., *Sulfur-Mediated Rearrangements I*, Ed. Schaumann, E., Springer Berlin Heidelberg, **2007**, Vol. 274, ch. 105, pp 1-34.
12. Farina, V.; Reeves, J. T.; Senanayake, C. H.; Song, J. J., *Chem. Rev.*, **2006**, *106*, 2734-2793.
13. Oae, S., *J. Mol. Struct.: THEOCHEM*, **1989**, *55*, 321-45.
14. Harrison, P. W. B.; Kenyon, J.; Phillips, H., *J. Chem. Soc.*, **1926**, *129*, 2079-2090.
15. Federsel, H. J.; Larsson, M., *Asymmetric Catalysis on Industrial Scale*, **2004**, ch. 24, pp 413-436.
16. Berkowitz, B. A.; Sachs, G., *Mol. Interv.*, **2002**, *2*, 6-11.
17. Bentley, R., *Chem. Soc. Rev.*, **2005**, *34*, 609-624.
18. Kumar, R., *Drugs*, **2008**, *68*, 1803-1839.
19. Ternois, J.; Guillen, F.; Plaquevent, J. C.; Coquerel, G., *Tetrahedron: Asymmetry*, **2007**, *18*, 2959-2964.
20. Prisinzano, T.; Podobinski, J.; Tidgewell, K.; Luo, M.; Swenson, D., *Tetrahedron: Asymmetry*, **2004**, *15*, 1053-1058.
21. Wong, Y. N.; King, S. P.; Simcoe, D.; Gorman, S.; Laughton, W.; McCormick, G. C.; Grebow, P., *J. Clin. Pharmacol.*, **1999**, *39*, 281-8.
22. Legros, J.; Dehli, J. R.; Bolm, C., *Adv. Synth. Catal.*, **2005**, *347*, 19-31.
23. Moseley, J. D.; Moss, W. O., *Org. Process Res. Dev.*, **2002**, *7*, 53-57.

24. Paias, F. O.; Lanchote, V. L.; Takayanagui, O. M.; Bonato, P. S., *Electrophoresis*, **2001**, *22*, 3263-9.
25. Hwang, D. R.; Helquist, P.; Shekhani, M. S., *J. Org. Chem.*, **1985**, *50*, 1264-1271.
26. Iimori, T.; Takahashi, Y.; Izawa, T.; Kobayashi, S.; Ohno, M., *J. Am. Chem. Soc.*, **1983**, *105*, 1659-1660.
27. Koiso, Y.; Li, Y.; Iwasaki, S.; Hanaoka, K.; Kobayashi, T.; Sonoda, R.; Fujita, Y.; Yaegashi, H.; Sato, Z., *J. Antibiot.*, **1994**, *47*, 765-73.
28. Maitro, G.; Prestat, G.; Madec, D.; Poli, G., *Tetrahedron: Asymmetry*, **2010**, *21*, 1075-1084.
29. Bryliakov, K. P.; Talsi, E. P., *Eur. J. Org. Chem.*, **2008**, *2008*, 3369-3376.
30. O'Mahony, G. E.; Kelly, P.; Lawrence, S. E.; Maguire, A. R., *Arkivoc*, **2011**, 1-110.
31. Rayner, D. R.; Gordon, A. J.; Mislow, K., *J. Am. Chem. Soc.*, **1968**, *90*, 4854-4860.
32. Rayner, D. R.; Miller, E. G.; Bickart, P.; Gordon, A. J.; Mislow, K., *J. Am. Chem. Soc.*, **1966**, *88*, 3138-3139.
33. Kagan, H. B., *Organosulfur Chemistry in Asymmetric Synthesis*, Eds. Toru, T.; Bolm, C., Wiley-VCH Verlag GmbH & Co. KGaA, **2009**, ch. 1, pp 1-29.
34. Mancha, G.; Cuenca, A. B.; Rodríguez, N.; Medio-Simón, M.; Asensio, G., *Tetrahedron*, **2010**, *66*, 6901-6905.
35. Fernández, I.; Khiar, N., *Organosulfur Chemistry in Asymmetric Synthesis*, Eds. Toru, T.; Bolm, C., Wiley-VCH Verlag GmbH & Co. KGaA, **2009**, ch. 8, pp 265-290.
36. Baldenius, K. U.; Kagan, H. B., *Tetrahedron: Asymmetry*, **1990**, *1*, 597-610.
37. Pellissier, H., *Tetrahedron*, **2006**, *62*, 5559-5601.
38. Dalko, P. I.; Moisan, L., *Angew. Chem., Int. Ed.*, **2004**, *43*, 5138-5175.
39. Chen, G.; Gui, J.; Li, L.; Liao, J., *Angew. Chem., Int. Ed.*, **2011**, *50*, 7681-7685.
40. Procter, D. J., *J. Chem. Soc., Perkin Trans. 1*, **2001**, 335-354.
41. Rayner, C. M., *Contemp. Org. Synth.*, **1996**, *3*, 499-533.
42. Smith, L. H. S.; Coote, S. C.; Sneddon, H. F.; Procter, D. J., *Angew. Chem., Int. Ed.*, **2010**, *49*, 5832-5844.
43. Capperucci, A.; Degl'Innocenti, A.; Lriverend, C.; Metzner, P., *J. Org. Chem.*, **1996**, *61*, 7174-7177.
44. Tillett, J. G., *Chem. Rev.*, **1976**, *76*, 747-772.
45. Akai, S.; Kita, Y., *Sulfur-Mediated Rearrangements I*, Ed. Schaumann, E., Springer Berlin Heidelberg, **2007**, *Vol. 274*, ch. 73, pp 35-76.
46. Sugimoto, H.; Nakamura, S.; Shibata, Y.; Shibata, N.; Toru, T., *Tetrahedron Lett.*, **2006**, *47*, 1337-1340.
47. Kagan, H. B.; Dunach, E.; Nemecek, C.; Pitchen, P.; Samuel, O.; Zhao, S. H., *Pure Appl. Chem.*, **1985**, *57*, 1911-1916.

48. Walker, A. J., *Tetrahedron: Asymmetry*, **1992**, 3, 961-998.
49. Mellah, M.; Voituriez, A.; Schulz, E., *Chem. Rev.*, **2007**, 107, 5133-5209.
50. Mikołajczyk, M.; Krysiak, J. A.; Midura, W. H.; Wieczorek, M. W.; Różycka-Sokołowska, E., *J. Org. Chem.*, **2006**, 71, 8818-8823.
51. Ferber, B.; Kagan, H. B., *Adv. Synth. Catal.*, **2007**, 349, 493-507.
52. Trost, B. M., *Chem. Rev.*, **1978**, 78, 363-382.
53. Kingsbury, C. A.; Cram, D. J., *J. Am. Chem. Soc.*, **1960**, 82, 1810-1819.
54. Cubbage, J. W.; Guo, Y.; McCulla, R. D.; Jenks, W. S., *J. Org. Chem.*, **2001**, 66, 8722-8736.
55. Kice, J. L.; Campbell, J. D., *J. Org. Chem.*, **1967**, 32, 1631-1633.
56. Hauser, F. M.; Ellenberger, S. R.; Clardy, J. C.; Bass, L. S., *J. Am. Chem. Soc.*, **1984**, 106, 2458-2459.
57. Posner, G. H.; Mallamo, J. P.; Miura, K., *J. Am. Chem. Soc.*, **1981**, 103, 2886-2888.
58. Posner, G. H., *Acc. Chem. Res.*, **1987**, 20, 72-78.
59. Posner, G. H.; Chapdelaine, M. J.; Lentz, C. M., *J. Org. Chem.*, **1979**, 44, 3661-3665.
60. Solladie, G.; Hamdouchi, C., *Synthesis*, **1991**, 1991, 979-982.
61. Itoh, N.; Matsuyama, H.; Yoshida, M.; Kamigata, N.; Iyoda, M., *Bull. Chem. Soc. Jpn.*, **1995**, 68, 3121-3130.
62. Bauder, C., *Tetrahedron Lett.*, **2008**, 49, 2243-2246.
63. Solladié, G.; Bauder, C.; Arce-Dubois, E.; Pasturel-Jacopé, Y., *Tetrahedron Lett.*, **2001**, 42, 2923-2925.
64. Marino, J. P.; de la Pradilla, R. F.; Laborde, E., *Synthesis*, **1987**, 1987, 1088-1091.
65. Sheldon, R. A.; Arends, I. W. C. E.; Hanefeld, U., *Green Chemistry and Catalysis*, Wiley-VCH Verlag GmbH & Co. KGaA, **2007**, pp 1-47.
66. Madesclaire, M., *Tetrahedron*, **1986**, 42, 5459-5495.
67. Napoletano, C.; Porta, E.; Allegrini, P.; Castaldi, G.
68. Braude, V.; Finkelstein, N.; Chen, K.; Pilarsky, G.; Liberman, A.; Singer, C.; Raizi, Y.
69. Westwell, A. Ph.D Thesis. University of Leeds, 1993.
70. K. Aggarwal, V.; Gultekin, Z.; S. Grainger, R.; Adams, H.; L. Spargo, P., *J. Chem. Soc., Perkin Trans. 1*, **1998**, 2771-2782.
71. Kowalski, P.; Mitka, K.; Ossowska, K.; Kolarska, Z., *Tetrahedron*, **2005**, 61, 1933-1953.
72. Kaczorowska, K.; Kolarska, Z.; Mitka, K.; Kowalski, P., *Tetrahedron*, **2005**, 61, 8315-8327.
73. Rayner, C. M., *Contemp. Org. Synth.*, **1994**, 1, 191-203.
74. Rayner, C. M., *Contemp. Org. Synth.*, **1995**, 2, 409-440.
75. Baird, C. P.; Rayner, C. M., *J. Chem. Soc., Perkin Trans. 1*, **1998**, 1973-2004.

76. Procter, D. J., *J. Chem. Soc., Perkin Trans. I*, **1999**, 641-668.
77. Kirihara, M.; Yamamoto, J.; Noguchi, T.; Itou, A.; Naito, S.; Hirai, Y., *Tetrahedron*, **2009**, *65*, 10477-10484.
78. Kinen, C. O.; Rossi, L. I.; de Rossi, R. H., *J. Org. Chem.*, **2009**, *74*, 7132-7139.
79. Matteucci, M.; Bhalay, G.; Bradley, M., *Org. Lett.*, **2003**, *5*, 235-237.
80. Mba, M.; Prins, L. J.; Licini, G., *Org. Lett.*, **2006**, *9*, 21-24.
81. Kumar, S.; Verma, S.; Jain, S. L.; Sain, B., *Tetrahedron Lett.*, **2011**, *52*, 3393-3396.
82. Secci, F.; Arca, M.; Frongia, A.; Piras, P. P., *Catal. Sci. Technol.*, **2014**, *4*, 1407-1415.
83. Imada, Y.; Iida, H.; Ono, S.; Murahashi, S. I., *J. Am. Chem. Soc.*, **2003**, *125*, 2868-2869.
84. Imada, Y.; Kitagawa, T.; Iwata, S.; Komiya, N.; Naota, T., *Tetrahedron*, **2014**, *70*, 495-501.
85. Jeon, H. B.; Kim, K. T.; Kim, S. H., *Tetrahedron Lett.*, **2014**, *55*, 3905-3908.
86. Adam, W.; Saha Möller, C. R.; Ganeshpure, P. A., *Chem. Rev.*, **2001**, *101*, 3499-3548.
87. Stingl, K. A.; Tsogoeva, S. B., *Tetrahedron: Asymmetry*, **2010**, *21*, 1055-1074.
88. Mahamuni, N. N.; Gogate, P. R.; Pandit, A. B., *Ind. Eng. Chem. Res.*, **2006**, *45*, 8829-8836.
89. Lacombe, S.; Cardy, H.; Simon, M.; Khoukh, A.; Soumillion, J. P.; Ayadim, M., *Photochem. Photobiol. Sci.*, **2002**, *1*, 347-354.
90. Hajipour, A. R.; Kooshki, B.; Ruoho, A. E., *Tetrahedron Lett.*, **2005**, *46*, 5503-5506.
91. Caron, S.; Dugger, R. W.; Ruggeri, S. G.; Ragan, J. A.; Ripin, D. H. B., *Chem. Rev.*, **2006**, *106*, 2943-2989.
92. Khatri, P. K.; Jain, S. L.; Sain, B., *Ind. Eng. Chem. Res.*, **2011**, *50*, 701-704.
93. Bahrami, K.; Khodaei, M. M.; Sheikh Arabi, M., *J. Org. Chem.*, **2010**, *75*, 6208-6213.
94. Surya Prakash, G. K.; Shakhmin, A.; Glington, K. E.; Rao, S.; Mathew, T.; Olah, G. A., *Green Chem.*, **2014**, *16*, 3616-3622.
95. Fogassy, E.; Nogradi, M.; Kozma, D.; Egri, G.; Palovics, E.; Kiss, V., *Org. Biomol. Chem.*, **2006**, *4*, 3011-3030.
96. Blaser, H. U.; Spindler, F.; Studer, M., *Appl. Catal., A*, **2001**, *221*, 119-143.
97. Maier, N. M.; Franco, P.; Lindner, W., *J. Chromatogr. A*, **2001**, *906*, 3-33.
98. Nishi, T.; Nakajima, K.; Iio, Y.; Ishibashi, K.; Fukazawa, T., *Tetrahedron: Asymmetry*, **1998**, *9*, 2567-2570.
99. Osorio-Lozada, A.; Prisinzano, T.; Olivo, H. F., *Tetrahedron: Asymmetry*, **2004**, *15*, 3811-3815.
100. Noguchi, T.; Miyagawa, T.; Satoh, T., *Tetrahedron: Asymmetry*, **2009**, *20*, 2073-2076.
101. Cope, A. C.; Caress, E. A., *J. Am. Chem. Soc.*, **1966**, *88*, 1711-1713.
102. Redondo, J.; Capdevila, A.; Latorre, I.; Bertrán, J., *J. Inclusion Phenom. Macrocyclic Chem.*, **2012**, *73*, 225-236.

103. Mikolajczyk, M.; Drabowicz, J.; Cramer, F., *J. Chem. Soc., Chem. Commun.*, **1971**, 317-318.
104. Bortolini, O.; Fantin, G.; Fogagnolo, M.; Medici, A.; Pedrini, P., *Chem. Commun.*, **2000**, 365-366.
105. Jin, Z.; Yong, Q.; Ze, H.; Fang Min, F.; Zhong Yuan, Z.; Jin Gen, D.; Yao Zhong, J.; Tay Yuan, C., *Tetrahedron: Asymmetry*, **1997**, 8, 2505-2508.
106. Toda, F.; Tanaka, K.; Nagamatsu, S., *Tetrahedron Lett.*, **1984**, 25, 4929-4932.
107. Pellissier, H., *Adv. Synth. Catal.*, **2011**, 353, 1613-1666.
108. Vedejs, E.; Jure, M., *Angew. Chem., Int. Ed.*, **2005**, 44, 3974-4001.
109. Mikolajczyk, M.; Para, M., *J. Chem. Soc. D*, **1969**, 1192-1193.
110. Mikolajczyk, M.; Drabowicz, J., *Phosphorus Sulfur Relat. Elem.*, **1976**, 1, 301-303.
111. Annunziata, R.; Borgogno, G.; Montanari, F.; Quici, S.; Cucinella, S., *J. Chem. Soc., Perkin Trans. 1*, **1981**, 113-118.
112. Hanlon, S. P.; Graham, D. L.; Hogan, P. J.; Holt, R. A.; Reeve, C. D.; Shaw, A. L.; McEwan, A. G., *Microbiology (Reading, England)*, **1998**, 144, 2247-53.
113. Boyd, D. R.; Sharma, N. D.; King, A. W.; Shepherd, S. D.; Allen, C. C.; Holt, R. A.; Luckarift, H. R.; Dalton, H., *Org. Biomol. Chem.*, **2004**, 2, 554-61.
114. Abo, M.; Tachibana, M.; Okubo, A.; Yamazaki, S., *Bioorg. Med. Chem.*, **1995**, 3, 109-112.
115. Marchese, G.; Naso, F.; Ronzini, L., *J. Chem. Soc., Chem. Commun.*, **1974**, 830-831.
116. Ohta, H.; Kato, Y.; Tsuchihashi, G. I., *Chem. Lett.*, **1986**, 15, 217-218.
117. Burgess, K.; Henderson, I., *Tetrahedron Lett.*, **1989**, 30, 3633-3636.
118. Kwiatkowska, M.; Janicki, I.; Kielbasiński, P., *J. Mol. Catal. B: Enzym.*, **2015**, 118, 23-28.
119. Serreqi, A. N.; Kazlauskas, R. J., *Can. J. Chem.*, **1995**, 73, 1357-1367.
120. Li, A.-T.; Yu, H.-L.; Pan, J.; Zhang, J.-D.; Xu, J.-H.; Lin, G.-Q., *Bioresour. Technol.*, **2011**, 102, 1537-1542.
121. Toda, F.; Mori, K.; Matsuura, Y.; Akai, H., *J. Chem. Soc., Chem. Commun.*, **1990**, 1591-1593.
122. Matlin, S. A.; Tiritan, M. E.; Cass, Q. B.; Boyd, D. R., *Chirality*, **1996**, 8, 147-152.
123. Gegenava, M.; Chankvetadze, L.; Farkas, T.; Chankvetadze, B., *J. Sep. Sci.*, **2014**, 37, 1083-1088.
124. Belaz, K. R.; Denadai, M.; Almeida, A. P.; Lima, R. T.; Vasconcelos, M. H.; Pinto, M. M.; Cass, Q. B.; Oliveira, R. V., *J. Pharm. Biomed. Anal.*, **2012**, 66, 100-8.
125. Cotton, H.; Elebring, T.; Larsson, M.; Li, L.; Sorensen, H.; von Unge, S., *Tetrahedron: Asymmetry*, **2000**, 11, 3819-3825.
126. Guan, J.; Li, J.; Yan, F.; Gu, H.; Li, F., *Chromatographia*, **2009**, 70, 1039-1044.

127. Tanaka, M.; Yamazaki, H.; Hakusui, H., *Chirality*, **1995**, *7*, 612-615.
128. West, C., *Curr. Anal. Chem.*, **2014**, *10*, 99-120.
129. Kalíková, K.; Šlechtová, T.; Vozka, J.; Tesařová, E., *Anal. Chim. Acta*, **2014**, *821*, 1-33.
130. Toribio, L.; Alonso, C.; del Nozal, M. J.; Bernal, J. L.; Jimenez, J. J., *J. Sep. Sci.*, **2006**, *29*, 1363-72.
131. del Nozal, M. J.; Toribio, L.; Bernal, J. L.; Nieto, E. M.; Jiménez, J. J., *J. Biochem. Biophys. Methods*, **2002**, *54*, 339-345.
132. Gargaro, G.; Gasparri, F.; Misiti, D.; Palmieri, G.; Pierini, M.; Villani, C., *Chromatographia*, **1987**, *24*, 505-509.
133. Altomare, C.; Carotti, A.; Cellamare, S.; Fanelli, F.; Gasparri, F.; Villani, C.; Carrupt, P. A.; Testa, B., *Chirality*, **1993**, *5*, 527-537.
134. Allenmark, S.; Nielsen, L.; Pirkle, W. H., *Acta Chem. Scand., Ser. B*, **1983**, *B37*, 325-8.
135. Tanaka, K.; Muraoka, T.; Hirayama, D.; Ohnishi, A., *Chem. Commun.*, **2012**, *48*, 8577-8579.
136. Nuzhdin, A. L.; Dybtsev, D. N.; Bryliakov, K. P.; Talsi, E. P.; Fedin, V. P., *J. Am. Chem. Soc.*, **2007**, *129*, 12958-12959.
137. Zhang, J. H.; Xie, S. M.; Chen, L.; Wang, B. J.; He, P. G.; Yuan, L. M., *Anal. Chem.*, **2015**.
138. Berthod, A.; Xiao, T. L.; Liu, Y.; Jenks, W. S.; Armstrong, D. W., *J. Chromatogr. A*, **2002**, *955*, 53-69.
139. Allenmark, S.; Bomgren, B.; Boren, H.; Lagerstrom, P. O., *Anal. Biochem.*, **1984**, *136*, 293-7.
140. Mitchell, C.; Desai, M.; McCulla, R.; Jenks, W.; Armstrong, D., *Chromatographia*, **2002**, *56*, 127-135.
141. Rodriguez, M. A.; Liu, Y.; McCulla, R.; Jenks, W. S.; Armstrong, D. W., *Electrophoresis*, **2002**, *23*, 1561-1570.
142. Anderson, J. L.; Ding, J.; McCulla, R. D.; Jenks, W. S.; Armstrong, D. W., *J. Chromatogr. A*, **2002**, *946*, 197-208.
143. Soloshonok, V. A., *Angew. Chem., Int. Ed.*, **2006**, *45*, 766-769.
144. Soloshonok, V. A.; Roussel, C.; Kitagawa, O.; Sorochinsky, A. E., *Chem. Soc. Rev.*, **2012**, *41*, 4180-4188.
145. Han, J.; Kitagawa, O.; Wzorek, A.; Klika, K. D.; Soloshonok, V. A., *Chem. Sci.*, **2018**.
146. Suzuki, Y.; Han, J.; Kitagawa, O.; Acena, J. L.; Klika, K. D.; Soloshonok, V. A., *RSC Adv.*, **2015**, *5*, 2988-2993.
147. Han, J.; Soloshonok, V. A.; Klika, K. D.; Drabowicz, J.; Wzorek, A., *Chem. Soc. Rev.*, **2018**.
148. Diter, P.; Taudien, S.; Samuel, O.; Kagan, H. B., *J. Org. Chem.*, **1994**, *59*, 370-373.

149. Wzorek, A.; Klika, K. D.; Drabowicz, J.; Sato, A.; Acena, J. L.; Soloshonok, V. A., *Org. Biomol. Chem.*, **2014**, *12*, 4738-4746.
150. Song, W.; Zhou, Y.; Fu, Y.; Xu, W., *Tetrahedron: Asymmetry*, **2013**, *24*, 909-912.
151. Baciocchi, R.; Zenoni, G.; Valentini, M.; Mazzotti, M.; Morbidelli, M., *J. Phys. Chem. A*, **2002**, *106*, 10461-10469.
152. Sun, J.; Zhu, C.; Dai, Z.; Yang, M.; Pan, Y.; Hu, H., *J. Org. Chem.*, **2004**, *69*, 8500-8503.
153. Tanaka, H.; Nishikawa, H.; Uchida, T.; Katsuki, T., *J. Am. Chem. Soc.*, **2010**, *132*, 12034-12041.
154. Andersen, K. K., *Tetrahedron Lett.*, **1962**, 93-95.
155. Andersen, K. K.; Gaffield, W.; Papanikolaou, N. E.; Foley, J. W.; Perkins, R. I., *J. Am. Chem. Soc.*, **1964**, *86*, 5637-5646.
156. Axelrod, M.; Bickart, P.; Goldstein, M. L.; Green, M. M.; Kjær, A.; Mislow, K., *Tetrahedron Lett.*, **1968**, *9*, 3249-3252.
157. Montanari, F., *Tetrahedron Lett.*, **1965**, *6*, 3367-3371.
158. Axelrod, M.; Bickart, P.; Jacobus, J.; Green, M. M.; Mislow, K., *J. Am. Chem. Soc.*, **1968**, *90*, 4835-4842.
159. Mislow, K.; Green, M. M.; Raban, M., *J. Am. Chem. Soc.*, **1965**, *87*, 2761-2762.
160. Maccioni, A.; Montanari, F.; Secci, M.; Tramontini, M., *Tetrahedron Lett.*, **1961**, *2*, 607-611.
161. Mioskowski, C.; Solladie, G., *Tetrahedron*, **1980**, *36*, 227-236.
162. Klunder, J. M.; Sharpless, K. B., *J. Org. Chem.*, **1987**, *52*, 2598-2602.
163. Pyne, S. G.; Hajipour, A. R.; Prabakaran, K., *Tetrahedron Lett.*, **1994**, *35*, 645-648.
164. Cherkaoui, M. Z.; Nicoud, J.-F., *New J. Chem.*, **1995**, *19*, 851-861.
165. Harpp, D. N.; Vines, S. M.; Montillier, J. P.; Chan, T. H., *J. Org. Chem.*, **1976**, *41*, 3987-3992.
166. Andersen, K. K.; Bujnicki, B.; Drabowicz, J.; Mikolajczyk, M.; O'Brien, J. B., *J. Org. Chem.*, **1984**, *49*, 4070-4072.
167. Whitesell, J. K.; Wong, M. S., *J. Org. Chem.*, **1991**, *56*, 4552-4554.
168. Whitesell, J. K.; Wong, M.-S., *J. Org. Chem.*, **1994**, *59*, 597-601.
169. Shibata, N.; Matsunaga, M.; Nakagawa, M.; Fukuzumi, T.; Nakamura, S.; Toru, T., *J. Am. Chem. Soc.*, **2005**, *127*, 5271-5271.
170. Lu, B. Z.; Jin, F.; Zhang, Y.; Wu, X.; Wald, S. A.; Senanayake, C. H., *Org. Lett.*, **2005**, *7*, 1465-1468.
171. Evans, D. A.; Faul, M. M.; Colombo, L.; Bisaha, J. J.; Clardy, J.; Cherry, D., *J. Am. Chem. Soc.*, **1992**, *114*, 5977-5985.

172. Oppolzer, W.; Froelich, O.; Wiaux-Zamar, C.; Bernardinelli, G., *Tetrahedron Lett.*, **1997**, 38, 2825-2828.
173. Nakamura, S.; Tateyama, M.; Sugimoto, H.; Nakagawa, M.; Watanabe, Y.; Shibata, N.; Toru, T., *Chirality*, **2005**, 17, 85-88.
174. Ridley, D. D.; Smal, M. A., *J. Chem. Soc., Chem. Commun.*, **1981**, 505-506.
175. Llera, J. M.; Fernández, I.; Alcudia, F., *Tetrahedron Lett.*, **1991**, 32, 7299-7302.
176. Fernandez, I.; Khiar, N.; Llera, J. M.; Alcudia, F., *J. Org. Chem.*, **1992**, 57, 6789-6796.
177. Khiar, N.; Fernández, I.; Alcudia, F., *Tetrahedron Lett.*, **1994**, 35, 5719-5722.
178. Fernández, I.; Khiar, N.; Roca, A.; Benabra, A.; Alcudia, A.; Espartero, J.; Alcudia, F., *Tetrahedron Lett.*, **1999**, 40, 2029-2032.
179. Balcells, D.; Ujaque, G.; Fernandez, I.; Khiar, N.; Maseras, F., *J. Org. Chem.*, **2006**, 71, 6388-6396.
180. Balcells, D.; Ujaque, G.; Fernández, I.; Khiar, N.; Maseras, F., *Adv. Synth. Catal.*, **2007**, 349, 2103-2110.
181. Chelouan, A.; Recio, R.; Alcudia, A.; Khiar, N.; Fernández, I., *Eur. J. Org. Chem.*, **2014**, 2014, 6935-6944.
182. Rebiere, F.; Kagan, H. B., *Tetrahedron Lett.*, **1989**, 30, 3659-3662.
183. Kagan, H. B.; Rebiere, F., *Synlett*, **1990**, 643-650.
184. Rebiere, F.; Samuel, O.; Ricard, L.; Kagan, H. B., *J. Org. Chem.*, **1991**, 56, 5991-5999.
185. Pelloux-Léon, N.; Gautier-Luneau, I.; Wendt, S.; Vallée, Y., *Tetrahedron: Asymmetry*, **1996**, 7, 1007-1010.
186. Wudl, F.; Lee, T. B. K., *J. Chem. Soc., Chem. Commun.*, **1972**, 61-62.
187. Wudl, F.; Lee, T. B. K., *J. Am. Chem. Soc.*, **1973**, 95, 6349-6358.
188. Benson, S. C.; Snyder, J. K., *Tetrahedron Lett.*, **1991**, 32, 5885-5888.
189. Han, Z.; Krishnamurthy, D.; Grover, P.; Fang, Q. K.; Senanayake, C. H., *J. Am. Chem. Soc.*, **2002**, 124, 7880-7881.
190. Han, Z.; Krishnamurthy, D.; Grover, P.; Wilkinson, H. S.; Fang, Q. K.; Su, X.; Lu, Z.-H.; Magiera, D.; Senanayake, C. H., *Angew. Chem., Int. Ed.*, **2003**, 42, 2032-2035.
191. Han, Z.; Krishnamurthy, D.; Grover, P.; Fang, Q. K.; Su, X.; Wilkinson, H. S.; Lu, Z.-H.; Magiera, D.; Senanayake, C. H., *Tetrahedron*, **2005**, 61, 6386-6408.
192. Han, Z.; Song, J. J.; Yee, N. K.; Xu, Y.; Tang, W.; Reeves, J. T.; Tan, Z.; Wang, X.-j.; Lu, B.; Krishnamurthy, D.; Senanayake, C. H., *Org. Process Res. Dev.*, **2007**, 11, 605-608.
193. García Ruano, J. L.; Alemparte, C.; Aranda, M. T.; Zarzuelo, M. M., *Org. Lett.*, **2003**, 5, 75-78.
194. Qin, Y.; Wang, C.; Huang, Z.; Xiao, X.; Jiang, Y., *J. Org. Chem.*, **2004**, 69, 8533-8536.
195. Balenović, K.; Bregant, N.; Francetić, D., *Tetrahedron Lett.*, **1960**, 1, 20-22.

196. Folli, U.; Iarossi, D.; Montanari, F.; Torre, G., *J. Chem. Soc. C*, **1968**, 1317-1322.
197. Pirkle, W. H.; Rinaldi, P. L., *J. Org. Chem.*, **1977**, *42*, 2080-2082.
198. Aoki, M.; Seebach, D., *Helv. Chim. Acta*, **2001**, *84*, 187-207.
199. Colonna, S.; Pironi, V.; Drabowicz, J.; Brebion, F.; Fensterbank, L.; Malacria, M., *Eur. J. Org. Chem.*, **2005**, *2005*, 1727-1730.
200. Dieva, S. A.; Eliseenkova, R. M.; Efremov, Y. Y.; Sharafutdinova, D. R.; Bredikhin, A. A., *Russ J Org Chem*, **2006**, *42*, 12-16.
201. Sato, Y.; Kunieda, N.; Kinoshita, M., *Chem. Lett.*, **1976**, *5*, 563-566.
202. Masayoshi, K.; Yoshiyasu, S.; Norio, K., *Chem. Lett.*, **1974**, *3*, 377-380.
203. Williamson, K. S.; Michaelis, D. J.; Yoon, T. P., *Chem. Rev.*, **2014**, *114*, 8016-8036.
204. Della Sala, G.; Lattanzi, A., *ACS Catal.*, **2014**, *4*, 1234-1245.
205. Davis, F. A., *J. Org. Chem.*, **2006**, *71*, 8993-9003.
206. Davis, F. A.; Sheppard, A. C., *Tetrahedron*, **1989**, *45*, 5703-5742.
207. Davis, F. A.; Jenkins, R.; Yocklovich, S. G., *Tetrahedron Lett.*, **1978**, *19*, 5171-5174.
208. Davis, F. A.; Lal, S. G.; Durst, H. D., *J. Org. Chem.*, **1988**, *53*, 5004-5007.
209. Davis, F. A.; Jenkins, R.; Rizvi, S. Q. A.; Panunto, T. W., *J. Chem. Soc., Chem. Commun.*, **1979**, 600-601.
210. Davis, F. A.; Jenkins, R. H.; Awad, S. B.; Stringer, O. D.; Watson, W. H.; Galloy, J., *J. Am. Chem. Soc.*, **1982**, *104*, 5412-5418.
211. Davis, F. A.; Billmers, J. M., *J. Org. Chem.*, **1983**, *48*, 2672-2675.
212. Davis, F. A.; McCauley, J. P.; Harakal, M. E., *J. Org. Chem.*, **1984**, *49*, 1465-1467.
213. Davis, F. A.; McCauley, J. P.; Chattopadhyay, S.; Harakal, M. E.; Towson, J. C.; Watson, W. H.; Tavanaiepour, I., *J. Am. Chem. Soc.*, **1987**, *109*, 3370-3377.
214. Davis, F. A.; Towson, J. C.; Weismiller, M. C.; Lal, S.; Carroll, P. J., *J. Am. Chem. Soc.*, **1988**, *110*, 8477-8482.
215. Davis, F. A.; Weismiller, M. C.; Murphy, C. K.; Reddy, R. T.; Chen, B. C., *J. Org. Chem.*, **1992**, *57*, 7274-7285.
216. Davis, F. A.; Reddy, R. T.; Han, W.; Reddy, R. E., *Pure Appl. Chem.*, **1993**, *65*, 633-40.
217. Davis, F. A.; Reddy, R. T.; Han, W.; Carroll, P. J., *J. Am. Chem. Soc.*, **1992**, *114*, 1428-1437.
218. Davis, F. A.; Thimmareddy, R.; Weismiller, M. C., *J. Am. Chem. Soc.*, **1989**, *111*, 5964-5965.
219. Schwan, A. L.; Pippert, M. F., *Tetrahedron: Asymmetry*, **1995**, *6*, 131-138.
220. Colombo, A.; Albericio, F.; Forns, P., *Tetrahedron: Asymmetry*, **2006**, *17*, 3327-3331.
221. Davis, F. A.; Reddy, R. T.; McCauley, J. P.; Przeslawski, R. M.; Harakal, M. E.; Carroll, P. J., *J. Org. Chem.*, **1991**, *56*, 809-815.

222. Davis, F. A.; Reddy, R. E.; Kasu, P. V. N.; Portonovo, P. S.; Carroll, P. J., *J. Org. Chem.*, **1997**, *62*, 3625-3630.
223. Page, P. C. B.; Heer, J. P.; Bethell, D.; Collington, E. W.; Andrews, D. M., *Tetrahedron Lett.*, **1994**, *35*, 9629-9632.
224. Bulman Page, P. C.; Heer, J. P.; Bethell, D.; Andrew Lund, B., *Phosphorus Sulfur Relat. Elem.*, **1999**, *153*, 247-258.
225. Bulman Page, P. C.; Heer, J. P.; Bethell, D.; Collington, E. W.; Andrews, D. M., *Tetrahedron: Asymmetry*, **1995**, *6*, 2911-2914.
226. Bethell, D.; Bulman Page, P. C.; Vahedi, H., *J. Org. Chem.*, **2000**, *65*, 6756-6760.
227. Hanquet, G.; Lusinchi, X.; Milliet, P., *Tetrahedron Lett.*, **1988**, *29*, 2817-2818.
228. Bohé, L.; Hanquet, G.; Lusinchi, M.; Lusinchi, X., *Tetrahedron Lett.*, **1993**, *34*, 7271-7274.
229. Bohé, L.; Lusinchi, M.; Lusinchi, X., *Tetrahedron*, **1999**, *55*, 155-166.
230. Akhatou, A.; Rahimi, M.; Cheboub, K.; Ghosez, L.; Hanquet, G., *Tetrahedron*, **2007**, *63*, 6232-6240.
231. del Río, R. E.; Wang, B.; Achab, S.; Bohé, L., *Org. Lett.*, **2007**, *9*, 2265-2268.
232. Jennings, W. B.; Kochanewycz, M. J.; Lovely, C. J.; Boyd, D. R., *J. Chem. Soc., Chem. Commun.*, **1994**, 2569-2570.
233. Higuchi, T.; Pitman, I. H.; Gensch, K.-H., *J. Am. Chem. Soc.*, **1966**, *88*, 5676-5677.
234. Tsuneo, I.; Hiroyasu, K., *Chem. Lett.*, **1986**, *15*, 967-968.
235. Tohma, H.; Takizawa, S.; Watanabe, H.; Fukuoka, Y.; Maegawa, T.; Kita, Y., *J. Org. Chem.*, **1999**, *64*, 3519-3523.
236. Ozanne-Beaudenon, A.; Quideau, S., *Tetrahedron Lett.*, **2006**, *47*, 5869-5873.
237. Tohma, H. T., S.; Morioka, H.; Maegawa, T.; Kita, Y., *Chem. Pharm. Bull.*, **2000**, *48*, 445-446.
238. Zhdankin, V. V., *J. Org. Chem.*, **2011**, *76*, 1185-1197.
239. Ladziata, U.; Zhdankin, V. V., *Synlett*, **2007**, *2007*, 0527-0537.
240. Zhdankin, V. V.; Smart, J. T.; Zhao, P.; Kiprof, P., *Tetrahedron Lett.*, **2000**, *41*, 5299-5302.
241. Ladziata, U.; Carlson, J.; Zhdankin, V. V., *Tetrahedron Lett.*, **2006**, *47*, 6301-6304.
242. Crini, G., *Chem. Rev.*, **2014**, *114*, 10940-10975.
243. Czarnik, A. W., *J. Org. Chem.*, **1984**, *49*, 924-927.
244. Drabowicz, J.; Mikołajczyk, M., *Phosphorus Sulfur Relat. Elem.*, **1984**, *21*, 245-248.
245. Surendra, K.; Krishnaveni, N. S.; Kumar, V. P.; Sridhar, R.; Rao, K. R., *Tetrahedron Letters*, **2005**, *46*, 4581-4583.
246. Mojz, V.; Budesinsky, M.; Cibulka, R.; Kraus, T., *Org. Biomol. Chem.*, **2011**, *9*, 7318-26.

247. Mojr, V.; Herzig, V.; Budesinsky, M.; Cibulka, R.; Kraus, T., *Chem. Commun.*, **2010**, 46, 7599-7601.
248. Cibulka, R., *Eur. J. Org. Chem.*, **2015**, 915-932.
249. Shinkai, S.; Yamaguchi, T.; Manabe, O.; Toda, F., *J. Chem. Soc., Chem. Commun.*, **1988**, 1399-1401.
250. Murahashi, S.-I., *Angew. Chem., Int. Ed. Engl.*, **1995**, 34, 2443-2465.
251. Jurok, R.; Cibulka, R.; Dvořáková, H.; Hampl, F.; Hodačová, J., *Eur. J. Org. Chem.*, **2010**, 2010, 5217-5224.
252. Jurok, R.; Hodačová, J.; Eigner, V.; Dvořáková, H.; Setnička, V.; Cibulka, R., *Eur. J. Org. Chem.*, **2013**, 2013, 7724-7738.
253. Liao, S.; Čorić, I.; Wang, Q.; List, B., *J. Am. Chem. Soc.*, **2012**, 134, 10765-10768.
254. Liu, Z.-M.; Zhao, H.; Li, M.-Q.; Lan, Y.-B.; Yao, Q.-B.; Tao, J.-C.; Wang, X.-W., *Adv. Synth. Catal.*, **2012**, 354, 1012-1022.
255. Jindal, G.; Sunoj, R. B., *Angew. Chem., Int. Ed.*, **2014**, 53, 4432-4436.
256. Held, F. E.; Stingl, K. A.; Tsogoeva, S. B., *Symmetry*, **2017**, 9, 9.
257. Firth, B. E.; Miller, L. L., *J. Am. Chem. Soc.*, **1976**, 98, 8272-8273.
258. Komori, T.; Nonaka, T., *J. Am. Chem. Soc.*, **1983**, 105, 5690-5691.
259. Komori, T.; Nonaka, T., *J. Am. Chem. Soc.*, **1984**, 106, 2656-2659.
260. Taghizadeh, M. J., *Iran. J. Sci. Technol., Trans. A: Sci.*, **2017**, 41, 355-361.
261. Guo, C.; Wu, Z.-L., *Enzyme Microb. Technol.*, **2017**, 106, 28-34.
262. Kylosova, T. I.; Elkin, A. A.; Grishko, V. V.; Ivshina, I. B., *J. Mol. Catal. B: Enzym.*, **2016**, 123, 8-13.
263. Holland, H. L., *Nat. Prod. Rep.*, **2001**, 18, 171-181.
264. Holland, H. L., *Chem. Rev.*, **1988**, 88, 473-485.
265. Dodson, R. M. N., N.; Tsuchiya, H. M., *J. Org. Chem.*, **1962**, 27, 2707-2708.
266. Auret, B. J.; Boyd, D. R.; Henbest, H. B.; Ross, S., *J. Chem. Soc. C*, **1968**, 2371-2374.
267. Holland, H. L.; Brown, F. M.; Larsen, B. G.; Zabic, M., *Tetrahedron: Asymmetry*, **1995**, 6, 1569-74.
268. Holland, H. L.; Gu, J.-X.; Kerridge, A.; Willetts, A., *Biocatal. Biotransform.*, **1999**, 17, 305-317.
269. Holland, H. L.; Brown, F. M.; Larsen, B. G., *Tetrahedron: Asymmetry*, **1994**, 5, 1241-1248.
270. Holland, H. L.; Brown, F. M.; Larsen, B. G., *Bioorg. Med. Chem.*, **1994**, 2, 647-652.
271. Holland, H. L.; Brown, F. M.; Larsen, B. G., *Tetrahedron: Asymmetry*, **1995**, 6, 1561-1567.
272. Holland, H. L.; Brown, F. M.; Lakshmaiah, G.; Larsen, B. G.; Patel, M., *Tetrahedron: Asymmetry*, **1997**, 8, 683-697.

273. Holland, H. L.; Bornmann, M. J.; Lakshmaiah, G., *J. Mol. Catal. B: Enzym.*, **1996**, *1*, 97-102.
274. Holland, H. L.; Brown, F. M.; Kerridge, A.; Turner, C. D., *J. Mol. Catal. B: Enzym.*, **1999**, *6*, 463-471.
275. Rossi, C.; Fauve, A.; Madesclaire, M.; Roche, D.; Davis, F. A.; Reddy, R. T., *Tetrahedron: Asymmetry*, **1992**, *3*, 629-636.
276. Pinedo-Rivilla, C.; Aleu, J.; Collado, I. G., *J. Mol. Catal. B: Enzym.*, **2007**, *49*, 18-23.
277. Ricci, L. C.; Comasseto, J. V.; Andrade, L. H.; Capelari, M.; Cass, Q. B.; Porto, A. L. M., *Enzyme Microb. Technol.*, **2005**, *36*, 937-946.
278. Barth, T.; Hilario, V. C.; Rocha, B. A.; Furtado, N.; Pupo, M. T.; de Oliveira, A. R. M., *Quim. Nova*, **2015**, *38*, 944-947.
279. Argoudelis, A. D.; Mason, D. J., *J. Antibiot.*, **1969**, *22*, 289-91.
280. Argoudelis, A. D.; Mason, D. J., *J. Antibiot.*, **1969**, *22*, 309-314.
281. Adam, W.; Heckel, F.; Saha-Möller, C. R.; Taupp, M.; Schreier, P., *Tetrahedron: Asymmetry*, **2004**, *15*, 983-985.
282. Ohta, H.; Okamoto, Y.; Tsuchihashi, G.-i., *Chem. Lett.*, **1984**, *13*, 205-208.
283. Ohta, H.; Okamoto, Y.; Tsuchihashi, G.-i., *Agric. Biol. Chem.*, **1985**, *49*, 671-676.
284. Ohta, H.; Okamoto, Y.; Tsuchihashi, G.-i., *Agric. Biol. Chem.*, **1985**, *49*, 2229-2231.
285. Elkin, A. A.; Kylosova, T. I.; Grishko, V. V.; Ivshina, I. B., *J. Mol. Catal. B: Enzym.*, **2013**, *89*, 82-85.
286. Mahmoudian, M.; Michael, A., *J. Biotechnol.*, **1993**, *27*, 173-179.
287. Olivo, H. F.; Osorio-Lozada, A.; Peeples, T. L., *Tetrahedron: Asymmetry*, **2005**, *16*, 3507-3511.
288. Daligault, F.; Nugier-Chauvin, C.; Patin, H., *Org. Biomol. Chem.*, **2006**, *4*, 1474-1477.
289. Tang, J.; Brackenridge, I.; Roberts, S. M.; Beecher, J.; Willetts, A. J., *Tetrahedron*, **1995**, *51*, 13217-13238.
290. Beecher, J.; Richardson, P.; Roberts, S.; Willetts, A., *Biotechnol. Lett.*, **1995**, *17*, 1069-1074.
291. Beecher, J.; Richardson, P.; Willetts, A., *Biotechnol. Lett.*, **1994**, *16*, 909-912.
292. Colonna, S.; Sordo, S. D.; Gaggero, N.; Carrea, G.; Pasta, P., *Heteroat. Chem.*, **2002**, *13*, 467-473.
293. Dembitsky, V. M., *Tetrahedron*, **2003**, *59*, 4701-4720.
294. van Deurzen, M. P. J.; van Rantwijk, F.; Sheldon, R. A., *Tetrahedron*, **1997**, *53*, 13183-13220.
295. Velde, F. v. d.; Rantwijk, F. v.; Sheldon, R. A., *Trends Biotechnol.*, **2001**, *19*, 73-80.
296. Morris, D. R.; Hager, L. P., *J. Biol. Chem.*, **1966**, *241*, 1763-1768.

297. Kobayashi, S.; Nakano, M.; Kimura, T.; Schaap, A. P., *Biochemistry*, **1987**, *26*, 5019-5022.
298. Colonna, S.; Gaggero, N.; Casella, L.; Carrea, G.; Pasta, P., *Tetrahedron: Asymmetry*, **1992**, *3*, 95-106.
299. Colonna, S.; Gaggero, N.; Carrea, G.; Pasta, P., *Chem. Commun.*, **1997**, 439-440.
300. van Deurzen, M. P. J.; Remkes, I. J.; van Rantwijk, F.; Sheldon, R. A., *J. Mol. Catal. A: Chem.*, **1997**, *117*, 329-337.
301. Vargas, R. R.; Bechara, E. J. H.; Marzorati, L.; Wladislaw, B., *Tetrahedron-Asymmetry*, **1999**, *10*, 3219-3227.
302. Lütz, S.; Steckhan, E.; Liese, A., *Electrochem. Commun.*, **2004**, *6*, 583-587.
303. Karmee, S. K.; Roosen, C.; Kohlmann, C.; Lutz, S.; Greiner, L.; Leitner, W., *Green Chem.*, **2009**, *11*, 1052-1055.
304. Perez, D. I.; Grau, M. M.; Arends, I. W. C. E.; Hollmann, F., *Chem. Commun.*, **2009**, 6848-6850.
305. Wang, W.; Xu, Y.; Wang, D. I. C.; Li, Z., *J. Am. Chem. Soc.*, **2009**, *131*, 12892-12893.
306. Tuynman, A.; Vink, M. K. S.; Dekker, H. L.; Schoemaker, H. E.; Wever, R., *Eur. J. Biochem.*, **1998**, *258*, 906-913.
307. Ozaki, S.-I.; Ortiz de Montellano, P. R., *J. Am. Chem. Soc.*, **1994**, *116*, 4487-4488.
308. Ozaki, S.-i.; Ortiz de Montellano, P. R., *J. Am. Chem. Soc.*, **1995**, *117*, 7056-7064.
309. Tuynman, A.; Schoemaker, H. E.; Wever, R., *Monatsh. Chem.*, **2000**, *131*, 687-695.
310. ten Brink, H. B.; Holland, H. L.; Schoemaker, H. E.; van Lingen, H.; Wever, R., *Tetrahedron: Asymmetry*, **1999**, *10*, 4563-4572.
311. ten Brink, H. B.; Tuynman, A.; Dekker, H. L.; Hemrika, W.; Izumi, Y.; Oshiro, T.; Schoemaker, H. E.; Wever, R., *Inorg. Chem.*, **1998**, *37*, 6780-6784.
312. Butler, A.; Walker, J. V., *Chem. Rev.*, **1993**, *93*, 1937-1944.
313. Sheffield, D. J.; Harry, T. R.; Smith, A. J.; Rogers, L. J., *Biotechnol. Tech.*, **1994**, *8*, 579-582.
314. Yu, H.; Whittaker, J. W., *Biochem. Biophys. Res. Commun.*, **1989**, *160*, 87-92.
315. Andersson, M.; Willetts, A.; Allenmark, S., *J. Org. Chem.*, **1997**, *62*, 8455-8458.
316. Allenmark, S. G.; Andersson, M. A., *Chirality*, **1998**, *10*, 246-252.
317. de Gonzalo, G.; Torres Pazmiño, D. E.; Ottolina, G.; Fraaije, M. W.; Carrea, G., *Tetrahedron: Asymmetry*, **2006**, *17*, 130-135.
318. Bordewick, S.; Beier, A.; Balke, K.; Bornscheuer, U. T., *Enzyme Microb. Technol.*, **2017**.
319. Goundry, W. R. F.; Adams, B.; Benson, H.; Demeritt, J.; McKown, S.; Mulholland, K.; Robertson, A.; Siedlecki, P.; Tomlin, P.; Vare, K., *Org. Process Res. Dev.*, **2017**, *21*, 107-113.

320. Rioz Martínez, A.; de Gonzalo, G.; Pazmiño, D. E. T.; Fraaije, M. W.; Gotor, V., *Eur. J. Org. Chem.*, **2010**, 2010, 6409-6416.
321. Pasta, P.; Carrea, G.; Holland, H. L.; Dallavalle, S., *Tetrahedron: Asymmetry*, **1995**, 6, 933-936.
322. Ottolina, G.; Pasta, P.; Carrea, G.; Colonna, S.; Dallavalle, S.; Holland, H. L., *Tetrahedron: Asymmetry*, **1995**, 6, 1375-1386.
323. Chen, G.; M. Kayser, M.; D. Mihovilovic, M.; E. Mrstik, M.; A. Martinez, C.; D. Stewart, J., *New J. Chem.*, **1999**, 23, 827-832.
324. Carrea, G.; Redigolo, B.; Riva, S.; Colonna, S.; Gaggero, N.; Battistel, E.; Bianchi, D., *Tetrahedron: Asymmetry*, **1992**, 3, 1063-1068.
325. Secundo, F.; Carrea, G.; Dallavalle, S.; Franzosi, G., *Tetrahedron: Asymmetry*, **1993**, 4, 1981-1982.
326. Zhang, J.-D.; Li, A.-T.; Yang, Y.; Xu, J.-H., *Appl. Microbiol. Biotechnol.*, **2010**, 85, 615-624.
327. Li, A.-T.; Zhang, J.-D.; Yu, H.-L.; Pan, J.; Xu, J.-H., *Process Biochem.*, **2011**, 46, 689-694.
328. Lee, K.; Brand, J. M.; Gibson, D. T., *Biochem. Biophys. Res. Commun.*, **1995**, 212, 9-15.
329. Boyd, D. R.; Sharma, N. D.; Byrne, B. E.; Haughey, S. A.; Kennedy, M. A.; Allen, C. C., *Org. Biomol. Chem.*, **2004**, 2, 2530-7.
330. Boyd, D. R.; Sharma, N. D.; Haughey, S. A.; Malone, J. F.; King, A. W. T.; McMurray, B. T.; Alves-Areias, A.; Allen, C. C. R.; Holt, R.; Dalton, H., *J. Chem. Soc., Perkin Trans. 1*, **2001**, 3288-3296.
331. R. Boyd, D.; D. Sharma, N.; A. Haughey, S.; A. Kennedy, M.; T. McMurray, B.; N. Sheldrake, G.; C. R. Allen, C.; Dalton, H.; Sproule, K., *J. Chem. Soc., Perkin Trans. 1*, **1998**, 1929-1934.
332. Boyd, D. R.; Sharma, N. D.; Ljubez, V.; Byrne, B. E.; Shepherd, S. D.; Allen, C. C. R.; Kulakov, L. A.; Larkin, M. J.; Dalton, H., *Chem. Commun.*, **2002**, 1914-1915.
333. Casella, L.; Granata, A.; Monzani, E.; Pievo, R.; Pattarello, L.; Bubacco, L., *Micron*, **2004**, 35, 141-142.
334. Pievo, R.; Gullotti, M.; Monzani, E.; Casella, L., *Biochemistry*, **2008**, 47, 3493-3498.
335. Sugimoto, T.; Kokubo, T.; Miyazaki, J.; Tanimoto, S.; Okano, M., *J. Chem. Soc., Chem. Commun.*, **1979**, 402-404.
336. Ogura, K.; Fujita, M.; Iida, H., *Tetrahedron Lett.*, **1980**, 21, 2233-2236.
337. Colonna, S.; Gaggero, N., *Tetrahedron Lett.*, **1989**, 30, 6233-6236.
338. Colonna, S.; Gaggero, N.; Leone, M., *Tetrahedron*, **1991**, 47, 8385-8398.
339. Katsuki, T.; Sharpless, K. B., *J. Am. Chem. Soc.*, **1980**, 102, 5974-5976.

340. Sharpless, K. B., *Angew. Chem., Int. Ed.*, **2002**, *41*, 2024-2032.
341. Ramón, D. J.; Yus, M., *Chem. Rev.*, **2006**, *106*, 2126-2208.
342. Hill, J. G.; Rossiter, B. E.; Sharpless, K. B., *J. Org. Chem.*, **1983**, *48*, 3607-3608.
343. Morrison, J. D., *Asymmetric synthesis*. Academic Press: New York, 1985; Vol. 5.
344. Pedersen, S. F.; Dewan, J. C.; Eckman, R. R.; Sharpless, K. B., *J. Am. Chem. Soc.*, **1987**, *109*, 1279-1282.
345. Ortega, R. B.; Tapscott, R. E.; Campana, C. F., *Inorg. Chem.*, **1982**, *21*, 672-676.
346. Finn, M. G.; Sharpless, K. B., *J. Am. Chem. Soc.*, **1991**, *113*, 113-126.
347. Pitchen, P.; Dunach, E.; Deshmukh, M. N.; Kagan, H. B., *J. Am. Chem. Soc.*, **1984**, *106*, 8188-8193.
348. Williams, I. D.; Pedersen, S. F.; Sharpless, K. B.; Lippard, S. J., *J. Am. Chem. Soc.*, **1984**, *106*, 6430-6431.
349. Joergensen, K. A.; Wheeler, R. A.; Hoffmann, R., *J. Am. Chem. Soc.*, **1987**, *109*, 3240-3246.
350. McKee, B. H.; Kalantar, T. H.; Sharpless, K. B., *J. Org. Chem.*, **1991**, *56*, 6966-6968.
351. Bradley, D. C.; Mehrotra, R. C.; Gaur, D. P., *Metal Alkoxides*. **1978**;
352. Di Furia, F.; Modena, G.; Seraglia, R., *Synthesis*, **1984**, *1984*, 325-326.
353. Massa, A.; Mazza, V.; Scettri, A., *Tetrahedron: Asymmetry*, **2005**, *16*, 2271-2275.
354. Zhao, S. H.; Samuel, O.; Kagan, H. B., *Tetrahedron*, **1987**, *43*, 5135-5144.
355. Brunel, J. M.; Kagan, H. B., *Synlett*, **1996**, 404-406.
356. Newhouse, T. R.; Li, X.; Blewett, M. M.; Whitehead, C. M. C.; Corey, E. J., *J. Am. Chem. Soc.*, **2012**, *134*, 17354-17357.
357. Potvin, P. G.; Fieldhouse, B. G., *Tetrahedron: Asymmetry*, **1999**, *10*, 1661-1672.
358. Pitchen, P.; France, C. J.; McFarlane, I. M.; Newton, C. G.; Thompson, D. M., *Tetrahedron Lett.*, **1994**, *35*, 485-488.
359. Maguire, A. R.; Papot, S.; Ford, A.; Touhey, S.; O'Connor, R.; Clynes, M., *Synlett*, **2001**, *2001*, 0041-0044.
360. Rodríguez, S.; Haddad, N.; Frutos, R. P.; Grinberg, N.; Krishnamurthy, D.; Senanayake, C. H., *Org. Process Res. Dev.*, **2017**, *21*, 444-447.
361. Song, Z. J.; King, A. O.; Waters, M. S.; Lang, F.; Zewge, D.; Bio, M.; Leazer, J. L.; Javadi, G.; Kassim, A.; Tschaen, D. M.; Reamer, R. A.; Rosner, T.; Chilenski, J. R.; Mathre, D. J.; Volante, R. P.; Tillyer, R., *Proc. Natl. Acad. Sci. U. S. A.*, **2004**, *101*, 5776-5781.
362. Makino, K.; Yoneda, T.; Ogawa, R.; Kanase, Y.; Tabata, H.; Oshitari, T.; Natsugari, H.; Takahashi, H., *Tetrahedron Lett.*, **2017**, *58*, 2885-2888.
363. Hogan, P. J.; Hopes, P. A.; Moss, W. O.; Robinson, G. E.; Patel, I., *Org. Process Res. Dev.*, **2002**, *6*, 225-229.

364. Bowden, S. A.; Burke, J. N.; Gray, F.; McKown, S.; Moseley, J. D.; Moss, W. O.; Murray, P. M.; Welham, M. J.; Young, M. J., *Org. Process Res. Dev.*, **2004**, *8*, 33-44.
365. Scettri, A.; Bonadies, F.; Lattanzi, A.; Senatore, A.; Soriente, A., *Tetrahedron: Asymmetry*, **1996**, *7*, 657-658.
366. Komatsu, N.; Nishibayashi, Y.; Sugita, T.; Uemura, S., *Tetrahedron Lett.*, **1992**, *33*, 5391-5394.
367. Komatsu, N.; Hashizume, M.; Sugita, T.; Uemura, S., *J. Org. Chem.*, **1993**, *58*, 4529-4533.
368. Komatsu, N.; Hashizume, M.; Sugita, T.; Uemura, S., *J. Org. Chem.*, **1993**, *58*, 7624-7626.
369. Jia, X.; Li, X.; Xu, L.; Li, Y.; Shi, Q.; Au-Yeung, T. T. L.; Yip, C. W.; Yao, X.; Chan, A. S. C., *Adv. Synth. Catal.*, **2004**, *346*, 723-726.
370. Pescitelli, G.; Di Bari, L.; Salvadori, P., *J. Organomet. Chem.*, **2006**, *691*, 2311-2318.
371. Chen, Y.; Yekta, S.; Yudin, A. K., *Chem. Rev.*, **2003**, *103*, 3155-3212.
372. Sahoo, S.; Kumar, P.; Lefebvre, F.; Halligudi, S. B., *J. Catal.*, **2009**, *262*, 111-118.
373. Bolm, C.; Dabard, O. A. G., *Synlett*, **1999**, *1999*, 360-362.
374. Chen, Y.; Yekta, S.; Martyn, L. J. P.; Zheng, J.; Yudin, A. K., *Org. Lett.*, **2000**, *2*, 3433-3436.
375. Martyn, L. J. P.; Pandiaraju, S.; Yudin, A. K., *J. Organomet. Chem.*, **2000**, *603*, 98-104.
376. Yamanoi, Y.; Imamoto, T., *J. Org. Chem.*, **1997**, *62*, 8560-8564.
377. Sun, J.; Yang, M.; Dai, Z.; Zhu, C.; Hu, H., *Synthesis*, **2008**, *2008*, 2513-2518.
378. Superchi, S.; Rosini, C., *Tetrahedron: Asymmetry*, **1997**, *8*, 349-352.
379. Donnoli, M. I.; Superchi, S.; Rosini, C., *J. Org. Chem.*, **1998**, *63*, 9392-9395.
380. Superchi, S.; Scafato, P.; Restaino, L.; Rosini, C., *Chirality*, **2008**, *20*, 592-596.
381. Naso, F.; Capozzi, M. A. M.; Bottoni, A.; Calvaresi, M.; Bertolasi, V.; Capitelli, F.; Cardellicchio, C., *Chem. - Eur. J.*, **2009**, *15*, 13417-13426.
382. Capozzi, M. A. M.; Terraneo, G.; Cavallo, G.; Cardellicchio, C., *Tetrahedron*, **2015**, *71*, 4810-4816.
383. Naso, F.; Cardellicchio, C.; Affortunato, F.; Capozzi, M. A. M., *Tetrahedron: Asymmetry*, **2006**, *17*, 3226-3229.
384. Zeng, Q.-L.; Tang, H.-Y.; Zhang, S.; Liu, J.-C., *Chin. J. Chem.*, **2008**, *26*, 1435-1439.
385. Bhadra, S.; Akakura, M.; Yamamoto, H., *J. Am. Chem. Soc.*, **2015**, *137*, 15612-15615.
386. Chen, Y. J.; Tan, R.; Zhang, Y. Y.; Zhao, G. W.; Yin, D. H., *ChemCatChem*, **2015**, *7*, 4066-4075.
387. Talsi, E. P.; Bryliakova, A. A.; Bryliakov, K. P., *Chem. Rec.*, **2016**, *16*, 924-939.
388. Xing, C.; Deng, J.; Tan, R.; Gao, M.; Hao, P.; Yin, D.; Dulin, Y., *Catal. Sci. Technol.*, **2017**.

389. Kiyohiko, N.; Caori, S.; Masaaki, K.; Tomonori, A.; Shigeru, O.; Yoshihiko, S.; Junnosuke, F., *Chem. Lett.*, **1987**, *16*, 2189-2192.
390. Saito, B.; Katsuki, T., *Tetrahedron Lett.*, **2001**, *42*, 3873-3876.
391. Saito, B.; Katsuki, T., *Tetrahedron Lett.*, **2001**, *42*, 8333-8336.
392. Tanaka, T.; Saito, B.; Katsuki, T., *Tetrahedron Lett.*, **2002**, *43*, 3259-3262.
393. Irie, R.; Uchida, T.; Matsumoto, K., *Chem. Lett.*, **2015**, *44*, 1268-1283.
394. Talsi, E. P.; Bryliakov, K. P., *Appl. Organomet. Chem.*, **2013**, *27*, 239-244.
395. Bryliakov, K. P.; Talsi, E. P., *Eur. J. Org. Chem.*, **2011**, *2011*, 4693-4698.
396. Nugent, W. A.; Harlow, R. L., *J. Am. Chem. Soc.*, **1994**, *116*, 6142-6148.
397. Di Furia, F.; Licini, G.; Modena, G.; Motterle, R.; Nugent, W. A., *J. Org. Chem.*, **1996**, *61*, 5175-5177.
398. Bonchio, M.; Calloni, S.; Di Furia, F.; Licini, G.; Modena, G.; Moro, S.; Nugent, W. A., *J. Am. Chem. Soc.*, **1997**, *119*, 6935-6936.
399. Bonchio, M.; Licini, G.; Modena, G.; Moro, S.; Bortolini, O.; Traldi, P.; A. Nugent, W., *Chem. Commun.*, **1997**, 869-870.
400. Nugent, W.; Licini, G.; Bonchio, M.; Bortolini, O.; Finn, M. G.; McClelland, B. W., *Pure Appl. Chem.*, **1998**, *70*, 1041-146.
401. Bonchio, M.; Licini, G.; Modena, G.; Bortolini, O.; Moro, S.; Nugent, W. A., *J. Am. Chem. Soc.*, **1999**, *121*, 6258-6268.
402. Licini, G.; Bonchio, M.; Modena, G.; Nugent, W. A., *Pure Appl. Chem.*, **1999**, *71*, 463-472.
403. Santoni, G.; Mba, M.; Bonchio, M.; Nugent, W. A.; Zonta, C.; Licini, G., *Chem. - Eur. J.*, **2010**, *16*, 645-654.
404. Bryliakov, K. P.; Talsi, E. P., *J. Mol. Catal. A: Chem.*, **2007**, *264*, 280-287.
405. Bera, P. K.; Ghosh, D.; Abdi, S. H. R.; Khan, N.-u. H.; Kureshy, R. I.; Bajaj, H. C., *J. Mol. Catal. A: Chem.*, **2012**, *361-362*, 36-44.
406. Chen, F. X.; Feng, X. M.; Jiang, Y. Z., *Arkivoc*, **2003**, 21-31.
407. Matsugi, M.; Fukuda, N.; Muguruma, Y.; Yamaguchi, T.; Minamikawa, J.; Otsuka, S., *Tetrahedron*, **2001**, *57*, 2739-2744.
408. Adam, W.; Korb, M. N.; Roschmann, K. J.; Saha Moller, C. R., *J. Org. Chem.*, **1998**, *63*, 3423-3428.
409. Scettri, A.; Bonadies, F.; Lattanzi, A., *Tetrahedron: Asymmetry*, **1996**, *7*, 629-632.
410. Antonioletti, R.; Bonadies, F.; Scettri, A., *Tetrahedron Lett.*, **1988**, *29*, 4987-4990.
411. Antonioletti, R.; Bonadies, F.; Lattanzi, A.; Monteagudo, E. S.; Scettri, A., *Tetrahedron Lett.*, **1992**, *33*, 5433-5436.
412. Lattanzi, A.; Bonadies, F.; Scettri, A., *Tetrahedron: Asymmetry*, **1997**, *8*, 2141-2151.

413. Lattanzi, A.; Bonadies, F.; Senatore, A.; Soriente, A.; Scettri, A., *Tetrahedron: Asymmetry*, **1997**, *8*, 2473-2478.
414. Lattanzi, A.; Bonadies, F.; Schiavo, A.; Scettri, A., *Tetrahedron: Asymmetry*, **1998**, *9*, 2619-2625.
415. Palombi, L.; Bonadies, F.; Pazienza, A.; Scettri, A., *Tetrahedron: Asymmetry*, **1998**, *9*, 1817-1822.
416. Lattanzi, A.; Scettri, A., *J. Organomet. Chem.*, **2006**, *691*, 2072-2082.
417. Massa, A.; Siniscalchi, F. R.; Bugatti, V.; Lattanzi, A.; Scettri, A., *Tetrahedron: Asymmetry*, **2002**, *13*, 1277-1283.
418. Lattanzi, A.; Iannece, P.; Scettri, A., *Tetrahedron: Asymmetry*, **2004**, *15*, 413-418.
419. Pellissier, H., *Coord. Chem. Rev.*, **2015**, *284*, 93-110.
420. Sutradhar, M.; Martins, L.; da Silva, M.; Pombeiro, A. J. L., *Coord. Chem. Rev.*, **2015**, *301*, 200-239.
421. Bolm, C., *Coord. Chem. Rev.*, **2003**, *237*, 245-256.
422. Bryliakov, K. P., *Chem. Rev.*, **2017**, *117*, 11406-11459.
423. Di Furia, F.; Modena, G.; Curci, R., *Tetrahedron Lett.*, **1976**, 4637-8.
424. Skarzewski, J.; Ostrycharz, E.; Siedlecka, R., *Tetrahedron: Asymmetry*, **1999**, *10*, 3457-3461.
425. Karpyshev, N. N.; Yakovleva, O. D.; Talsi, E. P.; Bryliakov, K. P.; Tolstikova, O. V.; Tolstikov, A. G., *J. Mol. Catal. A: Chem.*, **2000**, *157*, 91-95.
426. Bryliakov, K. P.; Karpyshev, N. N.; Fominsky, S. A.; Tolstikov, A. G.; Talsi, E. P., *J. Mol. Catal. A: Chem.*, **2001**, *171*, 73-80.
427. Skarzewski, J.; Wojaczyńska, E.; Turowska-Tyrk, I., *Tetrahedron: Asymmetry*, **2002**, *13*, 369-375.
428. Jeong, Y.-C.; Choi, S.; Hwang, Y. D.; Ahn, K.-H., *Tetrahedron Lett.*, **2004**, *45*, 9249-9252.
429. Jeong, Y.-C.; Huang, Y. D.; Choi, S.; Ahn, K.-H., *Tetrahedron: Asymmetry*, **2005**, *16*, 3497-3501.
430. Zeng, Q.; Wang, H.; Wang, T.; Cai, Y.; Weng, W.; Zhao, Y., *Adv. Synth. Catal.*, **2005**, *347*, 1933-1936.
431. Zeng, Q.; Wang, H.; Weng, W.; Lin, W.; Gao, Y.; Huang, X.; Zhao, Y., *New J. Chem.*, **2005**, *29*, 1125-1127.
432. Gao, A.; Wang, M.; Wang, D.; Zhang, L.; Liu, H.; Tian, W.; Sun, L., *Chin. J. Catal.*, **2006**, *27*, 743-748.
433. Hsieh, S.-H.; Kuo, Y.-P.; Gau, H.-M., *Dalton Trans.*, **2007**, 97-106.
434. Khiar, N.; Mallouk, S.; Valdivia, V.; Bougrin, K.; Soufiaoui, M.; Fernández, I., *Org. Lett.*, **2007**, *9*, 1255-1258.

435. Liu, H.; Wang, M.; Wang, Y.; Yin, R.; Tian, W.; Sun, L., *Appl. Organomet. Chem.*, **2008**, *22*, 253-257.
436. Romanowski, G.; Kwiatkowski, E.; Nowicki, W.; Kwiatkowski, M.; Lis, T., *Polyhedron*, **2008**, *27*, 1601-1609.
437. Koneva, E. A.; Volcho, K. P.; Korchagina, D. V.; Salakhutdinov, N. F.; Tolstikov, A. G., *Russ J Org Chem*, **2009**, *45*, 815-824.
438. Adão, P.; Kuznetsov, M. L.; Barroso, S.; Martins, A. M.; Avecilla, F.; Pessoa, J. C., *Inorg. Chem.*, **2012**, *51*, 11430-11449.
439. Stingl, K. A.; Weiß, K. M.; Tsogoeva, S. B., *Tetrahedron*, **2012**, *68*, 8493-8501.
440. Lazar, A.; Sharma, P.; Singh, A. P., *Microporous Mesoporous Mater.*, **2013**, *170*, 331-339.
441. Romanowski, G., *J. Mol. Catal. A: Chem.*, **2013**, *368-369*, 137-144.
442. Bolm, C.; Bienewald, F., *Angew. Chem., Int. Ed. Engl.*, **1996**, *34*, 2640-2642.
443. Bolm, C.; Bienewald, F., *Synlett*, **1998**, *1998*, 1327-1328.
444. Liu, G.; Cogan, D. A.; Ellman, J. A., *J. Am. Chem. Soc.*, **1997**, *119*, 9913-9914.
445. Cogan, D. A.; Liu, G.; Kim, K.; Backes, B. J.; Ellman, J. A., *J. Am. Chem. Soc.*, **1998**, *120*, 8011-8019.
446. Blum, S. A.; Bergman, R. G.; Ellman, J. A., *J. Org. Chem.*, **2002**, *68*, 150-155.
447. Weix, D. J.; Ellman, J. A., *Org. Lett.*, **2003**, *5*, 1317-1320.
448. Drago, C.; Caggiano, L.; Jackson, R. F., *Angew. Chem., Int. Ed. Engl.*, **2005**, *44*, 7221-3.
449. Kelly, P.; Lawrence, S. E.; Maguire, A. R., *Eur. J. Org. Chem.*, **2006**, *2006*, 4500-4509.
450. Kelly, P.; Lawrence, S. E.; Maguire, A. R., *Synlett*, **2006**, *2006*, 1569-1573.
451. Vetter, A. H.; Berkessel, A., *Tetrahedron Lett.*, **1998**, *39*, 1741-1744.
452. Suresh, P.; Srimurugan, S.; Babu, B.; Pati, H. N., *Tetrahedron: Asymmetry*, **2007**, *18*, 2820-2827.
453. Cucciolito, M. E.; Del Litto, R.; Roviello, G.; Ruffo, F., *J. Mol. Catal. A: Chem.*, **2005**, *236*, 176-181.
454. Chuo, T. H.; Boobalan, R.; Chen, C., *ChemistrySelect*, **2016**, *1*, 2174-2180.
455. Liu, H.; Wang, M.; Wang, Y.; Wang, Y.; Sun, H.; Sun, L., *Catal. Commun.*, **2009**, *11*, 294-297.
456. Aydin, A. E., *Tetrahedron: Asymmetry*, **2013**, *24*, 444-448.
457. Ben Zid, T.; Khedher, I.; Ksibi, Z.; Fraile, J. M., *J. Porous Mater.*, **2016**, *23*, 507-516.
458. Green, S. D.; Monti, C.; Jackson, R. F. W.; Anson, M. S.; Macdonald, S. J. F., *Chem. Commun.*, **2001**, 2594-2595.
459. Pelotier, B.; Anson, M. S.; Campbell, I. B.; Macdonald, S. J. F.; Priem, G.; Jackson, R. F. W., *Synlett*, **2002**, *2002*, 1055-1060.

460. Halterman, R. L.; Jan, S.-T.; Nimmons, H. L., *Synlett*, **1991**, 1991, 791-792.
461. Srour, H.; Jalkh, J.; Le Maux, P.; Chevance, S.; Kobeissi, M.; Simonneaux, G., *J. Mol. Catal. A: Chem.*, **2013**, 370, 75-79.
462. Palucki, M.; Hanson, P.; Jacobsen, E. N., *Tetrahedron Lett.*, **1992**, 33, 7111-7114.
463. Noda, K.; Hosoya, N.; Irie, R.; Yamashita, Y.; Katsuki, T., *Tetrahedron*, **1994**, 50, 9609-9618.
464. Noda, K.; Hosoya, N.; Yanai, K.; Irie, R.; Katsuki, T., *Tetrahedron Lett.*, **1994**, 35, 1887-1890.
465. Katsuki, T., *Coord. Chem. Rev.*, **1995**, 140, 189-214.
466. Kokubo, C.; Katsuki, T., *Tetrahedron*, **1996**, 52, 13895-13900.
467. Katsuki, T., *Adv. Synth. Catal.*, **2002**, 344, 131-147.
468. Dai, W.; Li, J.; Chen, B.; Li, G.; Lv, Y.; Wang, L.; Gao, S., *Org. Lett.*, **2013**, 15, 5658-5661.
469. Dai, W.; Shang, S. S.; Lv, Y.; Li, G. S.; Li, C. S.; Gao, S., *ACS Catal.*, **2017**, 7, 4890-4895.
470. Dai, W.; Mi, Y.; Lv, Y.; Chen, B.; Li, G. S.; Chen, G. W.; Gao, S., *Adv. Synth. Catal.*, **2016**, 358, 667-671.
471. Schoumacker, S.; Hamelin, O.; Pecaut, J.; Fontecave, M., *Inorg. Chem.*, **2003**, 42, 8110-6.
472. Gao, A.; Wang, M.; Shi, J.; Wang, D.; Tian, W.; Sun, L., *Appl. Organomet. Chem.*, **2006**, 20, 830-834.
473. Hirotsu, M.; Ohno, N.; Nakajima, T.; Kushibe, C.; Ueno, K.; Kinoshita, I., *Dalton Trans.*, **2010**, 39, 139-148.
474. Imagawa, K.; Nagata, T.; Yamada, T.; Mukaiyama, T., *Chem. Lett.*, **1995**, 24, 335-336.
475. Nagata, T.; Imagawa, K.; Yamada, T.; Mukaiyama, T., *Bull. Chem. Soc. Jpn.*, **1995**, 68, 3241-3246.
476. Alcón, M. J.; Corma, A.; Iglesias, M.; Sánchez, F., *J. Mol. Catal. A: Chem.*, **2002**, 178, 253-266.
477. Zhang, Z.; Guan, F.; Huang, X.; Wang, Y.; Sun, Y., *J. Mol. Catal. A: Chem.*, **2012**, 363-364, 343-353.
478. Voss, F.; Herdtweck, E.; Bach, T., *Chem. Commun.*, **2011**, 47, 2137-2139.
479. Groves, J. T.; Viski, P., *J. Org. Chem.*, **1990**, 55, 3628-3634.
480. Naruta, Y.; Tani, F.; Maruyama, K., *J. Chem. Soc. D*, **1990**, 1378-1380.
481. Naruta, Y.; Tani, F.; Maruyama, K., *Tetrahedron: Asymmetry*, **1991**, 2, 533-542.
482. Chiang, L.-c.; Konishi, K.; Aida, T.; Inoue, S., *J. Chem. Soc., Chem. Commun.*, **1992**, 254-256.

483. Mekmouche, Y.; Hummel, H.; Ho, R. Y. N.; Que, J. L.; Schünemann, V.; Thomas, F.; Trautwein, A. X.; Lebrun, C.; Gorgy, K.; Leprêtre, J.-C.; Collomb, M.-N.; Deronzier, A.; Fontecave, M.; Ménage, S., *Chem. - Eur. J.*, **2002**, *8*, 1196-1204.
484. Legros, J.; Bolm, C., *Chem. - Eur. J.*, **2005**, *11*, 1086-1092.
485. Bolm, C.; Legros, J.; Le Paih, J.; Zani, L., *Chem. Rev.*, **2004**, *104*, 6217-6254.
486. Legros, J.; Bolm, C., *Angew. Chem., Int. Ed.*, **2003**, *42*, 5487-5489.
487. Legros, J.; Bolm, C., *Angew. Chem., Int. Ed.*, **2004**, *43*, 4225-4228.
488. Korte, A.; Legros, J.; Bolm, C., *Synlett*, **2004**, *2004*, 2397-2399.
489. Egami, H.; Katsuki, T., *J. Am. Chem. Soc.*, **2007**, *129*, 8940-8941.
490. Egami, H.; Katsuki, T., *Synlett*, **2008**, *2008*, 1543-1546.
491. Bryliakov, K. P.; Talsi, E. P., *Angew. Chem., Int. Ed.*, **2004**, *43*, 5228-5230.
492. Bryliakov, K. P.; Talsi, E. P., *Chem. - Eur. J.*, **2007**, *13*, 8045-50.
493. Mohammadnezhad, G.; Debel, R.; Plass, W., *J. Mol. Catal. A: Chem.*, **2015**, *410*, 160-167.
494. Romanowski, G.; Kira, J., *Polyhedron*, **2016**, *117*, 352-358.
495. Zong, L.; Wang, C.; Moeljadi, A. M. P.; Ye, X. Y.; Ganguly, R.; Li, Y. X.; Hirao, H. M.; Tan, C. H., *Nat. Commun.*, **2016**, *7*.
496. Bonchio, M.; Carofiglio, T.; Di Furia, F.; Fornasier, R., *J. Org. Chem.*, **1995**, *60*, 5986-5988.
497. Basak, A.; Barlan, A. U.; Yamamoto, H., *Tetrahedron: Asymmetry*, **2006**, *17*, 508-511.
498. Barlan, A. U.; Zhang, W.; Yamamoto, H., *Tetrahedron*, **2007**, *63*, 6075-6087.
499. Carrasco, C. J.; Montilla, F.; Galindo, A., *Catal. Commun.*, **2016**, *84*, 134-136.
500. Chavarot, M.; Ménage, S.; Hamelin, O.; Charnay, F.; Pécaut, J.; Fontecave, M., *Inorg. Chem.*, **2003**, *42*, 4810-4816.
501. Li, Z.-Z.; Yao, S.-Y.; Wen, A. H.; Ye, B.-H., *Eur. J. Inorg. Chem.*, **2015**, *2015*, 4335-4342.
502. Bunce, S.; Cross, R. J.; Farrugia, L. J.; Kunchandy, S.; Meason, L. L.; Muir, K. W.; O'Donnell, M.; Peacock, R. D.; Stirling, D.; Teat, S. J., *Polyhedron*, **1998**, *17*, 4179-4187.
503. Plitt, P.; Pritzkow, H.; Oeser, T.; Kraemer, R., *J. Inorg. Biochem.*, **2005**, *99*, 1230-1237.
504. Zhu, H.-B.; Dai, Z.-Y.; Huang, W.; Cui, K.; Gou, S.-H.; Zhu, C.-J., *Polyhedron*, **2004**, *23*, 1131-1137.
505. Ayala, V.; Corma, A.; Iglesias, M.; Sánchez, F., *J. Mol. Catal. A: Chem.*, **2004**, *221*, 201-208.
506. Kelly, P.; Lawrence, S. E.; Maguire, A. R., *Synlett*, **2007**, *2007*, 1501-1506.
507. O'Mahony, G. E.; Ford, A.; Maguire, A. R., *J. Org. Chem.*, **2012**, *77*, 3288-3296.

508. O'Mahony, G. E.; Eccles, K. S.; Morrison, R. E.; Ford, A.; Lawrence, S. E.; Maguire, A. R., *Tetrahedron*, **2013**, *69*, 10168-10184.
509. Yamaguchi, T.; Matsumoto, K.; Saito, B.; Katsuki, T., *Angew. Chem., Int. Ed.*, **2007**, *46*, 4729-4731.
510. Matsumoto, K.; Yamaguchi, T.; Katsuki, T., *Chem. Commun.*, **2008**, 1704-1706.
511. Bonchio, M.; Licini, G.; Mantovani, S.; Modena, G.; Nugent, W. A., *J. Org. Chem.*, **1999**, *64*, 1326-1330.
512. Thakur, V. V.; Sudalai, A., *Tetrahedron: Asymmetry*, **2003**, *14*, 407-410.
513. Bigi, F.; Nimal Gunaratne, H. Q.; Quarantelli, C.; Seddon, K. R., *C. R. Chim.*, **2011**, *14*, 685-687.
514. Scarso, A.; Strukul, G., *Adv. Synth. Catal.*, **2005**, *347*, 1227-1234.
515. Kantam, M. L.; Prakash, B. V.; Bharathi, B.; Reddy, C. V., *J. Mol. Catal. A: Chem.*, **2005**, *226*, 119-122.
516. Malik, P.; Chakraborty, D., *Tetrahedron Lett.*, **2012**, *53*, 5652-5655.
517. Willsky, G. R., *Vanadium in Biological Systems: Physiology and Biochemistry*, Ed. Chasteen, N. D., Kluwer Academic Publishers, Dordrecht, The Netherlands, **1990**, pp 1-24.
518. Gaba, M.; Mohan, C., *Med. Chem. Res.*, **2016**, *25*, 173-210.
519. Federsel, H. J., *Chirality*, **2003**, *15*, S128-42.
520. Der, G., *Gastroenterol. Nurs.*, **2003**, *26*, 182-90.
521. Khetan, S. K.; Collins, T. J., *Chem. Rev.*, **2007**, *107*, 2319-64.
522. Mejia, A.; Kraft, W. K., *Expert Rev. Clin. Pharmacol.*, **2009**, *2*, 295-314.
523. Aronson, J. K., *BMC Med.*, **2016**, *14*, 172.
524. Lorentzon, P.; Bayati, A.; Lee, H.; Andersson, K., *Ann. N. Y. Acad. Sci.*, **1997**, *834*, 592-599.
525. Richardson, P.; Hawkey, C. J.; Stack, W. A., *Drugs*, **1998**, *56*, 307-35.
526. Strand, D. S.; Kim, D.; Peura, D. A., *Gut and liver*, **2017**, *11*, 27-37.
527. Lanas, A.; Chan, F. K. L., *Lancet (London, England)*.
528. Katz, P. O.; Zavala, S., *J. Gastrointest. Surg.*, **2010**, *14 Suppl 1*, S62-6.
529. Mossner, J.; Caca, K., *Eur. J. Clin. Invest.*, **2005**, *35*, 469-75.
530. Prinz, C.; Kajimura, M.; Scott, D.; Helander, H.; Shin, J.; Besancon, M.; Bamberg, K.; Hersey, S.; Sachs, G., *Yale J. Biol. Med.*, **1992**, *65*, 577-96.
531. Olbe, L.; Carlsson, E.; Lindberg, P., *Nat. Rev. Drug Discovery*, **2003**, *2*, 132-139.
532. Ward, R. M.; Kearns, G. L., *Paediatr. Drugs*, **2013**, *15*, 119-31.
533. <https://beta.nhs.uk/medicines/omeprazole>, (accessed 02/03/2018).
534. <http://www.who.int/mediacentre/news/releases/2017/essential-medicines-list/en/>, (accessed 24/02/2018).

535. Nguyen, T.; Cina, A.; Henriques, S., *J. Nurse Pract.*, **2017**, *13*, e95-e97.
536. Pali-Scholl, I.; Herzog, R.; Wallmann, J.; Szalai, K.; Brunner, R.; Lukschal, A.; Karagiannis, P.; Diesner, S. C.; Jensen-Jarolim, E., *Clin. Exp. Allergy*, **2010**, *40*, 1091-8.
537. Regardh, C. G., *Scand. J. Gastroenterol., Suppl.*, **1986**, *118*, 99-104.
538. Oosterhuis, B.; Jonkman, J. H., *Digestion*, **1989**, *44 Suppl 1*, 9-17.
539. Oriaifo, N.; Oriaifo, S. E.; Iruolagbe, C.; Okogbenin, E. O.; Egbeifo, J., *World J. Pharm. Pharm. Sci.*, **2017**, *6*, 218-237.
540. Lin, K.; Chen, X.; Zhang, L.; Wang, Y.; Shan, Z., *Eur. J. Pharmacol.*, **2013**, *718*, 435-40.
541. Nelson, C.; Lee, J.; Ko, K.; Sikora, A. G.; Bonnen, M. D.; Enkhbaatar, P.; Ghebre, Y. T., *Front. Pharmacol.*, **2017**, *8*, 16.
542. Almeida, G. T.; Lage, R. C.; Anderson, L.; Venancio, T. M.; Nakaya, H. I.; Miyasato, P. A.; Rofatto, H. K.; Zerlotini, A.; Nakano, E.; Oliveira, G.; Verjovski-Almeida, S., *PLoS Neglected Trop. Dis.*, **2015**, *9*, e0004086.
543. Perez Villanueva, J.; Romo Mancillas, A.; Hernandez Campos, A.; Yepez Mulia, L.; Hernandez Luis, F.; Castillo, R., *Bioorg. Med. Chem. Lett.*, **2011**, *21*, 7351-4.
544. Garcia-Torres, I.; dela Mora-de la Mora, I.; Marcial-Quino, J.; Gomez-Manzo, S.; Vanoye-Carlo, A.; Navarrete-Vazquez, G.; Colin-Lozano, B.; Gutierrez-Castellon, P.; Sierra-Palacios, E.; Lopez-Velazquez, G.; Enriquez-Flores, S., *Biochim. Biophys. Acta, Gen. Subj.*, **2016**, *1860*, 97-107.
545. Lapenna, D.; de Gioia, S.; Ciofani, G.; Festi, D.; Cuccurullo, F., *FEBS Lett.*, **1996**, *382*, 189-92.
546. Carlton, D. L.; Collin Smith, L. J.; Daniels, A. J.; Deaton, D. N.; Goetz, A. S.; Laudeman, C. P.; Littleton, T. R.; Musso, D. L.; Morgan, R. J.; Szewczyk, J. R.; Zhang, C., *Bioorg. Med. Chem. Lett.*, **2008**, *18*, 5451-5.
547. El-Nezhawy, A. O. H.; Biuomy, A. R.; Hassan, F. S.; Ismaiel, A. K.; Omar, H. A., *Bioorg. Med. Chem.*, **2013**, *21*, 1661-1670.
548. Ranganath, B.; Saleem Basha, V.; Jayapal, M. R.; Venkata Ramana, P., *Int. J. Pharm. Chem.*, **2015**, *1*, 7-11.
549. Ghandour, M. A.; Hassan, A.; Ali, H. M., *J. Anal. Chem.*, **2015**, *70*, 392-397.
550. Sachs, G.; Shin, J. M.; Vagin, O.; Lambrecht, N.; Yakubov, I.; Munson, K., *J. Clin. Gastroenterol.*, **2007**, *41*, S226-42.
551. Shin, J. M.; Munson, K.; Vagin, O.; Sachs, G., *Pflugers Arch. - Eur. J. Physiol.*, **2009**, *457*, 609-22.
552. Shin, J. M.; Sachs, G.; Cho, Y. M.; Garst, M., *Molecules (Basel, Switzerland)*, **2009**, *14*, 5247-80.

553. Barreiro, E. J.; Kummerle, A. E.; Fraga, C. A., *Chem. Rev.*, **2011**, *111*, 5215-46.
554. Wolfe, M. M.; Sachs, G., *Gastroenterology*, **2000**, *118*, S9-S31.
555. Shin, J. M.; Sachs, G., *Dig. Dis. Sci.*, **2006**, *51*, 823-33.
556. Lindberg, P.; Brandstrom, A.; Wallmark, B.; Mattsson, H.; Rikner, L.; Hoffmann, K. J., *Med. Res. Rev.*, **1990**, *10*, 1-54.
557. Lindberg, P.; Carlsson, E., *Analogue-based Drug Discovery*, Wiley-VCH Verlag GmbH & Co. KGaA, **2006**, pp 81-113.
558. Sachs, G.; Prinz, C.; Loo, D.; Bamberg, K.; Besancon, M.; Shin, J. M., *Yale J. Biol. Med.*, **1994**, *67*, 81-95.
559. Shin, J. M.; Kim, N., *Neurogastroenterol. Motil.*, **2013**, *19*, 25-35.
560. Lindberg, P.; Nordberg, P.; Alminger, T.; Brandstrom, A.; Wallmark, B., *J. Med. Chem.*, **1986**, *29*, 1327-9.
561. Al-Gousous, J.; Tsume, Y.; Fu, M.; Salem, I. I.; Langguth, P., *Mol. Pharmaceutics*, **2017**.
562. Shin, J. M.; Cho, Y. M.; Sachs, G., *J. Am. Chem. Soc.*, **2004**, *126*, 7800-7811.
563. Kohl, B.; Sturm, E.; Senn Bilfinger, J.; Simon, W. A.; Krueger, U.; Schaefer, H.; Rainer, G.; Figala, V.; Klemm, K., *J. Med. Chem.*, **1992**, *35*, 1049-1057.
564. Sturm, E.; Krueger, U.; Senn Bilfinger, J.; Figala, V.; Klemm, K.; Kohl, B.; Rainer, G.; Schaefer, H.; Blake, T. J., *J. Org. Chem.*, **1987**, *52*, 4573-4581.
565. Senn Bilfinger, J.; Krueger, U.; Sturm, E.; Figala, V.; Klemm, K.; Kohl, B.; Rainer, G.; Schaefer, H.; Blake, T. J., *J. Org. Chem.*, **1987**, *52*, 4582-4592.
566. Krueger, U.; Senn Bilfinger, J.; Sturm, E.; Figala, V.; Klemm, K.; Kohl, B.; Rainer, G.; Schaefer, H.; Blake, T. J., *J. Org. Chem.*, **1990**, *55*, 4163-4168.
567. Bhatt, P. M.; Desiraju, G. R., *Chem. Commun.*, **2007**, 2057-2059.
568. Larina, L. I., *Advances in Heterocyclic Chemistry*, Eds. Scriven, E. F. V.; Ramsden, C. A., Academic Press, **2018**, *Vol. 124*, pp 233-321.
569. Claramunt, R. M.; Lopez, C.; Alkorta, I.; Elguero, J.; Yang, R.; Schulman, S., *Magn. Reson. Chem.*, **2004**, *42*, 712-4.
570. Claramunt, R. M.; Lopez, C.; Elguero, J., *Arkivoc*, **2006**, 5-11.
571. Deng, J.; Chi, Y.; Fu, F.; Cui, X.; Yu, K.; Zhu, J.; Jiang, Y., *Tetrahedron: Asymmetry*, **2000**, *11*, 1729-1732.
572. Ohishi, H.; In, Y.; Ishida, T.; Inoue, M.; Sato, F.; Okitsu, M.; Ohno, T., *Acta Crystallogr., Sect. C: Cryst. Struct. Commun.*, **1989**, *45*, 1921-1923.
573. Vojcic, N.; Bregovic, N.; Cindro, N.; Pozar, J.; Horvat, G.; Piculjan, K.; Mestrovic, E.; Tomisic, V., *Chemistryselect*, **2017**, *2*, 4899-4905.
574. Brandstrom, A. E., Lamm, B.R., U.S. Patent 4,620,008, 1986.
575. Bullitt, O. H.; Maynard, J. T., *J. Am. Chem. Soc.*, **1954**, *76*, 1370-1371.

576. Al Badr, A. A., *Profiles of Drug Substances, Excipients and Related Methodology*, Ed. Harry, G. B., Academic Press, **2010**, Vol. Volume 35, pp 151-262.
577. Bhalerao, D. S.; Kondaiah, G. C. M.; Dwivedi, N.; Mylavarappu, R. K.; Reddy, L. A.; Roy, A.; Nagaraju, G.; Reddy, P. P.; Bhattacharya, A.; Bandichhor, R., *Synth. Commun.*, **2010**, *40*, 2983-2987.
578. Lind, T.; Rydberg, L.; Kyleback, A.; Jonsson, A.; Andersson, T.; Hasselgren, G.; Holmberg, J.; Rohss, K., *Aliment. Pharmacol. Ther.*, **2000**, *14*, 861-7.
579. Kahrilas, P. J.; Falk, G. W.; Johnson, D. A.; Schmitt, C.; Collins, D. W.; Whipple, J.; D'Amico, D.; Hamelin, B.; Joelsson, B., *Aliment. Pharmacol. Ther.*, **2000**, *14*, 1249-58.
580. Lindberg, P.; Keeling, D.; Fryklund, J.; Andersson, T.; Lundborg, P.; Carlsson, E., *Aliment. Pharmacol. Ther.*, **2003**, *17*, 481-488.
581. Scott, L. J.; Dunn, C. J.; Mallarkey, G.; Sharpe, M., *Drugs*, **2002**, *62*, 1503-38.
582. Spencer, C. M.; Faulds, D., *Drugs*, **2000**, *60*, 321-329.
583. Fock, K. M.; Ang, T. L.; Bee, L. C.; Lee, E. J., *Clin. Pharmacokinet.*, **2008**, *47*, 1-6.
584. Shen, Z.; Lv, C.; Zeng, S., *J. Pharm. Anal.*, **2016**, *6*, 1-10.
585. Andersson, T.; Rohss, K.; Bredberg, E.; Hassan Alin, M., *Aliment. Pharmacol. Ther.*, **2001**, *15*, 1563-1569.
586. Andersson, T.; Weidolf, L., *Clin. Drug Invest.*, **2008**, *28*, 263-79.
587. Tonini, M.; Vigneri, S.; Savarino, V.; Scarpignato, C., *Dig. Liver Dis.*, **2001**, *33*, 600-6.
588. Marom, H.; Pogodin, S.; Agranat, I., *Chirality*, **2014**, *26*, 214-227.
589. Caner, H.; Cheeseman, J. R.; Agranat, I., *Chirality*, **2006**, *18*, 10-6.
590. Asghar, W.; Pittman, E.; Jamali, F., *Daru, J. Pharm. Sci.*, **2015**, *23*, 7.
591. Tucker, G. T., *Lancet (London, England)*, **2000**, *355*, 1085-7.
592. Calcaterra, A.; D'Acquarica, I., *J. Pharm. Biomed. Anal.*, **2018**, *147*, 323-340.
593. Zhou, Q.; Yan, X. F.; Pan, W. S.; Zeng, S., *World J. Gastroenterol.*, **2008**, *14*, 2617-9.
594. Millership, J. S.; Fitzpatrick, A., *Chirality*, **1993**, *5*, 573-6.
595. Nunez, M. C.; Garcia Rubino, M. E.; Conejo Garcia, A.; Cruz Lopez, O.; Kimatrai, M.; Gallo, M. A.; Espinosa, A.; Campos, J. M., *Curr. Med. Chem.*, **2009**, *16*, 2064-74.
596. Mansfield, P.; Henry, D.; Tonkin, A., *Clin. Pharmacokinet.*, **2004**, *43*, 287-90.
597. Hellstrom, P. M.; Vitols, S., *Basic Clin. Pharmacol. Toxicol.*, **2004**, *94*, 106-11.
598. Hutt, A. J.; Valentova, j., *Acta Fac. Pharm. Univ. Comeniana*, **2003**, *50*, 7-23.
599. Agranat, I.; Caner, H.; Caldwell, J., *Nat. Rev. Drug Discovery*, **2002**, *1*, 753-68.
600. Federsel, H. J., *Bioorg. Med. Chem.*, **2010**, *18*, 5775-5794.
601. Erlandsson, P.; Isaksson, R.; Lorentzon, P.; Lindberg, P., *J. Chromatogr.*, **1990**, *532*, 305-19.
602. Raju, M. N.; Kumar, N. U.; Reddy, B. S.; Anitha, N.; Srinivas, G.; Bhattacharya, A.; Mukkanti, K.; Kolla, N.; Bandichhor, R., *Tetrahedron Lett.*, **2011**, *52*, 5464-5466.

603. Gallinella, B.; Ferretti, R.; Zanitti, L.; Sestili, I.; Mosca, A.; Cirilli, R., *J. Pharm. Anal.*, **2016**, *6*, 132-136.
604. Balmér, K.; Persson, B. A.; Lagerström, P. O., *J. Chromatogr. A*, **1994**, *660*, 269-273.
605. Dixit, S.; Dubey, R.; Bhushan, R., *Biomed. Chromatogr.*, **2014**, *28*, 112-9.
606. Ha, J. J.; Choi, H. J.; Jin, J. S.; Jeong, E. D.; Hyun, M. H., *J. Chromatogr. A*, **2010**, *8*, 6436-41.
607. Cairns, A. M.; Chiou, R. H. Y.; Rogers, J. D.; Demetriades, J. L., *J. Chromatogr. B: Biomed. Sci. Appl.*, **1995**, *666*, 323-328.
608. del Nozal, M. J.; Toribio, L.; Bernal, J. L.; Alonso, C.; Jimenez, J. J., *J. Sep. Sci.*, **2004**, *27*, 1023-9.
609. Taylor, L. T., *Anal. Chem.*, **2010**, *82*, 4925-4935.
610. Toribio, L.; Alonso, C.; del Nozal, M. J.; Bernal, J. L.; Martin, M. T., *J. Chromatogr. A*, **2006**, *22*, 30-5.
611. Andersson, S.; Nelander, H.; Ohlen, K., *Chirality*, **2007**, *19*, 706-15.
612. Raju, S. V. N.; Purandhar, K.; Reddy, P. P.; Reddy, G. M.; Reddy, L. A.; Reddy, K. S.; Sreenath, K.; Mukkanti, K.; Reddy, G. S., *Org. Process Res. Dev.*, **2006**, *10*, 33-35.
613. Kumar, M. K.; Purandhar, K.; Reddy, K. S.; Reddy, M. S.; Sreenath, K.
614. Reddy, L. A.; Malakondaiah, G. C.; Babu, K. S.; Bhattacharya, A.; Bandichhor, R.; Himabindu, V.; Reddy, P. P.; Anand, R. V., *Org. Process Res. Dev.*, **2008**, *12*, 66-68.
615. Mahale, R. D.; Rajput, M. R.; Maikap, G. C.; Gurjar, M. K., *Org. Process Res. Dev.*, **2010**, *14*, 1264-1268.
616. Delsarte, C.; Santraine, R.; Fours, B.; Petit, L., *Org. Process Res. Dev.*, **2018**, *22*, 321-327.
617. Babiak, P.; Kyslikova, E.; Stepanek, V.; Valesova, R.; Palyzova, A.; Maresova, H.; Hajicek, J.; Kyslik, P., *Bioresour. Technol.*, **2011**, *102*, 7621-6.
618. Balke, K.; Beier, A.; Bornscheuer, U. T., *Biotechnol. Adv.*, **2018**, *36*, 247-263.
619. Matsui, T.; Dekishima, Y.; Ueda, M., *Appl. Microbiol. Biotechnol.*, **2014**, 1-8.
620. Bong, Y. K.; Song, S.; Nazor, J.; Vogel, M.; Widegren, M.; Smith, D.; Collier, S. J.; Wilson, R.; Palanivel, S. M.; Narayanaswamy, K.; Mijts, B.; Clay, M. D.; Fong, R.; Colbeck, J.; Appaswami, A.; Muley, S.; Zhu, J.; Zhang, X.; Liang, J.; Entwistle, D., *J. Org. Chem.*, **2018**.
621. Yoshida, T.; Kito, M.; Tsujii, M.; Nagasawa, T., *Biotechnol. Lett.*, **2001**, *23*, 1217-1222.
622. Seenivasaperumal, M.; Federsel, H. J.; Ertan, A.; Szabo, K. J., *Chem. Commun.*, **2007**, 2187-2189.
623. Seenivasaperumal, M.; Federsel, H. J.; Szabó, K. J., *Adv. Synth. Catal.*, **2009**, *351*, 903-919.

624. Guoyong, C.; Jing, X.; Tian, T.; Qingfei, H.; Linfeng, C.; Jian, L.; Qiwei, W.; Jin, Z.; Jingen, D., *Tetrahedron: Asymmetry*, **2012**, *23*, 457-460.
625. Talsi, E. P.; Rybalova, T. V.; Bryliakov, K. P., *ACS Catal.*, **2015**, 4673-4679.
626. Talsi, E. P.; Bryliakov, K. P., *Catal. Today*, **2017**, *279*, 84-89.
627. Song, W.; Dong, L.; Zhou, Y.; Fu, Y.; Xu, W., *Synth. Commun.*, **2014**, *45*, 70-77.
628. Jiang, B.; Zhao, X. L.; Dong, J. J.; Wang, W. J., *Eur. J. Org. Chem.*, **2009**, *2009*, 987-991.
629. Khomenko, T. M.; Volcho, K. P.; Komarova, N. I.; Salakhutdinov, N. F., *Russ J Org Chem*, **2008**, *44*, 124-127.
630. Delamare, M.; Belot, S.; Caille, J. C.; Martinet, F.; Kagan, H. B.; Henryon, V., *Tetrahedron Lett.*, **2009**, *50*, 1702-1704.
631. Shen, C.; Qiao, J.; Zhao, L. W.; Zheng, K.; Jin, J. Z.; Zhang, P. F., *Catal. Commun.*, **2017**, *92*, 114-118.
632. Koneva, E. A.; Khomenko, T. M.; Kurbakova, S. Y.; Komarova, N. I.; Korchagina, D. V.; Volcho, K. P.; Salakhutdinov, N. F.; Tolstikov, A. G.; Tolstikov, G. A., *Russ. Chem. Bull.*, **2008**, *57*, 1680-1685.
633. Choi, J. Y.; Hwang, G. S.; Senapati, B. K.; Ryu, D. H., *Bull. Korean Chem. Soc.*, **2008**, *29*, 1879-1880.
634. Markovic, N.; Agotonovic Kustrin, S.; Glass, B.; Prestidge, C. A., *J. Pharm. Biomed. Anal.*, **2006**, *42*, 25-31.
635. Ray, P. C.; Mittapelli, V.; Rohatgi, A.; Tyagi, O. D., *Synth. Commun.*, **2007**, *37*, 2861-2868.
636. vonUnge, S.; Langer, V.; Sjolín, L., *Tetrahedron: Asymmetry*, **1997**, *8*, 1967-1970.
637. Hentschel, P.; Holtin, K.; Steinhauser, L.; Albert, K., *Chirality*, **2012**, *24*, 1074-6.
638. Tanaka, S.; Sugihara, Y.; Sakamoto, A.; Ishii, A.; Nakayama, J., *J. Am. Chem. Soc.*, **2003**, *125*, 9024-9025.
639. Redondo, J.; Capdevila, A.; Latorre, I., *Chirality*, **2010**, *22*, 472-478.
640. O'Mahony, G. E.; Ford, A.; Maguire, A. R., *J. Sulfur Chem.*, **2012**, *34*, 301-341.
641. Barraclough, C. G.; Martin, R. L.; Winter, G., *J. Chem. Soc.*, **1964**, 758.
642. Bradley, D. C.; Holloway, C. E., *J. Chem. Soc. A*, **1968**, 1316-1319.
643. Bradley, D. C.; Mehrotra, R. C.; Wardlaw, W., *J. Chem. Soc.*, **1952**, 4204-4209.
644. Bradley, D. C.; Mehrotra, R. C.; Swanwick, J. D.; Wardlaw, W., *J. Chem. Soc.*, **1953**, 2025-2030.
645. Bradley, D. C.; Mehrotra, R. C.; Wardlaw, W., *J. Chem. Soc.*, **1952**, 5020-5023.
646. Bradley, D. C.; Mehrotra, R. C.; Wardlaw, W., *J. Chem. Soc.*, **1952**, 2027-2032.
647. Finn, M. G.; Sharpless, K. B., *J. Am. Chem. Soc.*, **1991**, *113*, 113-126.
648. Bradley, D. C.; Gaze, R.; Wardlaw, W., *J. Chem. Soc.*, **1957**, 469-478.

649. Wenzel, T. J., *Stereoselective Synthesis of Drugs and Natural Products*, John Wiley & Sons, Inc., **2013**.
650. Wenzel, T. J.; Wilcox, J. D., *Chirality*, **2003**, *15*, 256-270.
651. Parker, D., *Chem. Rev.*, **1991**, *91*, 1441-1457.
652. Pirkle, W. H.; Hoekstra, M. S., *J. Am. Chem. Soc.*, **1976**, *98*, 1832-1839.
653. Sarfati, M.; Lesot, P.; Merlet, D.; Courtieu, J., *Chem. Commun.*, **2000**, 2069-2081.
654. Baillif, V.; Robins, R. J.; Billault, I.; Lesot, P., *J. Am. Chem. Soc.*, **2006**, *128*, 11180-11187.
655. Farjon, J.; Merlet, D.; Lesot, P.; Courtieu, J., *J. Magn. Reson.*, **2002**, *158*, 169-172.
656. Courtieu, J.; Lesot, P.; Meddour, A.; Merlet, D.; Aroulanda, C., *Encyclopedia of Nuclear Magnetic Resonance*, Ed. Harris, D. M. G. a. R. K., John Wiley & Sons, Ltd., Chichester, , **2002**, *Vol. 9*, pp 497-505.
657. Sackmann, E.; Meiboom, S.; Snyder, L. C., *J. Am. Chem. Soc.*, **1968**, *90*, 2183-2184.
658. Schmidt, M.; Sun, H.; Leonov, A.; Griesinger, C.; Reinscheid, U. M., *Magn. Reson. Chem.*, **2012**, *50*.
659. Sarfati, M.; Courtieu, J.; Lesot, P., *Chem. Commun.*, **2000**, 1113-1114.
660. Lesot, P.; Merlet, D.; Meddour, A.; Courtieu, J.; Loewenstein, A., *J. Chem. Soc., Faraday Trans.*, **1995**, *91*, 1371-1375.
661. Yamaguchi, S., *Asymmetric Synthesis*, Ed. Morrison, J. D., Academic, New York, **1983**, *Vol. 1*, pp 125-152.
662. Raban, M.; Mislow, K., *Tetrahedron Lett.*, **1965**, *6*, 4249-4253.
663. Gerlach, H.; Zagalak, B., *J. Chem. Soc., Chem. Commun.*, **1973**, 274-275.
664. Dale, J. A.; Dull, D. L.; Mosher, H. S., *J. Org. Chem.*, **1969**, *34*, 2543-2549.
665. Lee, S., *Chem. Educ.*, **2004**, *9*, 359-363.
666. Weisman, G. R., *Asymmetric Synthesis*, Ed. Morrison, J. D., Academic, New York, **1983**, *Vol. 1*, pp 153-171.
667. Gallou, I.; Senanayake, C. H., *Chem. Rev.*, **2006**, *106*, 2843-2874.
668. Thunhorst, M.; Holzgrabe, U., *Magn. Reson. Chem.*, **1998**, *36*, 211-216.
669. Wenzel, T. J., *Top. Curr. Chem.*, **2013**, *341*, 1-68.
670. Wenzel, T. J.; Freeman, B. E.; Sek, D. C.; Zopf, J. J.; Nakamura, T.; Yongzhu, J.; Hirose, K.; Tobe, Y., *Anal. Bioanal. Chem.*, **2004**, *378*, 1536-47.
671. Folli, U.; Iarossi, D.; Mucci, A.; Taddei, F., *J. Mol. Struct.*, **1995**, *350*, 115-128.
672. McCreary, M. D.; Lewis, D. W.; Wernick, D. L.; Whitesides, G. M., *J. Am. Chem. Soc.*, **1974**, *96*, 1038-1054.
673. Morrill, T. C., *Lanthanide shift reagents in stereochemical analysis*. Wiley: 1987;
674. Fraser, R. R., *Asymmetric Synthesis*, Ed. Morrison, J. D., Academic, New York, **1983**, *Vol. 1*, pp 173-196.

675. Mayo, B. C., *Chem. Soc. Rev.*, **1973**, 2, 49-74.
676. Whitesides, G. M.; Lewis, D. I. W., *J. Am. Chem. Soc.*, **1971**, 93, 5914-5916.
677. <http://www.sigmaaldrich.com/catalog/product/aldrich/164747?lang=en®ion=GB>, (accessed 27th July 2014).
678. <http://www.sigmaaldrich.com/catalog/product/aldrich/160938?lang=en®ion=GB>, (accessed 27th July 2014).
679. Jaime, C.; Virgili, A.; Claramunt, R. M.; Lopez, C.; Elguero, J., *J. Org. Chem.*, **1991**, 56, 6521-6523.
680. Pirkle, W. H.; Sikkenga, D. L.; Pavlin, M. S., *J. Org. Chem.*, **1977**, 42, 384-387.
681. Szawkało, J.; Zawadzka, A.; Wojtasiewicz, K.; Leniewski, A.; Drabowicz, J.; Czarnocki, Z., *Tetrahedron: Asymmetry*, **2005**, 16, 3619-3621.
682. Yuste, F.; Sánchez Obregón, R.; Díaz, E.; García Carrillo, M. A., *Tetrahedron: Asymmetry*, **2014**, 25, 224-228.
683. <http://www.sigmaaldrich.com/catalog/product/aldrich/211354?lang=en®ion=GB>, (accessed 27th July 2014).
684. <http://www.sigmaaldrich.com/catalog/product/aldrich/246956?lang=en®ion=GB>, (accessed 27th July 2014).
685. Baciocchi, R.; Juza, M.; Classen, J.; Mazzotti, M.; Morbidelli, M., *Helv. Chim. Acta*, **2004**, 87, 1917-1926.
686. Wenzel, T. J.; Bean, A. C.; Dunham, S. L., *Magn. Reson. Chem.*, **1997**, 35, 395-402.
687. Annunziata, R.; Cinquini, M.; Cozzi, F., *Org. Magn. Reson.*, **1983**, 21, 183-186.
688. Ema, T.; Tanida, D.; Sakai, T., *J. Am. Chem. Soc.*, **2007**, 129, 10591-10596.
689. Pirkle, W. H.; Beare, S. D.; Muntz, R. L., *Tetrahedron Lett.*, **1974**, 15, 2295-2298.
690. Charpin, P.; Duñach, E.; Kagan, H. B.; Theobald, F. R., *Tetrahedron Lett.*, **1986**, 27, 2989-2992.
691. Buist, P. H.; Marecak, D.; Holland, H. L.; Brown, F. M., *Tetrahedron: Asymmetry*, **1995**, 6, 7-10.
692. Fauconnot, L.; Nugier Chauvin, C.; Noiret, N.; Patin, H., *Tetrahedron Lett.*, **1997**, 38, 7875-7878.
693. Figueiras, A.; Sarraguça, J. M. G.; Carvalho, R.; Pais, A. A. C. C.; Veiga, F. B., *Pharm Res*, **2007**, 24, 377-389.
694. Muralidhara, R. D.; Parthasaradhi, R. B.; Raji, R. R.; Rathnakar, R. K.; Vamsi, K. B.
695. Coppi, L.; Berenguer Maimo, R.; Gasanz Guillen, Y.; Medrano Ruperez, J., WO2006094904A1.
696. Wain, C. P.; Hamied, Y. K.; Rao, D. R., WO2002098423A1.
697. Yang, L.; Wenzel, T.; Williamson, R. T.; Christensen, M.; Schafer, W.; Welch, C. J., *ACS Cent. Sci.*, **2016**, 2, 332-340.

698. Toda, F.; Mori, K.; Okada, J.; Node, M.; Itoh, A.; Oomine, K.; Fuji, K., *Chem. Lett.*, **1988**, 131-134.
699. Job, P., *Ann. Chim. Anal. Chim. Appl.*, **1928**, 9, 113-125.
700. Djedaini, F.; Lin, S. Z.; Perly, B.; Wouessidjewe, D., *J. Pharm. Sci.*, **1990**, 79, 643-646.
701. Fuller, A. L.; Aitken, R. A.; Ryan, B. M.; Slawin, A. M. Z.; Woollins, J. D., *J. Chem. Crystallogr.*, **2009**, 39, 407-415.
702. Mishra, M. K.; Ramamurty, U.; Desiraju, G. R., *J. Am. Chem. Soc.*, **2015**, 137, 1794-1797.
703. Allen, F. H.; Kennard, O.; Watson, D. G.; Brammer, L.; Orpen, A. G.; Taylor, R., *J. Chem. Soc.-Perkin Trans. 2*, **1987**, S1-S19.
704. Dolomanov, O. V.; Bourhis, L. J.; Gildea, R. J.; Howard, J. A. K.; Puschmann, H., *J. Appl. Crystallogr.*, **2009**, 42, 339-341.
705. Elguero, J.; Llouquet, G.; Marzin, C., *Tetrahedron Lett.*, **1975**, 16, 4085-4086.
706. Sun, C. L.; Li, X.; Zhu, Y., WO2009139834A1.
707. Dilarski, B., *Liebigs Ann. Chem.*, **1983**, 45, 1078-1082.
708. Yang, R.; Schulman, S. G.; Zavala, P. J., *Anal. Chim. Acta*, **2003**, 481, 155-164.
709. Redondo, J.; Jaime, C.; Marqués, A., *J. Pharm. Biomed. Anal.*, **2016**, 131, 454-463.
710. Wolfe, S.; Stolor, A.; LaJohn, L. A., *Tetrahedron Lett.*, **1983**, 24, 4071-4074.
711. Speers, P.; Laidig, K. E.; Streitwieser, A., *J. Am. Chem. Soc.*, **1994**, 116, 9257-9261.
712. Novak, P.; Meić, Z.; Vikić-Topić, D.; Smrečki, V.; Plavec, J., *Spectrochim. Acta, Part A*, **1998**, 54, 327-333.
713. Gottlieb, H. E.; Kotlyar, V.; Nudelman, A., *J. Org. Chem.*, **1997**, 62, 7512-7515.
714. Cosier, J.; Glazer, A. M., *J. Appl. Crystallogr.*, **1986**, 19, 105-107.
715. Rigaku Oxford Diffraction, CrysAlisPro Software, Rigaku Corporation, Oxford, UK.
716. Sheldrick, G., *Acta Crystallogr., Sect. A: Found. Adv.*, **2008**, 64, 112-122.
717. Palatinus, L.; Chapuis, G., *J. Appl. Crystallogr.*, **2007**, 40, 786-790.
718. Joseph, K. M.; Larraza Sanchez, I., *Tetrahedron Lett.*, **2011**, 52, 13-16.
719. Rosenblatt, K. M.; Bunjes, H.; Seeling, A.; Oelschlager, H., *Pharmazie*, **2005**, 60, 503-507.
720. Yang, C.; Jin, Q.; Zhang, H.; Liao, J.; Zhu, J.; Yu, B.; Deng, J., *Green Chem.*, **2009**, 11, 1401-1405.
721. Mohamed, G. G.; Nour El Dien, F. A.; Khalil, S. M.; Mohammad, A. S., *J. Coord. Chem.*, **2009**, 62, 645-654.
722. Ajiki, K.; Hirano, M.; Tanaka, K., *Org. Lett.*, **2005**, 7, 4193-4195.
723. M. Downie, I.; Heaney, H.; Kemp, G., *Tetrahedron*, **1988**, 44, 2619-2624.
724. Al-Karagully, H. J.; Razzak Mahmood, A. A., *J. Pharm. Sci. Res.*, **2017**, 9, 260-266.

725. Foucoin, F.; Caupène, C.; Lohier, J.-F.; Sopkova de Oliveira Santos, J.; Perrio, S.; Metzner, P., *Synthesis*, **2007**, 2007, 1315-1324.
726. Lewis, F. W.; McCabe, T. C.; Grayson, D. H., *Tetrahedron*, **2011**, 67, 7517-7528.
727. Kjaer, A.; Malver, O., *Tetrahedron Lett.*, **1982**, 23, 2687-2690.

Appendix: XRD Data

Contents

1.1	XRD data for Omeprazole 1.1	A2
1.2	XRD data for Pyrimetazole sulfide 3.17.....	A10
1.3	XRD data for Omeprazole sulfone 4.1	A17
1.4	XRD data for K-Omeprazole 3.38.....	A24
1.5	XRD data for NMe Omeprazole 5.22.....	A33
1.6	XRD data for Benzyl <i>p</i> -tolyl sulfoxide 4.10.....	A41
1.8	XRD data for Methyl 6(5)-OMe benzimidazole sulfoxide 4.11.....	A48
1.9	XRD data for Pyridyl <i>p</i> -tolyl sulfoxide 4.12	A55

1.1 XRD data for Omeprazole 1.1

Table 1 Crystal data and structure refinement for JS04_07_Cu.

Identification code	JS04_07_Cu
Empirical formula	C ₁₇ H ₁₉ N ₃ O ₃ S
Formula weight	345.41
Temperature/K	99.8(6)
Crystal system	triclinic
Space group	P-1
a/Å	9.6371(5)
b/Å	10.1691(6)
c/Å	10.4608(6)
α/°	90.477(5)
β/°	112.162(5)
γ/°	115.682(6)
Volume/Å ³	837.30(8)
Z	2
ρ _{calc} /mg/mm ³	1.370
m/mm ⁻¹	1.897
F(000)	364.0
Crystal size/mm ³	0.17 × 0.08 × 0.06
Radiation	CuKα (λ = 1.54184)
2θ range for data collection	9.32 to 133.14°
Index ranges	-11 ≤ h ≤ 11, -12 ≤ k ≤ 12, -12 ≤ l ≤ 12
Reflections collected	12305
Independent reflections	2860 [R _{int} = 0.0584, R _{sigma} = 0.0457]
Data/restraints/parameters	2860/0/245
Goodness-of-fit on F ²	1.058
Final R indexes [I ≥ 2σ (I)]	R ₁ = 0.0523, wR ₂ = 0.1336
Final R indexes [all data]	R ₁ = 0.0734, wR ₂ = 0.1506
Largest diff. peak/hole / e Å ⁻³	0.36/-0.38

Table 2 Fractional Atomic Coordinates ($\times 10^4$) and Equivalent Isotropic Displacement Parameters ($\text{\AA}^2 \times 10^3$) for JS04_07_Cu. U_{eq} is defined as 1/3 of the trace of the orthogonalised U_{ij} tensor.

Atom	<i>x</i>	<i>y</i>	<i>z</i>	U_{eq}
C1A	13675(4)	4596(4)	6504(5)	54.9(11)
O2A	13404(3)	5739(3)	6995(3)	49.8(7)
C3	11821(4)	5322(4)	6879(4)	58.7(10)
C4	11635(4)	6461(4)	7432(4)	58.1(9)
C5	10119(4)	6227(4)	7403(4)	59.0(9)
C6	8737(4)	4791(3)	6789(3)	52.6(8)
C7	8926(3)	3666(3)	6224(3)	51.5(8)
C8	10474(3)	3865(4)	6243(3)	53.3(8)
N9	7334(3)	2429(3)	5660(3)	49.2(7)
C10	6307(3)	2878(3)	5902(3)	51.4(8)
N11	7067(3)	4271(3)	6591(3)	56.1(7)
S12	4107.5(9)	1735.8(8)	5429.5(9)	50.8(3)
O13	3912(2)	322(2)	5960(2)	50.9(6)
C14	3481(4)	1263(4)	3566(3)	52.5(8)
C15	1567(3)	273(3)	2821(3)	43.9(7)
N16	676(3)	534(3)	3411(3)	49.9(7)
C17	-1019(4)	-253(4)	2766(4)	56.0(9)
C18	-1896(3)	-1310(4)	1522(4)	51.9(8)
C19	-934(3)	-1582(3)	949(3)	46.2(7)
C20	849(3)	-797(3)	1605(3)	44.1(7)
C21	-3820(4)	-2097(5)	802(5)	79.6(13)
O22	-1728(3)	-2596(2)	-303(2)	55.3(6)
C23	-2077(5)	-4081(4)	-110(4)	70.5(11)
C24	1889(4)	-1116(4)	993(4)	60.1(9)
C1B	13490(20)	8570(20)	8450(30)	63(7)
O2B	13466(13)	7326(13)	7771(13)	38(3)

Table 3 Anisotropic Displacement Parameters ($\text{\AA}^2 \times 10^3$) for JS04_07_Cu. The Anisotropic displacement factor exponent takes the form: $-2\pi^2[h^2a^*U_{11}+2hka^*b^*U_{12}+\dots]$.

Atom	U_{11}	U_{22}	U_{33}	U_{23}	U_{13}	U_{12}
C1A	36.4(17)	42.6(19)	75(3)	10.5(19)	17.6(18)	14.5(15)
O2A	24.6(11)	40.4(13)	63.7(18)	5.7(11)	9.3(11)	6.2(9)
C3	28.7(14)	65(2)	49(2)	21.6(17)	3.6(14)	5.3(14)
C4	40.9(16)	42.7(17)	49(2)	1.1(15)	2.0(14)	-0.3(13)
C5	37.7(16)	49.0(18)	47(2)	-0.7(15)	2.8(14)	-2.4(13)
C6	39.0(15)	45.9(17)	38(2)	-2.8(14)	6.3(14)	-0.4(13)
C7	30.6(14)	50.3(17)	38.7(19)	8.6(14)	5.9(13)	-2.7(13)
C8	32.2(14)	52.5(17)	46(2)	11.8(15)	7.5(13)	3.7(13)
N9	32.0(12)	44.0(14)	39.5(16)	-3.3(12)	9.2(11)	-3.5(11)
C10	30.8(14)	50.8(17)	36.5(19)	-7.5(14)	7.8(13)	-4.9(12)
N11	37.0(13)	50.9(15)	42.0(17)	-8.1(12)	9.5(12)	-4.7(11)
S12	31.4(4)	47.4(4)	43.5(5)	-8.5(3)	12.1(3)	-3.1(3)
O13	32.4(10)	51.2(12)	48.6(14)	1.8(10)	17.4(9)	2.6(9)
C14	31.9(14)	50.6(17)	43(2)	-1.9(14)	12.5(13)	-4.4(12)
C15	30.9(13)	38.9(14)	39.3(18)	2.3(13)	11.8(12)	0.2(11)
N16	34.9(12)	43.9(13)	48.4(17)	-1.6(12)	13.6(12)	3.4(10)
C17	35.4(15)	60.7(19)	57(2)	6.8(17)	18.2(15)	11.2(14)
C18	29.3(14)	53.6(17)	45(2)	6.4(15)	9.5(13)	2.1(12)
C19	32.5(13)	42.3(15)	36.1(18)	3.9(13)	8.7(12)	-0.4(12)
C20	32.4(13)	40.6(15)	35.4(17)	4.5(13)	10.4(12)	0.8(11)
C21	31.3(16)	100(3)	68(3)	7(2)	13.0(17)	5.1(17)
O22	38.9(10)	50.8(12)	36.4(13)	0.1(10)	7.8(9)	-5.1(9)
C23	70(2)	49.2(19)	47(2)	-5.8(16)	15.8(18)	-2.0(16)
C24	40.3(16)	71(2)	40(2)	-5.2(16)	14.2(14)	5.0(15)
C1B	23(9)	40(11)	90(20)	-5(11)	16(10)	-5(8)
O2B	26(6)	47(7)	32(8)	5(5)	13(5)	10(5)

Table 4 Bond Lengths for JS04_07_Cu.

Atom	Atom	Length/Å	Atom	Atom	Length/Å
C1A	O2A	1.427(4)	S12	C14	1.800(3)
O2A	C3	1.349(4)	C14	C15	1.522(4)
C3	C4	1.398(5)	C15	N16	1.335(4)
C3	C8	1.410(4)	C15	C20	1.394(4)
C4	C5	1.362(5)	N16	C17	1.338(4)
C5	C6	1.404(4)	C17	C18	1.386(5)
C6	C7	1.394(5)	C18	C19	1.391(5)
C6	N11	1.387(4)	C18	C21	1.515(4)
C7	C8	1.408(5)	C19	C20	1.405(4)
C7	N9	1.384(3)	C19	O22	1.380(4)
N9	C10	1.352(4)	C20	C24	1.511(4)
C10	N11	1.322(4)	O22	C23	1.432(4)
C10	S12	1.776(3)	C1B	O2B	1.43(3)
S12	O13	1.506(2)			

Table 5 Bond Angles for JS04_07_Cu.

Atom Atom Atom	Angle/°	Atom Atom Atom	Angle/°
C3 O2A C1A	116.2(3)	O13 S12 C10	107.11(14)
O2A C3 C4	114.2(3)	O13 S12 C14	105.52(15)
O2A C3 C8	122.6(4)	C15 C14 S12	109.5(2)
C4 C3 C8	123.2(3)	N16 C15 C14	115.0(3)
C5 C4 C3	121.7(3)	N16 C15 C20	124.3(2)
C4 C5 C6	117.4(4)	C20 C15 C14	120.7(3)
C7 C6 C5	120.6(3)	C15 N16 C17	117.7(3)
N11 C6 C5	129.0(3)	N16 C17 C18	123.9(3)
N11 C6 C7	110.3(3)	C17 C18 C19	117.1(3)
C6 C7 C8	123.6(3)	C17 C18 C21	121.1(3)
N9 C7 C6	106.0(3)	C19 C18 C21	121.7(3)
N9 C7 C8	130.4(3)	C18 C19 C20	120.8(3)
C7 C8 C3	113.5(3)	O22 C19 C18	120.1(2)
C10 N9 C7	105.2(3)	O22 C19 C20	119.1(3)
N9 C10 S12	125.2(2)	C15 C20 C19	116.1(3)
N11 C10 N9	115.2(3)	C15 C20 C24	123.3(2)
N11 C10 S12	119.5(3)	C19 C20 C24	120.6(3)
C10 N11 C6	103.2(3)	C19 O22 C23	113.1(2)
C10 S12 C14	96.55(14)		

Table 6 Torsion Angles for JS04_07_Cu.

A	B	C	D	Angle/°	A	B	C	D	Angle/°
C1A	O2A	C3	C4	177.2(3)	N11	C10	S12	O13	-127.8(3)
C1A	O2A	C3	C8	-3.3(5)	N11	C10	S12	C14	123.8(3)
O2A	C3	C4	C5	-179.8(3)	S12	C10	N11	C6	179.2(2)
O2A	C3	C8	C7	-179.7(3)	S12	C14	C15	N16	31.9(4)
C3	C4	C5	C6	-0.2(5)	S12	C14	C15	C20	-149.0(3)
C4	C3	C8	C7	-0.2(5)	O13	S12	C14	C15	71.5(3)
C4	C5	C6	C7	-0.6(5)	C14	C15	N16	C17	176.9(3)
C4	C5	C6	N11	-178.1(3)	C14	C15	C20	C19	-175.9(3)
C5	C6	C7	C8	1.0(5)	C14	C15	C20	C24	3.7(5)
C5	C6	C7	N9	-177.6(3)	C15	N16	C17	C18	-0.4(5)
C5	C6	N11	C10	176.6(4)	N16	C15	C20	C19	3.1(5)
C6	C7	C8	C3	-0.6(5)	N16	C15	C20	C24	-177.3(3)
C6	C7	N9	C10	0.5(4)	N16	C17	C18	C19	1.9(5)
C7	C6	N11	C10	-1.1(4)	N16	C17	C18	C21	-176.4(3)
C7	N9	C10	N11	-1.3(4)	C17	C18	C19	C20	-0.8(5)
C7	N9	C10	S12	-178.9(2)	C17	C18	C19	O22	-178.5(3)
C8	C3	C4	C5	0.6(5)	C18	C19	C20	C15	-1.5(4)
C8	C7	N9	C10	-178.0(3)	C18	C19	C20	C24	178.9(3)
N9	C7	C8	C3	177.7(3)	C18	C19	O22	C23	-90.2(4)
N9	C10	N11	C6	1.5(4)	C20	C15	N16	C17	-2.2(5)
N9	C10	S12	O13	49.7(3)	C20	C19	O22	C23	92.1(3)
N9	C10	S12	C14	-58.8(3)	C21	C18	C19	C20	177.4(3)
C10	S12	C14	C15	-178.7(2)	C21	C18	C19	O22	-0.3(5)
N11	C6	C7	C8	179.0(3)	O22	C19	C20	C15	176.3(3)
N11	C6	C7	N9	0.3(4)	O22	C19	C20	C24	-3.3(4)

Table 7 Hydrogen Atom Coordinates ($\text{\AA}\times 10^4$) and Isotropic Displacement Parameters ($\text{\AA}^2\times 10^3$) for JS04_07_Cu.

Atom	x	y	z	U(eq)
H1AA	12993	4242	5507	82
H1AB	13361	3786	6980	82
H1AC	14853	4991	6696	82
H4	12570	7402	7830	70
H5	10005	6989	7775	71
H8	10596	3108	5872	64
H9	7100(40)	1550(40)	5200(40)	46(9)
H14A	3802	2165	3192	63
H14B	4057	744	3401	63
H17	-1646	-81	3176	67
H21A	-4244	-3116	906	119
H21B	-4189	-2065	-182	119
H21C	-4245	-1608	1225	119
H23A	-2586	-4729	-1009	106
H23B	-2844	-4425	335	106
H23C	-1037	-4086	476	106
H24A	2729	-195	928	90
H24B	1158	-1741	69	90
H24C	2442	-1615	1592	90
H1BA	12445	8597	7929	94
H1BB	14425	9477	8475	94
H1BC	13618	8472	9392	94

Table 8 Atomic Occupancy for JS04_07_Cu.

<i>Atom</i>	<i>Occupancy</i>	<i>Atom</i>	<i>Occupancy</i>	<i>Atom</i>	<i>Occupancy</i>
C1A	0.848(4)	H1AA	0.848(4)	H1AB	0.848(4)
H1AC	0.848(4)	O2A	0.848(4)	C1B	0.152(4)
H1BA	0.152(4)	H1BB	0.152(4)	H1BC	0.152(4)
O2B	0.152(4)				

1.2 XRD data for Pyrimetazole sulfide 3.17

Table 1 Crystal data and structure refinement for JS04_68C_Mo.

Identification code	JS04_68C_Mo
Empirical formula	C ₁₇ H ₁₉ N ₃ O ₂ S
Formula weight	329.41
Temperature/K	119.99(10)
Crystal system	orthorhombic
Space group	P2 ₁ 2 ₁ 2 ₁
a/Å	6.8937(5)
b/Å	13.9553(12)
c/Å	16.8423(15)
α/°	90.00
β/°	90.00
γ/°	90.00
Volume/Å ³	1620.3(2)
Z	4
ρ _{calc} /g/cm ³	1.350
μ/mm ⁻¹	0.213
F(000)	696.0
Crystal size/mm ³	0.35 × 0.08 × 0.07
Radiation	MoKα (λ = 0.71073)
2θ range for data collection/°	6.32 to 52.72
Index ranges	-7 ≤ h ≤ 8, -15 ≤ k ≤ 17, -21 ≤ l ≤ 19
Reflections collected	7430
Independent reflections	3241 [R _{int} = 0.0670, R _{sigma} = 0.0894]
Data/restraints/parameters	3241/0/212
Goodness-of-fit on F ²	1.032
Final R indexes [I ≥ 2σ (I)]	R ₁ = 0.0530, wR ₂ = 0.1126
Final R indexes [all data]	R ₁ = 0.0637, wR ₂ = 0.1190
Largest diff. peak/hole / e Å ⁻³	0.56/-0.26
Flack parameter	0.02(11)

Table 2 Fractional Atomic Coordinates ($\times 10^4$) and Equivalent Isotropic Displacement Parameters ($\text{\AA}^2 \times 10^3$) for JS04_68C_Mo. U_{eq} is defined as 1/3 of the trace of the orthogonalised U_{ij} tensor.

Atom	x	y	z	U(eq)
C1	-18855(5)	1500(3)	83(2)	37.6(9)
O2	-17621(3)	762.7(17)	381.1(13)	32.0(6)
C3	-15950(4)	570(2)	-37.0(18)	22.8(7)
C4	-14849(4)	-190(2)	253.1(17)	23.0(7)
C5	-13175(4)	-416(2)	-167.9(17)	18.2(6)
C6	-12624(4)	70(2)	-863.3(17)	18.5(6)
C7	-13738(4)	840(2)	-1119.4(17)	21.8(6)
C8	-15402(4)	1089(2)	-708.5(18)	24.5(7)
N9	-11792(3)	-1116.9(17)	-63.5(14)	19.4(5)
C10	-10525(4)	-1031.2(19)	-677.2(17)	19.1(6)
N11	-10929(3)	-333.7(16)	-1172.7(14)	20.0(5)
S12	-8666.3(12)	-1875.6(5)	-743.6(5)	27.5(2)
C13	-7113(4)	-1280(2)	-1446.8(16)	18.1(6)
C14	-5560(4)	-1964(2)	-1720.1(16)	17.8(6)
N15	-5365(3)	-2780.0(17)	-1301.9(13)	18.2(5)
C16	-3963(4)	-3386(2)	-1520.0(16)	20.4(6)
C17	-2728(4)	-3253(2)	-2160.6(16)	18.0(6)
C18	-3002(4)	-2404(2)	-2593.1(16)	19.5(6)
C19	-4411(4)	-1740.5(19)	-2378.9(15)	16.7(6)
C20	-1196(5)	-3969(2)	-2375.9(18)	25.9(7)
O21	-1929(3)	-2254.6(15)	-3272.4(12)	25.5(5)
C22	-108(5)	-1821(3)	-3133(2)	35.3(8)
C23	-4684(5)	-822(2)	-2832.0(17)	24.0(7)

Table 3 Anisotropic Displacement Parameters ($\text{\AA}^2 \times 10^3$) for JS04_68C_Mo. The**Anisotropic displacement factor exponent takes the form: $-2\pi^2[h^2a^{*2}U_{11}+2hka^*b^*U_{12}+\dots]$.**

Atom	U_{11}	U_{22}	U_{33}	U_{23}	U_{13}	U_{12}
C1	24.6(16)	47(2)	41.5(19)	-2.1(16)	-0.4(17)	19.8(18)
O2	28.3(12)	38.7(13)	29.0(12)	5.2(10)	2.4(10)	9.7(12)
C3	15.3(15)	28.0(16)	25.0(15)	-12.3(13)	0.4(13)	2.3(14)
C4	20.3(15)	29.7(17)	19.1(15)	1.1(12)	-1.7(13)	0.6(14)
C5	15.7(14)	18.8(15)	20.1(15)	-0.7(12)	-3.3(12)	1.1(13)
C6	15.7(14)	20.0(14)	19.9(15)	0.5(12)	-1.1(12)	-2.0(12)
C7	18.0(14)	20.1(14)	27.3(15)	2.7(12)	0.0(14)	1.8(14)
C8	24.1(16)	19.7(14)	29.5(16)	0.1(14)	-6.0(15)	4.2(13)
N9	14.9(12)	23.6(13)	19.7(12)	7.6(10)	0.8(10)	0.2(11)
C10	15.7(14)	21.1(14)	20.7(14)	3.5(13)	3.4(13)	0.8(12)
N11	18.7(13)	17.6(12)	23.6(13)	3.5(10)	3.9(11)	2.5(11)
S12	21.1(4)	25.3(4)	36.0(4)	12.5(4)	10.1(4)	8.5(4)
C13	17.7(14)	17.1(14)	19.6(14)	2.1(11)	3.2(12)	0.6(13)
C14	18.0(14)	20.2(14)	15.0(13)	-2.4(12)	-2.9(12)	-0.1(13)
N15	18.9(13)	20.4(12)	15.4(11)	0.1(10)	-0.3(10)	2.4(11)
C16	21.4(15)	21.0(14)	18.7(14)	1.6(11)	0.2(13)	0.3(13)
C17	17.7(14)	17.3(14)	19.0(14)	-4.3(12)	-1.2(12)	0.5(13)
C18	17.4(14)	25.1(15)	16.0(14)	-2.0(12)	2.6(12)	-7.5(14)
C19	21.7(14)	16.6(13)	11.8(13)	-0.1(11)	-2.6(11)	-2.6(13)
C20	24.2(16)	24.1(15)	29.3(16)	-2.6(13)	6.0(15)	2.0(15)
O21	25.5(12)	30.9(11)	20.0(11)	-1.1(9)	6.6(9)	-4(1)
C22	26.2(17)	42(2)	37.1(19)	3.7(16)	4.1(15)	-9.2(19)
C23	27.4(17)	22.6(15)	22.1(15)	5.9(13)	1.3(14)	2.3(15)

Table 4 Bond Lengths for JS04_68C_Mo.

Atom	Atom	Length/Å	Atom	Atom	Length/Å
C1	O2	1.427(4)	S12	C13	1.800(3)
O2	C3	1.377(3)	C13	C14	1.506(4)
C3	C4	1.393(4)	C14	N15	1.346(4)
C3	C8	1.395(4)	C14	C19	1.399(4)
C4	C5	1.391(4)	N15	C16	1.335(4)
C5	C6	1.406(4)	C16	C17	1.387(4)
C5	N9	1.377(3)	C17	C18	1.404(4)
C6	C7	1.389(4)	C17	C20	1.498(4)
C6	N11	1.398(4)	C18	C19	1.390(4)
C7	C8	1.384(4)	C18	O21	1.378(3)
N9	C10	1.359(4)	C19	C23	1.503(4)
C10	N11	1.312(3)	O21	C22	1.414(4)
C10	S12	1.744(3)			

Table 5 Bond Angles for JS04_68C_Mo.

Atom	Atom	Atom	Angle/°	Atom	Atom	Atom	Angle/°
C3	O2	C1	117.4(2)	C10	S12	C13	99.62(13)
O2	C3	C4	115.2(3)	C14	C13	S12	109.34(19)
O2	C3	C8	122.7(3)	N15	C14	C13	116.6(2)
C4	C3	C8	122.2(3)	N15	C14	C19	123.2(3)
C5	C4	C3	116.5(3)	C19	C14	C13	120.2(2)
C4	C5	C6	122.6(3)	C16	N15	C14	117.6(2)
N9	C5	C4	132.1(3)	N15	C16	C17	125.0(3)
N9	C5	C6	105.2(2)	C16	C17	C18	115.7(2)
C7	C6	C5	118.9(3)	C16	C17	C20	122.2(2)
C7	C6	N11	131.1(3)	C18	C17	C20	122.2(2)
N11	C6	C5	110.0(2)	C19	C18	C17	121.5(2)
C8	C7	C6	119.8(3)	O21	C18	C17	119.1(3)
C7	C8	C3	120.0(3)	O21	C18	C19	119.3(2)
C10	N9	C5	106.6(2)	C14	C19	C23	121.5(3)
N9	C10	S12	117.49(19)	C18	C19	C14	117.0(2)
N11	C10	N9	114.4(2)	C18	C19	C23	121.6(3)
N11	C10	S12	128.1(2)	C18	O21	C22	113.8(2)
C10	N11	C6	103.9(2)				

Table 6 Torsion Angles for JS04_68C_Mo.

A	B	C	D	Angle/°	A	B	C	D	Angle/°
C1	O2	C3	C4	-176.7(3)	N11	C10	S12	C13	18.2(3)
C1	O2	C3	C8	2.6(4)	S12	C10	N11	C6	175.8(2)
O2	C3	C4	C5	178.5(2)	S12	C13	C14	N15	-12.5(3)
O2	C3	C8	C7	-177.8(3)	S12	C13	C14	C19	167.3(2)
C3	C4	C5	C6	-1.7(4)	C13	C14	N15	C16	-178.2(2)
C3	C4	C5	N9	-178.7(3)	C13	C14	C19	C18	179.7(2)
C4	C3	C8	C7	1.4(4)	C13	C14	C19	C23	-0.1(4)
C4	C5	C6	C7	3.4(4)	C14	N15	C16	C17	-2.1(4)
C4	C5	C6	N11	-177.7(3)	N15	C14	C19	C18	-0.6(4)
C4	C5	N9	C10	177.1(3)	N15	C14	C19	C23	179.7(3)
C5	C6	C7	C8	-2.6(4)	N15	C16	C17	C18	0.8(4)
C5	C6	N11	C10	0.4(3)	N15	C16	C17	C20	-179.4(3)
C5	N9	C10	N11	0.7(3)	C16	C17	C18	C19	0.8(4)
C5	N9	C10	S12	-176.20(19)	C16	C17	C18	O21	-175.2(2)
C6	C5	N9	C10	-0.4(3)	C17	C18	C19	C14	-0.8(4)
C6	C7	C8	C3	0.3(4)	C17	C18	C19	C23	178.9(3)
C7	C6	N11	C10	179.1(3)	C17	C18	O21	C22	-87.1(3)
C8	C3	C4	C5	-0.8(4)	C19	C14	N15	C16	2.0(4)
N9	C5	C6	C7	-178.9(2)	C19	C18	O21	C22	96.8(3)
N9	C5	C6	N11	0.0(3)	C20	C17	C18	C19	-179.1(2)
N9	C10	N11	C6	-0.7(3)	C20	C17	C18	O21	5.0(4)
N9	C10	S12	C13	-165.4(2)	O21	C18	C19	C14	175.1(2)
C10	S12	C13	C14	-169.37(19)	O21	C18	C19	C23	-5.2(4)
N11	C6	C7	C8	178.8(3)					

Table 7 Hydrogen Atom Coordinates ($\text{\AA} \times 10^4$) and Isotropic Displacement Parameters ($\text{\AA}^2 \times 10^3$) for JS04_68C_Mo.

Atom	x	y	z	U(eq)
H1A	-19312	1326	-436	56
H1B	-18142	2090	51	56
H1C	-19942	1581	433	56
H4	-15214	-528	705	28
H7	-13366	1187	-1566	26
H8	-16155	1602	-880	29
H9	-11740	-1528	316	23
H13A	-7870	-1065	-1898	22
H13B	-6521	-724	-1201	22
H16	-3803	-3939	-1219	24
H20A	42	-3747	-2191	39
H20B	-1157	-4045	-2942	39
H20C	-1491	-4574	-2133	39
H22A	545	-1722	-3629	53
H22B	663	-2230	-2801	53
H22C	-296	-1215	-2873	53
H23A	-5943	-819	-3075	36
H23B	-3705	-772	-3235	36
H23C	-4577	-289	-2475	36

1.3 XRD data for Omeprazole sulfone 4.1

Table 1 Crystal data and structure refinement for JS02_99_Cu.

Identification code	JS02_99_Cu
Empirical formula	C ₁₈ H ₂₃ N ₃ O ₅ S
Formula weight	393.45
Temperature/K	100.0(4)
Crystal system	triclinic
Space group	P-1
a/Å	8.9134(4)
b/Å	10.1893(5)
c/Å	11.0478(6)
α/°	94.295(4)
β/°	110.952(5)
γ/°	91.060(4)
Volume/Å ³	933.30(8)
Z	2
ρ _{calc} /mg/mm ³	1.400
m/mm ⁻¹	1.852
F(000)	416.0
Crystal size/mm ³	0.17 × 0.16 × 0.11
Radiation	CuKα (λ = 1.54184)
2θ range for data collection	8.6 to 133.04°
Index ranges	-10 ≤ h ≤ 10, -12 ≤ k ≤ 9, -13 ≤ l ≤ 13
Reflections collected	6452
Independent reflections	3189 [R _{int} = 0.0178, R _{sigma} = 0.0203]
Data/restraints/parameters	3189/0/257
Goodness-of-fit on F ²	1.038
Final R indexes [I ≥ 2σ (I)]	R ₁ = 0.0325, wR ₂ = 0.0839
Final R indexes [all data]	R ₁ = 0.0344, wR ₂ = 0.0854
Largest diff. peak/hole / e Å ⁻³	0.45/-0.32

Table 2 Fractional Atomic Coordinates ($\times 10^4$) and Equivalent Isotropic Displacement Parameters ($\text{\AA}^2 \times 10^3$) for JS02_99_Cu. U_{eq} is defined as 1/3 of the trace of the orthogonalised U_{ij} tensor.

Atom	<i>x</i>	<i>y</i>	<i>z</i>	$U(eq)$
C1	339(2)	10671.5(17)	13577.6(16)	24.1(4)
O2	-907.1(14)	9781.6(12)	12717.3(11)	25.7(3)
C3	-586.9(19)	9086.5(16)	11744.5(15)	18.2(3)
C4	834.7(18)	9220.5(15)	11524.2(15)	17.2(3)
C5	960.0(17)	8375.7(15)	10507.4(14)	14.8(3)
C6	-261.5(18)	7450.5(15)	9744.3(14)	15.8(3)
C7	-1709.8(18)	7359.2(16)	9975.0(15)	18.3(3)
C8	-1851.9(18)	8181.4(16)	10966.9(15)	19.3(3)
N9	2191.0(16)	8232.2(13)	10047.1(12)	15.2(3)
C10	1663.6(18)	7259.7(15)	9056.7(14)	15.1(3)
N11	215.2(15)	6750.7(13)	8825.8(12)	16.8(3)
S12	2876.4(4)	6736.7(4)	8171.8(3)	14.88(12)
O13	4415.4(13)	7435.1(11)	8817.5(11)	20.8(3)
O14	2043.8(14)	6868.1(11)	6814.2(10)	22.1(3)
C15	3059.6(18)	5029.1(15)	8420.0(14)	15.1(3)
C16	4085.9(18)	4418.6(15)	7720.4(14)	14.5(3)
N17	5676.0(15)	4580.1(13)	8376.9(12)	15.8(3)
C18	6658.2(18)	4076.3(15)	7809.0(15)	16.9(3)
C19	6140.3(19)	3383.1(15)	6585.8(15)	17.2(3)
C20	4480.7(19)	3206.2(15)	5942.4(14)	15.9(3)
C21	3405.0(18)	3737.8(15)	6486.2(14)	15.6(3)
C22	7318(2)	2857.8(18)	6007.3(16)	25.3(4)
C23	3710(2)	3119.6(18)	3658.5(15)	25.1(4)
O24	3888.3(14)	2423.4(11)	4781.8(10)	19.7(2)
C25	1611.0(19)	3552.3(17)	5791.4(15)	22.1(4)
O26	5205.1(17)	10082.6(14)	8525.3(14)	36.6(3)
C27	4516(2)	10074.0(19)	7146.2(18)	30.4(4)

Table 3 Anisotropic Displacement Parameters ($\text{\AA}^2 \times 10^3$) for JS02_99_Cu. The Anisotropic displacement factor exponent takes the form: $-2\pi^2[h^2a^{*2}U_{11}+2hka^*b^*U_{12}+\dots]$.

Atom	U_{11}	U_{22}	U_{33}	U_{23}	U_{13}	U_{12}
C1	27.8(9)	21.9(9)	21.6(8)	-5.8(6)	9.1(7)	0.3(7)
O2	25.9(6)	27.7(7)	25.1(6)	-9.4(5)	13.7(5)	-3.2(5)
C3	22.0(8)	18.6(8)	15.5(7)	0.9(6)	8.5(6)	2.9(6)
C4	17.2(7)	15.7(8)	17.0(7)	-0.2(6)	4.6(6)	-1.2(6)
C5	14.4(7)	14.8(7)	15.6(7)	3.8(6)	5.5(6)	1.6(6)
C6	17.3(7)	16.0(8)	13.9(7)	2.7(6)	5.0(6)	0.5(6)
C7	15.5(7)	20.5(8)	17.8(8)	0.0(6)	5.3(6)	-3.1(6)
C8	15.5(7)	23.7(9)	20.8(8)	2.8(6)	8.8(6)	-0.6(6)
N9	13.5(6)	15.3(7)	16.4(6)	-0.3(5)	5.3(5)	-2.2(5)
C10	16.9(7)	15.3(8)	14.0(7)	0.8(6)	7.0(6)	1.4(6)
N11	16.7(6)	18.3(7)	15.7(6)	0.1(5)	6.5(5)	-0.5(5)
S12	16.14(19)	15.3(2)	15.01(19)	0.44(13)	8.04(15)	-0.04(14)
O13	18.8(6)	18.2(6)	27.7(6)	-1.9(4)	12.2(5)	-3.2(4)
O14	28.1(6)	24.4(6)	16.7(6)	4.7(4)	10.8(5)	5.9(5)
C15	16.4(7)	15.5(8)	13.2(7)	0.5(5)	5.5(6)	-1.0(6)
C16	17.6(7)	13.3(7)	13.2(7)	2.8(5)	6.1(6)	0.2(6)
N17	17.4(6)	16.4(7)	13.4(6)	2.4(5)	5.1(5)	0.5(5)
C18	16.0(7)	18.5(8)	16.4(7)	4.8(6)	5.3(6)	2.3(6)
C19	22.4(8)	15.9(8)	15.9(7)	6.2(6)	9.2(6)	4.3(6)
C20	25.0(8)	11.1(7)	12.2(7)	1.4(5)	7.3(6)	0.1(6)
C21	18.8(8)	13.1(8)	14.8(7)	1.8(6)	6.0(6)	-1.6(6)
C22	26.7(9)	32(1)	20.6(8)	5.1(7)	11.8(7)	10.0(7)
C23	32.4(9)	28.2(9)	13.6(8)	2.5(6)	7.0(7)	-1.6(7)
O24	30.3(6)	16.2(6)	12.9(5)	-1.4(4)	8.8(5)	-0.4(5)
C25	19.6(8)	26.0(9)	18.7(8)	-5.8(6)	6.1(6)	-3.7(7)
O26	36.9(7)	26.3(7)	36.3(7)	4.0(6)	1.3(6)	-12.5(6)
C27	30.6(9)	28(1)	34.1(10)	2.6(8)	13.5(8)	0.6(8)

Table 4 Bond Lengths for JS02_99_Cu.

Atom	Atom	Length/Å	Atom	Atom	Length/Å
C1	O2	1.427(2)	S12	O14	1.4338(11)
O2	C3	1.3605(19)	S12	C15	1.7831(15)
C3	C4	1.379(2)	C15	C16	1.509(2)
C3	C8	1.418(2)	C16	N17	1.342(2)
C4	C5	1.401(2)	C16	C21	1.400(2)
C5	C6	1.404(2)	N17	C18	1.336(2)
C5	N9	1.3704(19)	C18	C19	1.392(2)
C6	C7	1.405(2)	C19	C20	1.395(2)
C6	N11	1.389(2)	C19	C22	1.499(2)
C7	C8	1.373(2)	C20	C21	1.399(2)
N9	C10	1.361(2)	C20	O24	1.3806(18)
C10	N11	1.312(2)	C21	C25	1.507(2)
C10	S12	1.7628(15)	C23	O24	1.4364(19)
S12	O13	1.4440(12)	O26	C27	1.424(2)

Table 5 Bond Angles for JS02_99_Cu.

Atom Atom Atom	Angle/°	Atom Atom Atom	Angle/°
C3 O2 C1	117.08(13)	O13 S12 C15	109.85(7)
O2 C3 C4	124.10(15)	O14 S12 C10	109.73(7)
O2 C3 C8	113.83(14)	O14 S12 O13	118.51(7)
C4 C3 C8	122.06(14)	O14 S12 C15	108.89(7)
C3 C4 C5	115.49(14)	C16 C15 S12	109.97(10)
C4 C5 C6	123.44(14)	N17 C16 C15	114.67(13)
N9 C5 C4	130.75(14)	N17 C16 C21	123.63(14)
N9 C5 C6	105.81(13)	C21 C16 C15	121.69(13)
C5 C6 C7	119.65(14)	C18 N17 C16	117.90(13)
N11 C6 C5	110.23(13)	N17 C18 C19	124.29(14)
N11 C6 C7	130.11(14)	C18 C19 C20	116.36(14)
C8 C7 C6	117.60(14)	C18 C19 C22	121.18(15)
C7 C8 C3	121.73(14)	C20 C19 C22	122.46(14)
C10 N9 C5	105.50(13)	C19 C20 C21	121.40(14)
N9 C10 S12	121.31(11)	O24 C20 C19	119.24(13)
N11 C10 N9	115.28(13)	O24 C20 C21	119.24(14)
N11 C10 S12	123.41(12)	C16 C21 C25	122.07(14)
C10 N11 C6	103.18(12)	C20 C21 C16	116.38(14)
C10 S12 C15	103.00(7)	C20 C21 C25	121.53(14)
O13 S12 C10	105.73(7)	C20 O24 C23	113.81(12)

Table 6 Torsion Angles for JS02_99_Cu.

A	B	C	D	Angle/°	A	B	C	D	Angle/°
C1	O2	C3	C4	-2.0(2)	N11	C10	S12	O14	57.19(15)
C1	O2	C3	C8	177.31(14)	N11	C10	S12	C15	-58.64(14)
O2	C3	C4	C5	177.39(14)	S12	C10	N11	C6	179.74(11)
O2	C3	C8	C7	-177.27(15)	S12	C15	C16	N17	83.19(14)
C3	C4	C5	C6	0.3(2)	S12	C15	C16	C21	-97.03(15)
C3	C4	C5	N9	-178.83(15)	O13	S12	C15	C16	-67.48(12)
C4	C3	C8	C7	2.0(2)	O14	S12	C15	C16	63.81(12)
C4	C5	C6	C7	1.1(2)	C15	C16	N17	C18	-179.31(13)
C4	C5	C6	N11	-179.43(14)	C15	C16	C21	C20	-179.47(13)
C4	C5	N9	C10	179.42(16)	C15	C16	C21	C25	-1.1(2)
C5	C6	C7	C8	-1.0(2)	C16	N17	C18	C19	-0.7(2)
C5	C6	N11	C10	0.01(16)	N17	C16	C21	C20	0.3(2)
C5	N9	C10	N11	-0.19(18)	N17	C16	C21	C25	178.68(15)
C5	N9	C10	S12	-179.82(11)	N17	C18	C19	C20	-0.8(2)
C6	C5	N9	C10	0.18(16)	N17	C18	C19	C22	179.41(14)
C6	C7	C8	C3	-0.5(2)	C18	C19	C20	C21	2.0(2)
C7	C6	N11	C10	179.39(16)	C18	C19	C20	O24	-173.99(13)
C8	C3	C4	C5	-1.8(2)	C19	C20	C21	C16	-1.8(2)
N9	C5	C6	C7	-179.57(14)	C19	C20	C21	C25	179.79(15)
N9	C5	C6	N11	-0.12(16)	C19	C20	O24	C23	-87.77(17)
N9	C10	N11	C6	0.11(17)	C21	C16	N17	C18	0.9(2)
N9	C10	S12	O13	5.68(14)	C21	C20	O24	C23	96.12(17)
N9	C10	S12	O14	-123.21(13)	C22	C19	C20	C21	-178.16(14)
N9	C10	S12	C15	120.96(13)	C22	C19	C20	O24	5.8(2)
C10	S12	C15	C16	-179.76(10)	O24	C20	C21	C16	174.21(13)
N11	C6	C7	C8	179.70(15)	O24	C20	C21	C25	-4.2(2)
N11	C10	S12	O13	-173.92(13)					

Table 7 Hydrogen Atom Coordinates ($\text{\AA}\times 10^4$) and Isotropic Displacement Parameters ($\text{\AA}^2\times 10^3$) for JS02_99_Cu.

Atom	x	y	z	U(eq)
H1A	599	11325	13092	36
H1B	1276	10193	13996	36
H1C	-21	11095	14224	36
H4	1655	9831	12017	21
H7	-2542	6763	9474	22
H8	-2803	8144	11133	23
H15A	3545	4925	9343	18
H15B	2002	4585	8095	18
H18	7760	4197	8261	20
H22A	7340	3388	5330	38
H22B	6999	1964	5650	38
H22C	8370	2885	6671	38
H23A	3438	2502	2903	38
H23B	4702	3593	3782	38
H23C	2870	3729	3539	38
H25A	1195	2885	6172	33
H25B	1379	3287	4888	33
H25C	1116	4367	5871	33
H27A	3929	9250	6787	46
H27B	5354	10184	6803	46
H27C	3799	10782	6919	46
H9	3070(20)	8660(20)	10335(19)	19(5)
H26	5100(30)	9300(30)	8770(30)	58(8)

1.4 XRD data for K-Omeprazole 3.38

Table 1 Crystal data and structure refinement for JS04_20_Cu_a.

Identification code	JS04_20_Cu_a
Empirical formula	C ₁₉ H ₂₆ KN ₃ O ₅ S
Formula weight	447.59
Temperature/K	99.9(6)
Crystal system	monoclinic
Space group	P2 ₁
a/Å	10.7149(5)
b/Å	7.3404(3)
c/Å	13.7741(5)
α /°	90.00
β /°	98.193(4)
γ /°	90.00
Volume/Å ³	1072.30(7)
Z	2
ρ_{calc} /mg/mm ³	1.386
m/mm ⁻¹	3.382
F(000)	472.0
Crystal size/mm ³	0.14 × 0.05 × 0.03
Radiation	CuK α (λ = 1.54184)
2 θ range for data collection	6.48 to 133.16°
Index ranges	-9 ≤ h ≤ 12, -7 ≤ k ≤ 8, -16 ≤ l ≤ 16
Reflections collected	4086
Independent reflections	2845 [R_{int} = 0.0375, R_{sigma} = 0.0632]
Data/restraints/parameters	2845/3/280
Goodness-of-fit on F ²	1.025
Final R indexes [$I \geq 2\sigma(I)$]	R_1 = 0.0360, wR_2 = 0.0803
Final R indexes [all data]	R_1 = 0.0422, wR_2 = 0.0837
Largest diff. peak/hole / e Å ⁻³	0.31/-0.29
Flack parameter	0.031(13)

Table 2 Fractional Atomic Coordinates ($\times 10^4$) and Equivalent Isotropic Displacement Parameters ($\text{\AA}^2 \times 10^3$) for JS04_20_Cu_a. U_{eq} is defined as 1/3 of the trace of the orthogonalised U_{ij} tensor.

Atom	x	y	z	U(eq)
K1	4304.9(6)	1518.9(10)	4933.0(5)	16.00(17)
O2	3486(2)	4972(3)	5229.6(18)	17.9(5)
S3	2190.8(8)	5468.1(11)	5439.6(6)	14.94(19)
C4	1242(3)	5997(4)	4291(2)	14.7(7)
N5	-5(3)	6084(4)	4266(2)	16.0(6)
C6	-395(3)	6522(5)	3290(2)	15.3(7)
C7	682(3)	6620(5)	2806(2)	16.7(7)
N8	1745(3)	6292(4)	3471(2)	16.7(6)
C9	-1604(3)	6811(5)	2780(2)	17.7(7)
C10	-1715(4)	7187(5)	1793(3)	19.5(8)
C11	-635(4)	7252(5)	1305(3)	19.6(8)
C12	562(4)	7003(5)	1790(3)	19.8(8)
O13	-924(3)	7599(4)	306.5(18)	27.7(6)
C14	101(4)	7587(7)	-245(3)	31.7(10)
N15	4476(3)	8670(4)	6444(2)	16.0(6)
C16	5459(4)	8893(5)	7146(3)	18.5(8)
C17	5439(4)	8506(5)	8142(3)	19.9(8)
C18	4290(3)	7889(5)	8383(2)	17.7(8)
C19	3245(3)	7621(5)	7679(2)	16.1(7)
C20	3384(4)	8047(5)	6702(3)	15.9(7)
C21	6585(4)	8756(6)	8888(3)	28.7(9)
O22	4230(3)	7446(4)	9354.5(17)	23.0(6)
C23	3744(4)	8903(6)	9891(3)	31.8(10)
C24	2008(3)	6962(5)	7943(3)	19.0(8)
C25	2326(3)	7835(5)	5867(3)	16.4(7)
O26	1772(2)	1486(4)	4474.4(17)	21.8(5)
C27	1219(3)	1440(6)	3474(3)	25.3(8)
O28	6035(3)	3320(4)	6314.6(19)	20.8(6)
C29	5718(4)	3758(6)	7250(3)	25.5(9)

Table 3 Anisotropic Displacement Parameters ($\text{\AA}^2 \times 10^3$) for JS04_20_Cu_a. The Anisotropic displacement factor exponent takes the form: $-2\pi^2[h^2a^{*2}U_{11}+2hka^*b^*U_{12}+\dots]$.

Atom	U_{11}	U_{22}	U_{33}	U_{23}	U_{13}	U_{12}
K1	14.3(4)	16.9(4)	16.8(3)	0.4(3)	2.0(2)	0.8(3)
O2	10.4(12)	20.3(14)	22.1(12)	-3.9(10)	-1.0(9)	1.7(10)
S3	13.3(4)	16.5(4)	14.4(4)	0.4(4)	0.0(3)	-0.4(3)
C4	14.2(18)	15.4(18)	13.7(16)	0.2(12)	-1.4(12)	-1.8(13)
N5	14.3(15)	16.2(16)	17.2(14)	-0.3(11)	0.9(11)	-1.9(11)
C6	16.2(17)	12.5(15)	16.4(16)	0.7(15)	-0.3(12)	-1.5(17)
C7	19.5(18)	12.8(16)	17.9(16)	-1.7(15)	3.0(12)	-0.4(16)
N8	15.1(15)	18.4(15)	16.6(14)	-0.2(13)	1.8(10)	-1.4(13)
C9	14.9(18)	19.0(19)	19.1(17)	-1.5(14)	1.7(13)	-1.1(15)
C10	14.9(19)	22(2)	20.5(18)	-0.4(14)	-1.0(13)	0.5(14)
C11	25(2)	18.4(18)	14.9(17)	-1.5(14)	2.2(14)	0.1(15)
C12	21(2)	24(2)	14.8(17)	-2.8(13)	4.3(14)	1.4(15)
O13	25.3(15)	43.5(16)	13.6(13)	5.1(12)	0.3(10)	4.4(13)
C14	29(2)	48(3)	19(2)	8.8(19)	6.0(16)	3(2)
N15	17.8(16)	14.3(14)	15.9(15)	-2.0(12)	3.1(12)	-1.4(12)
C16	16(2)	16.5(18)	23.5(19)	1.8(15)	5.9(15)	1.4(15)
C17	20(2)	16.9(17)	20.9(19)	-2.1(15)	-1.9(15)	4.2(15)
C18	24(2)	18.1(18)	10.5(16)	0.4(13)	1.2(13)	2.7(15)
C19	21.3(19)	12.3(16)	14.9(16)	-0.3(14)	2.7(13)	2.3(15)
C20	18.5(19)	12.8(17)	15.8(18)	-0.4(13)	0.6(14)	0.6(14)
C21	28(2)	30(2)	26(2)	0.9(17)	-3.1(16)	-2.7(19)
O22	28.9(15)	25.7(13)	13.9(13)	3.6(11)	1.3(10)	2.0(12)
C23	45(3)	32(2)	18.5(19)	-5.9(17)	6.1(17)	1(2)
C24	21(2)	17.5(19)	19.2(18)	1.5(14)	4.4(14)	-2.1(14)
C25	14.4(18)	16.4(18)	18.1(17)	2.5(14)	1.6(13)	-0.3(14)
O26	14.9(13)	30.3(13)	20.3(12)	4.7(13)	3.0(9)	-1.5(13)
C27	25(2)	29(2)	21.0(18)	-1.8(19)	1.5(13)	1(2)
O28	19.9(15)	25.4(14)	16.7(13)	-0.9(10)	1.1(10)	3.1(11)
C29	33(2)	27(2)	17.7(18)	-0.9(16)	7.4(16)	4.8(18)

Table 4 Bond Lengths for JS04_20_Cu_a.

Atom	Atom	Length/Å	Atom	Atom	Length/Å
K1	K1 ¹	3.9554(5)	C10	C11	1.420(5)
K1	K1 ²	3.9554(5)	C11	C12	1.372(5)
K1	O2	2.732(2)	C11	O13	1.389(4)
K1	O2 ²	2.664(3)	O13	C14	1.422(5)
K1	N15 ³	2.938(3)	N15	K1 ⁴	2.938(3)
K1	N15 ²	2.916(3)	N15	K1 ¹	2.916(3)
K1	C16 ²	3.392(4)	N15	C16	1.334(5)
K1	O26	2.697(2)	N15	C20	1.350(5)
K1	O28 ²	2.902(3)	C16	K1 ¹	3.392(4)
K1	O28	2.793(3)	C16	C17	1.404(5)
O2	K1 ¹	2.664(3)	C17	C18	1.395(5)
O2	S3	1.502(3)	C17	C21	1.496(5)
S3	C4	1.797(3)	C18	C19	1.387(5)
S3	C25	1.833(4)	C18	O22	1.388(4)
C4	N5	1.334(4)	C19	C20	1.409(5)
C4	N8	1.336(4)	C19	C24	1.503(5)
N5	C6	1.388(4)	C20	C25	1.504(5)
C6	C7	1.414(4)	O22	C23	1.439(5)
C6	C9	1.399(5)	O26	C27	1.421(4)
C7	N8	1.378(4)	O28	K1 ¹	2.902(3)
C7	C12	1.416(5)	O28	C29	1.415(4)
C9	C10	1.376(5)			

¹1-X,1/2+Y,1-Z; ²1-X,-1/2+Y,1-Z; ³+X,-1+Y,+Z; ⁴+X,1+Y,+Z

Table 5 Bond Angles for JS04_20_Cu_a.

Atom Atom Atom	Angle/°	Atom Atom Atom	Angle/°
K1 ¹ K1 K1 ²	136.22(4)	O2 S3 C4	107.74(15)
O2 K1 K1 ¹	168.74(6)	O2 S3 C25	104.98(15)
O2 ¹ K1 K1 ¹	43.53(5)	C4 S3 C25	94.99(15)
O2 ¹ K1 K1 ²	93.79(6)	N5 C4 S3	118.1(2)
O2 K1 K1 ²	42.19(5)	N5 C4 N8	119.6(3)
O2 ¹ K1 O2	135.76(7)	N8 C4 S3	122.2(3)
O2 K1 N15 ³	122.91(8)	C4 N5 C6	101.4(3)
O2 ¹ K1 N15 ³	77.85(8)	N5 C6 C7	108.4(3)
O2 ¹ K1 N15 ¹	71.96(8)	N5 C6 C9	130.6(3)
O2 K1 N15 ¹	77.18(8)	C9 C6 C7	121.0(3)
O2 K1 C16 ¹	73.38(8)	C6 C7 C12	120.7(3)
O2 ¹ K1 C16 ¹	88.50(9)	N8 C7 C6	109.4(3)
O2 ¹ K1 O26	148.54(9)	N8 C7 C12	129.9(3)
O2 ¹ K1 O28 ¹	69.11(8)	C4 N8 C7	101.2(3)
O2 K1 O28	69.83(7)	C10 C9 C6	118.0(3)
O2 K1 O28 ¹	145.42(8)	C9 C10 C11	120.9(3)
O2 ¹ K1 O28	75.37(8)	C12 C11 C10	122.3(3)
N15 ³ K1 K1 ¹	47.26(6)	C12 C11 O13	124.6(3)
N15 ³ K1 K1 ²	129.96(6)	O13 C11 C10	113.1(3)
N15 ¹ K1 K1 ¹	109.40(7)	C11 C12 C7	117.0(3)
N15 ¹ K1 K1 ²	47.73(6)	C11 O13 C14	116.6(3)
N15 ¹ K1 N15 ³	149.07(5)	K1 ² N15 K1 ⁴	85.01(8)
N15 ¹ K1 C16 ¹	22.84(9)	C16 N15 K1 ⁴	112.9(2)
N15 ³ K1 C16 ¹	163.56(9)	C16 N15 K1 ²	99.1(2)
C16 ¹ K1 K1 ¹	116.30(7)	C16 N15 C20	118.3(3)
C16 ¹ K1 K1 ²	59.33(7)	C20 N15 K1 ²	118.2(2)
O26 K1 K1 ²	112.27(7)	C20 N15 K1 ⁴	117.3(2)
O26 K1 K1 ¹	111.24(7)	N15 C16 K1 ²	58.09(19)
O26 K1 O2	73.11(9)	N15 C16 C17	124.3(4)
O26 K1 N15 ¹	112.42(8)	C17 C16 K1 ²	137.2(3)
O26 K1 N15 ³	96.83(9)	C16 C17 C21	121.4(4)

O26	K1	C16 ¹	90.03(9)	C18	C17	C16	115.7(3)
O26	K1	O28 ¹	79.44(9)	C18	C17	C21	122.8(3)
O26	K1	O28	135.38(9)	C19	C18	C17	122.1(3)
O28 ¹	K1	K1 ¹	44.89(5)	C19	C18	O22	119.8(3)
O28	K1	K1 ¹	101.44(6)	O22	C18	C17	118.0(3)
O28	K1	K1 ²	47.15(6)	C18	C19	C20	116.8(3)
O28 ¹	K1	K1 ²	142.48(6)	C18	C19	C24	121.9(3)
O28	K1	N15 ¹	82.63(8)	C20	C19	C24	121.3(3)
O28	K1	N15 ³	83.44(8)	N15	C20	C19	122.7(3)
O28 ¹	K1	N15 ³	80.42(8)	N15	C20	C25	114.9(3)
O28 ¹	K1	N15 ¹	94.76(8)	C19	C20	C25	122.4(3)
O28	K1	C16 ¹	102.11(9)	C18	O22	C23	113.1(3)
O28 ¹	K1	C16 ¹	86.21(8)	C20	C25	S3	111.1(2)
O28	K1	O28 ¹	143.29(7)	C27	O26	K1	119.6(2)
K1 ²	O2	K1	94.28(8)	K1	O28	K1 ²	87.96(7)
S3	O2	K1 ²	140.29(14)	C29	O28	K1 ²	109.2(2)
S3	O2	K1	125.38(13)	C29	O28	K1	120.4(2)

¹1-X,-1/2+Y,1-Z; ²1-X,1/2+Y,1-Z; ³+X,-1+Y,+Z; ⁴+X,1+Y,+Z

Table 6 Torsion Angles for JS04_20_Cu_a.

A	B	C	D	Angle/°	A	B	C	D	Angle/°
K1 ¹	K1	O2	K1 ²	87.9(3)	C12	C11	O13	C14	3.6(6)
K1 ²	K1	O2	S3	-178.0(2)	O13	C11	C12	C7	-178.5(3)
K1 ¹	K1	O2	S3	-90.1(3)	N15 ¹	K1	O2	K1 ²	-39.09(8)
K1 ¹	K1	O26	C27	-86.2(3)	N15 ⁴	K1	O2	K1 ²	115.15(9)
K1 ²	K1	O26	C27	88.8(3)	N15 ¹	K1	O2	S3	142.90(17)
K1 ¹	K1	O28	K1 ²	144.78(5)	N15 ⁴	K1	O2	S3	-62.86(18)
K1 ²	K1	O28	C29	111.2(3)	N15 ¹	K1	O26	C27	36.9(3)
K1 ¹	K1	O28	C29	-104.1(2)	N15 ⁴	K1	O26	C27	-132.8(3)
K1	O2	S3	C4	-93.37(17)	N15 ¹	K1	O28	K1 ²	36.39(8)
K1 ²	O2	S3	C4	89.7(2)	N15 ⁴	K1	O28	K1 ²	-171.30(8)
K1 ²	O2	S3	C25	-10.6(2)	N15 ¹	K1	O28	C29	147.5(3)
K1	O2	S3	C25	166.25(16)	N15 ⁴	K1	O28	C29	-60.1(2)
K1 ³	N15	C16	K1 ²	-88.38(16)	N15	C16	C17	C18	-1.4(5)
K1 ²	N15	C16	C17	-128.5(3)	N15	C16	C17	C21	178.8(4)
K1 ³	N15	C16	C17	143.1(3)	N15	C20	C25	S3	97.9(3)
K1 ²	N15	C20	C19	119.4(3)	C16 ¹	K1	O2	K1 ²	-62.39(9)
K1 ³	N15	C20	C19	-141.1(3)	C16 ¹	K1	O2	S3	119.60(17)
K1 ²	N15	C20	C25	-60.4(3)	C16 ¹	K1	O26	C27	32.2(3)
K1 ³	N15	C20	C25	39.1(4)	C16 ¹	K1	O28	K1 ²	24.40(10)
K1 ²	C16	C17	C18	-79.6(5)	C16 ¹	K1	O28	C29	135.6(2)
K1 ²	C16	C17	C21	100.7(4)	C16	N15	C20	C19	-0.2(5)
O2 ¹	K1	O2	K1 ²	7.38(5)	C16	N15	C20	C25	-180.0(3)
O2 ¹	K1	O2	S3	-170.63(17)	C16	C17	C18	C19	1.9(5)
O2	K1	O26	C27	104.8(3)	C16	C17	C18	O22	178.5(3)
O2 ¹	K1	O26	C27	-55.0(4)	C17	C18	C19	C20	-1.6(5)
O2	K1	O28	K1 ²	-42.62(7)	C17	C18	C19	C24	-179.8(3)
O2 ¹	K1	O28	K1 ²	109.59(8)	C17	C18	O22	C23	96.6(4)
O2 ¹	K1	O28	C29	-139.2(3)	C18	C19	C20	N15	0.7(5)
O2	K1	O28	C29	68.5(2)	C18	C19	C20	C25	-179.6(3)
O2	S3	C4	N5	165.4(2)	C19	C18	O22	C23	-86.8(4)
O2	S3	C4	N8	-14.2(3)	C19	C20	C25	S3	-81.9(4)

O2 S3 C25 C20	-53.4(3)	C20 N15 C16 K1 ²	129.1(3)
S3 C4 N5 C6	179.5(2)	C20 N15 C16 C17	0.6(5)
S3 C4 N8 C7	179.6(3)	C21 C17 C18 C19	-178.3(4)
C4 S3 C25 C20	-163.3(3)	C21 C17 C18 O22	-1.8(5)
C4 N5 C6 C7	1.3(4)	O22 C18 C19 C20	-178.1(3)
C4 N5 C6 C9	179.9(4)	O22 C18 C19 C24	3.7(5)
N5 C4 N8 C7	-0.1(4)	C24 C19 C20 N15	178.9(3)
N5 C6 C7 N8	-1.5(4)	C24 C19 C20 C25	-1.3(5)
N5 C6 C7 C12	178.4(3)	C25 S3 C4 N5	-87.1(3)
N5 C6 C9 C10	-178.3(4)	C25 S3 C4 N8	93.3(3)
C6 C7 N8 C4	0.9(4)	O26 K1 O2 K1 ²	-157.63(9)
C6 C7 C12 C11	-0.7(5)	O26 K1 O2 S3	24.36(15)
C6 C9 C10 C11	0.9(5)	O26 K1 O28 K1 ²	-78.22(12)
C7 C6 C9 C10	0.2(6)	O26 K1 O28 C29	32.9(3)
N8 C4 N5 C6	-0.8(4)	O28 K1 O2 K1 ²	47.67(7)
N8 C7 C12 C11	179.2(4)	O28 ¹ K1 O2 K1 ²	-118.71(13)
C9 C6 C7 N8	179.7(3)	O28 K1 O2 S3	-130.35(17)
C9 C6 C7 C12	-0.3(6)	O28 ¹ K1 O2 S3	63.3(2)
C9 C10 C11 C12	-2.0(6)	O28 ¹ K1 O26 C27	-53.9(3)
C9 C10 C11 O13	178.3(3)	O28 K1 O26 C27	139.6(3)
C10 C11 C12 C7	1.8(5)	O28 ¹ K1 O28 K1 ²	124.46(12)
C10 C11 O13 C14	-176.7(4)	O28 ¹ K1 O28 C29	-124.4(2)
C12 C7 N8 C4	-179.0(4)		

¹1-X,-1/2+Y,1-Z; ²1-X,1/2+Y,1-Z; ³+X,1+Y,+Z; ⁴+X,-1+Y,+Z

Table 7 Hydrogen Atom Coordinates ($\text{\AA}\times 10^4$) and Isotropic Displacement Parameters ($\text{\AA}^2\times 10^3$) for JS04_20_Cu_a.

Atom	x	y	z	U(eq)
H9	-2312	6751	3099	21
H10	-2508	7401	1441	23
H12	1265	7082	1466	24
H14A	-209	7804	-924	47
H14B	514	6424	-177	47
H14C	690	8525	-7	47
H16	6150(40)	9280(50)	6970(30)	8(9)
H21A	7273	9172	8569	43
H21B	6806	7616	9209	43
H21C	6413	9641	9365	43
H23A	3655	8488	10539	48
H23B	2937	9276	9558	48
H23C	4316	9915	9936	48
H24A	2134	6496	8601	29
H24B	1681	6014	7498	29
H24C	1420	7956	7898	29
H25A	2478	8620	5330	20
H25B	1540	8208	6079	20
H26	1160(30)	1340(80)	4850(30)	41(13)
H27A	1860	1197	3069	38
H27B	832	2594	3295	38
H27C	593	497	3381	38
H28	6700(30)	2550(60)	6400(40)	44(15)
H29A	4988	4531	7175	38
H29B	6412	4380	7627	38
H29C	5539	2659	7582	38

1.5 XRD data for NMe Omeprazole 5.22

Table 1 Crystal data and structure refinement for JS_NMeOmep_Cu.

Identification code	JS_NMeOmep_Cu
Empirical formula	C ₁₈ H ₂₁ N ₃ O ₃ S
Formula weight	359.44
Temperature/K	120.00(10)
Crystal system	triclinic
Space group	P-1
a/Å	7.6932(5)
b/Å	9.8933(6)
c/Å	12.3472(8)
α/°	95.341(5)
β/°	107.606(6)
γ/°	103.055(6)
Volume/Å ³	859.30(10)
Z	2
ρ _{calc} /cm ³	1.389
μ/mm ⁻¹	1.870
F(000)	380.0
Crystal size/mm ³	0.17 × 0.12 × 0.06
Radiation	CuKα (λ = 1.54184)
2θ range for data collection/°	7.62 to 134.14
Index ranges	-9 ≤ h ≤ 9, -8 ≤ k ≤ 11, -14 ≤ l ≤ 14
Reflections collected	5898
Independent reflections	2971 [R _{int} = 0.0546, R _{sigma} = 0.0778]
Data/restraints/parameters	2971/0/239
Goodness-of-fit on F ²	1.066
Final R indexes [I ≥ 2σ (I)]	R ₁ = 0.0531, wR ₂ = 0.1213
Final R indexes [all data]	R ₁ = 0.0737, wR ₂ = 0.1373
Largest diff. peak/hole / e Å ⁻³	0.31/-0.32

Table 2 Fractional Atomic Coordinates ($\times 10^4$) and Equivalent Isotropic Displacement Parameters ($\text{\AA}^2 \times 10^3$) for JS_NMeOmep_Cu. U_{eq} is defined as 1/3 of the trace of the orthogonalised U_{ij} tensor.

Atom	x	y	z	U(eq)
S13	686.5(11)	7813.2(8)	2440.1(6)	24.0(2)
O23	908(3)	6915(2)	7019.9(18)	29.5(5)
O2A	5331(4)	13518(2)	-151.9(19)	28.7(5)
O14	2153(4)	7071(2)	2941(2)	33.3(6)
N11	1350(4)	8534(3)	482(2)	22.7(5)
N21	-2013(4)	8038(3)	3979(2)	24.9(6)
N9	2575(4)	10329(3)	2007(2)	23.7(5)
C17	968(4)	8051(3)	5387(2)	21.2(6)
C16	-115(4)	8391(3)	4362(2)	21.6(6)
C18	-60(5)	7280(3)	5993(2)	23.9(7)
C10	1615(4)	9003(3)	1615(2)	22.0(6)
C6	2259(4)	9667(3)	108(3)	22.9(6)
C20	-2927(5)	7340(3)	4606(3)	27.2(7)
C15	779(4)	9143(3)	3585(2)	22.9(6)
C19	-2019(5)	6926(3)	5625(3)	25.6(7)
C5	3007(4)	10765(3)	1058(3)	23.1(6)
C7	2490(5)	9817(3)	-955(3)	27.9(7)
C4	4053(4)	12074(3)	960(3)	26.2(7)
C8	3489(4)	11115(3)	-1050(3)	27.4(7)
C12	372(5)	7135(3)	-201(3)	27.3(7)
C22	3092(4)	8523(3)	5823(3)	29.5(7)
C25	-3111(5)	6177(4)	6321(3)	34.2(8)
C3	4279(5)	12231(3)	-99(3)	28.8(7)
C1A	5326(5)	13803(4)	-1273(3)	28.4(8)
C24	1387(5)	5615(3)	6864(3)	36.0(8)
O2B	4310(40)	11750(30)	-1660(20)	27(6)
C1B	5020(50)	13120(40)	-1820(30)	21(7)

Table 3 Anisotropic Displacement Parameters ($\text{\AA}^2 \times 10^3$) for JS_NMeOmep_Cu. The Anisotropic displacement factor exponent takes the form: $-2\pi^2[h^2a^{*2}U_{11}+2hka^*b^*U_{12}+\dots]$.

Atom	U_{11}	U_{22}	U_{33}	U_{23}	U_{13}	U_{12}
S13	30.5(4)	19.4(4)	25.8(4)	4.3(3)	14.5(3)	6.7(3)
O23	42.2(14)	23.5(11)	23.8(11)	4.9(9)	11(1)	10.3(10)
O2A	36.3(14)	26.1(13)	26.2(12)	4.8(10)	16.7(11)	4.5(10)
O14	45.2(15)	32.0(13)	36.9(12)	14.4(10)	22.5(11)	22.5(11)
N11	26.1(14)	23.2(13)	21.8(12)	5.3(10)	10(1)	9.0(11)
N21	23.5(14)	26.1(14)	26.3(13)	2.2(11)	9.7(11)	7.8(11)
N9	25.6(14)	21.9(13)	25.7(12)	4.7(10)	11.2(11)	6.8(11)
C17	26.0(16)	13.7(14)	23.9(14)	0.7(11)	11.3(12)	2.2(11)
C16	25.6(16)	17.8(15)	23.9(14)	0.3(11)	12.2(12)	6.5(12)
C18	37.1(18)	15.9(15)	21.1(14)	1.0(11)	13.0(13)	8.2(13)
C10	23.6(15)	22.3(15)	22.2(14)	3.3(12)	10.4(12)	6.8(12)
C6	21.1(16)	25.4(16)	26.9(15)	8.3(12)	9.3(12)	12.0(13)
C20	28.0(17)	23.0(16)	31.8(16)	0.6(13)	14.2(14)	5.2(13)
C15	27.4(16)	18.8(15)	24.7(14)	4.5(12)	11.0(13)	7.2(12)
C19	33.6(18)	14.7(14)	32.2(16)	-1.0(12)	19.0(14)	4.7(13)
C5	22.1(16)	23.8(16)	28.0(15)	7.4(12)	11.2(13)	9.9(12)
C7	31.4(18)	33.2(18)	26.9(15)	8.7(13)	13.4(14)	18.0(14)
C4	22.4(16)	26.4(16)	30.8(16)	4.1(13)	9.7(13)	7.4(13)
C8	29.4(17)	33.6(18)	27.6(15)	10.5(14)	14.8(14)	15.4(14)
C12	31.7(18)	25.1(16)	24.3(15)	2.4(12)	7.9(13)	8.3(13)
C22	26.9(17)	31.1(18)	29.7(16)	5.8(13)	7.9(13)	7.8(14)
C25	39(2)	31.2(18)	38.1(18)	6.0(14)	22.3(16)	7.0(15)
C3	24.0(16)	29.9(17)	42.7(18)	17.5(15)	17.8(15)	13.1(13)
C1A	37(2)	23.9(18)	31.9(18)	9.3(16)	21.0(16)	7.8(15)
C24	41(2)	21.7(16)	44.2(19)	9.6(15)	12.0(16)	7.8(15)

Table 4 Bond Lengths for JS_NMeOmeP_Cu.

Atom	Atom	Length/Å	Atom	Atom	Length/Å
S13	O14	1.494(2)	C17	C16	1.406(4)
S13	C10	1.794(3)	C17	C18	1.399(4)
S13	C15	1.812(3)	C17	C22	1.502(4)
O23	C18	1.389(4)	C16	C15	1.499(4)
O23	C24	1.428(4)	C18	C19	1.385(5)
O2A	C3	1.365(4)	C6	C5	1.400(4)
O2A	C1A	1.437(4)	C6	C7	1.393(4)
N11	C10	1.370(4)	C20	C19	1.390(5)
N11	C6	1.377(4)	C19	C25	1.506(4)
N11	C12	1.456(4)	C5	C4	1.398(4)
N21	C16	1.341(4)	C7	C8	1.376(5)
N21	C20	1.334(4)	C4	C3	1.388(4)
N9	C10	1.314(4)	C8	C3	1.411(5)
N9	C5	1.392(4)	O2B	C1B	1.39(5)

Table 5 Bond Angles for JS_NMeOmep_Cu.

Atom Atom Atom	Angle/°	Atom Atom Atom	Angle/°
O14 S13 C10	107.23(14)	N9 C10 S13	125.3(2)
O14 S13 C15	107.36(14)	N9 C10 N11	115.2(3)
C10 S13 C15	96.82(13)	N11 C6 C5	105.6(2)
C18 O23 C24	113.4(2)	N11 C6 C7	131.6(3)
C3 O2A C1A	117.3(3)	C7 C6 C5	122.8(3)
C10 N11 C6	105.4(2)	N21 C20 C19	123.5(3)
C10 N11 C12	128.7(3)	C16 C15 S13	107.1(2)
C6 N11 C12	125.9(2)	C18 C19 C20	116.9(3)
C20 N21 C16	118.5(3)	C18 C19 C25	121.5(3)
C10 N9 C5	103.0(2)	C20 C19 C25	121.6(3)
C16 C17 C22	122.1(3)	N9 C5 C6	110.9(3)
C18 C17 C16	115.8(3)	N9 C5 C4	129.4(3)
C18 C17 C22	122.1(3)	C4 C5 C6	119.7(3)
N21 C16 C17	123.4(3)	C8 C7 C6	117.2(3)
N21 C16 C15	114.5(3)	C3 C4 C5	117.7(3)
C17 C16 C15	122.0(3)	C7 C8 C3	120.9(3)
O23 C18 C17	119.3(3)	O2A C3 C4	115.9(3)
C19 C18 O23	118.9(3)	O2A C3 C8	122.5(3)
C19 C18 C17	121.8(3)	C4 C3 C8	121.6(3)
N11 C10 S13	119.5(2)		

Table 6 Torsion Angles for JS_NMeOmep_Cu.

A	B	C	D	Angle/°	A	B	C	D	Angle/°
O23	C18	C19	C20	178.6(2)	C6	C5	C4	C3	1.0(4)
O23	C18	C19	C25	0.9(4)	C6	C7	C8	C3	1.5(4)
O14	S13	C10	N11	87.5(3)	C20	N21	C16	C17	0.8(4)
O14	S13	C10	N9	-91.9(3)	C20	N21	C16	C15	178.7(3)
O14	S13	C15	C16	-74.5(2)	C15	S13	C10	N11	-161.9(2)
N11	C6	C5	N9	0.0(3)	C15	S13	C10	N9	18.7(3)
N11	C6	C5	C4	179.0(3)	C5	N9	C10	S13	178.4(2)
N11	C6	C7	C8	179.8(3)	C5	N9	C10	N11	-1.0(3)
N21	C16	C15	S13	-80.4(3)	C5	C6	C7	C8	-0.6(4)
N21	C20	C19	C18	0.5(4)	C5	C4	C3	O2A	-179.1(3)
N21	C20	C19	C25	178.2(3)	C5	C4	C3	C8	-0.1(5)
N9	C5	C4	C3	179.8(3)	C7	C6	C5	N9	-179.7(3)
C17	C16	C15	S13	97.5(3)	C7	C6	C5	C4	-0.7(4)
C17	C18	C19	C20	1.6(4)	C7	C8	C3	O2A	177.7(3)
C17	C18	C19	C25	-176.1(3)	C7	C8	C3	C4	-1.2(5)
C16	N21	C20	C19	-1.7(4)	C12	N11	C10	S13	0.0(4)
C16	C17	C18	O23	-179.4(2)	C12	N11	C10	N9	179.5(3)
C16	C17	C18	C19	-2.4(4)	C12	N11	C6	C5	-179.1(3)
C18	C17	C16	N21	1.2(4)	C12	N11	C6	C7	0.6(5)
C18	C17	C16	C15	-176.6(3)	C22	C17	C16	N21	-176.9(3)
C10	S13	C15	C16	175.0(2)	C22	C17	C16	C15	5.3(4)
C10	N11	C6	C5	-0.6(3)	C22	C17	C18	O23	-1.2(4)
C10	N11	C6	C7	179.1(3)	C22	C17	C18	C19	175.7(3)
C10	N9	C5	C6	0.6(3)	C1A	O2A	C3	C4	-169.5(3)
C10	N9	C5	C4	-178.3(3)	C1A	O2A	C3	C8	11.5(4)
C6	N11	C10	S13	-178.4(2)	C24	O23	C18	C17	-87.7(3)
C6	N11	C10	N9	1.0(3)	C24	O23	C18	C19	95.2(3)

Table 7 Hydrogen Atom Coordinates ($\text{\AA}\times 10^4$) and Isotropic Displacement Parameters ($\text{\AA}^2\times 10^3$) for JS_NMeOmep_Cu.

Atom	x	y	z	U(eq)
H20	-4242	7119	4347	33
H15A	2082	9657	4012	27
H15B	95	9805	3267	27
H7	1990	9070	-1573	33
H4	4580	12814	1584	31
H8	3645	11260	-1752	33
H12A	1270	6707	-388	41
H12B	-555	7212	-899	41
H12C	-245	6565	234	41
H22A	3569	8113	5276	44
H22B	3562	8225	6549	44
H22C	3504	9531	5924	44
H25A	-2753	5323	6462	51
H25B	-4442	5954	5902	51
H25C	-2832	6775	7044	51
H1AA	4044	13631	-1776	43
H1AB	5941	13200	-1583	43
H1AC	5989	14770	-1208	43
H24A	260	4878	6448	54
H24B	1975	5390	7604	54
H24C	2249	5702	6435	54

Table 8 Atomic Occupancy for JS_NMeOmeP_Cu.

<i>Atom</i>	<i>Occupancy</i>	<i>Atom</i>	<i>Occupancy</i>	<i>Atom</i>	<i>Occupancy</i>
O2A	0.92	C1A	0.92	H1AA	0.92
H1AB	0.92	H1AC	0.92	O2B	0.08
C1B	0.08				

1.6 XRD data for Benzyl *p*-tolyl sulfoxide 4.10

Table 1 Crystal data and structure refinement for JS03_91_Cu.

Identification code	JS03_91_Cu
Empirical formula	C ₁₄ H ₁₄ OS
Formula weight	230.31
Temperature/K	99.9(5)
Crystal system	orthorhombic
Space group	P2 ₁ 2 ₁ 2 ₁
<i>a</i> /Å	5.66476(12)
<i>b</i> /Å	11.6755(2)
<i>c</i> /Å	17.5269(4)
α /°	90.00
β /°	90.00
γ /°	90.00
Volume/Å ³	1159.21(4)
Z	4
ρ_{calc} /mm ³	1.320
<i>m</i> /mm ⁻¹	2.257
F(000)	488.0
Crystal size/mm ³	0.27 × 0.13 × 0.09
Radiation	CuK α (λ = 1.54184)
2 θ range for data collection	9.1 to 133.2°
Index ranges	-6 ≤ <i>h</i> ≤ 6, -13 ≤ <i>k</i> ≤ 13, -20 ≤ <i>l</i> ≤ 20
Reflections collected	10499
Independent reflections	2053 [<i>R</i> _{int} = 0.0286, <i>R</i> _{sigma} = 0.0187]
Data/restraints/parameters	2053/0/146
Goodness-of-fit on <i>F</i> ²	1.088
Final <i>R</i> indexes [<i>I</i> ≥ 2 σ (<i>I</i>)]	<i>R</i> ₁ = 0.0254, <i>wR</i> ₂ = 0.0621
Final <i>R</i> indexes [all data]	<i>R</i> ₁ = 0.0267, <i>wR</i> ₂ = 0.0631
Largest diff. peak/hole / e Å ⁻³	0.16/-0.23
Flack parameter	-0.012(16)

Table 2 Fractional Atomic Coordinates ($\times 10^4$) and Equivalent Isotropic Displacement Parameters ($\text{\AA}^2 \times 10^3$) for JS03_91_Cu. U_{eq} is defined as 1/3 of the trace of the orthogonalised U_{ij} tensor.

Atom	<i>x</i>	<i>y</i>	<i>z</i>	U(eq)
C1	-4563(4)	2400.7(15)	-3501.6(11)	27.1(4)
C2	-3815(3)	1596.7(14)	-4128(1)	19.3(4)
C3	-1666(3)	1015.8(14)	-4100.8(9)	20.7(4)
C4	-1000(3)	276.9(14)	-4683(1)	20.2(4)
C5	-2494(3)	116.4(15)	-5297.6(10)	17.8(4)
C6	-4636(3)	695.7(15)	-5343.5(10)	19.3(4)
C7	-5274(3)	1429.1(14)	-4757.2(10)	19.7(4)
S8	-1658.4(7)	-822.3(3)	-6060.9(2)	18.93(11)
O9	841(2)	-1182.1(11)	-5923.8(7)	25.4(3)
C10	-3527(3)	-2026.5(14)	-5784.6(9)	19.6(4)
C11	-3441(3)	-2946.9(14)	-6382.9(9)	18.0(3)
C12	-1522(3)	-3687.6(14)	-6442.4(10)	19.4(3)
C13	-1466(3)	-4525.0(14)	-7002.1(10)	21.2(4)
C14	-3336(3)	-4647.5(14)	-7505.9(10)	22.1(4)
C15	-5261(3)	-3913.7(14)	-7449.7(10)	22.0(4)
C16	-5313(3)	-3065.8(14)	-6898.1(10)	20.2(4)

Table 3 Anisotropic Displacement Parameters ($\text{\AA}^2 \times 10^3$) for JS03_91_Cu. The Anisotropic displacement factor exponent takes the form: $-2\pi^2[h^2a^{*2}U_{11}+2hka^*b^*U_{12}+\dots]$.

Atom	U_{11}	U_{22}	U_{33}	U_{23}	U_{13}	U_{12}
C1	29.8(10)	23.4(9)	28(1)	-4.4(8)	-1.6(9)	-1.8(8)
C2	20.9(9)	16.5(8)	20.6(9)	2.5(6)	3.2(7)	-4.7(7)
C3	18.9(8)	22.4(8)	20.9(9)	3.2(6)	-5.5(7)	-5.2(7)
C4	15.2(9)	19.7(8)	25.6(9)	5.2(7)	0.0(7)	0.8(7)
C5	17.0(8)	16.4(8)	20.1(9)	2.5(7)	0.4(7)	-2.3(6)
C6	16.1(8)	22.0(9)	19.8(8)	0.2(7)	-3.6(7)	-1.1(7)
C7	14.5(8)	18.8(8)	25.8(10)	3.2(7)	0.3(7)	0.6(7)
S8	16.6(2)	19.52(19)	20.6(2)	0.82(17)	3.08(17)	0.28(17)
O9	15.2(6)	26.2(6)	34.7(8)	-4.3(5)	5.1(5)	1.3(5)
C10	16.7(8)	21.4(8)	20.7(8)	2.6(7)	4.3(7)	-2.9(8)
C11	16.3(8)	19.0(8)	18.6(8)	4.1(6)	3.3(7)	-0.9(7)
C12	17.1(8)	22.5(8)	18.4(8)	5.3(6)	0.4(8)	0.6(8)
C13	21.1(8)	17.2(8)	25.2(9)	5.8(6)	3.1(8)	3.3(7)
C14	27.4(9)	17.8(8)	21.0(9)	1.2(7)	2.6(9)	-2.2(8)
C15	20.0(9)	23.5(9)	22.5(9)	1.4(7)	-2.3(7)	-2.0(7)
C16	16.8(9)	18.8(8)	25.0(9)	4.3(7)	0.9(7)	0.6(7)

Table 4 Bond Lengths for JS03_91_Cu.

Atom	Atom	Length/Å	Atom	Atom	Length/Å
C1	C2	1.505(2)	S8	C10	1.8254(17)
C2	C3	1.394(2)	C10	C11	1.502(2)
C2	C7	1.392(2)	C11	C12	1.393(2)
C3	C4	1.389(3)	C11	C16	1.400(2)
C4	C5	1.383(2)	C12	C13	1.385(2)
C5	C6	1.391(2)	C13	C14	1.387(3)
C5	S8	1.7931(18)	C14	C15	1.390(3)
C6	C7	1.386(2)	C15	C16	1.384(2)
S8	O9	1.4965(12)			

Table 5 Bond Angles for JS03_91_Cu.

Atom	Atom	Atom	Angle/°	Atom	Atom	Atom	Angle/°
C3	C2	C1	121.61(16)	O9	S8	C5	107.55(8)
C7	C2	C1	119.88(16)	O9	S8	C10	106.86(8)
C7	C2	C3	118.51(16)	C11	C10	S8	110.30(11)
C4	C3	C2	120.94(16)	C12	C11	C10	121.46(16)
C5	C4	C3	119.37(16)	C12	C11	C16	118.79(16)
C4	C5	C6	120.87(16)	C16	C11	C10	119.76(16)
C4	C5	S8	120.16(13)	C13	C12	C11	120.60(17)
C6	C5	S8	118.96(13)	C12	C13	C14	120.41(17)
C7	C6	C5	119.02(16)	C13	C14	C15	119.38(16)
C6	C7	C2	121.29(16)	C16	C15	C14	120.47(17)
C5	S8	C10	96.88(8)	C15	C16	C11	120.35(16)

Table 6 Torsion Angles for JS03_91_Cu.

A	B	C	D	Angle/°	A	B	C	D	Angle/°
C1	C2	C3	C4	-179.99(16)	C7	C2	C3	C4	-0.7(2)
C1	C2	C7	C6	179.94(16)	S8	C5	C6	C7	-179.44(13)
C2	C3	C4	C5	0.0(2)	S8	C10	C11	C12	77.35(18)
C3	C2	C7	C6	0.6(2)	S8	C10	C11	C16	-102.24(16)
C3	C4	C5	C6	0.8(2)	O9	S8	C10	C11	-75.79(13)
C3	C4	C5	S8	179.36(13)	C10	C11	C12	C13	-179.46(15)
C4	C5	C6	C7	-0.9(2)	C10	C11	C16	C15	-179.68(16)
C4	C5	S8	O9	-7.18(16)	C11	C12	C13	C14	-0.8(2)
C4	C5	S8	C10	102.97(15)	C12	C11	C16	C15	0.7(2)
C5	C6	C7	C2	0.2(2)	C12	C13	C14	C15	0.7(2)
C5	S8	C10	C11	173.47(13)	C13	C14	C15	C16	0.2(2)
C6	C5	S8	O9	171.40(13)	C14	C15	C16	C11	-0.9(3)
C6	C5	S8	C10	-78.45(14)	C16	C11	C12	C13	0.1(2)

Table 7 Hydrogen Atom Coordinates ($\text{\AA}\times 10^4$) and Isotropic Displacement Parameters ($\text{\AA}^2\times 10^3$) for JS03_91_Cu.

Atom	x	y	z	U(eq)
H1A	-3556	2297	-3066	41
H1B	-6167	2241	-3361	41
H1C	-4442	3177	-3678	41
H3	-664	1125	-3687	25
H4	438	-106	-4660	24
H6	-5624	592	-5762	23
H7	-6706	1817	-4785	24
H10A	-2991	-2334	-5301	24
H10B	-5141	-1766	-5721	24
H12	-267	-3619	-6103	23
H13	-165	-5008	-7040	25
H14	-3303	-5215	-7878	26
H15	-6523	-3993	-7785	26
H16	-6599	-2572	-6870	24

1.8 XRD data for Methyl 6(5)-OMe benzimidazole sulfoxide 4.11

Table 1 Crystal data and structure refinement for JS03_82_Cu.

Identification code	JS03_82_Cu
Empirical formula	C ₉ H ₁₀ N ₂ O ₂ S
Formula weight	210.25
Temperature/K	120.00(12)
Crystal system	monoclinic
Space group	P2 ₁ /c
a/Å	8.0080(3)
b/Å	14.5693(6)
c/Å	16.4409(4)
α/°	90.00
β/°	95.840(3)
γ/°	90.00
Volume/Å ³	1908.20(11)
Z	8
ρ _{calc} /g/cm ³	1.464
μ/mm ⁻¹	2.826
F(000)	880.0
Crystal size/mm ³	0.25 × 0.05 × 0.03
Radiation	CuKα (λ = 1.54184)
2θ range for data collection/°	8.12 to 134.16
Index ranges	-9 ≤ h ≤ 9, -15 ≤ k ≤ 17, -19 ≤ l ≤ 19
Reflections collected	6999
Independent reflections	3410 [R _{int} = 0.0892, R _{sigma} = 0.1038]
Data/restraints/parameters	3410/0/257
Goodness-of-fit on F ²	0.989
Final R indexes [I ≥ 2σ (I)]	R ₁ = 0.0663, wR ₂ = 0.1536
Final R indexes [all data]	R ₁ = 0.1027, wR ₂ = 0.1849
Largest diff. peak/hole / e Å ⁻³	0.63/-0.50

Table 2 Fractional Atomic Coordinates ($\times 10^4$) and Equivalent Isotropic Displacement Parameters ($\text{\AA}^2 \times 10^3$) for JS03_82_Cu. U_{eq} is defined as 1/3 of the trace of the orthogonalised U_{ij} tensor.

Atom	x	y	z	U(eq)
C1	-2347(5)	10002(4)	1023(3)	41.7(11)
O2	-1067(4)	10548(2)	730.7(18)	40.3(8)
C3	453(5)	10584(3)	1196(2)	32.9(9)
C4	757(5)	10204(3)	1961(2)	32.7(9)
C5	2378(5)	10336(3)	2355(2)	31.2(9)
C6	3634(5)	10816(3)	2001(2)	32.6(9)
C7	3291(5)	11177(3)	1215(3)	37.5(10)
C8	1700(6)	11074(3)	823(3)	36.2(10)
N9	3087(4)	10079(3)	3120(2)	35.1(8)
C10	4698(5)	10400(3)	3183(2)	34.8(10)
N11	5106(5)	10835(3)	2539(2)	35.4(8)
S12	6017.3(14)	10202.8(8)	4111.7(6)	36.7(3)
O13	6361(4)	9186(2)	4136.7(16)	37.9(7)
C14	7851(6)	10759(4)	3822(3)	43.8(11)
C15	2611(5)	8440(3)	944(2)	35.9(10)
O16	3862(4)	7896(2)	622.4(16)	36.0(7)
C17	5382(5)	7826(3)	1091(2)	27.4(8)
C18	5715(5)	8198(3)	1859(2)	26.9(8)
C19	7321(5)	8041(3)	2252(2)	25.2(8)
C20	8551(5)	7542(3)	1893(2)	30.3(9)
C21	8166(5)	7167(3)	1117(2)	35(1)
C22	6606(5)	7309(3)	722(2)	31.9(9)
N23	8048(4)	8303(3)	3012.8(18)	29.2(8)
C24	9647(5)	7959(3)	3071(2)	31.4(9)
N25	10020(4)	7501(3)	2429.5(19)	33.4(8)
S26	10954.4(13)	8088.6(8)	4013.0(5)	34.5(3)
O27	11215(3)	9101(2)	4138.4(16)	35.4(7)
C28	12817(5)	7624(4)	3666(3)	41.2(11)

Table 3 Anisotropic Displacement Parameters ($\text{\AA}^2 \times 10^3$) for JS03_82_Cu. The Anisotropic displacement factor exponent takes the form: $-2\pi^2[h^2a^2U_{11}+2hka*b*U_{12}+\dots]$.

Atom	U_{11}	U_{22}	U_{33}	U_{23}	U_{13}	U_{12}
C1	28(2)	46(3)	52(2)	10(2)	9.6(17)	1(2)
O2	29.8(15)	38(2)	54.1(16)	15.4(14)	11.5(12)	6.5(14)
C3	27(2)	26(3)	47(2)	1.9(18)	9.5(16)	5.6(18)
C4	31(2)	24(2)	46(2)	5.3(17)	17.3(16)	4.8(18)
C5	34(2)	21(2)	40.6(19)	2.2(16)	13.2(16)	4.0(18)
C6	34(2)	21(2)	44.7(19)	-1.7(17)	15.0(16)	-2.1(18)
C7	36(2)	32(3)	47(2)	1.9(19)	16.0(18)	-2.4(19)
C8	40(2)	26(3)	44(2)	9.3(18)	13.1(17)	5(2)
N9	38.4(19)	29(2)	39.9(16)	1.4(15)	12.5(14)	-1.2(17)
C10	38(2)	26(3)	41.4(19)	-4.9(17)	8.7(16)	2.7(19)
N11	39(2)	28(2)	40.6(16)	-1.2(15)	9.8(14)	-0.1(17)
S12	43.5(6)	32.8(7)	35.2(5)	-3.0(4)	10.6(4)	1.0(5)
O13	42.1(17)	31.4(19)	41.8(14)	3.1(13)	11.1(12)	1.0(15)
C14	45(3)	41(3)	45(2)	0(2)	1.5(18)	-12(2)
C15	24.3(19)	40(3)	42.7(19)	-4.4(19)	-1.8(15)	8.2(19)
O16	28.1(14)	40(2)	38.1(13)	-7.1(13)	-4.3(11)	4.1(14)
C17	22.0(18)	26(2)	33.9(17)	0.2(15)	0.4(14)	-0.5(17)
C18	24.0(18)	25(2)	31.8(16)	0.1(15)	4.5(13)	-6.6(17)
C19	25.5(18)	17(2)	33.3(16)	0.8(15)	4.8(14)	-3.9(16)
C20	25.9(19)	27(2)	37.8(18)	5.6(17)	2.7(15)	0.8(18)
C21	35(2)	31(3)	39.3(18)	-3.3(17)	5.1(16)	7.5(19)
C22	35(2)	28(3)	32.2(17)	-2.5(16)	2.4(15)	3.9(19)
N23	26.3(16)	30(2)	31.2(14)	0.4(14)	1.8(12)	-0.7(15)
C24	28(2)	28(2)	37.9(18)	8.4(17)	1.2(15)	-3.1(18)
N25	27.3(16)	35(2)	36.2(16)	3.4(15)	-3.2(13)	0.8(16)
S26	32.1(5)	38.4(7)	32.2(4)	5.6(4)	-1.5(3)	-4.1(5)
O27	30.1(15)	36(2)	40.0(13)	-3.5(12)	1.5(11)	-3.8(13)
C28	33(2)	39(3)	48(2)	3(2)	-9.2(18)	3(2)

Table 4 Bond Lengths for JS03_82_Cu.

Atom	Atom	Length/Å	Atom	Atom	Length/Å
C1	O2	1.419(5)	C15	O16	1.421(5)
O2	C3	1.371(5)	O16	C17	1.376(5)
C3	C4	1.373(6)	C17	C18	1.376(5)
C3	C8	1.416(6)	C17	C22	1.421(6)
C4	C5	1.404(6)	C18	C19	1.398(5)
C5	C6	1.399(6)	C19	C20	1.402(6)
C5	N9	1.378(5)	C19	N23	1.378(5)
C6	C7	1.397(6)	C20	C21	1.394(6)
C6	N11	1.400(6)	C20	N25	1.397(5)
C7	C8	1.376(6)	C21	C22	1.364(6)
N9	C10	1.366(6)	N23	C24	1.369(5)
C10	N11	1.304(6)	C24	N25	1.308(6)
C10	S12	1.790(4)	C24	S26	1.789(4)
S12	O13	1.506(4)	S26	O27	1.501(3)
S12	C14	1.784(5)	S26	C28	1.783(5)

Table 5 Bond Angles for JS03_82_Cu.

Atom Atom Atom	Angle/°	Atom Atom Atom	Angle/°
C3 O2 C1	117.6(3)	C17 O16 C15	116.7(3)
O2 C3 C4	124.1(4)	O16 C17 C22	114.2(3)
O2 C3 C8	113.8(4)	C18 C17 O16	124.2(4)
C4 C3 C8	122.2(4)	C18 C17 C22	121.6(4)
C3 C4 C5	115.9(4)	C17 C18 C19	116.3(4)
C6 C5 C4	123.1(4)	C18 C19 C20	122.9(3)
N9 C5 C4	131.3(4)	N23 C19 C18	131.1(4)
N9 C5 C6	105.5(4)	N23 C19 C20	106.0(3)
C5 C6 N11	110.1(4)	C21 C20 C19	119.2(4)
C7 C6 C5	119.4(4)	C21 C20 N25	130.9(4)
C7 C6 N11	130.6(4)	N25 C20 C19	109.8(3)
C8 C7 C6	118.5(4)	C22 C21 C20	118.9(4)
C7 C8 C3	120.9(4)	C21 C22 C17	121.1(4)
C10 N9 C5	105.9(4)	C24 N23 C19	105.5(3)
N9 C10 S12	118.7(3)	N23 C24 S26	118.9(3)
N11 C10 N9	114.7(4)	N25 C24 N23	114.8(3)
N11 C10 S12	126.5(4)	N25 C24 S26	126.2(3)
C10 N11 C6	103.7(4)	C24 N25 C20	103.9(3)
O13 S12 C10	105.76(19)	O27 S26 C24	106.46(18)
O13 S12 C14	107.5(2)	O27 S26 C28	107.9(2)
C14 S12 C10	97.5(2)	C28 S26 C24	96.8(2)

Table 6 Torsion Angles for JS03_82_Cu.

A	B	C	D	Angle/°	A	B	C	D	Angle/°
C1	O2	C3	C4	-6.9(6)	C15	O16	C17	C18	4.2(6)
C1	O2	C3	C8	174.5(4)	C15	O16	C17	C22	-177.3(4)
O2	C3	C4	C5	-178.0(4)	O16	C17	C18	C19	178.7(4)
O2	C3	C8	C7	179.6(4)	O16	C17	C22	C21	-179.0(4)
C3	C4	C5	C6	-0.6(6)	C17	C18	C19	C20	0.6(6)
C3	C4	C5	N9	177.8(4)	C17	C18	C19	N23	-179.3(4)
C4	C3	C8	C7	0.9(7)	C18	C17	C22	C21	-0.4(7)
C4	C5	C6	C7	-0.8(7)	C18	C19	C20	C21	-1.2(6)
C4	C5	C6	N11	179.9(4)	C18	C19	C20	N25	179.9(4)
C4	C5	N9	C10	-179.2(4)	C18	C19	N23	C24	-179.8(4)
C5	C6	C7	C8	2.2(7)	C19	C20	C21	C22	1.0(7)
C5	C6	N11	C10	-1.2(5)	C19	C20	N25	C24	0.0(5)
C5	N9	C10	N11	-0.2(5)	C19	N23	C24	N25	-0.3(5)
C5	N9	C10	S12	179.4(3)	C19	N23	C24	S26	-175.6(3)
C6	C5	N9	C10	-0.6(5)	C20	C19	N23	C24	0.3(4)
C6	C7	C8	C3	-2.3(7)	C20	C21	C22	C17	-0.2(7)
C7	C6	N11	C10	179.5(5)	C21	C20	N25	C24	-178.7(5)
C8	C3	C4	C5	0.5(7)	C22	C17	C18	C19	0.2(6)
N9	C5	C6	C7	-179.5(4)	N23	C19	C20	C21	178.7(4)
N9	C5	C6	N11	1.2(5)	N23	C19	C20	N25	-0.2(5)
N9	C10	N11	C6	0.9(5)	N23	C24	N25	C20	0.2(5)
N9	C10	S12	O13	69.4(4)	N23	C24	S26	O27	-63.8(4)
N9	C10	S12	C14	-180.0(4)	N23	C24	S26	C28	-174.8(4)
N11	C6	C7	C8	-178.6(4)	N25	C20	C21	C22	179.6(4)
N11	C10	S12	O13	-111.1(4)	N25	C24	S26	O27	121.5(4)
N11	C10	S12	C14	-0.5(5)	N25	C24	S26	C28	10.5(4)
S12	C10	N11	C6	-178.6(3)	S26	C24	N25	C20	175.0(3)

Table 7 Hydrogen Atom Coordinates ($\text{\AA}\times 10^4$) and Isotropic Displacement Parameters ($\text{\AA}^2\times 10^3$) for JS03_82_Cu.

Atom	x	y	z	U(eq)
H1A	-3324	10012	632	63
H1B	-2628	10243	1535	63
H1C	-1956	9382	1098	63
H4	-61	9878	2203	39
H7	4119	11480	961	45
H8	1440	11329	308	43
H9	2613	9778	3484	42
H14A	8106	10527	3303	66
H14B	8778	10640	4226	66
H14C	7656	11408	3783	66
H15A	1627	8460	559	54
H15B	3030	9052	1043	54
H15C	2332	8177	1448	54
H18	4916	8536	2104	32
H21	8959	6826	872	42
H22	6340	7064	203	38
H23	7593	8616	3375	35
H28A	12638	6990	3525	62
H28B	13725	7675	4092	62
H28C	13089	7958	3194	62

1.9 XRD data for Pyridyl *p*-tolyl sulfoxide 4.12

Table 1 Crystal data and structure refinement for JS03_90_Cu.

Identification code	JS03_90_Cu
Empirical formula	C ₁₆ H ₁₉ NO ₂ S
Formula weight	289.38
Temperature/K	100.0(5)
Crystal system	monoclinic
Space group	P2 ₁ /c
<i>a</i> /Å	20.2700(6)
<i>b</i> /Å	4.89800(15)
<i>c</i> /Å	15.8506(5)
α /°	90.00
β /°	108.354(3)
γ /°	90.00
Volume/Å ³	1493.63(8)
Z	4
ρ_{calc} /mm ³	1.287
<i>m</i> /mm ⁻¹	1.929
F(000)	616.0
Crystal size/mm ³	0.24 × 0.14 × 0.07
Radiation	CuK α (λ = 1.54184)
2 Θ range for data collection	9.2 to 134.08°
Index ranges	-24 ≤ <i>h</i> ≤ 23, -5 ≤ <i>k</i> ≤ 5, -18 ≤ <i>l</i> ≤ 18
Reflections collected	11126
Independent reflections	2654 [<i>R</i> _{int} = 0.0387, <i>R</i> _{sigma} = 0.0280]
Data/restraints/parameters	2654/9/233
Goodness-of-fit on <i>F</i> ²	1.060
Final <i>R</i> indexes [<i>I</i> ≥ 2 σ (<i>I</i>)]	<i>R</i> ₁ = 0.0445, <i>wR</i> ₂ = 0.1069
Final <i>R</i> indexes [all data]	<i>R</i> ₁ = 0.0540, <i>wR</i> ₂ = 0.1136
Largest diff. peak/hole / e Å ⁻³	0.22/-0.24

Table 2 Fractional Atomic Coordinates ($\times 10^4$) and Equivalent Isotropic Displacement Parameters ($\text{\AA}^2 \times 10^3$) for JS03_90_Cu. U_{eq} is defined as 1/3 of the trace of the orthogonalised U_{ij} tensor.

Atom	<i>x</i>	<i>y</i>	<i>z</i>	U(eq)
C1A	362.1(19)	8136(9)	9324(2)	49.6(9)
C1B	536(5)	7080(20)	9583(7)	59(3)
C2A	782(3)	6878(18)	8784(3)	39(2)
C2B	809(10)	6510(30)	8792(9)	50(6)
C3A	704(3)	7795(14)	7941(4)	42.6(17)
C3B	671(8)	8140(30)	8034(9)	47(5)
C4A	1076(2)	6649(10)	7424(2)	35.1(8)
C4B	974(6)	7521(17)	7384(5)	39(3)
C5A	1532.0(15)	4543(7)	7779(3)	29.1(6)
C5B	1425(4)	5306(16)	7495(4)	27(2)
C6A	1619.2(16)	3576(7)	8630(3)	42.0(8)
C6B	1548(4)	3643(13)	8240(5)	34(2)
C7A	1241(2)	4800(9)	9121(3)	45.3(10)
C7B	1252(6)	4282(19)	8898(5)	45(3)
S8A	2015.0(3)	2972.0(14)	7137.7(5)	35.9(3)
S8B	1782.1(7)	4537(3)	6624.8(11)	31.5(6)
O9A	1590.4(12)	3085(7)	6180.9(17)	54.8(7)
O9B	1826(3)	1521(11)	6567(4)	42.8(13)
C10	2670.7(9)	5637(4)	7283.2(12)	34.4(4)
C11	3217.1(9)	4699(4)	6887.7(12)	32.0(4)
C12	3267.8(9)	5742(4)	6090.5(12)	32.5(4)
C13	3813.9(9)	4744(4)	5816.6(12)	34.5(4)
C14	4269.5(10)	2784(4)	6296.7(13)	39.9(5)
C15	4153.2(11)	1873(5)	7066.8(15)	47.0(5)
N16	3646.2(8)	2790(4)	7367.4(11)	42.7(4)
C17	2766.9(11)	7815(4)	5549.4(14)	45.9(5)
O18	3911.8(7)	5832(3)	5058.4(9)	46.2(4)
C19	3630.8(13)	4191(6)	4283.3(14)	61.9(7)
C20	4861.7(11)	1646(5)	6016.4(16)	53.3(6)

Table 3 Anisotropic Displacement Parameters ($\text{\AA}^2 \times 10^3$) for JS03_90_Cu. The Anisotropic displacement factor exponent takes the form: $-2\pi^2[h^2a^{*2}U_{11}+2hka^*b^*U_{12}+\dots]$.

Atom	U_{11}	U_{22}	U_{33}	U_{23}	U_{13}	U_{12}
C1A	41.9(18)	72(3)	46(2)	-18(2)	30.2(16)	-4.6(19)
C2A	24(2)	59(3)	40(3)	-26.4(19)	17.6(15)	-15.1(16)
C3A	30(2)	51(3)	52(3)	-8(2)	20.3(17)	8.0(15)
C4A	34(2)	42(2)	31.9(17)	0.6(14)	14.9(12)	-1.0(18)
C5A	28.1(14)	29.1(16)	34.4(18)	-0.4(15)	16.0(13)	-0.8(12)
C6A	36.8(16)	50(2)	38(2)	8.3(15)	11.0(16)	4.5(13)
C7A	40(2)	70(3)	29.0(17)	-5(2)	15.8(15)	-22.1(18)
S8A	35.6(4)	31.1(4)	48.5(5)	-7.5(4)	24.0(3)	-0.5(3)
S8B	30.7(8)	36.6(11)	29.9(10)	-2.3(7)	13.4(6)	2.7(6)
O9A	41.1(13)	82(2)	44.6(15)	-34.2(16)	18.0(11)	-8.3(14)
O9B	45(3)	37(3)	54(3)	-16(3)	26(2)	-6(2)
C10	34.8(9)	37.6(10)	36.1(10)	-7.7(8)	19.0(8)	-2.8(8)
C11	30.0(9)	36.6(10)	33.5(9)	-6.7(8)	16.0(7)	-2.5(7)
C12	35.5(9)	32.1(10)	33.4(9)	-6.4(7)	15.7(7)	-5.3(7)
C13	37.9(10)	39.1(10)	33.0(9)	-9.6(8)	20.2(8)	-11.4(8)
C14	34.9(10)	47.7(12)	43.2(11)	-10.0(9)	21.2(8)	-2.5(9)
C15	38.9(11)	58.7(14)	49.5(12)	7.4(10)	22.4(9)	14.6(10)
N16	37.7(9)	57.2(11)	39.7(9)	4.6(8)	21.3(7)	8.2(8)
C17	50.0(12)	45.9(12)	47.7(12)	6.9(9)	23.7(10)	5.2(10)
O18	52.4(8)	59.3(9)	35.8(7)	-7.2(7)	26.7(6)	-14.4(7)
C19	60.0(14)	93(2)	36.3(12)	-16.0(12)	20.8(10)	-11.7(14)
C20	42.4(12)	65.6(15)	63.6(14)	-10.1(12)	33.3(11)	2.9(11)

Table 4 Bond Lengths for JS03_90_Cu.

Atom Atom	Length/Å	Atom Atom	Length/Å
C1A C2A	1.516(5)	S8A O9A	1.490(3)
C1B C2B	1.547(11)	S8A C10	1.825(2)
C2A C3A	1.370(5)	S8B O9B	1.484(5)
C2A C7A	1.368(7)	S8B C10	1.855(2)
C2B C3B	1.3927(17)	C10 C11	1.506(2)
C2B C7B	1.3901(10)	C11 C12	1.397(2)
C3A C4A	1.394(6)	C11 N16	1.339(2)
C3B C4B	1.3901(10)	C12 C13	1.398(2)
C4A C5A	1.381(5)	C12 C17	1.500(3)
C4B C5B	1.3926(17)	C13 C14	1.382(3)
C5A C6A	1.386(5)	C13 O18	1.385(2)
C5A S8A	1.792(3)	C14 C15	1.388(3)
C5B C6B	1.3898(10)	C14 C20	1.512(3)
C5B S8B	1.789(5)	C15 N16	1.339(2)
C6A C7A	1.390(6)	O18 C19	1.428(3)
C6B C7B	1.3934(17)		

Table 5 Bond Angles for JS03_90_Cu.

Atom Atom Atom	Angle/°	Atom Atom Atom	Angle/°
C3A C2A C1A	120.2(6)	O9A S8A C10	105.44(14)
C7A C2A C1A	121.0(4)	C5B S8B C10	93.6(3)
C7A C2A C3A	118.8(4)	O9B S8B C5B	107.7(3)
C3B C2B C1B	124.8(8)	O9B S8B C10	104.9(2)
C7B C2B C1B	115.1(8)	S8A C10 S8B	35.06(6)
C7B C2B C3B	120.01(10)	C11 C10 S8A	109.32(13)
C2A C3A C4A	121.5(5)	C11 C10 S8B	112.85(13)
C4B C3B C2B	120.01(10)	C12 C11 C10	122.57(17)
C5A C4A C3A	118.5(3)	N16 C11 C10	114.09(16)
C3B C4B C5B	119.97(10)	N16 C11 C12	123.34(16)
C4A C5A C6A	121.0(2)	C11 C12 C13	116.36(18)
C4A C5A S8A	120.3(3)	C11 C12 C17	122.39(16)
C6A C5A S8A	118.7(3)	C13 C12 C17	121.25(17)
C4B C5B S8B	118.3(5)	C14 C13 C12	121.93(17)
C6B C5B C4B	120.00(10)	C14 C13 O18	119.46(16)
C6B C5B S8B	121.5(5)	O18 C13 C12	118.58(18)
C5A C6A C7A	118.3(3)	C13 C14 C15	116.00(17)
C5B C6B C7B	119.97(10)	C13 C14 C20	123.29(18)
C2A C7A C6A	121.9(3)	C15 C14 C20	120.7(2)
C2B C7B C6B	119.95(10)	N16 C15 C14	124.6(2)
C5A S8A C10	97.32(11)	C11 N16 C15	117.79(17)
O9A S8A C5A	108.53(17)	C13 O18 C19	113.73(17)

Table 6 Torsion Angles for JS03_90_Cu.

A	B	C	D	Angle/°	A	B	C	D	Angle/°
C1A	C2A	C3A	C4A	-179.0(6)	S8A	C5A	C6A	C7A	-179.8(3)
C1A	C2A	C7A	C6A	178.5(5)	S8A	C10	C11	C12	106.63(18)
C1B	C2B	C3B	C4B	176.5(17)	S8A	C10	C11	N16	-73.43(18)
C1B	C2B	C7B	C6B	-177.8(13)	S8B	C5B	C6B	C7B	-179.0(7)
C2A	C3A	C4A	C5A	-0.1(9)	S8B	C10	C11	C12	69.1(2)
C2B	C3B	C4B	C5B	-1(3)	S8B	C10	C11	N16	-110.92(17)
C3A	C2A	C7A	C6A	-0.9(10)	O9A	S8A	C10	S8B	27.53(13)
C3A	C4A	C5A	C6A	0.2(6)	O9A	S8A	C10	C11	-74.99(18)
C3A	C4A	C5A	S8A	179.3(4)	O9B	S8B	C10	S8A	-35.2(2)
C3B	C2B	C7B	C6B	-1(3)	O9B	S8B	C10	C11	56.2(3)
C3B	C4B	C5B	C6B	2.7(18)	C10	C11	C12	C13	178.08(16)
C3B	C4B	C5B	S8B	178.2(11)	C10	C11	C12	C17	-2.1(3)
C4A	C5A	C6A	C7A	-0.7(5)	C10	C11	N16	C15	-179.10(18)
C4A	C5A	S8A	O9A	-31.1(3)	C11	C12	C13	C14	1.5(3)
C4A	C5A	S8A	C10	77.9(3)	C11	C12	C13	O18	-176.21(15)
C4B	C5B	C6B	C7B	-3.7(14)	C12	C11	N16	C15	0.8(3)
C4B	C5B	S8B	O9B	-143.4(8)	C12	C13	C14	C15	-0.1(3)
C4B	C5B	S8B	C10	109.8(8)	C12	C13	C14	C20	179.56(19)
C5A	C6A	C7A	C2A	1.1(7)	C12	C13	O18	C19	-99.4(2)
C5A	S8A	C10	S8B	-84.07(18)	C13	C14	C15	N16	-1.0(3)
C5A	S8A	C10	C11	173.42(19)	C14	C13	O18	C19	82.9(2)
C5B	C6B	C7B	C2B	2.9(19)	C14	C15	N16	C11	0.7(3)
C5B	S8B	C10	S8A	74.2(3)	N16	C11	C12	C13	-1.9(3)
C5B	S8B	C10	C11	165.6(3)	N16	C11	C12	C17	177.99(18)
C6A	C5A	S8A	O9A	148.0(3)	C17	C12	C13	C14	-178.38(18)
C6A	C5A	S8A	C10	-103.0(3)	C17	C12	C13	O18	4.0(3)
C6B	C5B	S8B	O9B	32.0(8)	O18	C13	C14	C15	177.51(18)
C6B	C5B	S8B	C10	-74.8(7)	O18	C13	C14	C20	-2.8(3)
C7A	C2A	C3A	C4A	0.4(12)	C20	C14	C15	N16	179.3(2)
C7B	C2B	C3B	C4B	0(3)					

Table 7 Hydrogen Atom Coordinates ($\text{\AA}\times 10^4$) and Isotropic Displacement Parameters ($\text{\AA}^2\times 10^3$) for JS03_90_Cu.

Atom	<i>x</i>	<i>y</i>	<i>z</i>	U(eq)
H1AA	349	10083	9249	74
H1AB	574	7699	9941	74
H1AC	-103	7424	9124	74
H1BA	694	5666	10020	88
H1BB	37	7106	9376	88
H1BC	707	8811	9843	88
H3A	396	9216	7709	51
H3B	376	9632	7964	57
H4A	1018	7288	6853	42
H4B	877	8589	6874	47
H6A	1923	2146	8865	50
H6B	1827	2104	8298	41
H7A	1301	4189	9696	54
H7B	1351	3218	9409	54
H10A	2455	7300	6992	41
H10B	2883	6021	7911	41
H10C	2682	7613	7323	41
H10D	2779	4917	7882	41
H15	4448	533	7397	56
H17A	2311	7026	5334	69
H17B	2912	8373	5055	69
H17C	2757	9373	5913	69
H19A	3748	4983	3795	93
H19B	3134	4105	4140	93
H19C	3821	2383	4394	93
H20A	4697	148	5615	80
H20B	5224	1020	6531	80
H20C	5041	3048	5725	80

Table 8 Atomic Occupancy for JS03_90_Cu.

Atom	Occupancy	Atom	Occupancy	Atom	Occupancy
C1A	0.690(2)	H1AA	0.690(2)	H1AB	0.690(2)
H1AC	0.690(2)	C1B	0.310(2)	H1BA	0.310(2)
H1BB	0.310(2)	H1BC	0.310(2)	C2A	0.690(2)
C2B	0.310(2)	C3A	0.690(2)	H3A	0.690(2)
C3B	0.310(2)	H3B	0.310(2)	C4A	0.690(2)
H4A	0.690(2)	C4B	0.310(2)	H4B	0.310(2)
C5A	0.690(2)	C5B	0.310(2)	C6A	0.690(2)
H6A	0.690(2)	C6B	0.310(2)	H6B	0.310(2)
C7A	0.690(2)	H7A	0.690(2)	C7B	0.310(2)
H7B	0.310(2)	S8A	0.690(2)	S8B	0.310(2)
O9A	0.690(2)	O9B	0.310(2)	H10A	0.690(2)
H10B	0.690(2)	H10C	0.310(2)	H10D	0.310(2)